

**Atmospheric Transport Processes:
Part 2: Chemical Tracers**

By
Elmar R. Reiter

Department of Atmospheric Science
Colorado State University
Fort Collins, Colorado

US Atomic Energy Commission- Division of Technical Information
1971

**Colorado
State
University**

**Department of
Atmospheric Science**

Paper No. 133

*Atmospheric
Transport
Processes*

*Part 2:
Chemical Tracers*

Elmar R. Reiter

Department of Atmospheric Science
Colorado State University, Fort Collins, Colorado

U. S. ATOMIC ENERGY COMMISSION Division of Technical Information

1971

Available as TID-25314 for \$6.00 from
National Technical Information Service
U. S. Department of Commerce
Springfield, Virginia 22151

Library of Congress Catalog Card Number: 76-603262

Printed in the United States of America
USAEC Technical Information Center, Oak Ridge, Tennessee
January 1971; latest printing, August 1972

PREFACE

In Part 1 of this four-part series, the energy transfers and transformations that maintain the large-scale atmospheric circulation patterns were considered. As was pointed out in Part 1, energy transport processes are usually accompanied by mass transports. The mass transports are tied intimately to the transfer of conservative properties of air masses. As such we may consider, among other things, chemical admixtures which react only slowly with the surrounding constituents of the atmosphere and with the earth's surface and which are generated in specific source regions.

A number of such constituents, for example, ozone (O_3), have received detailed attention in meteorological research. There are, however, other trace constituents, such as atomic oxygen (O) or carbon monoxide (CO), whose potential use as tracers for atmospheric motions has scarcely been explored. Refined chemical-analysis techniques which have been developed during the past few years and which are still subject to improvement have put a wealth of information at the meteorologist's disposal. Much of the presently available data are still controversial, and we have to proceed with caution in their interpretation. Especially as we penetrate into higher regions of the atmosphere above the stratopause, where direct wind information becomes sparse and tracers assume a dominant role in obtaining drift information, controversial evidence of such drift motions has to be weighed carefully. The chemistry and photochemistry of the upper atmosphere has to be considered in detail in the interpretation of tracer abundance in these regions.

The use of trace constituents of the atmosphere in estimating the effects of the general circulation has opened into a wide field of research, as may be seen from the long list of references concerned with this subject matter. Excellent monographs have

dealt with certain aspects of chemical tracers and their movement in the atmosphere. This review attempts to avoid unnecessary duplication of these standard reference texts wherever this could be accomplished without sacrificing continuity. The large amount of literature on the problems of small-scale diffusion and the spread of pollutants over relatively small areas has been ignored; instead, attention has been focused on the large-scale aspects of the atmospheric circulation and on its effect on tracer distributions.

This study, again, reveals the need for chemists, atmospheric dynamicists, and synopticians to extend their dialogues and to overcome the barriers of specialization. After all, the atmosphere is their common, and virtually limitless, hunting ground. Future research in this fertile field may see more cooperation between these specialists and thus provide better returns from the intricate and complex experiments that will be needed to explore the many aspects of our global atmosphere and of the atmospheres of other planets.

The major part of this review, as with Part 1 of this series, was compiled during a year of sabbatical leave which I spent at European universities and libraries. My thanks go to Prof. Dr. Herfried Hoinkes, University of Innsbruck, and to Prof. Dr. Hermann Flohn, University of Bonn, who placed their excellent facilities at my disposal. I am also indebted to Prof. Dr. Christian Junge, Mainz, to Dr. Myron Corrin, Fort Collins, to Dr. Jerry Mahlman, Monterey, and to many other individuals, who, in numerous discussions, helped to clarify and generate ideas put forth in this review.

Mrs. Sandra Olson and Mrs. Peggy Stollar typed the manuscript. Mr. Dennis Walts and Mr. J. E. Lovill supervised the drafting of figures and helped in proofreading and editing the typed copy.

This review, sponsored by the U. S. Atomic Energy Commission under Contract No. AT(11-1)-1340, expresses my views and not necessarily those of the sponsoring agency.

Elmar R. Reiter, *Head*
Department of Atmospheric Science
Colorado State University

CONTENTS

Preface	iii
1. Introduction and Theoretical Considerations	1
The Spreading of Tracers	2
The Structure of the Upper Atmosphere	24
General Comments on the Photochemistry of the Upper Atmosphere	56
2. Water Vapor as a Tracer	65
Tropospheric Distributions	65
Water Vapor in the Stratosphere	72
Water Vapor in the Mesosphere	86
3. Carbon Dioxide	95
The Secular Trend of CO ₂ Concentrations	96
Diurnal Variations	98
Seasonal Variations and Interhemispheric Exchange	100
4. Ozone	113
The Chemistry and Photochemistry of Ozone	114
The Vertical Distribution of Ozone	117
Surface [O ₃] and Its Variations	145
Solar Relations of Ozone Variations	155

Ozone and the Biennial Oscillation	157
Theoretical Models of Ozone Transport	162
5. Oxygen as a Tracer	167
Molecular and Atomic Oxygen	167
The Oxygen Green Line, 5577 Å	169
The Oxygen Red Line, 6300 Å	176
The Hydroxyl Radical	182
6. Other Chemical Tracers	185
Carbon Monoxide, CO	185
Methane, CH ₄	188
Sulfur, S	191
Nitrogen Compounds	218
The Halogens	229
Sodium (Na) and Other Alkali Metals	233
Dust	268
7. Conclusions and Outlook	289
List of Symbols	293
References	297
Author Index	355
Subject Index	369

1 INTRODUCTION AND THEORETICAL CONSIDERATIONS

In Part 1 I discussed in detail the dynamics of atmospheric flow patterns and the energetics of the general circulation which provide the physical mechanisms of large-scale transport processes. Computations of momentum, heat, and water-vapor fluxes revealed the existence of mean meridional circulation cells in the troposphere and stratosphere as well as the dominant effects of large-scale eddy motions on the fluxes of quasi-conservative atmospheric parameters.

In recent years abundant material has been accumulated on the distribution of man-made and natural chemical and radioactive trace substances in the lower and upper atmosphere. Part 2 provides a short review of work by various authors dealing with the distribution of chemical tracers in the atmosphere. Radioactive tracers will be dealt with in Part 4 and hydrodynamic tracers in Part 3. The results from these studies are compared with those obtained from the investigations of atmospheric-motion patterns and of energy-flux processes given in Part 1. Chemical and radiochemical evidence thus may be used successfully to augment our understanding of the global transport processes in the atmosphere and of the general circulation, especially in regions outside and above the dense radiosonde networks.

THE SPREADING OF TRACERS

For each tracer with mixing ratio χ , we can write a continuity equation of the form

$$\nabla(\chi\mathbf{v}) = \chi\nabla \cdot \mathbf{v} + \mathbf{v} \cdot \nabla\chi = -\frac{\partial\chi}{\partial t} + S \quad (1.1)$$

where S is a source function that specifies the generation or destruction of the particular tracer under consideration (Murgatroyd, 1965a). We now consider fluctuations of χ with time, whereby $\chi = [\chi]_{(t)} + (\chi)_{(t)}$, and fluctuations of velocity. The mathematical notation in describing mean values and departures therefrom has been described in Part 1, Chap. 1. Substitution of average and departure values into Eq. 1.1 and subsequent averaging with time yields

$$\begin{aligned} \frac{\partial[\chi]_{(t)}}{\partial t} + \left\{ \frac{\partial}{\partial x} [u]_{(t)}[\chi]_{(t)} + \frac{\partial}{\partial y} [v]_{(t)}[\chi]_{(t)} + \frac{\partial}{\partial z} [w]_{(t)}[\chi]_{(t)} \right\} \\ + \left\{ \frac{\partial}{\partial x} [(u)_{(t)}(\chi)_{(t)}]_{(t)} + \frac{\partial}{\partial y} [(v)_{(t)}(\chi)_{(t)}]_{(t)} + \frac{\partial}{\partial z} [(w)_{(t)}(\chi)_{(t)}]_{(t)} \right\} \\ = [S]_{(t)} \end{aligned} \quad (1.2)$$

assuming that $[\partial(\chi)_{(t)}/\partial t]_{(t)} = 0$. Similar expressions can be derived for averaging and departure-forming with respect to longitude, λ , latitude, ϕ , area, A , or pressure, p . A combination of coordinates yields more complicated terms (see Part 1, pp. 92 ff; E. R. Reiter, 1969b). The terms in the first set of braces constitute the transport by the mean meridional or mass circulation (depending on whether a geographic or curvilinear coordinate system is adopted; see Part 1, Chap. 5). The terms in the second set of braces indicate the eddy transports. As has been shown in Part 1, Chap. 3, these terms can be reduced further into standing and transient eddy transports.

In interpreting observed tracer distributions in terms of large-scale transport processes, we will have to abandon the Fickian concept of diffusion, whereby the flux, F , of an atmospheric tracer (e.g., heat, momentum, or radioactive or chemical admixtures) is proportional to, and directed along, the gradient of the tracer distribution (Starr, 1968; E. R. Reiter, 1969a)

$$\begin{aligned} F_y = -\rho K_y \frac{\partial[\chi]_{(\lambda,t)}}{\partial y} = \rho[(\chi)_{(\lambda,t)}(v)_{(\lambda,t)}]_{(\lambda,t)} \\ F_z = -\rho K_z \frac{\partial[\chi]_{(\lambda,t)}}{\partial z} = \rho[(\chi)_{(\lambda,t)}(w)_{(\lambda,t)}]_{(\lambda,t)} \end{aligned} \quad (1.3)$$

where $\chi = c/\rho$ is the mixing ratio of the tracer (c being its concentration), K_y and K_z are the (positive) eddy diffusivity coefficients in the y and z directions, respectively, and λ and t indicate zonal and time averages and departures, respectively.

In Part 1, Chap. 3, we demonstrated that countergradient fluxes of momentum, heat, water vapor, etc., characterize many large-scale transport processes. The Fickian diffusion equations cannot account for such countergradient transport processes. Reed and German (1965) have developed a more general concept of the flux of conservative tracer substances, χ , based upon the mixing-length concept of turbulence theory. Let $\ell(\ell_y, \ell_z)$ be the displacement vector (with its horizontal and vertical components as indicated) equivalent to the mixing length. This vector indicates the distance and direction traveled by an air parcel with the characteristic property, χ , before the parcel mixes this property completely with its new environment. The fluctuations of the property, therefore, may be written as

$$\overline{(\chi)}_{(\lambda, t)} = -\ell \cdot \nabla [\chi]_{(\lambda, t)} = -\left\{ \ell_y \frac{\partial [\chi]_{(\lambda, t)}}{\partial y} + \ell_z \frac{\partial [\chi]_{(\lambda, t)}}{\partial z} \right\} \quad (1.4)$$

Substitution of Eq. 1.4 into Eq. 1.3 yields the flux components

$$\begin{aligned} F_y &= -\rho \left(K_{yy} \frac{\partial [\chi]_{(\lambda, t)}}{\partial y} + K_{yz} \frac{\partial [\chi]_{(\lambda, t)}}{\partial z} \right) \\ F_z &= -\rho \left(K_{zy} \frac{\partial [\chi]_{(\lambda, t)}}{\partial y} + K_{zz} \frac{\partial [\chi]_{(\lambda, t)}}{\partial z} \right) \end{aligned} \quad (1.5)$$

$$\begin{aligned} \text{where } K_{yy} &= [\ell_y(v)_{(\lambda, t)}]_{(\lambda, t)} \\ K_{yz} &= [\ell_z(v)_{(\lambda, t)}]_{(\lambda, t)} \\ K_{zy} &= [\ell_y(w)_{(\lambda, t)}]_{(\lambda, t)} \\ K_{zz} &= [\ell_z(w)_{(\lambda, t)}]_{(\lambda, t)} \end{aligned} \quad (1.6)$$

Equations 1.5 reduce to the form of Eq. 1.3 only if the covariances of ℓ_z and $(v)_{(\lambda, t)}$ and ℓ_y and $(w)_{(\lambda, t)}$ reduce to zero, i.e., if these terms are uncorrelated. As has been shown by Molla and Loisel (1962), however, this is not the case: northward flow in the stratosphere most frequently coincides with sinking motion and southward flow with rising motion (see Part 1, Chap. 3, p. 70), although there may be exceptions to such a pattern, especially during winter in high latitudes (Miller, 1967; Mahlman, 1966).

R. J. Reed and German (1965) assume that the velocity vectors and displacement vectors have the same direction,

$$\frac{(w)_{(\lambda, t)}}{(v)_{(\lambda, t)}} = \frac{\ell_z}{\ell_y} \quad (1.7)$$

This assumption appears justified if the mixing lengths, ℓ_y and ℓ_z , are small in comparison to the eddy sizes involved in the mixing process. (Mixing lengths were estimated to be of the order of 100 km, whereas large-scale eddies, according to Part 1, Chap. 4, p. 165ff, are of the order of 1000 km.)

From Eq. 1.7 and Fig. 1.1, we can derive the following relations:

$$\begin{aligned}
 (v)_{(\lambda,t)} &= (V_\ell)_{(\lambda,t)} \cos \alpha = (V_\ell)_{(\lambda,t)} \left(1 - \frac{\alpha^2}{2!} + \dots\right) \approx (V_\ell)_{(\lambda,t)} \\
 \ell_y &= \ell \cos \alpha = \ell \left(1 - \frac{\alpha^2}{2!} + \dots\right) \approx \ell \\
 (w)_{(\lambda,t)} &= (V_\ell)_{(\lambda,t)} \sin \alpha = (V_\ell)_{(\lambda,t)} (\alpha - \dots) \approx (V_\ell)_{(\lambda,t)} \alpha \\
 \ell_z &= \ell \sin \alpha = \ell(\alpha - \dots) \approx \ell \alpha
 \end{aligned} \tag{1.8}$$

where V_ℓ is the wind-speed component along the mixing-path vector, ℓ , and v is the horizontal wind component toward north. Higher-order terms of α may safely be neglected since for large-scale motions α is of the order of 1 : 1000. For such small angles $\alpha \approx \tan \alpha$; hence it may be referred to as the *slope of the mixing path* (or of the mixing surface).

Substitution of Eq. 1.8 into Eq. 1.6 yields

$$\begin{aligned}
 K_{yy} &\approx [(V_\ell)_{(\lambda,t)} \ell]_{(\lambda,t)} \equiv K \\
 K_{yz} &= K_{zy} \approx [(V_\ell)_{(\lambda,t)} \ell \alpha]_{(\lambda,t)} = [\alpha]_{(\lambda,t)} K \\
 K_{zz} &= [(V_\ell)_{(\lambda,t)} \ell \alpha^2]_{(\lambda,t)} = \{[\alpha]_{(\lambda,t)}^2 + [(\alpha)_{(\lambda,t)}^2]_{(\lambda,t)}\} K
 \end{aligned} \tag{1.9}$$

In arriving at Eq. 1.9, it was assumed by R. J. Reed and German (1965) that $[\alpha]_{(\lambda,t)}$ and $[(\alpha)_{(\lambda,t)}^2]_{(\lambda,t)}$ are independent of V_ℓ and ℓ , i.e., the slope of the mixing path and its variance do not depend on the wind speed and the length of the path.

Defining the mean slope of the surfaces of constant χ

$$[\beta]_{(\lambda,t)} = \tan [\beta]_{(\lambda,t)} = - \frac{\frac{\partial [\chi]_{(\lambda,t)}}{\partial y}}{\frac{\partial [\chi]_{(\lambda,t)}}{\partial z}} \tag{1.10}$$

we can rewrite the expressions for the flux components, Eq. 1.5, as

$$F_y = -\rho K \left\{ 1 - \frac{[\alpha]_{(\lambda,t)}}{[\beta]_{(\lambda,t)}} \right\} \frac{\partial [X]_{(\lambda,t)}}{\partial y}$$

$$F_z = -\rho K \{ [\alpha]_{(\lambda,t)}^2 + [(\alpha)_{(\lambda,t)}^2]_{(\lambda,t)} - [\alpha]_{(\lambda,t)}[\beta]_{(\lambda,t)} \} \frac{\partial [X]_{(\lambda,t)}}{\partial z} \quad (1.11)$$

or, with sufficient approximation,

$$F_y = -\rho K_{yy} \left\{ 1 - \frac{[\alpha]_{(\lambda,t)}}{[\beta]_{(\lambda,t)}} \right\} \frac{\partial [X]_{(\lambda,t)}}{\partial z}$$

$$F_z = -\rho K_{zz} \left\{ 1 - \frac{[\alpha]_{(\lambda,t)}[\beta]_{(\lambda,t)}}{[\alpha]_{(\lambda,t)}^2 + [(\alpha)_{(\lambda,t)}^2]_{(\lambda,t)}} \right\} \frac{\partial [X]_{(\lambda,t)}}{\partial z} \quad (1.12)$$

The flux of the property with mixing ratio χ will be countergradient if $[\alpha]_{(\lambda,t)} > [\beta]_{(\lambda,t)}$, as illustrated in Fig. 1.1 (see also Newell, 1964c). According to Eady (1949),

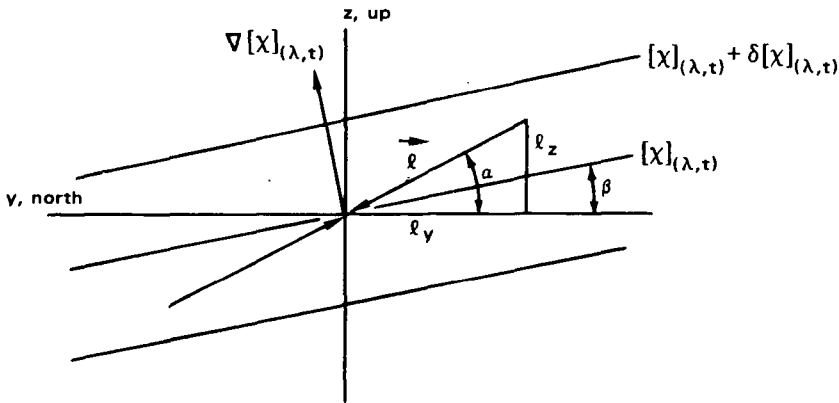


Fig. 1.1 Model for the eddy flux of a property by exchange along a sloping mixing path. [From R. J. Reed and K. E. German, *Monthly Weather Review*, 93(5): 315 (1965).]

in the baroclinically most active part of the extratropical troposphere, the optimal slope of the mixing surfaces is about one-half the slope of the undisturbed isentropic surfaces, $[\alpha]_{(\lambda,t)} \approx (1/2)[\beta]_{(\lambda,t)}$. Hence the heat flux in this region is in the direction of the gradient (see Part 1, Chap. 3, p. 49).

In the absence of sources and sinks of the tracer substance and if eddy transports are considered only in the meridional and vertical directions of a zonally mixed property, the continuity equation 1.1 reduces to

$$\begin{aligned}
\frac{\partial}{\partial t} [c]_{(\lambda,t)} = & - [\mathbf{v}]_{(\lambda,t)} \cdot \nabla [c]_{(\lambda,t)} - \Gamma [wc]_{(\lambda,t)} - \frac{\partial}{\partial y} \rho [(\chi)_{(\lambda,t)}(v)_{(\lambda,t)}]_{(\lambda,t)} \\
& - \frac{\partial}{\partial z} \rho [(\chi)_{(\lambda,t)}(w)_{(\lambda,t)}]_{(\lambda,t)} \\
& + \frac{\tan \phi}{a} \rho [(\chi)_{(\lambda,t)}(v)_{(\lambda,t)}]_{(\lambda,t)} \quad (1.13)
\end{aligned}$$

where \mathbf{v} is the wind vector, $c = \chi\rho$, $\Gamma \equiv (1/\rho) \partial\rho/\partial z$, a is the earth's radius, and ϕ is the geographic latitude. The last term in Eq. 1.13 arises from the convergence of meridians in a coordinate system in which y is oriented northward and x eastward. In the preceding equation fluctuations of ρ have been neglected in comparison to fluctuations of χ and \mathbf{v} . Also, terms arising because of the divergence of the vertical coordinate, z , have been ignored. Standing and transient eddy-transport terms are considered together in this formulation.

Introducing Eq. 1.5 into 1.13, R. J. Reed and German (1965) arrive at

$$\begin{aligned}
\frac{\partial}{\partial t} [c]_{(\lambda,t)} = & - [\mathbf{v}]_{(\lambda,t)} \cdot \nabla [c]_{(\lambda,t)} - \Gamma [wc]_{(\lambda,t)} + \frac{\partial}{\partial y} \left(\rho K_{yy} \frac{\partial [\chi]_{(\lambda,t)}}{\partial y} \right) \\
& + \frac{\partial}{\partial y} \left(\rho K_{yz} \frac{\partial [\chi]_{(\lambda,t)}}{\partial z} \right) + \frac{\partial}{\partial z} \left(\rho K_{yz} \frac{\partial [\chi]_{(\lambda,t)}}{\partial y} \right) \\
& + \frac{\partial}{\partial z} \left(\rho K_{zz} \frac{\partial [\chi]_{(\lambda,t)}}{\partial z} \right) - \frac{\rho \tan \phi}{a} \left(K_{yy} \frac{\partial [\chi]_{(\lambda,t)}}{\partial y} \right) \\
& + K_{yz} \frac{\partial [\chi]_{(\lambda,t)}}{\partial z} \quad (1.14)
\end{aligned}$$

and, since in the relation $[c]_{(\lambda,t)} = \rho[\chi]_{(\lambda,t)}$, ρ may be assumed to be constant,

$$\begin{aligned}
\frac{\partial [c]_{(\lambda,t)}}{\partial t} = & - [\mathbf{v}]_{(\lambda,t)} \cdot \nabla [c]_{(\lambda,t)} - \Gamma [wc]_{(\lambda,t)} + \frac{\partial}{\partial y} \left(K_{yy} \frac{\partial [c]_{(\lambda,t)}}{\partial y} \right) \\
& + \frac{\partial}{\partial y} \left(K_{yz} \frac{\partial [c]_{(\lambda,t)}}{\partial z} \right) + \frac{\partial}{\partial z} \left(K_{yz} \frac{\partial [c]_{(\lambda,t)}}{\partial y} \right) \\
& + \frac{\partial}{\partial z} \left(K_{zz} \frac{\partial [c]_{(\lambda,t)}}{\partial z} \right) + \frac{\partial}{\partial z} (\Gamma K_{zz} [c]_{(\lambda,t)}) \\
& - \frac{\tan \phi}{a} \left(K_{yy} \frac{\partial [c]_{(\lambda,t)}}{\partial y} + K_{yz} \frac{\partial [c]_{(\lambda,t)}}{\partial z} + \Gamma K_{yz} [c]_{(\lambda,t)} \right) \quad (1.15)
\end{aligned}$$

If the values of K_{yy} , K_{yz} , and K_{zz} were known, this equation could be used to estimate the distribution $[c]_{(\lambda,t)}$ numerically. R. J. Reed and German (1965) pointed out a number of difficulties that present themselves, however, not the least of which is the fact that in Eq. 1.5 only two equations are given for these three variables. To circumvent this difficulty, they use Eady's (1949) aforementioned finding that $[\alpha]_{(\lambda,t)} = (1/2)[\beta]_{(\lambda,t)}$ in the baroclinically active troposphere of mid-latitudes. The heat flux in this tropospheric region is then given by

$$H_y = - \frac{\rho c_p K_{yy}}{2} \frac{\partial [\theta]_{(\lambda,t)}}{\partial y} \quad (1.16)$$

From heat-flux and temperature data published by Peixoto (1960), R. J. Reed and German (1965) were able to estimate K_{yy} for this limited region. Assuming that K_{yy} is proportional to the variance of the meridional wind component, they were able to estimate K_{yy} for other levels and other latitudes, using data published by Buch (1954), Murakami (1962), and Peng (1963). From heat-flux data by Oort (1963), the distribution of $[\alpha]_{(\lambda,t)}$ was estimated, and from Eq. 1.9 values of K_{yz} could be derived. Since, for reasons of symmetry, on the equator we may assume $[\alpha]_{(\lambda,t)} = 0$, Eq. 1.9 also yields for equatorial regions

$$[(\alpha)_{(\lambda,t)}^2]_{(\lambda,t)} = \frac{K_{zz}}{K_{yy}} \quad (1.17)$$

From the spread of tungsten, ^{185}W , Friend et al. (1961) estimated K_{zz} in the lower stratosphere over the equator to be of the order of $10^3 \text{ cm}^2/\text{sec}$. Together with values of K_{yy} estimated by R. J. Reed and German (1965) for the same region, Eq. 1.17 was used to obtain the magnitude of $[(\alpha)_{(\lambda,t)}^2]_{(\lambda,t)}$. Since its variation with latitude and height was not known, this value was assumed to be constant. From Eq. 1.9 the distribution of K_{zz} can now be estimated.

Results of the computations by R. J. Reed and German (1965) are shown in Table 1.1 for the four seasons. Table 1.2 contains the values derived for $[\alpha]_{(\lambda,t)}$ and $[\beta]_{(\lambda,t)}$. A graphical interpretation is given in Fig. 1.2. In this diagram the short line segments give the distribution of $[\alpha]_{(\lambda,t)}$, the slopes of the mixing surfaces. They indicate well the northward and downward mixing of trace substances, such as ozone, during winter conditions in the stratosphere. Nearly everywhere these slopes of the mixing surfaces are greater than the slopes of the undisturbed isentropes, indicating the existence of countergradient-flux conditions. The angles $[\alpha]_{(\lambda,t)}$ are nearly equal, or slightly less, than the inclination of lines of equal ozone mixing ratio. Evidently the slopes $[\alpha]_{(\lambda,t)}$ obtained from heat-flux data are slightly too small to account for the countergradient flux of ozone (and of other quasi-conservative tracers). The reason for this underestimate is sought by R. J. Reed and German (1965) in the diabatic effects of radiation.

Table 1.1
EDDY EXCHANGE COEFFICIENTS BASED ON HEAT-FLUX DATA*

	Latitude, degrees							
	10	20	30	40	50	60	70	80
January–March								
Pressure Level, 100 mb								
$K_{yy}(10^{10} \text{ cm}^2/\text{sec})$	2.2	3.2	3.7	3.6	4.1	5.0	5.9	5.4
$K_{yz}(10^6 \text{ cm}^2/\text{sec})$	-8.4	-16.1	-31.5	-26.7	-22.5	-15.4	-4.9	-5.7
$K_{zz}(10^3 \text{ cm}^2/\text{sec})$	6.1	12.6	31.0	25.0	17.7	9.6	6.1	5.9
Pressure Level, 50 mb								
$K_{yy}(10^{10} \text{ cm}^2/\text{sec})$	0.9	1.0	1.3	2.1	3.4	4.4	6.4	7.1
$K_{yz}(10^6 \text{ cm}^2/\text{sec})$	-1.2	-3.0	-7.1	-12.3	-17.9	-18.9	-22.0	-11.4
$K_{zz}(10^3 \text{ cm}^2/\text{sec})$	1.0	1.9	5.1	9.4	12.9	12.4	13.6	8.7
Pressure Level, 30 mb								
$K_{yy}(10^{10} \text{ cm}^2/\text{sec})$	0.7	0.8	1.2	2.2	4.6	5.3	6.0	6.1
$K_{yz}(10^6 \text{ cm}^2/\text{sec})$	-1.3	-1.7	-3.0	-5.6	-10.5	-15.3	-15.5	-8.4
$K_{zz}(10^3 \text{ cm}^2/\text{sec})$	1.0	1.2	2.0	2.6	6.9	9.6	9.9	7.2
April–June								
Pressure Level, 100 mb								
$K_{yy}(10^{10} \text{ cm}^2/\text{sec})$	1.4	1.9	2.3	2.4	2.1	1.7	1.5	1.0
$K_{yz}(10^6 \text{ cm}^2/\text{sec})$	-4.8	-8.5	-16.9	-21.3	-15.1	-10.7	-4.3	0.8
$K_{zz}(10^3 \text{ cm}^2/\text{sec})$	3.6	6.4	15.1	21.4	13.5	9.2	3.3	1.4
Pressure Level, 50 mb								
$K_{yy}(10^{10} \text{ cm}^2/\text{sec})$	0.6	0.5	0.6	1.0	1.1	0.9	1.0	0.9
$K_{yz}(10^6 \text{ cm}^2/\text{sec})$	-0.9	-1.1	-2.0	-4.8	-5.4	-5.7	-4.5	1.4
$K_{zz}(10^3 \text{ cm}^2/\text{sec})$	0.9	0.9	1.4	3.8	4.3	5.1	3.2	1.4
Pressure Level, 30 mb								
$K_{yy}(10^{10} \text{ cm}^2/\text{sec})$	0.5	0.4	0.4	0.7	0.8	0.9	1.0	0.7
$K_{yz}(10^6 \text{ cm}^2/\text{sec})$	-0.7	-0.8	-0.7	-1.3	-2.4	-5.0	-3.5	2.2
$K_{zz}(10^3 \text{ cm}^2/\text{sec})$	0.8	0.7	0.6	1.2	1.8	3.7	2.5	1.6
July–September								
Pressure Level, 100 mb								
$K_{yy}(10^{10} \text{ cm}^2/\text{sec})$	1.5	2.0	2.7	2.6	2.1	1.2	0.7	0.6
$K_{yz}(10^6 \text{ cm}^2/\text{sec})$	-3.8	-5.8	-12.4	-22.2	-16.0	-7.0	-3.7	-1.7
$K_{zz}(10^3 \text{ cm}^2/\text{sec})$	2.9	4.3	9.3	22.2	14.9	6.1	3.2	1.2
Pressure Level, 50 mb								
$K_{yy}(10^{10} \text{ cm}^2/\text{sec})$	0.7	0.9	0.9	0.8	0.6	0.5	0.4	0.5
$K_{yz}(10^6 \text{ cm}^2/\text{sec})$	0.02	-0.5	-1.8	-3.8	-3.6	-2.8	-0.5	-1.1
$K_{zz}(10^3 \text{ cm}^2/\text{sec})$	1.0	1.2	1.6	2.8	3.0	2.2	0.6	0.9

Table 1.1 (Continued)

	Latitude, degrees							
	10	20	30	40	50	60	70	80
Pressure Level, 30 mb								
$K_{yy}(10^{10} \text{ cm}^2/\text{sec})$	0.8	1.1	0.9	0.8	0.6	0.5	0.4	0.3
$K_{yz}(10^6 \text{ cm}^2/\text{sec})$	-0.2	-0.6	-1.3	-2.3	-2.4	-0.4	-0.5	0.6
$K_{zz}(10^3 \text{ cm}^2/\text{sec})$	1.1	1.5	1.4	1.8	1.7	4.3	0.6	0.5
October–December								
Pressure Level, 100 mb								
$K_{yy}(10^{10} \text{ cm}^2/\text{sec})$	2.5	3.5	4.6	4.6	4.1	4.2	2.9	2.1
$K_{yz}(10^6 \text{ cm}^2/\text{sec})$	-6.5	-11.4	-28.2	-35.0	-24.7	-16.0	8.6	18.2
$K_{zz}(10^3 \text{ cm}^2/\text{sec})$	5.1	8.2	23.7	32.7	20.7	11.6	6.3	18.1
Pressure Level, 50 mb								
$K_{yy}(10^{10} \text{ cm}^2/\text{sec})$	0.9	1.2	1.6	1.9	2.7	3.8	4.0	1.7
$K_{yz}(10^6 \text{ cm}^2/\text{sec})$	-1.0	-2.2	-5.1	-9.2	-14.1	-6.7	14.6	11.6
$K_{zz}(10^3 \text{ cm}^2/\text{sec})$	1.3	2.0	3.7	7.0	11.1	6.2	10.6	10.4
Pressure Level, 30 mb								
$K_{yy}(10^{10} \text{ cm}^2/\text{sec})$	1.0	0.9	1.1	1.6	2.7	4.6	5.2	2.1
$K_{yz}(10^6 \text{ cm}^2/\text{sec})$	-1.1	-0.7	0.1	-0.4	-4.9	-2.7	16.2	8.0
$K_{zz}(10^3 \text{ cm}^2/\text{sec})$	1.4	1.3	1.5	2.2	4.5	6.3	11.9	6.0

*From R. J. Reed and K. E. German, *Monthly Weather Review*, 93(5): 316-317 (1965).

The foregoing example illustrates that observed tracer distributions may be used successfully to check on the magnitudes and the direction of large-scale atmospheric transport processes. Average distributions of tracers may serve to illustrate the eddy exchange mechanisms governing the various layers and regions of the atmosphere, as has been done by R. J. Reed and German (1965). Distribution measurements of individual tracers, conducted at a certain time and over certain locations, may serve equally well to illustrate transport processes attached to certain weather situations and flow patterns. The subsequent chapters will attempt to list the results of a number of tracer studies and to compare them with the behavior of the general circulation of the atmosphere as described in Part 1 of this review.

In the foregoing discussion, values of K_{yy} , K_{yz} , etc., were estimated from actual atmospheric observations and from plausible assumptions. An order of magnitude of 10^{10} to 10^{11} cm^2/sec appears to be valid for K_{yy} in the stratosphere. Earlier estimates by Defant (1921a, 1921b) (see also Defant and Defant, 1958) from meridional mass-transport fluctuations in temperate latitudes yielded 10^7 to 10^8 $\text{g}/\text{cm}/\text{sec}$ for a tropospheric "exchange coefficient," $A = \rho K$, for large-scale motions.

Table 1.2
ESTIMATES OF $[\alpha]_{(\lambda,t)}$ AND $[\beta]_{(\lambda,t)}$ *

	Latitude, degrees							
	10	20	30	40	50	60	70	80
January–March								
Pressure Level, 100 mb								
$[\beta]_{(\lambda,t)}(10^{-4})$	-2.7	-4.8	-7.8	-5.9	-1.6	0.8	0.2	-0.9
$[\alpha]_{(\lambda,t)}(10^{-4})$	-3.8	-5.1	-8.4	-7.5	-5.5	-3.1	-0.8	-1.1
Pressure Level, 50 mb								
$[\beta]_{(\lambda,t)}(10^{-4})$	-1.7	-2.6	-3.7	-3.3	-1.1	0.7	0.2	-0.8
$[\alpha]_{(\lambda,t)}(10^{-4})$	-1.4	-3.0	-5.4	-5.9	-5.3	-4.3	-3.4	-1.6
Pressure Level, 30 mb								
$[\beta]_{(\lambda,t)}(10^{-4})$	-1.5	-1.2	-1.0	-0.3	0.6	0.8	0.4	0.6
$[\alpha]_{(\lambda,t)}(10^{-4})$	-2.0	-2.2	-2.6	-2.6	-2.3	-2.9	-2.6	-1.4
April–June								
Pressure Level, 100 mb								
$[\beta]_{(\lambda,t)}(10^{-4})$	-2.1	-3.3	-5.9	-6.9	-4.2	-2.8	-1.5	-0.4
$[\alpha]_{(\lambda,t)}(10^{-4})$	-3.5	-4.5	-7.2	-8.7	-7.1	-6.4	-2.9	-0.8
Pressure Level, 50 mb								
$[\beta]_{(\lambda,t)}(10^{-4})$	-1.6	-2.2	-2.6	-3.2	-2.1	-2.2	-1.4	0.2
$[\alpha]_{(\lambda,t)}(10^{-4})$	-1.5	-2.1	-3.2	-4.9	-5.1	-6.6	-4.3	1.6
Pressure Level, 30 mb								
$[\beta]_{(\lambda,t)}(10^{-4})$	-1.6	-1.0	-0.5	-0.4	-0.8	-1.7	-1.4	0.4
$[\alpha]_{(\lambda,t)}(10^{-4})$	-1.3	-1.8	-1.5	-1.9	-3.0	-5.2	-3.4	3.0
July–September								
Pressure Level, 100 mb								
$[\beta]_{(\lambda,t)}(10^{-4})$	-1.8	-2.0	-4.2	-7.4	-5.5	-2.9	-2.4	-1.4
$[\alpha]_{(\lambda,t)}(10^{-4})$	-2.5	-2.9	-4.6	-8.5	-7.6	-6.1	-5.7	-2.6
Pressure Level, 50 mb								
$[\beta]_{(\lambda,t)}(10^{-4})$	-0.4	-1.0	-2.0	-3.2	-2.7	-2.2	-2.1	-1.8
$[\alpha]_{(\lambda,t)}(10^{-4})$	0.3	-0.5	-2.1	-4.8	-6.2	-5.6	-1.3	-2.2
Pressure Level, 30 mb								
$[\beta]_{(\lambda,t)}(10^{-4})$	$-(10^{-5})$	-0.5	-1.2	-1.3	-1.2	-1.3	-2.0	-1.5
$[\alpha]_{(\lambda,t)}(10^{-4})$	-0.3	-0.5	-1.4	-3.0	-3.8	-0.9	-1.4	2.1

Table 1.2 (Continued)

	Latitude, degrees							
	10	20	30	40	50	60	70	80
October–December								
Pressure Level, 100 mb								
$[\beta](\lambda, t)(10^{-4})$	-2.2	-3.1	-5.7	-6.2	-2.9	-0.2	3.2	4.9
$[\alpha](\lambda, t)(10^{-4})$	-2.6	-3.2	-6.2	-7.6	-6.1	-3.8	2.9	8.5
Pressure Level, 50 mb								
$[\beta](\lambda, t)(10^{-4})$	-1.0	-1.3	-1.9	-2.0	-0.7	1.4	3.7	3.9
$[\alpha](\lambda, t)(10^{-4})$	-1.1	-1.9	-3.2	-4.8	-5.3	-1.8	3.7	7.0
Pressure Level, 30 mb								
$[\beta](\lambda, t)(10^{-4})$	-1.1	-0.4	0.6	1.5	1.1	1.6	3.3	2.4
$[\alpha](\lambda, t)(10^{-4})$	-1.1	-0.8	0.1	-0.3	-1.8	-0.6	3.1	3.9

*From R. J. Reed and K. E. German, *Monthly Weather Review*, 93(5): 318 (1965).

With air density, ρ , of the order of 10^{-3} g/cm³ characterizing the lower troposphere, Defant's results agree very well with those by R. J. Reed and German (1965).

A summary of tropospheric estimates of K over various locations and during different seasons has been given by Drozdov and Grigor'eva (1965). Most of these estimates are in fair agreement with the preceding values. From this study it appears that latitudinal and longitudinal exchange coefficients have the same order of magnitude in the lower troposphere (see Table 1.3).

A theoretical estimate of large-scale exchange coefficients based upon spectrum considerations was given recently by Panchev (1968). Assuming two-dimensional isotropy and statistical stationarity of large-scale motions (scale $\ell \lesssim 10^3$ km), the exchange coefficient, $K(\ell)$, relates to the energy spectrum, $\Phi_{cc}(k)$, of the horizontal wind distribution as follows:

$$K(\ell) = \gamma_s \left[\int_{1/\ell}^{\infty} \Phi_{cc}^{s/2}(k) k^{[-(s/2)-1]} dk \right]^{1/s} \quad (1.18)$$

where $\gamma_s \approx 1$ is a dimensionless constant, $k = 1/\ell$ is the wave number, equal to the reciprocal value of scale, and s is an arbitrary parameter. It has been shown by Buell (1958, 1960) and by Panchev (1967) that the correlation functions and spectrum functions of velocity and geopotential height of an isobaric surface are geostrophically related. One may write

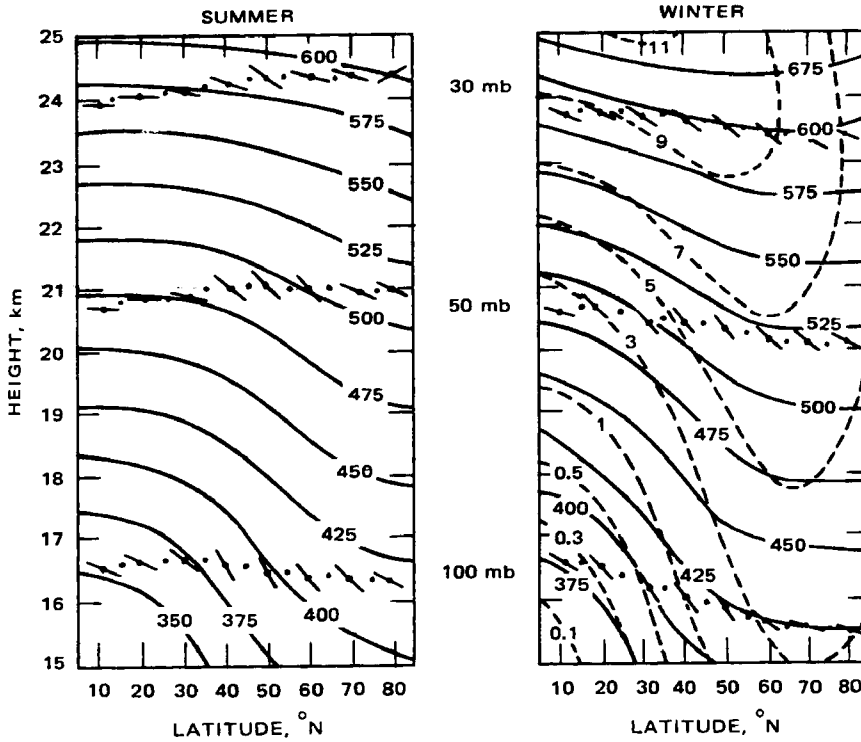


Fig. 1.2 Slopes of surfaces of preferred mixing (short line segments) for summer and winter seasons as derived from heat-flux data. Solid lines represent mean potential temperature ($^{\circ}\text{K}$) and dashed lines mean ozone mixing ratio ($\mu\text{g/g}$) according to Newell (1964a). [From R. J. Reed and K. E. German, *Monthly Weather Review*, 93(5): 317 (1965).]

$$\Phi_{cc}(k) = \frac{1}{f^2} k^2 \Phi_{HH}(k) \tag{1.19}$$

where $\Phi_{HH}(k)$ is the spectrum function for geopotential height, and f is the Coriolis parameter.

Substitution of Eq. 1.19 into Eq. 1.18 yields

$$K(\ell) = \frac{\gamma_s}{f} \left[\int_1^{\infty} \Phi_{HH}^{s/2}(k) k^{[(s/2)-1]} dk \right]^{1/s} \tag{1.20}$$

From this equation we see that the horizontal exchange coefficient depends on the scale ℓ of the largest eddies that enter into the diffusion consideration and on the wind or height fluctuations that are contained in the spectrum function Φ_{HH} , which is defined by

Table 1.3
ZONAL K_λ AND MERIDIONAL K_ϕ EXCHANGE COEFFICIENTS FOR
MOISTURE AS AN AVERAGE FOR THE EUROPEAN USSR
(10^{10} CM²/SEC)*

Coefficient	At earth's surface	At 850 mb	At 700 mb	At 500 mb	Integral exchange coefficient
January					
K_λ	1 to 2	5 to 6	6 to 7	1 to 2	5 to 6
K_ϕ	2 to 3	6 to 7	6 to 7	2 to 3	6 to 7
July					
K_λ	1 to 2	2 to 3	3 to 4	3 to 4	3 to 4
K_ϕ	0.5 to 1	2 to 3	3 to 4	3 to 4	2 to 3

*From Drozdov and Grigor'eva (1965).

$$\int_0^\infty \Phi_{HH}(k) dk = \sigma_H^2 \quad (1.21)$$

σ_H^2 being the variance of the height fluctuations. This quantity may be assumed to be a constant under conditions of isotropy. The maximum value of the horizontal eddy exchange coefficient, K_∞ , will be found if the integration in Eq. 1.20 is performed over all eddy sizes from $k = 0$ to $k = \infty$.

Panchev (1968) estimated the effect of the various parameters appearing in Eq. 1.20 on the magnitude of K_∞ , using empirical models of the spectrum function $\Phi_{HH}(k)$.

He arrived at the general conclusion that

$$K_\infty = \frac{\gamma}{f} \sigma_H \quad (1.22)$$

where $\gamma \approx 1$. We find that σ_H in the mid-troposphere is of the order of 10 geopotential decameters (1 geopotential decameter is equal to 98 m²/sec²). Thus one arrives at a value $K_\infty \approx 10^{11}$ cm²/sec. The magnitude of K apparently depends only slightly on the values assumed for the arbitrary parameters used in Eq. 1.18 and in the subsequent equations. (The variation of K due to different values of s is less than 30%.) The magnitude of K_∞ , given in Eq. 1.22, does not depend on any of the characteristic scales of macroturbulence (about 10³ km) that entered into Panchev's derivations. The main quantity determining the magnitude of K_∞ seems to be the standard deviation, σ_H . Thus it would appear that the large-scale character of the eddy fluctuations in geopotential height and consequently in wind velocities determines the

large-scale horizontal exchange coefficients and thereby the global dispersal of long-lived atmospheric trace substances. As σ_H changes with height, latitude, and season, changes in K_∞ have to be expected.

Panchev (1968) found also that, by extending the integration of Eq. 1.20 from $1/\ell$ to ∞ , with $\ell \approx 10^3$ km, instead of from zero to infinity, the horizontal exchange coefficients will amount to 60% to 90% of K_∞ . Thus the long and ultralong waves in the atmosphere ($\ell > 10^3$ km) contribute only little toward the dispersal of atmospheric trace constituents.

According to Eq. 1.18, one may also attempt to estimate the magnitude of $K(\ell)$ from the spectrum function of velocity, $\Phi_{cc}(k)$. In Part 1, Chap. 4, p. 165ff, several such spectrum estimates of the kinetic energy of the large-scale atmospheric motions have been presented. Wiin-Nielsen (1967) estimated the kinetic-energy distribution to follow a relation of the form

$$K_E = an^{-b} \quad (K_E \text{ in units of } \text{kJ/m}^2) \quad (1.23)$$

where n is the hemispheric wave number and b is approximately 2.8 for $8 \leq n \leq 15$. Kao (1965) computed normalized energy spectra from

$$F(n) = 4 \int_0^\infty R(\tau) \cos 2\pi n\tau \, d\tau \quad (1.24)$$

where $F(n)$ is expressed in hours per cycle and n is the frequency (cycles per hour). Autocorrelation coefficients, $R(\tau)$, were computed for time lags, τ , in Eulerian and Lagrangian coordinate systems. In both cases the spectrum slope was approximately -2 for zonal velocities in the frequency range between 0.008 and 0.030 cycle/hr.

Pinus et al. (1967) have shown from aircraft measurements that, for horizontal eddy dimensions less than 700 km, the spectrum slope appears to be approximately $-5/3$ (Fig. 1.3 and Table 1.4).

More recently, Kao and Al-Gain (1968) (see also Kao, 1968) derived Lagrangian spectrum estimates from isobaric trajectories constructed at the 850-, 500-, and 200-mb surfaces. These estimates yielded a spectrum slope of approximately -3 for both zonal and meridional velocity components (Fig. 1.4). GHOST balloon analyses by Wooldridge and Reiter (1970) also reveal a -3 slope in the zonal component for periods of less than 5 days and slightly steeper slopes in the meridional component.

Assuming an exponential relation of the type expressed in Eq. 1.23, with $b = 3$, Eq. 1.18 yields, for $\gamma_s = 1$ and $s = 2$,

$$K(\ell) = \left(\int_{1/\ell}^\infty ak^{-5} \, dk \right)^{1/2} = \frac{a^{1/2}}{2} k^{-2} \Big|_{1/\ell}^\infty = \frac{a^{1/2}}{2} \ell^2 \quad (1.25)$$

For $b = 2$, $\gamma_s = 1$, and $s = 2$,

$$K(\ell) = \frac{a^{1/2}}{\sqrt{3}} \ell^{3/2} \quad (1.26)$$

Table 1.4
POWER SPECTRA OF TURBULENCE IN THE FREE ATMOSPHERE (FIG. 1.3)*

Spectrum No.	Source	Characteristics (turbulence components given with respect to course of aircraft)
1	Shur (1962)	w-component, severe clear air turbulence (CAT), near jet-stream level, stable stratification.
2	E. R. Reiter and Burns (1965)	u- and v-components, moderate CAT, jet-stream level, stable stratification.
3	E. R. Reiter and Burns (1965)	w-component, flight parallel to wind, moderate CAT, jet-stream level, stable stratification.
4	E. R. Reiter and Burns (1965)	w-component, flight nearly normal to wind, moderate CAT, jet-stream level, stable stratification.
5	Vinnichenko et al. (1965)	u-component, no CAT, near jet-stream level, stable stratification.
6	E. R. Reiter and Burns (1965)	u-, v-, and w-components, light turbulence at 100 m altitude, unstable stratification.
7	Vinnichenko et al. (1965)	u-component, light turbulence at 1000-m altitude, unstable stratification
8	Kao and Woods (1964)	u-component, jet-stream level, flight parallel to jet stream.
9	Kao and Woods (1964)	v-component, jet-stream level, flight parallel to jet stream.
10	Kao and Woods (1964)	u- and v-components, jet-stream level, flight normal to jet stream.
11	Pinus (1963)	u-component, severe CAT, under core of jet stream, flight normal to jet stream.
12	Pinus (1963)	u-component, moderate CAT, under core of jet stream, flight normal to jet stream.
13	Pinus (1963)	u-component, light CAT, over core of jet stream, flight normal to jet stream.
14	Shur (1962)	w-component, moderate CAT, jet-stream level, stable stratification.
15	Shur (1962)	w-component, moderate CAT, jet-stream level, stable stratification.

*From N. Z. Pinus, E. R. Reiter, G. N. Shur, and N. K. Vinnichenko, *Tellus*, 19(2): 209 (1967).

For $b = 3$, $\gamma = 1$, and $s = 1$,

$$K(\ell) = \frac{a^{1/2}}{2} \ell^2 \quad (1.27)$$

and for $b = 2$, $\gamma = 1$, and $s = 1$,

$$K(\ell) = \frac{2a^{1/2}}{3} \ell^{3/2} \quad (1.28)$$

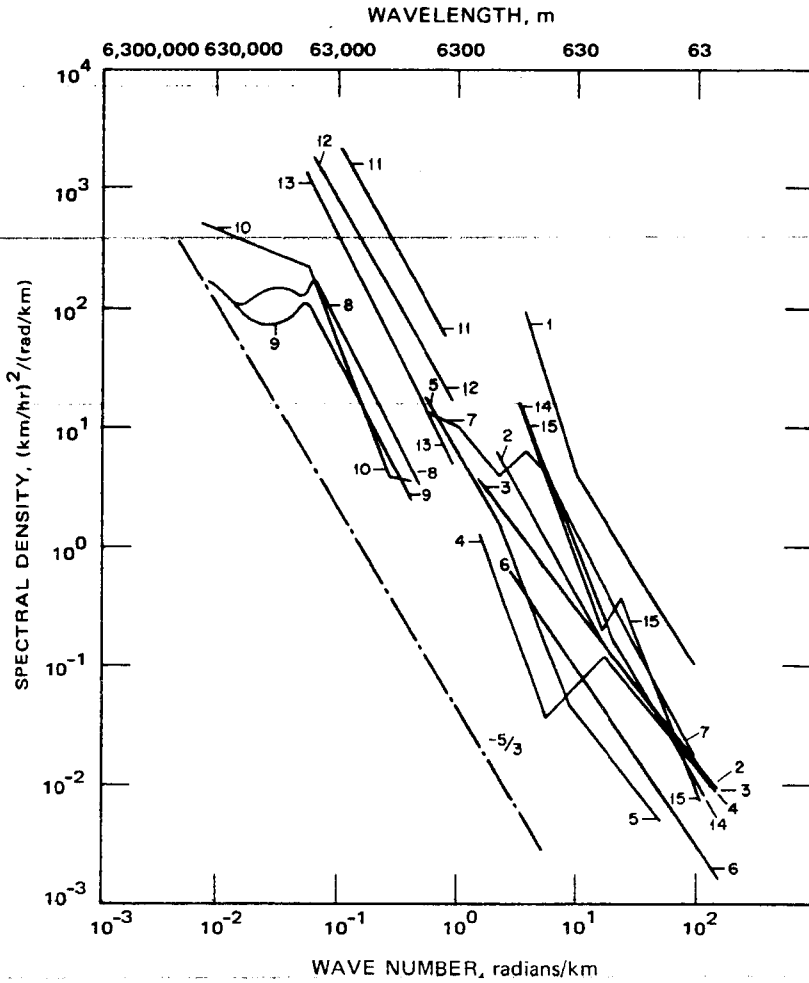


Fig. 1.3 Power spectra of atmospheric turbulence (see Table 1.4). [From N. Z. Pinus, E. R. Reiter, G. N. Shur, and N. K. Vinnichenko, *Tellus*, 19(2): 208 (1967).]

Thus it appears that the magnitude of the eddy diffusion coefficient depends on the following: (1) the diffusion model (i.e., the value of s adopted in Eq. 1.18), which influences the effect of the factor a , the dimensions of which depend on the value of the exponent b (under suitable conditions, a assumes the role of a “dissipation rate” of energy); (2) the magnitude of a ; and (3) the exponent b , i.e., the slope of the spectrum curves.

From Fig. 1.4 a is computed to be of the order of 10^{-4} cycle²/hr², or approximately 7×10^{-12} cycle²/sec². If we choose Eq. 1.25, we obtain, for $\ell \approx 10^8$

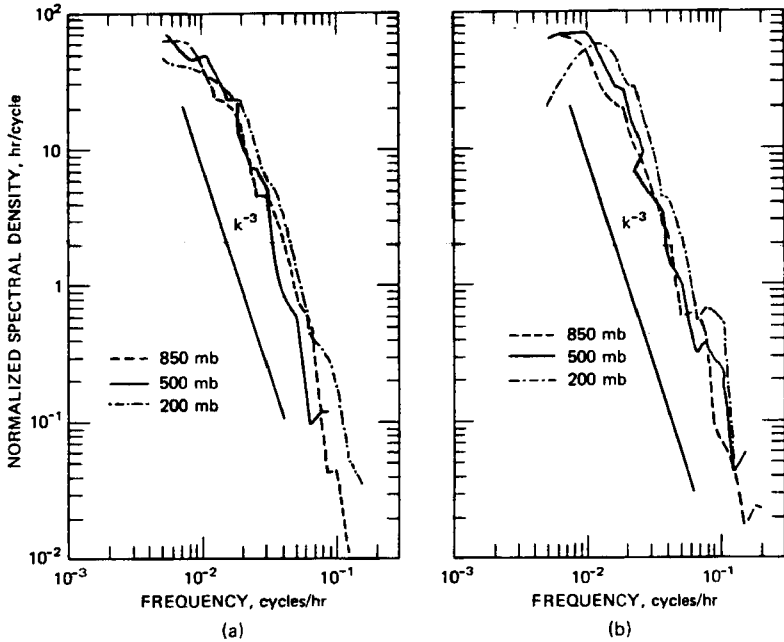


Fig. 1.4 Normalized power spectra of the zonal (a) and meridional (b) components of the relative velocity defined as the rate of separation of a diffusing cluster of particles. [From S.-K. Kao and A. A. Al-Gain, *Journal of Atmospheric Science*, 25(2): 217, 218 (1968).]

cm/cycle, $K(l) \approx 2.6 \times 10^{10}$ cm²/sec. This is close to the magnitude of this quantity derived by R. J. Reed and German (1965) and by Panchev (1968).

The effect of diffusion is measured by the separation that a cluster of particles undergoes. For short-range and short-period diffusion problems, this is expressed by Pasquill's (1962) diffusion equation,

$$c = \frac{Q}{2\pi\sigma_y\sigma_z\bar{V}} \exp\left[-\frac{1}{2}\left(\frac{y^2}{\sigma_y^2} + \frac{z^2}{\sigma_z^2}\right)\right] \tag{1.29}$$

where c = concentration of the diffusing contaminant (e.g., in $\mu\text{g}/\text{cm}^3$)

Q = source release rate (e.g., g/sec)

\bar{V} = mean wind speed in the plume direction

y = crosswind distance

z = vertical distance from the plume axis

σ_y and σ_z = standard deviations of the displacement of the material particles in the direction of the coordinate axes indicated by subscripts

The σ_y and σ_z deviations are defined as

$$\sigma_y^2 = \frac{\int_0^\infty y^2 c \, dy}{\int_0^\infty c \, dy} \quad (1.30)$$

A similar equation holds for σ_z^2 .

Estimates of the short-term dilution of (radioactive) contaminants in the atmosphere rely heavily on such equations as Eq. 1.29, which help to assess expected concentrations of the pollutant within the diffusing plume (see United States Weather Bureau, 1955; United States Atomic Energy Commission, 1968). Instead of measuring concentration fluctuations, as indicated by Eq. 1.29, one may evaluate detailed records of wind fluctuations (Pasquill, 1962; for additional literature and practical examples, see E. R. Reiter, 1967).

In this review we will be concerned only with large-scale aspects of atmospheric diffusion. Along such scales it is usually difficult and costly to arrive at statistics of σ_y^2 or σ_z^2 from concentration measurements, as expressed in Eq. 1.30 and used in Eq. 1.29. Kao and Al-Gain (1968) have made estimates of particle separation or dispersion, $[X_r^2]_{(n)}$ and $[Y_r^2]_{(n)}$, as functions of time in a Lagrangian coordinate system by constructing isobaric trajectories of large-scale air motions (see also Kao and Bullock, 1964, 1967; Murgatroyd, 1969).^{*} Results are shown in Fig. 1.5. Diffusion, as measured by the dispersion rates X/t and Y/t , according to this figure increases with height in the troposphere. This holds especially for the zonal component of the relative particle displacement. The values $[X_r^2]_{(n)}$ and $[Y_r^2]_{(n)}$ are approximately proportional to t^2 except at the 850-mb level where a proportionality to t^3 appears to be more appropriate. The dispersion rates decrease again in the middle and upper stratosphere (Kao and Powell, 1969).

Figure 1.6 shows the normalized dispersion of pairs of particles, σ_u and σ_v symbolizing the standard deviations of the respective velocity-component fluctuations. This diagram shows that planetary waves affect mainly the dispersion in the meridional direction for at least 6 days after release. Kao (1967) also states that results of computations for simultaneously and serially released particles are quite similar.

The exponents $\alpha = 2$ and 3 in the relation t^α found by Kao and Al-Gain (1968) agree well with earlier findings by Mesinger and Milovanović (1963) derived from particle trajectories on the 500-mb surface. For particle clusters these two authors find a relation

$$\sigma^2 - \sigma_0^2 \propto t^\alpha \quad (1.31)$$

with $1.95 \leq \alpha \leq 2.05$ for "small" times. In Eq. 1.31 σ^2 is the variance of particle dispersion with respect to the center of gravity of the cluster, and σ_0^2 is the initial value

^{*}Brackets with subscript (n) refer to average values over n observations.

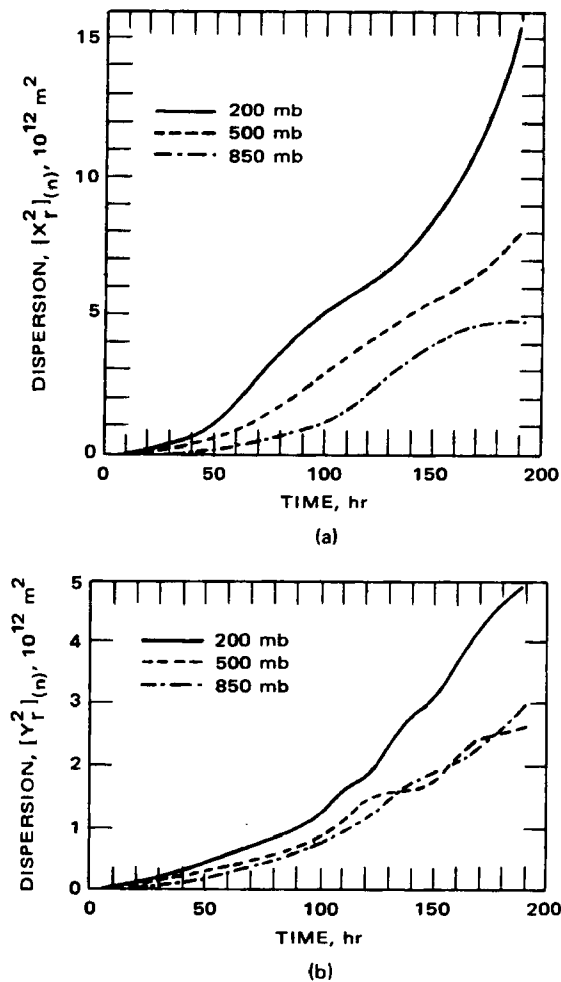


Fig. 1.5 Mean squares of the (a) zonal and (b) meridional components of the relative particle displacement. [From S.-K. Kao and A. A. Al-Gain, *Journal of Atmospheric Science*, 25(2): 218, 219 (1968).]

of this dispersion. For the expression

$$\sigma^2 \propto t^\beta \tag{1.32}$$

Mesinger and Milovanović found values of $1.40 \leq \beta \leq 1.60$ at time intervals of 6 to 8 days after release of the cluster (Fig. 1.7). Batchelor (1950) postulated relations of the form $\sigma^2 - \sigma_0^2 \propto t^2$ for small time intervals t and $\sigma^2 \propto t^3$ for intermediate t . The division between small and intermediate t is given by

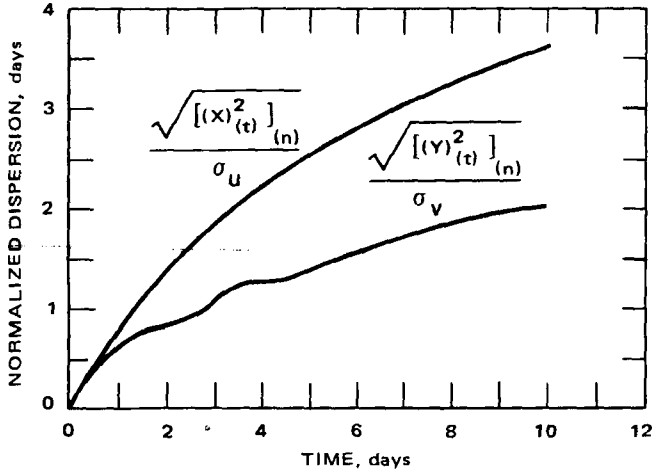


Fig. 1.6 Normalized dispersion of pairs of particles in the zonal and meridional directions. [From S.-K. Kao, *Quarterly Journal of the Royal Meteorological Society*, 93(397): 390 (1967).]

$$t_1 = \sigma_0^2 \epsilon^{-1/2} \quad (1.33)$$

where ϵ is the rate of dissipation of kinetic energy.

Actual results of computations of particle dispersions at 500 mb during an 8-day period [starting at 00 Greenwich Mean Time (GMT) on Aug. 26, 1958] from an originally square area are shown in Fig. 1.8.

Figure 1.9 shows the diagonal components of the relative particle displacement tensor in a Lagrangian coordinate system. The almost persistently negative values of the quantity $[X_r Y_r]_{(n)}$ indicate that at all levels the major axis of particle dispersion in the temperate latitudes of the northern hemisphere (where the particle trajectories were computed) is oriented from ESE to WNW. This agrees with the slight differences between zonal and meridional exchange coefficients ($5.90 \times 10^{10} \text{ cm}^2/\text{sec}$ and $2.30 \times 10^{10} \text{ cm}^2/\text{sec}$, respectively) found by Kao and Bullock (1964).

Even though the estimates on dispersion and large-scale diffusion in the atmosphere given by Kao and Al-Gain (1968) approach the correct order of magnitude, they do not portray the actual dispersion of contaminants. If we are to obtain the latter, isentropic trajectories on surfaces, $\theta = \text{constant}$ or $\theta_E = \text{constant}$ (the latter indicating constancy of equivalent potential temperature for moist adiabatic processes) should be considered instead of isobaric trajectories. Because of the large computational requirements inherent in the construction of such trajectories (Danielsen, 1961, 1967), no such statistics are available as yet. We may conclude, however, that Kao and Al-Gain's (1968) values constitute a slight underestimate of diffusion processes: Because of the larger vertical particle displacements in the baroclinic regions of middle latitudes along isentropic surfaces as compared with displacements on isobaric surfaces, particle-cluster separation should be expected to be

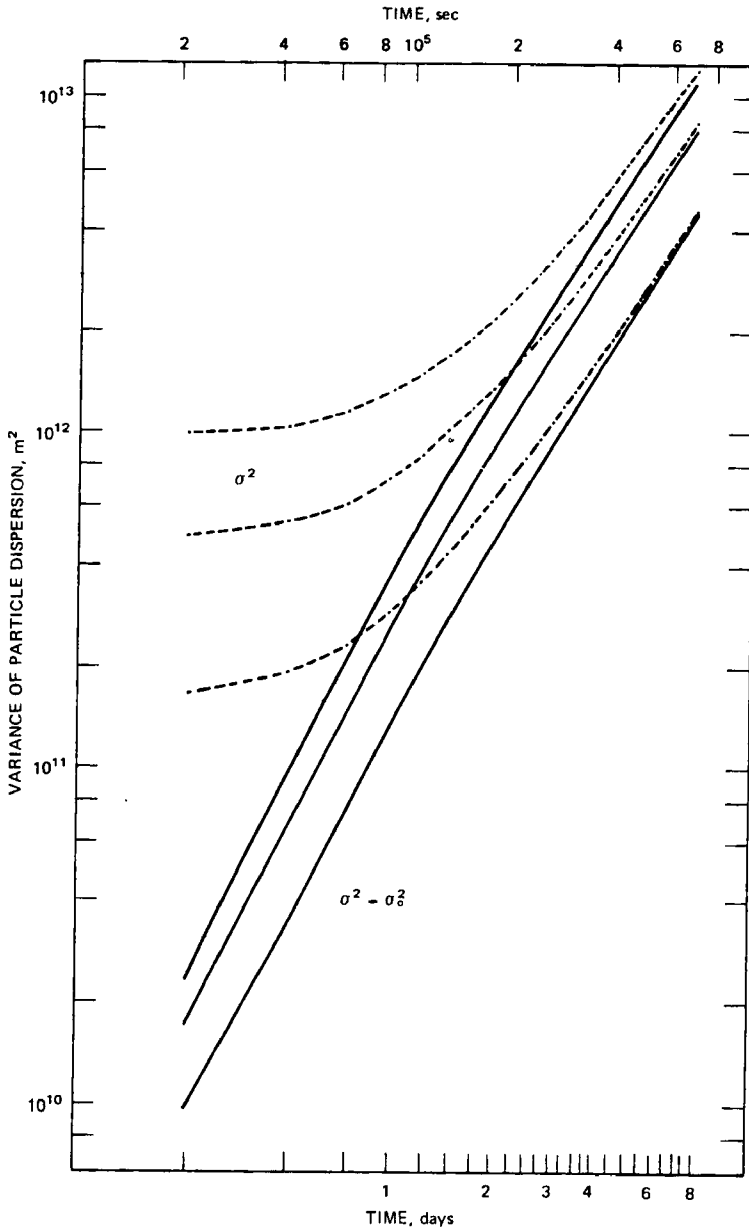


Fig. 1.7 Mean-square particle dispersion, σ^2 (---), and increase of mean-square particle dispersion relative to its initial value, σ_0^2 (—), for three sorts of initially square-formed clusters consisting of 9, 25, and 49 particles, respectively, with initial standard deviations, σ_0 , about the gravity centers of 393, 681, and 964 km, respectively. [From F. Mesinger and O. Milovanović, *Geofisica Pura e Applicata*, 55: 168 (1963).]

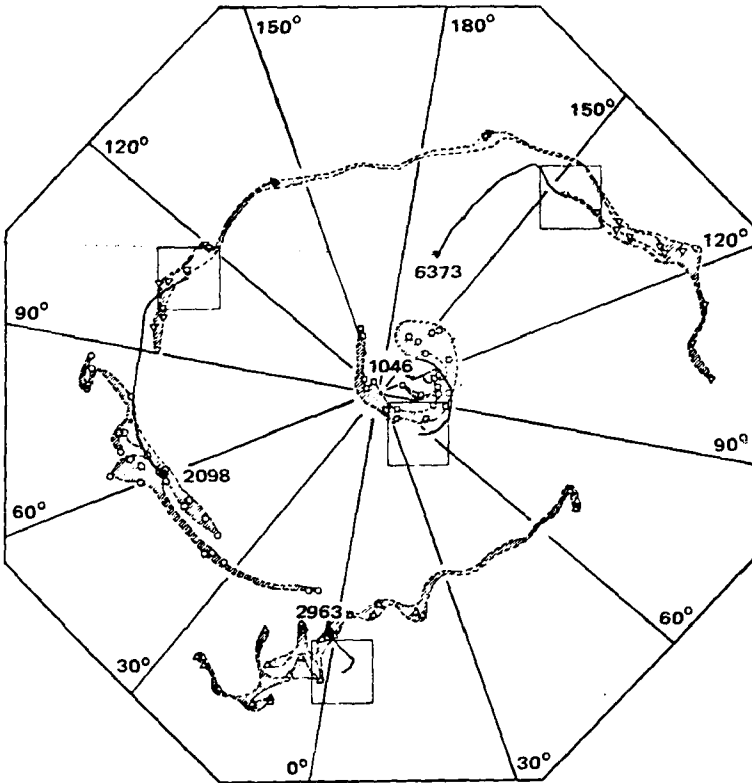


Fig. 1.8 Shape of four selected 25-point clusters after an 8-day period using 500-mb numerical forecasts for August 1958. Same geometrical signs denote the 25 particles of a particular cluster; full sign of the same form denotes their gravity center. Four squares represent the initial positions of the clusters and shaded areas their approximate 8-day positions. Full lines are the trajectories of the gravity centers of the four clusters, and numbers at their ends are the 8-day standard deviations (in kilometers) of the particles of the clusters. [From F. Mesinger and O. Milovanović, *Geofisica Pura e Applicata*, 55: 173 (1963).]

larger in a θ -coordinate system. Especially in the jet-stream region, convergent flow on an isobaric surface may actually signal strong directional wind shears with height that may give rise to rapid diffusion processes when individual particles are traced on isentropic surfaces (E. R. Reiter and Nania, 1964).* The intrusion of stratospheric air

*A preliminary study of the effect of directional wind shear on mesoscale atmospheric diffusion has been made by Gee (1967). Similar considerations have yet to be applied to large-scale diffusion processes. It is to be expected that vertical changes in wind direction are of importance especially in the wavelength range of baroclinic cyclone waves ($n \geq 8$; see Part 1, Chap. 4).

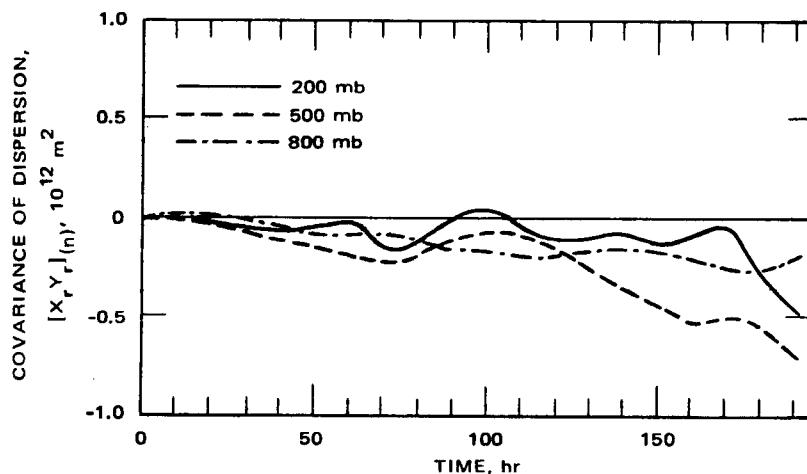


Fig. 1.9 Mean correlations of the zonal and meridional components of the relative particle displacement. [From S.-K. Kao and A. A. Al-Gain, *Journal of Atmospheric Sciences*, 25(2): 219 (1968).]

into the troposphere, which frequently occurs in the vicinity of jet streams, is brought to light by isentropic trajectories but not nearly as well by isobaric trajectories (Danielsen, 1961; E. R. Reiter, 1963b).

For similar reasons underestimates of atmospheric diffusion should also be expected from constant-density balloon experiments. From the dispersion rate of pairs of "constant-level" balloon flights near the 300-mb level over the United States, C. B. Moore et al. (1954) estimated exchange coefficients of 0.035 to 20×10^7 cm²/sec (3.6×10^7 cm²/sec average value). In comparison with Table 1.1, these values appear to be almost three orders of magnitude too low. GHOST balloon data that are presently accumulated over the southern hemisphere lend themselves to similar estimates of large-scale eddy exchange coefficients (Solot, 1968). Again, however, their quasi-isobaric trajectories will not fully portray actual air motions on isentropic surfaces. Wooldridge and Reiter (1970) estimated values of $K_{xx} = 5.03 \times 10^{10}$ cm²/sec and $K_{yy} = 2.11 \times 10^{10}$ cm²/sec for the southern hemisphere summer and $K_{xx} = 10.9 \times 10^{10}$ cm²/sec and $K_{yy} = 1.26 \times 10^{10}$ cm² sec for the southern hemisphere winter. Slightly higher values were obtained by Kao and Hill (1970).

Atmospheric exchange coefficients become even more difficult to estimate if moist adiabatic processes of a convective nature are involved. Under such conditions large-scale air trajectories may not reveal at all the effect of vertical mixing that takes place in small-scale and mesoscale convective cloud systems and in the subsidence regions between clouds. Chemical- or radiochemical-tracer experiments will give the only reliable information under such complex atmospheric conditions.

It should be expected that the effectiveness of planetary-scale eddies in dispersing atmospheric contaminants depends on, among other things, the kinetic

energy associated with these eddies. It was shown in Part 1 that the kinetic energy as a function of planetary wave number may vary drastically with season as well as during shorter periods of time. So does the relative importance of various wave numbers in accomplishing the energy transports necessary to maintain the general circulation of the atmosphere. We may assume, therefore, that the transport of contaminants by large-scale eddies is subject to a similar variability. [In a recent study, Murgatroyd (1969) found lowest values of K_{xx} and K_{yy} prevailing in the (lower) summer stratosphere and highest values in the spring stratosphere and upper troposphere.] From dishpan experiments in which the dispersion rate of dye was measured (Coté, 1968), it appears that low-wave-number regimes (preponderance of long planetary waves) lead to an enhancement of longitudinal dispersion and to a suppression of latitudinal dispersion. High-wave-number regimes reveal marked latitudinal dispersion of dye particles and decreased longitudinal spreading. Similar to Eq. 1.31, the dispersion in the dishpan could be expressed by a relation in nondimensional form

$$\frac{r_i^2 - r_0^2}{r_c^2} \sim (\Omega t)^\alpha \quad (1.34)$$

where r_i = separation distance between two particles in the i th photographic frame following particle injection

r_0 = initial separation of the same particles

r_c = parameter describing the dimensions of the dishpan

Ω = angular rotation of the dishpan, rad/sec

t = time

The exponent α turned out to be $1 < \alpha \leq 2$ for the experiments described by Coté; thus it is in good agreement with atmospheric conditions mentioned earlier in this chapter.

THE STRUCTURE OF THE UPPER ATMOSPHERE

The dispersion of atmospheric trace constituents, expressed, for instance, by the large-scale eddy exchange coefficients described in the previous section, depends on the characteristic structure and on the large-scale mean and eddy motions of the atmosphere. In Part 1 it was pointed out that the relative importance of various eddy sizes in the wave-number domain may vary strongly with time. It will be difficult, therefore, to arrive at a characteristic state of the atmosphere that will describe all possible large-scale diffusion processes of natural and artificial tracers. As we proceed into the layers above the lower stratosphere, the sparsity of direct observations of the temperature and wind structure makes itself felt adversely. In these higher regions of the atmosphere, the study of the behavior of trace substances yields especially valuable contributions toward an understanding of the general circulation of the atmosphere.

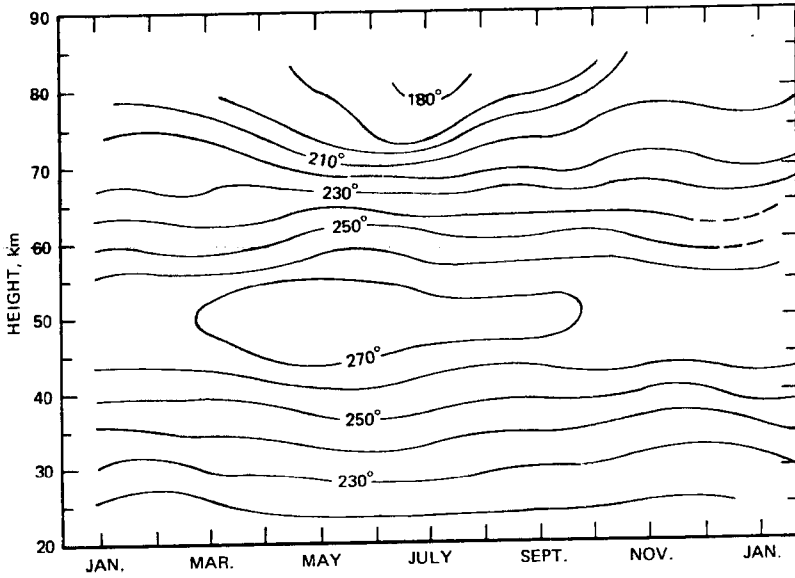


Fig. 1.11 Mean monthly temperature ($^{\circ}$ K) for 30° N. (From A. E. Cole, 1967.)

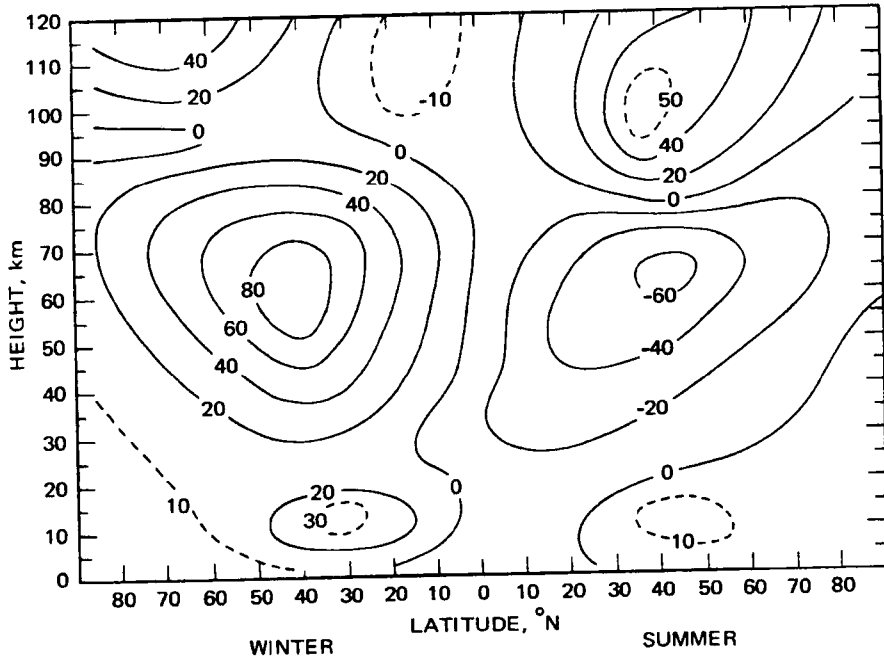


Fig. 1.12 Meridional cross section of mean zonal wind (m/sec). Positive winds are from the west. [From R. E. Newell, *Meteorological Monographs*, 9(31): 104 (1968).]

pole, mesopause temperatures may attain approximately 150°K during summer and 230°K during winter. Near the stratopause (50 to 60 km) the following temperatures are observed: approximately 270 to 290°K over the summer pole, approximately 270°K over the equator, and approximately 250°K over the winter pole (Figs. 1.13

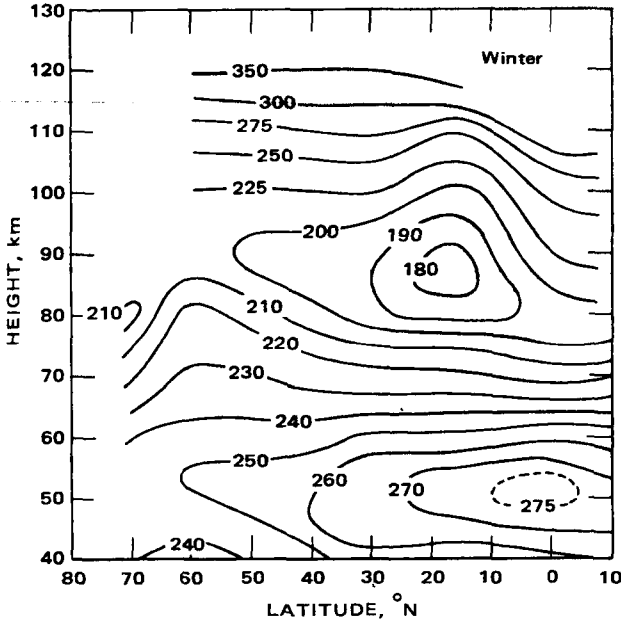


Fig. 1.13 Meridional temperature cross section in winter ($^{\circ}\text{K}$). [From R. E. Newell, *Meteorological Monographs*, 9(31): 99 (1968).]

and 1.14) (Newell, 1968a; see also Kellogg, 1964; Murgatroyd, 1965b, 1968; Labitzke, 1968; Cole, 1969). Thus the horizontal temperature gradient reverses from the stratosphere into the mesosphere. This would suggest that radiative processes exercise a dominant control over the stratospheric temperature distribution in the vicinity of the stratopause, whereas dynamic warming through sinking motions and chemical processes, such as the recombination of atomic oxygen, may be held mainly responsible for the high winter temperatures in the polar mesopause region (Haurwitz, 1961; Kellogg, 1961; K. Maeda, 1963; Newell, 1964a).

Radiative heating effects in the lower thermosphere have been estimated by Newell (1968a) and are shown in Fig. 1.15. Effects of horizontal and vertical motions were not included in these computations. Heating rates near the mesopause due to the presence of CO_2 and H_2O have been considered in detail by Houghton (1969). Radiational heating of this region should be expected from various infrared CO_2 bands (as much as 2°C per 12 hr).

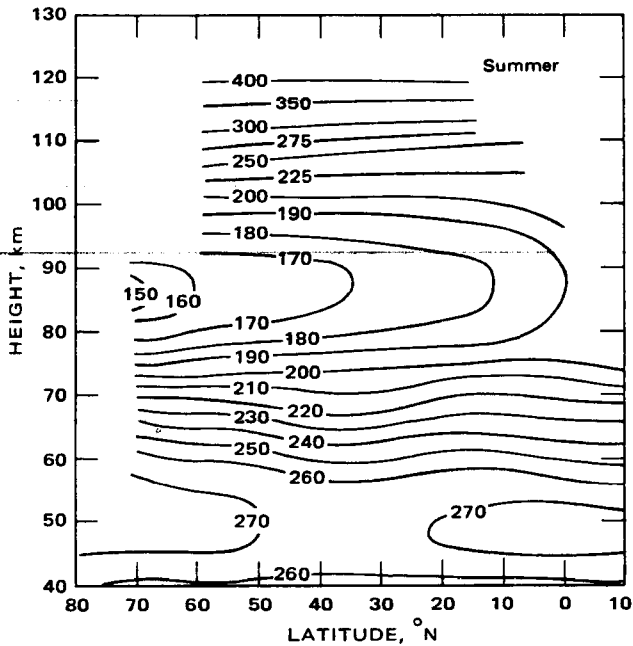


Fig. 1.14 Meridional temperature cross section in summer ($^{\circ}\text{K}$). [From R. E. Newell, *Meteorological Monographs*, 9(31): 99 (1968).]

Murgatroyd and Singleton (1961) have estimated the meridional circulation patterns that would result in the stratosphere and mesosphere from the requirement of heat transport between source and sink regions. Results of their computations were shown in Part 1 but are reproduced again in Fig. 1.16 for easier reference. As was mentioned in Part 1, stratospheric mean meridional motions in the northern hemisphere reveal a two-cell pattern with strongest sinking in northern middle latitudes [recently confirmed by Vincent (1968)]. Such a pattern is not evident from Murgatroyd and Singleton's circulation model. But then their model does not account for the effect of eddy transport processes. We may conclude, therefore, in line with the reasoning presented in Part 1, that the additional northward and downward transport of heat, ozone, and other contaminants of the atmosphere, which is accomplished by large-scale eddies in the stratosphere, and possibly also in the mesosphere, will significantly change the pattern shown in Fig. 1.16: Rising motions and adiabatic cooling associated with such motions may prevail in mean cross sections through the winter stratosphere over the northern polar regions, thus balancing some of the eddy influx of heat into these regions. If one allows for large-scale eddy diffusion, as, for instance, estimated by Prabhakara (1963) from the spread of radioactive tungsten in the stratosphere, only about 70% of the Murgatroyd–Singleton meridional circulation would have to be added to these eddy processes to account for

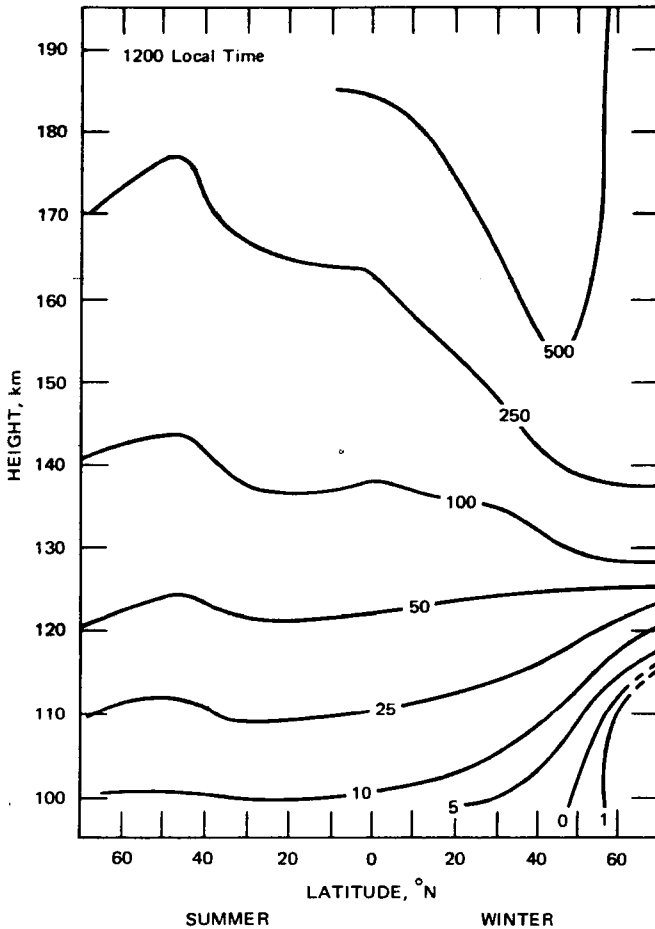


Fig. 1.15 Meridional cross section of radiative heating rate in lower thermosphere ($^{\circ}\text{K}/\text{day}$). [From R. E. Newell, *Meteorological Monographs*, 9(31): 102 (1968).]

the observed seasonal distribution of ozone (Gebhart, 1968). This confirms the overestimate of the role of the meridional circulations shown in Fig. 1.16.

It was also mentioned in Part 1 that the stratosphere of the southern hemisphere might possibly reveal a mean circulation pattern differing from the one found over the northern hemisphere. At least in the lower stratosphere, sinking motions seem to prevail over the south pole during winter. As we shall see in a subsequent chapter, the characteristic annual variation of ozone concentrations in the south-polar regions is different from that in the northern hemisphere, giving additional support to the existence of such subsidence motions over Antarctica. We might speculate that the eddy transport processes in the stratosphere are less effective in the southern

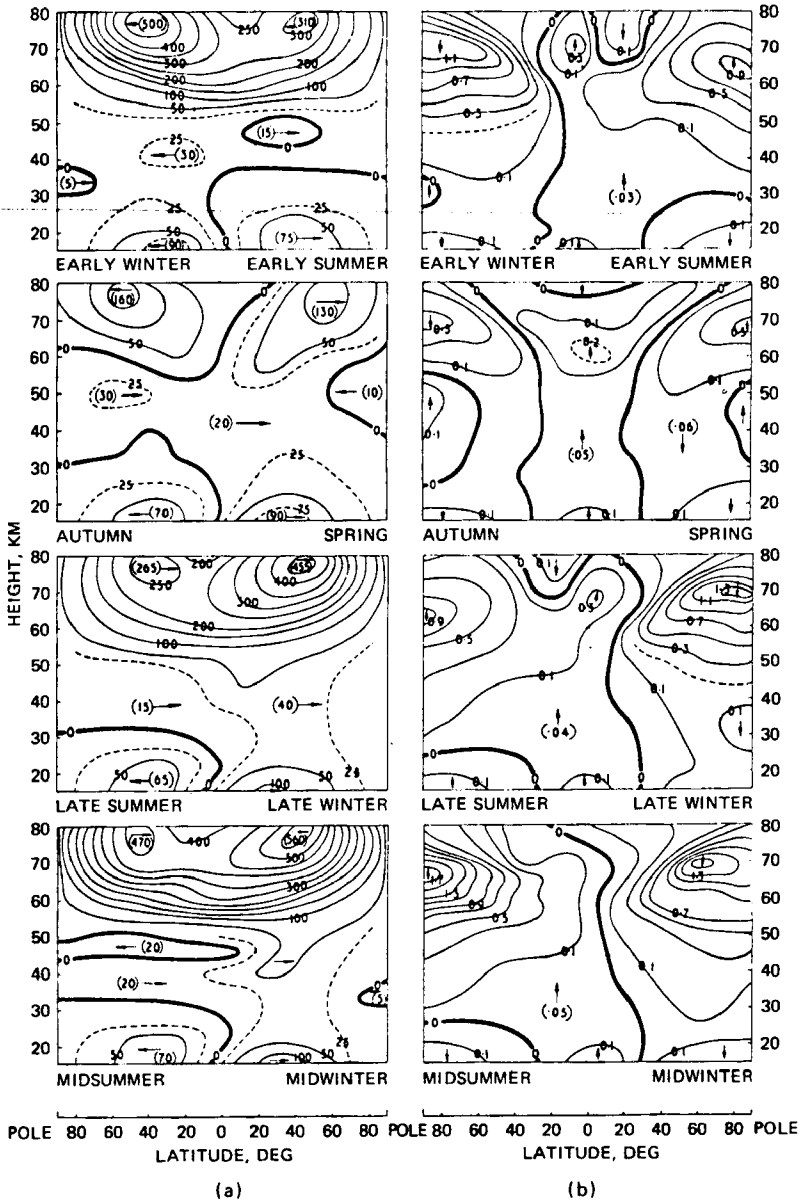


Fig. 1.16 Cross sections of (a) meridional and (b) vertical velocities (cm/sec) from pole to pole at different times of the year. [From R. J. Murgatroyd and F. Singleton, *Quarterly Journal of the Royal Meteorological Society*, 87(372): 130 (1961).]

hemisphere than in the northern one, thus leaving more of the actual transports to be accomplished by mean meridional circulations. Unfortunately we are still lacking sufficient wind data from the southern stratosphere to be able to prove these speculations. If we were to accept them, however, for the sake of argument, the circulation patterns in the stratosphere shown in Fig. 1.16 may describe conditions over the southern hemisphere more adequately than those over the northern hemisphere.

As we proceed into the higher regions of the atmosphere, temperatures become more and more difficult to measure directly. Already in the middle and upper stratosphere there are discrepancies between the temperature readings received from different sensors. These discrepancies appear to increase with altitude (Schmidlin, 1969; see also Finger and Woolf, 1966, and R. J. Reed, 1968a). Estimates of the temperature distribution will have to be made from wind measurements by use of the thermal wind equation (see Murgatroyd, 1957; Cole, 1967) or from density estimates made from drag measurements by falling spheres or by (reentering) satellites. Thus density becomes a primary meteorological variable in the upper atmosphere.

From data published by the Environmental Science Services Administration et al. (1966) (see also Anderson and Francis, 1966), it appears that the density distribution above approximately 180 km depends strongly on the thermospheric and exospheric temperature model used in the computations. Thus the thermal structure of the high atmosphere cannot yet be determined uniquely from available density observations. The sparsity of coordinated measurements from these high regions of the atmosphere poses a severe handicap to a detailed understanding of the general circulation in these layers (Teweles, 1967; Kellogg, 1968).

Observation points toward a strong seasonal variation of density, especially at high latitudes. These variations appear to attain a maximum near the 65-km level and decrease again toward the mesopause (Fig. 1.17) (see also Nordberg, 1964). Such a decrease is to be expected from the reversal of the horizontal temperature gradient that takes place between the stratopause and the mesopause (see Champion, 1967; Murgatroyd, 1968; Kantor, 1969a). The temperature distribution in the stratosphere and mesosphere described earlier causes relatively high pressures [approximately 130% of the 1962 U. S. Standard Atmosphere values (see National Aeronautics and Space Administration et al., 1962)] in the stratopause region of the summer pole and low pressures (about 70% of the 1962 U. S. Standard Atmosphere) at the same level near the winter pole. Departures of *density* have approximately the same percentage level. There probably is a broad isopycnic layer in both hemispheres near 90 km (Cole and Kantor, 1964). L. B. Smith (1969) observed higher densities in winter than in summer above 80 km over Hawaii, in conjunction with relatively warm winter mesopause temperatures.

A *semiannual* cycle in stratospheric temperatures and densities is observed in equatorial latitudes (R. J. Reed, 1962). This cycle is also reflected in wind observations (Loon and Jenne, 1969; Quiroz and Miller, 1967). According to Cole, the amplitude of the semiannual temperature wave is best developed near the 37.5- and the 52.5-km levels. The phase of the wave appears to proceed downward from higher

levels. Temperature variations appear to be at a minimum at 67.5 km. Above this level the annual temperature variation begins to dominate (Fig. 1.18). The semiannual variation in temperatures and densities is caused by the change of direct absorption of ultraviolet radiation by ozone with solar inclination (Murgatroyd, 1968). Loon and Jenne (1969) ascribe it to an intensification of vertical motions from autumn to winter. Maximum effects apparently are experienced near the stratopause over the equator. The amplitude of this temperature wave decreases rapidly with distance from the equator.

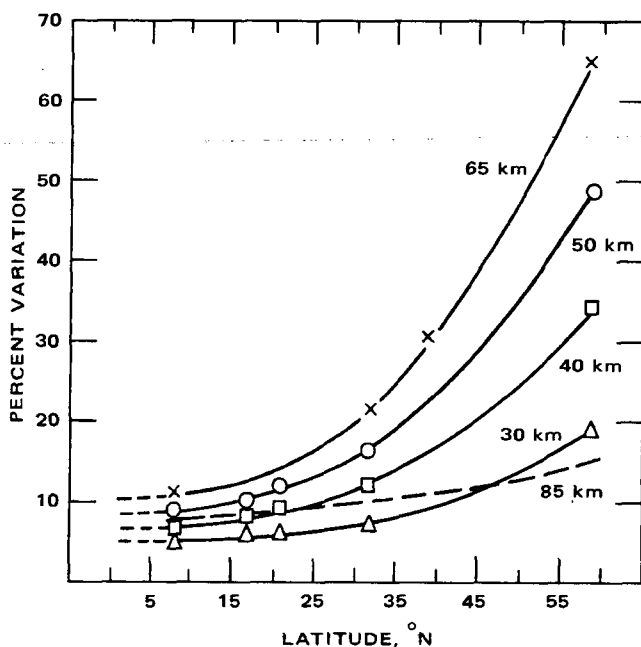


Fig. 1.17 Observed range of mean monthly densities as a function of latitude and altitude as a percentage of standard. [From A. E. Cole, (1967).]

Newell (1968b) comments on a semiannual variability of density observed near the 190-km level in the thermosphere (see also I. Harris and Priester, 1969). Besides pressure and temperature changes in the atmospheric layers beneath this level and the effect of vertical motions, the Joule heating by ionospheric current systems, steady as well as disturbed ones, may have a significant effect on the densities in those thermospheric layers, as will be discussed in conjunction with Fig. 1.27 (Jacchia et al., 1967; Blumen and Hendl, 1969).

Above the thermopause (500 km) in the exosphere, the semiannual variation of density again becomes important. This may be seen from density estimates at 1130 km derived by Cook and Scott (1966) from Echo II satellite drag observations (Fig. 1.19).

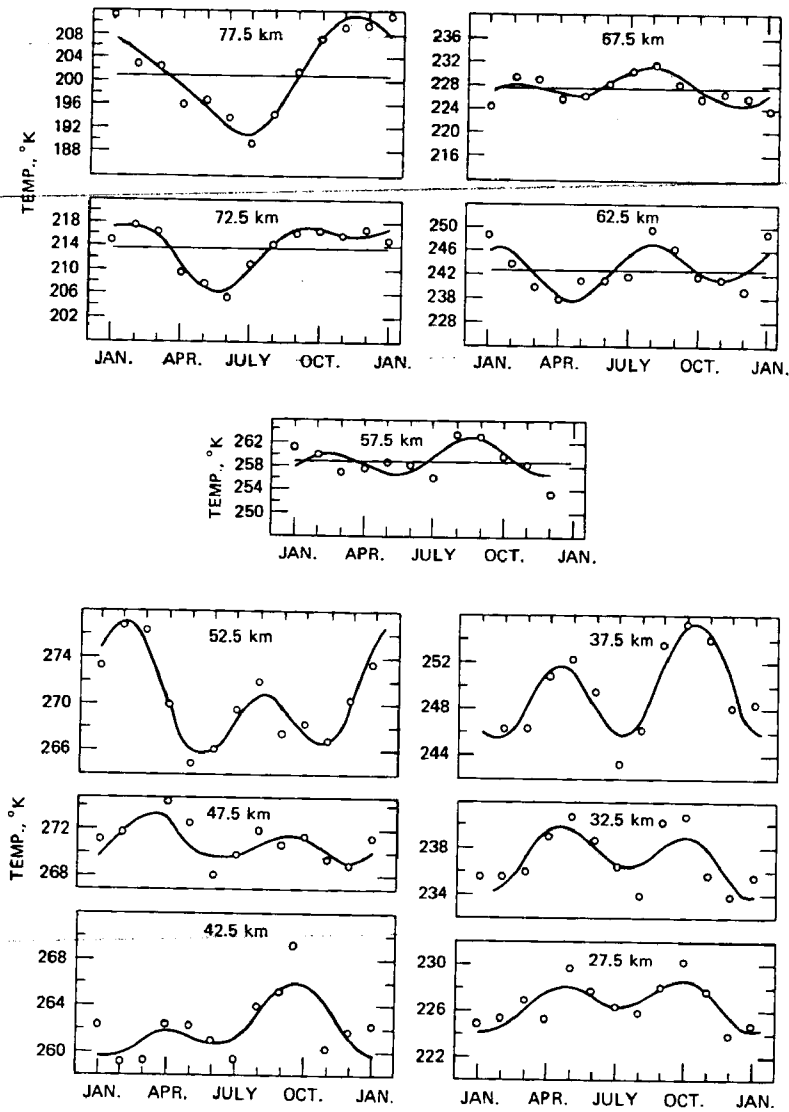


Fig. 1.18 Extrapolated annual temperature regimes for 15°N (solid curves represent the sum of the first and second harmonics of extrapolated data). (From A. E. Cole, 1967.)

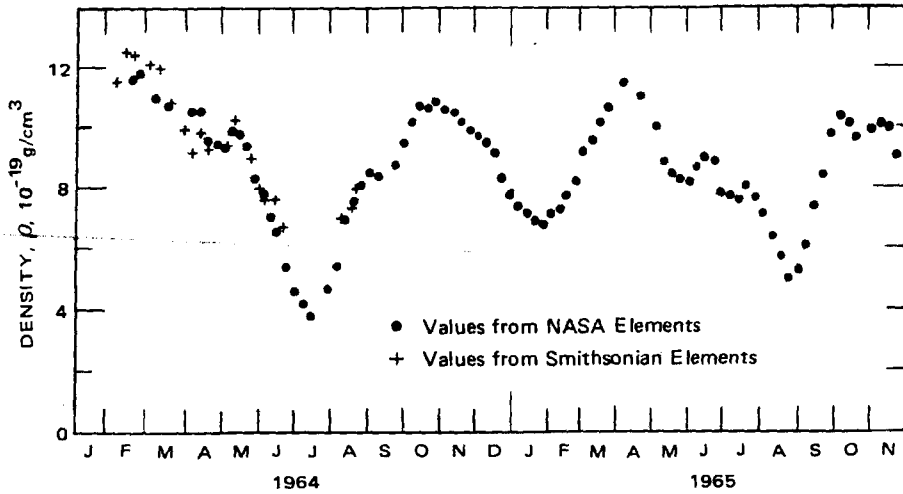


Fig. 1.19 Variation of atmospheric density at a height of 1130 km, derived from Echo II. [From G. E. Cook and D. W. Scott, *Planetary Space Science*, 14: 1149 (1966); see also I. Harris and W. Priester, *Meteorological Monographs*, 9(31): 74 (1968).]

Synoptic events may also cause large changes in stratospheric temperature, pressure, and density distribution. The “explosive” warming events, probably aided by the dynamic instability of the stratospheric polar vortex during the northern hemisphere winter, may serve as an example. Eddy and mean meridional transport processes associated with such events are discussed in Part I. Further references to explosive and final warming of the stratosphere during the middle and the end of the winter season will be made, especially in the discussion of the ozone distribution in Chap. 4.

During the easterly stratospheric wind regime of summer, Muench (1968) observed planetary long waves with amplitudes of the order 4 m/sec in the stratosphere (see also Scherhag, 1960; Deland, 1965; Eliassen and Machenhaur, 1965; Boville, 1966; Merilees, 1966). These waves propagate westward at a rate of approximately 30° longitude per day (10° to 90° longitude per day according to other investigators) and are most likely associated with a hemispheric wave number 1.

Finger and McInturff (1968) made an empirical study of the diurnal temperature variation in the middle stratosphere using regular rawinsonde data (see also Sparrow, 1967; Harris et al., 1965; Finger et al., 1964, 1965). The diurnal temperature range, according to their findings, depends on the solar elevation angle. It increases with altitude and decreases with latitude over the range investigated (essentially 24 to 36 km over the United States and Canada). Results are shown in Table 1.5. Computations are based on temperature differences, ΔT , observed during 12-hr time periods. Depending on the season, such stations may have both standard observation times (00 and 12 GMT) during daytime hours or during the dark hours. Differences in

Table 1.5
STATISTICS FOR THE DOUBLE-DAYLIGHT AND THE DOUBLE-DARKNESS
MEAN TEMPERATURE RANGES*

Scatter diagram		n	$[R]_{(n)}$, °C	95% confidence intervals	SE
Level, mb	Latitude, °N				
Double Daylight					
30	30 to 40	9711	0.484	$0.477 \leq R \leq 0.491$	0.63
30	40 to 50	9102	0.500	$0.492 \leq R \leq 0.508$	0.49
30	50 to 60	4859	0.340	$0.335 \leq R \leq 0.345$	0.43
30	60 to 70	6621	0.203	$0.173 \leq R \leq 0.233$	0.38
30	70 to 80	4021	0.179	$0.170 \leq R \leq 0.188$	0.33
10	30 to 40	7642	1.005	$0.940 \leq R \leq 1.070$	1.17
10	40 to 50	6041	0.952	$0.903 \leq R \leq 1.001$	0.97
10	50 to 60	2879	0.723	$0.680 \leq R \leq 0.766$	1.04
10	60 to 70	3239	0.471	$0.396 \leq R \leq 0.546$	1.01
10	70 to 80	2069	0.347	$0.343 \leq R \leq 0.351$	0.86
5	30 to 60	400	1.946	$1.846 \leq R \leq 2.046$	1.58
5	60 to 80	117	1.322	$0.875 \leq R \leq 1.769$	1.50
Double Darkness					
30	30 to 40	3045	0.333	$0.330 \leq R \leq 0.336$	0.44
30	40 to 50	2795	0.178	$0.169 \leq R \leq 0.187$	0.44
30	50 to 60	2206	0.253	$0.246 \leq R \leq 0.260$	0.46
30	60 to 70	1659	0.201	$0.168 \leq R \leq 0.234$	0.47
30	70 to 80	2067	0.077	$0.038 \leq R \leq 0.116$	0.48
10	30 to 40	1793	0.438	$0.408 \leq R \leq 0.468$	1.09
10	40 to 50	1377	0.593	$0.559 \leq R \leq 0.627$	1.24
10	50 to 60	641	0.736	$0.563 \leq R \leq 0.909$	1.53
10	60 to 70	837	0.134	$0.116 \leq R \leq 0.152$	1.89
10	70 to 80	1073	0.230	$0.180 \leq R \leq 0.280$	1.04

*From F. G. Finger and R. M. McInturff, *Journal of the Atmospheric Sciences*, 25(6): 1122 (1968).

the mean temperature range, $[R]_{(n)} = [T(00) - T(12)]_{(n)}$, for such extreme conditions are shown in Table 1.5, which also lists the number of observations, the 95% confidence limits, and the standard error, SE . From Finger and McInturff's statistics, it appears that maximum temperatures are reached near sunset and minimum temperatures near sunrise.

Diurnal and tidal effects on the temperature and wind distribution are appreciable in the mesosphere (a summary has been given by Haurwitz, 1964). The exact magnitudes of these effects, by some investigators estimated from observations to be on the order of 10°C, are still in doubt because of the difficulties encountered in measuring temperatures (Beyers and Miers, 1965; Finger and Woolf, 1967; Webb, 1969). J. S. A. Green (1965) and Lindzen (1967) have made detailed theoretical estimates of tidal effects. Figures 1.20 to 1.22 show the complex behavior of

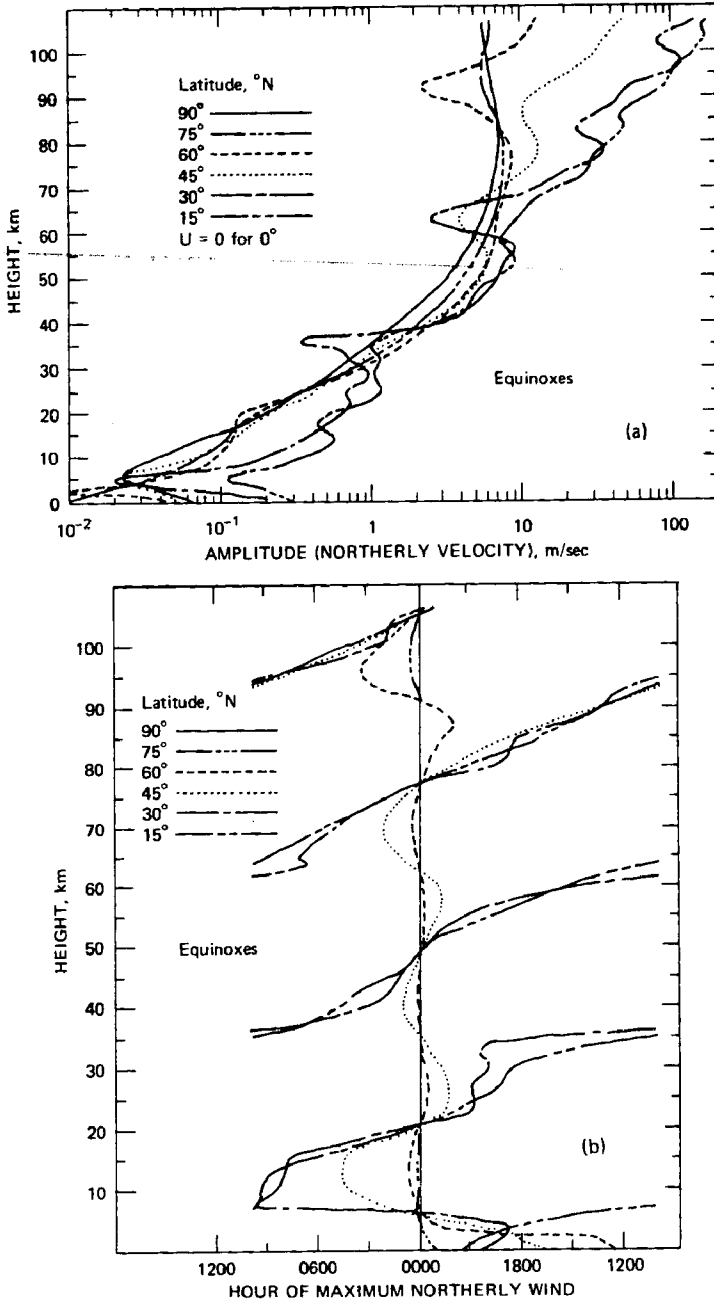


Fig. 1.20 Altitude distribution of the amplitude (a) and of the phase (b) of the solar diurnal component of v at 15° intervals of latitude for equinoctial conditions. [From R. S. Lindzen, *Quarterly Journal of the Royal Meteorological Society*, 93(395): 25, 26 (1967).]

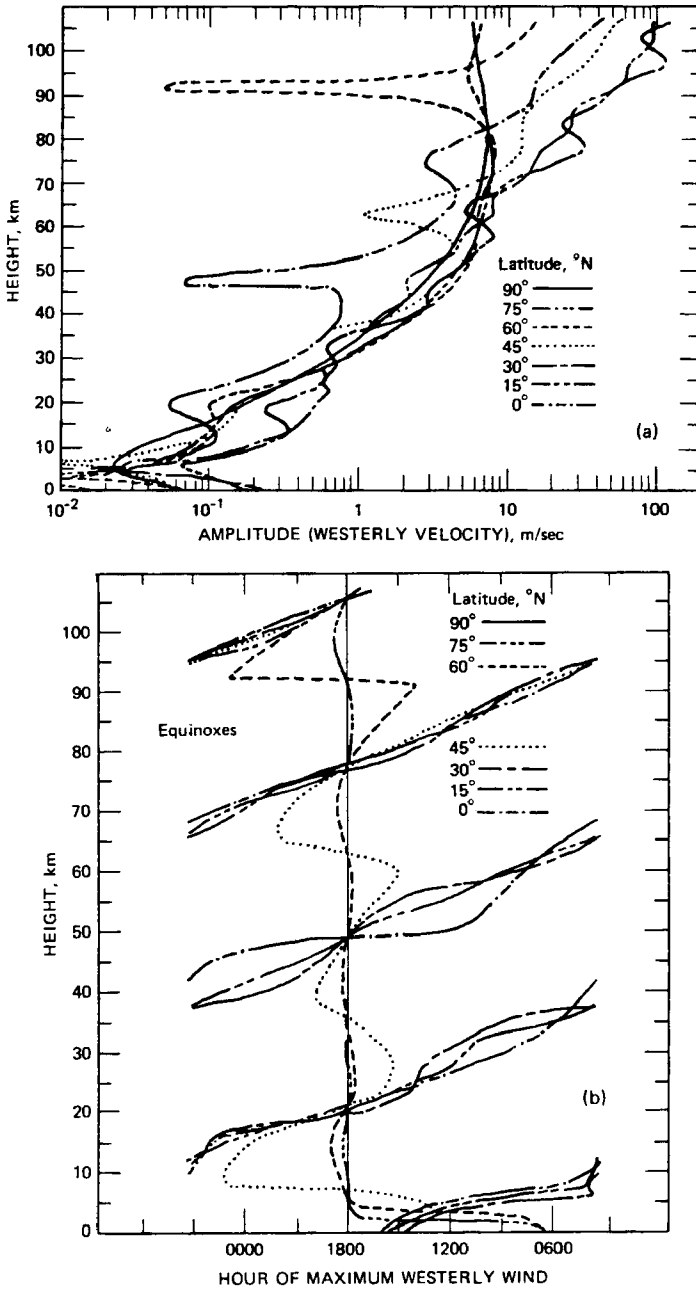


Fig. 1.21 Altitude distribution of the amplitude (a) and of the phase (b) of the solar diurnal component of u at 15° intervals of latitude for equinoctial conditions. [From R. S. Lindzen, *Quarterly Journal of the Royal Meteorological Society*, 93(395): 27, 28 (1967).]

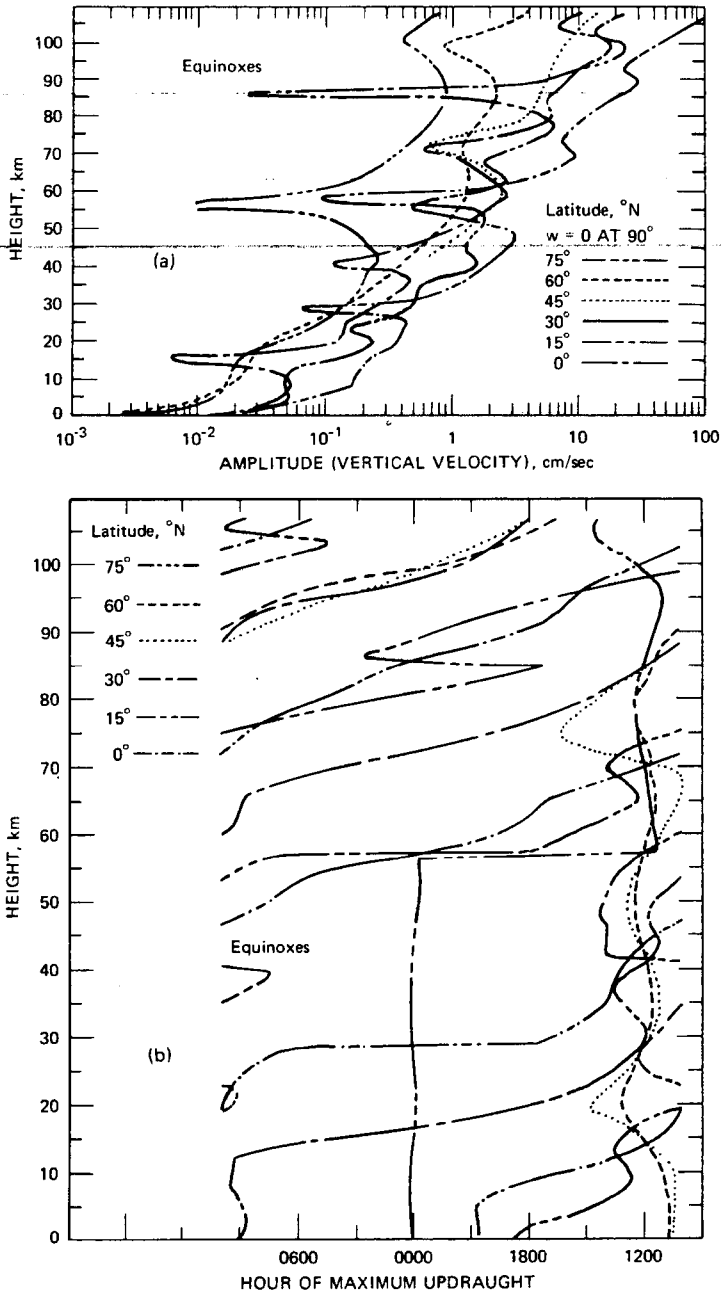


Fig. 1.22 Altitude distribution of the amplitude (a) and of the phase (b) of the solar diurnal component of w at 15° intervals of latitude for equinoctial conditions. [From R. S. Lindzen, *Quarterly Journal of the Royal Meteorological Society*, 93(395): 40 (1967).]

amplitudes and phases of the northerly, westerly, and vertical wind components at 15° latitude intervals. In Figs. 1.23 and 1.24, a comparison is made between observations and Lindzen's (1967) theoretical results at 30°N latitude. Allowing for the uncertainties in observations mentioned before, agreement between actual data and theory is fairly good (see Morris and Kays, 1968, 1969; Justus and Montgomery, 1969; Beyers and Miers, 1968; Lenhard, 1963). It appears that Lindzen's data, shown in Figs. 1.20 and 1.21, do not show enough lateral wind shear in the tidal components of motion to call for the existence of a "tidal jet" near the stratopause, as postulated by Webb (1966b, 1966c). Reed and Oard (1969) have also made comparisons between Lindzen's (1967) theory and actual observations (see also Reed, 1968a). They find small, but systematic, discrepancies that they attribute to the possibility that Lindzen has underestimated the strength of the trapped modes relative to the strength of the propagating modes. This makes the phase of the theoretical tidal oscillations appear progressively earlier than the observed ones at increasing height above 55 km. Reed and Oard suggest that the underlying estimates of ozone heating, which causes the trapped modes in the upper stratosphere and lower mesosphere, may have to be revised (see Chap. 4, p. 142). Randhawa (1969a, 1969b), for instance, found that balloon measurements of ozone near the stratopause showed considerably higher concentrations than spectrometric methods.

In the lower thermosphere diurnal and semidiurnal variations become of importance and, especially in the wind patterns, are perhaps the major feature between 100 and 150 km (see Figs. 1.20 to 1.22; see also Newell and Dickinson, 1967; Rao and Rao, 1969; Taffe, 1969). Upper atmospheric densities at these levels fluctuate accordingly in winter by as much as 6% of the mean value at 52°N and at 85 km, by 17% at 100 km in the diurnal wave, and by approximately half as much in the semidiurnal wave (Greenhow and Hall, 1960; see also Greenhow and Neufeld, 1961; Rosenberg and Edwards, 1964; C. H. Murphy et al., 1966; Istomin et al., 1969). The large tidal-wind velocities near and above the mesopause, shown in Figs. 1.20 to 1.22, may have a significant effect on the rapid dispersion of atmospheric trace substances at these levels. As pointed out by Justus and Roper (1968), tidal motions may influence drastically the turbulence regime above the mesopause [see also Lindzen (1968) and Fig. 1.35].

Diurnal temperature variations near the thermopause (500 km) have an amplitude of several hundred degrees centigrade. There also are significant differences in the thermospheric diurnal variation of ion temperatures and electron temperatures (Farley et al., 1967; W. E. Gordon, 1967; Walker and Spencer, 1968). I. Harris and Priester (1962, 1965, 1968) computed the diurnal temperature variations that should result at this level as an effect of extreme solar ultraviolet radiation absorption in the wavelength range from 100 to 1000 \AA [see also Mahoney (1968) for computation in the range from 10 to 1775 \AA]. As shown in Fig. 1.25, agreement with observed temperature fluctuations is poor in amplitudes as well as in phase. The temperature maximum calculated by considering radiation effects only lags behind the observed temperature maximum by approximately 3 hr. The calculated amplitude of the diurnal wave is considerably too large. Taking into account the diurnal wind system shown in

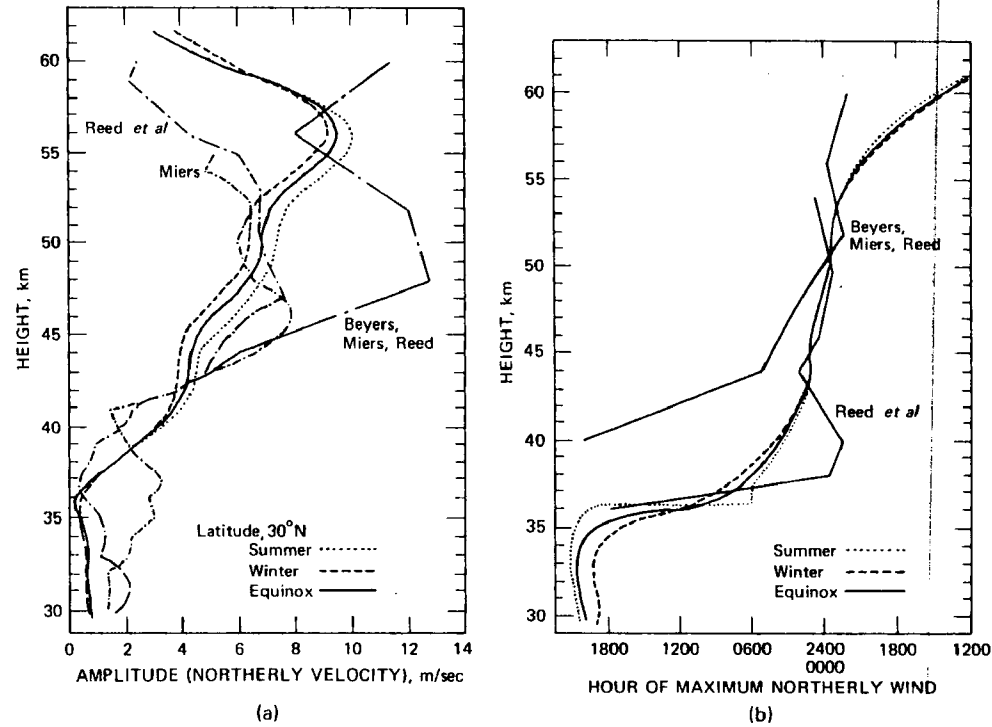


Fig. 1.23 Altitude distribution of the amplitude (a) and of the phase (b) of the solar diurnal component of v at 30° latitude for winter, equinoctial, and summer conditions. Also shown are some distributions based on observations by Miers (1965), Beyers, Miers, and Reed (1966), and Reed et al. (1966). [From R. S. Lindzen, *Quarterly Journal of the Royal Meteorological Society*, 93(395): 30, 31 (1967).]

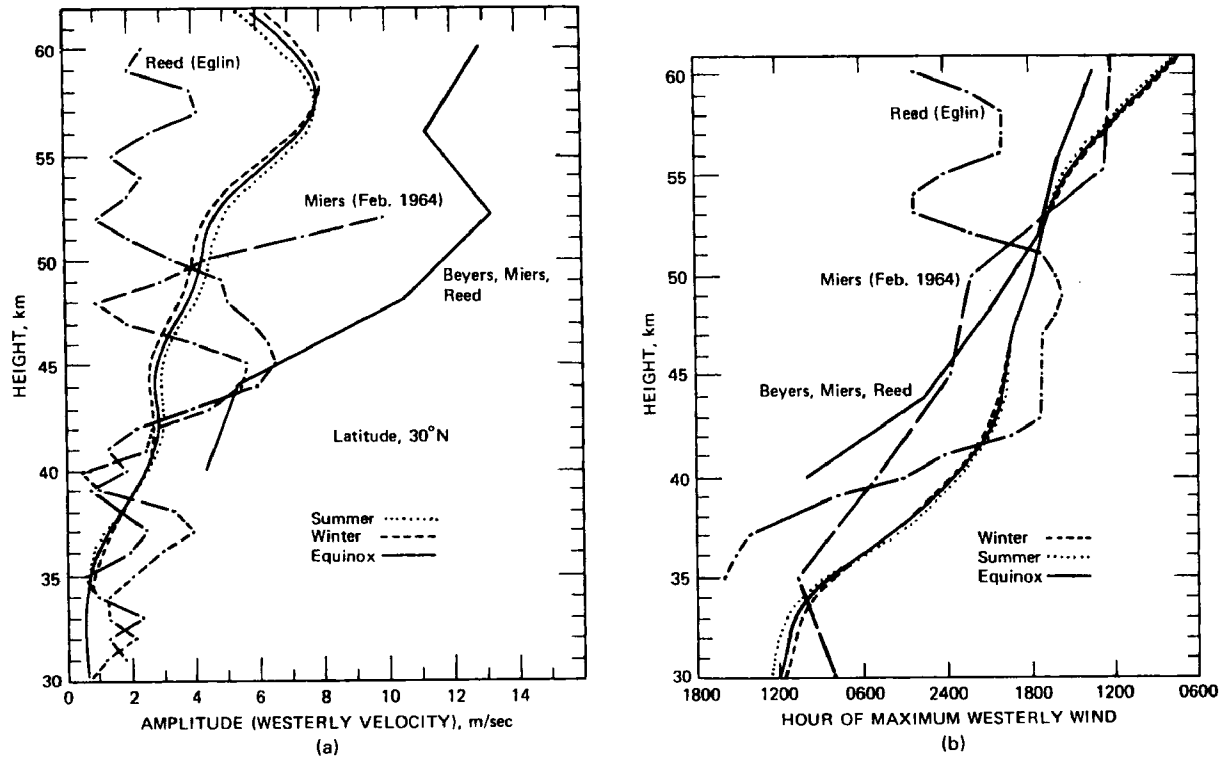


Fig. 1.24 Altitude distribution of the amplitude (a) and of the phase (b) of the solar diurnal component of u at 30° latitude for winter, equinoctial, and summer conditions. Also shown are some distributions based on observations by Miers (1965), Beyers, Miers, and Reed (1966), and Reed (personal communication to R. S. Lindzen). [From R. S. Lindzen, *Quarterly Journal of the Royal Meteorological Society*, 93(395): 32, 33 (1967).]

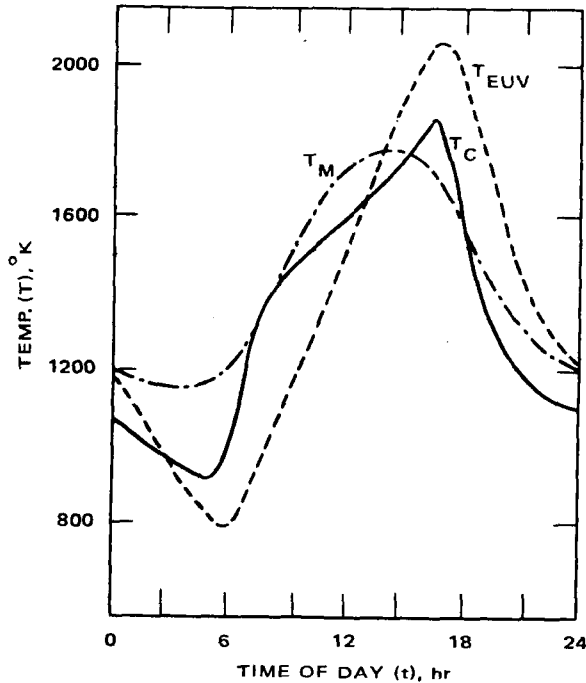


Fig. 1.25 Diurnal variation of the temperature at the thermopause (500 km). The abscissa is the local time, t . The observed temperature (T_M) (dashed-dotted curve, inferred from density measurements) is compared with calculated temperature variations. The dashed curve (T_{EUV}) is calculated under the assumption of heating by the absorption of solar extreme ultraviolet radiation and no horizontal advection. The solid curve (T_C) is obtained when the effect of horizontal advection in the equatorial plane is included. [From I. Harris and W. Priester, *Meteorological Monographs*, 9(31): 76 (1968).]

Fig. 1.26 reduces the amplitudes and yields better agreement with the observed values (see Fig. 1.25). The ion drag in the equatorial plane has to be relatively small to achieve wind velocities of the magnitudes shown in Fig. 1.26. One has to assume that the ion drag will especially affect the flow of the neutral gas in the direction perpendicular to the magnetic-field lines, i.e., in the direction parallel to the equator. I. Harris and Priester (1968) found that earlier assumptions by I. Harris (1966) on number densities of ions, by Chandra (1963) on electron-density profiles, and by Chapman (1956) on collision frequencies between neutrals and ions yielded rather small wind velocities in the equatorial plane which had no significant effect on the diurnal temperature distribution. Only when the ion drag was reduced to about 10% of the foregoing assumptions could wind velocities of the magnitude shown in Fig. 1.26 be obtained in the equatorial plane. The basic feature of the wind variation is an east-to-west wind in the morning and a west-to-east wind in the late evening. Meridional winds in the neutral air of the F-region (about 300 km) tend to blow toward the pole

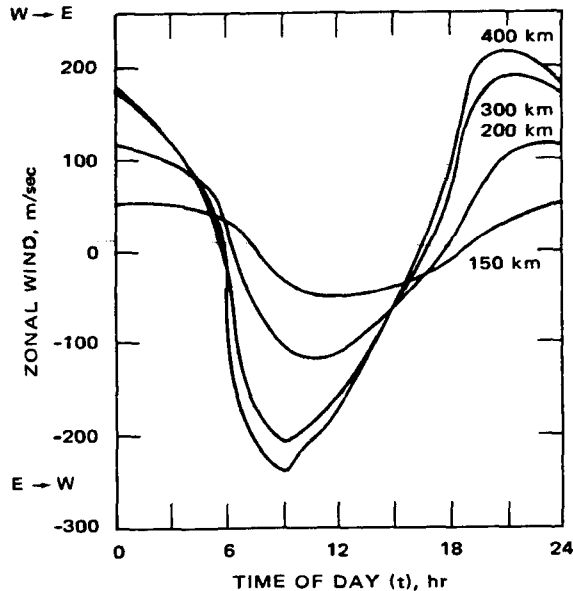


Fig. 1.26 The wind velocities in the equatorial plane for four different heights from 150 to 400 km as a function of local time, t . These high velocities were obtained when the ion drag was considerably suppressed. [From I. Harris and W. Priestler, *Meteorological Monographs*, 9(31): 78 (1968).]

by day and toward the equator by night (for a literature review, see Rishbeth, 1968). As shown in Fig. 1.25, the effect of high wind velocities on the temperature distribution in the upper thermosphere is appreciable. The heat transport associated with these winds, therefore, cannot be neglected. A similar effect of these winds on the transport of atmospheric trace substances may be anticipated. The presence of such wind systems may also explain the discrepancies between theoretical and observed tides (Webb, personal communication).

The temperature maximum shown in curve T_C (Fig. 1.25) at 1600 hr does not yet agree with the observed bulge at 1400 hr local time. This discrepancy may be explained by the restriction of the wind effect to the equatorial plane. The ion drag will be much less effective for other wind directions.

From model calculations Lagos (1967) (see also Dickinson et al., 1968; Dickinson and Geisler, 1968) was able to show that diurnal vertical-motion patterns, by the adiabatic heating and cooling associated with them, may provide a heat source for the thermosphere that may significantly shift the phase of the diurnal temperature wave. Consideration of vertical motions (order of magnitude 6 m/sec) makes it possible to shift the temperature maximum from 1800 local time to 1400 local time (compare with curve T_M in Fig. 1.25). Such diurnal vertical-motion patterns may also have a significant effect upon the dispersion and mixing of atmospheric constituents.

The solar response of the thermosphere reveals itself in the variations of upper atmosphere densities and temperatures with the sunspot cycle (Wasko and King, 1963). It is also evident from the semiannual (Fig. 1.18) and the diurnal (Fig. 1.25) temperature variations and becomes even more striking when one considers non-periodic solar events (I. Harris and Priester, 1962; Environmental Science Services Administration et al., 1966; Gregory, 1968; P. B. Rao, 1968). These may be characterized by various parameters, such as the solar flux in the 10.7-cm wave band (expressed in units of 10^{-22} watt/m²/Hz). Figure 1.27 shows the correlation between this solar parameter, the geomagnetic index, a_p , and the exospheric temperatures and densities derived from the drag of the Explorer IX satellite. The short-term variations revealed in this diagram may be expected to have some influence on the horizontal atmospheric structure and flow patterns at high levels as well, especially in the F-region of the ionosphere.

With the increased accuracy and resolution of measurements in the upper atmosphere, one becomes aware of the fact that the detailed vertical wind and temperature structure of the atmosphere above the stratopause is as complex as that of the troposphere and stratosphere (Boer and Mahoney, 1968; Jones and Peterson, 1968; Miller et al., 1968; W. S. Smith et al., 1968; Theon, 1968; Reed, 1968b). It will be shown in Chap. 6 that layers of positive and negative wind shears of several kilometers thickness appear quite regularly in the upper mesosphere and lower thermosphere. The formation of sporadic E-layers depends on the presence of such shearing layers. Meteorological Rocketsonde Network data also revealed such layers in the upper stratosphere and lower mesosphere. Measurements with the Robin falling sphere over Eglin Air Force Base indicate that certain smaller scale details (a few hundred meters thick) are of a highly transient nature, having lifetimes of the order of minutes and a horizontal extent of several hundred meters. Other features, however, with a vertical extent of the order of 10^3 m, seem to be relatively long lived and show up on successive soundings spaced at time intervals of slightly less than 1 hr (Webb, 1966a; Webb et al., 1966; Cole and Kantor, 1968; Mahoney and Boer, 1968).

In the lower stratosphere FPS-16 radar wind soundings have revealed an abundance of structural details in vertical wind profiles (Scoggins, 1963, 1965; Stinson et al., 1964). Some of these details are even evident from GMD soundings, although, because of the larger time interval between measurement points and the decreased tracking accuracy, the vertical extent and the amplitudes of wind fluctuations in vertical profiles are not reliably measured by GMD equipment (E. R. Reiter, 1958; Danielsen and Duquet, 1967). E. R. Reiter (1963c) has shown that certain structural details in the vertical wind profiles are quite persistent in time and tend to correlate with details in the vertical temperature structure (Figs. 1.28 and 1.29). An orientation *c.* wind details along isentropic surfaces may also be detected. The formation of such shearing layers could be explained by the action of gravity inertia waves occurring in layers with different mean wind speeds stacked upon each other (Weinstein and Reiter, 1965; Weinstein et al., 1966). Danielsen and Duquet (1967) find that the wind oscillations may be decomposed into a mean wind vector and a perturbation wind

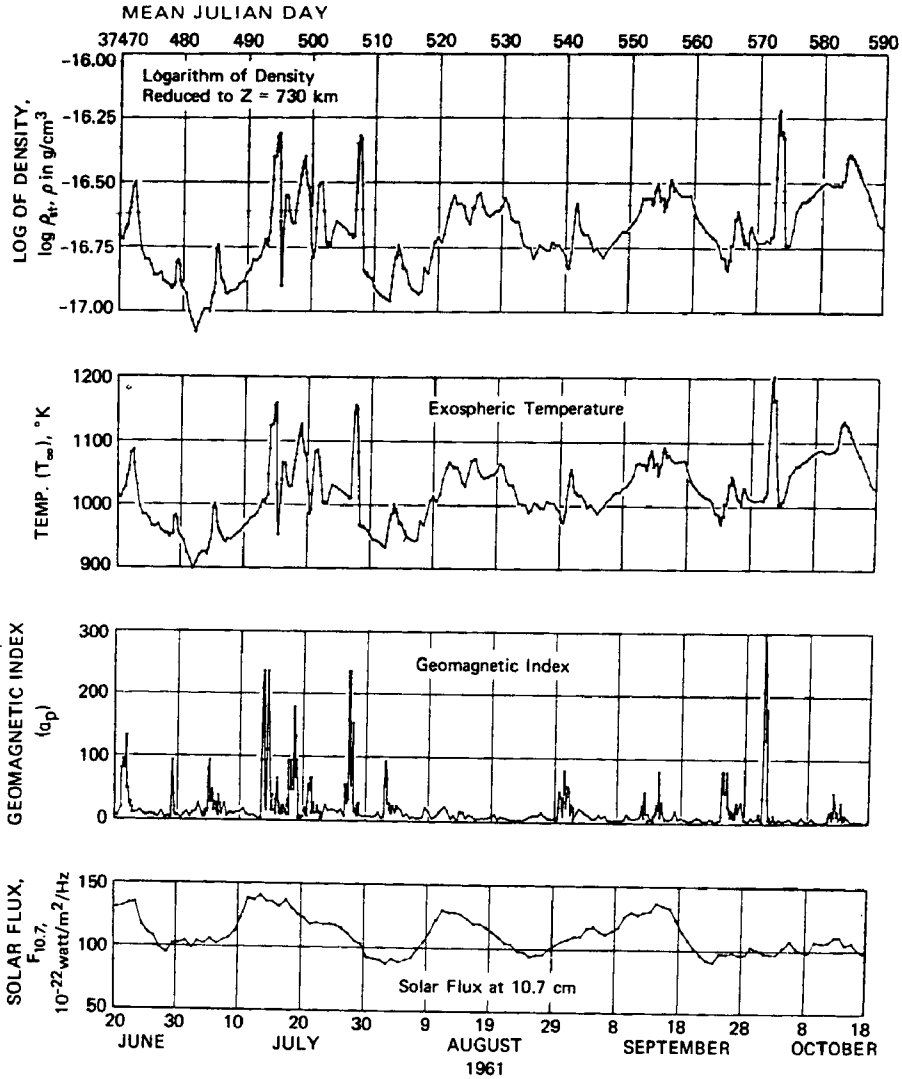


Fig. 1.27 Densities and temperatures derived from the drag of the Explorer IX satellite (196181) compared with the geomagnetic index, a_p , and the 10.7-cm solar flux. (From Environmental Science Services Administration, NASA, and U. S. Air Force, *U. S. Standard Atmosphere Supplements*, p. 58, U. S. Government Printing Office, Washington, 1966.)

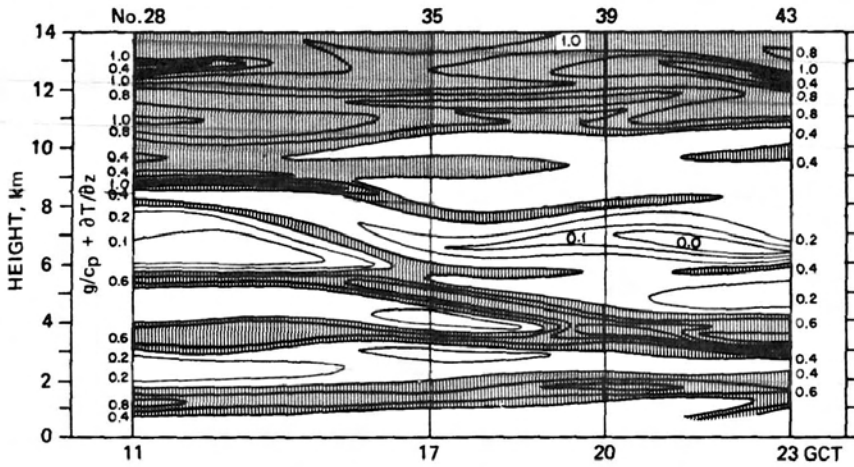


Fig. 1.28 Time section of stability, $(g/c_p + \partial T/\partial z)$ (in units of $^{\circ}\text{C}/100\text{ m}$), where c_p is the specific heat at constant pressure, Cape Kennedy, Jan. 3, 1963, 1100 to 2300 GCT. [From E. R. Reiter, *Atmospheric Science Technical Paper No. 47*, Colorado State University, 1963.]

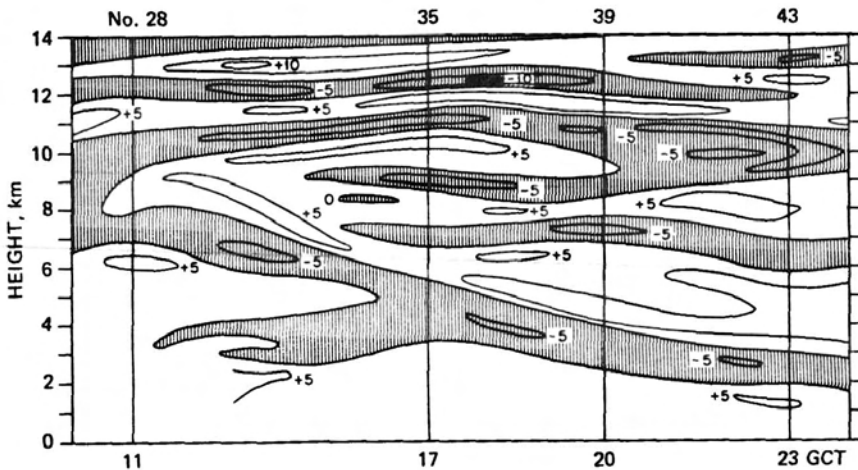


Fig. 1.29 Time section of mesostructure of wind speeds, Cape Kennedy, Jan. 3, 1963, expressed in terms of anomalies (m/sec) from smoothed wind profiles. Negative anomalies are shaded. [From E. R. Reiter, *Atmospheric Science Technical Paper No. 47*, Colorado State University, 1963.]

Hines (1959, 1960) associated the structural details observed in the upper atmosphere with internal gravity waves (see also Nelson, 1968; Hines, 1968c, 1968d, 1968e; Bowman, 1968; Hooke, 1968; Gossard and Paulson, 1968; Goodwin, 1968). Difficulties in interpreting drift data when several wave modes are superimposed have been analyzed by Hines and Rao, 1968. These waves may be considered as the

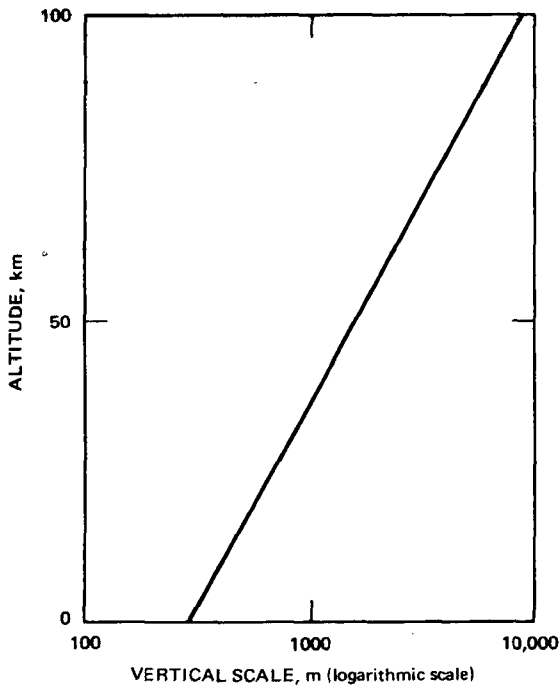
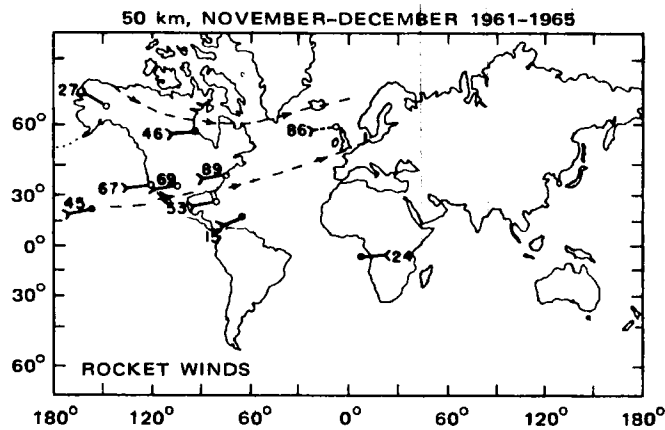
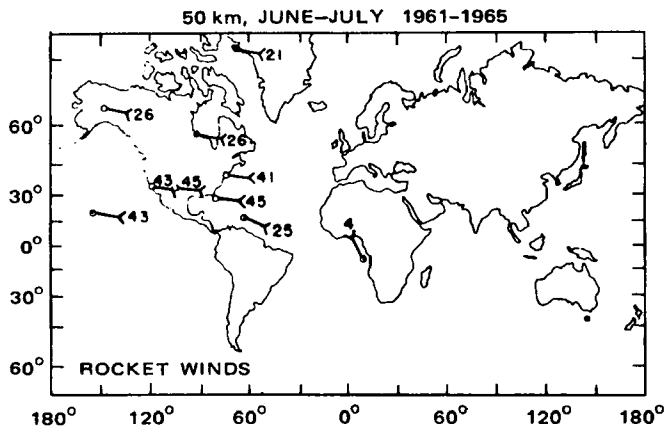
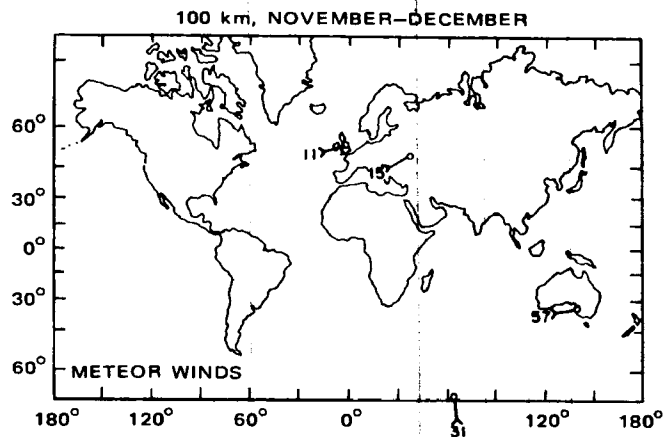
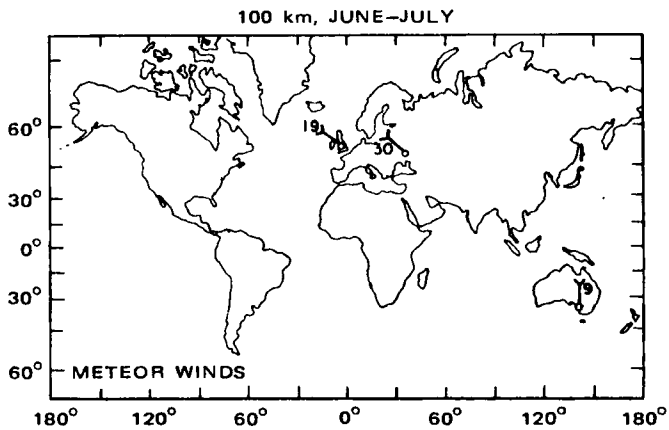
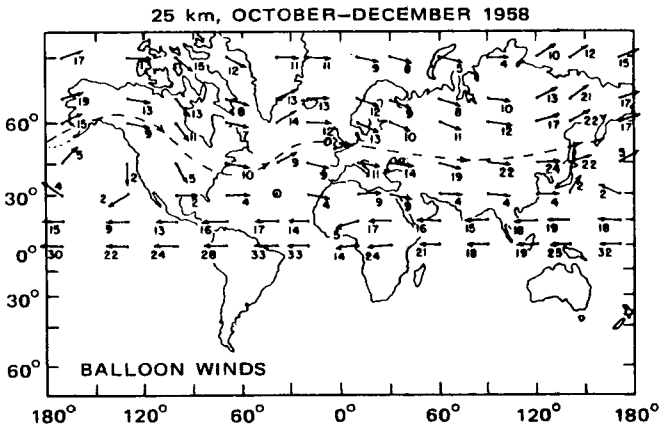


Fig. 1.30 Scale size in the vertical of stratospheric circulation detail features. [From W. L. Webb, J. Giraytys, H. B. Tolefson, R. C. Forsberg, R. I. Vick, O. H. Daniel, and R. L. Tucker, *Bulletin of the American Meteorological Society*, 47(10): 797 (1966).]

low-frequency counterparts of acoustic waves; if Coriolis forces are included in their treatment, they also comprise tidal waves. Such “internal waves” may have a substantial vertical component of phase propagation. This fact has led Charney and Drazin (1961), Lindzen (1968), and others to believe that appreciable energy of planetary-scale waves may reach the upper mesosphere from the troposphere, especially during winter when strong westerly winds prevail in the lower atmosphere. This is brought out by Fig. 1.31, which shows mean upper winds in the middle stratosphere (lower diagrams), near the stratopause (middle diagrams), and above the mesopause (upper diagrams) for summer and winter (Newell, 1968a). The planetary-wave configuration, revealing a trough over eastern North America, seems to propagate



STRUCTURE OF THE UPPER ATMOSPHERE



s. Speeds are in meters per second. [From R. E. Newell,
: 105 (1968).]

upward from the troposphere (where this trough is orographically generated) only during winter.

J. M. Wallace and Kousky (1968a) and D. D. Houghton and Jones (1968) attribute the existence of the biennial oscillation in the tropics to the vertical flux and final trapping of internal-wave energy. Hines (1968a) considers the vertical energy flux by gravity waves into the upper atmosphere to be considerable. This energy flux may contribute effectively to the heat budget in the ionospheric E- and F-regions (see also Mahoney, 1966).

Internal atmospheric gravity waves, produced either by tidal waves in situ or by the wind systems in the lower atmosphere (Georges, 1968; Jones, 1969), according to Hines (1960), exist for periods exceeding the critical value

$$\tau_g = \frac{2\pi C}{g(\gamma - 1)^{1/2}} \quad (1.41)$$

but smaller than $\tau_a = 4\pi C/\gamma g$. Here C is the speed of sound ($\cong 280$ m/sec at meteor-trail altitudes), g is the acceleration of gravity ($\cong 9.5$ m/sec² in the same region), and $\gamma = c_p/c_v$ is the ratio of specific heats ($\cong 1.4$). Near the mesopause τ_g is about 4.9 min.

From asymptotic relations between parameters that characterize these waves, Hines (1960) arrives at

$$\frac{\lambda_x}{\lambda_z} \approx \frac{\tau}{\tau_g} \quad (1.42)$$

describing the ratio of horizontal (λ_x) to vertical wavelengths (λ_z). For periods $\tau = 200$ min and $\lambda_z = 12$ km, one arrives at $\lambda_x = 490$ km. From ARCAS Robin measurements, Cole and Kantor (1968, 1969) conclude that features with a vertical wavelength, λ_z , of 3 to 4 km and with an amplitude of 4 to 12 m/sec have a horizontal wavelength, λ_x , of 1000 to 1300 km. Oscillations with $\lambda_z = 1$ to 3 km and amplitudes of 1 to 2 m/sec decrease rapidly with horizontal distance. From a second relation

$$\frac{u}{w} \approx \frac{\lambda_x}{\lambda_z} \quad (1.43)$$

one may see that the horizontal wind velocity, u , exceeds the vertical velocity, w , in such waves by a factor of 40 (see also Figs. 1.20 to 1.22) [for details of derivation of these relations, see Hines (1960)].

It has been shown by Hines (1960) that the exponential growth factor, $\exp(\gamma g z/2C^2)$, which was derived from linear perturbation theories, does not hold any longer above the mesopause. Observed drift velocities in the thermosphere are smaller than those predicted by this factor.

Lomax and Nielson (1968) observed, from perturbations issuing from high-altitude nuclear tests, that the amplitude of the traveling ionospheric disturbance

strongly depends on the orientation of the wave front traveling in the ionosphere with respect to the local geomagnetic field. The amplitude decreased as the angle of the wave normal to the magnetic field approached orthogonality. This could be brought about by an essentially unchanged wave in the neutral medium, which caused large-scale and rapid changes in the F-region electron densities as a result of the interaction of the ions traveling with the neutral wave and the earth's magnetic field. The velocity of the wave seemed to be unaffected by the magnetic-field orientation.

Certain wave modes will be reflected at "thermal barriers," thus being prevented from traveling upward through the atmosphere. Such reflections may occur at levels somewhat below 90 km, leading to minimum amplitudes of gravity waves in this region (Goodwin, 1968). Figure 1.32 shows the propagation modes of internal gravity waves in the vicinity of the mesopause. Observations by Vincent (1969) of

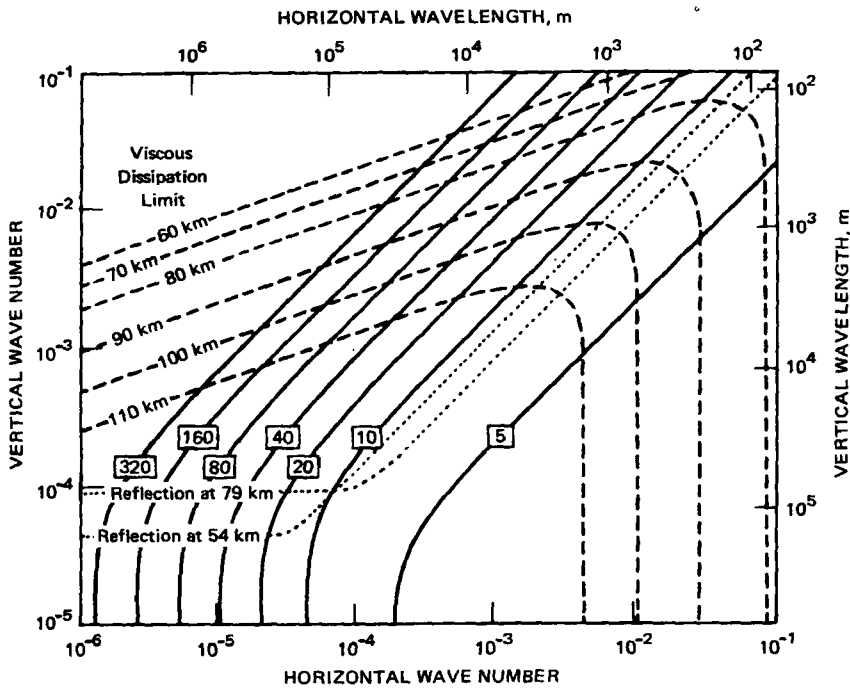


Fig. 1.32 Dispersion of internal gravity waves for atmospheric properties typical of 90 and 100 km. The periods, measured in minutes, are shown in boxes on the corresponding constant-period contours (solid lines). The following parameters have been applied: $\gamma = 1.4$; $g = 9.5 \text{ m/sec}^2$; $H = C^2/\gamma g = 6.0 \text{ km}$, with $C = 280 \text{ m/sec}$, $\tau_a = 4.4 \text{ min}$, and $\tau_g = 4.9 \text{ min}$. The approximate limits of the permitted spectrum, as determined by viscous damping, are shown for heights of 60, 70, 80, 90, 100, and 110 km (broken curves); modes lying above and to the right of these curves are excluded. The modes subject to reflection at heights of 54 and 79 km are also shown (dotted lines). [Reproduced by permission of the National Research Council of Canada from C. O. Hines, *Canadian Journal of Physics*, 38: 1472 (1960).]

phase-height variations in the E-region, most likely produced by internal gravity waves, agree with the propagation modes depicted in this diagram. Modes lying below the curves, indicating reflection of waves at 54 and 79 km, cannot proceed into the high atmosphere. Modes lying above and to the right of the dashed curves are also prohibited by viscous damping, which becomes stronger with increasing altitude.

At yet higher levels in the atmosphere, different parameters prevail. Figure 1.33 indicates propagation modes at 225 km. The assumptions underlying this diagram are

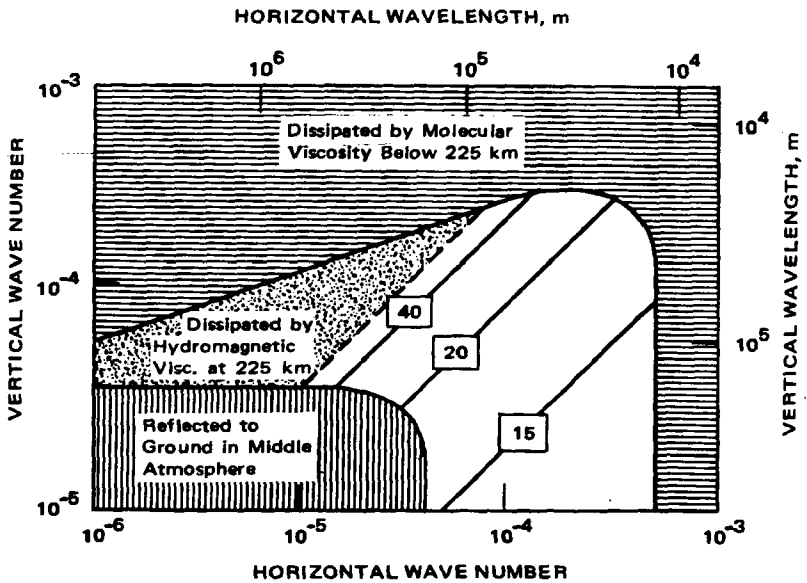


Fig. 1.33 Propagation modes at a height of 225 km ($\gamma = 1.40$; $g = 9.15 \text{ m/sec}^2$; $H = C^2/\gamma g = 51.3 \text{ km}$ (scale height of the atmosphere), where $\tau_a = 13.2 \text{ min}$, and $\tau_g = 14.7 \text{ min}$; dH/dz is assumed to be 0). The periods, measured in minutes, are shown in boxes on the corresponding constant-period contours. Modes removed by reflection in the middle atmosphere and those removed by molecular viscosity in the upper atmosphere are represented by the hatched areas; those damped severely by hydromagnetic viscosity in the upper atmosphere (during daytime) are shown by the shaded area. [Reproduced by permission of the National Research Council of Canada from C. O. Hines, *Canadian Journal of Physics*, 38: 1473 (1960).]

listed in the legend ($H = C^2/\gamma g$ is the "scale height" of the atmosphere and $\tau_a = 4\pi C/\gamma g$). It appears from this diagram that long-period oscillations that might lead to characteristic details in vertical wind profiles are effectively dissipated in the middle and upper thermosphere.

Schilling (1968) points out that between 160 and 200 km satellite drag observations rather consistently indicate a sharp relative density increase that could be associated with an ionospheric inversion between the E- and the F₁-layers (Fig. 1.34).

Thus some of the structure present in the upper atmosphere, not yet fully explored, may be of other than gravity or tidal-wave origin.

The effect of the small-scale structure of the atmosphere on the dispersion of trace constituents has not yet been explored systematically. From analyses by Danielsen and Duquet (1967), one may guess that the rotation of the perturbation wind vector with height may result in appreciable differences between trajectories following the air motions in different but adjacent layers. Weinstein and E. R. Reiter

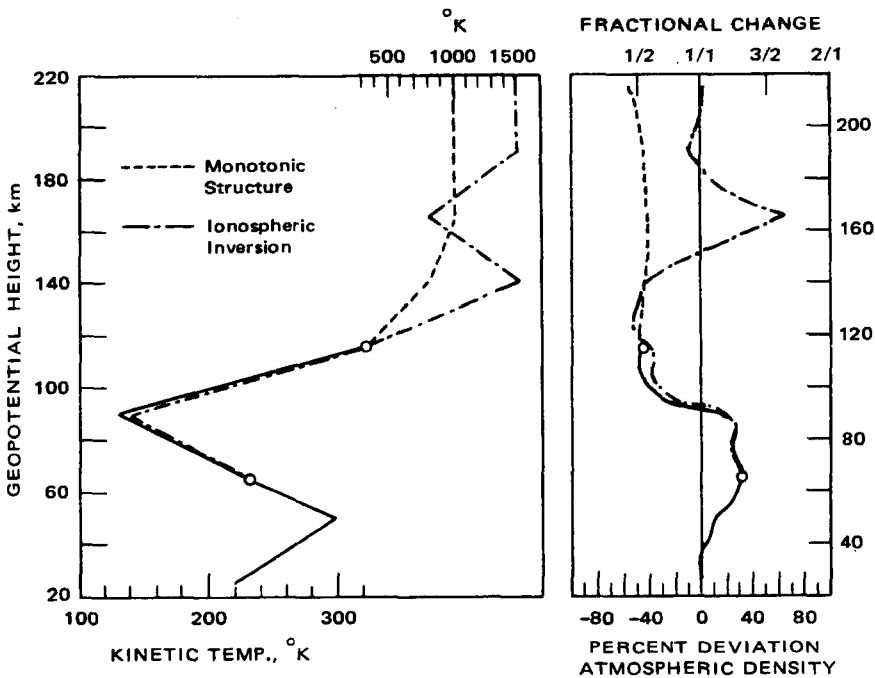


Fig. 1.34 Schematic characteristics of atmospheric structure with monotonic distribution and with a temperature inversion in the ionosphere. [From G. F. Schilling, *Meteorological Monographs*, 9(31): 87 (1968).]

(1965) suggested that the mesoscale vertical wind shears resulting from the superposition of layers undergoing inertial oscillations at times may reach critical Richardson numbers. On such occasions turbulent flow conditions and the dispersion of atmospheric trace substances will be enhanced. Lindzen (1968) postulates that the vertical distribution of tidal effects near the mesopause may also lead to critical Richardson numbers, which may be indicative of strong turbulent mixing in these regions (Fig. 1.35) (see also Justus and Roper, 1968).

E. R. Reiter (1968b) points out that turbulence in a stably stratified atmosphere may lead to the formation of relatively sharp discontinuities in temperature, wind

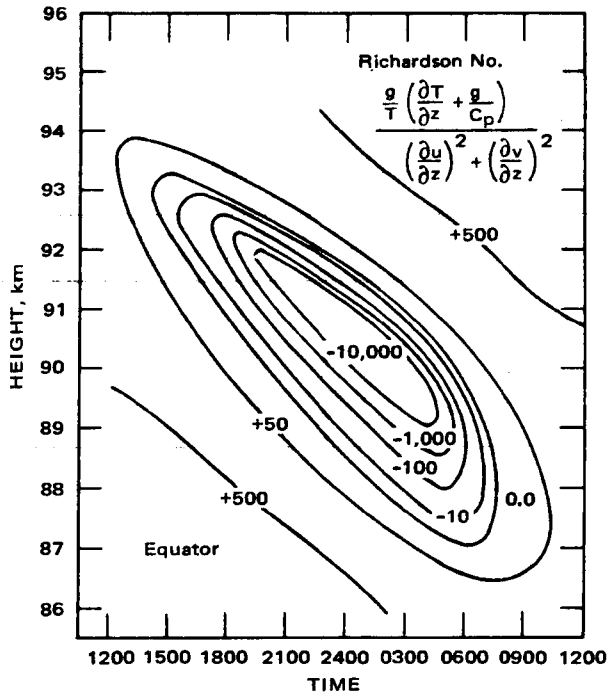


Fig. 1.35 Theoretically computed time-height cross section for the Richardson number due to the diurnal thermal tide over the equator. [From R. S. Lindzen, *Meteorological Monographs*, 9(31): 45 (1968).]

speed, and admixtures, such as water vapor. This is illustrated schematically in Fig. 1.36. The trace substance in this case is assumed to be water vapor. If a vertical gradient of water-vapor mixing ratio, χ_w , is present before the onset of turbulence, there will be sharp increases in $\partial\chi_w/\partial z$ at the top and bottom of the layer, which is thoroughly mixed after the establishment of turbulent flow conditions. As shown in Fig. 1.36, a "haze horizon" may even form along the upper boundary of the turbulent layer. Similar conditions may be expected for other atmospheric admixtures, such as ozone, radioactive material, etc., which show vertical gradients in their mixing ratios.

GENERAL COMMENTS ON THE PHOTOCHEMISTRY OF THE UPPER ATMOSPHERE

As will be shown in several of the subsequent chapters, the study of trace constituents in the upper atmosphere is beginning to throw considerable light on the intricate motion patterns that prevail above the reach of our conventional sounding systems.

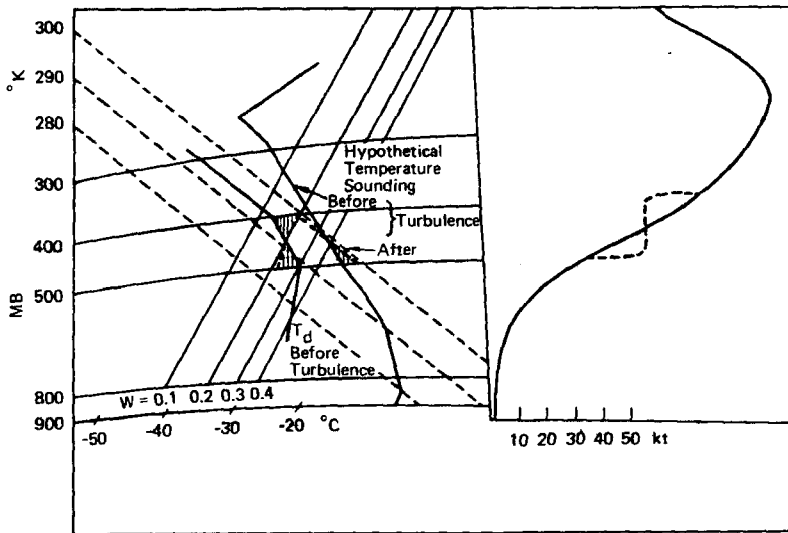


Fig. 1.36 Schematic view of effects of turbulence on vertical wind, temperature, and humidity profiles: A stable lapse rate will change into an adiabatic layer bounded by two inversions; at the same time the momentum exchange within the adiabatic layer will cause the formation of a "nose" on the vertical wind profile. (Similar noses are frequently observed in FPS-16 wind soundings.) Vertical wind shears will be concentrated at the top and bottom of the adiabatic layer. Vertical mixing in this layer will also equalize the water-vapor mixing ratio in the adiabatic layer. If there were a vertical gradient in the mixing ratio to start with, strong gradients of the quantity will result at the top and bottom of the adiabatic layer. Turbulence elements of a certain size will now generate larger fluctuations in atmospheric radio-wave refractivity "n" at the bottom and top of this layer than they did before turbulence started under moderately stable conditions. Solid lines indicate conditions before the onset of turbulence; dashed lines are after the establishment of a turbulent layer. Note that under favorable conditions a haze layer may develop on top of the turbulent region. [From E. R. Reiter, in *Proceedings of the Symposium on Clear Air Turbulence and Its Detection*, Seattle, Wash., Aug. 14-16, 1968, p. 19, Plenum Press, Inc., New York, 1969.]

High-energy solar radiation penetrating through the gaseous envelope of the earth at low pressures and densities causes dissociation of the normal atmospheric constituents and chemical reactions between the various resulting components. The energy budget of the high atmosphere is significantly influenced by these chemical reactions. This has been hinted at in Part I and in this chapter, as the relatively warm mesospheric temperatures prevailing during winter were described.

The energy-balance requirements in the upper atmosphere are satisfied by radiative fluxes, chemical processes, and heat and momentum transports by atmospheric motions. The heat and momentum transports lead by necessity to transports of trace constituents and thus to a modification of those chemical processes which would be encountered under equilibrium conditions in a stationary atmosphere.

It becomes quite obvious, therefore, that an understanding of the transport phenomena in the upper atmosphere is tied intimately to the knowledge of photochemical processes under equilibrium conditions. For the ozone layer this has been demonstrated by Dütsch (1968). (A detailed discussion will be given in a subsequent chapter.) For a discussion of photochemical processes in the ionosphere, see Rishbeth and Garriott, 1969.

With the rapid development of ground-based optical and airborne rocket sensing equipment, as well as of laboratory simulation techniques that allow one to "model" the upper atmosphere, we have come to realize that a large number of chemical reactions may have an important bearing on the structure and the energetics of the high atmosphere. Research in this field is still continuing at a rapid pace. The following summary, therefore, may be considered only as a tentative guideline.

Earlier studies of the chemical reactions leading to the observed ozone layer in the upper stratosphere took into account only the reactions of molecular and atomic oxygen. It has been brought to light recently, however, that reactions involving hydrogen and its compounds should not be neglected. The presence of other gases, such as molecular nitrogen, may be of importance even in the upper stratosphere if one wishes to consider in detail the possible three-body collisions influencing the ozone budget at these levels. Less-abundant constituents may have an effect of their own on the photochemical balance in the upper atmosphere. Methane, for instance, may influence the water-vapor budget of the upper stratosphere. Many of these detailed processes have not been sufficiently explored to allow a complete description of the chemistry and photochemistry of the earth's atmosphere. Computer modeling of the manifold chemical reactions possible under the environmental conditions of the upper atmosphere has become an important research tool in arriving at a more complete picture of atmospheric constituents and their behavior (Keneshea, 1967).

Chemical reactions in the high atmosphere involving hydrogen and its compounds, together with oxygen, have been studied by a number of authors (e.g., Bates and Nicolet, 1950, 1965; Hesstvedt, 1963, 1964, 1965a, 1965c, 1967a, 1967b, 1968a, 1968b; Hunt, 1966a; Schiff, 1968; Schofield, 1967; Crutzen, 1969; Mitra, 1969). Characteristic reactions used in Hesstvedt's (1968a) latest model of the upper atmosphere, together with the recombination rate coefficients, k_i , and the dissociation rates, J_i , are given in Tables 1.6 to 1.8. (Some of the recombination rate coefficients are listed as temperature dependent; for others this dependence is not known.) These reactions, according to Hunt (1966a), give fairly good agreement with satellite-observed ozone profiles. Reactions between hydrogen and nitrogen were excluded since, according to Nicolet (1965a), they appear to be of minor importance (see also Wayne, 1967). For further reference on nitrogen reactions, see p. 223. The reactions involving the hydroxyl radical, OH, are of particular interest in the study of day and night glow phenomena (Ballif and Venkateswaran, 1962; L. Wallace, 1962; Hampson, 1964; Hesstvedt, 1965b, 1967b; Hunt, 1966a). The notations $O(^3P)$ and $O(^1D)$ refer to two states of electronic excitation (Wayne, 1967). A wide variety of such states is possible in the atoms of the various atmospheric constituents, and considerable refinement in atmospheric modeling could be achieved by taking them

Table 1.6
CHEMICAL REACTIONS IN THE UPPER ATMOSPHERE *

(1)	$O(^3P) + O(^3P) + M \rightarrow O_2 + M$	$k_1 = 2.7 \times 10^{-33}$ (Reeves, Manella, and Harteck, 1960)
(2)	$O(^3P) + O_2 + M \rightarrow O_3 + M$	$k_2 = 8.2 \times 10^{-35} \exp(890/RT)$ (Benson and Axworthy, 1965)
(3)	$O(^3P) + O_3 \rightarrow 2 O_2$	$k_3 = 8 \times 10^{-12} \exp(-3260/RT)$ (Campbell and Nudelman, 1960)
(4a)	$O_2 + h\nu \rightarrow O(^3P) + O(^3P)$	J_{2a} (1750 A < λ < 2424 A) } $J_{2a} + J_{2b} = J_2$
(4b)	$O_2 + h\nu \rightarrow O(^3P) + O(^1D)$	
(5a)	$O_3 + h\nu \rightarrow O(^3P) + O_2$	J_{3a} (λ > 3100 A) } $J_{3a} + J_{3b} = J_3$
(5b)	$O_3 + h\nu \rightarrow O(^1D) + O_2$	
(6)	$OH + O(^3P) \rightarrow H + O_2$	$k_6 = 5 \times 10^{-11}$ (Kaufman, 1964)
(7)	$HO_2 + O(^3P) \rightarrow OH + O_2$	$k_7 = 10^{-11}$ (Kaufman, 1964)
(8)	$H + O_2 + M \rightarrow HO_2 + M$	$k_8 = 7.4 \times 10^{-32}$ (Larkin and Thrush, 1964)
(9)	$H + O_3 \rightarrow OH + O_2$	$k_9 = 2.6 \times 10^{-11}$ (Kaufman, 1964)
(10)	$OH + HO_2 \rightarrow H_2O + O_2$	$k_{10} = 10^{-11}$ (Kaufman, 1964)
(11)	$H_2O_2 + h\nu \rightarrow 2 OH$	$J_{H_2O_2}$ (1875 A < λ < 3825 A)
(12)	$O(^3P) + H_2O_2 \rightarrow OH + HO_2$	$k_{12} = 10^{-15}$ (Foner and Hudson, 1962)
(13)	$HO_2 + HO_2 \rightarrow H_2O_2 + O_2$	$k_{13} = 3 \times 10^{-12}$ (Kaufman, 1964)
(14)	$OH + H_2O_2 \rightarrow H_2O + HO_2$	$k_{14} = 4 \times 10^{-13}$ (Foner and Hudson, 1962)
(15)	$OH + OH \rightarrow H_2O + O(^3P)$	$k_{15} = 2.8 \times 10^{-12}$ (Kaufman, 1964)
(16)	$H_2O + h\nu \rightarrow OH + H$	J_{H_2O} (1350 A < λ < 2375 A + Ly α)
(17)	$H + HO_2 \rightarrow H_2O + O(^3P)$	$k_{17} = 2 \times 10^{10} \exp(-4000/RT)$ (Bates and Nicolet, 1950)
(18)	$H + HO_2 \rightarrow H_2 + O_2$	$k_{18} = 2 \times 10^{-13}$ (Clyne and Thrush, 1963)
(19)	$H + H + M \rightarrow H_2 + M$	$k_{19} = 2.6 \times 10^{-32}$ (Larkin and Thrush, 1964)
(20)	$O(^1D) + M \rightarrow O(^3P) + M$	$k_{20} = 10^{-10}$ for M = O ₂ (Schiff, 1964) $k_{20} = 2.2 \times 10^{-11}$ for M = N ₂ (More and Raper, 1964)
(21)	$O(^1D) + H_2 \rightarrow OH + H$	$k_{21} = 10^{-11}$ (Hunt, 1966a)
(22)	$O(^3P) + H_2 \rightarrow OH + H$	$k_{22} = 4.1 \times 10^{-11} \exp(-7700/RT)$ (Fenimore and Jones, 1958)
(23)	$HO_2 + O_3 \rightarrow OH + 2 O_2$	$k_{23} = 10^{-14}$ (Hunt, 1966a)
(24)	$OH + O_3 \rightarrow HO_2 + O_2$	$k_{24} = 5 \times 10^{-13}$ (Kaufman, 1964)
(25)	$H + H_2O_2 \rightarrow H_2 + HO_2$	$k_{25} = 10^{-13}$ (Foner and Hudson, 1962)
(26)	$H + O(^3P) + M \rightarrow OH + M$	$k_{26} = 8 \times 10^{-33}$ (Bates and Nicolet, 1950)
(27)	$H + O_3 \rightarrow HO_2 + O(^3P)$	$k_{27} = 2 \times 10^{-10} \exp(-4000/RT)$ (Bates and Nicolet, 1950)
(28)	$H + O_2 \rightarrow OH + O(^3P)$	$k_{28} = 1 \times 10^{-9} \exp(-16800/RT)$ (Kaufman, 1964)
(29)	$O(^1D) + H_2O \rightarrow 2 OH$	$k_{29} = 10^{-11}$ (Hunt, 1966a)
(30)	$H + HO_2 \rightarrow 2 OH$	$k_{30} = 10^{-11}$ (Kaufman, 1964)
(31)	$H + OH + M \rightarrow H_2O + M$	$k_{31} = 2.5 \times 10^{-31}$ (Kaufman, 1964)
(32)	$O(^3P) + OH + M \rightarrow HO_2 + M$	$k_{32} = 1.4 \times 10^{-31}$ (Petersen and Kretschmer, 1960)
(33)	$H + OH \rightarrow H_2 + O(^3P)$	$k_{33} = 1.8 \times 10^{-12} \exp(-5800/RT)$ (Kaufman, 1964)
(34)	$H_2 + OH \rightarrow H_2O + H$	$k_{34} = 10^{-10} \exp(-5900/RT)$ (Kaufman, 1964)
(35)	$O(^1D) + O_3 \rightarrow 2 O_2$	$k_{35} = 10^{-11}$ (Fitzsimmons and Bair, 1964)
(36)	$HO_2 + h\nu \rightarrow OH + O(^3P)$	J_{HO_2}

*Adapted from Hessstvedt (1967b, 1968a).

Table 1.7
TEMPERATURES, AIR NUMBER DENSITIES, AND DISSOCIATION RATES (SEC⁻¹)*

Height, km	Temp., °K	M, cm ⁻³	J ₂	J _{3a}	J _{3b}	J _{H₂O₂} = J _{HO₂}	J _{H₂O}
40	254	8.6 × 10 ¹⁶	5.1 × 10 ⁻¹⁰	7.2 × 10 ⁻⁴	1.6 × 10 ⁻³	3.7 × 10 ⁻⁵	1.8 × 10 ⁻¹⁰
35	243	1.8 × 10 ¹⁷	2.2 × 10 ⁻¹⁰	7.2 × 10 ⁻⁴	6.2 × 10 ⁻⁴	1.9 × 10 ⁻⁵	7.5 × 10 ⁻¹¹
30	232	3.8 × 10 ¹⁷	5.7 × 10 ⁻¹¹	7.1 × 10 ⁻⁴	2.4 × 10 ⁻⁴	8.9 × 10 ⁻⁶	1.8 × 10 ⁻¹¹
25	221	8.4 × 10 ¹⁷	6.5 × 10 ⁻¹²	6.9 × 10 ⁻⁴	9.0 × 10 ⁻⁵	4.7 × 10 ⁻⁶	2.4 × 10 ⁻¹²
20	207	2.0 × 10 ¹⁸	4.2 × 10 ⁻¹³	6.8 × 10 ⁻⁴	5.0 × 10 ⁻⁵	3.6 × 10 ⁻⁶	1.6 × 10 ⁻¹³
15	199	4.8 × 10 ¹⁸	7.7 × 10 ⁻¹⁵	6.7 × 10 ⁻⁴	4.2 × 10 ⁻⁵	3.3 × 10 ⁻⁶	1.9 × 10 ⁻¹⁵

*From Hesstvedt (1967b).

Table 1.8
DISSOCIATION RATES AS A FUNCTION OF OPTICAL THICKNESS OF O₂ *

Optical thickness of O ₂ , cm ⁻²	Approximate height, km	J _{H₂O₂}	J _{H₂O}	J _{2a}	J _{2b}	J _{3a}	J _{3b}
1 × 10 ¹⁷	120	1.2 × 10 ⁻⁴	1.0 × 10 ⁻⁵	1.6 × 10 ⁻⁸	2.9 × 10 ⁻⁶	7.5 × 10 ⁻⁴	8.4 × 10 ⁻³
3 × 10 ¹⁷	110	1.2 × 10 ⁻⁴	8.6 × 10 ⁻⁶	1.6 × 10 ⁻⁸	1.4 × 10 ⁻⁶	7.5 × 10 ⁻⁴	8.4 × 10 ⁻³
1 × 10 ¹⁸	102	1.2 × 10 ⁻⁴	6.6 × 10 ⁻⁶	1.6 × 10 ⁻⁸	3.9 × 10 ⁻⁷	7.5 × 10 ⁻⁴	8.4 × 10 ⁻³
3 × 10 ¹⁸	94	1.2 × 10 ⁻⁴	5.2 × 10 ⁻⁶	1.5 × 10 ⁻⁸	6.9 × 10 ⁻⁸	7.5 × 10 ⁻⁴	8.4 × 10 ⁻³
1 × 10 ¹⁹	87	1.2 × 10 ⁻⁴	4.4 × 10 ⁻⁶	1.2 × 10 ⁻⁸	2.3 × 10 ⁻⁹	7.5 × 10 ⁻⁴	8.4 × 10 ⁻³
3 × 10 ¹⁹	81	1.2 × 10 ⁻⁴	3.5 × 10 ⁻⁶	8.9 × 10 ⁻⁹	6.2 × 10 ⁻¹²	7.5 × 10 ⁻⁴	8.4 × 10 ⁻³
1 × 10 ²⁰	75	1.2 × 10 ⁻⁴	1.6 × 10 ⁻⁶	5.5 × 10 ⁻⁹	6.2 × 10 ⁻²⁰	7.5 × 10 ⁻⁴	8.4 × 10 ⁻³
3 × 10 ²⁰	68	1.2 × 10 ⁻⁴	1.8 × 10 ⁻⁷	3.5 × 10 ⁻⁹	8.7 × 10 ⁻⁴³	7.5 × 10 ⁻⁴	8.4 × 10 ⁻³
1 × 10 ²¹	60	1.2 × 10 ⁻⁴	2.4 × 10 ⁻⁹	2.3 × 10 ⁻⁹		7.5 × 10 ⁻⁴	8.4 × 10 ⁻³
3 × 10 ²¹	52	1.2 × 10 ⁻⁴	9.2 × 10 ⁻¹⁰	1.6 × 10 ⁻⁹		7.5 × 10 ⁻⁴	8.0 × 10 ⁻³
1 × 10 ²²	44	8.0 × 10 ⁻⁵	3.9 × 10 ⁻¹⁰	1.2 × 10 ⁻⁹		7.5 × 10 ⁻⁴	5.0 × 10 ⁻³

*From Hesstvedt (1968a).

into account (Swider, 1969a; for excitation cross sections, see A. E. S. Green et al., 1969). Many of these states are of minor significance, however (Ratcliffe, 1960). The symbol "M" in Table 1.6 refers to a molecule involved in a three-body collision. Specification of the type of molecule, e.g., O₂ or N₂, leads to further refinement. The height dependence of the dissociation rates, J₁, can be seen from Tables 1.7 and 1.8.

The reactions listed in Table 1.6 depend on the concentrations of the individual constituents, which, in turn, will be changed by such reactions until an equilibrium state is reached. (For details of such concentration changes, see Hesstvedt, 1968a.) Our knowledge of the concentrations of various molecular and atomic constituents of the upper atmosphere is still in flux and is continuously augmented by improved model calculations and by evidence from rocket experiments. Estimates of the number densities of various constituents of the high atmosphere are available from the 1962 U. S. Standard Atmosphere (National Aeronautics and Space Administration et al., 1962), COSPAR (1965), and other publications (Champion, 1968; Hesstvedt, 1968a; Johnson, 1968). Figure 1.37 shows a comparison of number densities measured by rocket experiments (Hedin et al., 1964; Hedin and Nier, 1965; see also Jursa et al., 1965) and those computed in the 1966 U. S. Standard Atmosphere Supplements (Environmental Science Services Administration et al., 1966). Agreement between measurements and the postulated model values is good near 120 km. At 200 km the ratios of model to measured densities are 3.4 for O₂, 2.5 for O, and 2.1 for N₂. Some of these discrepancies may be due to measurement difficulties [Zahn (1967) points out the possibility of systematically too low values of [O]* at 120 km observed by mass spectrometers] as well as to a certain variability of atmospheric composition near the turbopause (i.e., the top of the homosphere or turbosphere near 100 km; above this level in the heterosphere, diffusive separation becomes important). Hall et al. (1967) report on an interdiurnal variability of atmospheric composition near 200 km during daytime of less than 25% (see also Hinteregger, 1964; Champion et al., 1967; Spencer et al., 1968). According to work referenced by Champion (1968), some of this variability may be caused by two separate bulges in the thermosphere: A bulge of atomic oxygen near the equator during summer and a helium bulge at high latitudes during winter in the hemisphere opposite the sun. Agreement on atmospheric models incorporating such possibilities is still very much in flux (Newell, 1968b).

Ionized species have been measured on various occasions by mass spectrometers that were carried aloft by rockets (Narcisi and Bailey, 1965a, 1965b; Narcisi et al., 1966; see also Champion, 1968). Examples are given in Figs. 1.38 and 1.39. Ions are tentatively identified as follows: 18 H₂O⁺, 19 H₃O⁺, 24 Mg⁺, 30 NO⁺, 32 O₂⁺, 37 H₅O₂⁺, 40 Ca⁺, and 56 Fe⁺. The metallic ions are believed to have contributed significantly to the sporadic E-layer phenomenon near 87 km observed in the measurements shown in Fig. 1.38. There may have been corresponding layers of neutral metallic atoms of meteoric origin. Of interest are the ions incorporating hydrogen. They presumably

*Values in brackets without subscripts indicate chemical concentrations.

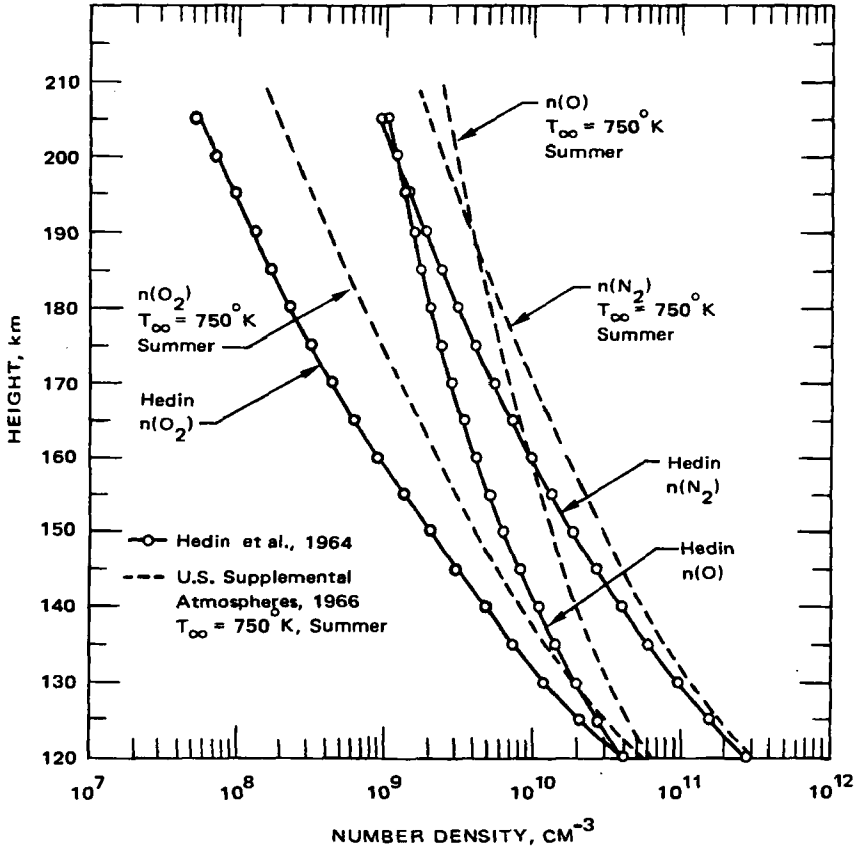


Fig. 1.37 Measured N_2 , O_2 , and O profiles at White Sands, N. Mex., compared with values from the appropriate 1966 U. S. Standard Atmosphere Supplements. [From K. S. W. Champion, *Meteorological Monographs*, 9(31): 51 (1968).]

derive from neutral water molecules transported upward through the mesosphere. This problem, which is not without controversy, will be discussed in the subsequent chapter.

From this brief discussion it becomes obvious that the chemistry and photochemistry of the upper atmosphere with all its complex diurnal, seasonal, and latitudinal variations become major factors in utilizing any of the atmospheric constituents as trace substances for estimating large- or small-scale motions at these levels. Some of the problems associated with upper atmospheric chemistry will be reemphasized in subsequent chapters.

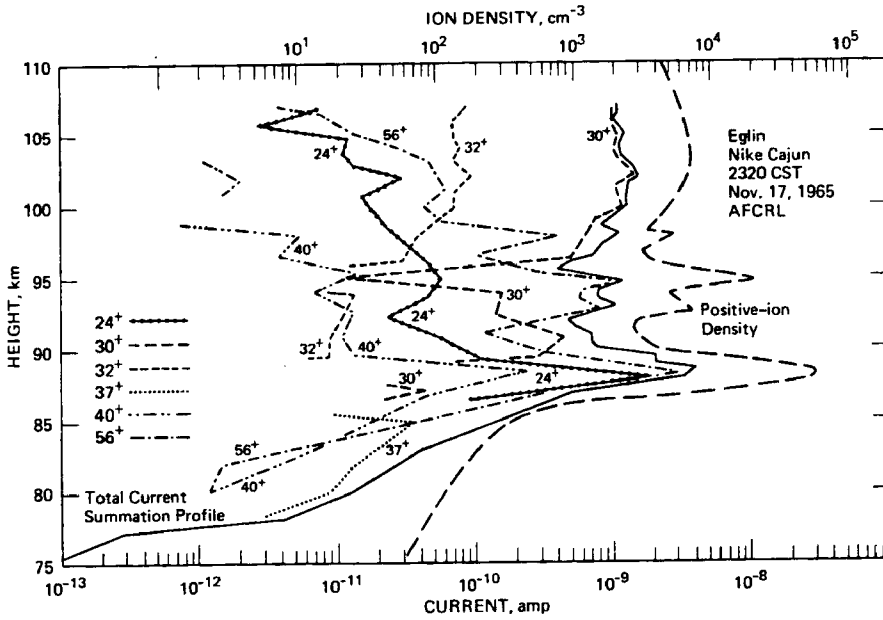


Fig. 1.38 Nighttime measurement of positive ion species in the lower E-region at Eglin Air Force Base, Fla. For further explanation see text. [From Narcisi et al, (1966).]

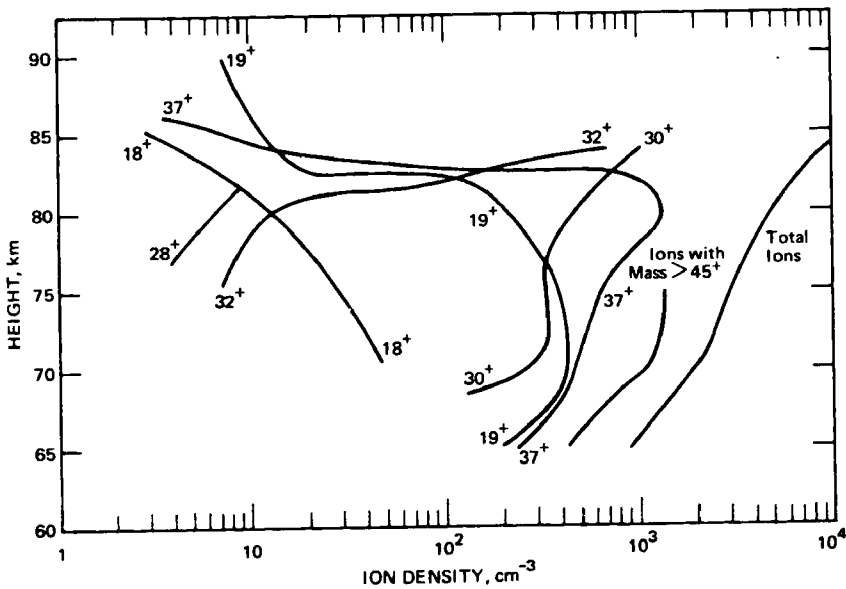


Fig. 1.39 Measurement of positive ion species in the D-region at Eglin Air Force Base, Fla. [From Narcisi (1965b).]

2 WATER VAPOR AS A TRACER

TROPOSPHERIC DISTRIBUTIONS

In Part 1, Chaps. 3 and 4, detailed accounts were given of the eddy and mean transports of water vapor. It was pointed out that, in the wave-number space of transport processes, the wave $n = 2$ plays a dominant role because of the land-sea distribution and its influence on the evaporation process. This is also evident from the vapor distribution in the lower atmosphere (Bannon and Steele, 1960). In the upper troposphere and at still higher levels, routine radiosonde data are of poor reliability in estimating water-vapor concentrations. Other measurement techniques have to be employed to arrive at reasonable estimates on $[H_2O]$.^{*} For instance, data from satellites can be used in analyzing the global distribution and the seasonal fluctuations of water vapor in the upper troposphere (Raschke, 1967; Raschke and Bandeen, 1967).

In the troposphere, with all its transient weather phenomena, water vapor may not be considered as a conservative quantity, except under very special conditions in the free atmosphere, when subsidence motions prevail in the absence of clouds. Kleinschmidt (1959) and Danielsen and E. R. Reiter (1960) have described cases of isentropic trajectory analyses in which the conservation of specific humidity was used successfully to check on the accuracy of the trajectory computations. Even in these cases it had to be pointed out, however, that the present reliability of humidity measurements obtained routinely above the middle troposphere leaves much to be

^{*}Brackets around chemical symbols denote concentrations of this compound.

desired. It is difficult, therefore, to construct topographies of constant specific humidity surfaces and trajectories of air parcels moving on such surfaces assuming that specific humidity is conserved during the flow process.

In several other case studies of air-mass transports, humidity measurements were used in a qualitative manner to establish, or to confirm, flow trajectories. Stratospheric air subsiding underneath the jet stream is characterized by excessive dryness. The distribution of "motorboating" humidity values (so called because of the low-frequency audio signal emitted by the radiosonde under very dry conditions) along such trajectories, therefore, may help to establish the extent of stratospheric air intrusions into the moist lower troposphere. An example of such a moisture analysis is given in Fig. 2.1. It shows the relative humidity distribution on the 295°K isentropic surface. The area outlined by irregular shading roughly coincides with the extent of the intrusion of radioactively contaminated stratospheric air (E. R. Reiter, 1963a, 1963b; E. R. Reiter and Mahlman, 1964a, 1964b, 1965a).

The cross section shown in Fig. 2.2 also pertains to the same case of stratospheric air intrusion. It shows an extremely dry atmospheric layer near 300°K potential temperature in the lower right corners of the diagrams. This layer has been advected from the stratosphere. It descended through the "jet-stream front" underneath the jet core and finally ended up in the lower troposphere on the south side of an extensive anticyclone.

As mentioned before, the humidity sensors used on standard radiosondes are not sensitive enough or do not have a short enough time lag to reveal the detailed moisture structure of the atmosphere. Only if the latter could be measured accurately could one use specific humidity more effectively as a tracer of atmospheric motions. In the

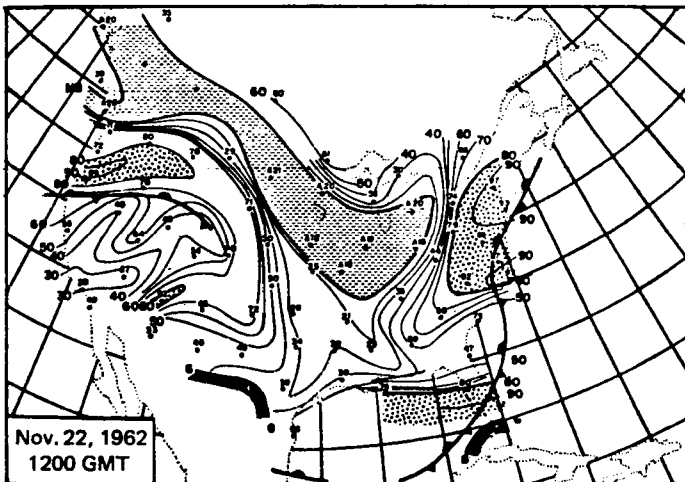


Fig. 2.1 (See page 67 for legend.)

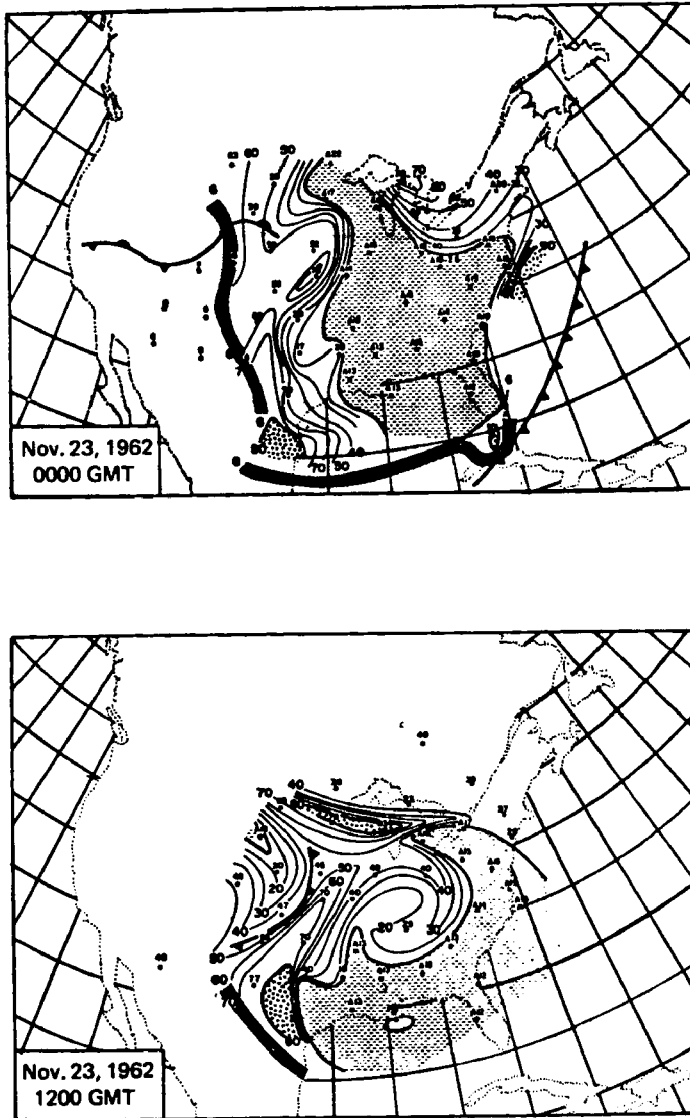


Fig. 2.1 Relative humidities (percent) on 295°K isentropic surface and for map times as indicated. Frontal systems at the earth's surface are indicated by conventional symbols. Areas with relative humidities in excess of 80% are shaded with dots; those with motorboating reports are shaded with dashes. Stations in motorboating region are prefixed by letter A and give maximum possible humidity under such conditions. Intersection of 295°K surface with ground is shown by heavy line, hatched band, and G. [From E. R. Reiter and J. D. Mahlman, *Journal of Geophysical Research*, 70(18): 4509 (1965).]

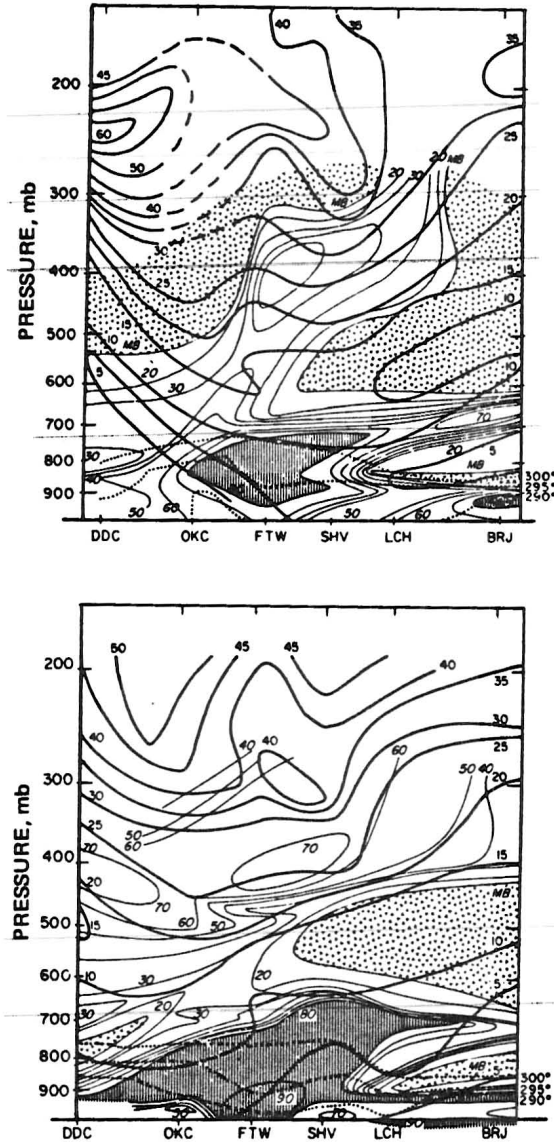


Fig. 2.2 Cross sections through the atmosphere from Dodge City (DDC), Kans., to Burrwood (BRJ), La., for Nov. 24, 1962, 0000 GMT, and Nov. 24, 1962, 1200 GMT. Heavy lines, isotachs (m/sec, vertical numbers); thin lines, relative humidities (percent, slanting numbers). Areas with motorboating reports and with humidities exceeding 80% are marked with dotted and vertical shadings, respectively. Dotted lines indicate potential temperatures of 290, 295, and 300°K. (DDC, Dodge City, Kans.; OKC, Oklahoma City, Okla.; FTW, Fort Worth, Tex.; SHV, Shreveport, La.; LCH, Lake Charles, La.; BRJ, Burrwood, La.) [From E. R. Reiter and J. D. Mahlman, *Journal of Geophysical Research*, 70(18): 4517 (1965).]

regions above the middle troposphere, radiometer measurements from satellites may eventually give the desired information (W. L. Smith, 1967).

The radio refractive index, n , or the radio refractivity, N , defined as

$$N = (n - 1) \times 10^6 \tag{2.1}$$

has been used to measure detailed moisture fluctuations and distributions (Bean, 1966; Yaglom and Tatarski, 1967; see also Bean et al., 1966; Thompson et al., 1968). Since N depends critically on the vapor pressure, e , for frequencies up to 30,000 Mc/sec, according to

$$N = 77.6 \frac{P}{T} + 3.73 \times 10^5 \frac{e}{T^2} \tag{2.2}$$

(E. K. Smith and Weintraub, 1953), discontinuities in e will lead to sharp gradients in N . Turbulent fluctuations in regions of such gradients may lead to the backscatter of radar signals (Atlas et al., 1966; Stephens and Reiter, 1966). Radar and radiowave probing of the atmosphere, therefore, may be employed successfully in revealing details of its moisture structure as long as the moisture effect in Eq. 2.2 dominates significantly over the temperature effect. This will usually be the case in the lower and middle troposphere.

An example of the use of N -measurements in tracing mesoscale atmospheric motions over mountain ranges has been given by Fukushima (1967). Airborne refractometer measurements were conducted over a mountain range between Tokyo (0 km in Fig. 2.3) and Sendai (310 km in Fig. 2.3). The mean-square values of the

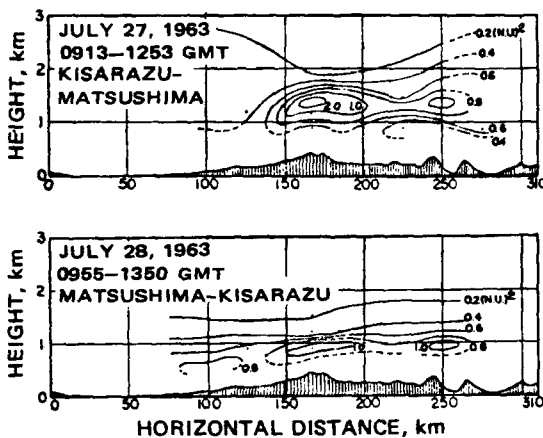


Fig. 2.3 Examples of the spatial distribution of mean-square values of deviation of refractivity, in $(N\text{-units})^2$, from mean values of N obtained along horizontal flight legs and for observation times as indicated in the diagrams (Japan standard time). [From M. Fukushima, *Journal of the Meteorological Society of Japan*, 45(4): 335 (1967).]

departures of N from the average value measured along the flight route, x , $[(N)_{(x)}^2]_{(x)}$, shown in Fig. 2.3, reveal a distinct correlation with terrain features, indicating the presence of lee waves. The pattern of vertical gradients of N , shown in Fig. 2.4, agrees well with model calculations of streamlines, thus indicating the potential use of water-vapor pressure as a tracer of mesoscale motions.

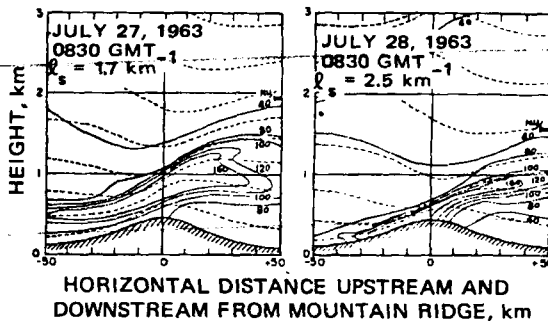


Fig. 2.4 The distribution of the vertical gradient of N (solid lines, N -units/km) and the streamlines (dashed lines) calculated for idealized models. The scorer parameters $s^2 = [g(\partial\theta/\partial z)/\theta U^2] - (1/U)(\partial^2 U/\partial z^2)$ (θ is the potential temperature and U is the wind component normal to ridge) assumed in the model calculations is given in the upper left corner of each diagram. [From M. Fukushima, *Journal of the Meteorological Society of Japan*, 45(4): 336 (1967).]

Figure 2.2 reveals several shortcomings of water vapor as a tropospheric tracer: Near the station of Shreveport (SHV), the dry and radioactively contaminated layer of stratospheric air is "punctured" by moist air that contains convective precipitation processes. Consequently considerable amounts of radioactivity were detected in rainwater samples collected from this region. If we were to trace the trajectories of air parcels moving from the dry, contaminated, stable layer into the region of moist air with convective activity, the specific humidities of such air parcels could no longer be regarded as conservative quantities. From the fact that advection takes place across the lines of constant specific humidity, s , ($ds/dt \neq 0$), E. R. Reiter and Mahlman (1965a) (see also E. R. Reiter, 1966) were able to make a rough estimate of the mixing between dry stratospheric air and moist air from the lower troposphere. Under the assumption that the increase in water-vapor mixing ratio along an air trajectory was produced by turbulent mixing of dry air having motorboating humidity values with saturated air from the Gulf of Mexico, they estimated that approximately 3 parts of radioactively contaminated air were diluted in 10 parts of moist tropospheric air.

Even in the region where no precipitation and washout processes occurred during this November 1962 case of radioactive fallout, turbulent mixing in the lowest layers of the troposphere rendered specific humidities nonconservative. Figure 2.5 shows that convective processes in the adiabatic layer produced by diurnal heating tap the dry layer of stratospheric air and thus transport radioactivity toward the ground. The low

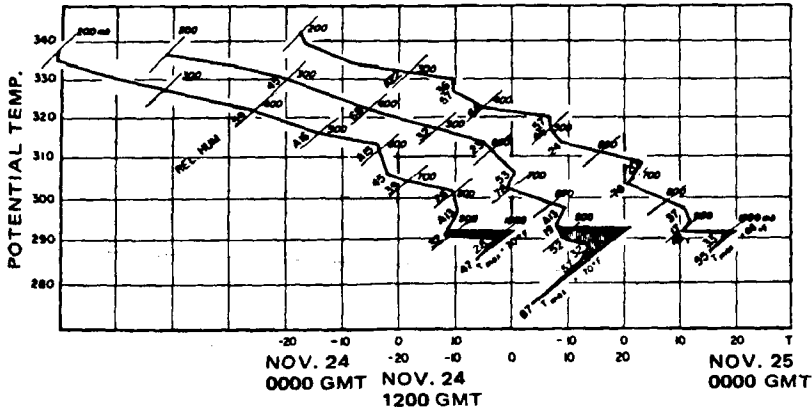


Fig. 2.5 Temperature soundings at Jackson, Miss., on Nov. 24, 1962, 0000 and 1200 GMT, and on Nov. 25, 0000 GMT, plotted on a tephigram. Soundings have been shifted by 20°C along the temperature coordinate for successive observation times. Relative humidities are plotted along soundings (maximum humidities possible with motorboating are prefixed with letter A). Standard pressure levels along sounding are indicated by short lines and are labeled with small slanting numbers. The adiabat through the observed surface-temperature maximum is assumed to determine the depth of the adiabatic mixing layer (marked by hatching). [From E. R. Reiter and J. D. Mahlman, *Journal of Geophysical Research*, 70(18): 4518 (1965a).]

specific humidities of this dry layer will be thoroughly mixed with the relatively moist air of the planetary boundary layer.

In general terms, we may state that changes of specific humidity, ds/dt , within a given volume of air are produced by turbulent mixing processes, M , across the boundary of this volume and by evaporation, E , into and precipitation, P , from the air volume (Palmén and Söderman, 1966):

$$\frac{ds}{dt} = -M + E - P \tag{2.3}$$

The specific humidity is defined as $s = \rho_w / (\rho_w + \rho_d)$, where ρ_w is the density of water vapor and ρ_d is the density of dry air. If, instead of the specific humidity, s , we consider the mixing ratio $\chi_w = \rho_w / \rho_d$, the mixing effects can be computed from Eq. 1.15, in which $c = \rho_w$. The total derivative in Eq. 2.3 then consists of the partial derivative on the left side and of the first two terms on the right side of Eq. 1.15. If we use diffusion coefficients K_{yy} , K_{zz} , and K_{yz} in Eq. 1.15 characteristic of large-scale mixing across latitude circles, the values of ds/dt thus computed will apply to large-scale aspects only.

In Eq. 2.3 E is the rate of evaporation and P is the rate of precipitation applicable to the air volume under consideration. Both parameters have to be expressed in units of grams of H_2O per gram of dry air per unit of time, dt . For known

sources of evaporating water (e.g., a lake in a desert environment), Eq. 2.3 could be used to estimate mixing processes by treating H_2O as a trace substance (Dittmann, 1966).

In the free atmosphere E reduces to the effect of evaporation from precipitation falling through the air parcel under consideration and P constitutes precipitation forming, or growing, within the volume under consideration. In the absence of such processes, i.e., in the absence of clouds, E and P will vanish, and s or χ_w will be controlled entirely by the transport processes described in Eq. 1.15.

The volume over which the moisture change is computed may be considered to extend throughout the vertical extent of the atmosphere. Then s denotes the vector transport of specific humidity

$$s(\lambda, \phi, t) = \frac{1}{g} \int_0^{p_0} s \, v \, dp \quad (2.4)$$

whose time-averaged divergence relates to evaporation and precipitation as follows:

$$\nabla \cdot [s]_{(t)} = \frac{1}{R \cos \phi} \left[\frac{\partial [s_\lambda]_{(t)}}{\partial \lambda} + \frac{\partial ([s_\phi]_{(t)} \cos \phi)}{\partial \phi} \right] = [E - P]_{(t)} \quad (2.5)$$

assuming that

$$\int_0^{p_0} \left[\frac{\partial s}{\partial t} \right]_{(t)} dp = 0$$

Subscripts λ and ϕ without parentheses indicate longitudinal and latitudinal components of the transport vector s , respectively. The symbolism of averaging has been explained in Part 1. Estimates of $\nabla \cdot [s]_{(t)}$ have been made by V. P. Starr and Peixoto (1958) and V. P. Starr et al. (1965). Mean and eddy fluxes have been considered in Part 1 (see also Drozdov and Grigor'eva, 1965).

Vertically integrated moisture conditions above the 500-mb level have been estimated from satellite data (Raschke and Bandeen, 1967). Results are shown in Fig. 2.6. Even though clouds are present in some of the regions considered in this latitude-time section, the characteristic moisture distribution is mainly affected by vertical and horizontal transport processes. The convective upward transport in tropical regions and in temperate latitudes during the summer of the northern hemisphere is well documented by this diagram. Transport processes during this season are strongly influenced by the summer monsoon over Asia, as can be seen, for instance, from data on precipitable water (Tuller, 1968).

WATER VAPOR IN THE STRATOSPHERE

For general conditions in the stratosphere, we may neglect E and P safely in Eq. 2.3. In still higher regions of the atmosphere, there may be several effects

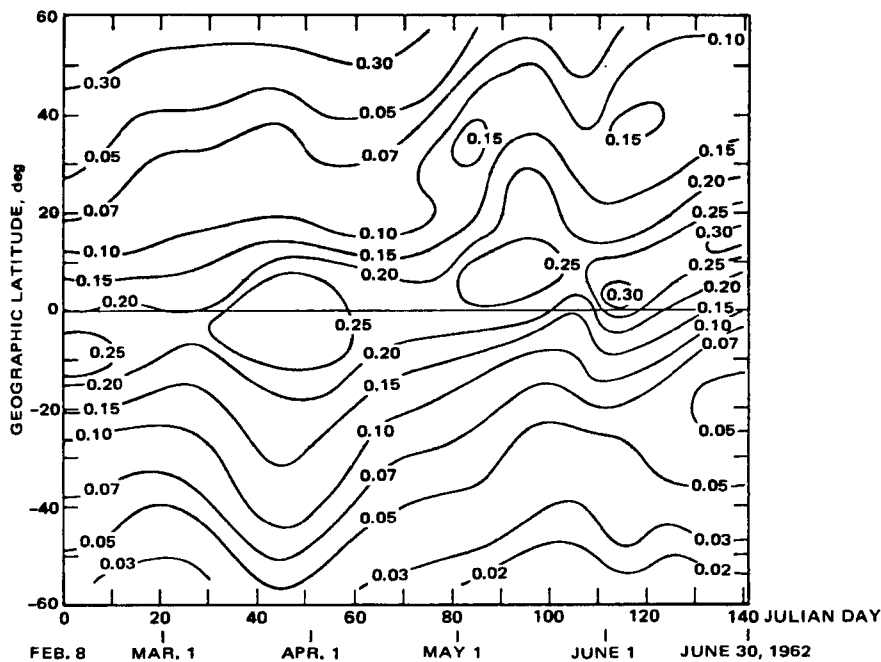


Fig. 2.6 Zonal averages of the water-vapor mass in g/cm^2 above 500 mb inferred from coordinated TIROS IV radiometric measurements. These averages were determined for 10-day periods within zones of approximately 5° of latitude. [From E. Raschke and W. R. Bandeen, *Journal of Applied Meteorology*, 6(3): 480 (1967).]

endangering this assumption; however, none of these are well known at this time: (1) Condensation products may form at the levels of mother-of-pearl clouds and of noctilucent clouds and fall into adjacent layers, thereby slightly changing the water-vapor mixing ratio; (2) vaporization of meteors may introduce small amounts of H_2O ; and (3) space vehicles traversing these regions of the atmosphere may, among other chemical compounds, introduce large amounts of H_2O as a form of man-made “air pollution” (Manabe, 1967; Manabe and Wetherald, 1967).

The last effect may become quite pronounced even in the stratosphere should supersonic transport flights be conducted in large numbers. The effects of such man-made air pollution on the atmospheric radiation budget might reach proportions that may no longer be neglected. A “moist” stratosphere of 5% relative humidity would show a radiation budget quite different from the one of a “dry” stratosphere (Jurica, 1966). In theoretical model computations, Manabe and Wetherald (1967) have estimated the effect of different stratospheric moisture contents at a constant mixing ratio [3×10^{-6} g/g, suggested by Mastenbrook (1963b) and J. T. Houghton (1963); 15×10^{-6} g/g and 75×10^{-6} g/g conforming to “moist” conditions]. The resulting equilibrium temperatures are shown in Fig. 2.7. Increasing stratospheric moisture

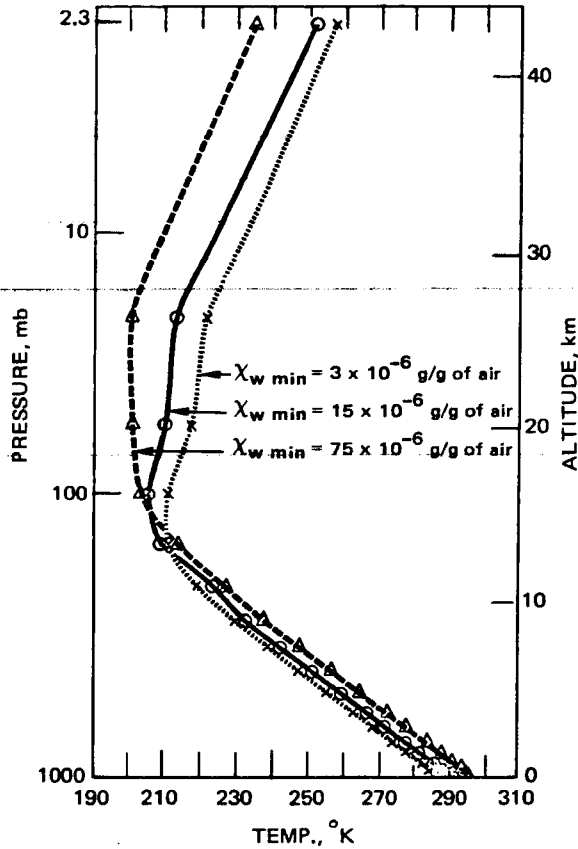


Fig. 2.7 Vertical distributions of radiative convective equilibrium temperature for various values of water-vapor mixing ratio (x_w) in the stratosphere. [From S. Manabe and R. T. Wetherald, *Journal of the Atmospheric Sciences*, 24(3): 248 (1967).]

content will lead to a cooling above 100 mb and to a warming of the troposphere, the former effect being much larger than the latter. The presence of H_2O at mesopause level will also influence the CO_2 heating rate (J. T. Houghton, 1969).

If air traffic is conducted along certain routes and within preferred layers of the stratosphere, H_2O will not be uniformly distributed but will have source regions along such traffic corridors. This will complicate matters to a certain extent. It would be of great practical interest, however, to estimate the effects of a "layered" H_2O distribution, allowing for the diffusion rates estimated by other investigators, such as Reed and German (1965).

Not taking into account the preceding problems, Brewer's (1949) assumption of a dry stratosphere appears reasonable, especially in view of the mean circulation patterns postulated in Fig. 1.16. According to these diagrams and according to

Brewer's reasoning, air ascending in equatorial regions would lose H_2O vapor when passing through the "cold trap" of the equatorial tropopause region. Radiational heating of this ascending air would partly compensate for the dynamic cooling. The reverse holds for higher latitudes where sinking motions and dynamic warming (partly compensated by radiational cooling) remove the air from the saturation point and thus make extremely dry conditions in the stratosphere very plausible. Such a circulation would also account for the observed high ozone concentrations in the Arctic spring (Dobson, Harrison, and Lawrence, 1929; Dobson, 1956). From the nearly homogeneous distribution of helium measured in the stratosphere, Brewer (1949) concluded that considerable turbulent mixing is associated with this meridional circulation. Thus in his model turbulence accounts for the thoroughly mixed helium distribution (the same should also hold for other conservative trace substances that do not have sources or sinks in the stratosphere, such as CO_2) whereas the dynamics of the large-scale circulation are responsible for the observed water-vapor distribution.

The rather general conclusions by Brewer may need some refinements in light of recent investigations. First, it was shown in Part 1, Fig. 3.11, that mean ascending motions are found in the winter stratosphere over the pole, where tropopause temperatures are considerably higher than over the equator (see also Vincent, 1968). Therefore a not yet determined amount of water vapor—higher than that allowed for by the Brewer–Dobson model—may seep into the stratosphere after all. Second, eddy-transport processes, in conjunction with pronounced polar-front or subtropical jet maxima, may cause considerable inflow of (moist) tropospheric air into the stratosphere in the vicinity of these jet streams. It has been demonstrated by E. R. Reiter et al. (1967) that such flow processes seem to take place above the isentropic level of the jet core ($\theta > 330^\circ K$ in the case of the polar-front jet) and ahead of the jet maximum. According to R. M. Smith (1968), such intrusions of tropospheric air—in conjunction with ascending stratospheric air motions in high latitudes—might constitute an efficient mechanism of moisture influx into the stratosphere. Such a moisture flux may also have a significant effect on the tritium balance of the stratosphere. Figure 2.8 indicates that return flow of water vapor and of tritium from the troposphere into the stratosphere is well correlated with the jet-stream position, as suggested by E. R. Reiter et al. (1967). Direct and accurate moisture measurements at stratospheric levels will shed further light on such a moisture flux.

A number of such measurements are available. Kitaoka (1963) published results of frost-point measurements over Japan (Fig. 2.9). Mixing ratios in the lower stratosphere appeared to be higher during winter and spring than during summer and autumn. Over Japan this seasonal variation amounted to almost one order of magnitude above 20 km. No significant seasonal variations of humidity have been found over England up to 50,000 ft, where generally dry conditions (2×10^{-6} mixing ratio) prevail (Bannon et al., 1952; Murgatroyd et al., 1955; Helliwell et al., 1957). Figure 2.9 also reveals a lack of seasonal variation below approximately 16 km. The moisture content, however, is considerably higher in the Japanese measurements.

Figure 2.9 shows that the mixing ratio increases with heights above 18 to 20 km (Barclay et al., 1960; Laboratory of Astrophysics and Physical Meteorology, 1960;

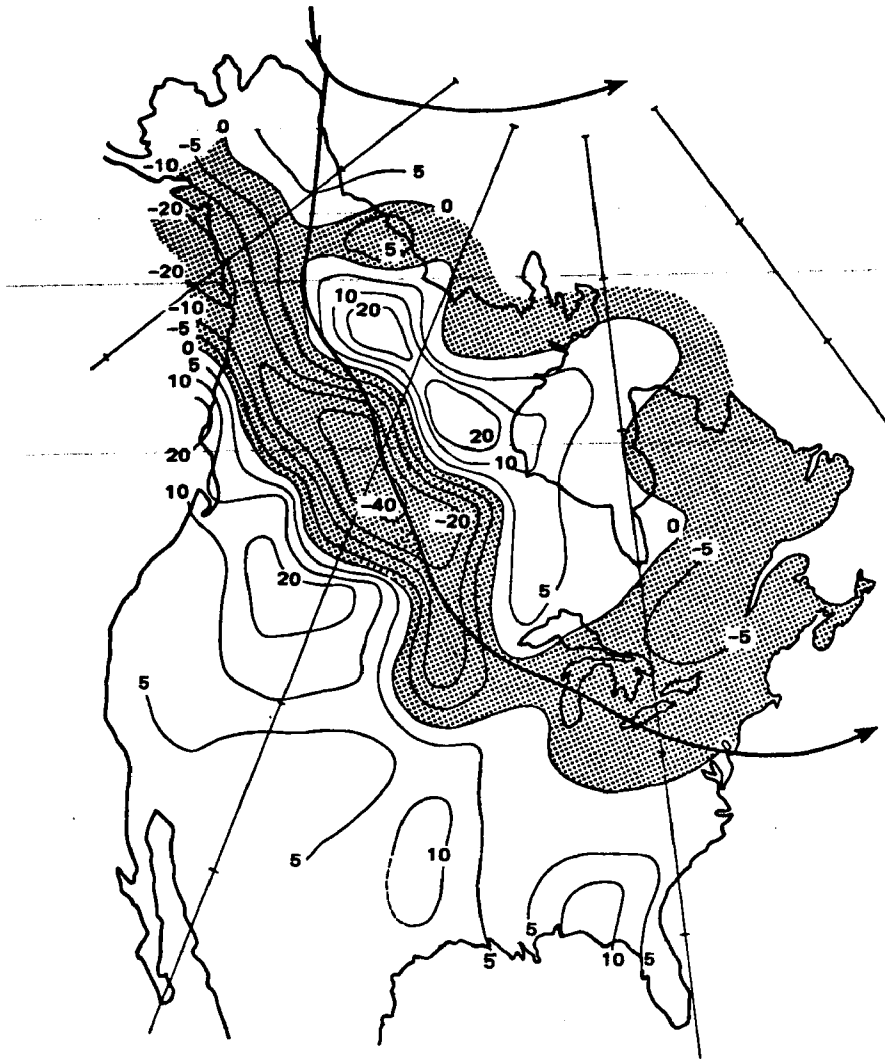


Fig. 2.8 Mean transport of tritium through the tropopause in July 1962 at 0000 GMT. Units in $10^3 \text{ TU} \cdot \text{cm}$. Dotted regions indicate ascending (negative) motions. Long thick arrows denote mean positions of jet axes. [From R. M. Smith, *Tellus*, 20(1): 78 (1968).]

Mastenbrook and Dinger, 1960, 1961; Murcray et al., 1960; F. Brown et al., 1961; Gutnick, 1961; Junge, 1962c; Murcray et al., 1966; Webb, 1966a; for a review, see Junge, 1963a). According to data compiled by Gutnick (1962), which agree well with those given by Kitaoka (1963), the average mixing ratio at 30 km appears to be $1.5 \times 10^{-4} \text{ g/g}$, or 0.15 g/kg. This is considerably higher than median values obtained by Mastenbrook (1968). Mother-of-pearl clouds, or nacreous clouds, observed

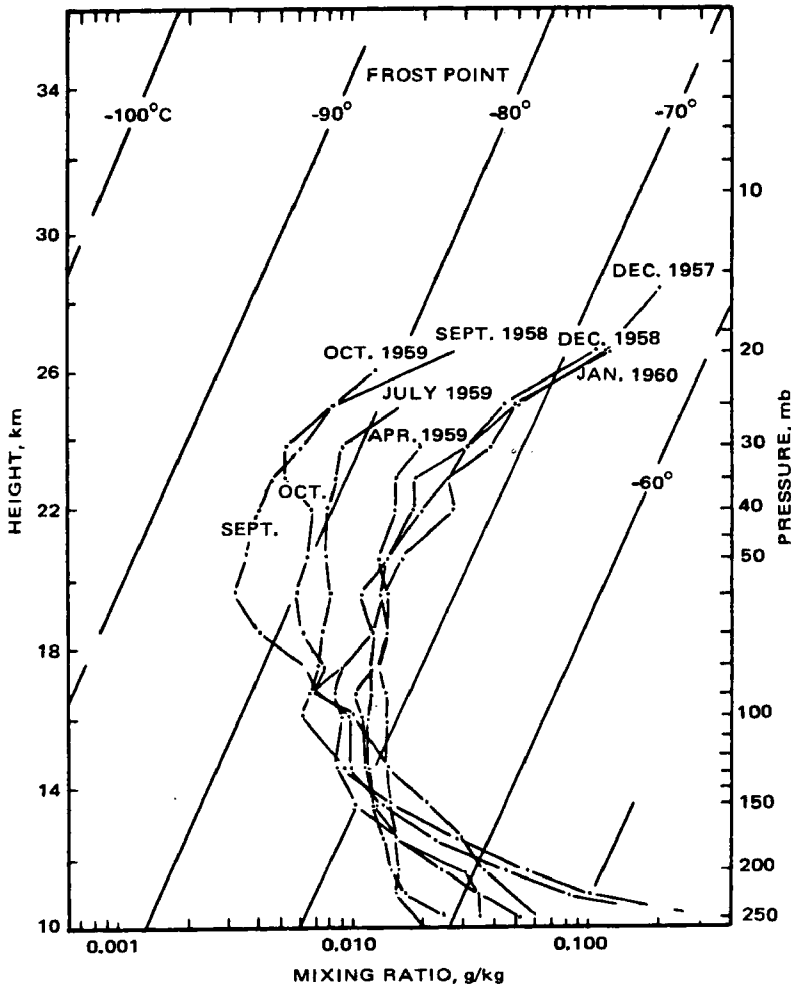


Fig. 2.9 Vertical distribution of mixing ratio at Tateno, Japan. [From T. Kitaoka, *Meteorologische Abhandlungen*, 36: 128 (1963).]

occasionally near levels of 25 km would indicate the presence of moisture in the middle stratosphere (Størmer, 1940; Hesstvedt, 1959, 1969b). Temperatures of -88°C at 25 km would produce saturation with respect to ice. These clouds usually have a lenticular shape and are in all likelihood produced by orographic lee waves. Sufficiently low temperatures may be achieved by adiabatic cooling in the rising branch of the wave motion. In spite of such cloud observations, the high mixing ratios reported by Gutnick have to be viewed with suspicion. Contamination of the atmosphere by the ascending balloon may be a major cause of erroneous measurements, as will be described. Earlier measurements by Barrett et al. (1950) appear to

agree with data shown in Fig. 2.9 as far as the relatively moist middle stratosphere (near 26 km) is concerned. Barrett's data, however, showed an almost equally large amount of water vapor in the lower stratosphere. This has not been borne out by the investigations cited previously.

Mastenbrook's (1963a) and Goldsmith's (1964) measurements also reveal no increase in the mixing ratio with height. Their data lie close to a constant value of 1.8×10^{-6} g/g, indicating considerably dryer conditions than those evident from the preceding measurements. The balloon flights analyzed by Mastenbrook and Dinger (1961) show the usual increase of mixing ratio with height except for one occasion over Denver (Apr. 28, 1959) when the mixing ratio remained nearly constant (3×10^{-5} g/g) above the tropopause. Measurements by Williamson and Houghton (1965) over England indicate mixing ratios of 3×10^{-6} g/g to prevail at least to 25 km (about 20 mb).

Spectrum measurements by J. T. Houghton (1963) would fit either a uniform mixing ratio above the 150-mb level of approximately 2.5×10^{-6} g/g or a "dry" lower stratosphere (about 1.5×10^{-6} g/g) and a "wet" upper stratosphere (up to 5×10^{-5} g/g) above 25 mb. The latter values still are considerably dryer than those obtained from most of the older balloon measurements; thus the accuracy of these earlier direct-measurement techniques appears questionable. Spectrometer flights over Russia (Neporent et al., 1968) also indicate dry stratospheric conditions (12×10^{-6} g/g at 11 km, 2.5×10^{-6} g/g at 17 km, and constant thereafter; at $z > 25.3$ km, the mean mixing ratio was 4×10^{-6} g/g). Murcay et al. (1969) report water-vapor mixing ratios of 2.5×10^{-6} to 3.0×10^{-6} g/g in the region from 25 to 30 km. These data were obtained over New Mexico with a balloon-borne spectrometer. Far infrared measurements by aircraft in temperate latitudes (California) yielded similar magnitudes of water vapor above 12 km. Large variations were encountered, however, on different flights (Eddy et al., 1969).

Recent studies by Mastenbrook (1966, 1968) also cast some doubt on earlier measurements that show relatively moist conditions in the upper stratosphere, such as those reported by Kitaoka (1963). Figure 2.10 indicates some of the instrumental difficulties encountered with frost-point hygrometers carried aloft by balloons. Contamination of the air by the ascending balloon (Brousailles and Morrissey, 1967; Zander and Bottema, 1967) may lead to high frost-point temperature readings during the ascent and to considerably lower moisture values during the descending phase of the measurements (see also Sissenwine et al., 1968a, 1968b). The ascent curve shown in Fig. 2.10 would, for instance, indicate an increase of water-vapor mixing ratio with height above the 100-mb level (see Fig. 2.9). The curve obtained from the descent measurements, on the other hand, indicates mixing ratios that are almost constant with height. Figure 2.11 summarizes measurements over Washington, D. C., and Trinidad, West Indies. From these data it appears that the most frequent conditions encountered over the two stations conform to nearly constant water-vapor mixing ratios above 100 mb of the order of 2 to 3×10^{-6} g/g. On occasion conditions are encountered, however, in which mixing ratios increase with height, especially above the 30-mb level. The fairly uniform moisture conditions between the 100- and 40-mb

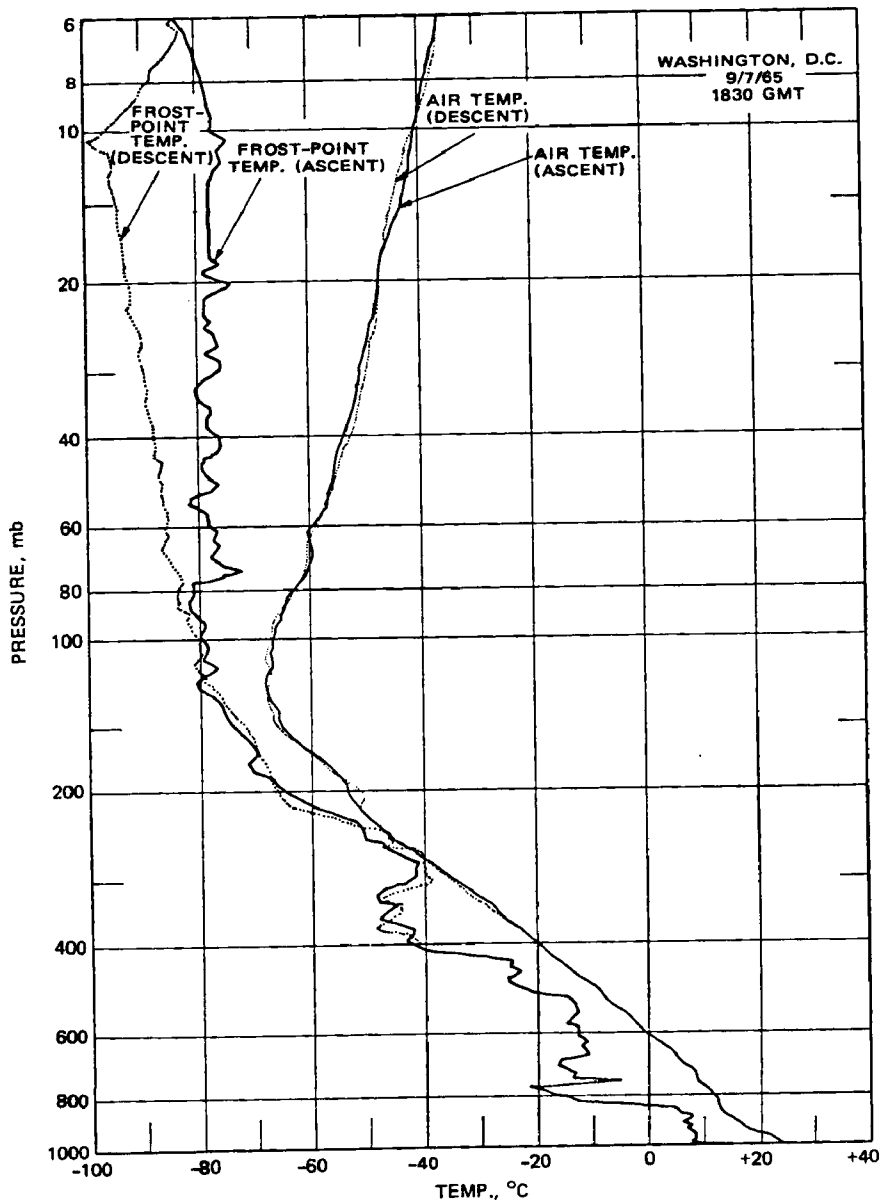


Fig. 2.10 A typical ascent-descent water-vapor sounding. The descent after turnaround adjustment is taken as the measure of stratospheric moisture. [From H. J. Mastenbrook, *Journal of the Atmospheric Sciences*, 25(2): 302 (1968).]

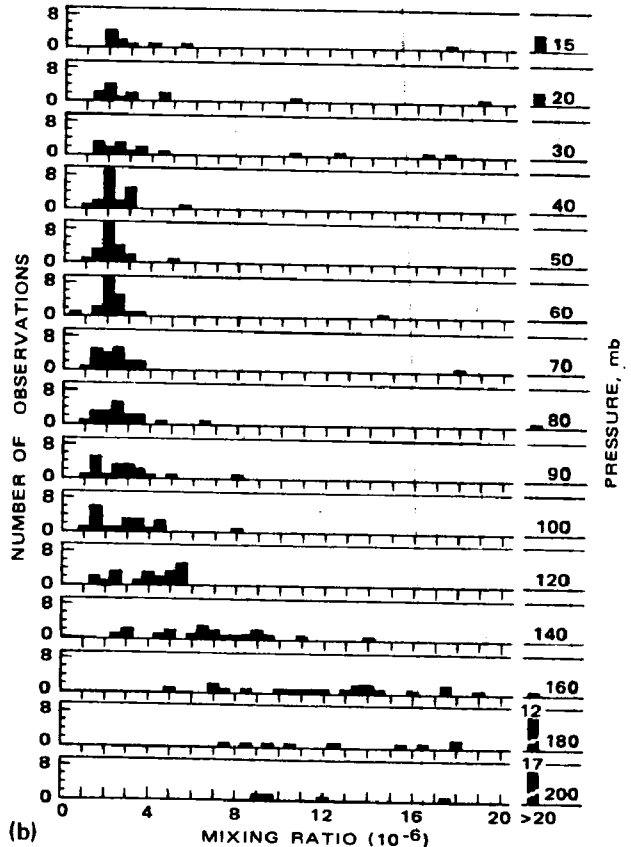
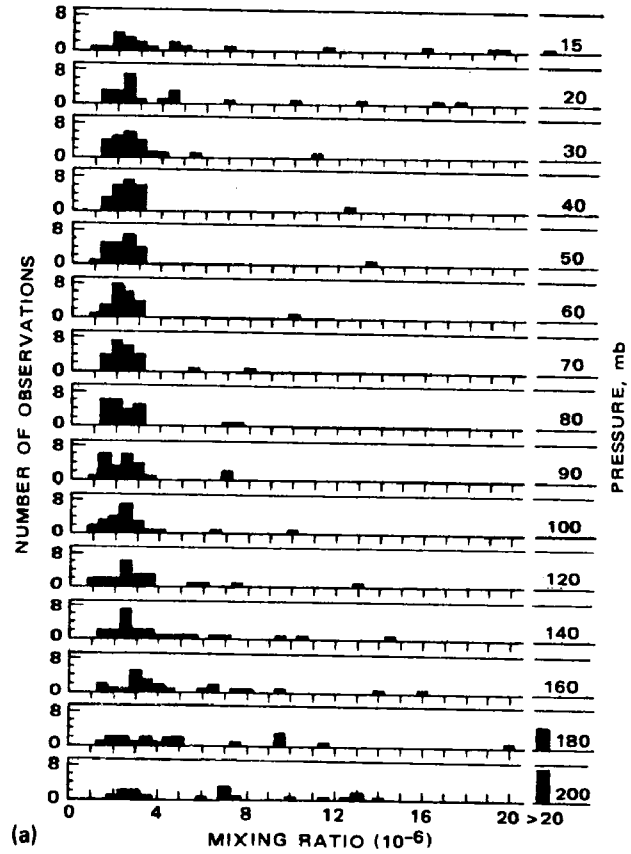


Fig. 2.11 Frequency distribution of mixing ratio for selected pressure levels over (a) Washington, D. C., and (b) over Trinidad, West Indies, for the years 1964 and 1965. [From H. J. Mastenbrook, *Journal of the Atmospheric Sciences*, 25(2): 303 (1968).]

levels are also reflected from a tabulation of median values of mixing ratios (Table 2.1). The moist conditions of the low stratosphere and the decreasing moisture values between 200 and 100 mb encountered over Washington, D. C., and Trinidad, West Indies, conform to earlier measurements by Gutnick (1962), Kitaoka (1963), and other investigators. The much dryer conditions in the upper stratosphere encountered by Mastenbrook (1968) are ascribed by him to the extra care taken against contamination of the atmosphere by degassing of the ascending balloon.

Table 2.1
MEDIAN DISTRIBUTION OF MIXING RATIO
FOR THE STRATOSPHERE AND HIGH TROPOSPHERE DURING 1964
AND 1965 AT WASHINGTON, D. C., AND TRINIDAD, WEST INDIES*

Level, mb	Median mixing ratio (10^{-6} g/g)†		
	Washington, D. C.	Trinidad, W. I.	Both
15	3.0(21)	3.3(14)	3.2(35)
20	2.6(23)	3.0(16)	2.7(39)
25	2.5(23)	2.8(16)	2.6(39)
30	2.5(23)	2.8(16)	2.6(39)
40	2.4(23)	2.1(20)	2.3(43)
50	2.3(23)	2.1(20)	2.2(43)
60	2.2(23)	2.1(20)	2.2(43)
70	2.3(23)	2.3(20)	2.3(43)
80	2.2(23)	2.5(19)	2.4(42)
90	2.4(23)	2.6(18)	2.4(41)
100	2.4(23)	2.8(19)	2.5(42)
120	2.7(22)	4.3(20)	3.2(42)
140	3.1(25)	6.8(20)	5.1(43)
160	3.7(23)	13.0(21)	8.0(45)
180	5.0(24)	24.0(21)	11.0(45)
200	11.5(25)	33.0(21)	24.2(46)

*From H. J. Mastenbrook, *Journal of the Atmospheric Sciences*, 25(2): 304 (1968).

†Number of cases in parentheses.

Sissenwine et al. (1968a) found similar low-humidity values between approximately 12 and 20 km over Chico, Calif. Near 25 km, however, a secondary maximum of mixing ratios is encountered with values near 17×10^{-6} g/g (Table 2.2 and Fig. 2.12). Again the observation of nacreous clouds (mother-of-pearl clouds) between 20 and 30 km would agree with a moisture maximum at such levels. Sissenwine et al. (1968a) quote Captain Joseph W. Kittenger, a U. S. Air Force parachutist, who, after jumping from a balloon-borne gondola at 102,800 ft, stated: "I am making an exciting discovery. There are clouds at my altitude. They are so thin I see them only when my vision comes within 30° of the sun, but they reflect the sun with dazzling whiteness."

Table 2.2
BASIS FOR OBTAINING MEAN MIXING RATIOS
ABOVE 34 MB AT CHICO, CALIFORNIA*

Layer, mb	Weighting factor	Mean mixing ratio for Chico extension, ppm
34 to 25	9	13.0
25 to 15	10	17.0
15 to 10	5	17.0
10 to 6	4	15.5
6 to 3	3	14.0
3 to 1	2	10.4
1 to 0.5	0.5	6.8
0.5 to 0.01	0.5	1.8

*From N. Sissenwine, D. D. Grantham, and H. A. Salmela,
Journal of the Atmospheric Sciences, 25(6): 1138 (1968).

Mastenbrook's (1968) measurements also reveal a seasonal trend of stratospheric moisture: Lowest mixing ratios are encountered in the lower stratosphere during late winter [during spring, according to Sissenwine et al. (1968a, 1968b)] and highest mixing ratios during late summer over both stations, Washington, D. C., and Trinidad, West Indies. The amplitude of the seasonal trend, according to Sissenwine et al., decreases with altitude in the middle stratosphere. This seasonal trend is consistent with the removal of water vapor by the cold region near the tropical tropopause. Figure 2.13 shows that the tropical tropopause tends to lie relatively high and is found at low temperatures during winter, whereas summer conditions are characterized by higher tropopause temperatures that permit higher saturation mixing ratios. This seasonal trend is confirmed by estimates made by Calfee and Gates (1966) over Florida using spectrographic absorption measurements from aircraft. In the lower stratosphere average mixing ratios of 3.2×10^{-6} g/g were obtained during summer and 2.4×10^{-6} g/g during winter.

The seasonal variation of moisture conditions near the level of the tropical tropopause described causes a seasonal reversal of the vertical gradient of mixing ratios over both Washington, D. C., and Trinidad, West Indies. The gradient, $-(\partial s/\partial z)$, is directed downward during late winter and upward during late summer in the layer 90 to 50 mb.

The greater care exercised in the measurements reported by Mastenbrook as well as apparent control of mid-stratospheric moisture conditions by the temperature characteristics of the tropical tropopause lend far more credence to these data and the seasonal trends derived therefrom than to those reported by earlier investigators. We may conclude, therefore, that the eddy motions near 20 km (or 50 mb) exercise a dominant influence upon the establishment of a dry middle stratosphere. The same motions are responsible for exporting ozone-rich air from low to high latitudes,

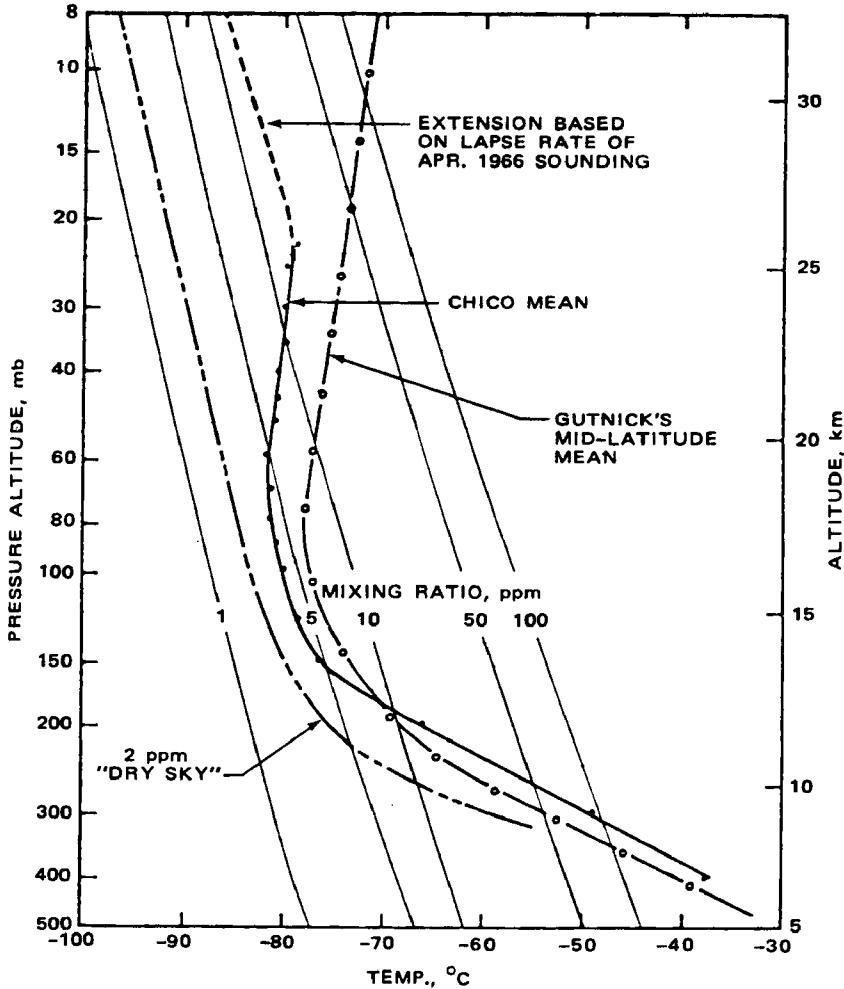


Fig. 2.12 Comparison of frost-point profiles between measurements over Chico, Calif., “dry” measurements over England, and the probably erroneous “moist” results obtained by Gutnick. [From N. Sissenwine, D. D. Grantham, and H. A. Salmela, *Journal of the Atmospheric Sciences*, 25(6): 1138 (1968).]

especially during late winter, as will be shown in a later chapter. Variability of water-vapor mixing ratios in the lower stratosphere over one order of magnitude may also be indicative of eddy processes (Sissenwine et al., 1968a).

Figure 2.14 shows measurements of stratospheric water-vapor mixing ratios over Thule, Greenland, during the summer of 1965. The distribution is essentially the same as that reported earlier for Washington, D. C., and Trinidad, West Indies. This suggests that the latitudinal variations of moisture in the stratosphere are very small, a fact that

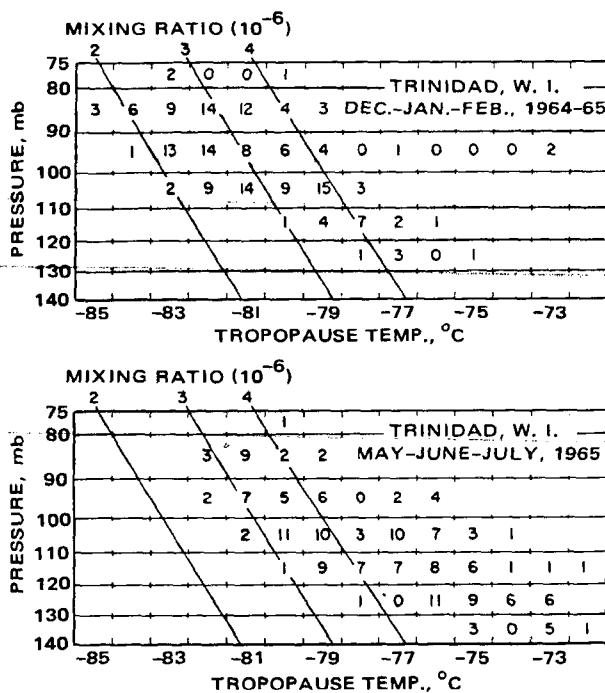


Fig. 2.13 The distribution of tropopause temperature and pressure at Trinidad, West Indies, for three months in winter and three months in summer. Numbers indicate the frequency of tropopause occurrence within the given temperature and pressure intervals. Sloping lines are lines of constant-saturation mixing ratio. [From H. J. Mastenbrook, *Journal of the Atmospheric Sciences*, 25(2): 306 (1968).]

also contradicts earlier measurements by Kitaoka (1963) over Japan. More measurements, possibly by satellite (Bolle, 1965), may make it possible, eventually, to estimate latitudinal variations of stratospheric moisture more accurately. The relatively high low-stratospheric moisture values over Thule may be brought about by the influx of tropospheric air into the stratosphere in the jet-stream region, as suggested earlier. Reliable winter measurements of H_2O are not yet available in the polar stratosphere. Such measurements would allow one to check the effect of ascending motions in the winter stratosphere over the north polar regions on water-vapor transport processes.

Sissenwine et al. (1968a) also suggest that the influx of tropospheric air into the stratosphere by large-scale eddy processes near the jet stream is one process by which the mid-stratospheric water-vapor content can be enriched. Another process, by which H_2O can be transported into the 20-km region, may be sought in high-reaching thunderstorms of continental mid-latitudes during summer. Cloud tops of 22 km have been observed by radar and aircraft (Long, 1966; Grantham and Kantor, 1967). Haze layers at heights ≤ 50 km above tropical storms observed from the Gemini V flight

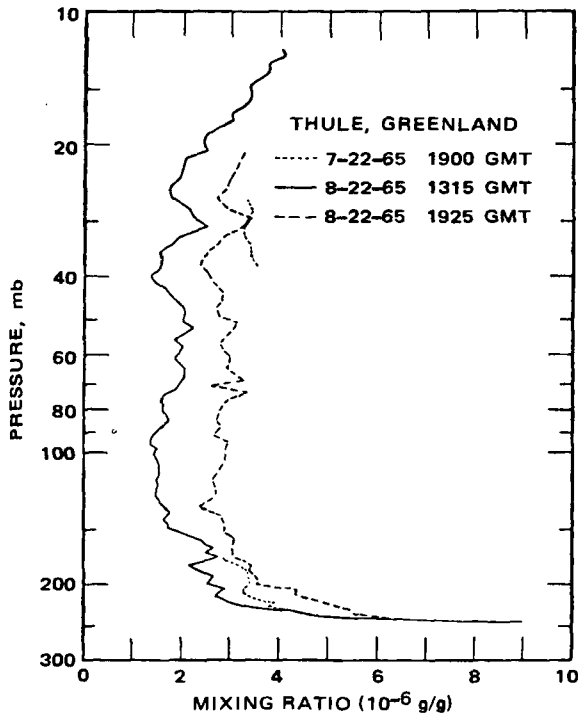


Fig. 2.14 Stratospheric mixing-ratio distributions over Thule, Greenland, during the summer of 1965. [From H. J. Mastenbrook, *Journal of the Atmospheric Sciences*, 25(2): 310 (1968).]

suggest that the upward motion in the stratosphere above such storms may also have an effect on the eddy water-vapor transport (Remsberg and Weinman, 1969).

In the foregoing discussion it has been assumed that the only source for stratospheric and mesospheric H_2O lies at the earth's surface and in the evaporation processes acting there. Methane, CH_4 , which has been identified as a trace constituent of the atmosphere (see Chap. 6), might conceivably oxidize under the presence of atomic oxygen, and water molecules may be generated in the process (Dilleuth, Skidmore, and Schubert, 1960). Such a source of moisture might possibly contribute to the slight increase of mixing ratios above 40 mb suggested by data by Mastenbrook (1968) over Washington, D.C., Trinidad, West Indies, and Thule, Greenland (Figs. 2.11 and 2.14) and by Sissenwine et al. (1968a) over California (Fig. 2.12). Kyle et al. (1969), however, found, from spectrometric measurements, that the main decrease in CH_4 concentrations occurs in the height layer between 13 and 20 km, i.e., in the lower stratosphere. These observations are in disagreement with the "methane-burning" hypothesis because the oxidation of CH_4 would occur in the driest region of the stratosphere.

With a new rocket sampling technique, Martell (oral communication) measured mean water-vapor concentrations of 32.2×10^{-6} g/g in the stratopause region. (This

value may still be subject to a 5 to 10% correction.) Both stratospheric and mesospheric air were contained in this sample. Assuming only stratospheric conditions as in Mastenbrook's measurement, as much as 60×10^{-6} g/g of water-vapor mixing ratio may prevail in the stratosphere. These high values of humidity are probably in error. They could not be produced by oxidation of methane. A quantity of 2.4 ppm of methane, measured in the lower troposphere (see Chap. 6), would produce an increase of 2.4 ppm of CO_2 and 4.8 ppm of H_2O . This CO_2 increase is within the range of measurements reported by Martell. However, 4.8 ppm of H_2O will contribute only $(4.8 \times 18/29) \times 10^{-6} = 3.0 \times 10^{-6}$ g/g of mixing-ratio increase. Whereas this increase is in line with Mastenbrook's measurements (see Fig. 2.14), it is less than was postulated by Sissenwine (see Fig. 2.12) and certainly not enough to account for the moist conditions indicated by Martell. Should the latter be verified by additional measurements, one will have to look for additional sources of moisture in the upper stratosphere and in the mesosphere, brought there, possibly by large-scale eddy-exchange processes.

WATER VAPOR IN THE MESOSPHERE

In the upper stratosphere and in the mesosphere, information on water-vapor concentrations is very sparse indeed. One would imagine that, in the absence of sources of H_2O other than methane, the increase of mixing ratio with height, shown, for instance, in the Chico measurements (Fig. 2.12), should level off somewhere in the middle stratosphere. If we assume that the mean mixing ratio of 1.5×10^{-4} g/g, found by Gutnick (1962), prevails throughout the upper stratosphere and mesosphere, a "moist" model of the upper atmosphere results. Values of 1.8×10^{-6} g/g, measured by Mastenbrook (1963a) and Goldsmith (1964), would yield a "dry" model. Sissenwine, Grantham, and Salmela (1968b) proposed the humidity model shown in Fig. 2.15. This model is based on the humidity atlas by Gringorten et al. (1966), on the Chico measurements described in the preceding section, and on noctilucent-cloud observations. According to Fig. 2.15, the mixing ratio is envisioned to decrease from about 25 km to the mesopause, the mean value coming close to the "dry" values of 1.8×10^{-6} g/g. If methane is assumed to be a significant source of H_2O in the middle stratosphere, a photochemical sink in the mesosphere could explain the decrease in the mixing ratio of H_2O with altitude.

Turbulent mixing and large-scale transport processes are expected to exercise a strong influence on H_2O distribution in the mesosphere. Hesstvedt (1967a, 1969c) assumes vertical eddy diffusion coefficients ranging from 5×10^5 cm^2/sec at 65 km to 3×10^6 and even 7×10^6 cm^2/sec at 100 km. These values are considerably higher than those given in Table 1.1 for the lower and middle stratosphere where stable lapse rates prevail for K_{zz} . Vertical turbulent exchange of moisture, therefore, should be appreciable in the mesosphere and will cause an abundance of H_2O vapor at mesopause levels and above (Hesstvedt, 1967b, 1968a, 1968b). Hesstvedt also assumes horizontal moisture gradients to be small. (Actual estimates of such gradients are not

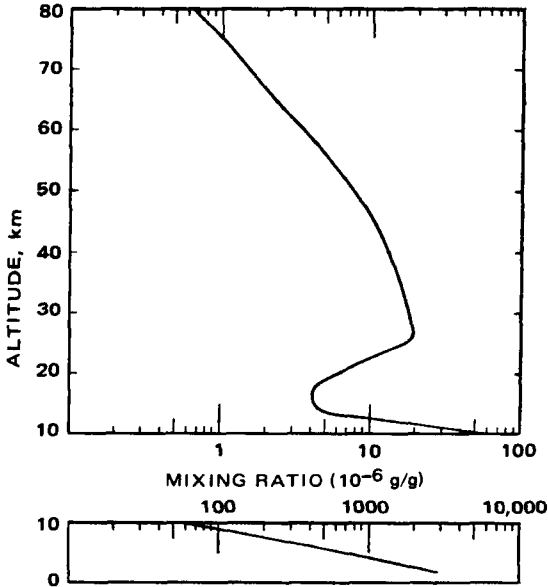


Fig. 2.15 Model of mid-latitude mean annual mixing ratio for H₂O. [From N. Sissenwine, D. D. Grantham, and H. A. Salmela (1968b).]

available.) Therefore horizontal transport processes should be of little consequence on the overall mesospheric moisture distribution. Whether or not Hesstvedt's assumption is justified has yet to be proved. The study by R. J. Reed and German (1965) revealed that large-scale horizontal eddy diffusion coefficients in the stratosphere are several orders of magnitude larger than vertical ones (Table 1.1). Even though with the lesser degree of thermal stability prevailing in the mesosphere the differences in magnitude between K_{yy} , K_{yz} , and K_{zz} will be considerably smaller there than in the stratosphere, horizontal gradients and transport processes of moisture may turn out not to be negligible.

The distribution of H₂O in the mesosphere depends not only on vertical and horizontal transports but also on photochemical processes. According to Hesstvedt (1965a, 1967a), H₂O is the most important hydrogen component up to 75 km. Above this level H₂O predominates under the assumption of "moist" conditions (1.5×10^{-4} g/g mixing ratio of water vapor), which are too moist according to Mastenbrook (1968) and Sissenwine et al. (1968a). Dissociated H becomes the main hydrogen constituent above 85 km (Fig. 2.16). Characteristic half-life times of H₂O and H₂ seem to be quite long below the mesopause, on the order of 1 week; thus the aforementioned transport processes have enough time to exercise their influence. Dissociation of H₂O at the level of noctilucent clouds might, therefore, be less than has been assumed previously (Hesstvedt, 1967c). This is evident from Fig. 2.17, which contains estimates by Hesstvedt (1965a) of relative concentrations of H₂O, defined as

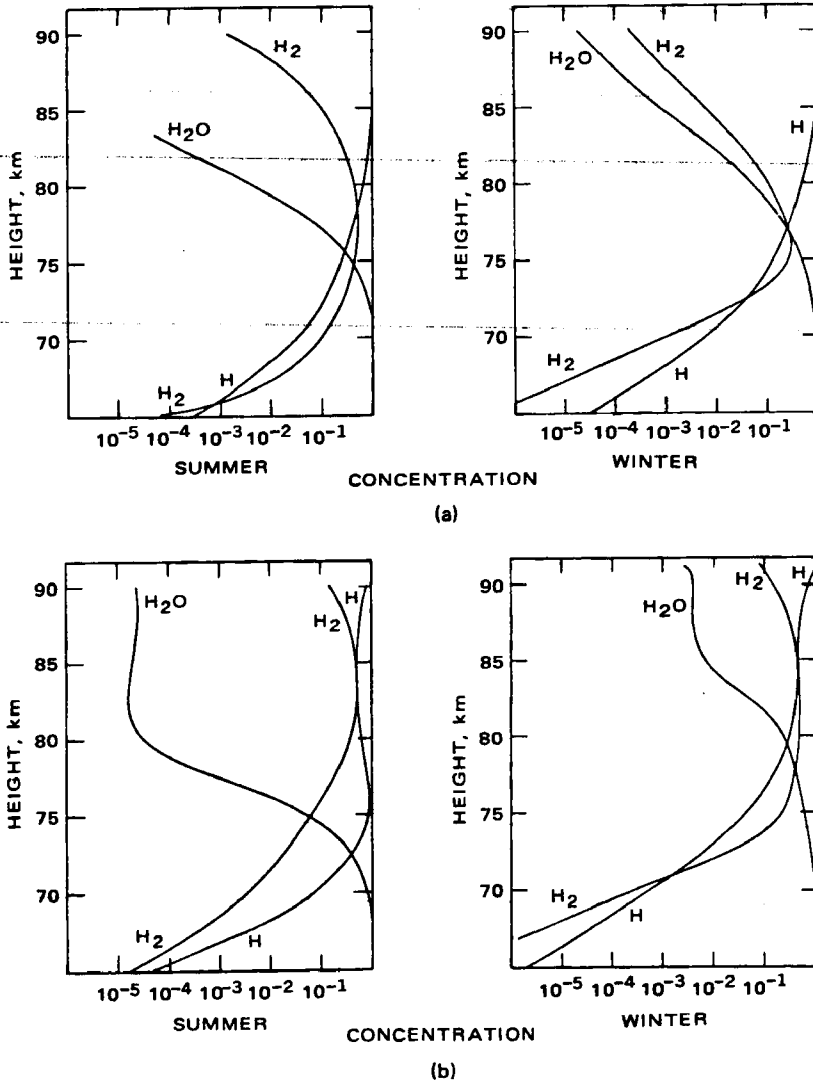


Fig. 2.16 Relative concentration of H, H₂, and water vapor for latitude 45°, summer and winter. (a) "Dry" case. (b) "Moist" case. Units are in terms of (concentration of constituent)/(total number of H atoms per cubic centimeter) (see text). [From E. Hesstvedt, *Tellus*, 17(3): 347, 348 (1965).]

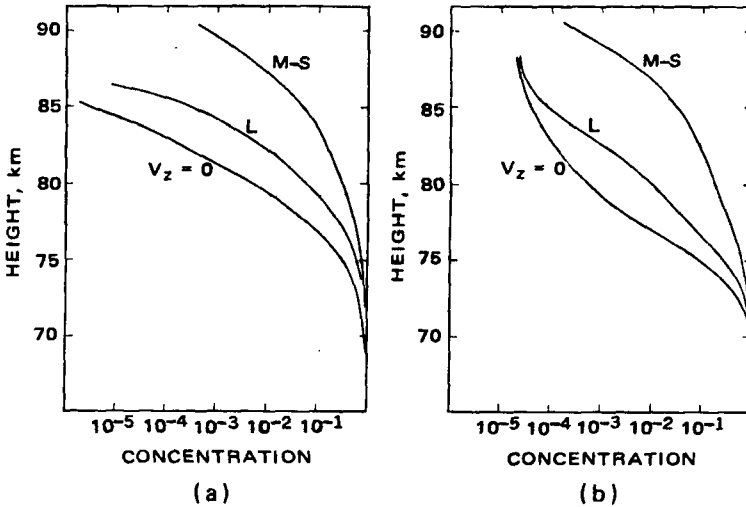


Fig. 2.17 Relative concentration of water vapor, high-latitude summer, for zero vertical motions ($V_z = 0$) and for vertical velocity profiles according to Leovy (L) and Murgatroyd and Singleton (M-S). (a) "Dry" case. (b) "Moist" case. Units are in terms of (concentration of constituent)/(total number of H atoms per cubic centimeter) (see text). [From E. Hessvedt, *Tellus*, 17(3): 348 (1965).]

the ratio $2[H_2O]/\Sigma_H$, where Σ_H denotes the total number of hydrogen atoms per cubic centimeter. Concentration estimates are shown in this diagram for zero vertical motions and for vertical velocities estimated by Murgatroyd and Singleton (1961) and Leovy (1964). Typical values at $45^\circ N$ were given by the former authors as 1 cm/sec (Fig. 1.16) and by the latter as 0.25 cm/sec. As shown in this diagram, Leovy's mesospheric circulation model raises the water-vapor regime by insignificant amounts, whereas Murgatroyd and Singleton's model would ensure sufficient moisture concentrations at the mesopause to permit the formation of noctilucent clouds.

According to Jesse (1896), noctilucent clouds (NLC) occur between 78 and 90 km, with an average height of 82 km (see also Fogle, 1966). From more recent data (Størmer, 1935; Paton, 1949; Burov, 1959; Witt, 1962), it appears that noctilucent clouds are associated with the mesopause and have their lower boundary at about 80 to 85 km. They drift predominantly from a direction between north and east (Murgatroyd, 1957; Murgatroyd and Singleton, 1961; Leovy, 1964), suggesting the presence of meridional transport processes of appreciable magnitude from the north. [Figure 3.21 in Part 1, after Haurwitz (1961), on the other hand, indicated a slight frictionally induced wind component from the south to be present at noctilucent-cloud levels during summer, which would tend to reduce the northerly wind components below magnitudes to be expected from conservation of absolute angular momentum.] The occurrence of these clouds depends on exceptionally low mesopause temperatures (about $130^\circ K$; Schröder, 1967d; Witt, 1968; Christie, 1969c; see

Fig. 2.18). Their visibility is contingent upon the sun's position below the horizon (Dietze, 1969). These factors cause a predominance of observations at high latitudes during June and July (Schröder, 1966a, 1966d, 1967a, 1967b, 1967e, 1968c; Paton, 1969). According to Fogle (1968), the peak activity of NLC shifts to higher latitudes with the progression of the summer season. The same factors are also responsible for certain diurnal variations, especially in brightness and to a lesser degree in frequency (Schröder, 1966b, 1967c, 1968a). More complete NLC observations may become feasible from satellites (Joseph, 1967). An extensive bibliography on noctilucent clouds has been compiled by Schröder (1966c).

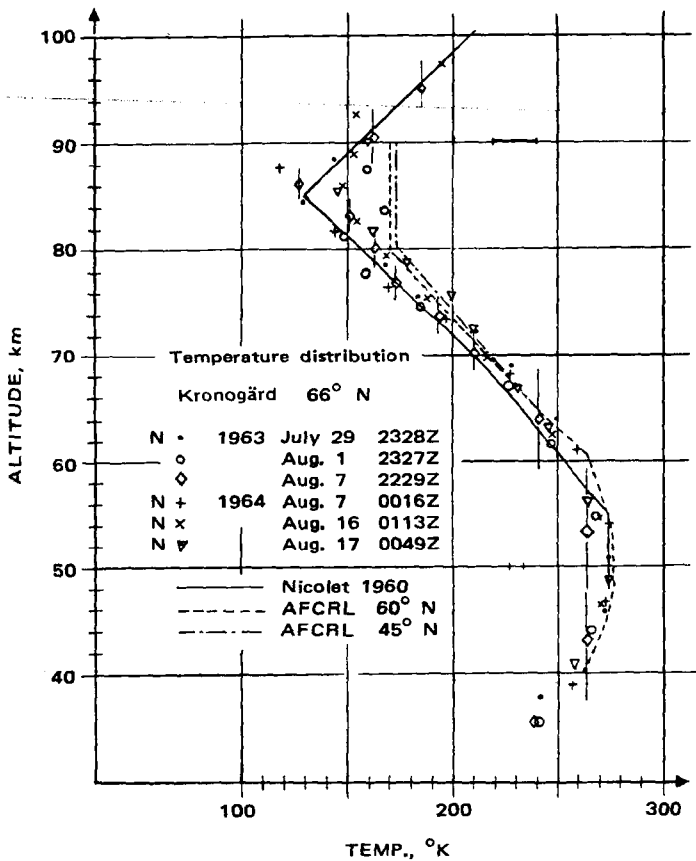


Fig. 2.18 Temperature as a function of altitude from rocket-grenade soundings over Kronogård (66° N), Sweden. The presence of visible noctilucent clouds is indicated by an N preceding the launching date. The estimated error at 50- and 90-km altitudes is shown by horizontal lines. Notice that the symbols denote the average temperature in layers of varying geometric thickness as indicated by short vertical lines. Profiles derived by Nicolet (1960) and the AFCRL Standard Atmosphere (Environmental Science Services Administration et al., 1966) have been entered for comparison. [From G. Witt, *Tellus*, 20(1): 100 (1968).]

Rocket samples from the height region of noctilucent clouds seem to substantiate the presence of moisture (Linscott et al., 1964; Skrivanek and Soberman, 1964; Soberman et al., 1964), probably in the form of ice shells surrounding meteoric dust particles, many of them nickel-based micrometeorites (Hemenway, Fullam, et al., 1964; Hemenway, Soberman, and Witt, 1964; Witt et al., 1964; Chapman and Kendall, 1965). These measurements indicate that two to three orders of magnitude more nuclei of probably meteoric origin are present in the noctilucent-cloud layer when such clouds are observed than during their absence. Size distributions of particles follow the form $n \propto r^{-p}$, where n is the number of particles, r is their radius, and p ranges from 3 to 4 (Witt et al., 1963; Skrivanek, 1969). Fiocco and Grams (1969), using optical radar for their measurements, were able to associate thin aerosol layers (less than 1-km thick) with the passage of noctilucent clouds. Height variations of the cloud layer of about 2 km could be assessed from these data. Rocket measurements described by Narcisi (1966) indicate the presence of the water-vapor-like ions of H_3O^+ and $H_5O_2^+$ in the D-region of the ionosphere below 82 km (see Figs. 1.38 and 1.39). The possibility of contamination of the atmosphere by the rocket itself still remains.

Temperatures in the vicinity of the mesopause and in the regions where noctilucent clouds were observed appear to be low enough, especially during summer, to cause supersaturation (Stroud et al., 1960; Theon et al., 1967; Witt, 1968) (Fig. 1.14).

Hesstvedt (1967a) assumes a water-vapor mixing ratio of 1.8×10^{-6} g/g to be present at the mesopause. This value corresponds approximately to minimum mixing ratios in the lower stratosphere (Fig. 2.12) and also agrees well with Mastenbrook's (1968) findings (Fig. 2.11). The "dry sky" conditions extrapolated from British measurements (Fig. 2.12) would also meet Hesstvedt's assumptions. Mean conditions measured by Sissenwine et al. (1968a) over Chico, Calif., would easily provide enough mesospheric moisture to account for noctilucent clouds. An extrapolation of Gutnick's data, shown in the same diagram, would call for a noctilucent-cloud cover over most of the earth, in disagreement with observations.

Although sublimation into ice crystals could occur with such low humidity values, the growth rate would be too small to yield visible cloud particles within reasonable time. In an earlier paper, Hesstvedt (1961) arrived at a plausible growth rate of 0.004×10^{-4} cm of radius increase per minute. The billows and waves observed by Witt (1962) and others in noctilucent-cloud displays, therefore, seem to be not so much an effect of sublimation and reevaporation of moisture moving through a wave pattern, nor are they likely to be caused by a wavelike pattern in the number density of dust particles (McLone, 1967), but they may rather be explained by geometrical reasoning: The optical path length through the cloud layer of almost uniform thickness changes with the phase angle of the wave phenomenon, thus producing "billows" of brightness. In an NLC viewed vertically from below, billows are not visible (Dietze, 1969) because the optical thickness is the same in the crests and troughs of these waves.

The cause of the wave motions observed in the noctilucent-cloud layer has not yet been fully explored. Shearing gravity waves would produce wavelengths shorter

than those observed (λ_x observed \approx 30 to 40 km). Internal gravity waves propagated into the cloud layer from elsewhere appear more likely to be sources of the observed phenomenon. Hines (1968b) excludes orographic lee waves because noctilucent-cloud waves usually show a speed of horizontal progression (order of magnitude, 10 m/sec). He speculates that tropospheric frontal systems and jet streams more than 700 km upstream may serve as sources of upward-propagating internal gravity waves [see also Christie (1969a), who speculates that such wave activity may enhance the vertical turbulent transfer of water vapor].

Small extraterrestrial particles of 0.1 to 100 μ will reach terminal velocities near 80 to 100 km (Shafir and Humi, 1967). This fact may account for the relatively large number of particles [8×10^{10} particles per square meter in the layer 75 to 98 km, according to Hemenway et al. (1964)] found in the presence of noctilucent clouds. According to Witt (1962), these small particles might stay within the cloud layer long enough to be able to grow to visible size.

Rising motions near the mesopause over the summer pole, shown in Fig. 1.16, may transport enough water vapor upward to yield supersaturation (Schröder, 1968b). Furthermore, these ascending motions would help generate the low mesopause temperatures needed for NLC formation (Christie, 1969b). The southward flow near the mesopause, estimated by Leovy (1964) (about 0.5 m/sec), would cause only small departures in the water-vapor distribution from photochemical equilibrium. With a meridional velocity of 4 m/sec, assumed by Murgatroyd and Singleton (1961), a southward displacement of relatively high moisture concentrations by as much as 15° to 20° latitude could be achieved within the characteristic half-life times of H₂O. Thus the moisture at mesopause level will not be seriously reduced in the southward flow before latitudes of about 50° to 60° are reached. The latitudinal distribution of noctilucent-cloud observations might thus be explained. These meridional velocities, of course, need not necessarily be produced only by a mean meridional circulation; they can also be produced by planetary-scale eddies, which were not considered by Murgatroyd and Singleton. Descending motions near the mesopause over the winter pole would lower the water-vapor regime, especially in the model by Murgatroyd and Singleton, inhibiting the formation of noctilucent clouds.

Chapman and Kendall (1965) also reached the conclusion that convective processes in the mesosphere transport enough moisture upward to permit noctilucent-cloud formation. They furthermore postulate that noctilucent clouds will appear only if the following conditions are met simultaneously:

1. Low mesopause temperature minimum.
2. Adequate supply of water vapor from below by convection.
3. Generation of a "dust ledge" by coincidence of mesopause and "turbopause."

The turbopause is defined as the level above which turbulent processes cease or become negligible. (The coefficients of molecular and eddy diffusion are nearly the same above this level.) From sodium cloud experiments (see p. 243) conducted at latitudes of 30° to 35°N, it appears that the turbopause is located near 100 km; it thus lies higher than the average mesopause level. The persistence of noctilucent clouds for

several hours would suggest that on such occasions the turbopause has descended to mesopause level. The sharp change of the magnitude of the diffusion coefficients at the turbopause may cause a dust maximum to appear at this level. This maximum is further enhanced if large-scale upward convective velocities of 18 cm/sec occur in the noctilucent-cloud layer at mesopause level. This is shown schematically in Fig. 2.19. Such vertical velocity values of exactly the right magnitude are unlikely to persist near the mesopause, however.

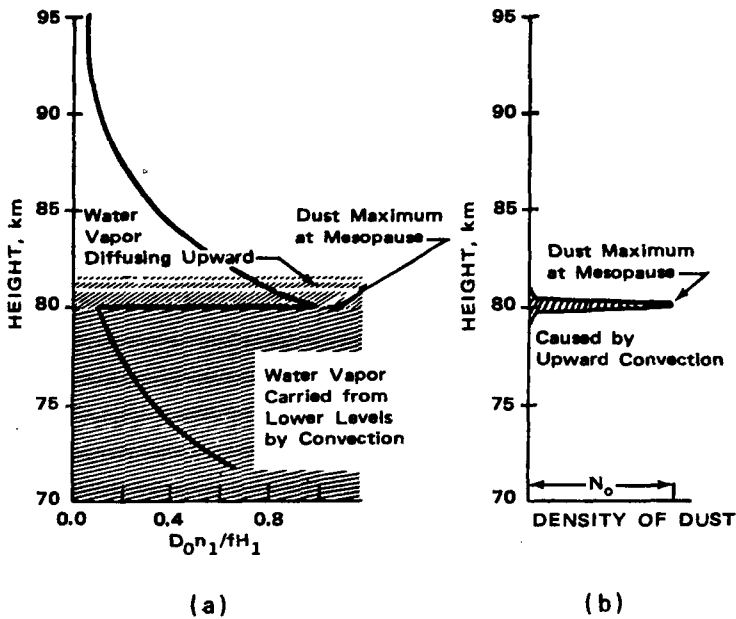


Fig. 2.19 (a) The steady-state dust profile when the turbopause is at the same level as the mesopause. The heavy shading denotes the presence of water vapor below the mesopause. The lighter shading denotes water vapor diffusing into the thermosphere and decreasing in density as it does so. (b) The steady distribution of dust given by a large-scale upward convective velocity of 18 cm/sec (see text). The thickness of the layer is exaggerated. The maximum number density is taken to be N_0 . D_0 is the coefficient of molecular diffusion at the mesopause or turbopause; H_1 is the scale height of dust particles [$= kT/m_1g \approx 0.216$ cm, where k is the Boltzmann constant (1.380×10^{-16} erg/deg) and m_1 is the mass per molecule of dust particles]; n_1 is the number density of dust particles; and f is the flux of dust ($g/cm^2/sec$) from a great height. [From S. Chapman and P. C. Kendall, *Quarterly Journal of the Royal Meteorological Society*, 91(388): 130 (1965).]

Chapman and Kendall (1965) conclude, furthermore, that, if the micrometeorites involved in noctilucent-cloud formation were compact and spherical, they would descend through the mesopause too quickly and be dispersed in the mesosphere too rapidly to have a visible effect. They suggest, therefore, that these particles are strongly nonspherical, being either needle-shaped or flaky.

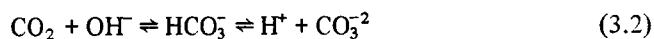
Figure 2.16 shows that H_2 and H become the predominant hydrogen constituents above 85 km. Tinsley (1969) suggests that the altitude profile of H in the thermosphere depends strongly on the temperature distribution, which, in turn, determines the rate of escape of H into interplanetary space. Between the maximum 24-hr average temperatures of 1600°K observed during the solar maximum of 1958 and the minimum 24-hr average temperatures of 800°K at the solar minimum of 1964, a change in the column density of H above 500 km from $5 \times 10^{11} \text{ cm}^{-2}$ to $2 \times 10^{13} \text{ cm}^{-2}$ was predicted. High temperatures cause large escape rates and hence lower column densities. Increased escape rates will have to result in increased upward transport of H from lower layers of the thermosphere and from the mesosphere. Observations of the variations of [H] with season and with the solar cycle may shed some light on these transport processes. According to Tinsley (1969), actual observations of H abundance, mainly derived from airglow observations, exceeded the theoretically predicted buildup between 1958 and 1964.

3 CARBON DIOXIDE

Carbon dioxide is a minor but not unimportant, because of its radiation bands in the infrared (among others near 2.7, 4.2, and, most important, 15 μ) (Hoffmann, 1967), constituent of the atmosphere. Its radiance at 15 μ especially has been used successfully to map temperature distributions in the lower stratosphere and near the stratopause, and from these maps estimates of the stratospheric motion patterns have been made (Kennedy and Nordberg, 1967; Belmont et al., 1968; Gille, 1968; Shen et al., 1968; Zak and Panofsky, 1968). Its molecular weight is 44.0, and its density with respect to air is 1.529. Under the influence of ultraviolet radiation, it dissociates into atomic oxygen (O) and carbon monoxide (CO) (Ratcliffe, 1960).

Fluctuations of the CO₂ content of the atmosphere have long been thought of as insignificant and within the accuracy limits of the measurement techniques. Hann and Süring (1939) report in their classical textbook that the CO₂ content tends to be somewhat higher over the continents than over the oceans since the latter act as reservoirs or sinks (Kanwisher, 1960).

The exchange of atmospheric CO₂ with the sea is governed by the following equations (Bolin, 1960; Kanwisher, 1960; Takahashi, 1967):



which express the fact that in ocean water dissolved carbon dioxide, carbonic acid, and bicarbonate and carbonate ions are in approximate equilibrium (for laboratory results,

see Hoover and Berkshire, 1969). Equation 3.1 dominates for $\text{pH} \leq 8$ and Eq. 3.2 for $\text{pH} \geq 10$ (Mills and Urey, 1940). Enzymes, such as carbonic anhydrase, may possibly have a controlling influence in the exchange of CO_2 between air and ocean (Berger and Libby, 1969).

A slight decrease of CO_2 concentration with altitude was also quoted by Hann and Süring (1939) (see also Bray, 1959; Bischof, 1960; Kelley, 1969b).

Carbon dioxide constitutes only about 0.03 vol.% of the total atmosphere. In a homogeneous atmosphere of height $H_0 = 7991$ m, CO_2 would occupy $H_0 p'_0/p_0 = 2.40$ m (p'_0 is the partial pressure of CO_2 at the surface, equal to 0.23 mm Hg, and p_0 is the normal pressure of the total atmosphere, equal to 760 mm Hg).

Recent refinements in measurement techniques (Fonselius and Wärme, 1960; see also Junge, 1963a) revealed significant fluctuations in CO_2 concentration as well as in the relative abundance of ^{13}C and ^{12}C (Keeling, 1958, 1960). These will be described later. Thus this long-neglected atmospheric constituent achieved new significance as an atmospheric tracer. Measurement networks for monitoring CO_2 fluctuations have been set up, notably in Scandinavia (Eriksson, 1954; Fonselius et al., 1955; Anonymous, 1958, 1959, 1960; Fonselius, 1958; Bischof, 1960, 1962; Steinhauser, 1960a).

THE SECULAR TREND OF CO_2 CONCENTRATIONS

Bray (1959) compared a long list of old and new (1868–1956) measurements of CO_2 concentrations in order to reach a conclusion about the much-argued secular trend of CO_2 that might be expected from increasing industrialization. Callendar (1940, 1958) had argued earlier in favor of such a trend, whereas Slocum (1955) questioned its existence from the available data. Bray (1959) went into great detail in examining the various sources of information on CO_2 concentrations for their reliability. He rejected data prior to the 1850's because of uncertain analysis techniques. These data actually showed a decrease in concentrations from the 1750's to the 1850's because of improved chemical techniques (Effenberger, 1951). A further difficulty in comparing data arises from the fact that CO_2 values show extreme variability near the ground. There are, apparently, higher concentrations at ground level, with a rapid decrease within the lowest few centimeters and possibly a slight increase above approximately 2 m (Kreutz, 1941; Midorikawa, 1957; Bischof, 1960). Bischof (1960) actually found an increase of CO_2 up to a height of approximately 800 m and constancy above this level.

Urban areas, on the average, show higher CO_2 values than rural areas, but the magnitude of these excess amounts varies greatly. Owing to the variability in atmospheric diffusion conditions (controlled by thermal stability and wind speeds) and in home and industrial combustion processes, urban areas have a large *interdiurnal* variation of CO_2 concentrations. This variation reaches a maximum in the winter months (Steinhauser; 1958, 1960a). For the same reasons a considerable *diurnal*

variation in CO₂ values should be expected (Bischof, 1960). Latitudinal and seasonal fluctuations of CO₂ must also be considered when examining long-term records.

Taking all these limitations into account, Bray (1959) concluded that CO₂ concentrations could have increased slightly over the continents during the past 100 years. This increase was probably due to industrial activity (see also Bolin, 1966). A less likely alternative is that it might have been, in part, produced by systematic changes in the relative location of sampling stations (e.g., by a preponderance of nonurban stations during the first part of the period and by urban stations during the second part) and by improved analysis techniques. Records from well-maintained sampling stations for a shorter time period also point toward a slow secular increase of CO₂. Data from the Mauna Loa Observatory, Hawaii, reveal a trend of 0.7 ppm per year (Bolin and Keeling, 1963; Pales and Keeling, 1965). Measurements over Antarctica, far away from any industrial sources and vegetation sinks, indicate a very similar trend (Keeling, 1958, 1960; Brown and Keeling, 1965).

Bolin and Eriksson (1959) and Kanwisher (1960) argued that the "buffering" effect of the oceans may not be nearly as large as commonly assumed. The water above the oceanic thermocline, constituting the mixing layer and containing less than 2% of the total ocean water, is in diffusion equilibrium with the atmosphere. Thus any increase in atmospheric CO₂ would have only a small fraction of total ocean water available for buffering. Only over longer time periods, as the marine mixing layer exchanges its waters with the deep sea (Montgomery, 1959; Plass, 1956), is the full effect of the ocean's buffering capability brought to bear upon the atmosphere. These effects, however, might be offset if fossil-fuel combustion continues to increase at an exponential rate. The relatively small secular increase of CO₂, in spite of its inefficient buffering by ocean water, suggests that the biosphere on land plays a very important role in removing CO₂ from the atmosphere. This is also emphasized in studies by Lieth (1963, 1965), who reports that the turnover time of the total CO₂ contained in an atmospheric column of unit cross section would be 2 years in a European forest and 0.8 year in a Malayan forest (assuming the mass of CO₂ to be 30 metric tons per hectare, or 3 kg/m²). The world vegetation at its present production capacity could remove the entire CO₂ content of the atmosphere in 23 to 26 years.

From Bray's (1959) study and from the foregoing discussion, it appears that the secular trend in CO₂ values, although definitely present, may be considered small enough so that its effect on the atmosphere's radiation and heat budget is negligible so far. This may be seen by the estimates of the equilibrium temperature reached under various CO₂ concentrations (Fig. 3.1) (Manabe and Wetherald, 1967; see also Kaplan, 1960). Infrared contributions of the 15- μ CO₂ band to the heat budget between 30 and 110 km were also computed by Kuhn and London (1969); other vibrational bands were considered by J. T. Houghton (1969).

The secular trend, until now, has produced a CO₂ increase of the order of 20 ppm (Bray, 1959). Thus it falls considerably short of the large variations assumed in Fig. 3.1. Such variations could only be realized with drastic changes in ocean temperatures or with strong variations in the biological activity in the oceans (Eriksson, 1963a; see also Plass, 1956). Small variations of the order of 30 ppm may

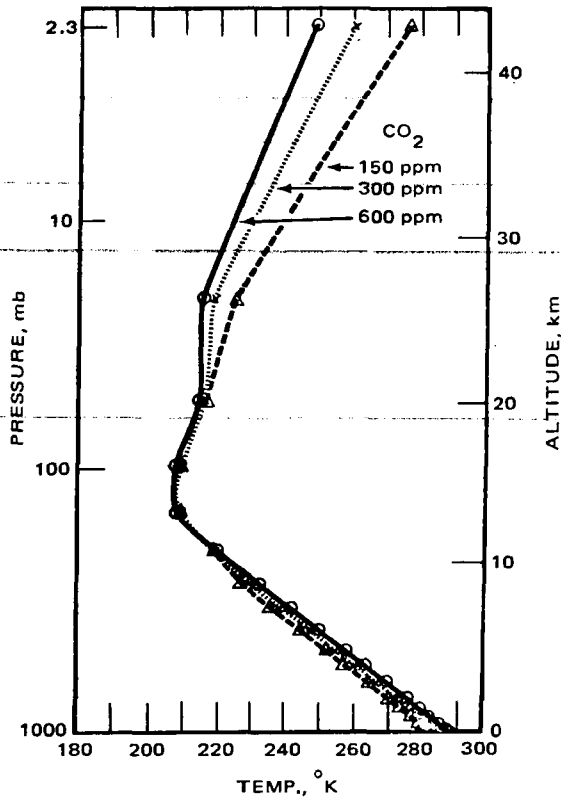


Fig. 3.1 Vertical distributions of temperature in radiative convective equilibrium for various values of CO_2 content. [From S. Manabe and R. T. Wetherald, *Journal of the Atmospheric Sciences*, 24(3): 250 (1967).]

be compensated by changes in humidity and cloudiness without affecting the temperature (Möller, 1963, 1964; see also Plass, 1964). Injections of excessive amounts of water vapor into the stratosphere by dense supersonic air traffic may have much more serious effects on the atmospheric radiation and heat balance than "air pollution" by CO_2 (see Fig. 2.7). In the following discussion, we will disregard the secular trend of CO_2 altogether.

DIURNAL VARIATIONS

The diurnal variation of CO_2 has been analyzed by Bischof (1960) for a golf course (golfbanan) near Stockholm, for a location 1 km east of the course (bryggan) on the shore of a narrow bay of the Baltic Sea, which is exposed to easterly winds, and for a small island (Dalarö). Results are shown in Fig. 3.2. Measurements taken around

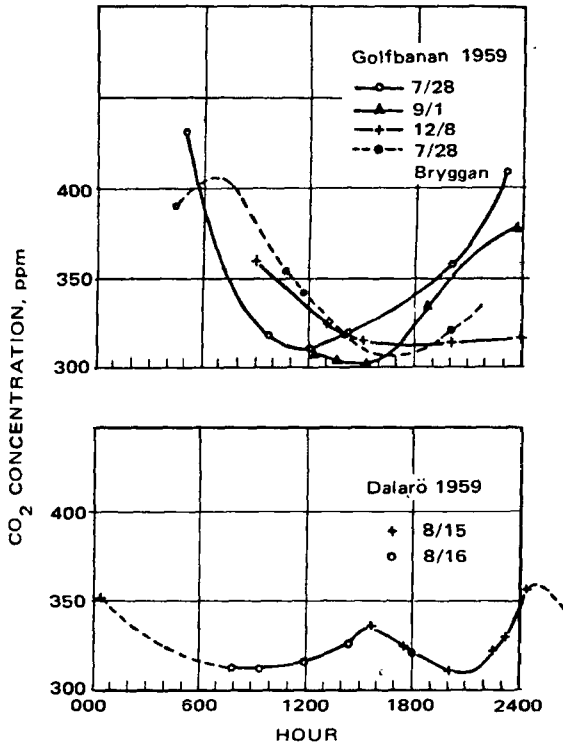


Fig. 3.2 Daily cycle of CO₂ content at the golf course (golfbanan) on several occasions and comparison with a place 1 km away at the Baltic Sea (bryggan) and with a small island (Dalarö). [From W. Bischof, *Tellus*, 12(2):225 (1960).]

1300 local time appear to be least “contaminated” by local conditions because of the increased vertical turbulent exchange processes at this time of the day. Daytime minimums of [CO₂] during the growing season at a rural location have been measured by Clarke (1969).

The diurnal variation shown here from Swedish data is not universally applicable. Measurements on Mauna Loa, Hawaii, for instance, reveal a characteristic afternoon dip in CO₂ concentrations around 1600 local time (Fig. 3.3). This dip is best developed during the months of July, August, and September, when, on the average, it amounts to 1.3 to 1.4 ppm. Pales and Keeling (1965) ascribe this deficit in CO₂ values to the uptake by vegetation along the lower slopes of Mauna Loa. The low concentration values are advected to the observation site in the diurnal upslope breeze. Figure 3.3 shows a comparison of the Mauna Loa observations with measurements taken at Point Barrow, Alaska (Kelley, 1964), and at Mount Olympus, Washington (Kelley and LaChapelle, 1966). The Arctic station is almost void of any diurnal variation. On Mount Olympus, however, a pronounced variation exists which is completely different from that on Mauna Loa. The valley breezes during the afternoon

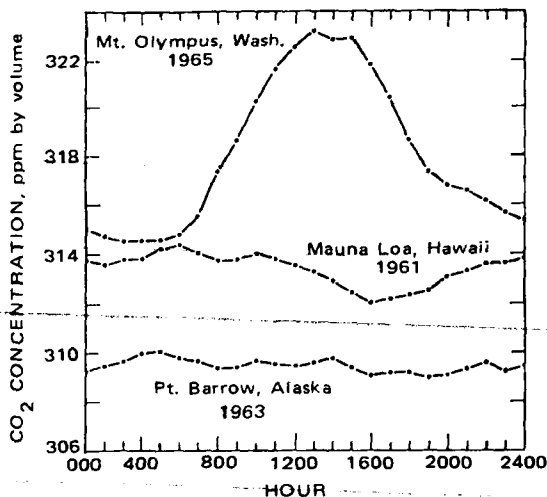


Fig. 3.3 Diurnal variation of atmospheric CO₂, August 1965. [From J. J. Kelley, Jr., and E. LaChapelle, *Journal of Geophysical Research*, 71(8):2174 (1966).]

hours (Thyer and Buettner, 1962; Buettner, 1967) import CO₂-rich air from the cities on Puget Sound and on the Straits of Juan de Fuca. This circulation is intense enough to suffer only little depletion of CO₂ in daytime assimilation by plants (Kelley, 1969a).

From the foregoing one can see that CO₂ serves well as a tracer for mesoscale circulation patterns.

SEASONAL VARIATIONS AND INTERHEMISPHERIC EXCHANGE

The seasonal march of CO₂ values is quite pronounced. Table 3.1 indicates this clearly for the city of Vienna, Austria (Steinhauser, 1960a). Measurements cover the period 1957–1960. This table also shows that the scatter of measurement values is rather broad during the months of January to April, probably because of the effects of highly variable diffusion conditions and of increased CO₂ input into the atmosphere by home incineration of fossil fuels during this season. Figure 3.4 exhibits winter maximums of CO₂. It also reveals the aforementioned different behavior of an urban region (Vienna, Austria), a small provincial town (Klagenfurt, Austria), and rural climates (Retz, Austria).

The seasonal trend of CO₂ concentrations at Mauna Loa Observatory, Hawaii (19.5°N, 155.6°W) is shown in Fig. 3.5. Regular peaks appear in May and June and minimum values in September and October (Pales and Keeling, 1965). Similar trends have been measured by aircraft in the free atmosphere (Keeling et al., 1968). Figure

Table 3.1
 PERCENT FREQUENCY DISTRIBUTION OF DAILY CO₂ CONCENTRATION
 AT NOON, VIENNA, AUSTRIA*

Milliliters of CO ₂ / 10 liters of air													Annual percent frequency	
	J	F	M	A	M	J	J	A	S	O	N	D		
3.91 to 4.00	1													0
3.81 to 3.90	9		1	1								2		1
3.71 to 3.80	11	2	1	1							1	6		2
3.61 to 3.70	12	10	7	4	2	4					6	20		5
3.51 to 3.60	14	13	15	5		5		3		5	18	20		9
3.41 to 3.50	17	17	19	15	6	9	4	14	1	18	24	23		14
3.31 to 3.40	16	20	21	23	22	18	14	22	8	18	18	14		18
3.21 to 3.30	10	16	17	21	26	16	30	25	25	31	25	10		21
3.11 to 3.20	4	7	6	11	25	19	25	20	36	17	7	5		15
3.01 to 3.10	4	5	4	7	15	14	15	9	22	11	1			8
2.91 to 3.00	1	7	5	6	4	12	10	5	7					5
2.81 to 2.90	1	2	4	3		3	2	2	1					2
2.71 to 2.80		1		3										0

*From F. Steinhauser, *Wetter und Leben*, 12(9-10) (1960).

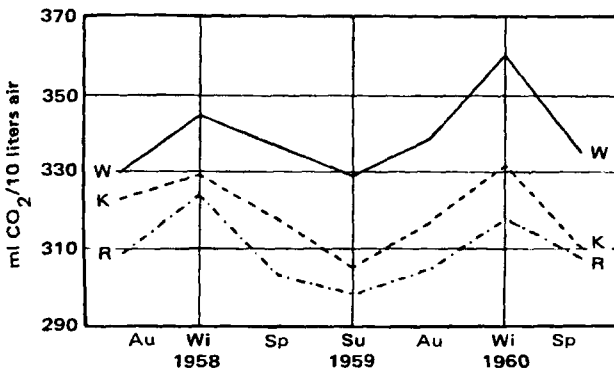


Fig. 3.4 Seasonal mean values of CO₂ content of air (milliliters of CO₂ per 10 liters of air) at Vienna (W), Klagenfurt (K), and Retz (R), Austria, from autumn 1958 to spring 1960. [From F. Steinhauser, *Wetter und Leben*, 12(9-10) (1960).]

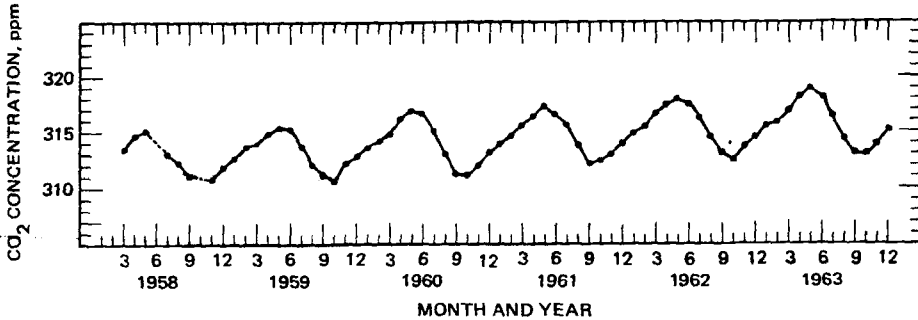


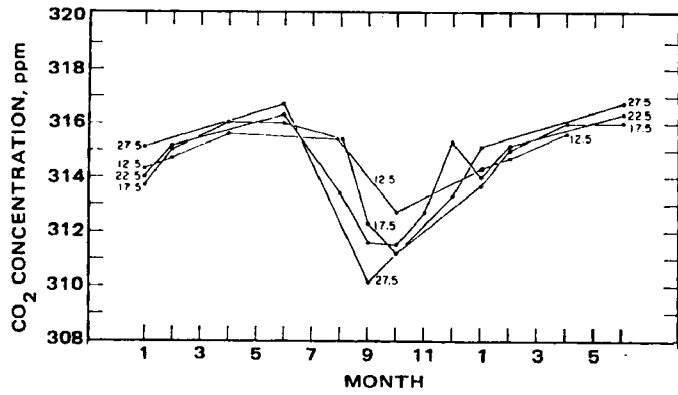
Fig. 3.5 Monthly average concentration of atmospheric CO₂ at Mauna Loa Observatory vs. time. [From J. C. Pales and C. D. Keeling, *Journal of Geophysical Research*, 70(24): 6066 (1965).]

3.6 indicates an increasing amplitude with increasing northern latitude as well as a shift in the occurrence of maximums and minimums (in subtropical latitudes the maximum is shown in June and the minimum in October; in high latitudes a shift to May and August, respectively, is observed). The difference in flight levels (700 and 500 mb) is thought to have no consequence on the sampling because of the well-mixed conditions of the troposphere.

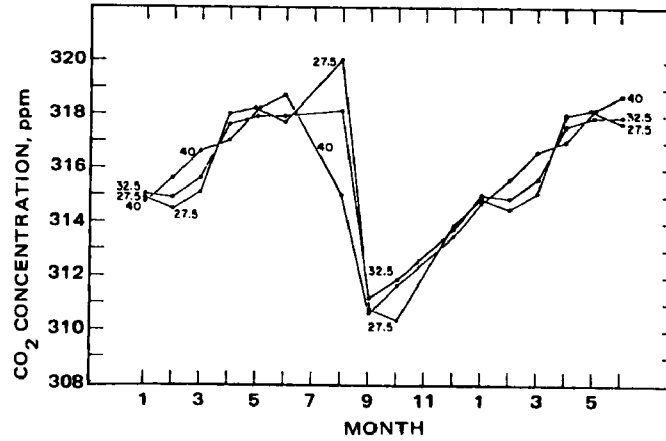
The seasonal variations shown in Figs. 3.5 and 3.6 are rather well established (see also Bray, 1959). On the other hand, Effenberger (1951) computed, from older records, a double oscillation of CO₂ during the year with maximums of CO₂ in February and March and August and September. He found minimums in June and July and in December. Using Scandinavian data from 1955 to 1959, Bischof (1960) also found two maximums and two minimums. However, their time of occurrence near the surface varies greatly from year to year as well as from station to station. This may be caused, at least in part, by large-scale changes in seasonal and annual CO₂ concentration patterns produced by changing frequencies and intensities of circulation patterns and of diffusion regimes acting on low-level sources. At some distance above the ground (>1000 m), the seasonal march of CO₂ behaves much more uniformly, with minimums in (late) summer and maximums in (late) winter and spring (Bischof, 1962; Bischof and Bolin, 1966). The fact that many stations collect CO₂ samples only three times a month does not seem to affect the establishment of a seasonal trend in CO₂ concentrations too drastically (Steinhauser, 1958).

The effect of atmospheric circulation patterns is also indicated from CO₂ concentrations measured near the tropopause on flights between Copenhagen and Los Angeles (Bischof, 1965). The CO₂ values in the upper troposphere seemed to be higher by about 4 ppm than those in the lower stratosphere.

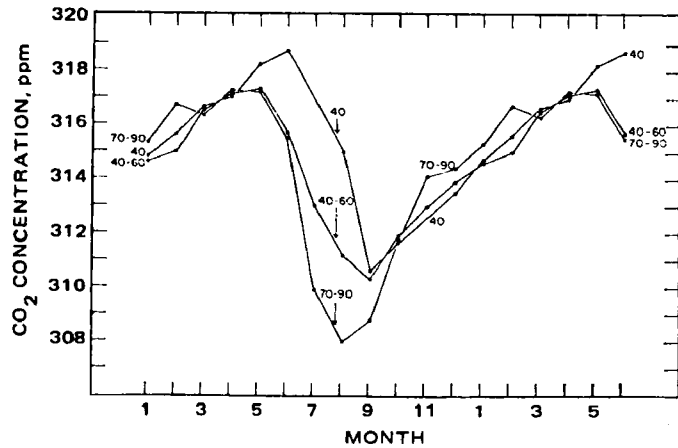
Bolin and Keeling (1963) found a strongly pronounced CO₂ minimum over the Arctic regions during summer (Fig. 3.7). For comparison, Fig. 3.8 shows the seasonal trend of CO₂ over Antarctica for the period 1958–1963. Peak concentrations are found there in November and December (summer) and a minimum in March (Brown



(a)



(b)



(c)

Fig. 3.6 Average monthly values of CO₂ concentration at 700 mb, 10°N to 30°N (a), 500 mb, 20°N to 41°N (b), and 500 mb, 40°N to 90°N (c), based on data for the years 1958 to 1961. Months 1 to 6 (January to June) are plotted twice to reveal the seasonal pattern more fully. [From C. D. Keeling, T. B. Harris, and E. M. Wilkins, *Journal of Geophysical Research*, 73(14):4527 (1968).]

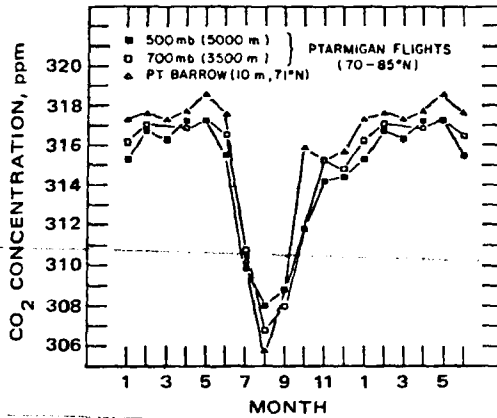


Fig. 3.7 Average monthly values of the concentration of atmospheric CO₂ at the surface, at 700 mb, and at 500 mb in the Arctic. [From B. Bolin and C. D. Keeling, *Journal of Geophysical Research*, 68(13):3918 (1963).]

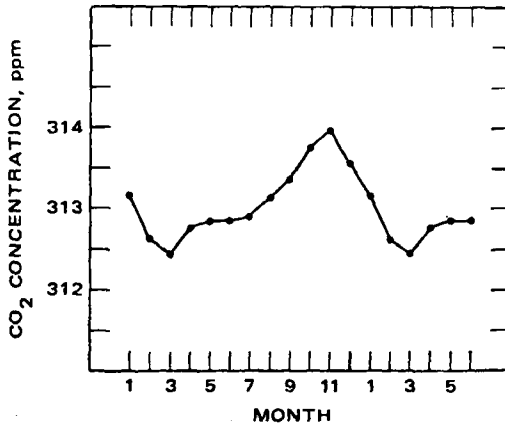


Fig. 3.8 Concentration of atmospheric CO₂ in Antarctica (1958--1963) as a function of the month of the year. Values have been referred to a January 1960 datum. Months 1 to 6 (January to June) are plotted twice to reveal the seasonal pattern more fully. [From C. W. Brown and C. D. Keeling, *Journal of Geophysical Research*, 70(24):6084 (1965).]

and Keeling, 1965). (A correction for the average annual increase of 0.7 ppm has been applied to these data.) The amplitude of this seasonal variation is small in comparison to the ones found in the northern hemisphere. The out-of-phase relation with the growing season suggests the presence of rather strong interhemispheric exchange processes. Wilkins (1961) estimated these to be about one-fifth of the air in one hemisphere within every half year (see also Junge, 1962b).

From actual measurement data, Bolin and Keeling derived the smoothed curves of latitudinal CO_2 distribution shown in Fig. 3.9. They admit to the possibility that the concentrations shown for the south pole in this diagram may be too low by as much as 1.0 ppm because of the measurement techniques used there. If this is the case, the CO_2 values assumed for the southern hemisphere will have to be adjusted accordingly. Such a grave error, however, is not suggested from Fig. 3.8. Figure 3.10

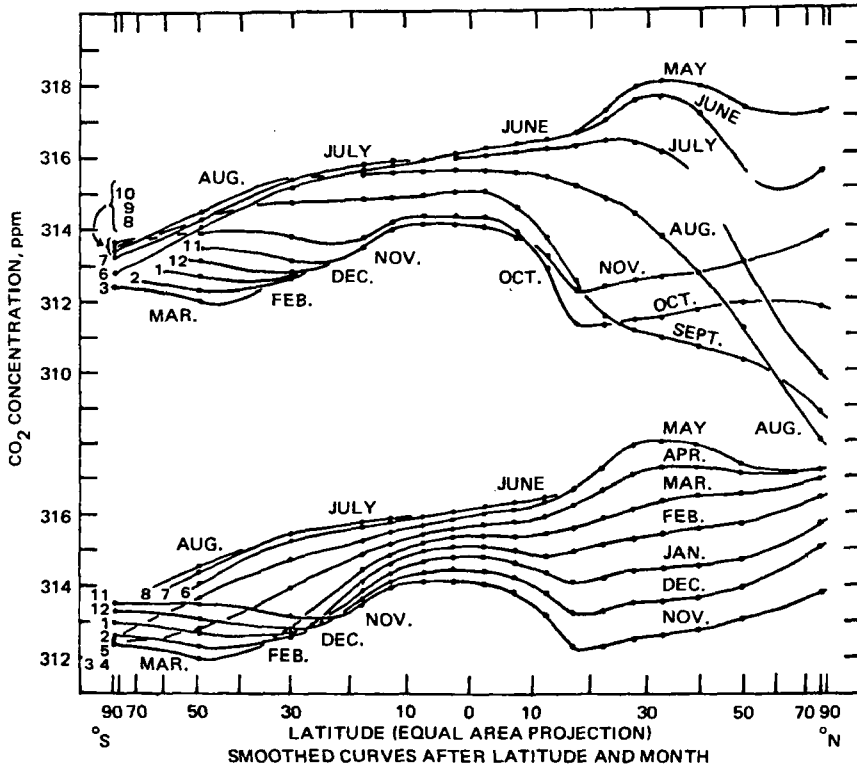


Fig. 3.9 Smoothed curves of the concentration of atmospheric CO_2 as a function of latitude for each calendar month. [From B. Bolin and C. D. Keeling, *Journal of Geophysical Research*, 68(13):3911 (1963).]

contains annual average CO_2 values as a function of latitude. In the northern hemisphere a differentiation is made in this diagram between surface, 700-mb, and 500-mb observations. The data suggest a source region for CO_2 near the equator, presumably a result of the natural release from the ocean surface (Takahashi, 1961), which is compensated by oceanic absorption in higher latitudes. This conclusion is confirmed by data reported recently by Keeling and Waterman (1968). An example of their findings is given in Fig. 3.11. Wherever the partial pressure of CO_2 in surface water exceeds that in the atmosphere, the ocean acts as a CO_2 source. These two

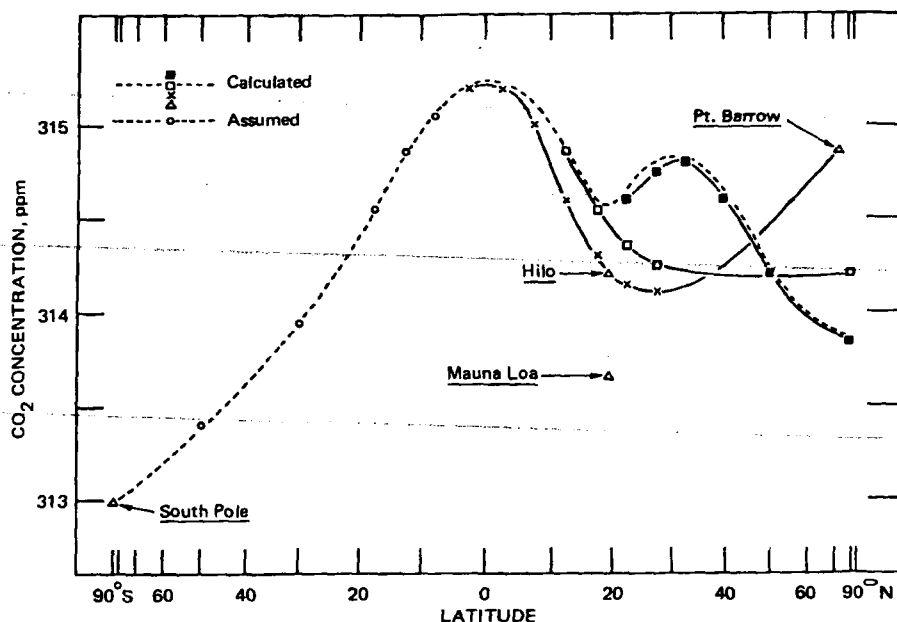


Fig. 3.10 Annual average concentration of atmospheric CO₂ as a function of latitude at the surface, at 700 mb, and at 500 mb, shown by the symbols x, □, and ■, respectively. Plotted points from 5°S to 85°S (○) are assumed values. [From B. Bolin and C. D. Keeling, *Journal of Geophysical Research*, 68(13): 3912 (1963).]

authors have observed longitudinal and seasonal variations in partial pressure differences over various oceans, which further complicates the picture. The global distribution of CO₂ partial pressure excess of surface waters over atmospheric partial pressures—mainly inferred from summer conditions—is shown in Fig. 3.12. High pressures in the equatorial Pacific and in the subtropical regions of upwelling coastal waters constitute the dominant features of this map.

Bolin (1960) argues that transfer velocities of CO₂ in the ocean of 7×10^{-3} cm/sec derived for a smooth ocean surface would lead to a residence time of about 5 years for CO₂ in the atmosphere (see also Bolin and Eriksson, 1959; Bolin, 1966). The residence time is 4 to 10 years according to H. Craig's (1957) estimate from radiocarbon data and 10 years according to Revelle and Suess (1957). Keeling (1965), in a rough estimate, arrived at slightly lower residence times of the same order of magnitude.

For rough ocean surfaces the transfer velocities may be 1 to 2 orders of magnitude larger. If this wind factor is included, CO₂ will be more readily exchanged in the southern oceans during both seasons than in the oceans of the northern hemisphere (Kanwisher, 1963). The gas exchange depends on the partial pressure difference of CO₂ between ocean and atmosphere (see Fig. 3.12) and on the time

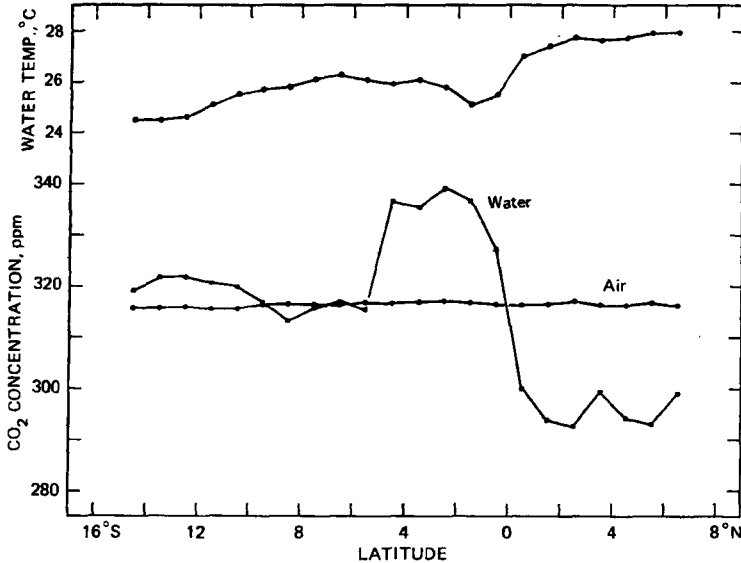


Fig. 3.11 Concentration of CO₂ near the ocean surface in the atmosphere and in ocean water and surface ocean water temperature as a function of latitude in the eastern Atlantic Ocean, June 28 to July 7, 1963. [From C. D. Keeling and L. S. Waterman, *Journal of Geophysical Research*, 73(14):4540 (1968).]

integral of V^2 . The area distribution of the latter is shown in Fig. 3.13. Such refined considerations will lead to slight modifications of Bolin and Keeling's CO₂ exchange model described later.

A second source region of CO₂ may be identified from Fig. 3.10 at the 500-mb level in temperate latitudes. This source is caused by the combustion of fossil fuels. It leads to the observed negative vertical CO₂ gradients over the oceans in these latitudes.

In spite of the uncertainties in the data, Bolin and Keeling (1963) attempted to fit to the observed annual CO₂ distribution a numerical model that would allow for large-scale exchange processes, thereby regarding CO₂ as a trace constituent of the atmosphere that is transported between source and sink regions.

The simple equation

$$\frac{\partial c}{\partial t} = \frac{K}{a^2} \frac{\partial}{\partial \sin \phi} \left[(1 - \sin^2 \phi) \frac{\partial c}{\partial \sin \phi} \right] + Q(\sin \phi, t) \quad (3.3)$$

is thought to account for the observed mean annual distribution of CO₂ with latitude. In this equation c is the CO₂ concentration, Q describes the sources and sinks of CO₂, and a is the earth's radius; K is an exchange coefficient that is assumed to be independent of latitude in the Bolin and Keeling model. The problem consists of finding an appropriate value of K and the proper latitudinal distribution of Q to

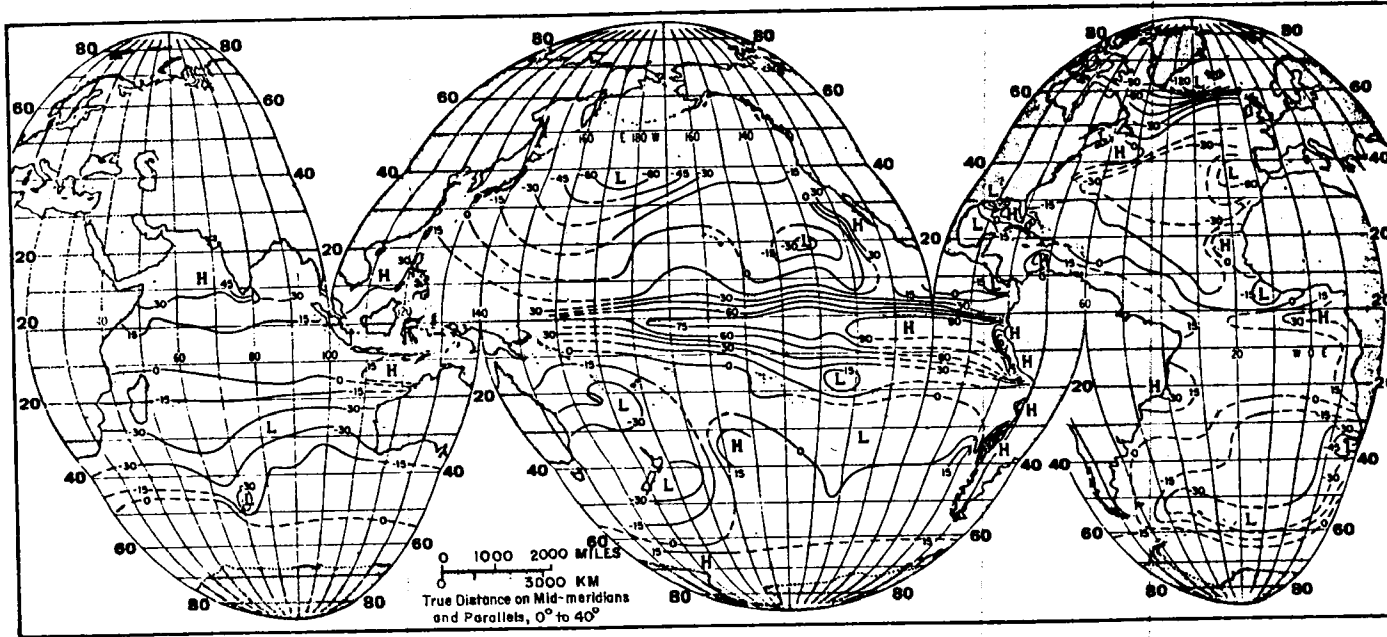


Fig. 3.12 The distribution of partial pressure of CO₂ of the world's oceans expressed as the departure (in ppm) from equilibrium with atmospheric CO₂. [From C. D. Keeling, *Journal of Geophysical Research*, 73(14):4547 (1968).]

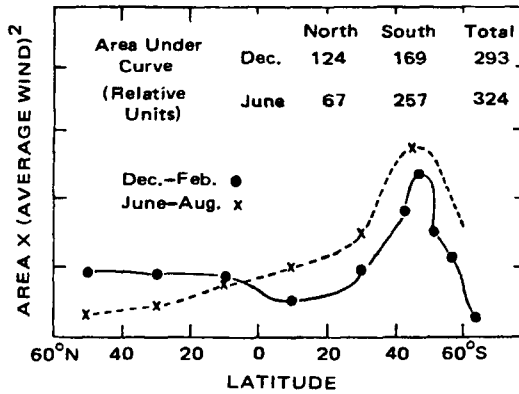


Fig. 3.13 Wind effect on the gas exchange between ocean and atmosphere as measured by the quantity $\text{area} \times (\text{average wind})^2$ (see text). [From J. Kanwisher, *Journal of Geophysical Research*, 68(13):3923 (1963).]

account for the observed latitudinal dependence of the concentration values c . In a more refined model, Junge and Czeplak (1968) allow K to be a function of latitude. However, model calculations are rather insensitive to variations of K and of Q .

To estimate K and Q , Bolin and Keeling assumed that Q was divided into *natural* sources and sinks, which were globally balanced, and into *industrial* sources. The latter are balanced by a slow secular increase in CO_2 concentration and, in view of the slow transfer rates of CO_2 into the ocean, by sinks, which are much more widely distributed than the source regions. Specifically, Bolin and Keeling assume that the sinks of industrial CO_2 are independent of latitude. (For the mathematical formulation of the problem, the reader is referred to the original paper; see also Junge and Czeplak, 1968.) Assuming, furthermore, that the natural sources and sinks are the same in both hemispheres when averaged over the year and that industrial sources are confined to the northern hemisphere, Bolin and Keeling determined the distribution of Q as shown in Fig. 3.14 together with a value of $K = 3.5 \times 10^{10} \text{ cm}^2/\text{sec}$. This value is in agreement with observed magnitudes of exchange coefficients of about $10^{10} \text{ cm}^2/\text{sec}$ in the surface layer and of $10^{11} \text{ cm}^2/\text{sec}$ in the upper troposphere of middle latitudes. The maximum of industrial output is found near 45°N . Close to 90% of the man-made CO_2 release appears to be between latitudes 30°N and 60°N .

The distribution of natural sources of CO_2 shown in Fig. 3.14 calls for a net flow of carbon dioxide from low to high latitudes. Approximately 2×10^{10} tons per year will have to be transferred into the ocean poleward of 30° in each hemisphere and 4×10^{10} tons per year will have to be released into the atmosphere by the tropical oceans. In the latter regions there should be a partial pressure of CO_2 of about 50 ppm above that of the atmosphere in order to accomplish such a transfer (see Fig. 3.12 for comparison).

The most likely value of K for large-scale mixing processes may also be determined from the observed seasonal variations of CO_2 (see Fig. 3.9). Most of this

variation, presumably, is caused by land vegetation and thus originates mainly in the northern hemisphere. In searching for that value of K which would give the largest values in the ratio of northern and southern hemisphere sources, Bolin and Keeling (1963) arrived at $K = 2.5 \times 10^{10} \text{ cm}^2/\text{sec}$, which is in close agreement with the value derived earlier from the annual mean distribution of CO_2 ($3.5 \times 10^{10} \text{ cm}^2/\text{sec}$). Taking the former value for K , the two authors arrived at the distribution with latitude

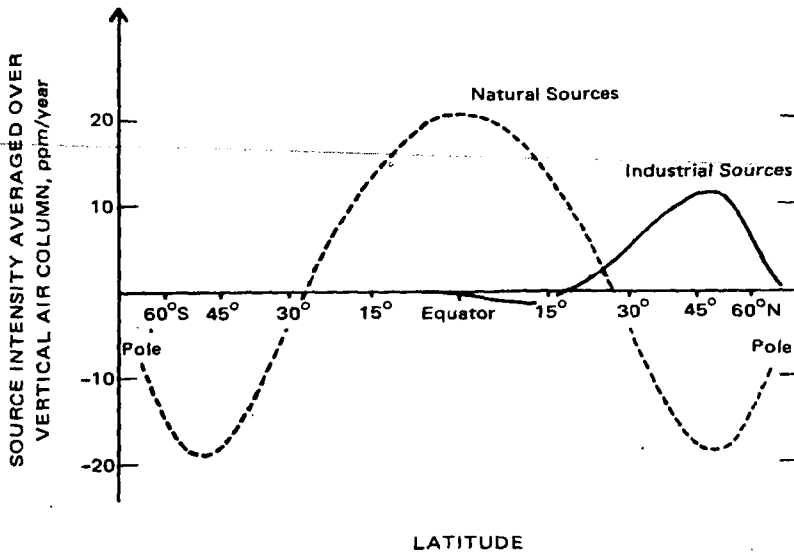


Fig. 3.14 Computed time-average sources and sinks of CO_2 as a function of latitude. The solid horizontal line (abscissa) gives the latitudinal average of the natural source function. The ordinate is in units of parts per million per year averaged over the total vertical air column. [From B. Bolin and C. D. Keeling, *Journal of Geophysical Research*, 68(13):3914 (1963).]

of the seasonally varying sources shown in Fig. 3.15. This diagram shows that the seasonal main sink in north polar latitudes acts only between June and August. In equatorial latitudes and in the southern hemisphere, seasonal sources and sinks are insignificant. The total sink north of 45°N during summer amounts to 1.5×10^{10} tons, which is about 0.5% of the total CO_2 of the atmosphere. This may be considered as the consumption of CO_2 by land vegetation north of 45°N during the vegetation period of summer. The agreement between Fig. 3.15 and the seasonal trends, evident from Table 3.1 and Figs. 3.4 to 3.6, is rather striking. The trend computed for the south pole overemphasizes the dip in September and October as compared with the data shown in Fig. 3.8. The maximum in November and December, however, is too small in Bolin and Keeling's model. Discrepancies are not large enough to affect Bolin

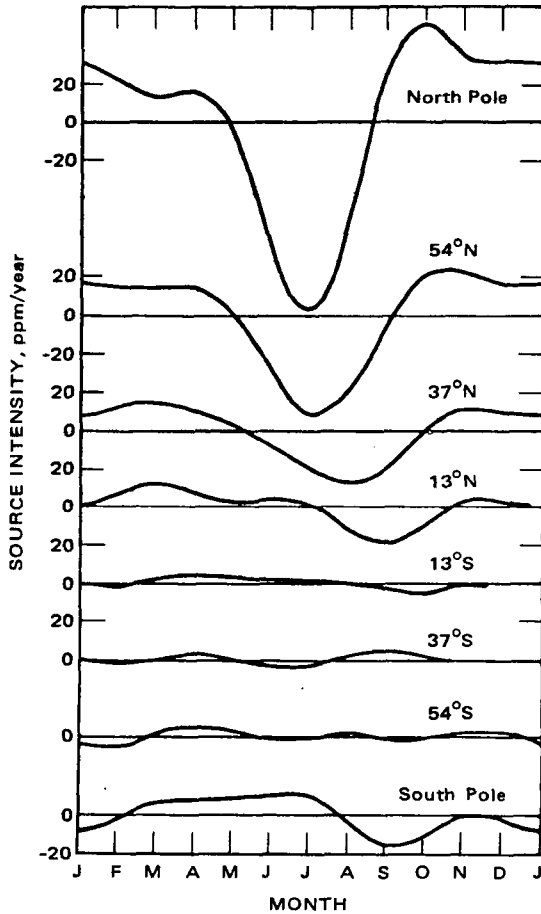


Fig. 3.15 Variation of the intensity of the CO_2 source with time for selected latitudes. Abscissa is in units of parts per million per year averaged over the total air column. [From B. Bolin and C. D. Keeling, *Journal of Geophysical Research*, 68(13):3918 (1963).]

and Keeling's reasoning. Junge and Czeplak's (1968) model of CO_2 variation produces reasonable results even at low southern latitudes. This is shown in Figs. 3.16 and 3.17 (c is the CO_2 concentration; see Eq. 3.3). The dotted line in Fig. 3.17 assumes K to be varying between approximately $1 \times 10^{10} \text{ cm}^2/\text{sec}$ at the equator to slightly more than $4 \times 10^{10} \text{ cm}^2/\text{sec}$ at 60° latitude and $2 \times 10^{10} \text{ cm}^2/\text{sec}$ over the pole.

The foregoing discussion indicates that, in spite of the complexity of source and sink distributions, CO_2 may serve as a tracer for large-scale atmospheric transport processes. In this chapter we have considered only the total CO_2 concentrations. Additional implications arise from the various isotopes of carbon (^{12}C , ^{13}C , and ^{14}C). These will be considered in more detail in Part 4.

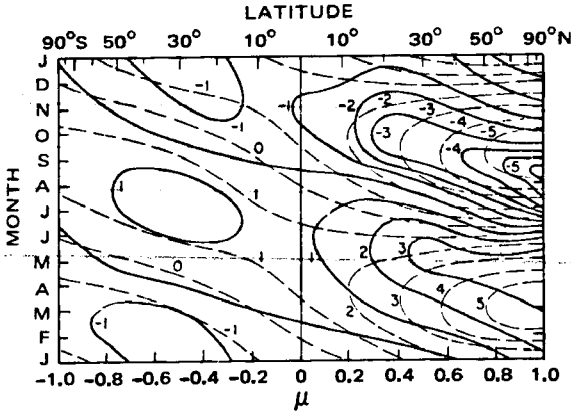


Fig. 3.16 Isopleths of the variation of CO₂ in parts per million as a function of time and geographic latitude. Solid lines, observed values according to Bolin and Keeling. Dashed lines, calculated $c(\mu, t)$ values for $K = 3 \times 10^{10} \text{ cm}^2/\text{sec}$ (c is the CO₂ concentration, μ is $\sin \phi$, where ϕ is the geographic latitude). [From C. E. Junge and G. Czeplak, *Tellus*, 20(3):428 (1968).]

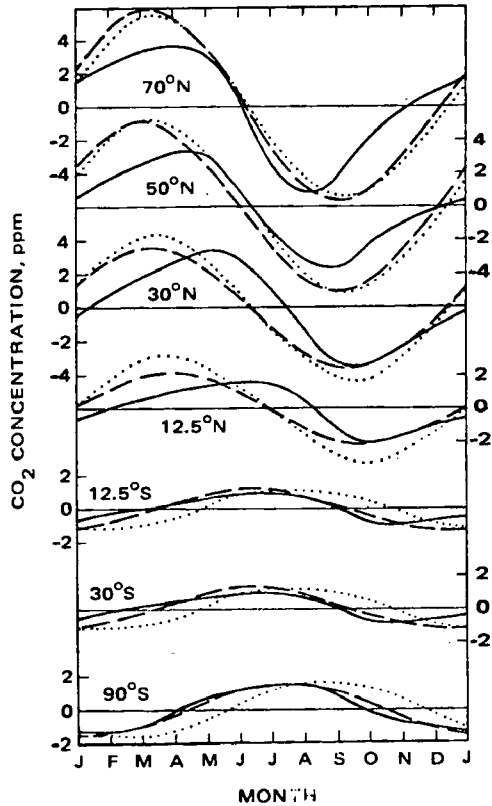


Fig. 3.17 Same as Fig. 3.16 but for discrete latitudes to show more detail. Solid lines are the observed values according to Bolin and Keeling (1963). Dashed lines are calculated $c(\mu, t)$ values for $K = 3 \times 10^{10} \text{ cm}^2/\text{sec}$. Dotted lines are calculated $c(\mu, t)$ values for varying K (see text). [From C. E. Junge and G. Czeplak, *Tellus*, 20(3):429 (1968).]

4 OZONE

Ozone, O_3 , plays an important role in the radiation and heat budget of the upper stratosphere and mesosphere. The temperature peak near 50 km, coinciding with the stratopause, is a direct effect of the absorption of ultraviolet radiation. [For infrared bands of ozone, see Hoffmann, 1967; the $9.6\text{-}\mu$ band was studied by Walshaw (1955); rotational bands at shorter wavelengths were considered by Caton et al. (1967). The $14.1\text{-}\mu$ infrared band of O_3 is the most intense.]

The long half-life of O_3 , especially in the lower stratosphere, makes it an ideal tracer of atmospheric motions. The main source of O_3 lies in the middle and upper stratosphere and in the mesosphere. (For global considerations, one can safely neglect small industrial sources of air pollution and generation by electric discharges in thunderstorms.) Its main sink is the earth's surface, continents as well as oceans (Junge, 1962a; Warmbt, 1965; Aldaz, 1969), as revealed by a downward gradient of $[O_3]$ near the earth's surface (Teichert, 1955; Kelley and McTaggart-Cowan, 1968). Junge (1963a) and, more recently, Dütsch (1969) have given excellent and comprehensive reviews of these tracer qualities. (For a short summary, see also Mirtov, 1964.) The subsequent résumé is restricted mainly to additional investigations not covered in these reviews.

Ozone, in addition to its usefulness as a tracer, has recently also received attention by aviation systems engineers and meteorologists. High-flying supersonic transport aircraft may be exposed to its adverse oxidizing effects. Crews and passengers may have to be shielded against its highly toxic qualities (Koch, 1961; Brabets, 1963; General Electric Co., 1963; Jaffe and Estes, 1963; Jurkevich, 1964; Berggren and Labitzke, 1966).

Umkehr measurements, described, for instance, by Mateer and Dütsch (1964) and R. A. Craig (1965), provide the bulk of information on the global distribution of O_3 (Dütsch, 1964). Even though the Mateer-Dütsch method appears to be superior to the "classical" approaches, the Umkehr measurements tend to yield smaller ozone concentrations at the level of the ozone peak than measurements made by ozone soundings (Bojkov, 1966; R. A. Craig, DeLuisi, and Stuetzer, 1967). The Umkehr method also appears to be susceptible to the presence of haze (DeLuisi, 1967, 1969; Kulkarni, 1968b). Measurements with the ozonometer M-83, carried out mainly in the Soviet Union, show about 6% less total ozone at solar angles less than 57° and about 20 to 30% more ozone at solar angles greater than 60° than equivalent measurements with the Dobson spectrophotometer (Bojkov, 1969a). According to a theoretical study by Dave and Mateer (1967), satellite measurements of ozone with a modified Umkehr method are within the realm of feasibility (see also Herman and Yarger, 1969; Sellers and Yarger, 1969; Twomey, 1969; Iozenas et al., 1969a, 1969b). The first successful attempts to determine ozone profiles from the NIMBUS III IRIS (Infrared Interferometer Spectrometer) records at 9.6μ have been reported by Prabhakara (1969a, 1969b). Such measurements might eventually provide a more continuous monitoring system of atmospheric O_3 than ground-based sensors and soundings. It would exceed the scope of this monograph to present details on ozone measurement techniques and problems associated therewith.

THE CHEMISTRY AND PHOTOCHEMISTRY OF OZONE

The photochemical and chemical reactions leading to ozone generation and destruction are listed in Tables 1.6 and 1.7 for a "moist" atmosphere (Hunt, 1966a; Hessvedt, 1967b, 1968a; Leovy, 1969; Crutzen, 1969). Additional details as to the electronic excitation state of O and O_2 in these reactions can be taken from recent papers by Chamberlain (1961), Schiff and Megill (1964), Hunt (1965, 1966b), McGrath and McGarvey (1967), Wayne (1967), and LeLevier and Branscomb (1968). Reactions with nitrogen have not been included in Hessvedt's table. The effect of such reactions has been considered in detail for a "dry" atmosphere by Keneshea (1962, 1963, 1967) (see also Cadle, 1963; Barth, 1964; Schiff, 1964; Batey et al., 1965; Fehsenfeld et al., 1965a, 1965b, 1965c; Brewer, 1966; Hunten and McElroy, 1966; McGrath and McGarvey, 1967). In a dry atmosphere, photodissociation of oxygen (reactions 4a and 4b in Table 1.6) and the three-body collision given in reaction 2 are mainly responsible for the generation of O_3 and photodissociation (reactions 5a and 5b), as well as the three-body collision of reactions 3 and 35, for its destruction (Hessvedt, 1963; Dütsch, 1969). In addition, reactions 4a and 4b and 1 are important in a "dry" atmosphere (Blankenship and Crutzen, 1966). As is clearly evident from this table, hydrogen components play an important role (Crutzen, 1969; Leovy, 1967, 1969; Newell, 1967, 1968a). The presence of the hydroxyl group, OH, as shown, for instance, in reaction 24, has been demonstrated from airglow measurements.

Dütsch (1969) pointed out that, owing to the slow reactions of O_3 in the lower stratosphere, ozone becomes an ideal tracer element at these levels. There O_3 is more conservative than any of the "hydrodynamic tracers," such as potential temperature or potential vorticity. This is brought out by the so-called relaxation time or time of half-restoration, i.e., the time needed for a nonequilibrium concentration $[O_3]$ to approach the photochemical equilibrium concentration by one-half of the value of the original discrepancy. Typical values are shown in Table 4.1.

Table 4.1
TIME OF HALF-RESTORATION (τ) OF O_3 *

Height, km	Latitude, °N						
	0		45		60		80
	Summer	Summer	Winter	Summer	Winter	Summer	
	$\tau = \text{Hours}$						
50	1.5	1.4	2.7	1.8	5.3	1.8	
45	3.9	3.3	8.0	4.7	18.1	5.5	
40	13.6	12.5	36.1	17.8	86.2	20.9	
	$\tau = \text{Days} = \frac{\text{Number of hours}}{\text{Number of sunlit hours per day}}$						
35	5.8	4.0	23	4.5	121	4.3	
30	35	23	151	26	804	25	
25	254	162	1.2×10^3	166	3.5×10^3	173	
20	3.2×10^3	1.5×10^3	7.1×10^3	1.4×10^3	1.6×10^4	1.4×10^3	
15	10^5	2.7×10^4	5.2×10^4	2.4×10^4	8.6×10^4	1.6×10^4	

*From H. U. Dütsch, *World Survey of Climatology*, Vol. IV, H. Landsberg (Ed.), p. 388, Elsevier, Amsterdam, 1969.

Although, in general, we may assume that ozone has a source in the stratosphere and a sink at the ground, there may be localized regions in the lower troposphere where ozone is formed in polluted, urban atmospheres by photochemical reactions involving hydrocarbons and oxides of nitrogen (Bartel and Temple, 1952; Haagen-Smit, 1958; Renzetti, 1959; Wanta et al., 1961; Ripperton, 1965). Irradiation of aldehydes, for instance, leads to the production of ozone (Leighton, 1961). Plant damage and eye irritation have been observed as a consequence of oxidizing effects of O_3 in air pollution (Mukammal, 1963; Davis and Dean, 1966). The damaging effects of ozone on plants appear to increase with increasing relative humidity and with the presence of moisture on the leaves (Leone and Brennan, 1969).

An example of pollution-produced ozone in a low-level inversion is given in Fig. 4.1. This diagram shows an "ozonogram" designed and described in detail by Godson (1962). As we shall see later, O_3 may be treated as a quasi-conservative air-mass property at tropospheric levels. The spectacularly high concentrations of O_3 or, more properly, of total oxidant shown in Fig. 4.1 within the temperature inversion

above the ground cannot be explained by subsidence of a stratospheric air mass. If the latter were the case, a direct descent without mixing from the 75-mb level would have to be postulated, an impossibility if the enormous range of diabatic cooling that would be required to accomplish such a vertical transfer of air is considered. Lea (1968)

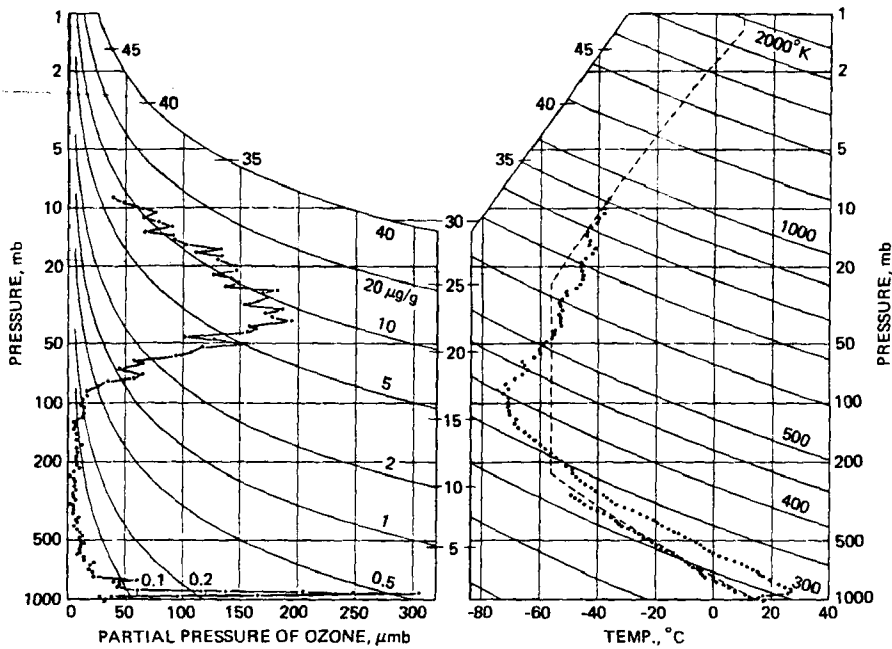


Fig. 4.1 Ozonagram for Point Mugu sounding, 0925 PST (1725 GMT) Oct. 7, 1965. (a) Ozone partial pressure; sloping curves are lines of equal ozone mixing ratio ($\mu\text{g/g}$). (b) Temperature and dew-point temperature; sloping curves are lines of equal potential temperature ($^{\circ}\text{K}$). [From D. A. Lea, *Journal of Applied Meteorology*, 7(2):255 (1968).]

considered the Los Angeles air pollution basin as a likely source of these high ozone values (see also Miller and Ahrens, 1969). According to Fig. 4.2, a correlation seems to exist between the metropolitan population (Bureau of Census, 1967), which produces air pollutants, and the frequency with which high $[\text{O}_3]$ values are observed in low-tropospheric inversions.

Ozone measurements within a growing plant canopy away from industrial pollution sources indicate that, especially during fall, the olefins emitted by plants (noticeable by their fragrance) may be decomposed by photochemical oxidation (Rasmussen, 1965). During this process, ozone may be formed, leading to a gradient of $[\text{O}_3]$ that is directed upward immediately above plant canopy level (Kelley and McTaggart-Cowan, 1968).

Figure 4.1 also shows that, in spite of the extremely high partial pressures of O_3 reached in the contaminated air of the temperature inversion, mixing ratios still remain

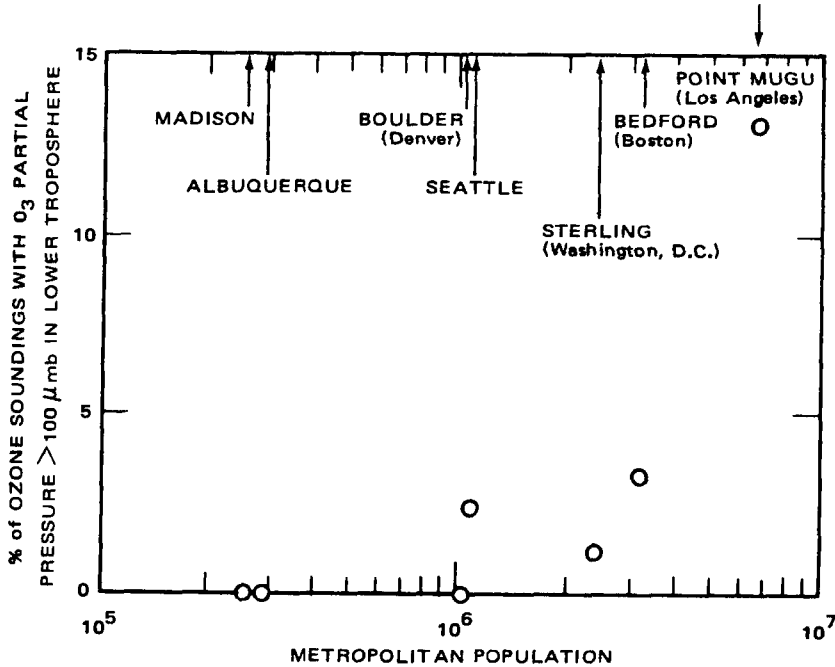


Fig. 4.2 Percent of soundings with an ozone maximum in lower troposphere exceeding 100 μmb vs. population of a nearby metropolitan area. [From D. A. Lea, *Journal of Applied Meteorology*, 7(2):257 (1968).]

much smaller than those observed in the stratosphere. Therefore, even with the existence of localized low-level sources of O₃, the major use of ozone as a tracer of atmospheric motions will be derived from the stratospheric source. Mesoscale motion patterns and trajectories in the lower troposphere in the vicinity of urban sources of O₃ may, however, be studied in some detail by utilizing measurements such as those reported by Lea (1968).

Ozone production by thunderstorms (lightning discharge) may be considered as a tropospheric source, but its effectiveness is still under dispute (Dobson et al., 1946; Dufay, 1949; Buettner et al., 1962; Kroening and Ney, 1962; Ney and Kroening, 1962; Orville, 1967), especially in view of the high temperatures within the ionized lightning channel.

THE VERTICAL DISTRIBUTION OF OZONE

Photochemical Theory

The vertical distribution of O₃ can be computed from the reactions listed in Table 1.6 if we assume that photochemical equilibrium prevails at each level. If we

neglect the presence of hydrogen compounds, and reactions with them, and neglect certain other small terms (see Dütsch, 1969), this equilibrium concentration of O_3 can be written as

$$[O_3] = [O_2]^{3/2} \sqrt{\frac{J_2 k_2}{J_3 k_3} s} \quad (4.1)$$

where $s = [M]/[O_2]$, M standing for air molecules. Brackets without subscripts written around chemical symbols signify concentrations of this chemical compound. The symbols J_2 , J_3 , k_2 , and k_3 are the dissociation and reaction rates defined in Table 1.6. (Small adjustments in the values of J_2 reported in Table 1.7 may be in order, incorporating the results of intensity measurements of direct radiation in the 2100 Å window by Brewer and Wilson, 1965.)

From the distribution of the quantities given in Eq. 4.1 with height, O_3 attains maximum concentrations between 20 and 25 km. Below these levels the dissipation, J_3 and k_3 , which is active in the near-ultraviolet and visible light, dominates over the formation processes J_2 and k_2 , leading to a rapid decrease of $[O_3]$ with decreasing altitude [Fig. 4.3(a)].

Table 4.1 shows that with decreasing height O_3 becomes an increasingly stable trace substance. Long relaxation times, or times of half-restoration, τ , will be needed before departures in $[O_3]$ will approach photochemical equilibrium conditions (Dütsch, 1956). These relaxation times exceed the seasonal variations of J_2 , J_3 , and k_2 , especially in the lower stratosphere. At these levels Eq. 4.1 still holds for an indication of instantaneous O_3 concentrations but not for seasonally averaged values, which will not be in photochemical equilibrium. Distributions of $[O_3]$, allowing for values of τ given in Table 4.1, are shown in Fig. 4.3(b). Discrepancies between these nonequilibrium values, as compared with those obtained from photochemical equilibrium [Fig. 4.3(a)], are appreciable in the lower stratosphere, where τ is comparable to, or larger than, the period of the seasonal forcing function (for details, see Dütsch, 1969).

Blankenship and Crutzen (1966) reported on an equilibrium model of $[O_3]$ distribution, based on the assumption of an infinite day, and on a nonequilibrium model that contains time-dependent concentrations of oxygen atoms and molecules and of ozone. Discrepancies between the two models are large, especially in predicting the latitude dependence of the ozone maximum.

The nonequilibrium theory of ozone distribution does not yet take into account any transport processes. These will modify actual O_3 concentrations drastically from those shown in Fig. 4.3, especially in regions in which vertical or horizontal flow components, or both, of mean and eddy motions have magnitudes comparable to, or larger than, L/τ , where L is the vertical or horizontal distance over which these flow processes are active and τ is the time of half-restoration. Since this will be the case, especially in the middle and lower stratosphere, actually observed $[O_3]$ distributions and their comparison with the theoretical ones shown in Fig. 4.3(b) will serve as valuable indicators of large-scale stratospheric motion patterns (Brewer, 1949; Martin,

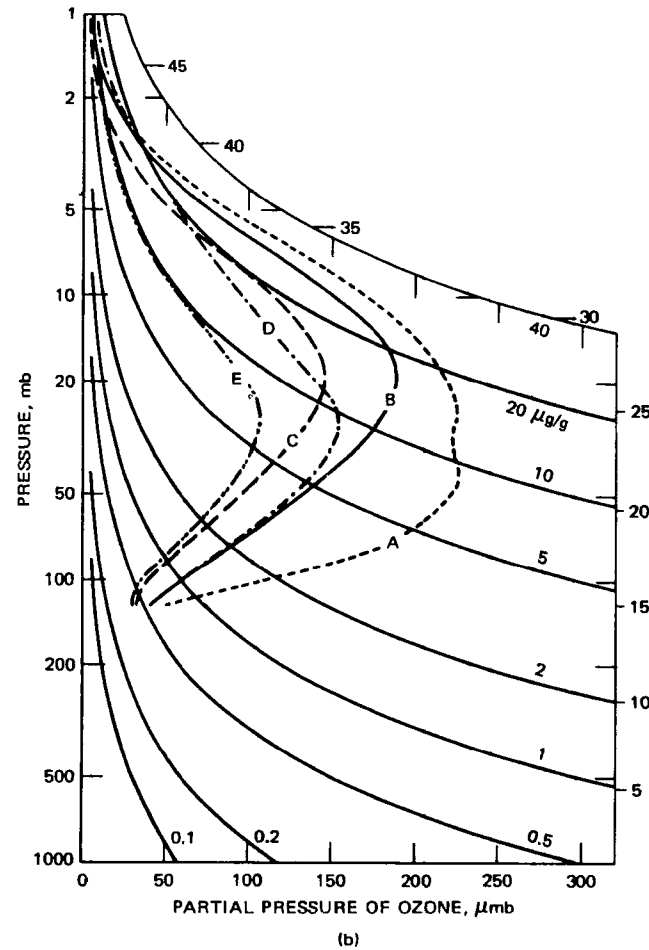
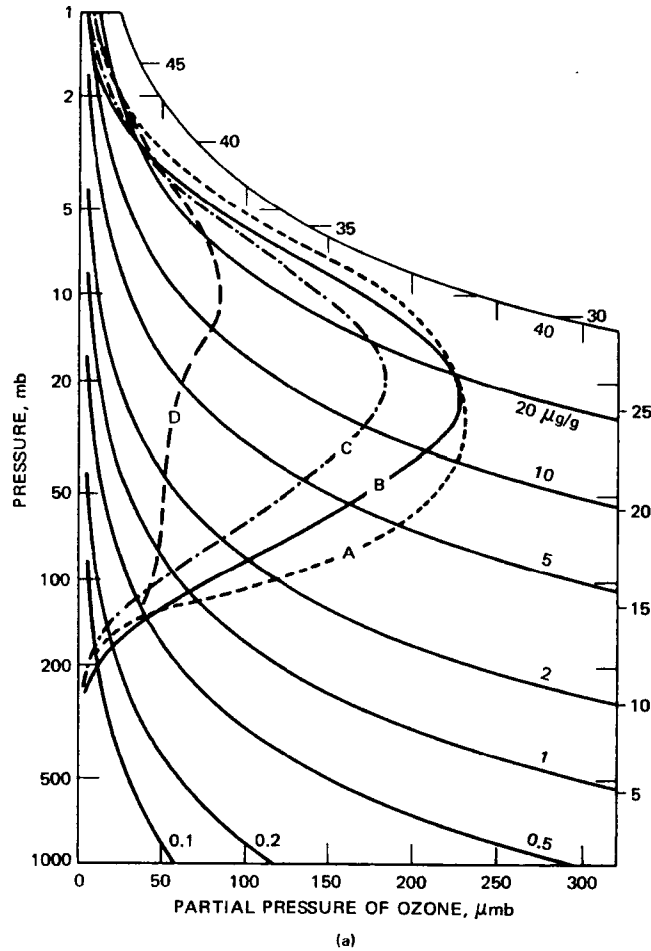


Fig. 4.3 Vertical ozone distribution according to (a) photochemical equilibrium theory and (b) photochemical nonequilibrium theory. A, equator, June; B, 45°N, June; C, 60°N, June; D, 45°N, December; E, 60°N, December. (From H. U. Dütsch, *World Survey of Climatology*, Vol. IV, H. Landsberg (Ed.), p. 387, Elsevier, Amsterdam, 1969.)

1956; Dütsch, 1960; Paetzold and Piscalar, 1961; Bolin, 1964; Byron-Scott, 1967; Craig and Clark, 1969; Gebhart, 1968; Brewer and Wilson, 1968).

The photochemical theories described do not yet take into account the important reactions with hydrogen compounds. Leovy (1967) pointed out that reactions 6, 7, 9, 23, 24, and 29 in Table 1.6 drastically influence the time constants given in Table 4.1. (For a summary of "moist" reactions influencing ozone, see also Dütsch, 1968; Mitra, 1969; Brewer and Wilson, 1968.) Especially at levels above the ozone peak, a "modified" photochemical theory, taking into account these hydrogen reactions, tends to reduce the time constants appreciably (Fig. 4.4). Figures 4.5 and

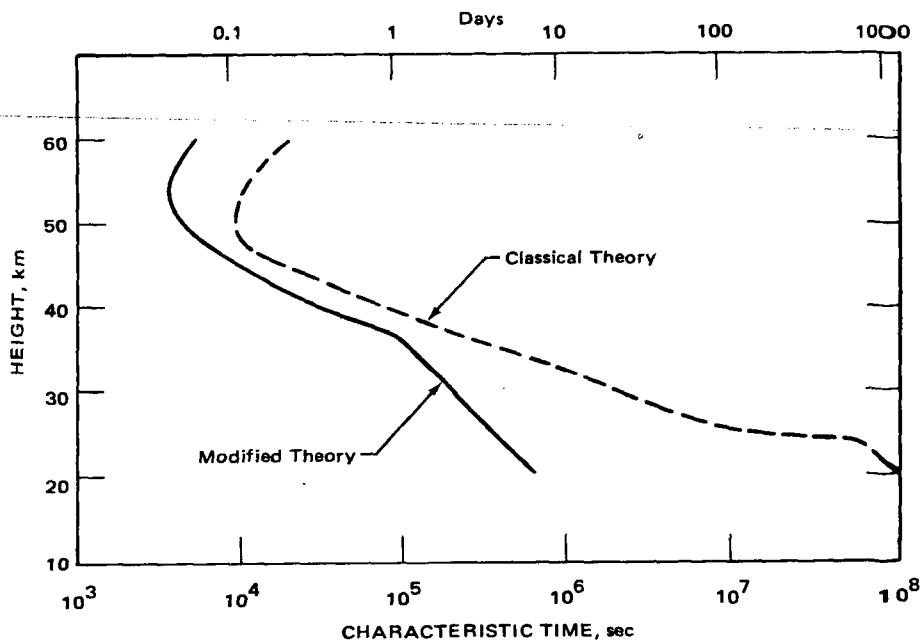


Fig. 4.4 Photochemical time constants for ozone based on the classical and modified theories, assuming vertically overhead sun. The reaction rates used to compute these times are those used by Hunt (1966a). [From unpublished data by C. Leovy (1967).]

4.6 show that the incorporation of hydrogen reactions also produces better agreement with observations of heating rates and ozone number densities than the classical theory of a "dry" atmosphere. Hunt (1969) (see also Hunt and Manabe, 1968) demonstrated that the inclusion of hydrogen reactions made the O_3 distribution obtained from an 18-level general-circulation model more realistic.

Observations from Sondes

Measurements from the North American Ozonesonde Network (Hering, 1964; Hering and Borden, 1964, 1965a) and earlier observations (e.g., Brewer, 1960) quite

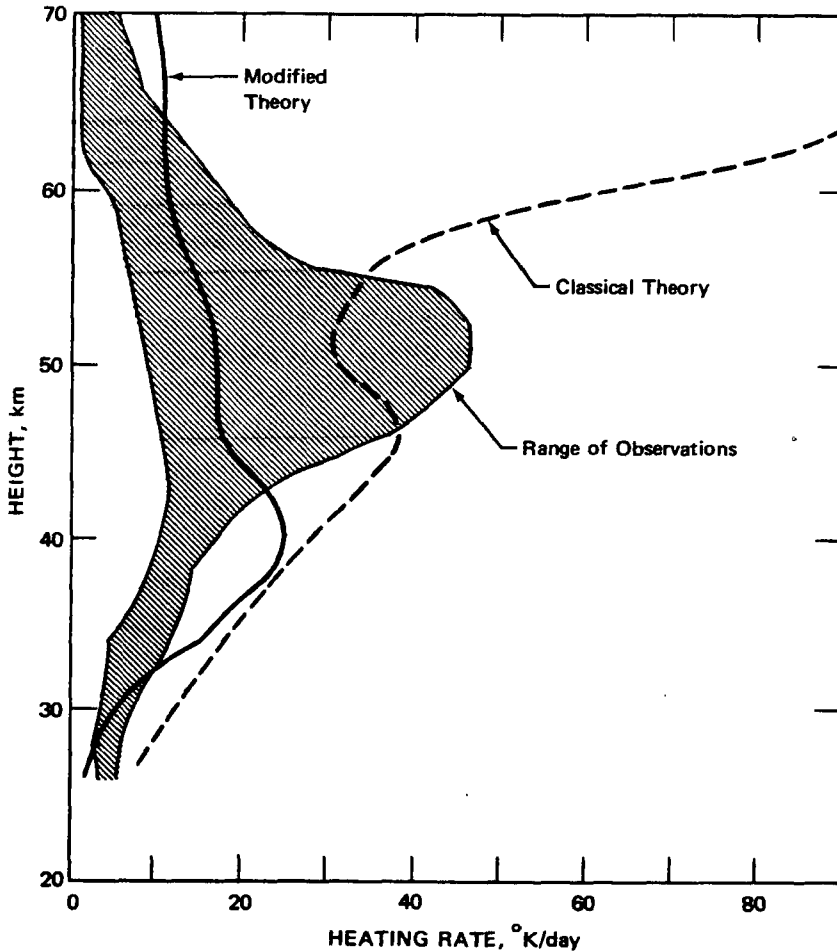


Fig. 4.5 Heating rates for different ozone number densities, assuming vertically overhead sun. The shaded area corresponds to the observational range of ozone number densities entering into the calculations. The solid and dashed curves correspond to the respective number densities shown in Fig. 4.6. The heating effect of scattered radiation has been neglected. [From unpublished data by C. Leovy (1967).]

distinctly reveal deviations of ozone concentrations from theoretical values (for a data summary, see Bojkov, 1969b). As an example, Fig. 4.7 shows overlapping bimonthly averages of the vertical ozone distribution for Albrook Field, Canal Zone (9.0°N , 79.6°W); Tallahassee, Fla. (30.4°N , 84.3°W); Albuquerque, N. Mex. (35.0°N , 106.0°W); and Fort Collins, Colo. (40.6°N , 105.1°W) (Hering and Borden, 1965b). In comparing these diagrams with Fig. 4.3, we find the following noteworthy results:

1. Maximum concentrations of O_3 are reached in temperate latitudes and not on the equator.

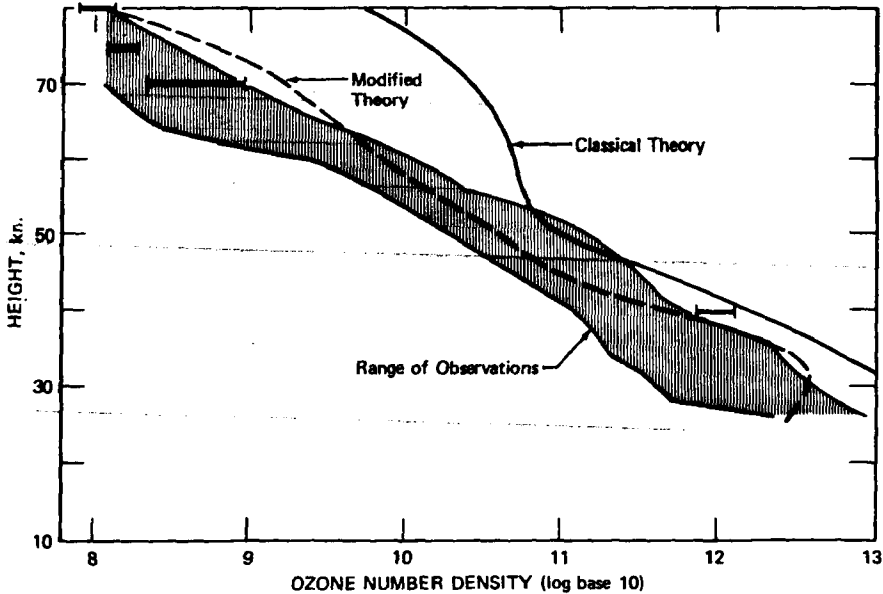


Fig. 4.6 Observational range in ozone number densities (shaded area) and observations by Rawcliffe et al. (1963) (bars) and by Rawcliffe and Elliott (1966). The theoretical curves are based on calculations by Hunt (1966a) for classical photochemistry and for photochemistry modified to allow for reactions involving $O(^1D)$ and H_2O . [From unpublished data by C. Leovy (1967).]

2. The altitude of the observed ozone peak over Albrook Field lies near 25 km instead of 21 km as suggested by curve A of Fig. 4.3(b). Actually, the photochemical equilibrium theory seems to predict the location of the peak in equatorial regions somewhat better than the nonequilibrium theory. This observed upward shift in the peak location can be explained by ascending air motions in the lower and middle stratosphere over the equator.

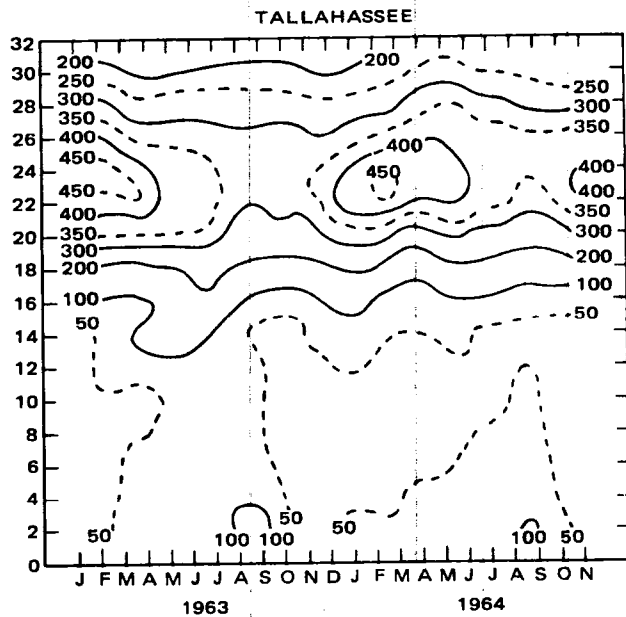
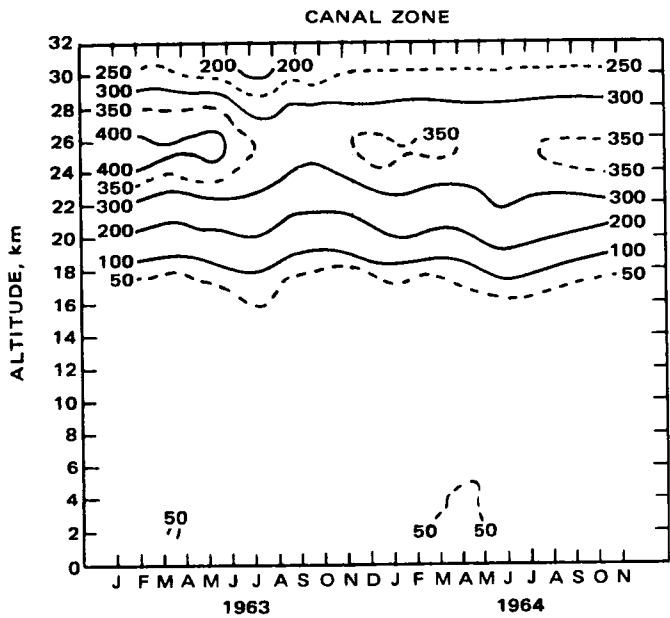
3. The altitude of the ozone peak decreases with increasing latitude. This is not indicated in Fig. 4.3(a) or (b) for the latitudes represented in Fig. 4.7. Again we may take recourse to the vertical-motion pattern, described in Part 1, Chap. 3, to explain the discrepancies between theory and observations. Descending motions and downward mixing (see also Fig. 1.16) account for the decreased altitude of the ozone peak.

4. The ozone peak lies higher in autumn (near 23 km over Fort Collins) than in winter and spring (near 21 km). Such an altitude shift is expressed in the nonequilibrium theory only at higher latitudes. The equilibrium theory indicates a shift in the opposite direction. Observations in the southern hemisphere (Christchurch, New Zealand, $43^\circ S$, $172^\circ E$) reveal shifts in the level of the ozone peak similar to those in the northern hemisphere (Bojkov and Christie, 1966; Bojkov, 1967b). The secondary maximum near 13 km, shown over Fort Collins in spring (Fig. 4.7), which accounts for a considerable fraction of the spring increase in total ozone, was also found over Christchurch.

5. The nonequilibrium theory yields maximum $[O_3]$ at the altitude of the ozone peak (near 26 km or 20 mb) and at $45^\circ N$ during July and August and minimum $[O_3]$ during February and March (Dütsch, 1969). (The longer lag in the occurrence of the minimum after the solistices is explained by the less rapid dissociation of O_3 as compared with the formation processes leading to the summer peak.) Figure 4.7, however, shows maximums of ozone in February and March in middle latitudes [and around March and April in polar latitudes, according to Dütsch (1969)], and minimums around September and October (see also Shimizu, 1962; Paetzold, 1955; Iozenas et al., 1969a, 1969b). Over Mirny, Antarctica, the maximum in total ozone was observed in October and November and the minimum in April (Skeib and Popp, 1961; see also Wexler et al., 1960; A. Vassy, 1962). More details on hemispheric differences will be given later in this chapter. These data indicate a slight retardation in the occurrence of ozone maximums and minimums over the south polar regions as compared with the northern hemisphere. As mentioned in Part 1, Chap. 3, no sudden midwinter breakdowns in the Antarctic stratospheric vortex have been observed. Since such breakdowns, frequent in the northern hemisphere, lead to major increases in O_3 , the delay in the spring maximum of ozone over the south pole may find its explanation. Not only is the observed ozone distribution (Fig. 4.7) almost 180 degrees out of phase with the theoretical one but also there is not much difference in the time lags of observed maximums and minimums behind the solistices. This, again, indicates that horizontal and vertical transport processes in the stratosphere completely overshadow the photochemical processes in a stationary atmosphere. The decrease in meridional transport processes during spring obviously reduces the supply of O_3 from low latitudes by a larger amount than the increased zenith angle of the sun and increased photochemical production *in loco* could make up for.

6. The extension of high $[O_3]$ values into the lower stratosphere during spring, which in Fig. 4.7 is strongly evident over Fort Collins, is an indicator of the downward mixing processes that take place during this season (see also Paetzold, 1955). As shown in Part 1, Chap. 3, as the stratospheric polar night vortex collapses, descending motions are well developed in the middle and lower stratosphere of middle latitudes (see also Vincent, 1968). These motions carry high ozone concentrations into the vicinity of the tropopause. Here they may be transported into the troposphere by intrusion processes associated with jet streams. The spring maximums of radioactive fallout and of ozone observed in temperate latitudes thus find their physical explanation.

There is a chance that the data of Fort Collins shown in Fig. 4.7 reveal unusually large downward mixing processes. This station is located east of the Rocky Mountains, where frequent cold outbreaks associated with deep upper troughs would enhance downward motions in the stratosphere. This is indicated by the total global ozone distribution, expressed in Dobson units (i.e., the thickness of the equivalent layer of pure O_3 at normal temperature and pressure, expressed in units of 10^{-3} cm), shown in Fig. 4.8 (London, 1962, 1963a). Even from a qualitative inspection of these diagrams we find, besides the well-documented spring maximum of ozone, that eddy motions,



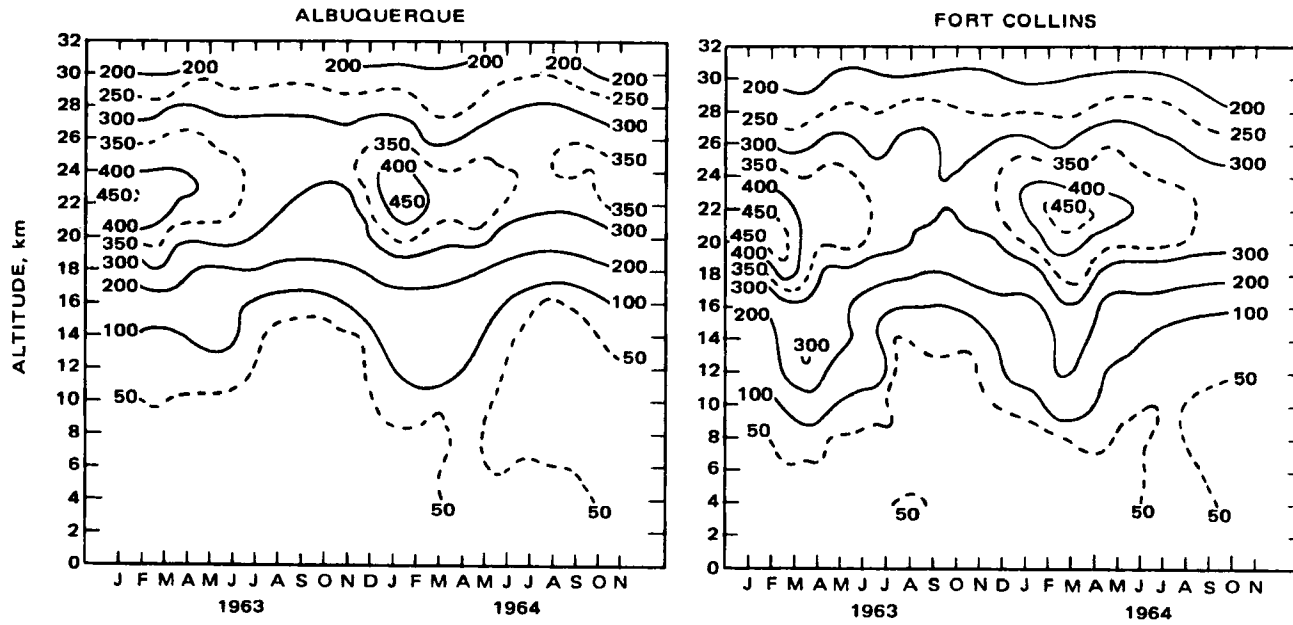
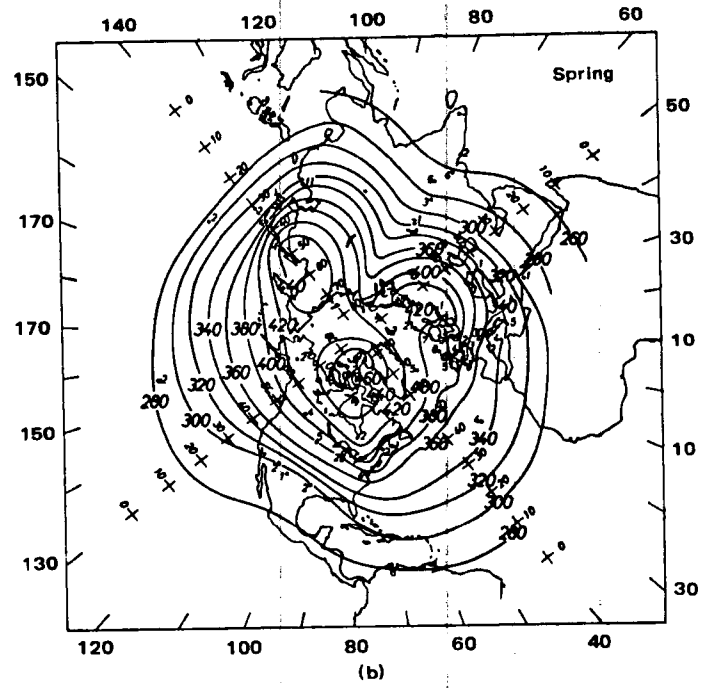
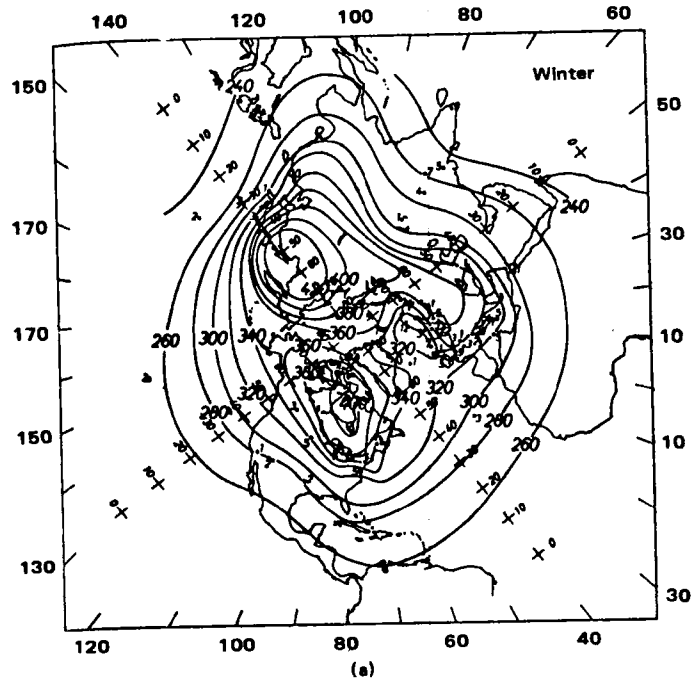


Fig. 4.7 Mean bimonthly distribution of ozone density ($\mu\text{g}/\text{m}^3$) at (a) Albrook Field, Canal Zone, (b) Tallahassee, Fla., (c) Albuquerque, N. Mex., and (d) Fort Collins, Colo., 1963-1964. [From W. S. Hering and T. R. Borden (1965b).]



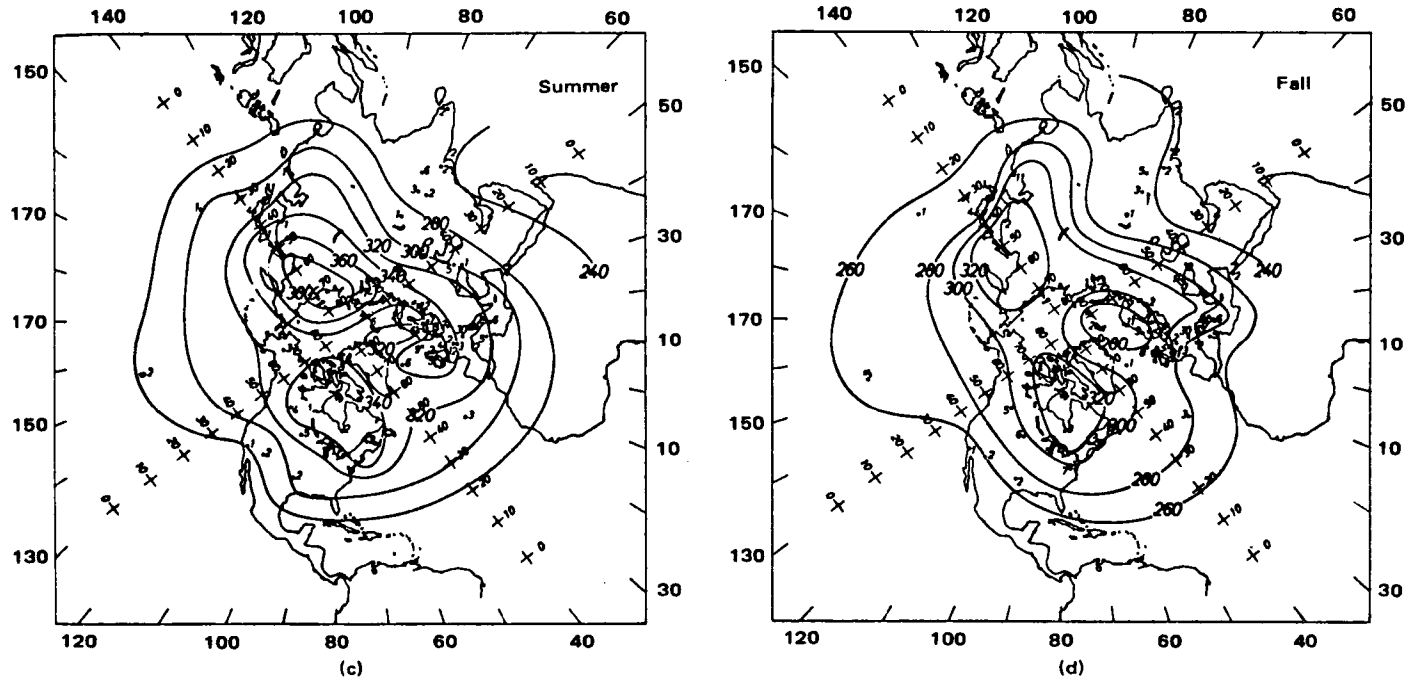
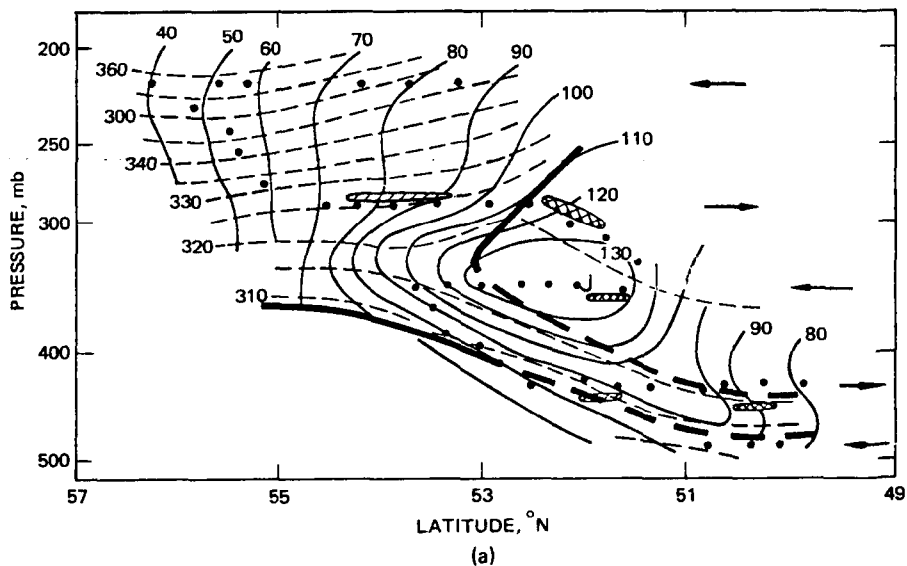


Fig. 4.8 Distribution of total ozone in the northern hemisphere (1926 to 1959). Dobson units (10^{-3} cm standard temperature and pressure). (a) Winter. (b) Spring. (c) Summer. (d) Fall. The numbers at each station represent the number of years for which data are available. [From J. London, *Beitraege zur Physik der Atmosphaere*, 36: 257 (1963).]

especially in hemispheric wave numbers 2 and 3, play a dominant role in horizontal and vertical ozone transport. The location of the three ozone maximums agrees closely with the major troughs in the upper-tropospheric mean flow patterns and with descending motions in the lower stratosphere (Miller, 1967). These stationary troughs, which appear in monthly and seasonal mean maps, are a manifestation of orographic forcing of the planetary wave pattern (see Part I, Chap. 4). From the ozone distribution shown in Fig. 4.8, we may conclude that this forcing persists well into the middle stratosphere. The three maximums of total O_3 evident from this diagram may be explained only by a combination of horizontal advection of O_3 from low latitudes with downward transport at, and below, the level of the ozone peak (as, for instance, postulated by Molla and Loisel, 1962). Thus one is forced to conclude that large-scale vertical motions in the "ozonosphere" are still, to a great extent, forced by the tropospheric flow and its orographic controls. Distribution patterns quite similar to those deduced from Figs. 4.7 and 4.8 may be expected to hold for radioactive contaminants injected into the middle and lower tropical stratosphere.

Detailed Vertical Ozone Distributions and Short-Term Variations.

Short-term variations in ozone concentrations also are strongly influenced by transport processes (R. J. Reed, 1950). Intrusions of stratospheric air into the troposphere near the jet stream favor the stable region (jet-stream front) underneath the jet core. Since stratospheric air, on the average, contains larger amounts of ozone than tropospheric air, large-scale mixing processes across the tropopause will reveal themselves in characteristic details of the vertical and horizontal ozone distribution (Penn, 1964).



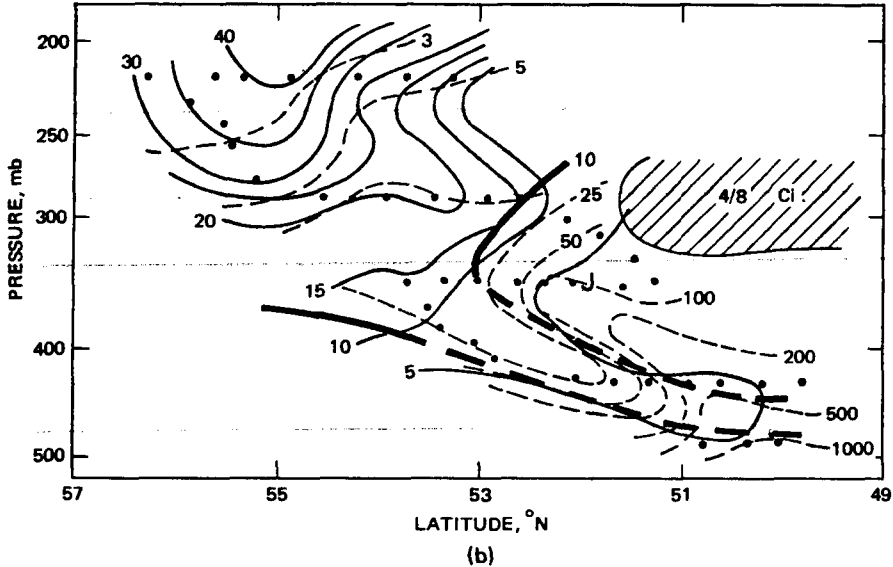


Fig. 4.9 Analysis of aircraft observations on flight of May 8, 1961. In both figures the heavy solid line indicates the tropopause, the heavy dashed line defines the jet-stream front "J" represents the jet axis, and the dots are points of observation.

- (a) ———, isotachs (kt).
- , potential temperature ($^{\circ}$ K).
- ▨▨▨, slight clear-air turbulence.
- ▩▩▩, moderate clear-air turbulence.
- Arrows and dots indicate flight path of aircraft.
- (b) ———, ozone mixing ratio (parts per hundred million).
- , humidity mixing ratio (μ g/g).
- A broken cloud deck of $\frac{4}{8}$ of cirrus is indicated by hatching.

[From J. Briggs and W. T. Roach, *Quarterly Journal of the Royal Meteorological Society*, 89(380): 241 (1963).]

Figure 4.9 shows cross sections of wind, potential temperature, and ozone and humidity mixing ratios across a jet stream blowing from the west-northwest over England (Briggs and Roach, 1963). The downward mixing in the jet-stream front, mainly along isentropic surfaces, is clearly evident from the "tongues" of relatively high ozone mixing ratios, high potential vorticity values, high radioactivity counts, and low humidity in this stable layer (see also Berggren and Labitzke, 1966; Danielsen, 1968; and statistical evidence presented by Pittock, 1969). Using the same reasoning that stratospheric air intrusions into the troposphere should be identifiable by higher-than-normal $[O_3]$ values, Penn (1965, 1966) has investigated the ozone distribution over hurricanes. Horizontal gradients of $[O_3]$ above cloud level, measured by U-2 aircraft, are only small, indicating that there is no significant "downward sucking" of stratospheric air in the hurricane eye.

Figure 4.9 shows also that ozone and humidity concentrations remain fairly constant in the upper portion of the jet-stream front (see, for comparison, Berggren,

1965; Sticksel, 1966). This would suggest that the vertical and horizontal transport processes caused by the dynamics of the jet stream in this region by far overshadow the smaller scale turbulent mixing processes with the air adjacent to this baroclinic zone. This conclusion is corroborated by the facts that potential vorticity is well conserved in such layers within time periods of synoptic scale and that isentropic trajectories portray the air motions in such layers to a high degree of accuracy (Danielsen, 1961, 1964, 1968; E. R. Reiter, 1963a, 1963b; E. R. Reiter and Mahlman, 1964a, 1964b, 1965a; Mahlman, 1965a; for further details see part 3 of this review). Both potential vorticity conservation and isentropic trajectory analyses would have to be modified under diabatic mixing processes. The negligible effects of such mixing during the early life history of the intrusion process, however, are evident from Fig. 4.9 and also from other case studies reported in the literature.

A hypothetical ozone sounding placed, for instance, at 51°N in Fig. 4.9 would reveal significant variations of $[O_3]$ in the vertical. There would also be a certain correlation between thermal stability and ozone concentrations. Such correlations have been found time and time again in detailed measurements of the vertical O_3 distribution (Hering, 1964; Hering and Borden, 1964, 1965a, 1967; Berggren, 1965; Breiland, 1968; Breiland and May, 1969). Breiland (1964, 1967) has pointed toward the fact that vertical details in temperature and in the wind field frequently are related to changes in $[O_3]$ (see also Dütsch, 1963). Especially on occasions when a polar and an extratropical tropopause are present simultaneously, the vertical ozone distribution may turn out to be a conglomerate of tropical conditions in its upper portion and of mid-latitude conditions in its lower part (Breiland, 1965, 1969).

Figure 4.10 shows typical cases of vertical ozone distributions governed by advective processes. A corresponding vertical cross section through the atmosphere from Tatoosh Island, Wash. (TTI), to Brownsville, Tex. (BRO), is given in Fig. 4.11. The three ozone soundings shown in Fig. 4.10 reveal a distinct maximum of O_3 near, or slightly above, 200 mb. According to Fig. 4.11, the extratropical tropopause is found near this level. The second ozone maximum near 50 mb over Albuquerque (ABQ) lies above the tropical tropopause. An inspection of the latter sounding, for instance, reveals a close agreement between a secondary maximum of O_3 near 300 mb and a shallow stable layer near 325°K in the University of New Mexico (UNM) sounding. At Fort Collins (FCL) this layer was located slightly higher in a semistable region near the 250-mb level just below the extratropical tropopause. Only a small "nose" appears on the ozone sounding at this station. Over Fort Collins, however, this "nose" has a mixing ratio of O_3 , almost the same as that over Albuquerque. Even though no baroclinic layers or frontal zones have been marked in Fig. 4.11, we can conclude that this lowest secondary ozone maximum at FCL and ABQ lies in the stable "jet-stream front," as was the case in Fig. 4.9.

Comparing smaller details in the ABQ ozone sounding above 200 mb with the temperature soundings of ABQ and UNM, we find that small ozone maximums tend to occur in layers with temperatures slightly higher than those found in adjacent regions. This, again, suggests the presence of strong advective controls on the stratospheric ozone distribution within the baroclinic layer above the tropopause jet stream.

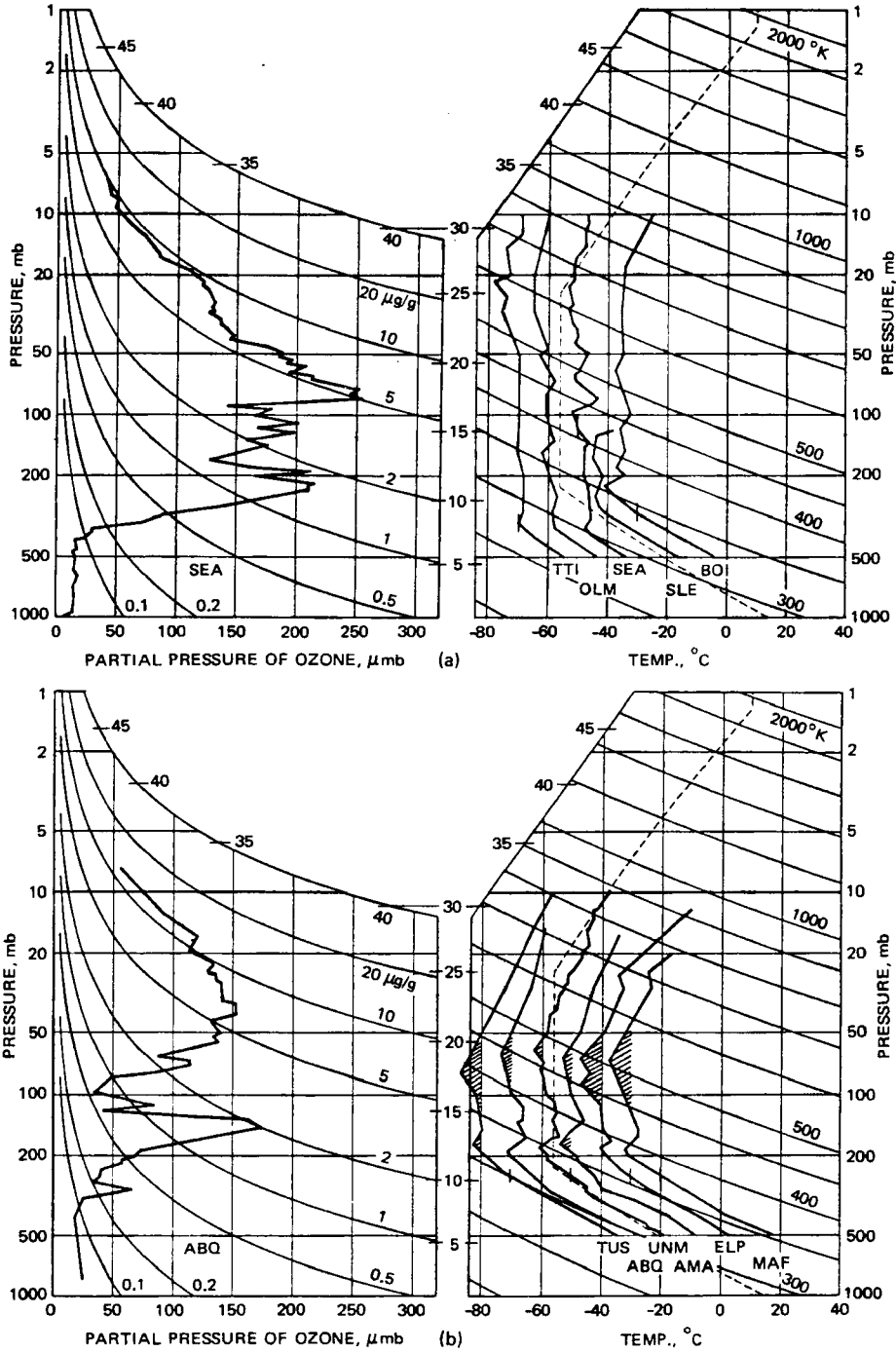


Fig. 4.10 (See page 132 for legend.)

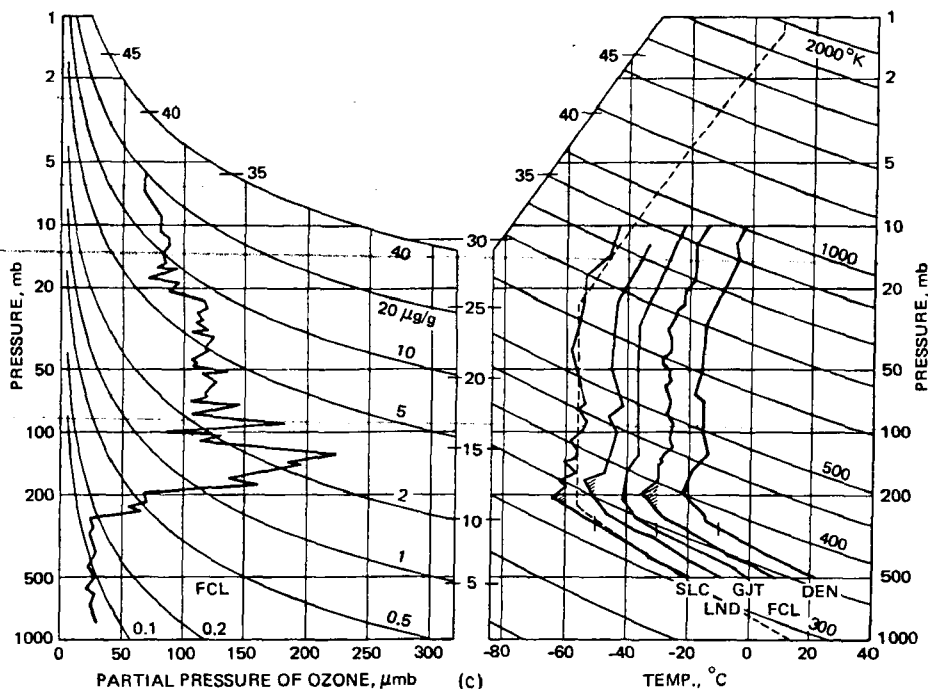


Fig. 4.10 Ozone and temperature soundings (the latter on a sliding scale) for indicated stations, 1200 GMT, May 1, 1963. The area to the left of the -60°C isotherm for each temperature sounding is shown by hatching; the -50°C isotherm is marked with a short vertical line. The stations used are: ABQ, Albuquerque, N. Mex.; SEA, Seattle, Wash.; TTI, Tatoosh Island, Wash.; OLM, Olympia, Wash.; SLE, Salem, Ore.; BOI, Boise, Idaho; TUS, Tucson, Ariz.; UNM, Univ. of New Mexico; AMA, Amarillo, Tex.; MAF, Midland, Tex.; FCL, Fort Collins, Colo.; SLC, Salt Lake City, Utah; GJT, Grand Junction, Colo.; DEN, Denver, Colo.; LND, Lander, Wyo.; ELP, El Paso, Tex. [From J. G. Breiland, *Journal of Geophysical Research*, 69(18): 3803-3805 (1964).]

Advection processes are also evident from the relatively large differences in detail between the Seattle, Fort Collins, and Albuquerque ozone soundings.

From a study by Lovill (1968) (see also Lovill and Miller, 1968), it becomes evident that not only details in the vertical temperature structure (in the low tropospheric inversion as well as in the stratosphere) show a certain correlation with the vertical distribution of $[\text{O}_3]$ but also details in the wind profiles appear to have some influence (Fig. 4.12). Especially above the tropopause these details in wind-profile structure may be associated with the presence of inertial gravity waves (see Chap. 1). Such waves may exercise a considerable advective control on $[\text{O}_3]$, especially if their wavelengths are of the order of 10^3 km.

Ozone concentrations, or, more properly, total oxidant concentrations, may be considerable in the vicinity of urban air-pollution sources. Trapping in the low-tropospheric inversion, especially over the cities on the U. S. west coast, has been determined by ozonesonde measurements (Lovill and Miller, 1968; Miller and Ahrens,

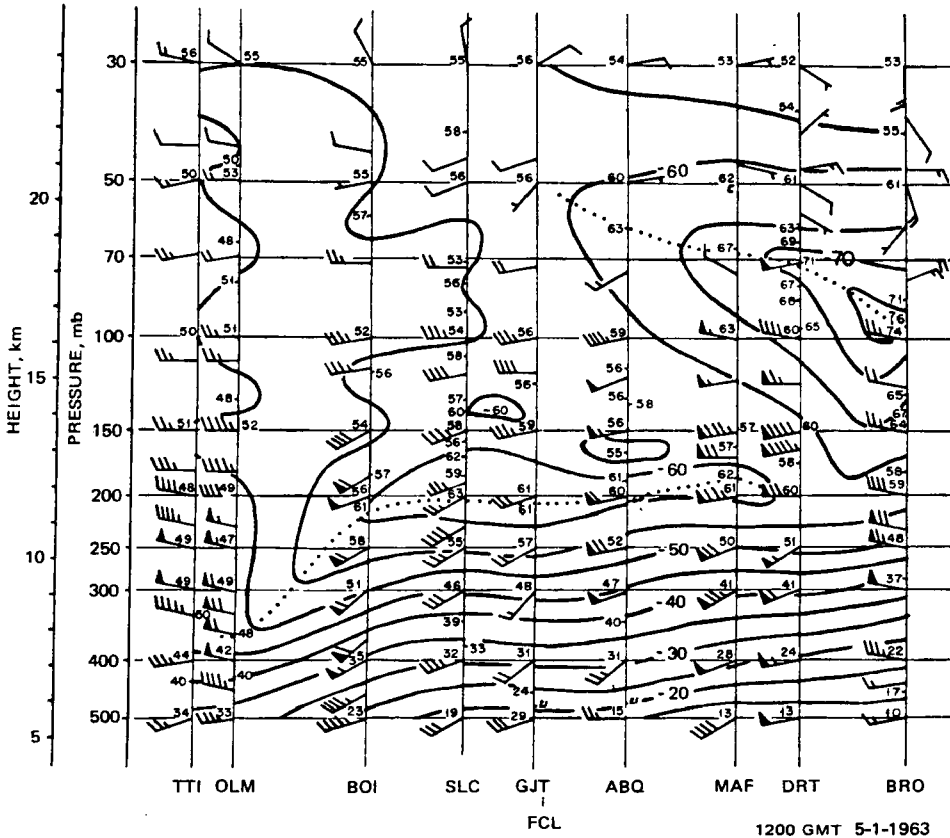


Fig. 4.11 Vertical cross section, 1200 GMT, May 1, 1963, through Tatoosh Island, Wash. (48°N, 125°W); Olympia, Wash. (47°N, 123°W); Boise, Idaho (44°N, 116°W); Salt Lake City, Utah (41°N, 112°W); Grand Junction, Colo. (39°N, 109°W); Albuquerque, N. Mex. (35°N, 107°W); Midland, Tex. (32°N, 102°W); Del Rio, Tex. (29°N, 101°W); and Brownsville, Tex. (26°N, 97°W). Plotted values are temperatures (°C) (minus signs omitted). Winds are shown by conventional symbols: each pennant represents 50 knots; full line, 10 knots; half line, 5 knots. Continuous lines are isotherms. The tropopause is shown by dots. [From J. G. Breiland, *Journal of Geophysical Research*, 69(18): 3802 (1964).]

1969). The oxidant concentration in the inversion depends not only on the temperature structure but also on the destruction rate. The latter is proportional to the eddy mixing in the boundary layer and inversely proportional to the depth of the mixing layer.

The vertical temperature structure in terms of thermal stability, $\partial\theta/\partial p$, where θ stands for potential temperature, and the wind structure in terms of the vertical vorticity component, Q_z , can be combined into an expression of potential vorticity

$$P = - Q_z \frac{\partial\theta}{\partial p} \tag{4.2}$$

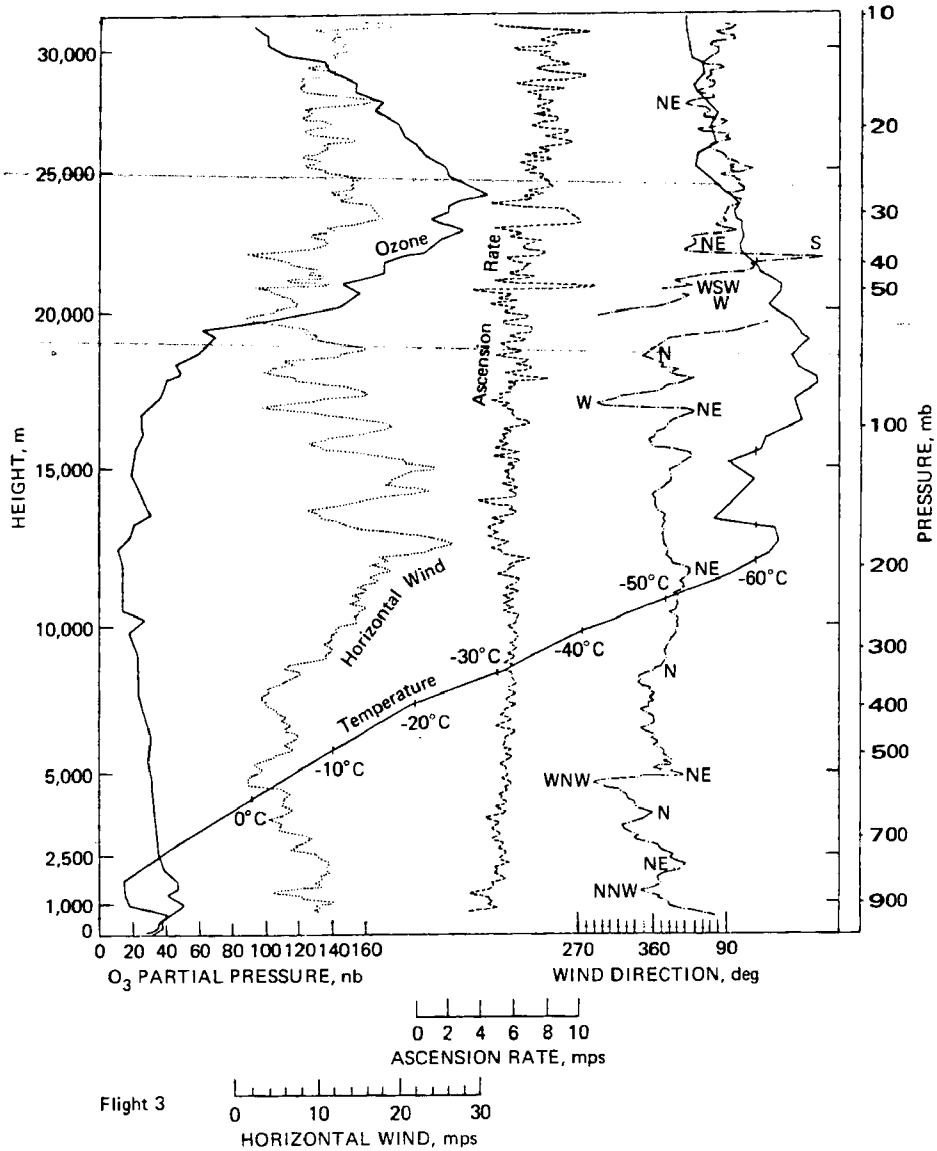


Fig. 4.12 Detailed vertical distribution of ozone, temperature, ascension rate of balloon, wind direction, and horizontal wind at Oakland, Calif., 0000 GMT, Feb. 5, 1967. (From J. E. Lovill, San Jose State College, Department of Meteorology, report under NSF grant GP-4248 and Department of the Navy, Order No. IPR 10-64-8050-WEPS, 1968.)

(θ is the potential temperature and p is the pressure). The P value is a conservative quantity for frictionless adiabatic motion and is high in the stratosphere and in intrusions of stratospheric air into the troposphere (see Part 3). It is not surprising, therefore, that vertical profiles of P show good agreement with the large-scale vertical structure of $[O_3]$ (Danielsen, 1968). An example is given in Fig. 4.13. Significant correlations between P and ozone mixing ratios have also been found along isentropic surfaces, the 330°K surface showing highest correlation coefficients among the surfaces, $320, 330, 350, 375,$ and 400°K (Berggren and Labitzke, 1968).

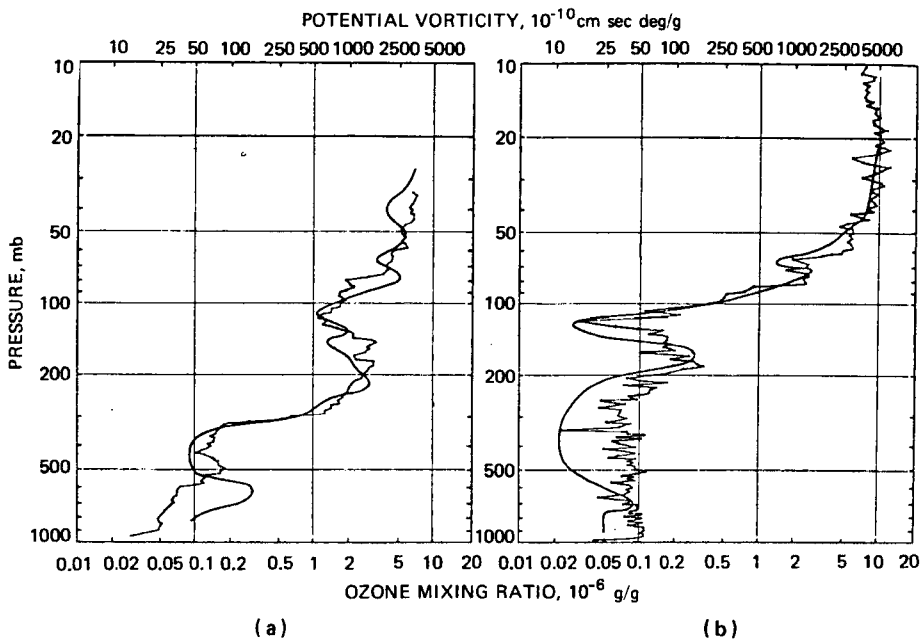


Fig. 4.13 Vertical profiles of ozone mixing ratio (thin line) and potential vorticity (heavy line). (a) over Bedford (Apr. 24, 1963; 1224 GMT) and (b) Tallahassee (Apr. 24, 1963; 1217 GMT). [From E. F. Danielsen, *Journal of the Atmospheric Sciences*, 25(3): 516 (1968).]

Pittock (1966) demonstrated that stratospheric anomalies in the vertical distribution of ozone may, at times, be rather long lived, especially when the horizontal advection processes are coupled with small values of K_z , the vertical eddy diffusion coefficient (measured over all scales smaller than those of the main advective process). He studied the example of an ozone minimum that occurred near 20 km over Boulder, Colo., during several days of March 1964. This ozone minimum coincided with a layer of volcanic dust from Agung Volcano (Bali); it could thus be traced back into tropical regions. Although volcanic debris may have a certain catalytic destruction effect on O_3 (Pittock, 1965), such processes are not believed to be significantly involved in generating the ozone minimum over Boulder. The persistent appearance of the debris during several successive days could be explained more readily by a low

diffusion coefficient, K_z , of the order of 2.5×10^2 cm²/sec or less. (As shown in Table 1.1, mean vertical diffusion coefficients during this season and at 50 mb, including the planetary scales of motion, are larger by more than one order of magnitude.)

Berggren and Labitzke (1966, 1968) have also shown from analyses of $[O_3]$ on isentropic surfaces, measured by the ozonesonde network, that well-defined horizontal ozone advection processes exist in the lower stratosphere (see also Breiland, 1969). Figure 4.14 shows, as an example, the ozone distribution on the 375°K isentropic surface on May 3 and 4, 1963, 1200 GMT. An ozone maximum, located above a tropospheric trough and a region with low tropopause heights, drifted eastward along lines of constant Montgomery stream function (the latter is defined as $M = c_p T + gz$, where z is the height of the isentropic surface). An ozone minimum, located above the ridge that follows the tropopause trough, also drifted eastward along the same lines.

The increase of $[O_3]$ above tropopause level, apparent from Fig. 4.10, does not necessarily hold in the tropics. Griggs (1963) reported on bubbler ozonesonde measurements over Nairobi, which, on occasion, revealed quite low $[O_3]$ values above the tropical tropopause. Upward transport of air might account for such observed distributions (see also explanation of "sulfate layer", p. 195).

Since jet streams, such as the one shown in Fig. 4.9, are associated with strong cold fronts, it is not surprising to find numerous reports in the literature of observed increases in total O_3 , as well as in $[O_3]$ of surface air, after the passage of such fronts or of troughs aloft (Dobson et al., 1946; Gupta, 1964).

In the stratosphere short-period variations in ozone concentrations are to be expected mainly in the region below the ozone peak, where relaxation times, τ , according to Table 4.1, are long. Vertical and horizontal transport processes acting in this region of the stratosphere will cause departures of ozone concentrations from seasonal mean values. Since restoration to photochemical equilibrium conditions will proceed only very slowly, these departures will remain active over considerable time periods unless they are removed by turbulent mixing processes. Neglecting photochemical restoration of the O_3 equilibrium, we can compute changes of the partial pressure of ozone, p_3 , from (Dütsch, 1963)

$$-\left(\frac{\partial p_3}{\partial t}\right)_p = \mathbf{V}_p \cdot \nabla_p p_3 - \omega \frac{\partial}{\partial \ln p} \left(\frac{p_3}{p}\right) \quad (4.3)$$

and the local change in temperature

$$\left(\frac{\partial T}{\partial t}\right)_p = -\mathbf{V}_p \cdot \nabla_p T + \omega \left(\frac{T}{p} \kappa - \frac{\partial T}{\partial p}\right) \quad (4.4)$$

where $\kappa = R/c_p = 0.286$ is Poisson's constant, with R expressing the gas constant for dry air and c_p the specific heat at constant pressure. Subscript p indicates processes on a constant-pressure surface. Local advection and changes in p_3 and T due to vertical motion may be of equal importance in the lower stratosphere. On occasion they may

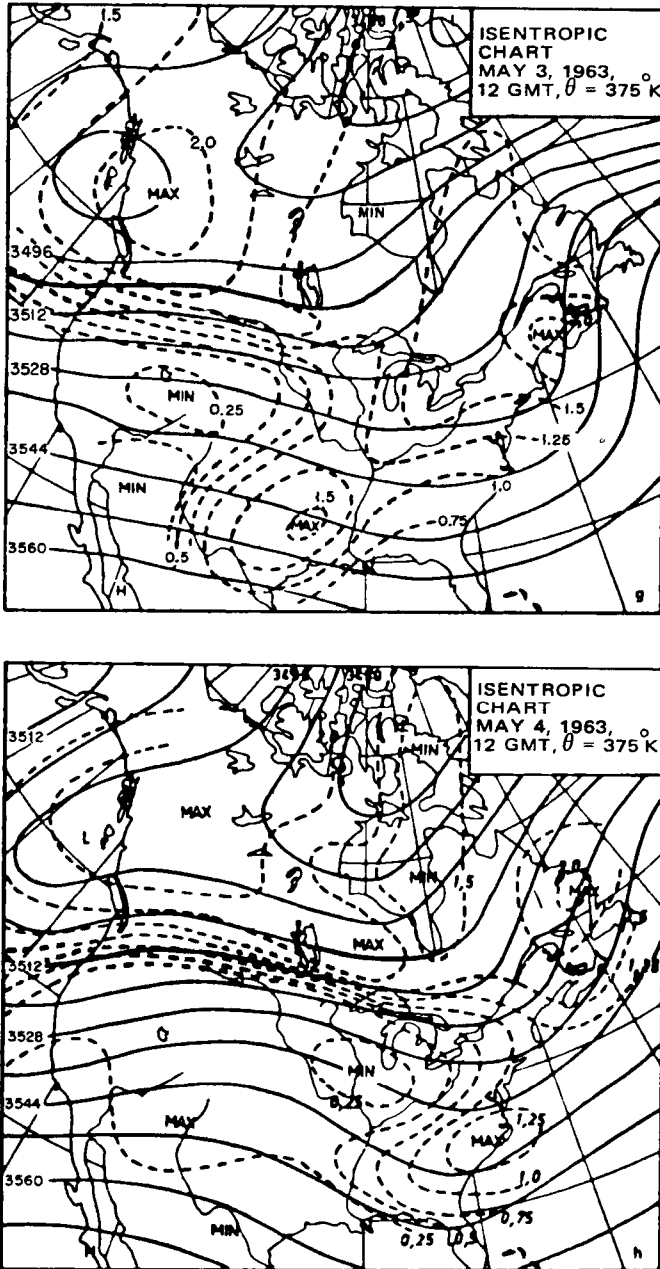


Fig. 4.14 Isentropic charts for May 3 and 4, 1963, 1200 GMT; Montgomery stream function is given in full lines (interval in 800 meter-ton-second units, numbering given with last two digits omitted); ozone mixing ratio (dashed lines) for every 0.25 $\mu\text{g/g}$. [From R. Berggren and K. Labitzke, *Tellus*, 18(4): 767 (1966).]

be of opposite sign. Therefore increases in $[O_3]$ do not necessarily correlate with increases in T (Canales, 1965), although such a correlation is frequently observed. In the lower stratosphere, below the ozone peak, we can assume $\partial T/\partial p \approx 0$ and $(\partial/\partial \ln p)/(p_3/p) < 0$ (the ozone concentration decreases with increasing pressure). Subsidence will thus increase both the local temperature and the $[O_3]$ at these levels. Since the same vertical-motion regime frequently prevails through a deep layer of the atmosphere, it is not surprising that correlations have been found between low tropopause height and large amounts of total ozone (Kulkarni, 1963, 1968a).

Horizontal advection is of importance in the observed increases of $[O_3]$, especially during periods of the so-called "sudden warming" (see Part 1, p. 63). Such increases are also reflected in the total amount of ozone measured over high-latitude stations (Sturrock, 1960; Kinisky et al., 1961; Komhyr, 1961; Sullivan et al., 1961). The positive correlation $[(\omega)_{(\lambda)}(v)_{(\lambda)}]_{(\lambda t)}$ observed in the lower stratosphere (Molla and Loisel, 1962; Miller, 1967) reaches high values during such breakdown periods of the polar vortex (Mahlman, 1966; for further references, see E. R. Reiter, 1969a), thus contributing toward a rapid and effective northward and downward transport of ozone. Again increases in T are accompanied by increases in $[O_3]$ because of the strong spatial correlation between ozone concentration and temperature (Dütsch, 1962a, 1963; Godson, 1963; London, 1963b; Shimizu, 1964; Kulkarni, 1968a). Figure 4.15 shows the correlation between the meridional wind component, which is mainly responsible for these horizontal advection processes, and total O_3 (Newell, 1964b; see

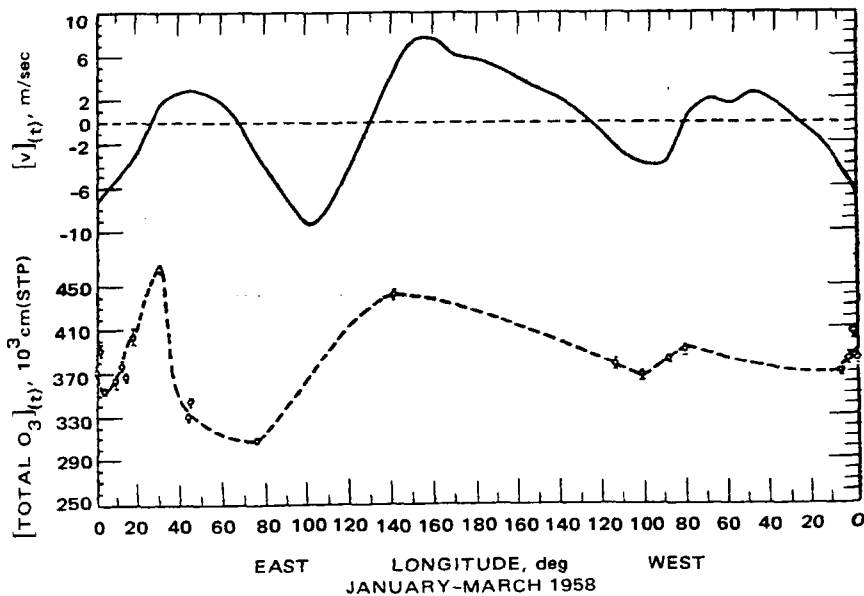


Fig. 4.15 Example of variation of total ozone amount and time-averaged meridional wind component at 100 mb with longitude at $50^\circ N$. [From R. E. Newell, *Pure and Applied Geophysics*, 59: 195 (1964b).]

also Newell, 1961). From this diagram we can conclude that wave numbers 2 and 3, characteristic for orographically induced standing planetary waves, play a dominant role in the meridional ozone transport (see also Fig. 4.8). Since these waves originate in the troposphere, Newell concluded that the flux of energy from troposphere to stratosphere controls ozone transport. These energy transports have been considered in detail in Part 1. In addition to the standing-eddy effect, which is expressed in Fig. 4.15, transient eddies will cause short-term fluctuations, expressed by the interdiurnal variability of total O_3 as well as of $[O_3]$ along vertical ozone profiles (Vigroux et al., 1966). The transient eddies act in the sense that in the lower stratosphere northward-moving air parcels are sinking (Newell, 1961). The large values of standard deviations in $[O_3]$ observed at levels below the ozone peak, shown in Fig. 4.16 for Boulder, Colo., prove the great interdiurnal variability of this atmospheric constituent (Dütsch, 1966; see also Dütsch, 1962b; Craig et al., 1967). (Over Boulder

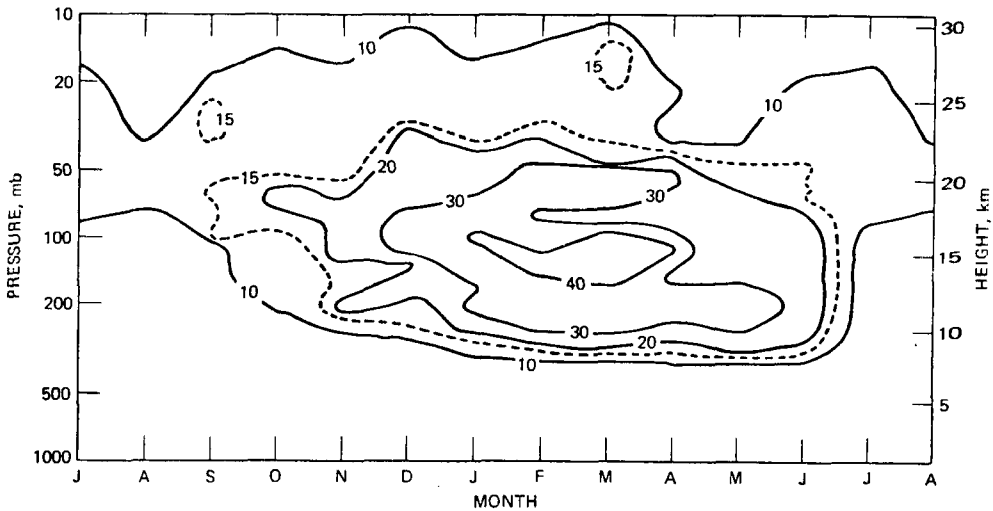


Fig. 4.16 Time cross section of standard deviation of $[O_3]$ from monthly mean values at the respective pressure levels, Boulder, Colo. (From H. U. Dütsch, Report NCAR-TN-10, p. 42, National Center for Atmospheric Research, 1966.)

the ozone peak is found near 23 km, slightly above the 50-mb level.) A similar behavior of the standard deviation is found in pole-to-pole cross sections (Bojkov, 1968b, 1969b). Synoptic-scale systems thus may be held responsible for much of the observed transports in the lower stratosphere. The importance of wave numbers 6 to 8 in atmospheric energetics, discussed in Part 1, Chap. 4, thus appears to be present also in ozone transports and, by analogy, in radioactive-debris transports.

The relative importance of standing and transient eddies and of the mean meridional circulation in transporting ozone has been estimated by Newell (1963a) [see also Newell and Miller (1968) for effects of these eddies on vertical velocities].

Using the mathematical notation given in Part 1, Chap. 1, we can describe the total meridional transport of ozone, averaged with time, by

$$[O_3 v]_{(t)} = [O_3]_{(t)} [v]_{(t)} + [(O_3)_{(t)} (v)_{(t)}]_{(t)} \quad (4.5)$$

Subsequent averaging with respect to longitude produces

$$[O_3 v]_{(t,\lambda)} = \left[[O_3]_{(t)} [v]_{(t)} \right]_{(\lambda)} + [(O_3)_{(t)} (v)_{(t)}]_{(t,\lambda)} \quad (4.6)$$

In a similar fashion we can write

$$[O_3 v]_{(\lambda)} = [O_3]_{(\lambda)} [v]_{(\lambda)} + [(O_3)_{(\lambda)} (v)_{(\lambda)}]_{(\lambda)} \quad (4.7)$$

or, by analogy,

$$\left[[O_3]_{(t)} [v]_{(t)} \right]_{(\lambda)} = [O_3]_{(\lambda,t)} [v]_{(\lambda,t)} + \left[[(O_3)_{(t)}]_{(\lambda)} [(v)_{(t)}]_{(\lambda)} \right]_{(\lambda)} \quad (4.8)$$

Introducing this expression into Eq. 4.6, we arrive at

$$[O_3 v]_{(t,\lambda)} = [O_3]_{(\lambda,t)} [v]_{(\lambda,t)} + \left[[(O_3)_{(t)}]_{(\lambda)} [(v)_{(t)}]_{(\lambda)} \right]_{(\lambda)} + [(O_3)_{(t)} (v)_{(t)}]_{(t,\lambda)} \quad (4.9)$$

The first term on the right side contains the effect of the mean meridional circulation, the second term the effect of standing eddies, and the third term the effect of transient eddies (see Eqs. 2.5 and 2.6 in Part 1 for comparison).

According to Mateer and Godson (1960), the correlation between the total amount of ozone and the ozone in the layer 12 to 24 km is +0.97 for a Canadian station. Bojkov (1967a) found correlation coefficients greater than 0.75 between changes in total ozone and simultaneous changes of $[O_3]$ in the layer 10 to 24 to 28 km. Newell (1963a), therefore, argues that the 12- to 24-km vertically-averaged winds, together with total ozone, can be used as a first approximation in Eq. 4.9. Results for meridional transports are reported in Table 4.2. This table also contains estimates of total transports necessitated by the month-to-month change of total ozone north of $50^\circ N$ and north of $40^\circ N$, respectively. The values given in this table were estimated by using 50-mb winds and by assuming that 35% of the total ozone was transported in a layer for which these winds may be considered representative. In arriving at the values of the transport by the mean meridional circulation, meridional motions given by Barnes (1961) were used.

Regener (1957) estimated from ozone measurements near the earth's surface that in middle latitudes 1.2×10^{11} molecules of O_3 per square centimeter and per second are transported toward the ground. Newell (1963a) assumed that half this value might be representative for the total area north of $40^\circ N$. This ozone would enter the

Table 4.2

OZONE BUDGET* (CUBIC CENTIMETERS OF OZONE AT STANDARD TEMPERATURE AND PRESSURE PER SECOND WHEN MULTIPLIED BY 10^9)

	July–Sept. 1957	Jan.–March 1958	July–Sept. 1958
Transport of ozone across 50°N			
By transient eddies	+2.9	+10.4	+2.0
By standing eddies	-0.1	+3.8	-0.8
By mean meridional motions	-2.9	?	?
Transport from content change north of 50°N	-5.2	+9.0	-5.2
Transport of ozone across 40°N			
By transient eddies	+0.4	+12.6	+0.5
By standing eddies	-0.1	+4.5	-0.9
By mean meridional motions	-4.9	?	?
Transport from content change north of 40°N	-7.4	+11.6	-7.4
Tropospheric downward flux	≈ 6		

*From R. E. Newell, *Quarterly Journal of the Royal Meteorological Society*, 89(380): 182 (1963).

troposphere mainly through the “tropopause gap” near jet streams, and it would amount to approximately 6×10^9 cm³/sec of northward flow in the stratosphere across the 40th parallel. As shown in Table 4.2, this value has the correct magnitude to balance the transports calculated by means of Eq. 4.9 and by assuming that the 50-mb winds are representative of the stratospheric transport processes.

Even though Newell’s (1963a) estimates admittedly are rather crude, they reveal the dominant role, especially during spring, of transient eddies. This conclusion is in agreement with results shown in Fig. 4.16. Transient eddies also play an important role in the zonal transport of ozone. Their effect can be estimated from a term similar to the last one in Eq. 4.9 but containing the zonal velocity component u instead of v . Results computed by Newell (1963a) are shown in Table 4.3. Largest transports by such eddies are realized again during the spring season and at latitudes characteristic of the stratospheric jet stream.

From the foregoing it appears that fluctuations in the total amount of ozone present in an air column are influenced mainly by the layer below the ozone peak, where large variations are only slowly affected by photochemical dissociation processes. Therefore this integrated value, easily measured with the Umkehr method, may also serve as an indicator of stratospheric transport processes. This is highlighted by the correlation that has been found between stratospheric temperatures and amounts of total ozone: Above-normal temperatures indicate that air masses underwent subsidence processes. These air motions import ozone-rich air from higher strata near the ozone peak and thus lead to an increase in the total ozone amount observed from the ground (Meetham, 1937; Martin and Brewer, 1959; Godson, 1960;

Table 4.3
ZONAL FLUX OF OZONE BY TRANSIENT EDDIES AT 50 Mb*†
 (CENTIMETERS OF OZONE AT STANDARD TEMPERATURE AND PRESSURE
 TIMES METER PER SECOND)

Latitude belts	July–Sept. 1957	Oct.–Dec. 1957	Jan.–Mar. 1958	Apr.–June 1958	July–Sept. 1958	Oct.–Dec. 1958
Marcus Island			+0.0485 (12)	–0.1135 (55)	–0.0054 (75)	–0.0357 (60)
Japan 30°N–43°N (3 stations)	–0.0095 (148)	+0.0501 (211)	+0.0066 (312)	+0.0898 (319)	–0.0472 (461)	+0.0544 (393)
38°N–45°N (6 stations)	–0.0424 (79)	+0.0665 (94)	–0.0480 (166)	+0.0925 (321)	–0.0253 (300)	+0.0312 (220)
45°N–55°N (7 stations)	–0.0317 (409)	+0.0827 (388)	–0.1429 (372)	+0.0825 (531)	–0.0378 (592)	+0.0550 (518)
55°N–60°N (5 stations)	–0.0292 (180)	+0.0506 (151)	–0.1739 (192)	+0.0870 (359)	–0.0165 (335)	+0.0207 (207)
Keflavik 64°N	–0.0328 (141)	–0.0055 (117)	–0.5801 (125)	+0.1550 (166)	–0.0351 (161)	–0.1132 (96)
Resolute 75°N	–0.0582 (25)	–0.0670 (13)	+0.0819 (4)	+0.1223 (87)	+0.0050 (110)	–0.5867 (14)
Alert 82.5°N	–0.0248 (113)	+0.1663 (5)	+0.3502 (7)	+0.1221 (126)	–0.0270 (121)	+0.1174 (9)

*From R. E. Newell, *Quarterly Journal of the Royal Meteorological Society*, 89(380): 192 (1963).

†Number of cases in parentheses.

Kulkarni, 1963, 1968a). This is demonstrated by Fig. 4.17, where the passage of a cold low in the middle stratosphere (indicated by a drop in 30-mb temperatures) coincides well with observed minimum amounts of ozone (Boville and Hare, 1961). Actually, close inspection of this diagram shows that the ozone minimum precedes the observed minimum temperatures by a day. This is to be expected since maximum ascending motions, hence minimum values of total ozone, are found in the southwesterly stratospheric current preceding the eastward-moving low and not in the cold center itself. Different time lags between ozone and temperature, and even differences in the sign of these lags, may be expected, depending on the location of the stratospheric circulation centers relative to the observation station (Boville and Hare, 1963).

Ozone Effects on Temperature

So far we have considered correlations between changes in temperature and total ozone or $[O_3]$ which were caused by horizontal or vertical flow processes or both. One should not disregard, however, the direct effects of O_3 and its vertical distribution on temperature (Sissenwine et al., 1962). The photochemical equilibrium theory mentioned earlier already bears out the fact that the temperature peak near 50 km is

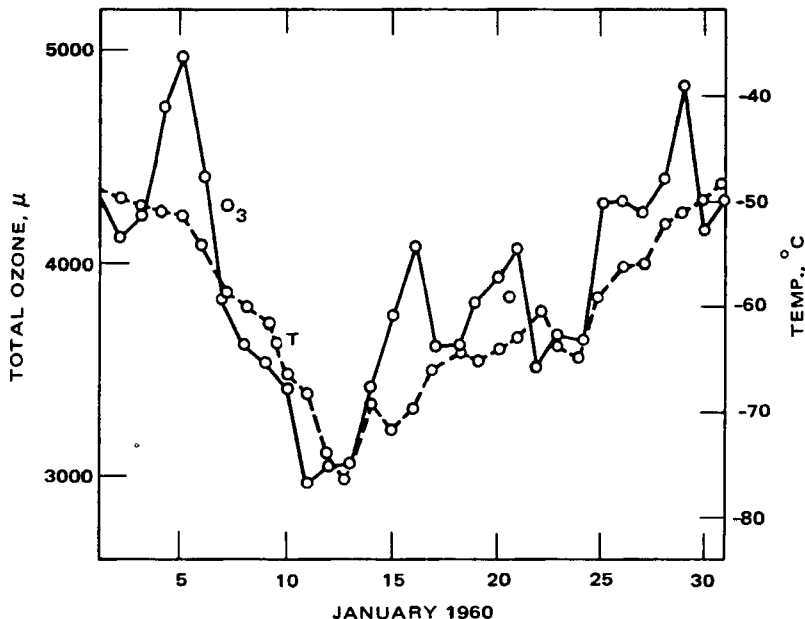


Fig. 4.17 Time sections of 30-mb temperature ($^{\circ}\text{C}$, dashed line) and total ozone (μ , solid line) at Moosonee, Ontario, January 1960. The curves show the profound ozone and temperature changes, almost in phase, associated with the passage of a cold low. [From B. W. Boville and F. K. Hare, *Quarterly Journal of the Royal Meteorological Society*, 87(374): 497 (1961).]

primarily caused by ultraviolet (UV) absorption to which O_3 owes its existence. As shown by Hering et al. (1967), the monthly mean temperatures in the ozone layer are controlled largely by the absorption effects of direct solar radiation, which depend on the sun's zenith angle and on the duration of sunlight. The high ozone concentrations at the ozone peak are produced by radiation in the "window" between 2000 and 2200 \AA . In this window region UV radiation penetrates relatively deep down into the stratosphere. Larger wavelengths are almost completely absorbed by O_3 at higher levels above the ozone peak. (The Hartley bands between 2000 and 3000 \AA , with a peak at 2550 \AA , are mainly responsible for the UV absorption. The weaker Huggins bands lie between 3200 and 3600 \AA . The weak Chappius bands between 4500 and 6500 \AA lie in the visible part of the spectrum.) Wavelengths less than 2000 \AA are absorbed by O_2 (Brewer and Wilson, 1965; Brewer et al., 1966; Dütsch, 1969).

Ozone, being a three-atom gas, also exercises its influence as an absorber in the infrared (4.7, 9.6, and 14.1 μ) similar to water vapor and CO_2 (Walshaw, 1955, 1957; Caton et al., 1967; Hoffmann, 1967). Radiative flux divergences and convergences may be produced by specific vertical $[\text{O}_3]$ distributions, which may, in turn, cause an adjustment in the radiative equilibrium temperatures (Manabe and Wetherald, 1967). Hitschfeld and Houghton (1961, 1962, 1963) demonstrated the importance of the 9.6- μ band of ozone, especially in the atmospheric layer below the ozone peak and in

the absence of clouds. Heating rates of 0.2 to 0.3°C per day produced by this band are comparable to the effects of CO₂ (see also Curtis, 1952; Godson, 1955; Clark and Hitschfeld, 1964; Leovy, 1967; Rodgers, 1967). A simple radiation chart for estimating the effects of ozone in this infrared band has been designed by Clark and Hitschfeld (1964).

Ozone in the Mesosphere

Above the ozone peak and in the mesosphere, relaxation times, according to Table 4.1, are small. There O₃ loses its effectiveness as a tracer. Short-term fluctuations, produced by diurnal insolation, become dominant. Above pressure levels of 0.6 mb, a daytime minimum caused by the photodissociation of O₃ and a nighttime maximum govern the diurnal variation of [O₃]. (London, 1967b; Dütsch, 1968). Actual ozone concentration values above the ozone peak are still somewhat in doubt. Randhawa (1969a, 1969b), for instance, reported on concentrations near the stratopause, measured by a balloon-borne sensor, which were one order of magnitude higher than concentrations determined by spectrometric techniques.

Ozone measurements during an eclipse also show an increase of mesospheric [O₃] in the absence of solar radiation (Stranz, 1961; Randhawa, 1967, 1968; Rodionov et al., 1967; Bojkov, 1968a; Ballard et al., 1969). Recent measurements of [O₃] near the stratopause (above the ozone peak) with a balloon-borne sensor also reveal an increase in concentration after sunset (Randhawa, 1969a, 1969b). According to Doherty (1968), the electron density of the ionospheric D-region (starting at about 70 to 80 km) may be influenced by ozone and atomic oxygen. Such reactions as $e + O_3 \rightarrow O^- + O_2$ tend to decrease the electron concentration with increasing [O₃]. Consequently probing of the D-region by low-frequency pulse signals revealed minimum [e] values in this region after sunset and during a solar eclipse, in agreement with enhanced ozone concentrations.

The amplitude of the diurnal variation of [O₃] appears to have a maximum near 0.01 mb (above 70 km). It is, however, small enough to have no measurable effect on total ozone, at least with the accuracy of present instrumentation (Shah, 1966). This diurnal variation also produces a secondary nighttime maximum of the vertical ozone distribution in the mesosphere near 70 km, postulated theoretically by Hunt (1964) and verified by rocket observations (E. I. Reed and Scolnik, 1965; Carver et al., 1966; Webb, 1966a; E. I. Reed, 1968; Hilsenrath et al., 1969). Estimates of [O₃] above the ozone peak by Venkateswaran et al. (1961), using the reflected light from the Echo satellite (1960 Iota 1) as it passed in and out of the earth's shadow, indicated a secondary ozone maximum near 55 km. Later measurements by Rawcliffe et al. (1963), using a satellite-borne radiometer during sunrise and sunset, did not reveal such a secondary ozone maximum. K. H. Stewart (1967) reported on additional measurements made by Soviet investigators with this technique which revealed rather striking spatial variations, on the synoptic scale, of ozone above the ozone peak (fluctuations as large as 30% of the mean value).

Data of the earth's radiance at 2840 Å, measured by satellite and reported by Rawcliffe and Elliott (1966), indicate that high-level O_3 (above 23 km) shows maximum values during summer and minimum values during winter, which is contrary to the seasonal O_3 variation depicted in Fig. 4.7 at, and below, the ozone peak. This is to be expected, however, because at high levels $[O_3]$ is governed almost exclusively by photochemical processes whereas the increasing relaxation times, τ , at lower elevations allow for an increasing role of transport processes. Above 40 km there seems to be a reversal of the seasonal variation of ozone. Using the Mateer-Dütsch (1964) Umkehr technique, Rangarajan (1969) computed maximum ozone concentrations at 45 km for winter and minimum concentrations for summer. The range of this seasonal variation seems to be fairly uniform at all stations between 25 and 51°N. It is difficult, therefore, to explain this variation with the seasonal change of temperature at these altitudes, which increases with latitude. Since the classical photochemical theory fails to produce a seasonal variation similar to the one observed by Rangarajan, we may have to include water-vapor fluxes into the computations of ozone concentrations above the ozone peak. Higher moisture concentrations during summer (when noctilucent clouds are observed) may be produced by an upward flux of H_2O in the 30- to 50-km region and may affect adversely the photochemical equilibrium concentrations of ozone.

According to Dütsch (1963), reactions 1, 2, and 35 in Table 1.6 are of importance during the nighttime hours in the mesosphere. Wagner (1963) pointed out the importance of O^- and O_2^- ions in these photochemical processes (see also Reid, 1964).

Gebhart (1967) postulated that in the mesosphere ozone, by its 9.6- μ band, and CO_2 , by its 15- μ band, have a strong influence on the mesospheric equilibrium temperature. Radiative flux convergence above the stratopause may actually lead to a warming of the upper mesosphere. This effect may contribute toward the relatively high mesospheric temperatures observed during the winter polar night (see Fig. 1.13).

SURFACE $[O_3]$ AND ITS VARIATIONS

The Spring Maximum of Ozone

In the discussion of Fig. 4.7, it was mentioned that $[O_3]$ at and below the level of the ozone peak shows a distinct maximum in middle latitudes during early spring (in the northern hemisphere during February and March). This figure shows that such a maximum would occur during the same months also in the values of total ozone. This has been shown by Dütsch (1969) from data obtained over Boulder, Colo.

Continuous records of $[O_3]$ near the earth's surface also reveal a prominent spring maximum. There is, however, a time lag of more than 2 months between stratospheric and low tropospheric maximums of $[O_3]$ at stations in the middle latitudes of the northern hemisphere (Junge, 1962a; Vigroux et al., 1965; Newell,

Brandli, and Widen, 1966). This is readily seen by comparing Fig. 4.18, which shows values obtained in the Boston area, with Fig. 4.7. During May a distinct maximum of $[O_3]$ appears in the surface air. The minimum of surface $[O_3]$ in November, on the other hand, reveals not much lag against the minimum of total ozone in October and November, found by Dütsch (1969) over Boulder.

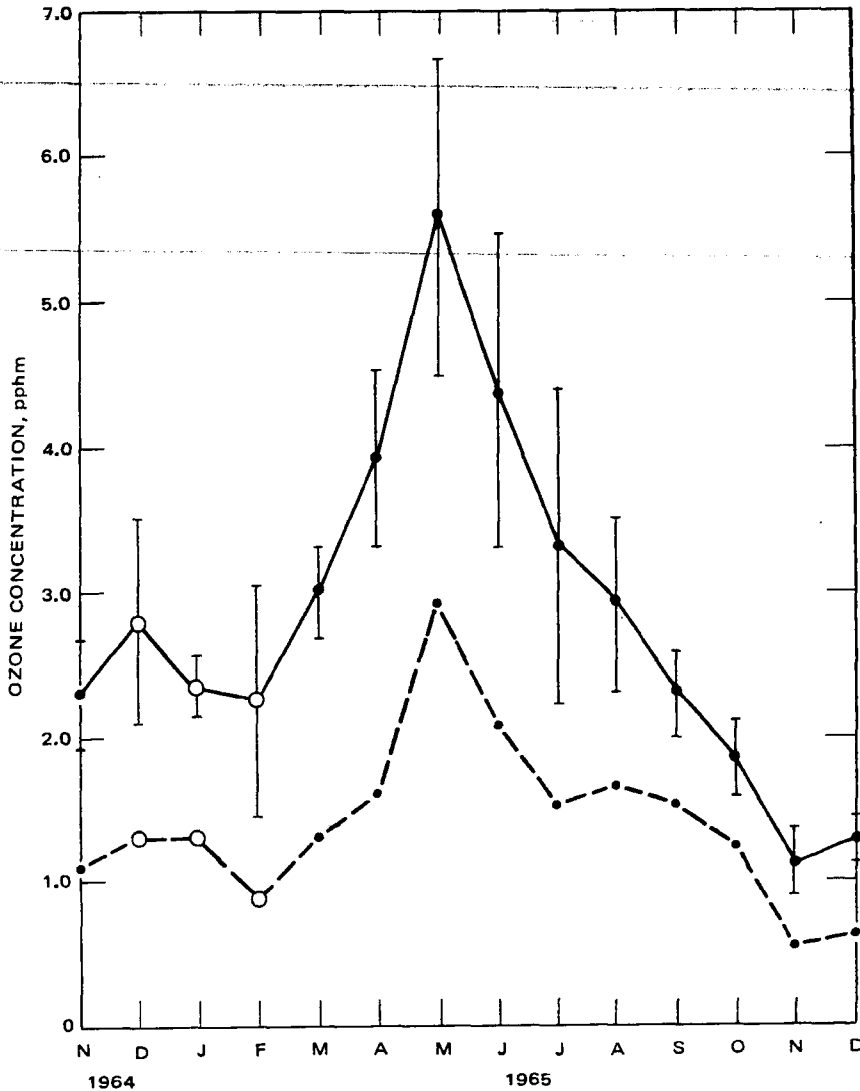


Fig. 4.18 Ozone concentration over greater Boston (in parts per hundred million), where bars represent one standard deviation. Number of days per month instrument was in operation were: 1964, 23,25; 1965, 24, 24, 19, 20, 30, 30, 31, 17, 22, 28, 28, and 11. —, average of 24-hr maximum reading. ---, monthly mean of all hours. [From R. E. Newell, H. W. Brandli, and D. A. Widen, *Journal of Applied Meteorology*, 5(5): 741 (1966).]

Steinhauser (1959a) found a maximum of surface [O₃] in Vienna during June and July. In Arosa, Switzerland, Perl (1965) noted a maximum in surface [O₃] during May and June. Values tended to be higher during clear days than during cloudy ones. Similar results were reported by Warmbt and Teichert (1956) for observations in East Germany. Clear-day readings are indicative of subsidence motions in the troposphere associated with anticyclonic weather regimes. Perl also found a 2-month lag between the total ozone maximum over Arosa and the surface [O₃] maximum.

The occurrence of the spring maximum of ozone concentrations near the earth's surface agrees well with the maximum of radioactive fallout observed in middle latitudes (Mahlman, 1965b). This close agreement enables us to describe reasonably well the transport mechanisms governing the transfer of O₃ from the ozonosphere to the ground. Seasonal changes in the large-scale stratospheric circulation patterns, especially in their eddy aspects, lead to a maximum of [O₃] during middle and late winter in the middle stratosphere. The role of the stratospheric vortex breakdown and of the "sudden warming" in such horizontal and meridional transport processes was discussed in Part 1. Large-scale turbulent exchange processes increase the radioactivity burden as well as the O₃ contents of the lower stratosphere by spring. These layers, however, are continuously "tapped" by cyclogenetic processes associated with jet streams, causing a transfer of low-stratospheric air into the troposphere by the mechanism described in conjunction with Fig. 4.9. Thus the observed late-spring maximum of surface ozone concentrations depends on the seasonal fluctuations of the "ozone reservoir" in the lower stratosphere, which lags somewhat behind the maximum [O₃] values at the level of the ozone peak (see Fig. 4.7), and on the synoptic-scale transport processes through the tropopause.

Junge (1962a, 1962c, 1963c) took the phase lag between the maximum in total O₃ and in surface [O₃] to be the result of the limited lifetime of tropospheric ozone. It is destroyed mainly by contact with the ground (neglecting the destruction by industrial air pollution) and has to be replenished through inflow from the stratosphere. The existence of the ozone sink at the ground is demonstrated by detailed measurements of vertical ozone gradients and flux rates in the lowest layers of the atmosphere (Regener and Aldaz, 1969; Galbally, 1969). For a phase lag of 2 months, the stratospheric residence time of O₃ is of the order of 3 to 5 years, the tropospheric residence time of the order of 3.3 months, and the vertical flow of ozone in the troposphere approximately 0.5×10^{-7} g/m²/sec, or 0.804×10^9 tons of ozone per year over the whole globe. (For further details, the reader is referred to Junge's original papers and to Fabian and Junge, 1970.) This compares to 1.3×10^9 tons of ozone per year on a global basis, computed by Aldaz from ozone flux measurements near the earth's surface over land and over the ocean. From this it appears that Junge's flux estimates in the troposphere may be too low and that the tropospheric and stratospheric residence times may have been assumed too high. The very efficient transport mechanisms between stratosphere and troposphere in the jet-stream region of temperate latitudes certainly would indicate shorter residence times of a passive contaminant of the lower stratosphere. According to estimates by Reiter and Mahlman (1964b, 1965a) and Mahlman (1966), derived from radioactive-debris transport near

the jet stream, residence times of 1 to 2 years of air masses in the stratosphere are more reasonable. This would imply that a factor slightly larger than 2 should be applied to Junge's ozone flux estimates, which would bring them closely in line with the values observed by Aldaz.

The transfer processes through the tropopause cause considerable interdiurnal variations of $[O_3]$ in surface air just as they cause large fluctuations of the radioactive-fallout rate (Vassy and Tanaevsky, 1964). Such fluctuations are, for instance, evident from the daily ozone measurements in Vienna reported by Steinhauser (1959a). Peak ozone concentrations observed under conditions of rapid transfer of air from the stratosphere to the ground may be large enough to cause "weather flecking" of tobacco leaves and of other crops (Davis and Dean, 1966).

Figure 2.5 shows that the diurnal heating of the ground causes convective mixing processes and the establishment of an adiabatic mixing layer that prevails, if winds are generally weak and mechanically induced turbulence is small, during the daytime hours only. Since the source of O_3 is to be sought in the upper atmosphere, its sink, however, being at the ground, the diurnal cycle of convective activity will be reflected strongly by the diurnal variation of $[O_3]$. This is evident from the studies by Perl (1965) and Steinhauser (1959a). Figure 4.19 shows the rather simple pattern of diurnal ozone variations in Vienna, Austria, and Arosa, Switzerland. The variations at Arosa studied by Perl are similar in their general nature to the ones in Vienna. They reveal, however, a secondary ozone maximum in the late evening, especially during summer, which is probably caused by mountain breezes. These downslope currents, which establish themselves with the radiative cooling of the air along the sides of the valley, apparently transport ozone-rich air from levels near the mountain tops toward the bottom of the valley. Worth et al. (1967), for similar reasons, found ozone maximums occurring almost 12 hr out of phase at mountain tops and in the valley. Maximum $[O_3]$ values are found during late night and early morning on the mountain top. Similar to CO_2 (see the discussion carried out in conjunction with Fig. 3.3), variations of $[O_3]$ near the earth's surface might thus be used to check on local circulation systems.

Hemispheric Differences

The preceding seasonal variations of surface $[O_3]$ refer to conditions in the northern hemisphere. Observations in the southern hemisphere also reveal a distinct seasonal trend, especially in middle latitudes. There are, however, remarkable differences between the two hemispheres, and these will be discussed in the following.

Figure 4.20 shows monthly mean values of total ozone observed at several sites in the southern hemisphere (R. N. Kulkarni, 1962, 1968a; see also Bojkov, 1967b; Pittcock, 1968). In comparing this diagram with Fig. 4.7, note that the ozone maximum occurs much later in the season in the southern hemisphere, especially in middle and high latitudes, than, on the average, in the northern hemisphere. As mentioned in Part 1, the stratospheric polar vortex of winter in the southern

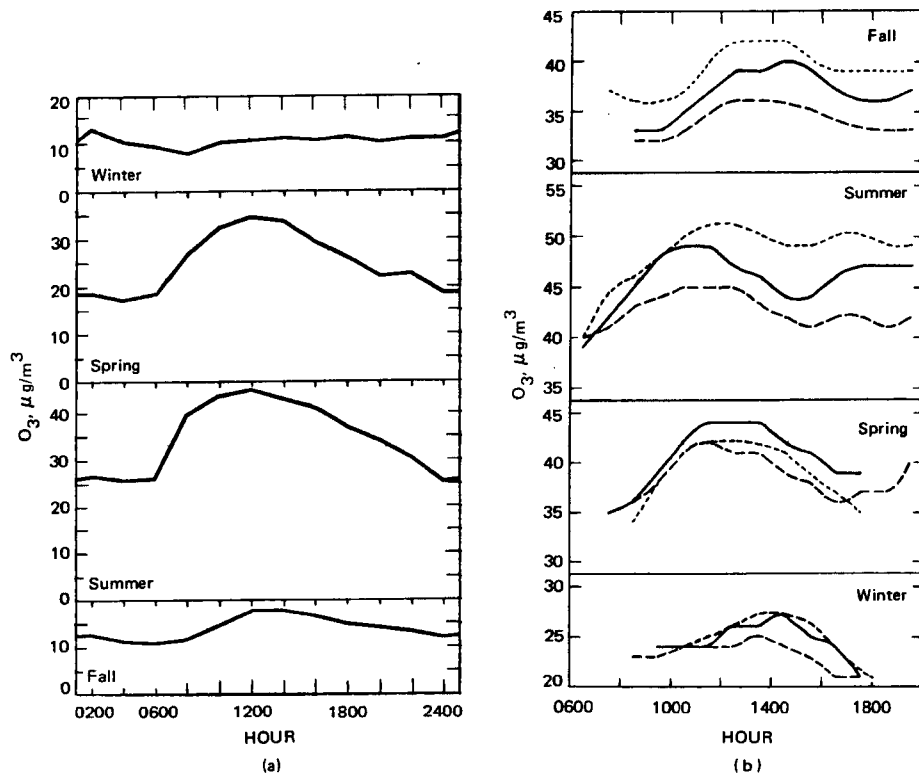


Fig. 4.19 Mean diurnal variation of surface ozone concentrations at (a) Vienna, Austria, and (b) Arosa, Switzerland, for seasons as indicated. Units are in $\mu\text{g}/\text{m}^3$. Dashed lines in (b) pertain to all days of observation, full lines to days without precipitation, and dotted lines to exceptionally clear days. [(a) From F. Steinhauser, *Archiv fuer Meteorologie, Geophysik und Bioklimatologie, Series A.*, 11(3): 378 (1959); (b) From G. Perl, *Archiv fuer Meteorologie, Geophysik und Bioklimatologie, Series A (Austria)*, 14: 453 (1965).]

hemisphere apparently suffers no major breakdown until the time of the spring equinoxes. In the northern hemisphere the stratospheric flow, on the average, is much more disturbed, and a breakdown of the vortex may already occur during midwinter. With what has been said in Part 1, Chap. 3, on vertical motions associated with the breakdown of the stratospheric vortex and with so-called "sudden warming" periods, we can expect the total ozone maximum to be correlated with the seasonal occurrence of this breakdown. Therefore the ozone maximum will show up earlier in the northern hemisphere than in the southern hemisphere.

From Umkehr observations over Pretoria (S. Africa) reported by Bojkov (1967b), it appears that the spring increase of total ozone follows the final warmings of the stratosphere in the southern hemisphere and not so much the minor midwinter warmings that are observed occasionally (Fig. 4.21). A similar observation was made by Wisse and Meerburg (1969) over Base King Baudouin, Antarctica ($70^{\circ}26'S$,

24° 19'E). Here, however, the total ozone variation seems to follow minor midwinter warmings also (Fig. 4.22). The spring warming and its associated increase of total ozone may occur in several surges, as is evident from Fig. 4.23.

As shown in Fig. 4.20, the latitudinal gradients in total ozone are strongest in winter and spring. Eddy motions in the stratosphere, therefore, will cause the largest interdiurnal variability of total ozone during that season (R. N. Kulkarni, 1962).

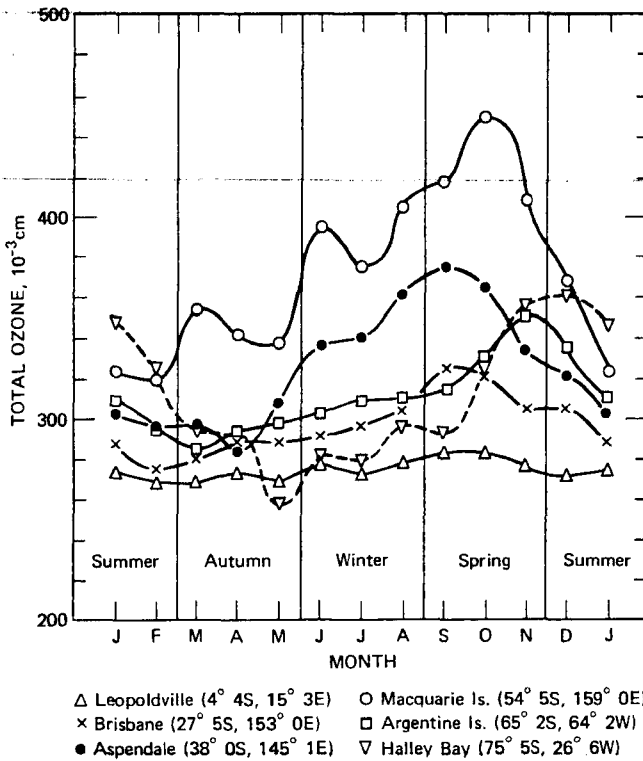


Fig. 4.20 Seasonal variations of total ozone. [From R. N. Kulkarni, *Quarterly Journal of the Royal Meteorological Society*, 88(378): 524 (1962).]

Figure 4.20 also reveals the interesting fact that Antarctic stations (Argentine Island and Halley Bay) show a late spring and early summer maximum of total ozone (see also Wexler et al., 1960; Dobson, 1966; Willett, 1968), mainly produced by conditions in the lower stratosphere (R. N. Kulkarni, 1966a). Such a phenomenon is not found in the northern hemisphere, as can be seen from a comparison of data from Halley Bay and Tromsø (Fig. 4.24). The latter station reveals an early spring maximum similar to that over Fort Collins (see Fig. 4.7). This maximum is much larger than the

late spring maximum in the southern hemisphere (see also Ramanathan, 1963a; E. Vassy, 1963). Kulkarni's (1962) observations over the southern hemisphere may be explained by referring to Part 1, Fig. 3.69. As shown in Fig. 3.69, Rubin and Weyant (1963) found descending motions prevailing throughout the year over the Antarctic

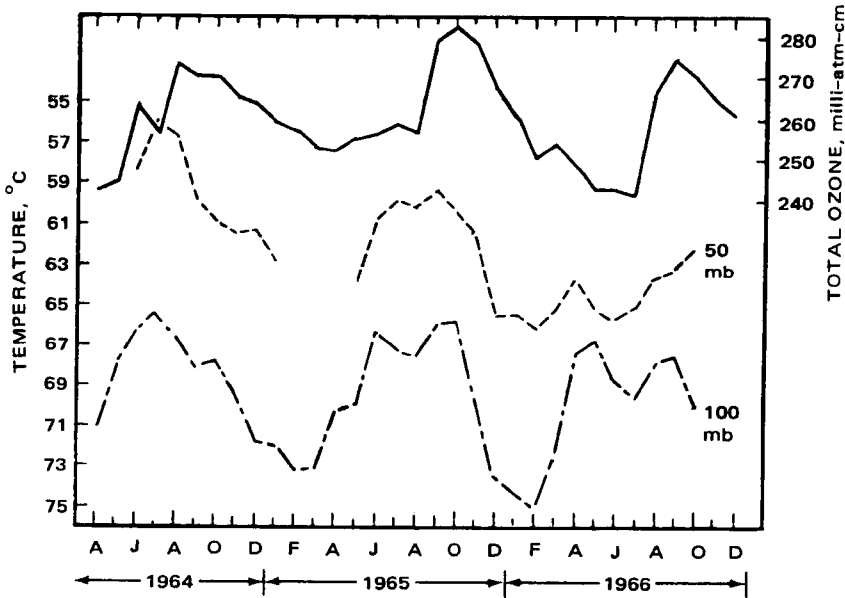


Fig. 4.21 Time variation of the total ozone and the temperature at 50 and 100 mb at Pretoria (25°S, 28°E; height, 1374 m). [From R. D. Bojkov, *Journal of Geophysical Research*, 72(22): 5587 (1967).]

continent in the troposphere and lower stratosphere. This vertical-motion regime can be expected to transport ozone downward after it has been brought to high latitudes mainly by horizontal eddy-transport processes. The well-organized outflow from the cold Antarctic vortex and the associated sinking motion thus produce a maximum of total ozone more than 2 months after maximum ozone amounts are observed in middle latitudes (see also Wexler et al., 1960; Wisse and Meerburg, 1969). There appears to be an interaction in the southern hemisphere between horizontal eddy motions of middle latitudes and a more or less stationary subsidence regime over polar regions (see also Pittock, 1968). In the northern hemisphere, however, the eddy processes are quite dominant even in polar latitudes.

Surface [O₃] observations in Antarctica reported by Aldaz (1965) and by Wisse and Meerburg (1969) give further evidence of the subsidence regime. Figure 4.25 shows monthly mean values for Amundsen-Scott Base, the South Pole station (90°S,

3050 m), Hallet station ($72^{\circ}18'S$, $170^{\circ}18'E$, 15 m), on the coast, and several other Antarctic locations. The maximum of total ozone at Amundsen–Scott, which was observed during November and December, was similar to that shown in Fig. 4.24 for Halley Bay. Surface $[O_3]$, according to Fig. 4.25, attains maximum values in June

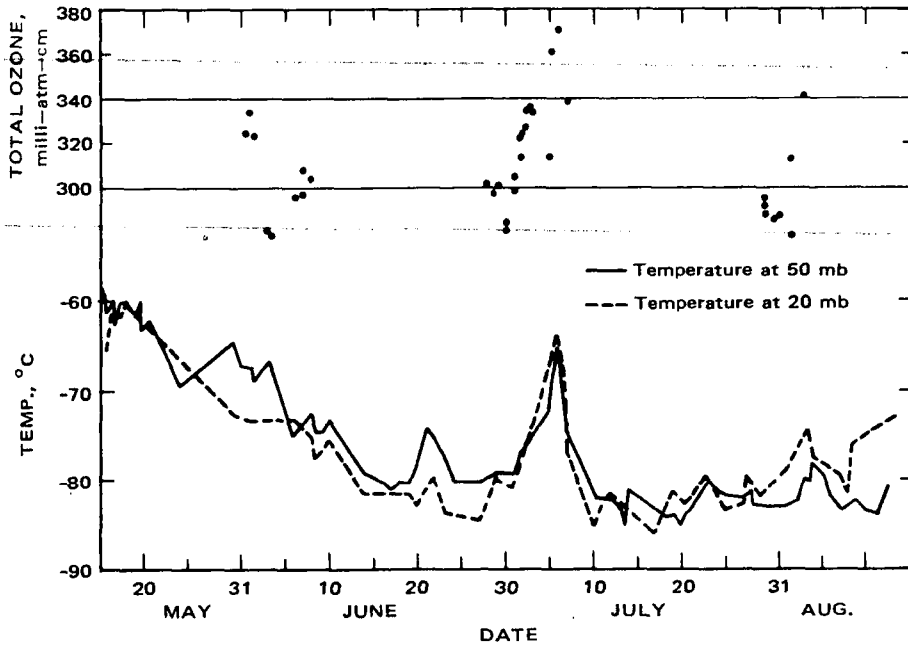


Fig. 4.22 Total ozone values from moon observations and 50-mb temperatures for Base King Baudouin, winter 1966. [From J. A. Wisse and A. J. Meerburg, *Archiv fuer Meteorologie, Geophysik und Bioklimatologie, Series A (Austria)*, 18(1-2): 52 (1969).]

both at the South Pole and at the coast of Antarctica, at a time when total ozone is at a minimum (see Fig. 4.24). Whereas on the coast surface $[O_3]$ values decrease markedly thereafter, the Amundsen–Scott station retains relatively high values throughout winter and spring. Aldaz reported minimum values at Little America ($78^{\circ}11'S$, $162^{\circ}10'W$, 44 m) and Amundsen–Scott during February and March and at Hallet and Halley Bay during December and January. Inland stations show generally higher values of surface ozone concentrations than coastal stations. This indicates a certain amount of destruction of ozone at the surface.

From the foregoing data samples, it becomes evident that there is also a significant difference between the two hemispheres in the time lag between maximums

of total ozone and of surface $[O_3]$. A comparison of Fig. 4.7 and Fig. 4.18 shows a 2-month lag between the maximum of total ozone, governed mainly by conditions in the middle stratosphere below the ozone peak, and the maximum of surface ozone concentrations. As shown, the latter depends mainly on discrete intrusions of stratospheric air into the troposphere which are associated with jet streams.

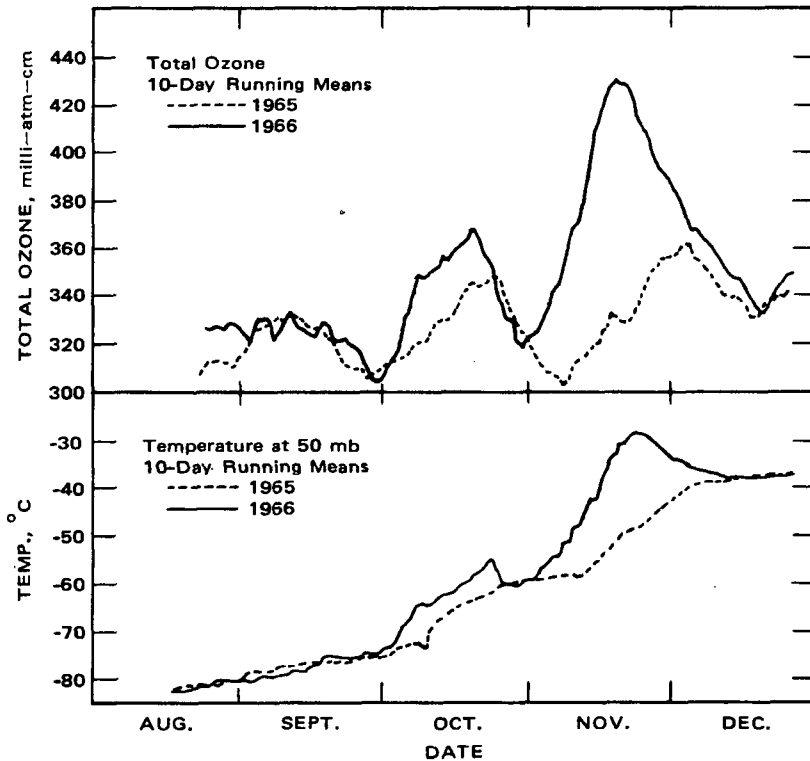


Fig. 4.23 Ten-day running means of total ozone content and of 50-mb temperature for Base King Baudouin, 1965–1966. [From J. A. Wisse and A. J. Meerburg, *Archiv fuer Meteorologie, Geophysik und Bioklimatologie, Series A (Austria)*, 18(1-2): 51 (1969).]

The south polar regions have a lag of 6 months between total ozone maximum and surface $[O_3]$ maximum. Figure 4.24 shows, with the exception of Antarctic stations, total ozone maximums occurring in nearly the same season in both hemispheres. We can conclude therefore that vertical transport processes through the jet stream and its associated tropopause break, if they were the dominant factor in stratospheric–tropospheric air-mass transports over Antarctica, should produce at best

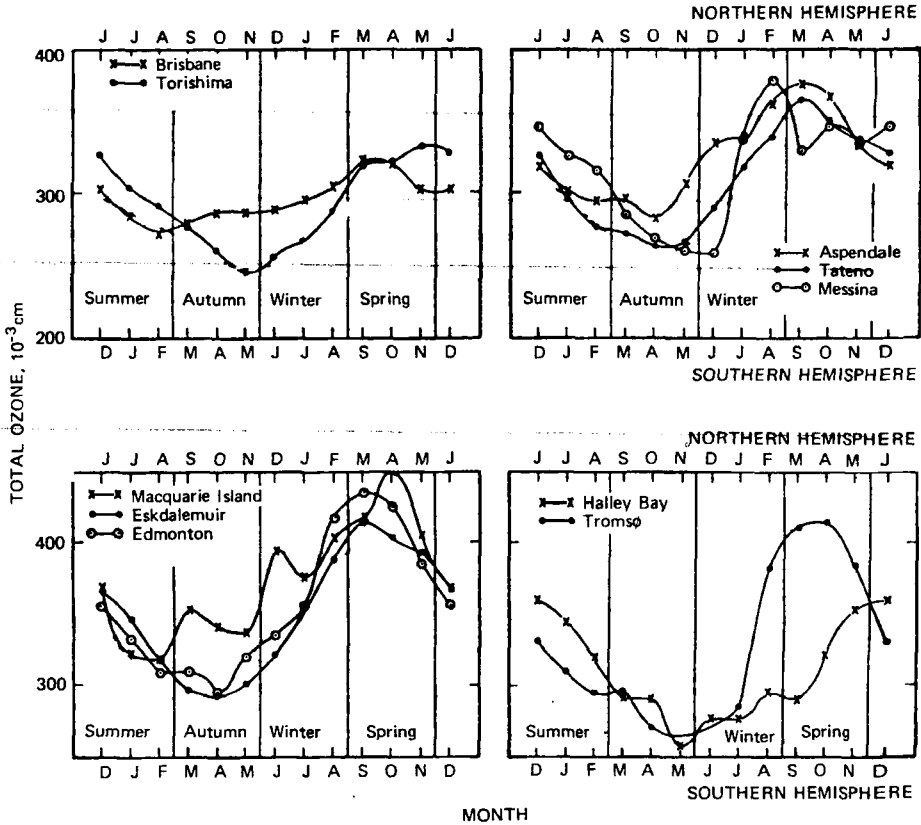


Fig. 4.24 Comparison of the seasonal variation of total ozone in the two hemispheres. [From R. N. Kulkarni, *Quarterly Journal of the Royal Meteorological Society*, 88(378): 526 (1962).]

a 2-month lag of maximum surface $[O_3]$ behind total O_3 , as they do in the northern hemisphere. The secondary surface $[O_3]$ maximum during December 1961 and January 1962 observed at the Amundsen–Scott station (Fig. 4.25) might be taken as an indication that such synoptic-scale exchange processes through the tropopause do exist. However, they appear not to be of major importance in Antarctica. The steady subsidence over the Antarctic continent, the inflow of air at high levels and the outflow at low levels, as shown in Part 1, Fig. 3.69, appears to dominate over the role of synoptic disturbances and of jet maxima. The decrease of surface $[O_3]$ from the interior of Antarctica toward the coast, along the direction of the low-level outflow, bespeaks the effect of the subsidence regime. Dobson (1966) arrived at similar conclusions. From the foregoing discussion, it appears unlikely that extraterrestrial effects, as suggested by Willett (1968) and manifest in the auroral displays, are of major importance in causing the observed hemispheric differences in stratospheric ozone concentrations.

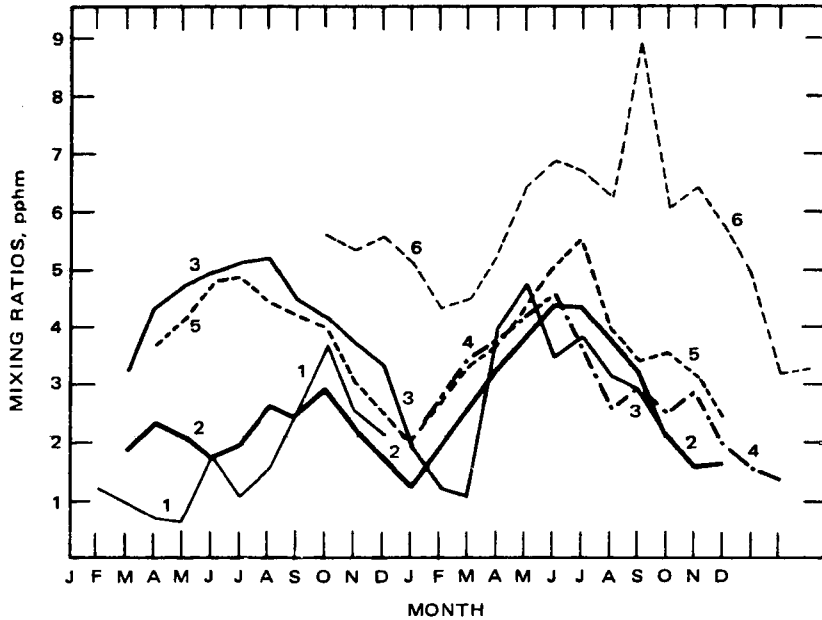


Fig. 4.25 Monthly mean surface ozone mixing ratios (in parts per hundred million) for (1) Dumont d'Urville, 1958; (2) Halley Bay, 1958-1959; (3) Little America, 1957-1958; (4) Hallett station, 1962; (5) Base King Baudouin, 1965-1966; (6) Amundsen-Scott Base, 1961-1962. [From J. A. Wisse and A. J. Meerburg, *Archiv fuer Meteorologie, Geophysik und Bioklimatologie, Series A (Austria)*, 18(1-2): 43 (1969).]

SOLAR RELATIONS OF OZONE VARIATIONS

The first part of this chapter shows that the vertical distribution of ozone depends, among other things, on the energy of ultraviolet (UV) solar radiation. It should be expected, therefore, that fluctuations in this energy would lead to corresponding fluctuations in ozone concentrations. The long relaxation times in the layers below the ozone peak, evident from Table 4.1, indicate that the chemical stability of ozone molecules in these regions exercises a strong "filtering" effect on fluctuations of UV intensity if these fluctuations have periods less than τ . The main response of ozone concentrations to short-period variations of solar UV radiation should be sought in the upper stratosphere and in the mesosphere where relaxation times are short. As shown before, however, these upper layers of the "ozonosphere" contribute little toward the total amount of ozone.

Long-period variations of UV radiation, such as might occur with the sunspot cycle (Leistner, 1967), might, at least theoretically, affect the ozone concentrations at all levels and thus be reflected in variations of total ozone. But even for such long cycles, it is difficult to estimate which of the reaction equations in Table 1.6, 2 or 5a

and 5b (photochemical generation or destruction of ozone), is most severely affected by the long periodic change in solar radiation (Mitchell, 1962). Short-period changes in UV, as they are expected, for instance, during solar eclipses, appear to lead to a temporary increase of total O₃ because of reduced photochemical ozone dissociation. As discussed earlier in this chapter, this short-term ozone increase is restricted mainly to the layers above the ozone peak, where relaxation times, τ , are small (Stranz, 1961).

Willett (1962) and Willett and Prohaska (1965) believe that they have found an effect of the sunspot cycle on ozone whereby the years of total ozone maximum occur approximately 0 to 3 years before the sunspot minimum. A similar shift in time is observed between ozone minimums and sunspot maximums. According to these investigations, the "ozone stimulating effect" cuts off sharply if sunspots move poleward of 12° heliographic latitude. Dütsch (1965, 1969), on the other hand, found an increase in the upper-stratospheric ozone over Arosa, Switzerland, before the sunspot maximum was reached and a corresponding decrease before the sunspot minimum was reached.

Dobson and Normand (1962) issued a word of caution against attempts to establish such correlations for total ozone from optical measurement data. Such measurements depend on the relative intensities of two wavelengths whose absorption by ozone is deduced by comparing them against the "extra-terrestrial intensity values." Long-term fluctuations of the latter are difficult to measure from the earth's surface because of calibration difficulties in the instruments. Satellite measurements would be desirable in an attempt to settle this problem (Rasool, 1963; Paetzold, 1963).

Furthermore, it is difficult to assess any secular changes of total ozone that might have been produced by circulation changes over the stations used in Willett's statistics (Mitchell, 1962). London and Haurwitz (1963) have shown that records of mean total ozone, of sunspot number, and of mean sunspot latitude each possess maximum autocorrelation coefficients near the period of 10 years. It remains to be seen, from observations made during future sunspot cycles, whether this 10-year periodicity in these three parameters occurs at a constant phase relation between these parameters, as Willett suggested from relatively short records, or whether the phase relation shifts in time. If the latter were the case, a sunspot dependence of total ozone probably would have to be denied.

The suggestion by Willett and Prohaska (1965) that corpuscular radiation "beamed" from sunspots at low heliographic latitude (it is difficult to postulate a "beaming" effect for UV wave radiation) may cause a response of total ozone to the sunspot cycle is not too attractive either. Although the "beaming" of corpuscular radiation from disturbed regions on the sun may explain the observed semianual geomagnetic variations (Priester and Cattani, 1962), it is doubtful if the reactions in the high atmosphere [as determined, for instance, by the braking of satellites in a denser-than-normal environment (Paetzold, 1963; Grigorevskii, 1964; Jacchia, 1964; Mikhnevich, 1964) or by an enhancement of ionospheric current systems (Akasofu and Chapman, 1963)] reach as far down as the ozonosphere. Ahmed and Halim (1961), for instance, found no significant correlation between total ozone and

geomagnetic activity or solar corpuscular radiation (see also Fritz, 1951; Götz, 1951). Rasool (1961), however, pointed toward the existence of such a correlation (see also Sekihara, 1961). According to Ahmed and Halim, there is a certain likelihood that the extraterrestrial intensity of UV radiation undergoes changes with solar activity, as suspected by Dobson and Normand (1962).

From the foregoing discussion, it appears that the dependence of total ozone on sunspot activity and on the sunspot cycle still awaits further corroborating evidence. A periodicity of 25 or 26 months in relative sunspot numbers (Shapiro and Ward, 1962), corresponding roughly to the "biennial oscillation" of stratospheric flow in tropical latitudes, has even less significance and should not be considered as the cause of this oscillation. This is also evident from a study by Lindzen (1965) (see also Lindzen and Goody, 1965), who concluded that minor changes in solar UV emission have only a negligible effect on the thermal structure of the equatorial stratosphere and mesosphere. Fluctuations of 12% in the UV bands of O_3 and O_2 would be needed to give rise to a $2^\circ C$ fluctuation of mesospheric temperatures. Only a 3 to 6% variation in visible radiation, however, would be needed to cause the same temperature variation at heights of 20 to 35 km. Lindzen notes that, on the average, 26% of the visible radiation at these levels is received in the form of reflected radiation from below. Thus variations in albedo, caused by large-scale variations in cloud cover, may have a significant influence on stratospheric and mesospheric temperatures.

OZONE AND THE BIENNIAL OSCILLATION

From the foregoing remarks it appears unlikely that the biennial oscillation is caused by a direct solar-terrestrial relation that would act upon the ozonosphere. The evidence of a biennial oscillation being present in total ozone records, therefore, will have to be interpreted differently. In light of recent investigations by J. M. Wallace and Kousky (1968a, 1968b), it appears more likely that the biennial oscillation is caused by the trapping of upward propagating internal Kelvin waves in a layer with supercritical vertical wind shear (see also Yanai and Maruyama, 1966; Maruyama, 1967; Maruyama and Yanai, 1967; Holton and Lindzen, 1968; Lindzen and Matsuno, 1968; Maruyama, 1968a, 1968b, 1969; Yanai et al., 1968; Yanai and Hayashi, 1969).

A comparison of total ozone records from tropical and extratropical stations made by Ramanathan (1963b) seems to indicate that years with above-normal ozone amounts in temperate and subtropical latitudes correspond to years with low total ozone near the equator. Rome, Italy ($42^\circ N$), and Tateno, Japan ($36^\circ N$), show a rather similar behavior of the biennial periodicity of ozone (Fig. 4.26). The records from Arosa, Switzerland ($46.5^\circ N$) (Fig. 4.27), fit the same pattern (J. M. Wallace and Newell, 1966). From Fig. 4.27, especially when compared with Fig. 4.26, the fallacy of establishing periodicities from records that are too short, pointed out by London and Haurwitz (1963; see also Farkas, 1969), becomes quite apparent. The biennial oscillation is well established in this data series only between 1952 and 1963. At the end of this time period, a breakdown or shift of the oscillation seemed to occur after

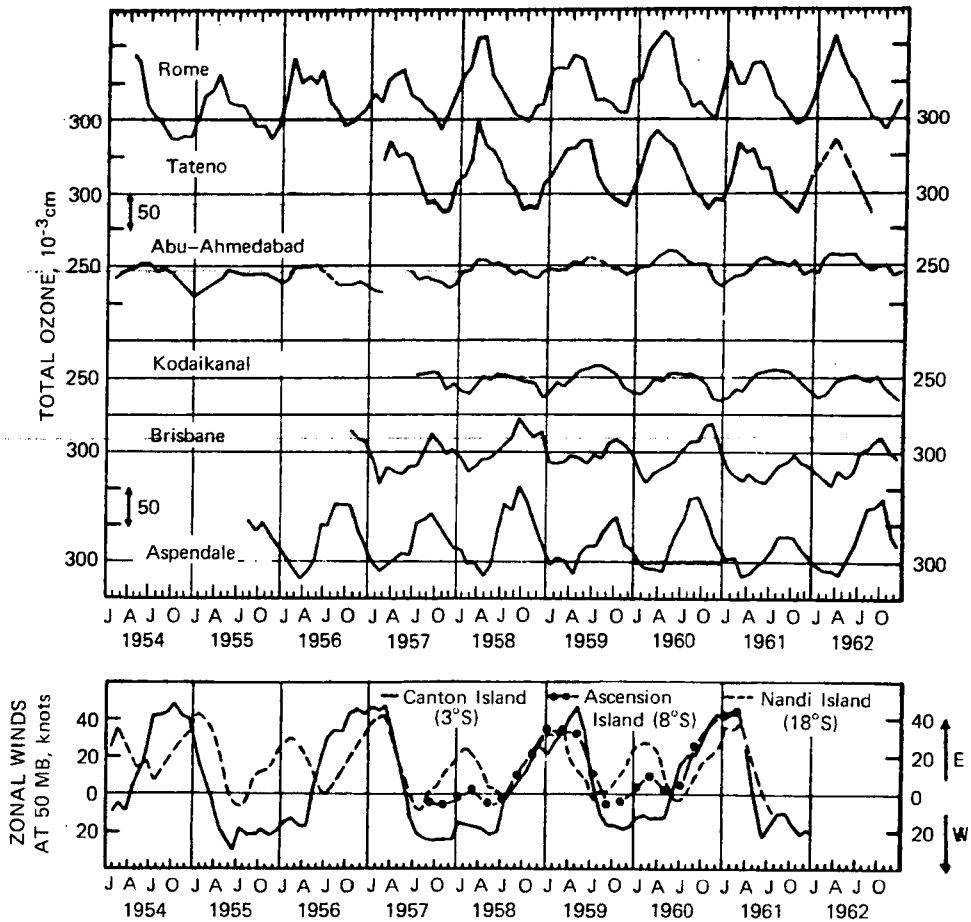


Fig. 4.26 Monthly mean ozone amounts for stations and years as indicated (a) and monthly mean zonal winds at 50 mb over equatorial stations (b). [From K. R. Ramanathan, *Quarterly Journal of the Royal Meteorological Society*, 89(382): 541 (1963).]

which the biennial oscillation reestablished itself (Hopwood, 1969). This breakdown in the biennial ozone oscillation has been commented on by several authors (Ramanathan, 1965; R. N. Kulkarni, 1966b; London, 1967a, 1969). Its causes have yet to be explored.

During the time period in which the biennial ozone oscillation did exist (see Fig. 4.26), above-normal spring maximums in the northern hemisphere appear to have been followed by above-normal spring maximums in the southern hemisphere. The stations of Mt. Abu and Ahmedabad (25–23°N) seem to have followed the 1-year phase shift between extratropical and tropical ozone maximums. Kodaikanal (10°N), however, was in phase with the biennial cycle of the northern hemisphere and out of phase with the cycle in the southern hemisphere. Shah (1967) deduced a “progres-

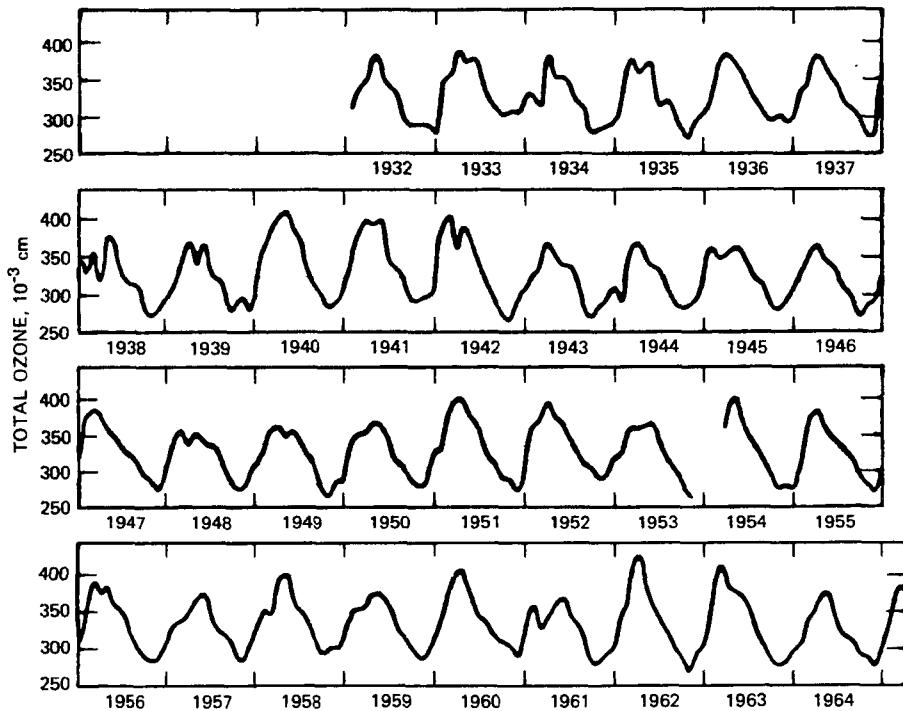


Fig. 4.27 Monthly mean total ozone amounts at Arosa, Switzerland (46.5°N , 9.4°E). [From J. M. Wallace and R. E. Newell, *Quarterly Journal of the Royal Meteorological Society*, **92**(394): 487 (1966).]

sion" of the phase of the biennial variation of total ozone from the equator to extratropical latitudes in the northern hemisphere (Fig. 4.28). Angell and Korshover (1964, 1967) arrived at similar conclusions, computing a poleward progression of the "biennial wave" of about 0.2 m/sec. Poleward of 40° the drift becomes indistinct. In the southern hemisphere, according to their study, phase shifts appeared to be similar to those shown in Fig. 4.28. However, in this hemisphere conditions are not a simple mirror-image of the ones in the northern hemisphere. Biennial maximums of total ozone at Aspendale and Brisbane (see also Funk and Garnham, 1962), for instance, appear about 9 months, and not 6 months, later than the maximums in corresponding latitudes of the northern hemisphere. The hemispheric differences in meridional transports, which lead to a late winter maximum of total ozone in the northern hemisphere and to a late spring maximum in the southern hemisphere, thus also exercise their influence on the biennial variation of ozone distribution. This would also suggest that the cause of the 26-month oscillation is not to be sought in extraterrestrial factors but rather in variations of the large-scale transport mechanism, horizontal ones as well as vertical ones, the latter in the form of vertically propagating Kelvin waves. There are also longitudinal differences in the occurrence of the total ozone maximums which make the biennial oscillation and its propagation a fairly complicated matter.

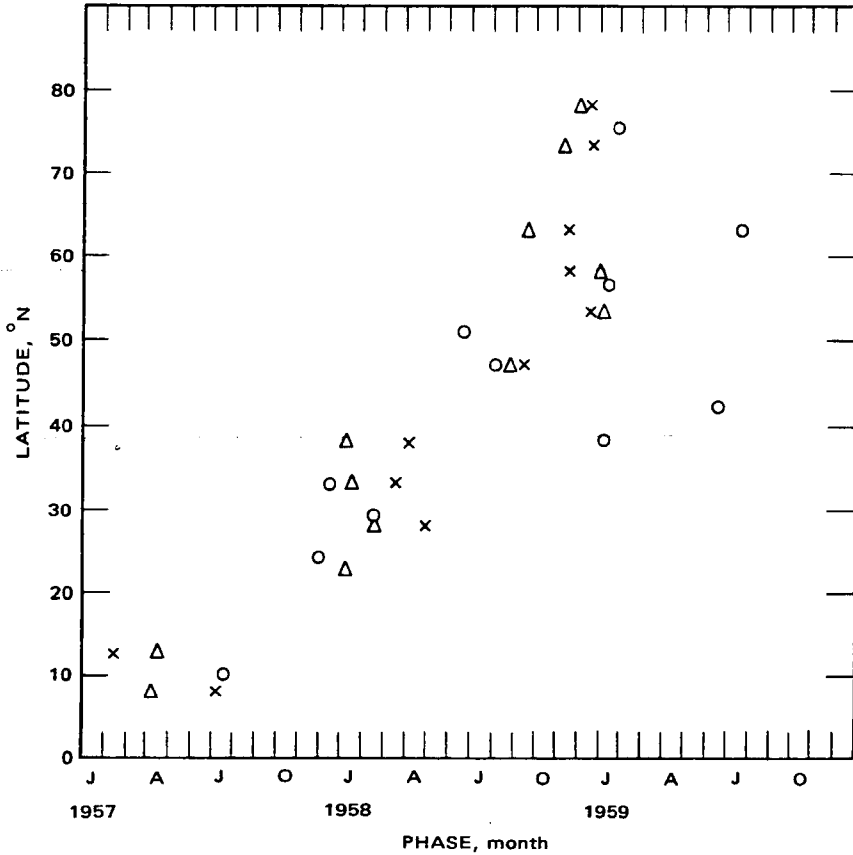


Fig. 4.28 Phase of the 26-month oscillation, averaged vectorially over 5 degrees of latitude, in ozone (\circ), temperature at 30 mb (Δ), and temperature at 50 mb (\times). [From G. M. Shah, *Journal of the Atmospheric Sciences*, 24(4): 399 (1967).]

It is of interest to note that the phases of the 26-month temperature maximums at 30, 50, and 60 mb agree well with the phase of the ozone variation. (The 30- and 50-mb temperature phases are shown in Fig. 4.28.) Shah (1967) found that the phase of the 50-mb temperature preceded the ozone oscillation by about 0.3 month on the average, whereas the 60-mb temperature phase lagged behind by about the same time span. There is only very little longitudinal variation in the occurrence of the biennial temperature maximums.

According to Sparrow and Unthank (1964), the ozone maximums appear to be 180° out of phase with the maximums in zonal winds, at least over Aspendale and Brisbane. Over the equator the total ozone starts to increase with the establishment of a westerly wind regime in the middle and lower stratosphere. It decreases with the appearance of easterlies in the middle stratosphere (Rangarajan, 1964). These observations are in good agreement with the vertical circulation model derived by R. J.

Reed (1964) and shown in Part 1, Fig. 3.16. Grasnck and Hoebbel (1967) found the correlation shown in Table 4.4, which is in agreement with the foregoing statements. (It has been mentioned that years with high total ozone amount in the tropics concur with years of low total ozone in the subtropics.) According to Table 4.4, there also is a correlation between tropical wind systems, ozone, the time of breakdown of the northern hemisphere polar vortex, and the direction of motion of the stratospheric warming centers (see Fig. 3.63, Part 1).

Table 4.4
CORRELATION BETWEEN OZONE AND STRATOSPHERIC
CIRCULATION CHARACTERISTICS*

Year	Winds in the stratosphere of the tropics (March)	Movement of stratospheric warmings	Type of final warming	Total ozone amount over the north- ern hemisphere (March)
1957	W	Eastward	Early	
1958	E	Westward	Late	
1959	W	Eastward	Early	
1960	E	Westward	Late	High
1961	W	Eastward	Early	Low
1962	E	Eastward	Late	High
1963	E	Westward	Late	High
1964	W	Eastward	Early	Low
1965	E	Eastward	Late	High
1966	E	Westward	Late	High

*From K.-H. Grasnck and W. Hoebbel, 1967.

Excluding extraterrestrial causes of the biennial ozone variation for reasons mentioned earlier, the preceding facts suggest a triggering of this oscillation within the earth's atmosphere. This conclusion is corroborated by a study by J. M. Wallace and Newell (1966), who found that during winters preceding those spring seasons with above-normal ozone maximums, the poleward eddy transport of heat and momentum is above normal. The biennial modulation of these transports is especially well developed above the 30-mb level. (For further details, see Part 1, Chap. 3.) As Newell (1964b, 1964d) suggests, eddy transports and their variability from year to year may cause the observed periodicities in total ozone and in stratospheric temperature and wind regimes. Tucker (1964) arrived at similar conclusions. The studies by J. M. Wallace and Kousky (1968a, 1968b) mentioned earlier, which indicate that the trapping of Kelvin waves is responsible for the biennial wind oscillation, might well be regarded as an explanation of the triggering mechanism that sets off the observed oscillation in ozone. Furthermore, the results of Lindzen's (1965) study should be recalled here, according to which stratospheric and mesospheric temperatures may react significantly to changes in the earth's albedo, which are produced mainly by

cloudiness. It might well be possible therefore that the observed biennial oscillation was the result of a feedback mechanism between atmospheric energetics and eddy transport processes in the stratosphere and troposphere, the latter resulting in specific cloud distributions. Such a variation in cloudiness could be brought about by systematic changes in pressure patterns (Murray and Moffitt, 1969; Angell, Korshover, and Cotten, 1969) and tropospheric wind regimes (Angell and Korshover, 1968; Newell, Kidson, and Vincent, 1969). According to Godshall et al. (1969), the biennial variation of cloud cover in the tropics leads the biennial wind oscillation by several months. The cloud-cover variation correlates well with ocean surface temperatures, which, in the Christmas Island region, also show a biennial variation. This evidence strengthens the hypothesis of a feedback mechanism within the earth-atmosphere system. Systematic measurements of the earth's albedo by satellites, together with numerical modeling of the atmospheric general circulation, might eventually shed some light on such a possible feedback.

A new slant on the problem of the biennial oscillation has been provided by Schove (1969), who considers, among other things, growth rings in trees as climatological indicators. He maintains that the 2.2-year oscillation is a subcycle, generated by the earth-atmosphere system, to the 11-year sunspot cycle (see also Berson and Kulkarni, 1968).

THEORETICAL MODELS OF OZONE TRANSPORT

In Chap. 1 a rather simple model of eddy transport, directed against the mean gradient of the quantity to be transported, is discussed. This model was applied by R. J. Reed and German (1965) to the observed ozone distribution. Since the results obtained were quite satisfactory, we can conclude that the premises on which this model was based, especially the derived eddy diffusion conditions, portray the eddy transports in the stratosphere reasonably well.

Other authors have dealt with the same problems of "modeling" atmospheric transport characteristics after the observed ozone distribution. London and Prabhakara (1963), for instance, arrived at a theoretical ozone distribution by assuming photochemical equilibrium to be disturbed by transport terms. The latter are based on estimates of eddy exchange coefficients, K_y and K_z , by Prabhakara (1962, 1963), which are slightly lower than the K_{yy} and K_{zz} derived by R. J. Reed and German (1965) and given in Table 1.1. Mean motions in the stratosphere were taken from estimates by Murgatroyd and Singleton (1961) (Fig. 1.16), but values were reduced by 80%. Hesstvedt (1965b) also found that the ozone distribution over the equator is modeled adequately by assuming vertical motions in the stratosphere to be less than those derived by Murgatroyd and Singleton (1961). Ascent rates in the troposphere, however, were assumed by Hesstvedt to be slightly higher.

Chapter 6 mentions, in conjunction with the water-vapor transports near the noctilucent-cloud level, that the mean-motion estimates by Murgatroyd and Singleton (1961) appear to have the correct magnitude. The circulation model of these two

investigators, however, contains only a "one-cell stratosphere" with rising motions near the equator and sinking motions throughout the winter polar stratosphere and mesosphere. Although this pattern might conform to the sinking motions found over Antarctica and shown in Part 1, Fig. 3.69, it does not take into account the "two-cell" structure of the northern hemispheric winter stratosphere. There, according to Part 1, Fig. 3.11, we find maximum sinking motions in middle latitudes and ascending motions again near the pole.

In spite of these shortcomings in the assumptions on which the London and Prabhakara (1963) model is based, the computed distribution of total ozone with latitude averaged over a whole year agrees well with the observed distribution. (Computed values are slightly too low except for equatorial latitudes, indicating that the transport processes have been underestimated.) Additional details are given in the paper by Prabhakara (1963).

The observed surface distributions of O_3 may also be utilized in arriving at models of large-scale atmospheric exchange properties. We may compare Junge's (1962a) estimate of hemispheric vertical ozone transport in the troposphere, 0.5×10^{-7} g/m²/sec, with Regener's (1967) value of 1.2×10^{11} molecules of O_3 per cubic centimeter and per second in middle latitudes quoted earlier. For the molecular weight of ozone in grams, 48, and for Avogadro's number, $N = 6.02486 \times 10^{23}$, giving the number of molecules per gram-mole, we arrive at the mass of 1 molecule of O_3 , 7.97×10^{-23} g. Hence the transfer of 1.2×10^{11} molecules/cm²/sec is equivalent to 9.56×10^{-12} g/cm²/sec, or 0.956×10^{-7} g/m²/sec. Thus Regener's (1957) estimate for midlatitudes is higher by almost a factor of 2 than Junge's (1962a) hemispheric value. This should not be surprising since we do find considerable latitudinal variation of tropospheric ozone (as well as of radioactive fallout of stratospheric origin) and hemispheric differences as well, which will be discussed later.

Junge and Czeplak (1968) arrived at a model of the variation of surface $[O_3]$ given by the amplitudes $c = c(\mu, t)$, where $\mu = \sin \phi$, $\phi =$ geographic latitude, and $t =$ time (see Eq. 3.3). The value $c(\mu, t)$ is expected to reach a balance between destruction of ozone at the ground and supply of O_3 by a high-level source located above the tropopause. The source function may be written as

$$Q(\mu, t) = b(\mu) \sin 2\pi t - d_0 c(\mu, t) \quad (4.10)$$

where $d_0 = 1/\tau$ is a constant, the exchange rate, τ being the tropospheric residence time of ozone. For $\tau \approx 3$ months, $d_0 \approx 3.6 \text{ years}^{-1}$. The term $b(\mu)$ is the latitude-dependent amplitude of the seasonally variable component of the O_3 source function. Values of $b(\mu)$ are shown in Fig. 4.29(a). Curve 1 represents the assumption that the flux of O_3 from the stratosphere to the troposphere occurs mainly during spring with an intensification of the polar-front and subtropical jet-stream activity and with intrusion processes as shown in Fig. 4.9. Curve 2 incorporates the idea that the polar tropopause permits additional intrusions (Lockhart et al., 1959, 1960; Martell and Drevinsky, 1960; Münnich and Vogel, 1963). Curve 3 is based on Staley's (1962) idea of lifting and lowering of the tropopause at all latitudes $\phi > 30^\circ$ as a process of

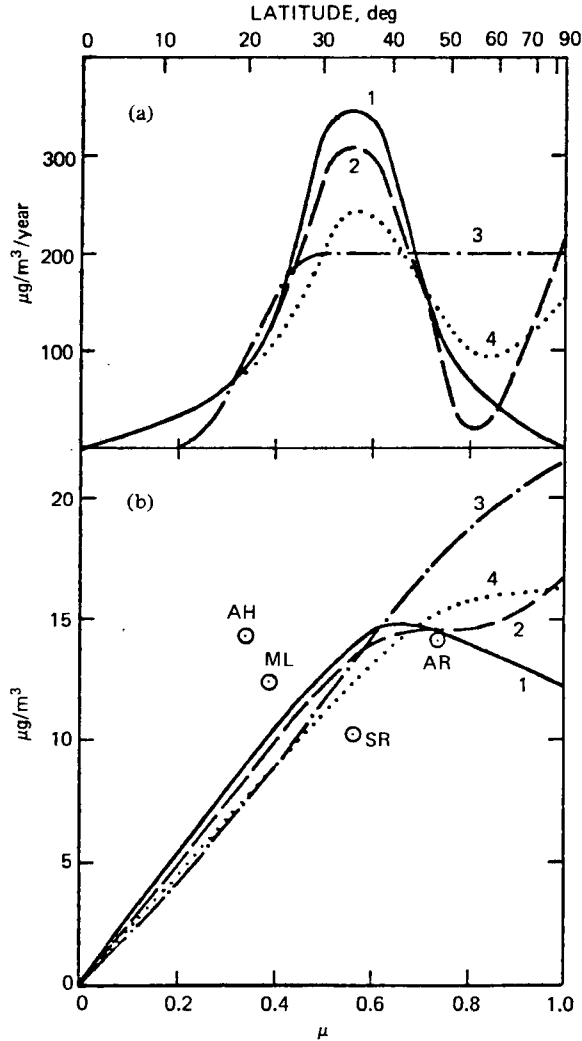


Fig. 4.29 (a) Assumed models of the $[\text{O}_3]$ amplitudes $b(\mu)$ based on various concepts about the exchange mechanism between stratosphere and troposphere. (b) Calculated amplitudes of $c(\mu, t)$ for the $b(\mu)$ models in (a) and $K = 3 \times 10^{10} \text{ cm}^2/\text{sec}$. Included are the observed amplitudes at the stations listed in Table 4.5: AR, Arosa; AH, Ahmedabad; ML, Mauna Loa; SR, Srinagar. [From C. E. Junge and G. Czeplak, *Tellus*, 20(3): 432 (1968).]

stratospheric–tropospheric mass exchange. Curve 4 is assumed to incorporate all aforementioned processes of such mass fluxes. It shows an amplitude of $b(\mu)$ in middle latitudes that is approximately twice as high as the hemispheric average value, in agreement with the “discrepant” estimates by Regener (1957) and Junge (1962a).

Figure 4.29(b) compares the values of the amplitudes $c(\mu, t)$ for corresponding values of $b(\mu)$ shown in Fig. 4.29(a) and for a constant exchange coefficient $K = 3 \times$

10^{10} cm²/sec (see Chap. 3) with surface [O₃] measurements at the stations given in Table 4.5. Junge and Czeplak (1968) were able to show that a slightly better fit of the model to the observations could be obtained by allowing K to vary with latitude. Any uncertainty in the values of $K(\mu)$ and any asymmetry of $b(\mu)$ between the northern

Table 4.5
INFORMATION ON THE SEASONAL VARIATION OF [O₃]
OVER FOUR STATIONS IN THE NORTHERN HEMISPHERE*

Station	Latitude	Amplitude of [O ₃] variation, μg/m ³	Spring maximum
Arosa, Switzerland	47°N	14	May
Srinager, India	34°N	10	May
Ahmedabad, India	23°N	14	February–March
Mauna Loa, Hawaii	19°N	12	April

*From C. E. Junge and G. Czeplak, *Tellus*, 20(3): 430 (1968).

and southern hemispheres affect primarily the c values at latitudes $\phi \leq 40^\circ$. At $\phi \geq 40^\circ$, c is influenced mainly by the assumed variation of b with latitude and not so much by K .

Junge and Czeplak (1968) conclude from this that more detailed information on tropospheric [O₃] in tropical and subtropical latitudes ($\phi < 30^\circ$) may shed considerable light on interhemispheric differences in stratospheric-tropospheric exchange processes, whereas [O₃] data at higher latitudes would yield information on the magnitude of transports through the polar tropopause.

As has been demonstrated, further refinements of the present models of ozone transport may be anticipated with a more accurate determination of the eddy diffusion coefficients as functions of height, latitude, and time. One should also be aware of the fact that transport models based upon the diffusion equation, such as the one outlined in Chap. 1, are rather crude approximations of actual atmospheric conditions. As shown in Part 1, Chaps. 3 and 4, transport mechanisms do not act uniformly throughout the spectrum of atmospheric eddies. Further developments might even resort to the definition of different diffusion coefficients for different scales of motion. We have stated, for instance, in Chap. 1 that large-scale eddy processes may lead to a countergradient non-Fickian flux of the quantity to be transported. At the same time, however, there are small-scale turbulent flux processes acting in the direction of local gradients trying to destroy them. By comparing theoretical transport models with observed ozone distributions, these small-scale effects have been included tacitly into our consideration. We will have to learn a lot more about the behavior and the turbulence characteristics of all eddy scales before more adequate transport models can be developed. Such models, once available, will aid greatly in the understanding of some of the intricate mechanisms of the general circulation described in Part 1.

5 OXYGEN AS A TRACER

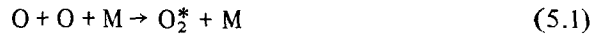
MOLECULAR AND ATOMIC OXYGEN

Table 1.6 lists a number of reaction equations that involve molecular and atomic oxygen besides ozone. Chapter 4 lists a number of literature references in which additional refinements of these oxygen reaction equations can be found with regard to various electronic excitation states of O and O₂. The advances of plasma physics and of physical chemistry which have been made in recent years begin to shed some light on the processes in which the upper atmosphere is involved. Several of these processes are made visible by light emission in specific wave bands of electromagnetic radiation. [A collection of papers on this subject was published recently by McCormac and Omholt (1969).] With the improvement of observation techniques, which measure these small amounts of radiation, we can begin to utilize the chemical constituents of the upper atmosphere as tracers of motions in these high regions.

Figure 1.16 shows horizontal and vertical circulations up to approximately mesopause level as postulated by Murgatroyd and Singleton (1961). These circulations were inferred from heat-transport requirements between equator and pole near the tropopause and between summer and winter poles in the mesosphere, not taking into account eddy transport processes. Criticism about the validity of the circulation schemes, shown in Fig. 1.16 for the stratosphere, has already been voiced: In Part 1, Chap. 3, it has been demonstrated that in the middle stratosphere of the northern hemisphere winter a two-cell pattern seems to exist with sinking motions in middle latitudes and ascending motions over the pole. This is not evident from Fig. 1.16.

In spite of these shortcomings in the lower layers of Murgatroyd and Singleton's circulation model, we will accept the mesospheric motion pattern at least as a working hypothesis while searching for further evidence to substantiate these drifts computed from the heat-balance requirement. We will also seek to extend the model to still higher altitudes.

Stroud et al. (1960) showed that mesospheric temperatures in the 70- to 95-km layer are up to 70°K warmer over the winter pole than over the summer pole. Yet, according to Murgatroyd and Goody (1958), we should expect a heat sink at these heights during winter mainly because of heat loss by infrared radiation from CO₂. To account for the observed high temperatures, Kellogg (1961) postulated the existence of a meridional circulation that carries atomic oxygen from low latitudes to the winter pole. Subsidence there would cause dynamic warming, and, in addition, sensible heat would be realized by the recombination process



where the asterisk indicates a state of electronic excitation. The molecule will be deactivated according to



Such deactivation may be observed in the spectrum bands of night airglow, especially at 5577 Å (oxygen green line) (Schröer, 1947). According to Evans et al. (1968), the infrared emission of O₂ at 1.27 μ may also serve as an indicator of deactivation processes. Decomposition of O₃ seems to play a major role in this emission (see also Hunten and McElroy, 1968). [For a complete spectrum of night airglow accessible from the ground, between 0.31 and 1.0 μ, see Broadfoot and Kendall (1968). Far ultraviolet (UV) airglow has been observed from rockets (Moos and Fastie, 1967).]

Seasonal variations in the 1.58-μ emission of O₂ have been observed by Vallance Jones and Gattinger (1963). (Dissociation of ozone in the mesosphere appears also to be responsible for emission in this airglow band, which is observed during the twilight hours.) Although this seasonal variation, which showed a late spring and early summer minimum in the relative brightness of the 1.58-μ radiation band over a Canadian station, could not be explained by Vallance Jones and Gattinger, it might well be that vertical transport processes (see, for example, Fig. 1.16 by Murgatroyd and Singleton) exercise a certain influence on the ozone dissociation processes that lead to this twilight phenomenon. There also appears to have been a decreasing trend in the relative brightness of the 1.58-μ O₂ emission between 1961 and 1964, which correlates well with the monthly average sunspot numbers (Gattinger and Vallance Jones, 1966). Such a correlation has also been detected for the 5577 Å green line, as will be discussed later.

Young and Epstein (1962) were able to show that moderate vertical motions of less than 1 cm/sec might conceivably transport enough atomic oxygen to lower altitudes, where it would recombine according to Eqs. 5.1 and 5.2 to account for the

warming mechanism postulated by Kellogg. Figure 5.1 shows the heating rates for different vertical velocities and different initial [O] concentrations. Figure 5.2 shows that vertical velocities also affect the height of the peak [O] concentrations as well as their magnitude (Nicolet, 1958).

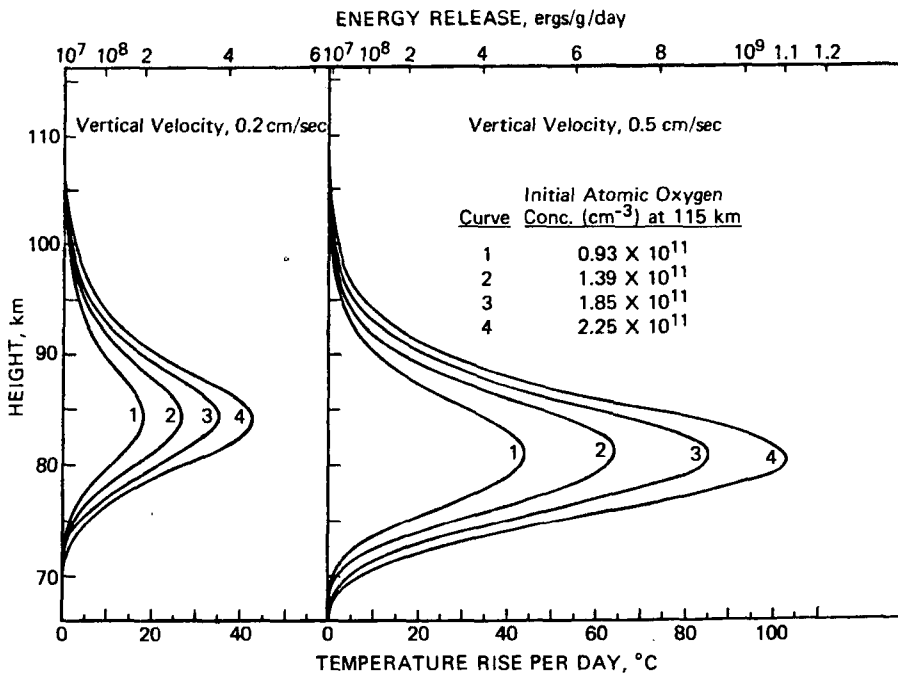


Fig. 5.1 Heating rates as a function of height for various vertical velocities and initial concentrations of atomic oxygen. [From Ch. Young and E. S. Epstein, *Journal of the Atmospheric Sciences*, 19(6):440 (1962).]

THE OXYGEN GREEN LINE, 5577 Å

If the 5577 Å oxygen green line of airglow and its intensity can be taken as an indicator of the recombination process (Eqs. 5.1 and 5.2), we can hope that the characteristic behavior of airglow patterns will be specific for certain high-atmospheric flow patterns. Tohmatsu and Nagata (1963) have given a summary of airglow observations that lend themselves to the study of the dynamics and kinematics of the upper atmosphere. For further references and details, see the original paper by these two authors.

The altitude distribution of 5577 Å airglow emissivity, as measured by rockets, reveals a maximum near the level of peak [O] concentration (Golomb et al., 1965;

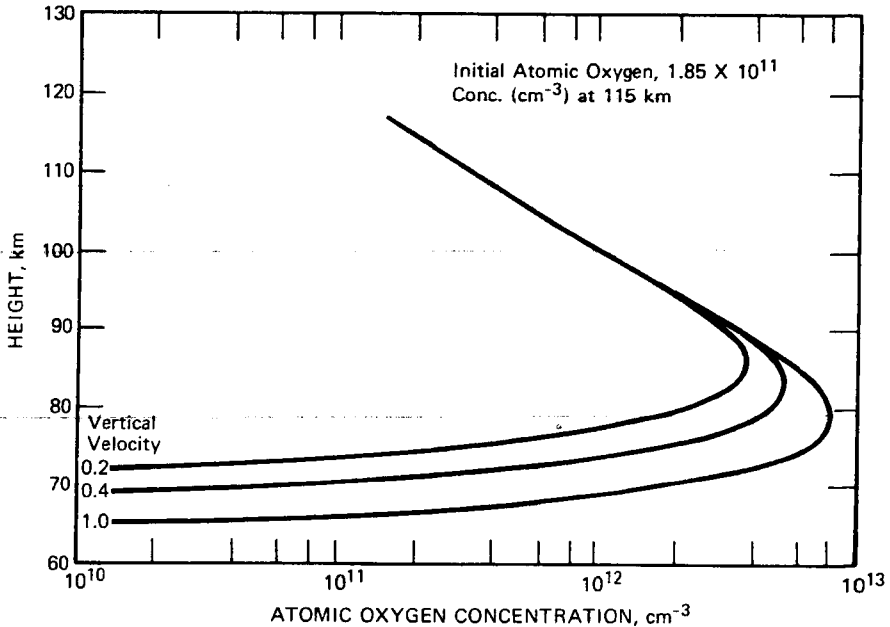


Fig. 5.2 Computed profiles of atomic oxygen concentration for vertical velocities of 0.2, 0.4, and 1.0 cm/sec. [From Ch. Young and E. S. Epstein, *Journal of the Atmospheric Sciences*, 19(6):438 (1962).]

Spindler, 1966; Golomb and Good, 1967; Greer and Best, 1967). According to Fig. 5.2, the peak of [O] reacts sensitively to vertical motions. Figure 5.3 shows emissivity as a function of altitude and vertical velocity, as computed by Tohmatsu and Nagata (1963) (see also P. V. Kulkarni, 1965). Figure 5.4 contains night-glow observations of the 5577 Å oxygen green line made over White Sands, N. Mex., on Apr. 28, 1966 (Baker and Waddoups, 1967, 1968). The continuum emission (see Ratcliffe, 1960, p. 225) was subtracted before values were entered into this diagram. The emission peaks sharply at 102 ± 5 km, which, according to Fig. 5.3, is indicative of sinking motion. This is in fair agreement with mesospheric circulation patterns below 80 km (Fig. 1.16).

Airglow patches of typical horizontal dimensions of 2500 km have been observed to move with speeds of about 100 m/sec (Chamberlain, 1961). A recent evaluation of data from the OSO-B2 satellite (March–October 1965) by Sparrow et al. (1968) revealed a patchiness of similar dimensions in longitudinal airglow profiles (see also Slack, 1967). Speeds of ≈ 50 m/sec are indicated on occasion from position shifts of such patches. These speeds, however, do not necessarily have to be wind velocities. They may, to some extent, camouflage the horizontal propagation of vertical motion patterns, which cause an enhancement of airglow emission. The patchiness of the

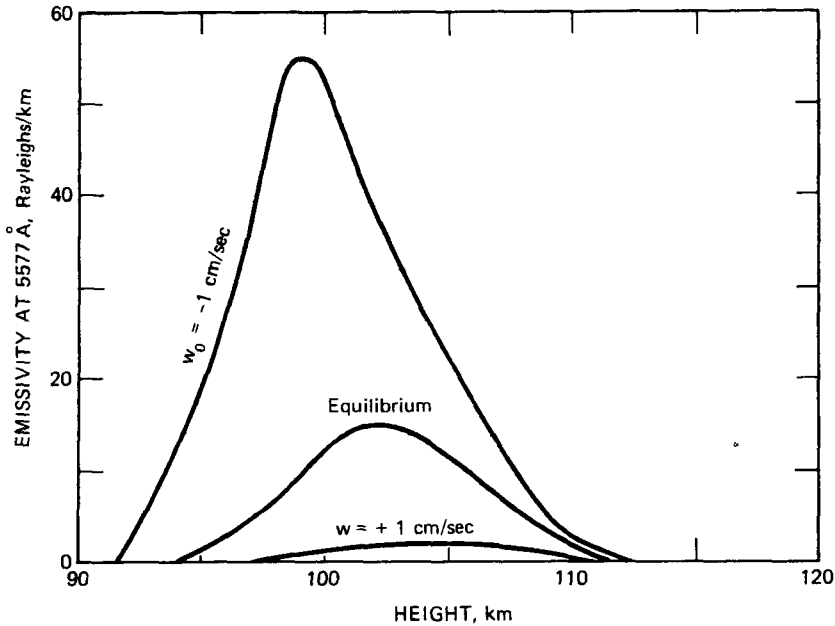


Fig. 5.3 Altitude distributions of the 5577 Å radiation emissivity at different vertical transport velocities (w). [From T. Tohmatsu and T. Nagata, *Planetary and Space Science*, 10:108 (1963).]

airglow phenomenon might serve as an indicator of large-scale eddy transport processes at these altitudes, which were neglected in Murgatroyd and Singleton's (1961) circulation model. Meteor-trail observations (Greenhow and Lovell, 1960) and ionospheric drift observations (Ratcliffe and Weeks, 1960) indicate that these eddy motions may be, to a large extent, of a tidal nature, showing semidiurnal and diurnal periodicities. Phase (expressed in local time) and amplitude of the semidiurnal component vary considerably with height and season in the layers adjacent to the mesopause (see Chap. 1). Eddy effects may also be inherent in the large temperature variations observed in the upper mesosphere and lower thermosphere within a few hours as well as from day to day (W. S. Smith et al., 1964; Hernandez and Turtle, 1965).

Lagos (1969) argues that the observed large diurnal variability of the 5577 Å (OI) emission cannot be explained satisfactorily by vertical motions if only the three-body recombinations $3O \rightarrow O_2 + O(^1S)$ were held responsible. A typical intensity variation of the emission of 100% would call for a variation of 30% or more in $[O]$, which would require very strong vertical motions in view of the short time scales involved. Lagos, therefore, holds a two-step mechanism important, whereby the reaction of Eq. 5.1 is followed by a second reaction of the form $O_2^* + O \rightarrow O_2^{**} + O(^1S)$. Here O_2^* and O_2^{**} symbolize different states of electronic excitation. Atomic oxygen in the state $O(^1S)$ causes the 5577 Å emission.

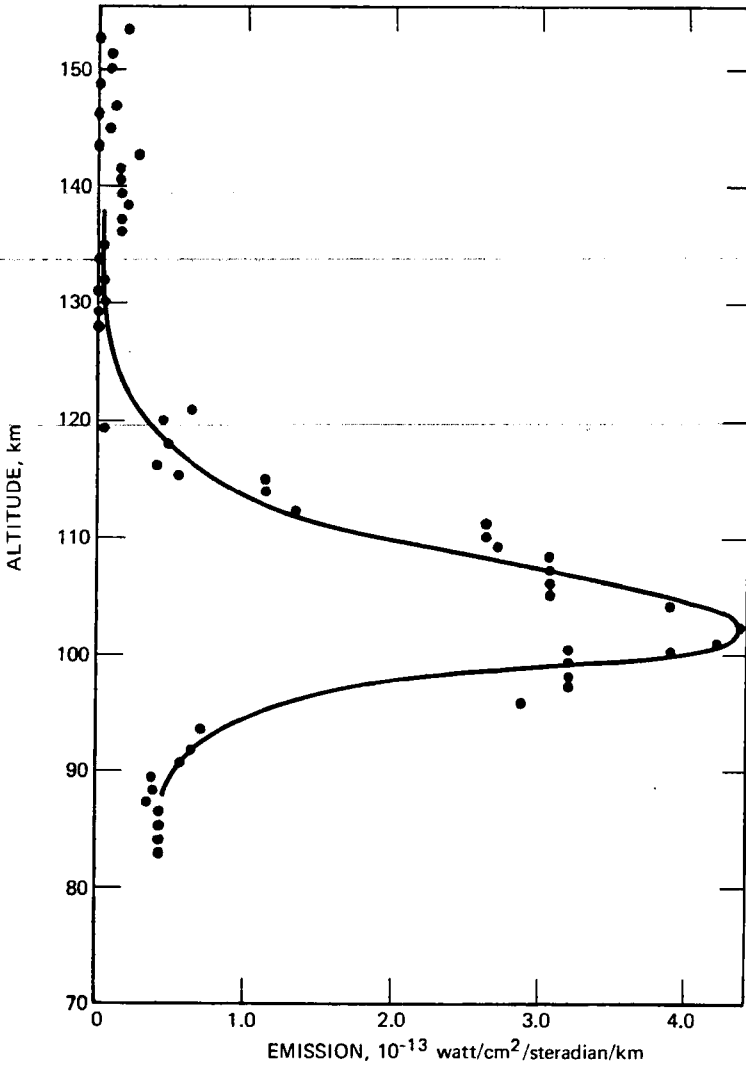


Fig. 5.4 Altitude profile of the night-sky airglow oxygen green line over White Sands, N. Mex., Apr. 28, 1966. The radiation of the night-glow continuum emission has been subtracted. [From D. J. Baker and R. O. Waddoups, *Journal of Geophysical Research*, 73(7):2547 (1968).]

Observations of the ionospheric F-region show that irregularities of a scale smaller than those revealed by airglow patches are present in the thermosphere. Essex and Hibberd (1968) found irregularities in the E- and F-regions with horizontal scale sizes of only a few hundred meters. Titheridge (1963, 1968a) observed waves with a periodicity of 15 to 60 min and a wavelength of 40 to 160 km in the F-layer, possibly

indicating the presence of gravity waves. Such disturbances were found mostly during daytime. They were absent during sunrise and sunset. Highest frequencies of occurrence were encountered during winter, with an increase toward higher latitudes (for a theoretical discussion, see Reid, 1968). N. N. Rao (1967) found gravity-wave disturbances of somewhat larger wavelength (250 to 750 km) characterizing the peak of the F-region (350-km height). As will be mentioned later in this chapter, the middle and high latitudes during the winter season are also characterized by anomalously strong F development with dominant large-scale irregularities.

If the large tidal periodicities are removed from the records, prevailing wind patterns can be studied. Gracade experiments (Webb, 1966a) and rocket network data (Faust, 1963; Teweles, 1964) indicate easterlies (i.e., winds from the east) near 70 and 80 km during summer and westerlies (i.e., winds from the west) during winter (see also Murgatroyd, 1957). Turbulence and vertical wind shears are considerable in this region, as measured from meteor-trail observations (Greenhow and Lovell, 1960) and from chemiluminescent releases (Spindler, 1966). The latter data also indicate that the seasonal variations in the zonal motion patterns observed at temperate latitudes in the stratosphere and mesosphere may change at still higher levels. In 1954, for instance, the 85-km level showed westerlies with the exception of April and May, when weak prevailing easterlies were observed. At 100 km, during the same year, westerlies were strongest during July and August and January and December (average speeds of 20 m/sec). Weaker easterlies were observed at this higher level during April and May and October (see also Murgatroyd, 1957).

At yet higher levels (200 to 300 km) satellite drag data reveal the predominance of westerlies (King-Hele, 1964; see also Jacchia, 1966; Marov, 1966). These flow processes may, in part, be geostrophic, i.e., governed by the larger scale temperature distribution and the resulting pressure field. Because of strong ionization at these levels, hydromagnetic effects may no longer be discounted in explaining such motions in which the angular velocity is larger than that of the earth (Hines, 1965; Krassovsky, 1965).

In addition to the patchiness and to the observed drifts, the 5577 Å emission shows a rather peculiar variation with latitude and season (Tohmatsu and Nagata, 1963; Silverman, 1969). Figure 5.5 shows mean seasonal variations of this emission at various stations. Spring and fall maximums seem to prevail at middle- and low-latitude stations. Figure 5.6 compares the data from Haute Provence taken during 1958 with the long-term average shown for that station in Fig. 5.5 (Christophe-Glaume, 1965; see also Barbier et al., 1963; Hernandez, 1965). Figure 5.7 shows monthly diurnal variations of the 5577 Å line at Kitt Peak (32°N) and at Haleakala (21°N). The semiannual variation is strongly evident, especially at the latter station (L. L. Smith and Steiger, 1968).

Spring and fall maximums of airglow have also been observed by Sparrow et al. (1968) from satellite data. From these measurements it also appears that changes in airglow intensity occur simultaneously in both hemispheres (see also Fig. 5.5). In the southern hemisphere such variations were also found by Davis and Smith (1965).

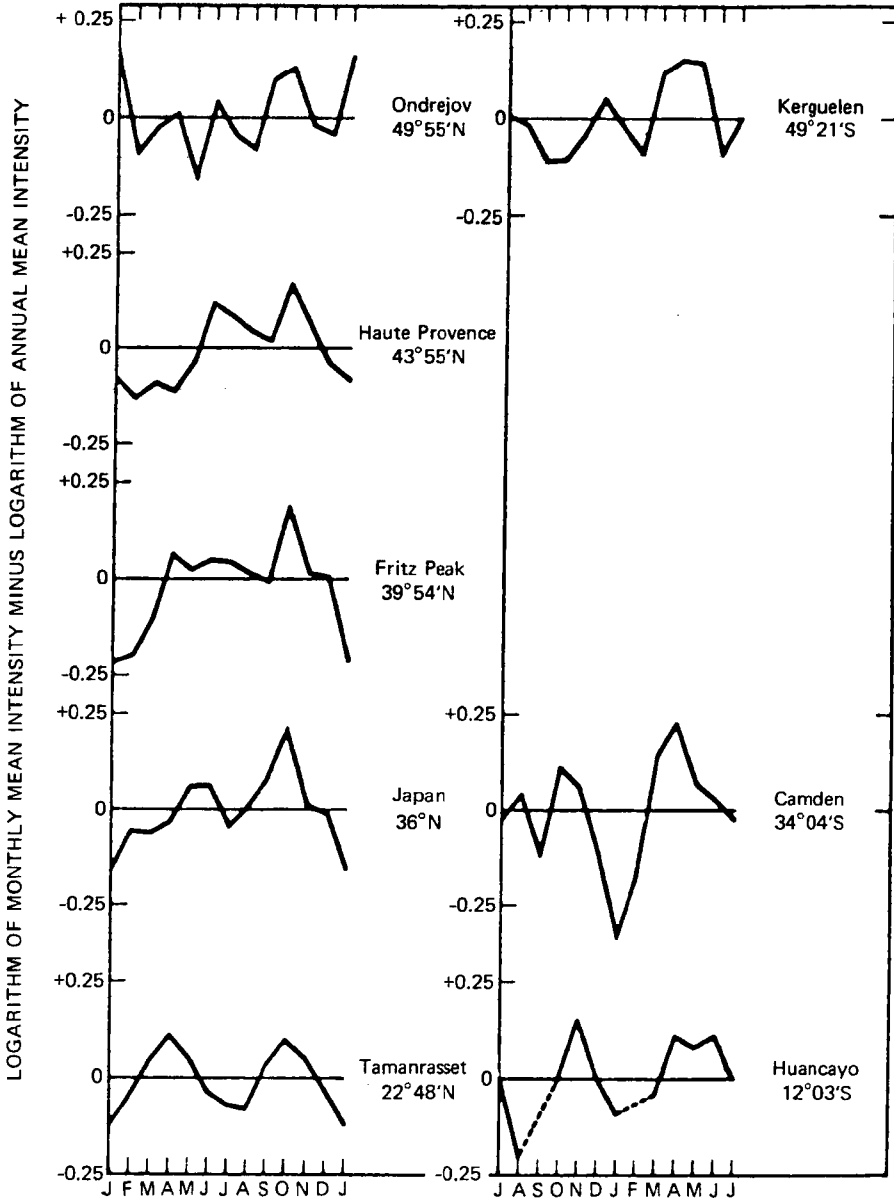


Fig. 5.5 Seasonal variation of the difference between the logarithm of the monthly mean intensity of the 5577 Å emission and the logarithm of the annual mean intensity for different stations as indicated. [From J. Christophe-Glaume, *Annales de Géophysique (France)*, 21(1):14 (1965).]

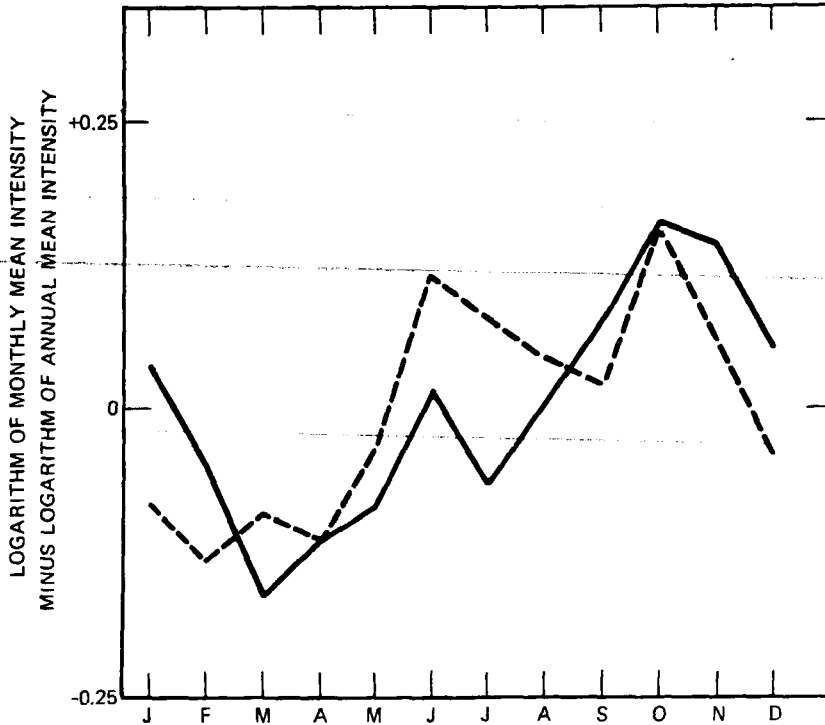


Fig. 5.6 Seasonal variation of the difference between the logarithm of the monthly mean intensity of the 5577 Å emission and the logarithm of the annual mean for Haute Provence, France. —, values shown in Fig. 5.5. - - -, values observed in 1958. [From J. Christophe-Glaume, *Annales de Géophysique (France)*, 21(1):22 (1965).]

Monthly mean values of the green-line emission intensity appear to be correlated with the mean sunspot number (Barbier, 1965a; Christophe-Glaume, 1965; for references on earlier work by Rayleigh pointing out this correlation, see Hernandez and Silverman, 1964; Silverman, 1969). Such a correlation also exists for nightly average values (Rosenberg and Zimmerman, 1967; Yano, 1967). This suggests a certain solar influence on the photochemistry and perhaps also on the motion patterns in the layers above, but adjacent to, the mesopause. (Such a solar influence on motion patterns is also suggested from the variation of sporadic E-layer occurrence with the solar cycle. See Chap. 6.)

In order to account for the latitudinal and seasonal variations, a mean circulation model was proposed which shows a multicellular structure above the 100-km level (Fig. 5.8). Each downward-moving branch of the thermospheric circulation (the thermosphere is the region above the mesopause) will enhance the concentration of atomic oxygen at relatively low altitudes, where it will recombine according to Eqs. 5.1 and 5.2, emitting the observed green airglow line. Dachs (1969) provides evidence

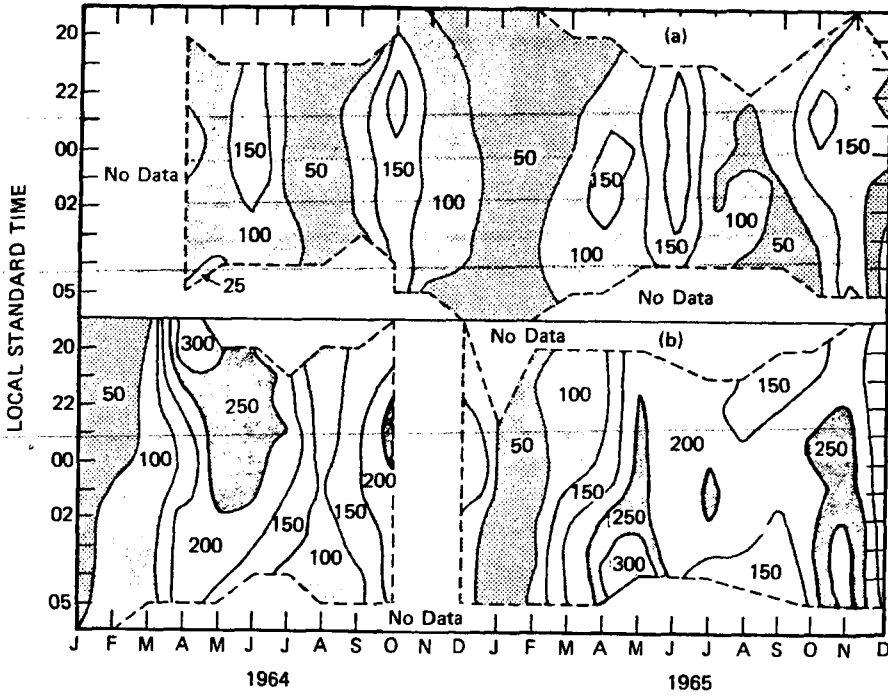


Fig. 5.7 Monthly diurnal average intensities (in Rayleighs) as a function of season at (a) Kitt Peak and (b) Haleakala for 5577 \AA emission during 1964 and 1965. [From L. L. Smith and W. R. Steiger, *Journal of Geophysical Research*, 73(7):2532 (1968).]

for such vertical motions by comparisons of green-line emissions with variations in the height of sporadic E-layers. Vertical velocities of the order of 1 cm/sec would suffice to explain this enhancement in [O]. A comparison of Figs. 5.8 and 1.37 would suggest, in view of the semiannual variation of the 5577 \AA emission, that the almost symmetric pattern of vertical motions in both hemispheres during autumn and spring, shown for the mesosphere, intensifies considerably above the mesopause.

The effect of high atmospheric circulation patterns on the 5577 \AA oxygen emission should be of considerable importance because of the long recombination times of atomic oxygen at the altitudes of green-line emission (Yano, 1967; G. E. Chapman, 1969). According to Nicolet (1960), the recombination time of O is more than a month at 100 km and more than a year at 120 km.

THE OXYGEN RED LINE, 6300 \AA

The "forbidden" oxygen red line at 6300 \AA originates primarily in the F_1 -region of the ionosphere (Zipf and Fastie, 1963). J. G. Moore and Rao (1965) observed an

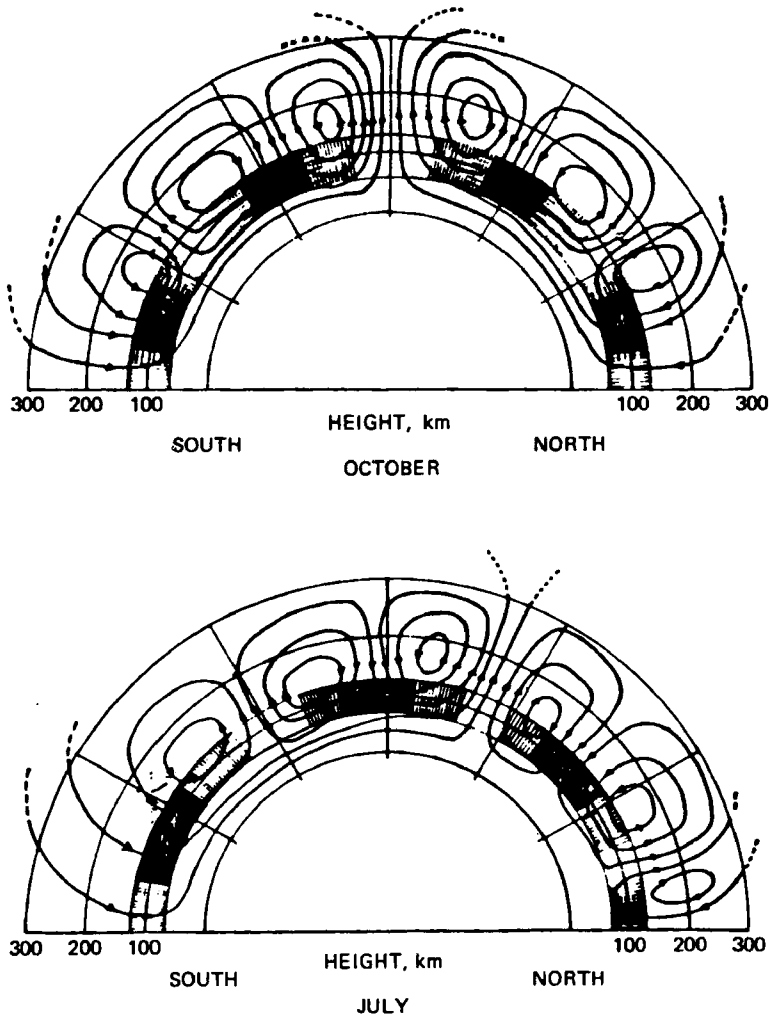


Fig. 5.8 Model of the upper atmospheric circulations as inferred from airglow distributions, the latter indicated schematically by hatched regions. [From T. Tohmatsu and T. Nagata, *Planetary and Space Science*, 10:113 (1963).]

enhancement of this line during a solar eclipse, which was probably caused by excitation of atomic oxygen by thermal electrons in the F_1 -region. (Excitation by photoelectrons and photodissociation would be minimized during a total eclipse.) The intensity of this line also shows a pronounced latitudinal variation (Fig. 5.9). Allowing for the fact that the observations on which this diagram is based were made from a ship and were averaged over a large time interval (March 24–September 1, 1962, data mainly), the cellular pattern is in good agreement with Fig. 5.8. A comparison of

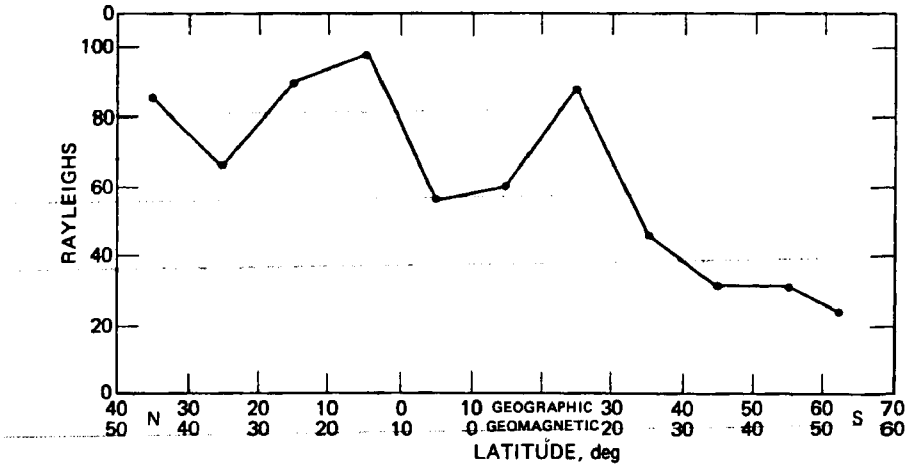


Fig. 5.9 Nightly averages of 6300 Å; 10° latitude averages vs. latitude. [From T. N. Davis and L. L. Smith, *Journal of Geophysical Research*, 70(5):1134 (1965).]

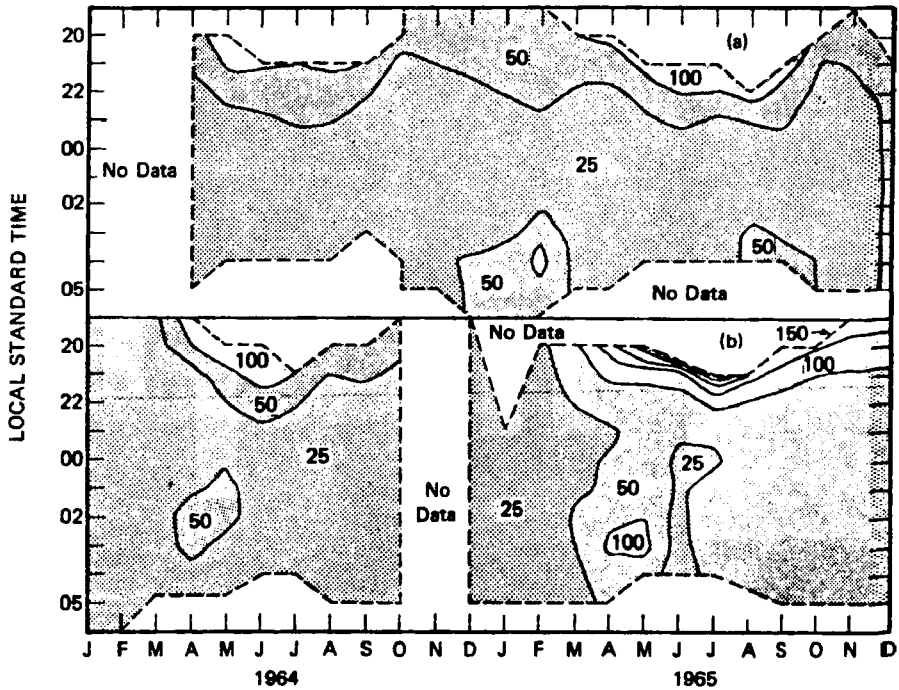


Fig. 5.10 Monthly diurnal average intensities (in Rayleighs) as a function of season at (a) Kitt Peak and (b) Haleakala for 6300 Å emission during 1964–1965. [From L. L. Smith and W. R. Steiger, *Journal of Geophysical Research*, 73(7):2534 (1968).]

6300 Å data taken over such a long time span appears to be permissible, however, in view of the very small seasonal variations (Fig. 5.10).

P. V. Kulkarni and Steiger (1967) report that normally there is a poor correlation between 5577 Å and 6300 Å lines, the former issuing near 100 km and the latter near 300 km. The correlation is improved, however, during periods of enhanced emission. A comparison of Figs. 5.10 and 5.7 reveals a poor correlation also in the seasonal trend. The 6300 Å line shows a tendency of weak summer maximums, whereas the 5577 Å emission has maximums in spring and fall. A better correlation exists between the 6300 Å and the 5200 Å intensities (Weill, 1969).

The 6300 Å emission, similar to the 5577 Å emission, varies with the solar cycle. Years with sunspot maximums coincide with those showing maximum 6300 Å intensity (Barbier, 1965a; see also L. L. Smith and Steiger, 1968). Figure 5.10, for instance, shows stronger 6300 Å emissions during the summer of 1965 than during 1964, in line with the increasing solar activity.

The circulation model shown in Fig. 5.8 may be used in viewing the red-line emission characteristics. This model is similar to the one proposed earlier by Yerg (1951). The northerly winds in polar latitudes of the northern hemisphere below the 100-km level agree with the observed drift direction (from N and E) of noctilucent clouds (see Chap. 2). Drift velocities of these noctilucent clouds, as well as of airglow patterns, are much less than those to be expected under conservation of absolute angular momentum within the meridional circulation cells shown in Fig. 5.8. However, absolute angular momentum should not be maintained in these circulation wheels for two reasons: (1) Above the mesopause viscous interaction between air layers moving in different directions will be appreciable because of the long mean-free-path length of air molecules (Yerg, 1951; Haurwitz, 1961). Thus a strong braking action on the mean meridional circulation may be expected. (2) Effects of horizontal eddies may cause angular momentum transports in a direction opposite to the one indicated by the mean meridional circulation shown in Fig. 5.8. These large-scale eddies may well be of a quasi-tidal nature, especially those observed in the ionosphere (Yerg, 1951; Greenhow and Lovell, 1960; Ratcliffe and Weeks, 1960; Rao and Rao, 1969).

Ionization of atomic oxygen and recombination by collision with a molecule XY play important roles in controlling the electron densities in the F-region of the ionosphere (about 250-km altitude) (King, 1964) (for a summary, see Rishbeth and Garriott, 1969). The ionizing effect of solar radiation may be expressed by



where e symbolizes an electron. Recombination, acting extremely slowly, may be expressed by the reactions



XY molecules may be either N_2 or O_2 (see also Keneshea, 1967; Thomas, 1969; Roach, 1969). As shown recently by Knudsen (1968), photoelectrons produced by such reactions as those in Eq. 5.3 are not the only ones contributing to the electron distribution in the F-region. Interaction of the Van Allen radiation belts with the upper atmosphere causes characteristic geographic variations of electron flux and electron concentrations (see also Mariani, 1963). The observed predawn enhancement of the red line may, at least in part, be caused by the influx of such electrons (R. W. Smith, 1969).

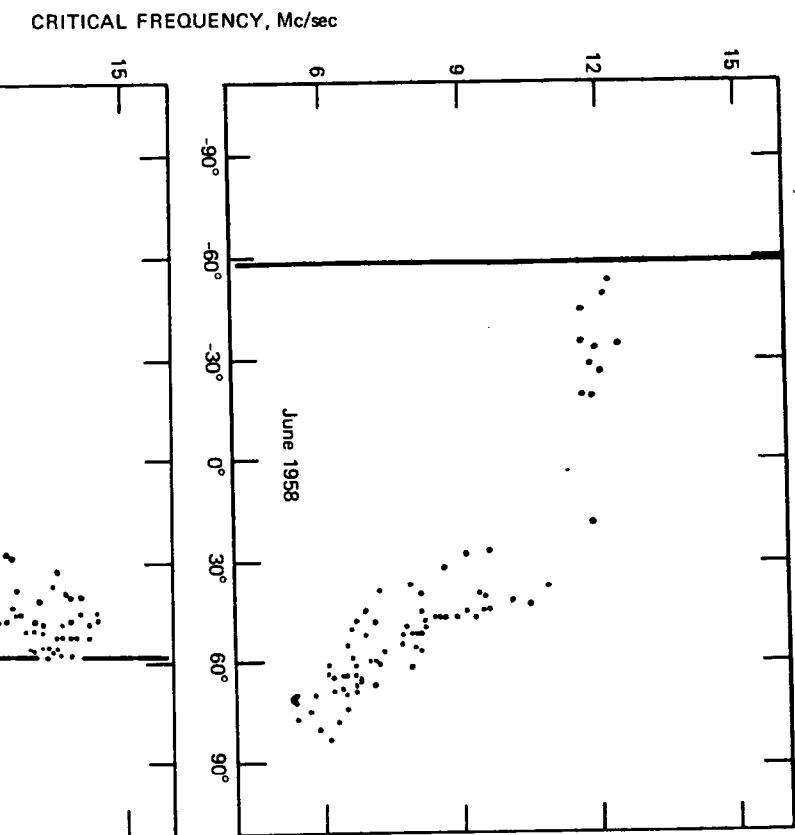
The recombination rate at which electrons are destroyed according to Eq. 5.5 thus depends on the supply of XO^+ ions, which, in turn, depends on the molecular concentrations $[XY]$ according to Eq. 5.4. In the lower layers of the F-region, $[XY]$ is large, and hence recombination of XO^+ ions occurs readily (F_1 -layer). In the upper part of the F-region, $[XY]$ is small, and recombination of O^+ occurs at a much slower rate (F_2 -layer).

The concentrations of O^+ and XY that control the recombination rate according to Eqs. 5.4 and 5.5 are influenced to a certain extent by vertical motions. King (1964) found that the maximum electron density in the F_2 -layer (which is practically equal to $[O^+]$ and is measured by the critical frequency f_oF_2 ; see Rishbeth and Garriott, 1969) is largest in the high latitudes of the winter hemisphere and drops continually to high latitudes of the summer hemisphere (Fig. 5.11) (see also J. W. Wright, 1964; Titheridge, 1968b). This anomalous seasonal and latitudinal variation of maximum electron density in F_2 has been explained by King (1964) as the effect of a meridional circulation from the summer to the winter pole. Undissociated gas wells up near the summer pole. As it travels toward the winter pole, it is dissociated by UV radiation. Ionized gas (particularly O^+) subsides over the winter polar regions and thus causes the observed large electron densities there. (For a summary of F-region behavior, see Rishbeth, 1968.)

The rather crude model developed by King (1964) is not quite consistent with the one shown in Fig. 5.8. Closer inspection of Fig. 5.11, however, reveals that the largest changes in f_oF_2 occur between 30° and 60° of the northern hemisphere during June. Comparing this diagram with Fig. 5.8 for July, we find that strong downwelling is postulated in this latitude sector of the northern hemisphere. It seems from this comparison that eddy or cellular effects of ionospheric flow patterns, not yet taken into account by King (1964), may be of significance in explaining observed electron densities. It should also be expected that there is a strong diurnal variation of vertical velocities that may affect ionization in the F-region (Doupnik and Nisbet, 1968).

Ion drifts in the ionosphere give rise to electric-current systems, which, in turn, cause measurable changes in the geomagnetic field. H. Maeda and Murata (1968) have demonstrated that nonperiodic meridional wind components in the ionosphere are more effective in producing current systems than are zonal components. Chapter 6 shows that the neutral wind field varies strongly along the vertical coordinate. It is difficult therefore to estimate the detailed neutral wind distribution from geomagnetic-field variations (Sugiura, 1968).

OXYGEN RED LINE, 6300 Å



The ionospheric E-layer (about 105 km), especially the "sporadic E-layer," also shows a well-marked seasonal dependence mainly in middle latitudes. Peak frequencies of occurrence of sporadic E (E_s) in these regions are reported for May–July and lowest frequencies for January and February (for references, see Ratcliffe and Weeks, 1960; E. K. Smith and Matsushita, 1962). It might well be that the subsidence motions indicated for these latitudes in the summer hemisphere (Fig. 5.8) may have some effect on sporadic E occurrence (Spizzichino and Taieb, 1964). It will be shown briefly in Chap. 6 how sporadic E occurrence correlates with wind shears adjacent to the wind maximum near 100 km, as detected by alkaline tracer experiments. A possible biennial variation of E_s was mentioned in Part 1, Chap. 3.

In addition to the oxygen emission lines, absorption characteristics of metastable excited states of O_2 in the near ultraviolet region of the spectrum (0.3μ) may become useful as tracers of atmospheric motions near the 50-km level (Krueger, 1969).

THE HYDROXYL RADICAL

In addition to the major photochemical processes involved in the phenomena described in the preceding sections, there are less conspicuous ones that have not yet been explored adequately.

Table 1.6 shows that photochemical reactions between oxygen and hydrogen atoms are of importance in a moist atmosphere. The hydroxyl group, OH, whose radiation bands have been detected in nightglow, appears in several of these reaction equations. According to Bates and Nicolet (1950) (see also Krassovsky, 1963), electronically activated OH^* (activation indicated by asterisk) may be formed by



Atomic hydrogen is regenerated by



A. F. Ferguson and Parkinson (1963) made a study of the process



suggested by other authors (for references, see the paper by Ferguson and Parkinson). Still other reactions were considered by L. Wallace (1962), who reviews the work by other investigators.

Deactivation of OH leads to the emission of the observed nightglow lines (green to far infrared). Maximum emission of the OH spectrum lines appears to lie somewhere between 80 and 100 km, as determined from rocket measurements (Baker and Waddoups, 1968). Hesstvedt (1969a) computed theoretically a sharp emission peak of

OH near 88 km. Temperatures at these levels, determined from the OH spectrum, do not show any significant and consistent latitudinal or seasonal trends (see, for example, Shepherd, 1969). There is, however, a seasonal trend in the intensities of the OH bands measured over Norway (Kvifte, 1967). Minimums are observed during winter. However, data are not reliable enough to allow any far-reaching conclusions to be drawn. Aircraft data collected by Huppi and Stair (1969) show a great variability of the OH emission in the infrared. There are indications of an increase in this emission to a maximum shortly after sunset. Lower nighttime levels are followed by a decrease at dawn. Improvement in observation techniques may render valuable information from OH emission, together with other airglow characteristics, on atmospheric circulation processes at these levels.

6 OTHER CHEMICAL TRACERS

In the foregoing chapters we have dealt with those trace constituents of the atmosphere, H_2O , CO_2 , and O_3 , which, as three-atom gases, leave a marked imprint on the radiation fluxes traversing the atmosphere. They are abundant enough to play a significant role in the energy budget of the atmosphere. There are, however, other chemical elements and compounds that have little effect as far as the maintenance or the modification of the general circulation is concerned. They may, nevertheless, be used in tracing atmospheric motions.

These chemical tracers can be divided into "natural" and "artificial" ones. The latter may be unavoidable by-products of man's activities, mainly in the form of air pollution, or they may be deliberately introduced into the atmosphere to study its structure or its motions. Some tracers will have both natural and artificial sources.

Junge (1963a), in an excellent summary, has dealt with a number of these tracers. For additional details the reader is referred to the review by Junge.

CARBON MONOXIDE, CO

Junge (oral communication, unpublished, 1968) pointed toward the fact that CO may have similar tracer qualities as CO_2 . It is generated mainly by incomplete combustion processes in the industrial regions of the northern hemisphere and thus qualifies as a man-made trace substance (for references, see Junge, 1963a).

Automotive traffic in urban areas plays a decisive role in the diurnal variation of [CO] (Fig. 6.1). McCormick and Xintaras (1962) were able to show the ventilating

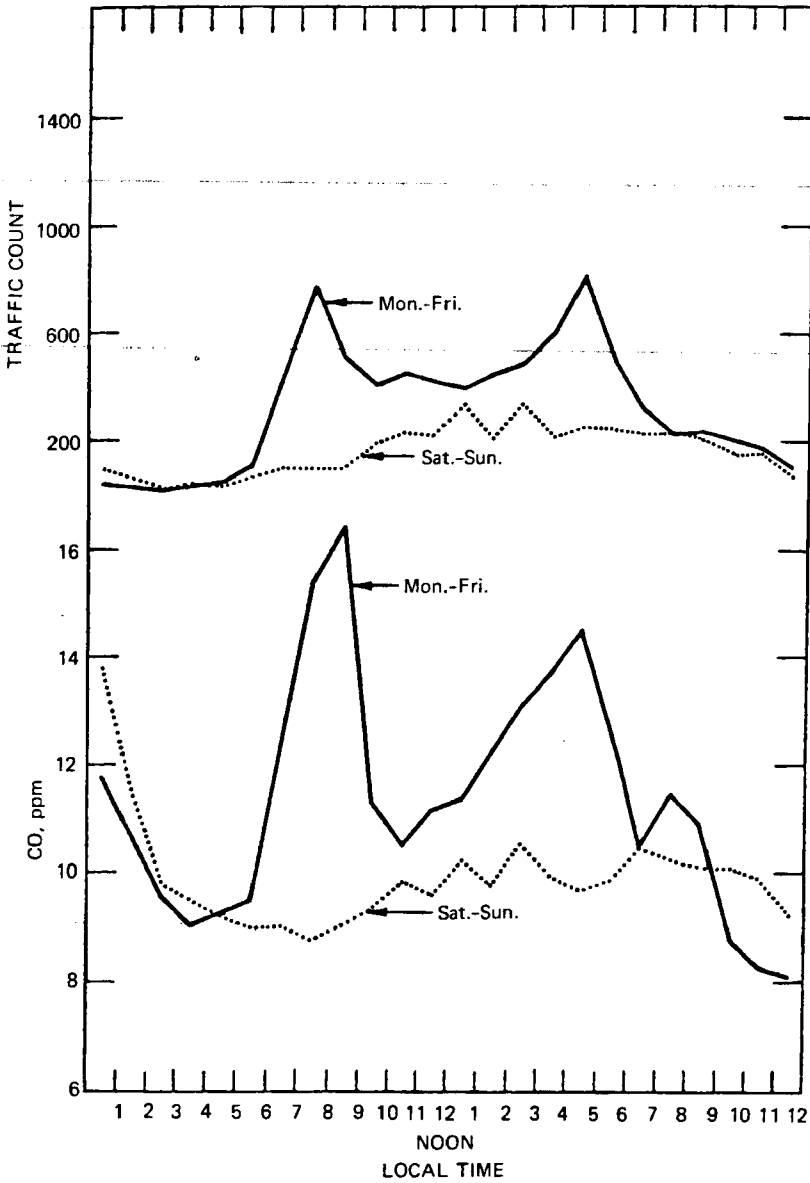


Fig. 6.1 Hourly traffic count and [CO], Nashville, Tenn. [From R. A. McCormick and C. Xintaras, *Journal of Applied Meteorology*, 1(2): 239 (1962).]

effects of winds in removing carbon monoxide from street-level source regions (Fig. 6.2). Although the multiple traffic and industrial sources of CO generate a complex concentration pattern that is highly variable in time and space, refined measuring systems monitoring this trace constituent might yield valuable insight into the ventilation properties of urban areas. Such information will be invaluable in the planning and design of population centers.

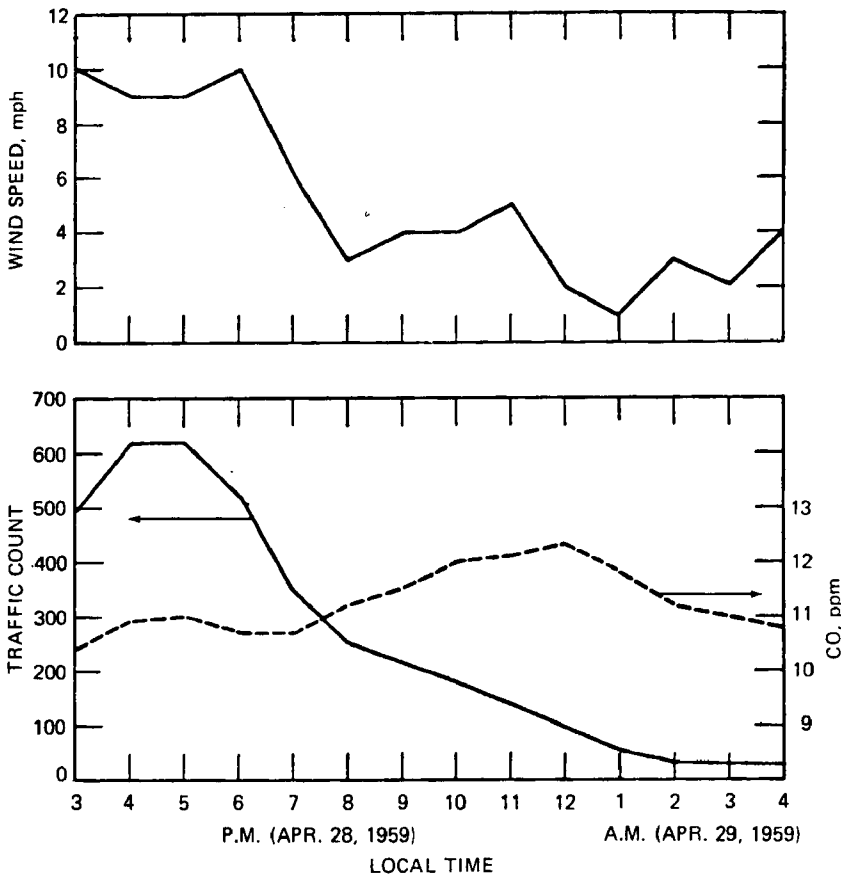


Fig. 6.2 Hourly values of CO, traffic count, and wind speed, Nashville, Tenn. [From R. A. McCormick and C. Xintaras, *Journal of Applied Meteorology*, 1(2): 240 (1962).]

Recently Robinson and Robbins (1968a) voiced the opinion that certain ocean areas may serve as CO sources. Especially between depths of 10 to 50 m, [CO] of 5 to 10 times the equilibrium value with atmospheric partial pressure characteristic of surface waters has been found. The production mechanism in the ocean is most likely biological. Such an additional source of CO would require an even larger sink of this

pollutant, which may conceivably also lie in the biosphere. Robinson and Robbins (1968b) speculated that biological take-up of CO, if it were directly related to that of CO₂, may compensate for the present CO in pollution emission.

Measurements from aircraft indicate that the present tropospheric burden of CO in the northern hemisphere is approximately 0.1 to 0.2 ppm. Carbon monoxide concentration decreases sharply above the tropopause (to below 0.03 ppm according to Seiler and Junge, 1969), indicating a ground-level source and a stratospheric sink of CO. Also, it appears that [CO] values in the southern hemisphere are about half as high as those in the northern hemisphere. This is evident from the measurements during *Eltanin* cruise No. 31, conducted between San Francisco and New Zealand in November and December 1967 (Robinson and Robbins, 1968a) (Fig. 6.3). Estimates of residence times of CO in the atmosphere vary between 4 years and 0.1 year (Weinstock, 1969).

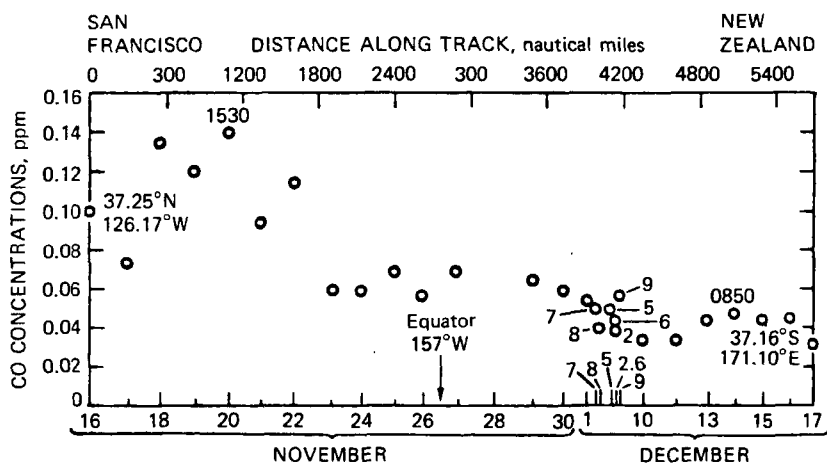


Fig. 6.3 Carbon monoxide concentrations at local noon in the Pacific Ocean during *Eltanin* cruise No. 31 (November and December 1967, United States to New Zealand). [From E. Robinson and R. C. Robbins, *Antarctic Journal of the United States*, 3(5): 195 (1968).]

More detailed measurements of the CO distribution on a global basis, using sophisticated measurement techniques (Seiler and Junge, 1967), will be needed before this constituent can become effective as a tracer of atmospheric transport processes.

METHANE, CH₄

Junge (1963a) summarized early measurements of this constituent, which is relatively abundant in surface air [2.4 ppm according to Shaw (1959)]. The source of CH₄ is the earth's surface (natural gas, animal sources, and decomposition of organic material) (Koyama, 1963). The sinks of CH₄ may be sought at high altitudes in

chemical reactions with oxidizing agents, such as O₃ or O, and in photodissociation (Dilleuth, Skidmore, and Schubert, 1960). Junge (1963a) has estimated residence times of 50 to 100 years for atmospheric methane. Koyama (1963, 1964) arrived at a considerably shorter lifetime of 16 years. The increase of the water-vapor mixing ratio in the upper stratosphere (see Fig. 2.12) found by some investigators but denied by others may largely be due to the oxidation of CH₄ (see comments at the end of Chap. 2). From spectrometric measurements with a balloon-borne sensor, Kyle et al. (1969) found that between 13 and 20 km CH₄ shows a decrease of approximately 80% from the concentration observed at tropopause level. According to Fig. 2.12, however, the water-vapor mixing ratios tend to remain relatively uniform at this height. Simultaneous measurements of water-vapor and methane concentrations in the stratosphere must be made before meaningful budgets of these two admixtures can be established.

Bishop et al. (1962) reported that tritium may be found in methane as CH₃T. Its content increased exponentially in the southern hemisphere between 1953 and 1958. Highest concentrations were found in the northern hemisphere (22×10^3 tritium units*) (still higher concentrations of tritium have been reported by Haines and Musgrave, 1968). In view of the long residence time of methane and of the half-life of tritium of 12.5 years, natural sources of tritium methane had to be discounted. The sharp decrease of tritium concentrations in methane in the stratosphere suggests a tropospheric source, possibly industry. From the data presented by Bishop et al., Junge (1962b) estimated an exchange rate, d_0 , between the northern and southern hemispheres of 0.26 or 0.25 year⁻¹ for an exponential or linear increase, respectively, in concentrations observed in the southern hemisphere. This would correspond to exchange times, $\tau = 1/d_0$, of 3.8 and 4.0 years, respectively. These values agree well with those derived from observed CO₂ distributions (see Chap. 3). Both atmospheric trace constituents, CH₃T and CO₂, may thus be considered to describe mainly tropospheric exchange processes between the northern and southern hemispheres.

Begemann and Friedman (1968a), using additional data by Bainbridge et al. (1961) (see also Martell, 1963) and their own measurements, extended the investigations of Bishop et al. The distribution of tritium in atmospheric methane shown in Fig. 6.4 resulted. The gradual increase in the southern hemisphere prior to 1958 would confirm the conclusion of an "industrial leak" in the northern hemisphere. An accidental release during a one-time event should be discounted in view of this gradual, but seemingly continuous, increase (Begemann, 1963). Leakage of tritium from tritium processing plants by reaction of tritium with stopcock grease and pump oil might account for the presence of CH₃T (Haines and Musgrave, 1964). Also, exchange reactions between the compound HT imported from the stratosphere and methane or methylene, CH₂ (Martell, 1963), will have to be discounted as a source of CH₃T with a high degree of probability since the strong stepwise increases in tritium concentrations from nuclear weapons tests are not reflected in the tritiated methane data (Begemann and Friedman, 1968b). Laboratory experiments (Cadle, 1967) also

*Tritium unit (TU) = T/H ratio of 1×10^{-18} .

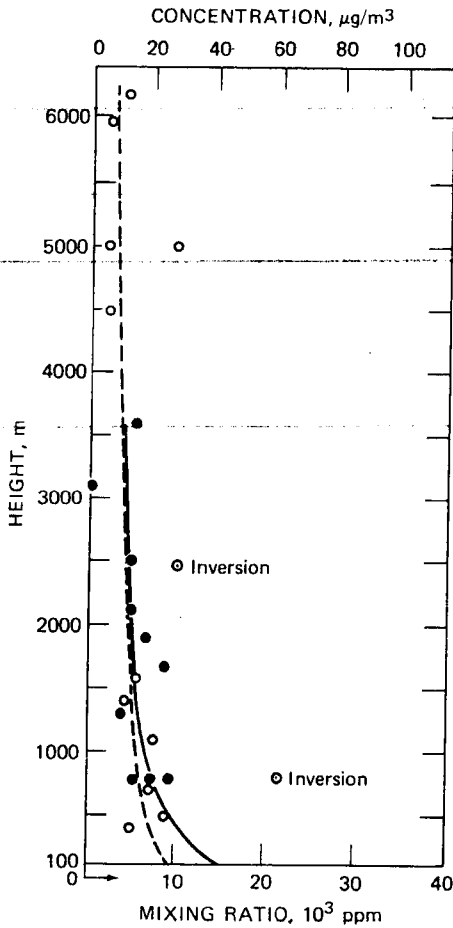


Fig. 6.6 Mean vertical distribution of SO₂ mixing ratios. Concentration values, also indicated along abscissa, have been reduced to atmospheric surface pressure. [From H.-W. Georgii and D. Jost, *Pure and Applied Geophysics*, 59:220(1964).]

Most of the sulfur passing through the atmosphere (365×10^6 tons per year, according to Eriksson, 1963b) appears to come from natural sources. Industrial pollution provides only 11% of the total; hence it plays only a minor role in the global atmospheric sulfur budget. It may be of importance, however, in the sulfur budget of confined regions of population concentration and industry (Vittori and Nucciotti, 1967; Nucciotti et al., 1968; Okita, 1968). Junge (1960) found that there had been no increase in $[\text{SO}_4^{2-}]$ since 1915 in ice deposited on the Greenland ice cap. The short residence time of industrial sulfur in the atmosphere, therefore, seems to prevent a worldwide increase. Sulfur concentrations in the Greenland ice are in good agreement with aerosol measurements there (Fenn, 1960; Fenn et al., 1963).

Beilke and Georgii (1968) have demonstrated by laboratory experiments and from data taken in the natural atmospheric environment that rainout and washout play important roles in the removal of gaseous SO₂ from the atmosphere. The

atmospheric SO_2 concentration and its vertical distribution thus affect $[\text{SO}_4^{2-}]$ in rainwater. The washout of SO_2 is of much greater importance for the sulfate concentration in precipitation than the washout of sulfate-containing aerosol particles (see also Okita, 1968). The latter effect depends mainly on giant nuclei and only negligibly on small Aitken nuclei. According to Heuvel and Mason (1963), the sulfate in giant nuclei of industrially polluted air may be formed by absorption of SO_2 and NH_3 in droplets.

The $[\text{SO}_2]$ in and near cities shows a marked annual variation with maximum values during the winter heating period. Figure 6.7 gives the mean annual variation for

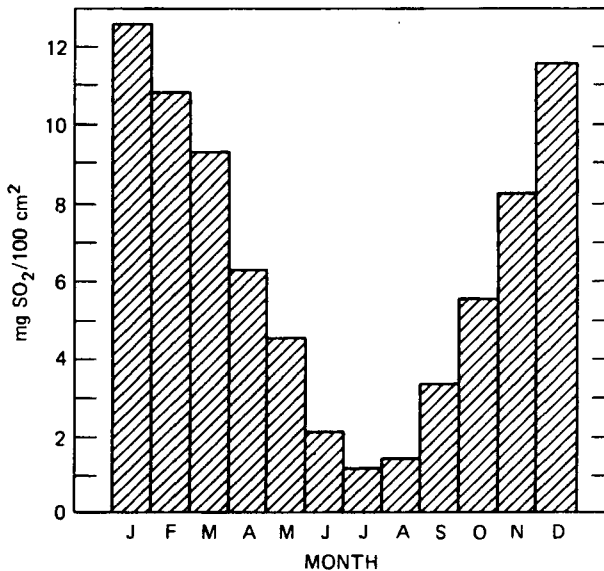


Fig. 6.7 Annual variation of the SO_2 deposition in Vienna, Austria (average values 1958–1966). [From F. Steinhauser, *Wetter und Leben*, 19: 49 (1967).]

Vienna. Steinhauser (1967) points out that large differences in $[\text{SO}_2]$ may occur from year to year, partly because of the fluctuations in the temperature regime and hence in the heating demand, partly because of changes in the advection and thermal stability patterns of the atmosphere. Figure 6.8 shows the tendency of larger SO_2 concentrations to occur during winter in downtown areas (Bangerl and Steinhauser, 1959; see also Steinhauser, 1964; Steinhauser and Chalupa, 1965; Höschele, 1966). Similar seasonal variations of SO_2 are reported by Jacobs (1959) over New York City. According to Jacobs, H_2S also shows a winter maximum. A diurnal cycle of SO_2 with a main maximum in the morning and a secondary maximum in the afternoon after convection dies down is indicated in urban areas (Jacobs, 1959).

From the foregoing SO_2 appears to have limited use as a short-term tracer of local circulation systems in the vicinity of industrial and home incineration sources.

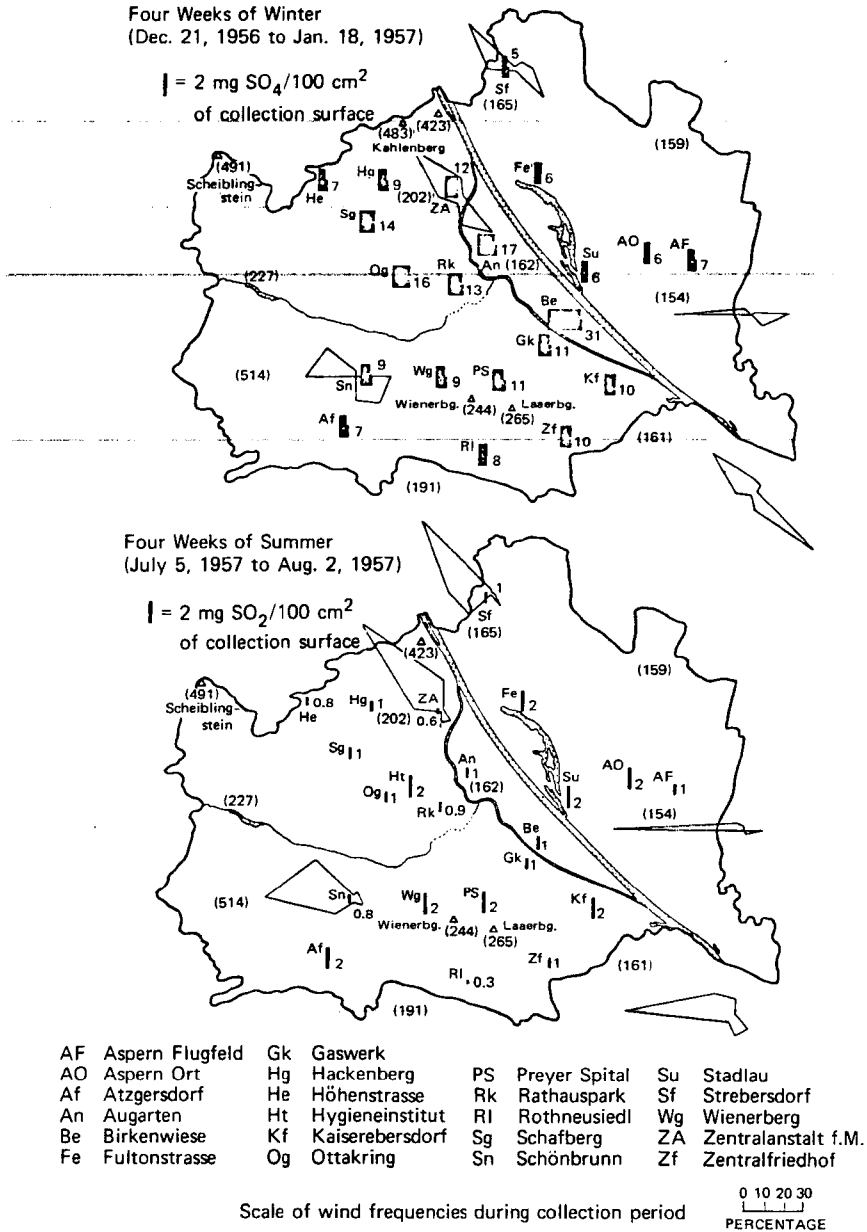


Fig. 6.8 Deposition of SO_2 in Vienna, Austria, during 4-week periods in winter (upper diagram) and in summer (lower diagram), in units of milligrams of $\text{SO}_2/100 \text{ cm}^2$ of collection surface. Frequencies of wind direction are given for four measurement sites during the respective collection periods. City boundaries and the Danube River are indicated on the maps. [From A. Bangerl and F. Steinhauser. *Archiv fuer Meteorologie, Geophysik und Bioklimatologie, Series B (Austria)*, 10(1): 144 (1959).]

Disadvantages lie in the fact that such sources are spread over a wide area, the dimensions of which are commensurate with the scale of the circulation phenomenon to be studied. Furthermore, SO_2 may not be considered as a quasi-permanent admixture of the atmosphere, even though its presence has been observed on a global basis. It is absorbed by plants and soil (for references see Junge, 1963a) and washed out by rain. Concerning the latter process, Junge and Ryan (1958) have reached the conclusion that oxidation of SO_2 into SO_4^{2-} in such quantities as observed in rain, fog, or smog depends on a catalyst, such as heavy metal ions, and on the pH value of the solution. The latter may be raised by absorption of NH_3 .

Photochemical oxidation of SO_2 seems to play only a minor role in its removal from the atmosphere because it could not account for the short half-life of 4 days observed for industrial SO_2 .

The $[\text{H}_2\text{S}]$ appears to show highest values in rural areas during summer (for details see Junge, 1963a). It enters the atmosphere by reduction of sulfate whenever there is an excessive decay of organic material. There is little information on the oxidation of H_2S in the atmosphere. It appears to react readily with O_3 . With average tropospheric ozone concentrations, the half-life of H_2S should be expected to be of the order of 2 days. Eriksson (1963b) arrived at residence times of a similar order of magnitude.

The "Junge" Layer Near 20 km

Atmospheric transport processes involving sulfur in the form of SO_2 , H_2S , or SO_4^{2-} become of paramount importance when explaining the sulfate layer between 15 and 23 km (peak near 18 to 20 km). Aerosol particles in the stratosphere have been characterized as being of tropospheric origin for particle sizes 0.01 to 0.1 μ , of stratospheric origin for 0.1 to 1.0 μ , and of extra-terrestrial origin for sizes larger than 1.0 μ (Junge et al., 1961). Particles with an average radius of 0.15 μ reveal a rather distinct vertical distribution that does not seem to change drastically in space or time. Figure 6.9 shows such aerosol profiles obtained by Chagnon and Junge (1961), Rossmann (1950), Reger and Siedentopf (1950), and Penndorf (1954). The aerosol layer centered at about 18 to 20 km and found with impactors is clearly evident from these measurements (see also Soviet measurements reported by Koprova, 1968). Quite similar conditions have been verified over Hyderabad, India (Fig. 6.10). Optical sounding systems also reveal this "Junge aerosol layer." Elterman and Campbell (1964) reported on the observation of this layer by searchlight techniques (see also Elterman, 1966, 1967, 1968). More sophisticated observations are now possible by optical radar (lidar) systems (Dietze and Seidel, 1967). Grams and Fiocco (1967) (see also Collis and Ligda, 1966) have monitored this aerosol layer over Lexington, Mass., and College, Alaska, with a lidar system (pulsed ruby laser); see also Fiocco and Smullins (1963), Fiocco and Grams (1964). A summary has been given by Goyer and Watson (1968). Over both stations the Junge layer appears quite persistently to be more pronounced and narrower during December 1964 than during March 1965 (Fig. 6.11) over the midlatitude station. The aerosol profiles obtained over Alaska

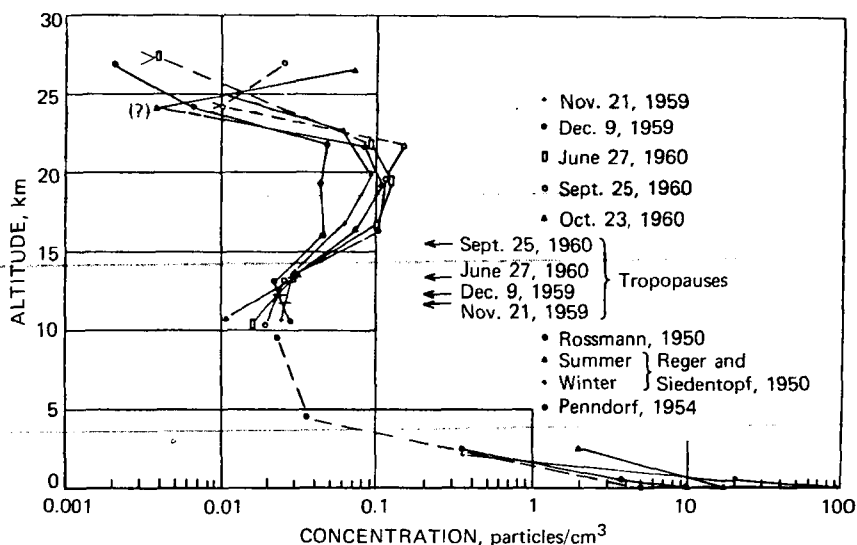


Fig. 6.9 Comparison of five vertical profiles of aerosol concentrations and tropospheric data available in the literature. The values of Rossmann (1950) and of Reger and Siedentopf (1950) were obtained from collections by aircraft impactors over Germany. These data represent average results of 18, 12, and 8 flights, respectively. Penndorf's (1954) values are based on calculations from radiation measurements and are normalized to match the present data at 10-km altitude. [From C. W. Chagnon and C. E. Junge, *Journal of Meteorology*, 18(6): 750 (1961).]

(Fig. 6.12) also reveal a characteristic layer, although at a slightly lower altitude (about 15 km).

Comparing Figs. 6.9 to 6.12 with each other, one finds a slight altitude variation of the Junge layer with latitude (see also Bigg, 1964). A much stronger dependence on latitude for the spread of Mt. Agung debris was found by Dyer and Hicks (1968) (Fig. 6.13).

A comparison between the height of the aerosol layer and the tropopause height (observed at Lexington, Mass., and Nantucket Island, respectively) suggests only an insignificant correlation, with a slope of the regression line of +0.1 (Fig. 6.14) (Grams and Fiocco, 1967).

The rather diffuse characteristics of the aerosol layer during March 1965 over Lexington (Fig. 6.11) as compared with the well-established peak during December 1964 might indicate the enhanced vertical eddy transports in the lower stratosphere in association with the breakdown of the stratospheric polar vortex during late winter. The enhancement of this transport is clearly evident from ozone data (see Chap. 4). A seasonal variation of the aerosol layer, indicative of the strong vertical transport during late winter and spring and leading to a midwinter maximum of aerosol, is evident from Fig. 6.15. The scattering ratio Σ/Σ_M , shown in this diagram, gives the ratios of the

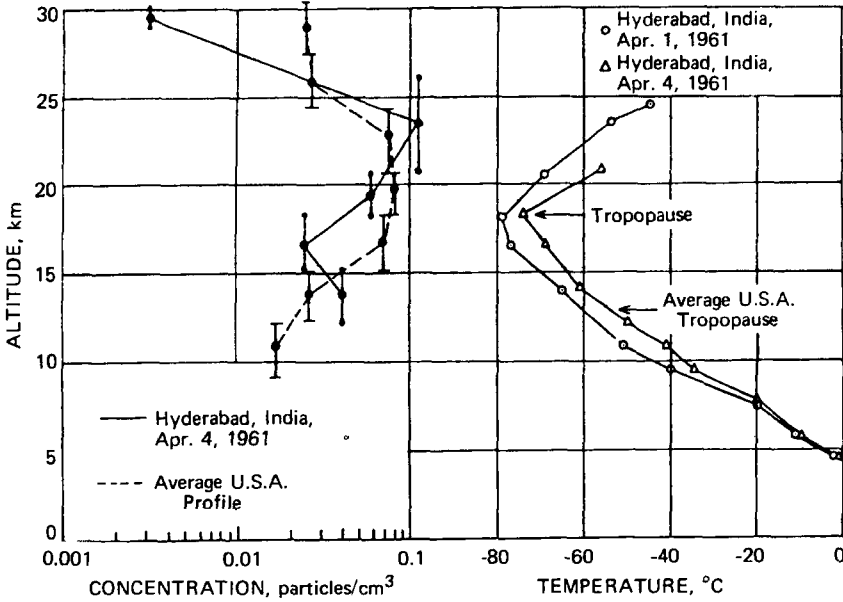


Fig. 6.10 Vertical profile of particles collected with the General Mills impactors at Hyderabad, India (17.5°N), on Apr. 4, 1961, and the temperature sounding for the same date and location. The vertical bars indicate the altitude interval over which the sample was collected. The point at 29.5 km gives only an upper limit of concentration. The average profile of particles collected in the United States at 43°N is plotted for comparison. [From C. W. Chagnon and C. E. Junge, *Journal of Meteorology*, 18(6): 750 (1961).]

lidar return and of values calculated from a model dust-free atmosphere (Σ), normalized by the ratios Σ_M calculated in a similar fashion for the 25- to 30-km region where backscatter is assumed to be due only to air molecules. Ratios Σ are expected to be abnormally large in the presence of aerosol $r \geq 0.1 \mu$. Twilight observations by Volz and Goody (1962) also indicate a winter maximum of aerosol to be present at all levels from above the tropopause to the top level of their measurements (near 60 km). Winter maximums of the Agung debris have been observed in both hemispheres, moving poleward at a rate of approximately 40 cm/sec in middle and high latitudes (Dyer and Hicks, 1968).

Junge, Chagnon, and Manson (1961) found sulfur, probably in the form of sulfate, to be the predominant elemental constituent of the particles in the aerosol layer near 20 km. Flight measurements by U-2 aircraft confirmed these conclusions (Junge and Manson, 1961). Shedlovsky and Paisley (1966) measured sulfur mixing ratios in this layer of $\leq 2.9 \times 10^{-9}$ g sulfur/g dry air. This aerosol layer may well be identical with the dust layer suspected from purple twilight observations (Gruner, 1958; Volz and Goody, 1962; Dave and Mateer, 1968).

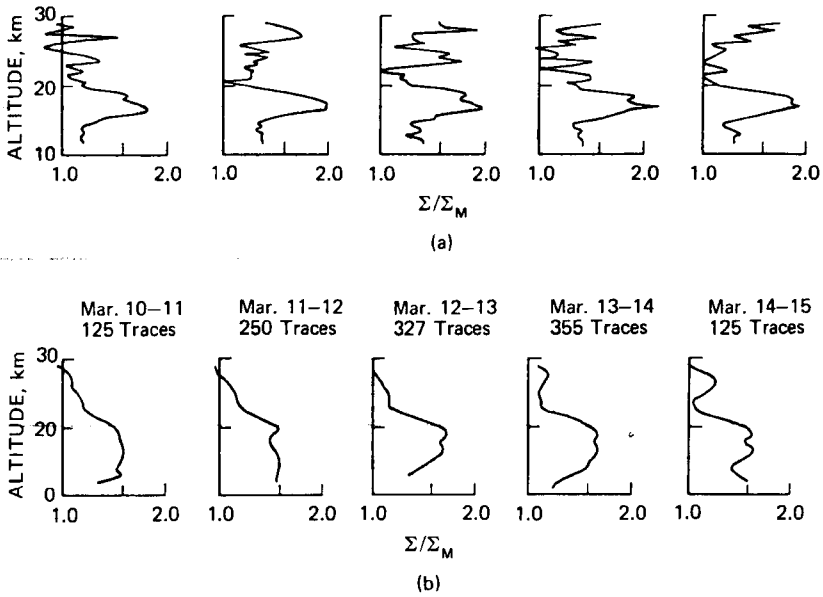


Fig. 6.11 Consecutive profiles of Σ/Σ_M obtained on Dec. 18–19, 1964, over Lexington, Mass., during the time interval 2300–2315 EST. Each profile is constructed from 35 consecutive optical radar traces recorded at about 5-sec intervals (a). Daily profiles obtained on five consecutive nights in March 1965 over the same station (b). [From G. Grams and G. Fiocco, *Journal of Geophysical Research*, 72(14): 3531, 3532 (1967).]

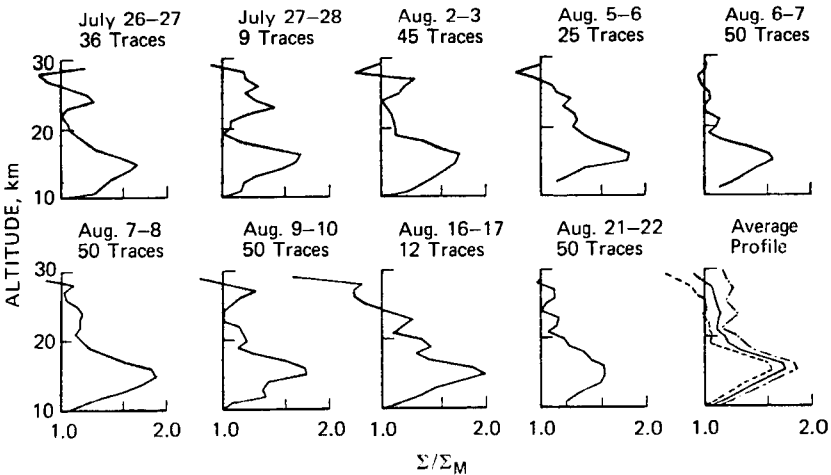


Fig. 6.12 Profiles of Σ/Σ_M obtained during summer 1964 in Alaska. [From G. Grams and G. Fiocco, *Journal of Geophysical Research*, 72(14): 3536 (1967).]

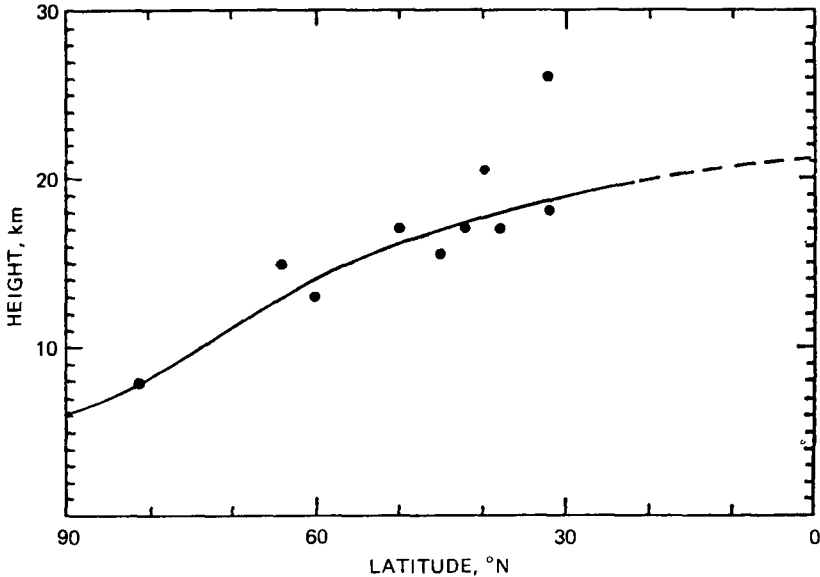


Fig. 6.13 Height of the dust layer of Mt. Agung debris as a function of latitude. [From A. J. Dyer and B. Hicks, *Quarterly Journal of the Royal Meteorological Society*, 94(402): 550 (1968).]

Measurements by Telford (1960) and by Bigg and Miles (1963) indicate that, in addition to the (hygroscopic) sulfate material in the Junge layer, there are large numbers of ice nuclei in the lower stratosphere of the northern and southern hemispheres exceeding the typical concentrations at ground level by almost two orders of magnitude. These particles are active at temperatures higher than -20° . Bigg and Miles (1963) speculate that these ice nuclei are of extraterrestrial origin. They have not explored the possibility of a terrestrial (volcanic) source. Cadle et al. (1969), on the other hand, speculate that ice nuclei sampled by aircraft in the upper troposphere and lower stratosphere are of terrestrial origin.

Additional details on aerosols as atmospheric tracers will be given later in this chapter. Here we shall concern ourselves mainly with the problem of the origin of the aerosol, and of the sulfur, which has been identified in the layer near 20 km. In view of the characteristic particle size (about 0.15μ), an extraterrestrial source is unlikely for this aerosol. Particles would have to be considerably larger to attain the appropriate sinking velocities to be found at such levels and in such concentrations. Computations of falling speeds of spherical particles have been made by Kasten (1968) (see also Kornblum, 1969a). Typical results are shown in Fig. 6.16. Rosen (1964) argues in favor of an extraterrestrial source for stratospheric dust, leading to a mixing ratio of dust that is constant with height. There is, however, too wide a scatter of observational data to substantiate this hypothesis. Balloon-borne coronagraph measurements up to a height of 25 km reported by Newkirk and Eddy (1963, 1964) (see

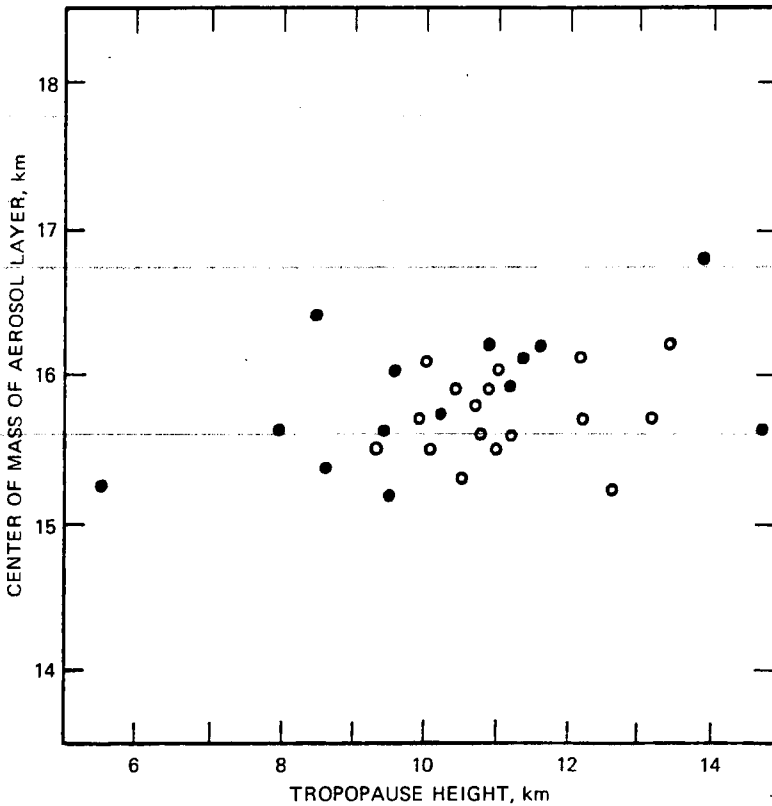


Fig. 6.14 Relation between the height of the center of mass of the aerosol layer and the height of the tropopause. Open circles represent measurements that incorporate an instrument correction. [From G. Grams and G. Fiocco, *Journal of Geophysical Research*, 72(14): 3537 (1967).]

also MacQueen, 1968) also show that constant mixing ratios are not realized for particles with $r = 0.1$ to 0.3μ , postulated to be of stratospheric origin (Fig. 6.17). A constant-mixing-ratio distribution in the stratosphere appears to approximate particles with $r > 2 \mu$, which are most likely of extraterrestrial origin, according to Junge's classification.

Twilight observations by Volz and Goody (1962) (see also Meinel and Meinel, 1963, 1964; Bigg, 1964; Flohn and Henning, 1964; Volz, 1964; see Unz, 1969, for polarization measurements), confirming the presence of the Junge layer, also indicate a more or less uniform mixing ratio of dust above 30 km, with some evidence of a weak secondary maximum recurring near 50 km. These mixing ratios, however, are lower than those postulated for the noctilucent-cloud layer, which suggests an extraterrestrial source of the nonaqueous particles in the latter. (For theoretical considerations on the detection of haze layers, see Volz, 1965b.)

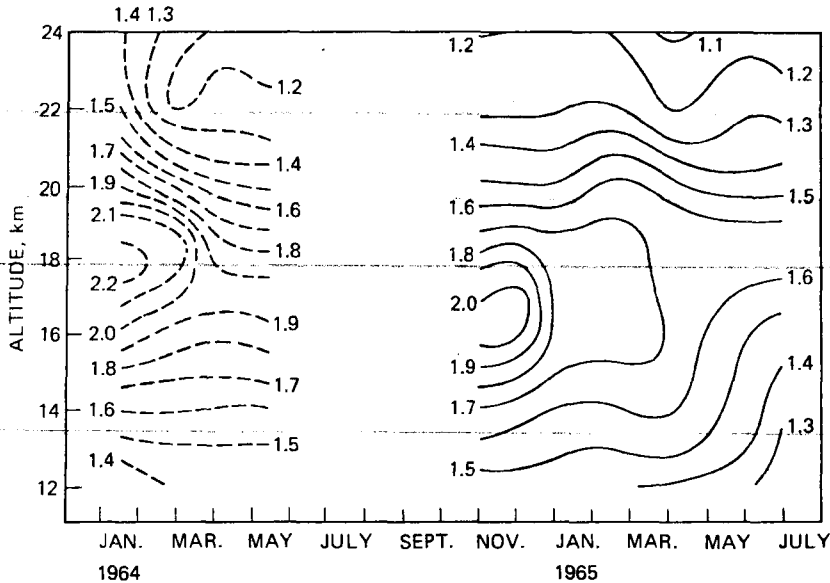


Fig. 6.15 Temporal variation of the stratospheric aerosol layer expressed as isopleths of mean bimonthly scattering ratios Σ/Σ_M at Lexington, Mass. The dotted lines indicate an observation period in early 1964 when a relatively small number of profiles were available to compute bimonthly mean profiles. [From G. Grams and G. Fiocco, *Journal of Geophysical Research*, 72(14): 3534 (1967).]

The coronagraph observations indicate the presence of very thin laminae of aerosol particles. Thus the Junge layer near 20 km, as well as aerosol layers above this level in the stratosphere, appears to be composed of an array of thin layers (laminae) with above-normal aerosol content of a thickness of the order of 30 m. The “dirty” layers are separated by layers of “clean” air with average vertical dimensions of 300 m. Ion-concentration measurements substantiate these findings (Newkirk and Eddy, 1964; Newkirk and Kroening, 1965) (Fig. 6.18). Observations of dust “striations” by Volz (1969a) would also point toward a thinly layered structure [so do attenuation measurements of direct solar radiation obtained from two balloon-borne Eppley normal-incidence pyrheliometers (Kosters, Kyle, and Murcay, 1969)]. The presence of such laminae would suggest advection controls in the formation of the aerosol layers similar to those responsible for the stable “laminae” observed by Danielsen (1959) and others in the troposphere.

Because of the pronounced minimum of particle concentrations near the midlatitude tropopause (Fig. 6.9), a tropospheric source for these sulfate particles was deemed unlikely by Junge if one postulated Fickian diffusion conditions to hold for the diffusion of this atmospheric trace constituent in the lower stratosphere. From this, Junge et al. (1961) concluded that sulfate is formed “in loco” by oxidation of

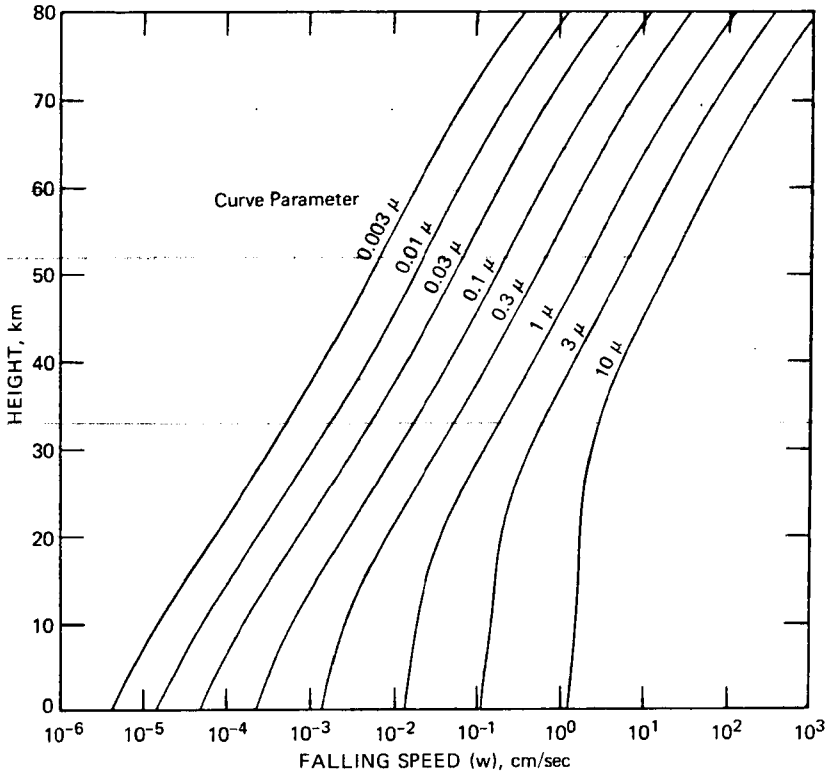
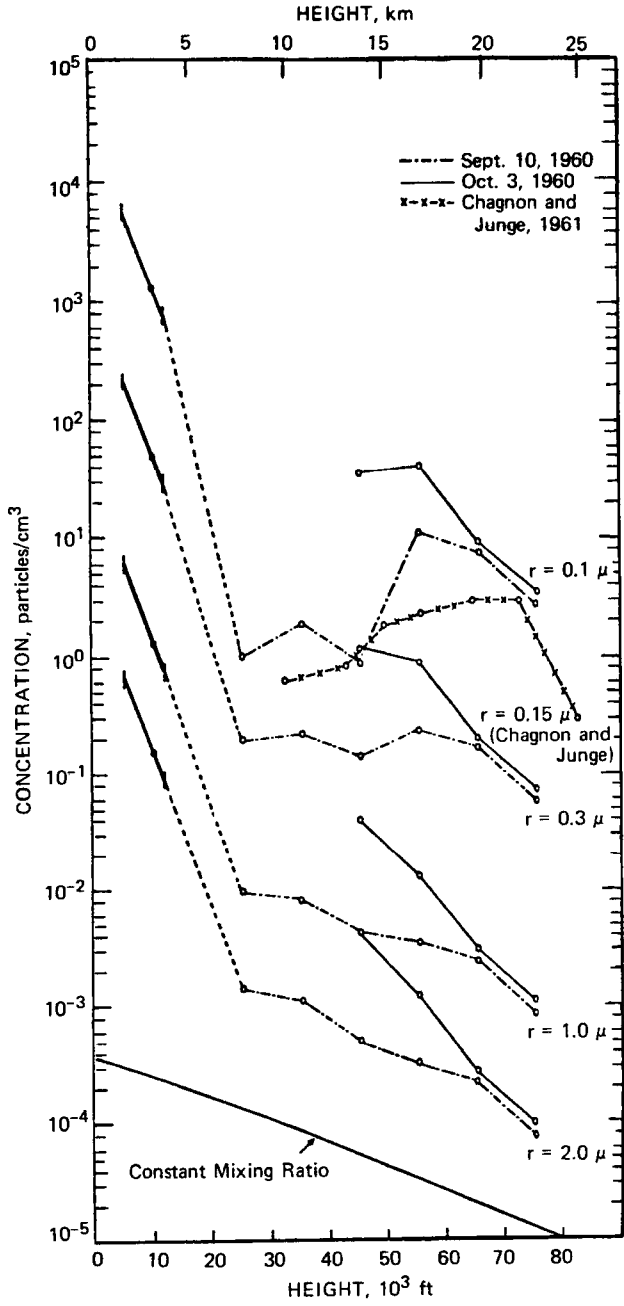


Fig. 6.16 Falling speed, w , of spherical particles of mass density 1.0 g/cm^3 in the 1962 U. S. Standard Atmosphere as a function of height, z , above mean sea level for several particle radii, r (in microns). [From F. Kasten, *Journal of Applied Meteorology*, 7(5): 946 (1968).]

H_2S and SO_2 . Mossop (1963, 1964) also argued in favor of the dust particles in the sulfate layer being generated within the stratosphere. According to his reasoning, they are largely introduced, however, as small, 0.1μ , particles that become coated by a moist hygroscopic material, resulting in the final size of 0.5 to 1.0μ . Since volcanic fumes seem to be very rich in sulfuric acid droplets (up to 95% of the fumes,

Fig. 6.17 Change in the concentration of particles of radius r with altitude. The concentrations above 7.6-km altitude from this investigation are to be compared with the distribution obtained for $r = 0.15 \mu$ by direct sampling. The heavy lines at approximately 3 km show the concentrations and scale height ($H = 1 \text{ km}$) inferred in an earlier investigation (Newkirk, 1956). Particles distributed with a constant mixing ratio with air would display a decrease in concentration with altitude parallel to the bottom curve. [From G. Newkirk and J. A. Eddy, *Journal of the Atmospheric Sciences*, 21(1): 50 (1964).]



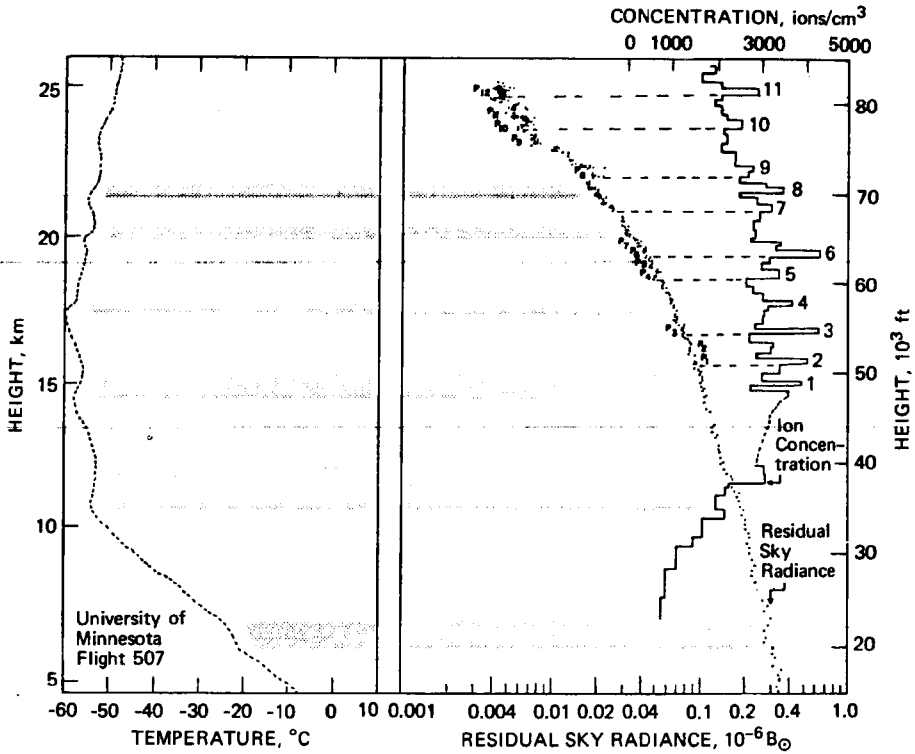


Fig. 6.18 Small-ion concentration (solid line), with thin layers numbered successively. These layers are about 300 m thick and are relatively free of aerosols. Residual sky radiance, B_M , at a scattering angle of 10.3° , $\lambda = 0.54 \mu$ (indicated by dots). The residual sky radiance (observed minus Rayleigh) has been multiplied by $\mu = \cos Z$, where Z is the zenith distance of the point of sky considered, to reduce the measurements to zenith. The unit of radiance, B_\odot , is that of the mean solar disk observed at the corresponding height and wavelength. Plateaus of constant residual radiance, which indicate layers relatively free of aerosol, are connected by dashed lines with corresponding layers of high ion concentration. The sharp drop of radiance above each plateau (approximately 30 m thick) indicates abnormally high concentrations of scattering particles. There is no consistent connection of these layers with the most stable regions in the atmosphere (indicated by shading). [From G. Newkirk, Jr., and J. L. Kroening, *Journal of the Atmospheric Sciences*, 22(5): 568 (1965).]

Anonymous, 1969), part of the sulfur found in the Junge layer could easily be of volcanic origin. Scott et al. (1969) considered anhydrous reactions between ammonia (NH_3) and SO_2 at low temperatures (below -10°C) as a possible aerosol-generating mechanism in the Junge layer, especially near levels of minimum temperature in the atmosphere.

According to Pilipowskyj et al. (1968), lidar measurements [by a pulsed ruby lidar system operating at a wavelength (λ) of 0.694μ] in the altitude range between

15 and 30 km agree well with aerosol concentrations observed from impactor collectors measuring particles with $r > 0.1 \mu$. (Above 30 km the backscatter of the laser beam is assumed to be accomplished entirely from air molecules.) A comparison of the lidar results with measurements of the downward-directed irradiance conducted by a radiometersonde (Suomi and Kuhn, 1958) reveals that there must be a large population of aerosols with $r < 0.1 \mu$ present in the stratosphere which normally escapes detection (see also Bary and Rössler, 1966).

Consulting, again, Figs. 6.9 and 6.10, one notes that the Junge layer is not far above the tropical tropopause. One might argue, therefore, that the aerosol in this layer is of terrestrial origin and is introduced into the 20-km region in the tropics. A process similar to the one postulated by Mossop (1963, 1964) and described previously may lead to a growth in particle size and to an enrichment in sulfur content by drawing on gaseous SO_2 and H_2S in an oxidation process.

Newkirk and Eddy found that the number of particles in the stratosphere in the size range $r = 0.3 \mu$ and 3.0μ follows a distribution proportional to $r^{-3.5}$. [An exponent of -4.0 seems more appropriate for particles collected in urban air pollution (Pasceri and Friedlander, 1965; W. E. Clark and Whitby, 1967; for more details, see Junge, 1963a) and also for water droplets (Dietze, 1956); for aerosol collected in Hawaii, Takeuchi (1966) found a size distribution approximately proportional to r^{-3} .]

From the size distribution of the aerosol in the sulfate layer, Junge (1963b) arrived at an average residence time, due to sedimentation, of about 0.5 year. He also speculated that some of the stratospheric radioactive debris might be removed by these aerosol particles, which would act as condensation nuclei. Near jet streams, with their dynamically produced downward motion within the tropopause gap, the above mentioned residence time might be shortened considerably. Estimates by Hidy and Brock (1967) indicate that particles with $r = 0.1 \mu$ would require approximately 10^3 days to sink from 100 km to 20 km. Photophoretic forces* may become appreciable below 30 km.

A transport model of sulfur, which is able to account for the sulfate layer in the 23-km region, will have to include the following considerations:

Tropospheric air may enter the stratosphere in the upwelling part of the tropical Hadley circulation. It may be carried into higher latitudes by mean and eddy transport processes above the tropopause (see Part 1). Tropospheric air may also intrude into the stratosphere by discrete surges associated with jet maxima (E. R. Reiter, Glasser, and Mahlman, 1967). Both processes, at a first glance, may appear equally important in transferring sulfur into the stratosphere. One should be aware of the fact, however, that upward motions in the troposphere are usually accompanied by condensation processes and by washout. Sulfate, therefore, does not appear to be carried into the stratosphere by extratropical jet streams to any large extent. If this were the case, one

*The force produced on a small particle by incident radiation. This radiation may produce temperature differences on the surface of particles with low conductivity, leading to differences in the kinetic energy of gas molecules impinging on the surface against molecules reflected from the particle surface.

should expect peak concentrations of sulfate particles above the extratropical tropopause and a decrease from thereon upward.

With this conclusion, Junge's hypothesis of "in loco" formation of sulfate by oxidation of H_2S and SO_2 appears intriguing. It might not be the only source, however. Rosen (1968) reported on relatively high dust concentrations, especially in tropical regions. Figure 6.19 shows results of two dust soundings made over Panama 50 hr apart, the full line representing the sounding of Sept. 14, 1966 (see Rosen,

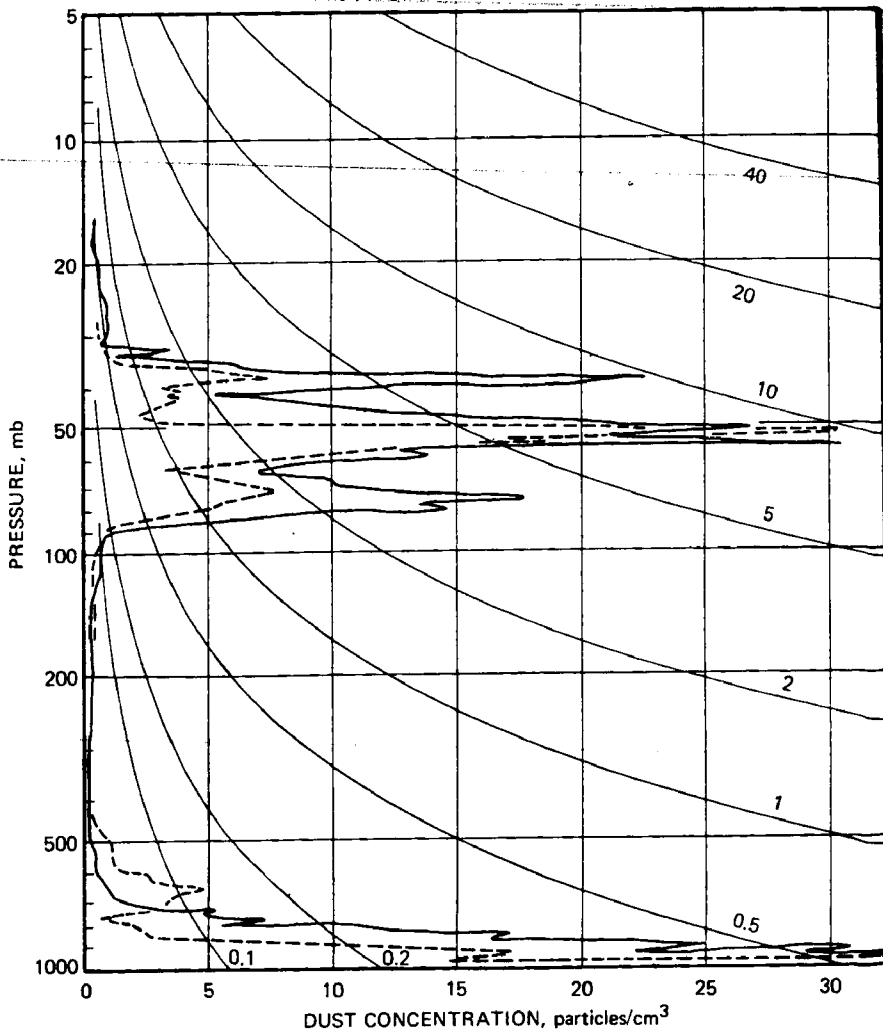


Fig. 6.19 A comparison of two dust soundings made over Panama 50 hr apart. Sounding of Sept. 14, 1966, given by full line. [From J. M. Rosen, *Journal of Geophysical Research*, 73(2): 483 (1968).]

1967). Measurements on different dates over Minneapolis (Minn.) and Churchill (Canada) indicate a marked decrease of dust with increasing latitude. This fact would point toward an equatorial dust source. Over Panama a considerable fraction of the particles was smaller than 0.2μ ; over Minneapolis and Churchill, most particles were larger than 0.8μ .

The seasonal variations in turbidity produced by dust, found by Volz and Goody (1962) at the Blue Hill Observatory (Milton, Mass.), and direct observations of the aerosol by lidar show a winter maximum (see also Fig. 6.15). This would also point toward quasi-horizontal transports from a low-latitude source, quite similar to the transport of ozone.

Junge's data indicate the presence of approximately $3 \times 10^{-15} \text{ g/cm}^3$ of sulfur at 20 km. Rosen's dust measurements, on the other hand, yield a total dust concentration of about 10^{12} g/cm^3 at the same level. Thus the sulfur content of stratospheric dust would account for only 0.3% of the total dust mass. Oxidation of H_2S and SO_2 into sulfate, therefore, does not account for the observed dust distribution.

From Rosen's investigation it would appear that most of the smaller dust particles are introduced into the stratosphere in tropical latitudes, if one may take the latitudinal dust distribution obtained from the soundings available so far as typical.

Part of the observed dust particles may be of volcanic origin (for references, see Rosen, 1968), but it is unlikely that all of them are. Dust clouds of the Mt. Agung (Bali) eruption (Mar. 17, 1963), observed later in the stratosphere near the level of the sulfate layer, contributed only to about one-half of the stratospheric aerosol in the southern hemisphere shortly after the eruption. One year after the injection date, only one-third of the dust seemed to have been of volcanic origin.

From the data of Grams and Fiocco (1967), the Mt. Agung activity appears to have influenced the stratospheric aerosol layer as late as summer 1965, when low values of lidar scattering (Fig. 6.20) as well as of turbidity (Volz, 1965a) were observed again. From a study by Volz (1965a) (Fig. 6.21), it appears that it takes on the order of 2 years after large volcanic eruptions before the aerosol concentration in the upper atmosphere returns to normal levels. From Fig. 6.21 we may also conclude that eruptions during autumn (curves c and d) lead to an increase of (stratospheric) aerosol in the appropriate hemisphere not later than the following spring. Eruptions during the spring and summer, especially at low latitudes (curves a and b), lead to a major increase during the spring season of the following year. This corroborates the stratospheric transport mechanisms in the Junge and ozone layers discussed earlier.

A study of the Linke turbidity factor, defined as

$$T = \frac{(\ln \ell_0 - \ln \ell)}{(\ln \ell_0 - \ln \ell')} \quad (6.1)$$

(where ℓ_0 is the solar constant, ℓ is the observed direct solar radiation, and ℓ' is the direct radiation transmitted through a dust-free atmosphere with 1 cm of precipitable water vapor), for Mauna Loa, Hawaii, does not reveal the decrease of aerosol content after the Mt. Agung event as postulated by Volz. Peterson and Bryson (1968) argued

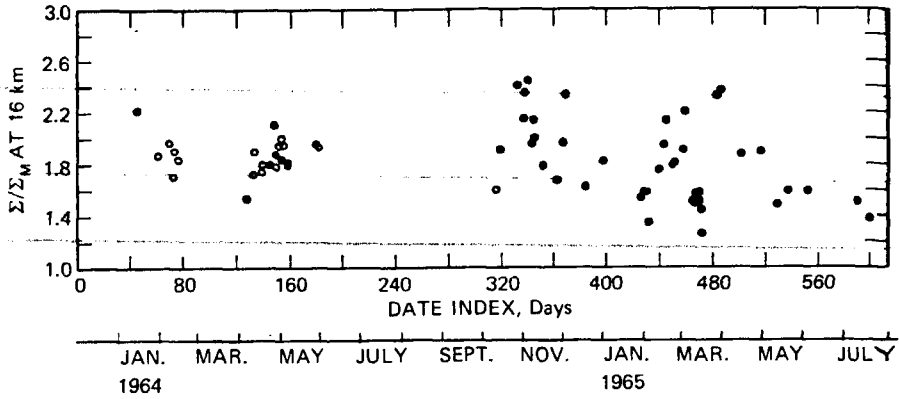


Fig. 6.20 Temporal variation of the stratospheric aerosol layer expressed as the day-to-day fluctuations of the scattering ratio Σ/Σ_M at 16 km at Lexington, Mass. (See also explanation to Fig. 6.11.) Open circles represent measurements that incorporate an instrument correction. [From G. Grams and G. Fiocco, *Journal of Geophysical Research*, 72(14): 3534 (1967).]

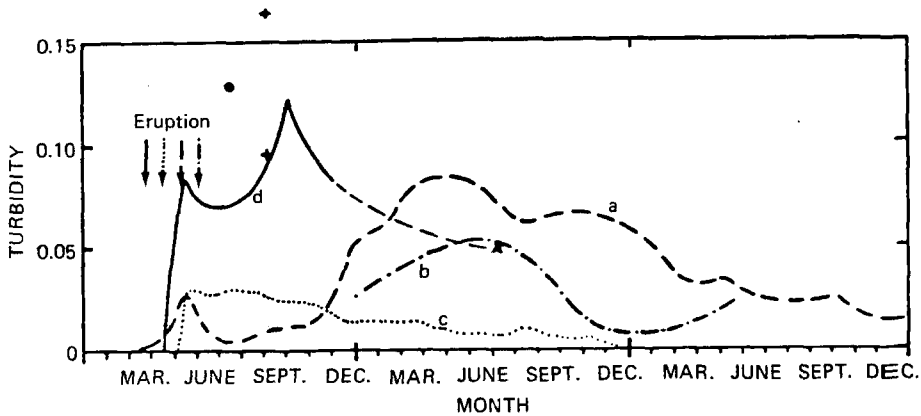


Fig. 6.21 Course of turbidity after great volcanic eruptions on the hemisphere of eruption. Curves a to d have been derived from monthly means of total solar radiation under approximate consideration of the annual course of water vapor and solar elevation. This results in a much smaller turbidity in winter than in summer for the same relative radiation depletion. (a) Mt. Pelee eruption, measurements at Washington, D. C., Warsaw, Lausanne, and in Russia; (b) Katmai eruption, measurements at Davos; (c) volcano in South American Andes, measurements at Mt. Stromlo, Australia; (d) Agung eruption, measurements in the southern hemisphere (o, Australian data; x, data from Chile.) [From F. E. Volz, *Tellus*, 17(4): 514 (1965).]

that either Agung debris was still present in the atmosphere in significant concentrations or that the Agung event was superimposed upon a long-term (possibly man-made) increase in turbidity, which seems to be evident even before this volcanic eruption (Fig. 6.22).

The effect of the Mt. Agung eruption also has been studied extensively in the southern hemisphere. The ashes reached South Africa in April (Bosua, 1963) and

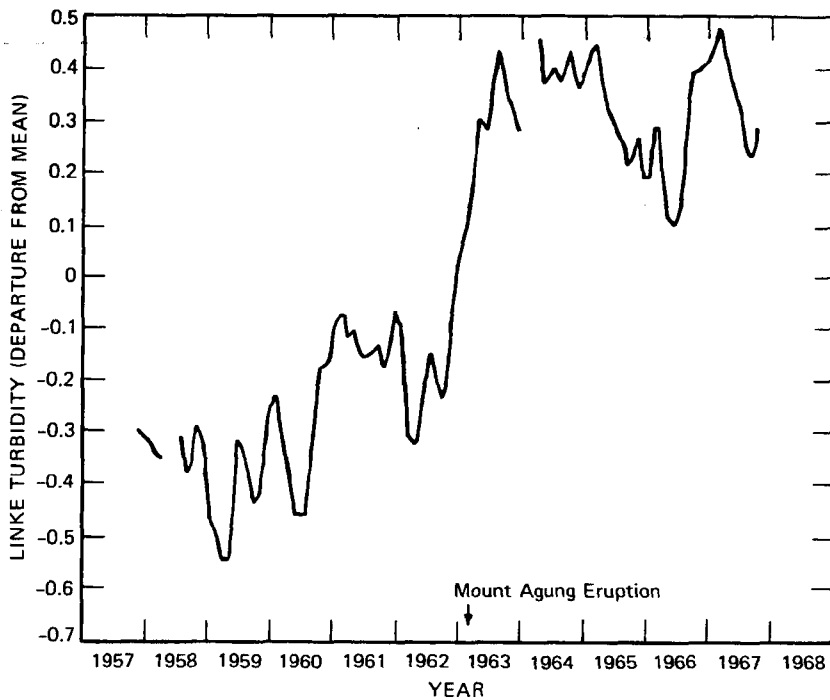


Fig. 6.22 Trend of monthly anomalies of Linke turbidity factor calculated from published normal-incidence radiation data for Mauna Loa, Hawaii. Three-point binomial smoothing has been used. [From J. T. Peterson and R. A. Bryson, *Science*, 162: 120 (1968). Copyright 1968 by the American Association for the Advancement of Science.]

Australia in March and April (Dyer and Hicks, 1965; Weinert, 1967), appearing there at a height of 21 to 25 km (B. Harris, 1964). The ashes were observed over Chile in May (Moreno and Stack, 1964) and over the South Pole in November (Flowers and Viebrock, 1965). Figure 6.23 shows the effect of Mt. Agung ashes on direct solar radiation at the Amundsen-Scott South Pole station (Viebrock and Flowers, 1968). Increased turbidity becomes noticeable toward the end of November 1963, after the spring weakening of the stratospheric polar vortex. From this diagram and from the discussion given by Viebrock and Flowers, it appears that the initial intrusions of Agung debris over the South Pole arrived in large eddies, leading to large-amplitude

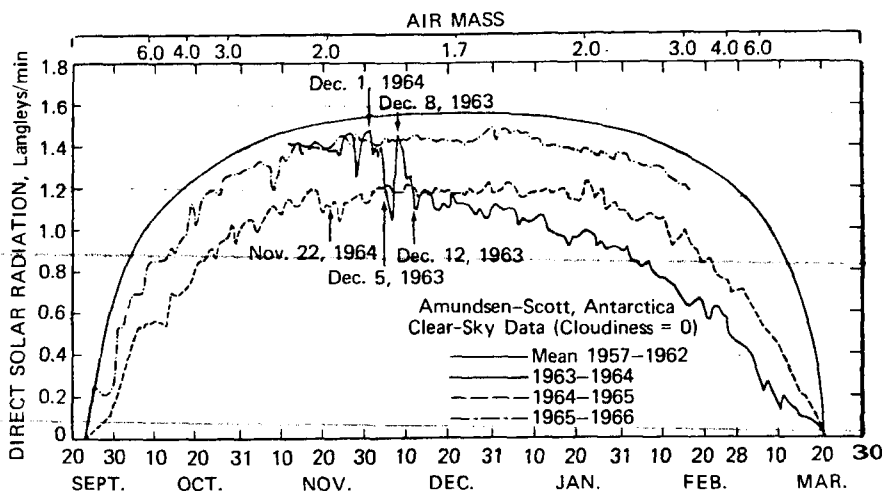


Fig. 6.23 Direct solar radiation data for Amundsen-Scott (South Pole) station. [From H. J. Viebrock and E. C. Flowers, *Tellus*, 20(3): 402 (1968).]

fluctuations of direct solar radiation, especially during December. This would confirm the importance of eddy-transport processes during and after the breakdown of the stratospheric circumpolar vortex. A trajectory study at the 50-mb level, characterizing the flow conditions in the Junge layer, is given in Fig. 6.24. As indicated in this diagram, the dust clouds, which occurred in late November and December 1963 over the South Pole, appeared to have been carried into this region by planetary waves, predominantly in the low-wave-number domain. (Wave number 1, the excentricity of the polar vortex, and wave number 2 are rather conspicuous in Viebrock and Flowers' trajectory analysis. A prominent wave number 1 appears to be a rather persistent feature of the southern vortex) (see, e.g., Astapenko, 1964). The relatively dust-free days, Nov. 26 and Dec. 1 and 8, 1963, were characterized by 50-mb trajectories that originated over the south polar region and indicated only little meridional mass transport.

Figure 6.23 also indicates that the aerosol content of the atmosphere over the south polar regions had returned close to normal values by the (southern) summer of 1966. Turbidity measurements of this summer were compared by Fischer et al. (1969) with data from the same season of 1950. The somewhat hasty conclusion was reached that "no pronounced change in turbidity in the Antarctic atmosphere has occurred over the intervening 16 years." In light of Fig. 6.23, this conclusion appears to be erroneous. Since during the 1964-1965 and 1965-1966 summer seasons the extinction of direct solar radiation did not change appreciably with time, Viebrock and Flowers (1968) concluded that the removal of stratospheric aerosol occurred mainly during the dark winter months when no direct observations of turbidity were

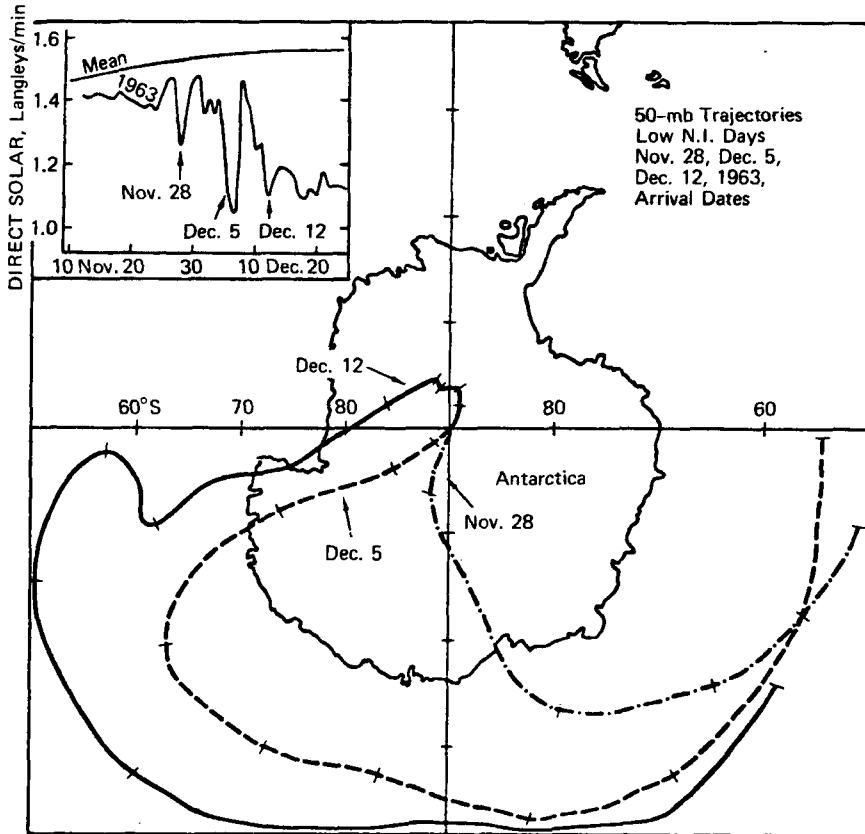


Fig. 6.24 Trajectories at 50 mb for air arriving at the South Pole on Nov. 28, Dec. 5, and Dec. 12, 1963. The diagram in the upper left shows the direct solar radiation at the South Pole on these dates. [From H. J. Viebrock and E. C. Flowers, *Tellus*, 20(3): 406 (1968).]

available. This conclusion is in excellent agreement with earlier statements on ozone transport (Chap. 4). Figure 3.69, Part 1, shows that sinking motions seem to prevail throughout the Antarctic troposphere and lower stratosphere during this season, with an influx of air into the Antarctic regions in the upper troposphere and lower stratosphere. The winter maximum of surface ozone may very well be correlated with the postulated downward flux and subsequent removal of stratospheric aerosol originally located in the Junge layer. Further evidence for such a downward transport of stratospheric air over the Antarctic interior has been gathered by Cadle et al. (1968), who found abnormally high concentrations of SO_4^{2-} anions in surface air over this continent. There may also have been $\text{S}_2\text{O}_8^{2-}$ anions, which would suggest a strong oxidizing mechanism as it could be expected in the Junge layer (Friend, 1966). Lorius et al. (1969) found SO_4^{2-} deposits increasing with depth in the ice of the coastal

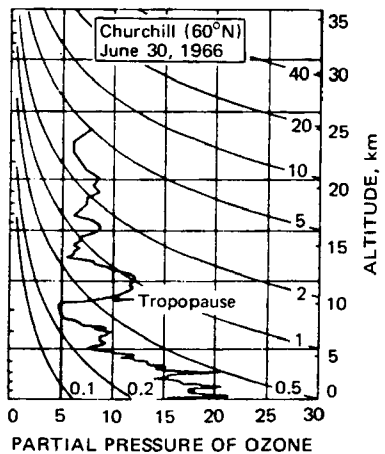
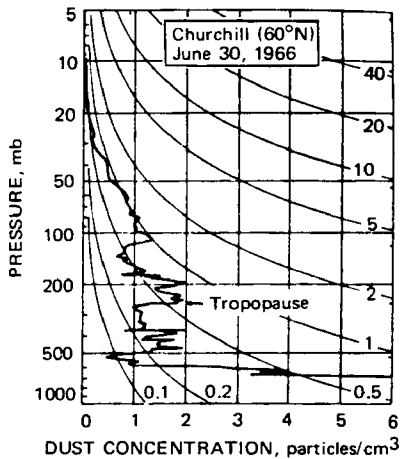
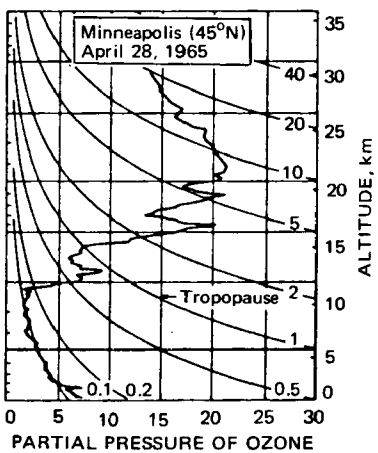
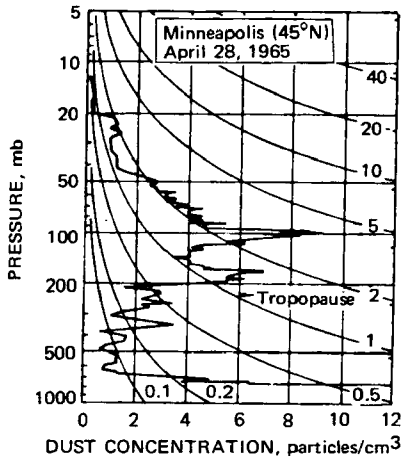
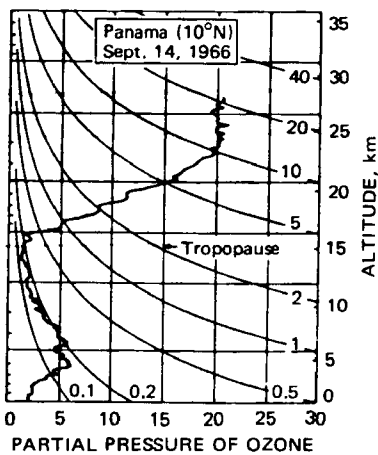
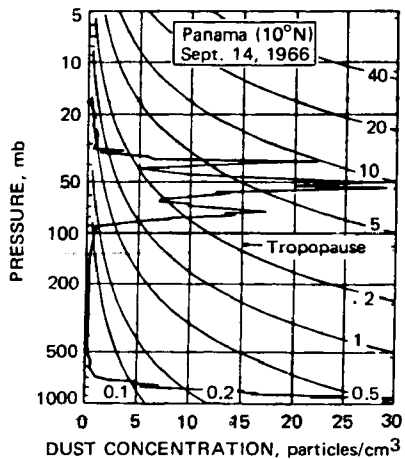
regions of Terre Adelie (Antarctica). The deep strata of ice originate inland and flow toward the shore, whereas the upper layers originate from local snow deposits. The enhancement of SO_4^{2-} in the inland ice confirms the findings on atmospheric aerosols reported by Cadle et al. (1968).

Viebrock and Flowers (1968) also stated that the aerosol particles observed over Antarctica were mainly scatterers and not absorbers of solar radiation since the loss in direct solar radiation was almost entirely compensated by an increase in diffuse radiation; thus the total radiation received at the surface was changed only slightly.

Rosen (1968) left the question concerning the origin of the non-volcanic particles in the lower stratosphere unanswered. It is not unlikely that high-reaching cumulonimbus clouds in the intertropical convergence zone, as they penetrate the tropical tropopause and evaporate into the stratosphere, act as an additional source of small nuclei that contain a certain amount of sulfate. These convective motions might also carry SO_2 into the stratosphere. These nuclei might even retain their moist coating (which was postulated by Mossop, 1963, 1964) after the evaporation process and act as scavengers for additional sulfur produced by SO_2 oxidation. Mean meridional and eddy motions would carry these aerosol particles poleward. In this context it is of interest to note that the sulfate layer does not lie far from the layer of minimum water-vapor mixing ratios (see, e.g., Fig. 2.12). The latter has already been explained earlier by the cold tropical tropopause, which traps ascending moisture.

A certain correlation between ozone and dust concentrations in thin layers above the tropopause in temperate latitudes led Rosen (1968) to the conclusion that both trace substances are advected by the same transport mechanisms (Fig. 6.25). Eddy effects seem to dominate in this "river-like" advection. In the tropics (Panama), however, no such correlation between dust and ozone seems to exist between the tropopause and the 25-km level. This fact confirms the conclusions that dust is introduced from below in these latitudes and is not transported from higher levels through the ozone layer. If the latter were the case, a positive correlation between $[\text{O}_3]$ and dust concentrations should also hold in the tropics. In extratropical latitudes, where horizontal eddy motions dominate, both O_3 and dust will be subject to the same advection patterns, even though the two contaminants have different sources. Grams and Fiocco (1967), on the other hand, found a slight negative correlation between stratospheric aerosol at 16 km and total ozone (data from observation sites in Massachusetts). That stratospheric aerosol may act as a catalytic sink for O_3 (Kroening, 1965; Pittcock, 1965) and that ozone and aerosol have different geographic source regions (Pittcock, 1966) are difficult to prove. It may also be that total ozone, in spite of its good correlation with $[\text{O}_3]$ in the 12- to 24-km altitude

Fig. 6.25 The vertical distribution of dust and ozone at three different latitudes. The dust profiles are for 0.25- μ -diameter particles. Note that the dust concentration scale is different at all three latitudes. The partial pressure of ozone is in relative units. The curved lines on the dust and ozone profiles are lines of constant mixing ratio in relative units. [From J. M. Rosen, *Journal of Geophysical Research*, 73(2): 481 (1968).]



interval (Mateer and Godson, 1960), does not reveal the effect of detailed layers shown in Fig. 6.25.

The fact that the sulfate layer and the dry region in the stratosphere coincide rather closely leads to the conclusion that the latter also owes its existence mainly to horizontal eddy-transport processes that bring dry equatorial air from the tropopause region into temperate and high latitudes. The mean meridional circulations sketched in Fig. 3.11 of Part 1 tend to support these eddy processes, but the latter dominate over the former in magnitude, at least in the lower stratosphere and outside the tropical regions. This we may infer by analogy from the conclusions reached from the momentum-flux data in Part 1.

Aircraft measurements reported by Cadle et al. (1969) show that stratospheric air intruding into the troposphere within the stable layer underneath a jet stream is characterized not only by relatively high radioactivity and high ozone, as shown by previous investigations, but also by relatively high sulfate-ion concentrations. Thus the removal of radioactive debris from the stratosphere, as well as the downward transport of O_3 and SO_4^{2-} , is strongly influenced by the eddy processes associated with jet streams.

The existence of Junge's sulfate layer and the dust layer near 20 km seems to confirm the meridional circulation shown in Fig. 3.11 of Part 1 for that level. Whether or not the biennial oscillation in the magnitude of the eddy transports has a marked influence on the sulfate layer cannot be ascertained from present data.

Figure 6.12 shows the Junge layer in subpolar regions. Rosen's (1968) data from Ft. Churchill also show such a layer in high latitudes, although at a lower level and with smaller concentrations than in middle latitudes (Fig. 6.25). Vertical eddy-transport processes and removal of stratospheric aerosol in the jet-stream belt of midlatitudes may be responsible for the smaller aerosol concentrations observed in the lower stratosphere of polar regions.

The question remains as to why the aerosol is concentrated in such a relatively shallow layer, as depicted, for example, in Fig. 6.25, instead of being spread out over the depth of the stratosphere. Two possible answers, or a combination thereof, offer themselves to this question:

1. From Figs. 1.10 and 1.12, we see that the 20- to 24-km region is characterized by a minimum in mean zonal winds, sometimes referred to as "stratonull layer" (Faust, 1960, 1967a; Faust and Attmannspacher, 1961; Webb, 1966a). This layer also coincides with the region in which a mean isothermal lapse rate of temperature, characterizing the lower stratosphere, especially in middle and high latitudes, gives way to an inversion lapse-rate characteristic of the upper stratosphere. This vertical gradient in lapse rate will reflect itself in the vertical eddy-exchange coefficient, K_{zz} , and in its distribution with altitude. [Compare values of this quantity in Table 1.5 between 100 and 50 mb. Note that the latter pressure level lies close to 21 km in middle latitudes (Environmental Science Services Administration et al., 1966).] An argument similar to the one proposed in connection with Fig. 2.19 may be advanced here: A sharp vertical gradient in K_{zz} might conceivably generate a dust ledge similar to the one proposed by Chapman and Kendall (1965) in explaining the noctilucent-cloud layer.

2. Meridional transport processes accomplished by eddy motions, and the ratio thereof to the mean meridional transports, may reach minimum values in this region and thus cause large and persistent imports of air from tropical latitudes by a mean meridional circulation cell. Teweles (1964) found considerable poleward air motions $[v]_{(t,\lambda)}$ in middle and low latitudes near 20 km during periods of stratospheric warming (Part 1, Fig. 3.11). Murgatroyd and Singleton (1961) indicate the same (Fig. 1.16).

D. A. Stewart and Essenwanger (1968) and D. A. Stewart (1968) confirmed this speculation on meridional transport processes near the stratonull layer from wind and temperature statistics collected along the 80°W meridian (see also Attmannspacher, 1963; Faust and Attmannspacher, 1962a, 1962b). Figure 6.26 shows the correlation between fluctuations in the (meridional) v -component of flow and in temperature. The 20-km region is characterized by a zero correlation, meaning that, at least near this geographic longitude, there is no organized eddy meridional transport of heat in this layer. During the winter months this fact may be explained by the presence of nearly isopycnic conditions (minimum meridional temperature gradients along isobaric surfaces), which agree with the minimum of westerly winds found near this level (Fig. 1.12) (see also Nolan, 1967). The resulting minimum meridional transport of heat is not necessarily reflected by a minimum in meridional aerosol and moisture, or "dryness," transport since the meridional gradients of these quantities do not vanish. Above this layer we note a sharp increase in correlation coefficients, which indicates strong eddy-transport processes of heat and of other quantities in the upper stratosphere above the Junge layer.

Further evidence of the idiosyncratic poleward transports in the 20-km region is presented in Fig. 6.27. This diagram shows the ^{90}Sr distribution resulting from the sixth Chinese nuclear test observed during January 1968 and computed from the Project Streak large-scale diffusion model (Seitz et al., 1968) (to be described in Part 4). We note that this model gives a relatively smooth distribution of $[^{90}\text{Sr}]$, which is indicative of the spreading of a midlatitude source. The actual distribution, however, reveals a striking anomaly: A "ledge" of minimum concentrations near 20 km, indicative of the northward penetration of clear tropical air that is not readily mixed with surrounding contaminated layers. This would suggest that the minimum in the horizontal eddy transport of heat revealed in Fig. 6.26 is also reflected in a minimum of vertical eddy transport of atmospheric admixtures. The mean isentropic surfaces in this nearly isopycnic layer of the winter stratosphere are almost horizontal. Large-scale eddy-transport processes, therefore, will have a minimum effect on vertical mixing (Newell, 1968a).

From the foregoing evidence, we may formulate the following tentative hypothesis of the formation of the Junge layer: In the region of minimum mean zonal winds, mean meridional transport processes will be augmented by eddy-transport processes. Since, during winter, these processes occur in a nearly isopycnic layer, vertical eddy mixing will be reduced to a minimum. Horizontal mean meridional and eddy motions will ensure a continuous influx of air contaminated by aerosol, SO_2 , or

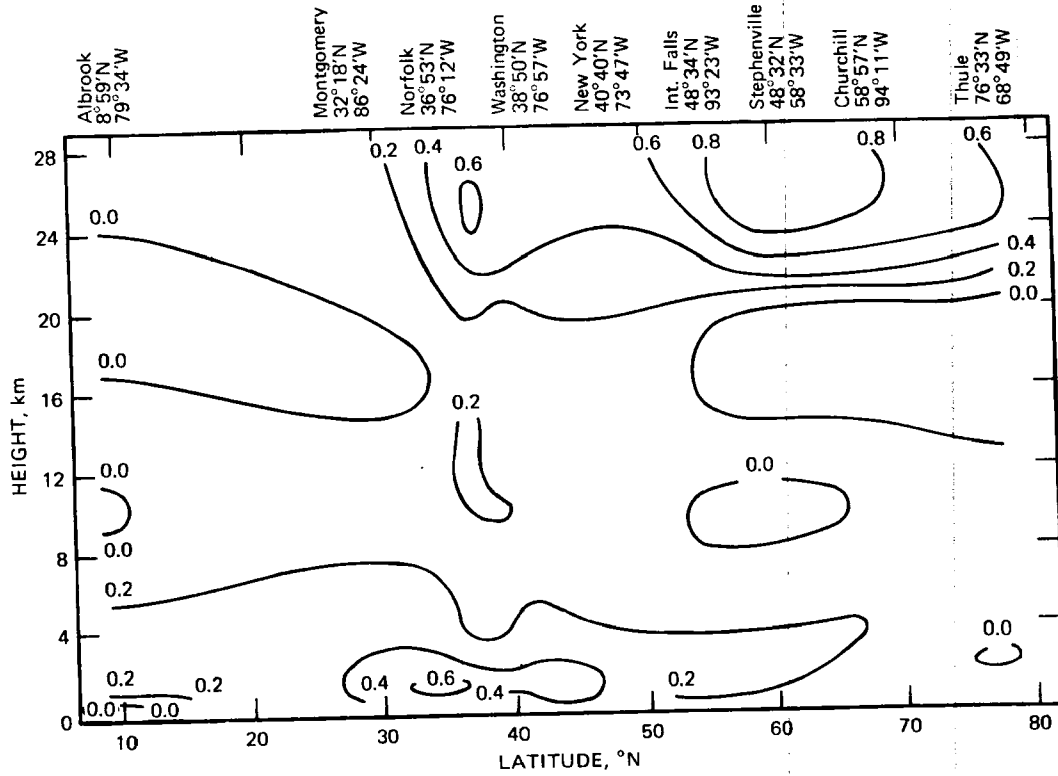


Fig. 6.26 Cross section of the correlation coefficient between temperature and the meridional wind component along 80°W during January. [From D. A. Stewart and O. M. Essenwanger, *Meteorologische Rundschau (West Germany)*, 21(5): 136 (1968).]

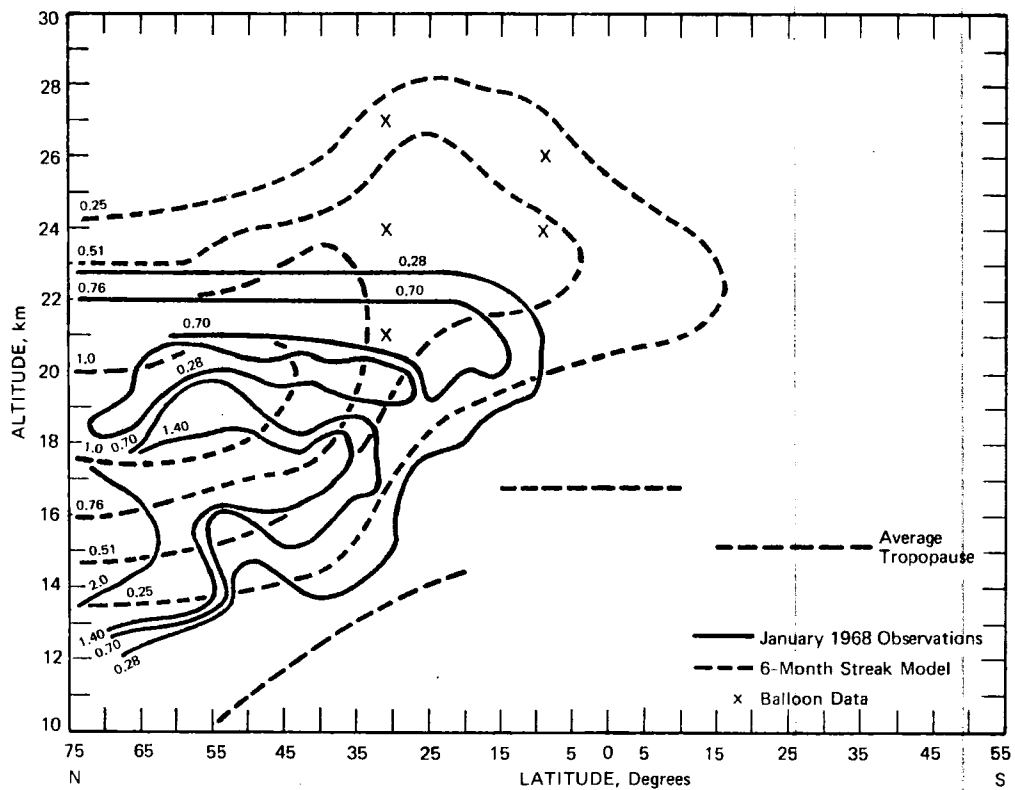


Fig. 6.27 Theoretical (---) and observed (—) distribution of ^{90}Sr concentrations (in picocuries per standard cubic meter) during January 1968. [From Seitz et al. (1968).]

both, thus providing the prerequisites for the formation of a sulfate layer. (By the same token this air shows low radioactivity concentrations, as revealed in Fig. 6.27.) The sharp vertical gradient in the eddy exchange coefficient K_{zz} for eddies smaller than planetary waves, which is to be expected with the change of vertical lapse rate in this layer, may help in generating an aerosol ledge from an otherwise inconspicuous layer.

According to Fig. 1.12, summer conditions are not expected to reveal an isopycnic layer in middle latitudes near 20 km. On the other hand, this figure suggests that meridional pressure gradients and mean zonal winds are zero near this level in middle latitudes (Faust, 1968). Yet, according to Fig. 6.9, even during this season the presence of an aerosol layer is suggested. This would mean that (1) the effect of vertical variations in K_{zz} is the predominant one in generating a dust layer; (2) for some unknown reason this layer shows large anisotropy between large-scale horizontal and vertical eddy-transport processes, as postulated for the winter case above; (3) the mean meridional motions computed by Murgatroyd and Singleton (1961) and shown in Fig. 1.16 maintain most of the transport; or (4) photochemical oxidation of SO_2 is restricted to a relatively narrow altitude range. In the absence of confirming or refuting evidence to argument (2), mechanisms (1), (3), or (4), or a combination thereof, appear to be the most important in generating the Junge layer.

NITROGEN COMPOUNDS

Junge (1963a) has given an exhaustive survey of nitrogen compounds as atmospheric tracers. Only little additional knowledge has been added since. Table 6.1 contains a summary of the most important tracer aspects of N_2O (nitrous oxide), NO (nitric oxide), NO_2 (nitrogen dioxide), and NH_3 (ammonia). The other compounds, such as N_2O_3 (dinitrogen trioxide), N_2O_4 (dinitrogen tetroxide), N_2O_5 (dinitrogen pentoxide), NO_3 (nitrogen trioxide), and N_2O_6 (dinitrogen hexoxide), seem to be of only minor importance as trace constituents of the atmosphere. Nitrates (NO_3^-) and NH_4^+ become important in precipitation processes, which wash them out (Yaalon, 1964). Nitrogen in organic compounds may have a source in sea spray, pollen, and other organic debris (Wilson, 1959a, 1959b; Munczak, 1960; Tarrant et al., 1968). According to Goetz (1966), organic material from the sea surface may surround small droplets, thus inhibiting their evaporation and causing a delay in sea fog dissipation. For further details, see Junge's (1963a) book.

A summary of possible sources and sinks of nitrogen compounds in the atmosphere is given in Fig. 6.28 (see also Altshuller, 1958; for a study of industrial sources, see Anonymous, 1966). Although thunderstorms have been entered in this diagram as a possible source of NO_2 , Georgii (1963) states, in agreement with Junge (1963a), that evidence to that effect is highly questionable. So, for instance, thunderstorms over Kampala (Uganda) did not seem to produce NO_2 that could be detected by an NO_3^- increase in precipitation.

Table 6.1
NITROGEN COMPOUNDS AS ATMOSPHERIC TRACERS

Compound	Concentration in atmosphere	Sources	Vertical distribution	Lifetime	Remarks
Nitrous oxide (N ₂ O)	0.25–0.60 ppm, or 500–1200 µg/m ³ at STP.	Probably biological by soil bacteria; photochemical production of minor importance.	Probably constant.	10 km 4000 days 20 km 800 days 30 km 50 days 40 km 20 days Residence time, about 4 years for total amount of 0.4 cm STP.	Similar residence time as CO ₂ . If production at ground dominates, one should expect similar amplitudes of fluctuations.
Nitric oxide (NO)	About 2.5 × 10 ⁻² ppm, or 33.5 µg/m ³ at STP.	Ionization in D-layer; bacterial reduction of nitrates to nitrites or from HNO ₂ .	Slight increase with altitude (?).		Night afterglow seems to indicate presence of NO at heights greater than 80 km.
Nitrogen dioxide (NO ₂)	16 µg/m ³ in London, 1 to 6 µg/m ³ in suburb.	Urban air pollution. Natural background, 2 to 3 µg/m ³ produced by anaerobic conditions in soils.	No definite conclusions.	2 months.	Lightning as source of NO ₂ appears to be unimportant.
Ammonia (NH ₃)	Mean: 0.013 cm STP, or 1.6 × 10 ⁻² ppm, or 10 µg/m ³ at STP, 15 to 20 µg/m ³ fluctuations.	Alkaline soils; possibly ocean. Anthropogenic production by special industries. Volcanic (Anonymous, 1969).			Annual variation: Maximum in summer and fall. Soil and ocean may act as sources and sinks.

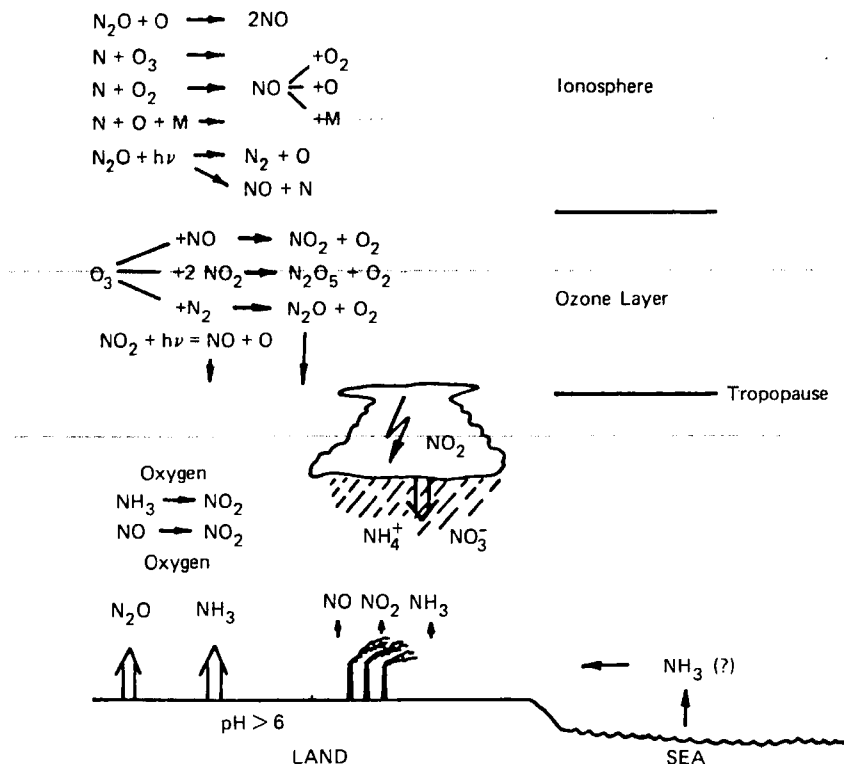


Fig. 6.28 Possible sources and sinks of oxides of nitrogen and of NH_3 in the different layers of the atmosphere. [From H.-W. Georgii, *Journal of Geophysical Research*, 68(13): 3969 (1963).]

R. Reiter (1966) found that NO_3^- ions in precipitation may play a certain role in thunderstorm electrification, irrespective of the origin of the nitrogen-oxygen compound. If there is an ion-concentration gradient in the solid ice particles, the fragmentation of a particle will yield a negative charge in the "splinter" that carries the higher NO_3^- ion concentration. By this process the correlation that exists between $[\text{NO}_3^-]$ measured in precipitation and atmospheric electric activity measured by the frequency of sign reversals of the potential gradient may be explained. This correlation is better established at higher elevations (Zugspitze Peak, 2964 m) than at lower ones (Wank Peak, 1780 m; Garmisch, 730 m) (Fig. 6.29). From this, R. Reiter concluded that charge separation effects and, consequently, the washout removal of NO_3^- are most pronounced in the strongly turbulent regions of convective clouds.

The ground-level source of NO_2 is further augmented by the sharp decrease of this trace constituent with height found by Georgii and Jost (1964) during measurement flights over Germany (Fig. 6.30).

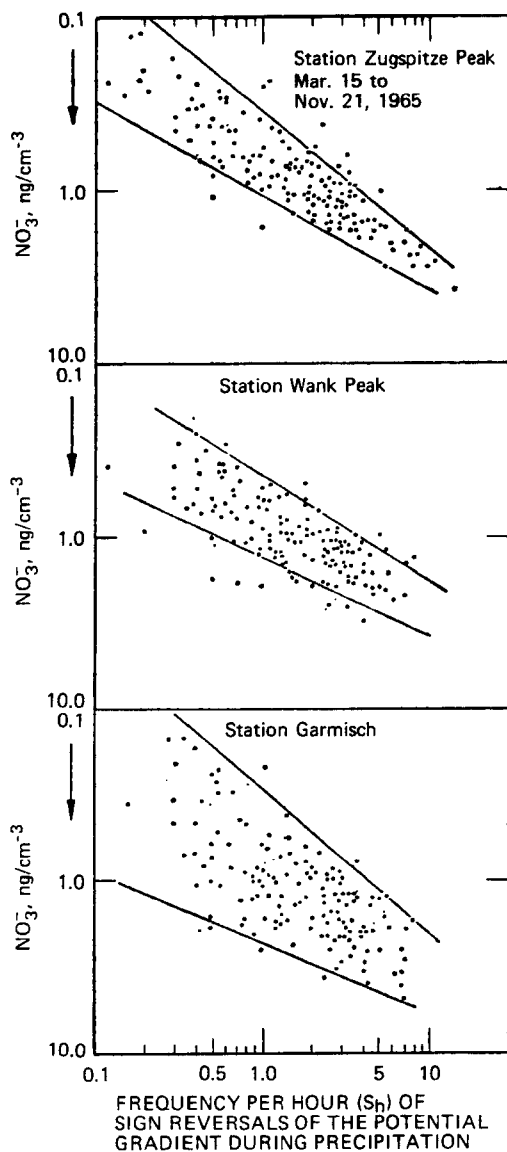


Fig. 6.29 Relation between NO_3^- ion concentration of precipitation and frequency per hour (S_h) of sign reversals of the potential gradient during precipitation at stations Garmisch, Wank Peak, and Zugspitze Peak. [From R. Reiter, *Journal of Atmospheric and Terrestrial Physics*, 28: 1074 (1966).]

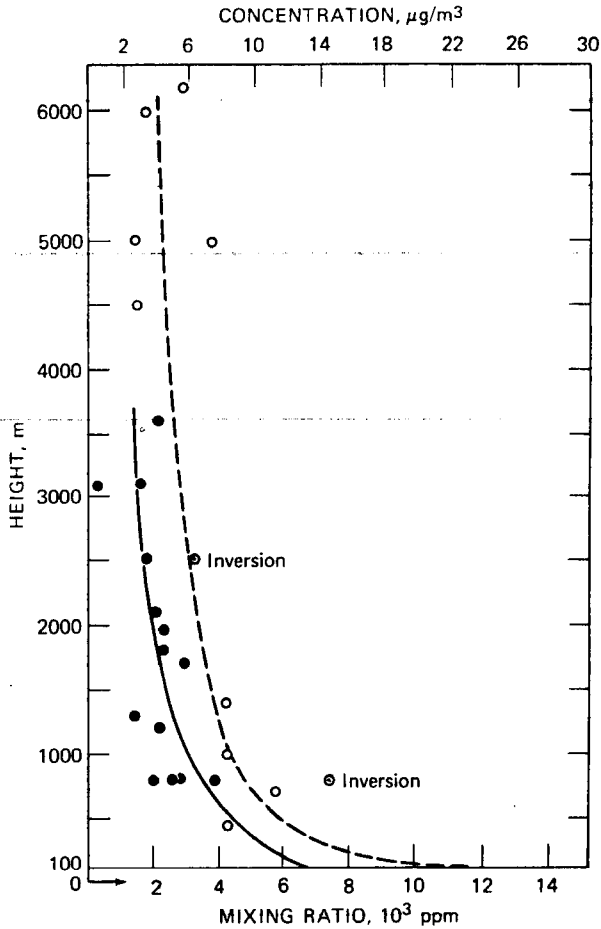


Fig. 6.30 Mean vertical distribution of NO₂ mixing ratios obtained from measurement flights over Germany. — and ●, Winter 1962–1963. - - - and ○, Summer 1963. Concentration values are reduced to surface pressure. [From H.-W. Georgii and D. Jost, *Pure and Applied Geophysics*, 59: 220 (1964).]

Nitric oxide production at ionospheric levels has recently been confirmed by rocket measurements of the day-glow spectrum (Barth, 1966). According to these measurements, the typical volume density of NO is 6.2×10^7 molecules/cm³ at 76 km and 6.0×10^7 molecules/cm³ at 95 km; it decreases from there on to 6.0×10^6 molecules/cm³ at 125 km.

Geisler and Dickinson (1968) reported that these excessively high concentrations of NO have been measured on a winter day of anomalous electromagnetic wave absorption in the ionospheric D-region. (This paper also contains references to work

by other authors pertaining to the winter anomaly of the D-region. For other references, see Thomas, 1969.)

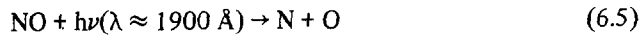
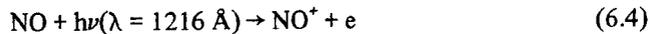
The photochemistry of NO and NO₂ has been studied by, among others, Nicolet (1965a, 1965b), Keneshea (1967), and Ghosh (1968) (for a summary, see Rishbeth and Garriott, 1969). The following reactions appear to be of main importance, especially in the part of the ionospheric D-region near 70 to 85 km (Nicolet, 1965a; see also Craig, 1965; Geisler and Dickinson, 1968):

Production of nitric oxide:

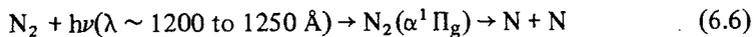


Hunten and McElroy (1968) suggest that the reaction rate involving O₂(¹Δ) could be as much as 3 × 10⁶ faster than k₇ characterizing the unexcited molecule O₂.

Destruction:



Atomic nitrogen is produced by radiation:



The reaction rates k₆ and k₇ are given by:

$$\left. \begin{aligned} k_6 &= (1.5 \pm 0.5) \times 10^{-12} T^{1/2} \text{ cm}^3/\text{sec} \\ k_7 &= 2 \times 10^{-13} T^{1/2} e^{-3000/T} \text{ cm}^3/\text{sec} \end{aligned} \right\} \quad (6.7)$$

The terms ¹Δ and α¹Π_g refer to electronic excitation (Ratcliffe, 1960); T is the absolute temperature. Swider (1969b) suggests that absorption of nonflare solar X rays at much shorter wavelengths than those given in Eq. 6.6, namely, between 1 and 100 Å, plays an important role in NO formation and in D- and E-region ionization.

In the mesosphere the lifetime of NO seems to be quite long. This compound, therefore, might conceivably serve as a tracer of atmospheric motions in this region once its distributions in time and space become better known.

The "winter anomalies" in the D- and F-regions express the fact that electron concentrations are higher and, consequently, electromagnetic wave absorption is stronger (with higher critical frequencies of the electromagnetic waves used in ionospheric probing) during this season than can be explained by the ionizing effect of

solar radiation (see Ratcliffe and Weeks, 1960). Whereas in the F_2 -layer O^+ ions appear to contribute the bulk of positive ions, in the D-region nitric oxide plays an important role, together with the attachment processes $e + O_3 \rightarrow O_2 + O^-$ and $e + O_3 \rightarrow O + O_2^-$ (Burkard, 1962; Doherty, 1968). (For a summary of ion reactions in the lower ionosphere, see also Horiuchi, 1962; Whitten and Poppoff, 1964; Keneshea and Fowler, 1966; E. Ferguson, 1967.) Newell (1968a) points out that vertical and horizontal atmospheric transport processes produce this winter anomaly of middle and high latitudes in the F_2 -region. Geisler and Dickinson (1968) hold such processes responsible for the observed anomalies in the D-region (see also Lauter, Sprenger, and Entzian, 1969, for an excellent summary on the D-region anomaly). Vertical velocities of the order of magnitude of centimeters per second or less would produce the desired effect. Hesstvedt and Jansson (1968) showed with the aid of model calculation that the effect of vertical eddy transports may drastically alter the photochemical equilibrium distribution of the nitrogen compounds in the upper atmosphere.

The out-of-phase relation of decreased and enhanced D-region absorption, hence of decreased and enhanced [NO] in the 70- to 85-km region, during winter over Europe and North America would suggest the effect of standing planetary waves (see also G. E. Chapman, 1969). Since periods of high absorption usually last about 5 days, transient planetary wave phenomena should play an important role. Such transient waves with large variations of amplitude and phase have been observed in the mesosphere by Theon et al. (1967). Transient-wave phenomena would also explain the fact that the winter anomaly of the D-region is not a constant phenomenon observed every day but a highly variable phenomenon occurring rather frequently on single days or during several successive days, leading to a great interdiurnal variability of the D-layer during this season (Dieminger et al., 1967; Lauter and Sprenger, 1968).

Aerosol particles, such as those found in the sodium layer which are partly of meteoric origin, may capture electrons and thus may have a certain effect on the D-region ionization. This effect will depend on the local dust concentrations and is inversely proportional to the ionization density (Parthasarathy and Rai, 1966).

The maintenance of [NO] in the upper mesosphere during summer is probably not so much due to planetary waves (such waves are not expected to penetrate to the mesosphere during this season) but possibly to a mean meridional circulation (see Fig. 1.16) active in the lower part of the D-region. Lauter and Nitzsche (1967) have shown that the winter anomaly appears at high critical frequencies, thus indicating conditions in the upper D-region, whereas low frequencies portraying conditions in the lower D-region reveal a summer anomaly (Fig. 6.31). (A solar zenith angle of 90° shown in this diagram corresponds to sunrise.) Minimum ionization levels in the D-region prevail during spring and autumn. The ionization maximum of summer develops already at negative sun heights and is completely built up by sunrise ($\Psi = 90^\circ$). The ionization maximum associated with the winter anomaly builds up after sunrise. Lauter and Sprenger (1968) speculated that the presunrise enhancement during summer might be caused either by an influx of cosmic radiation particles (see Maehlum, 1967, King, 1967, for winter disturbances) or by alterations in the concentrations of some minor constituents below the 80-km level. Quoting Cumme

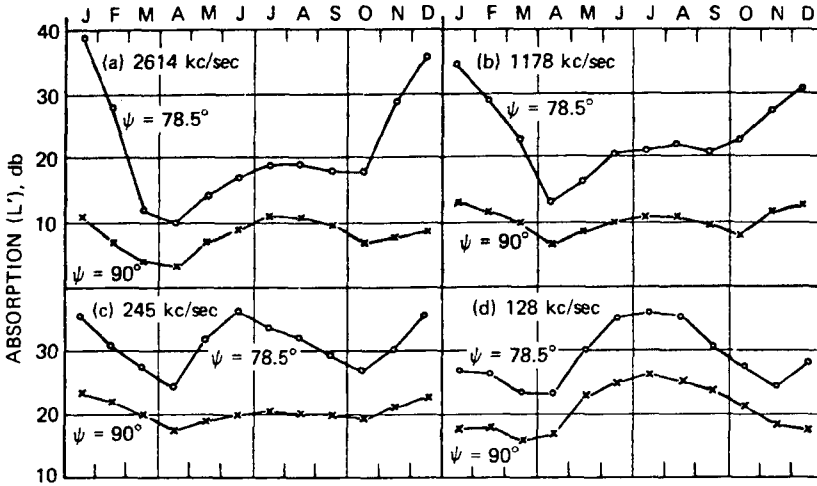


Fig. 6.31 Seasonal variations of ionospheric absorption L' in high-frequency, medium-frequency, and low-frequency bands at constant solar zenith angles ψ during the sunspot minimum 1963–1965 at latitudes 53° to 55°N . [From E. A. Lauter and K. Sprenger, *Meteorological Monographs*, 9(31): 130 (1968).]

et al. (1966), Lauter and Sprenger suggested an increased detachment mechanism by an increase in O_3^- ions. The effect of a mean meridional circulation cell upon the transport of NO, proposed by Geisler and Dickinson (1968), may also be present.

According to Fig. 6.32, the summer and winter anomalies in the D-region relate well to maximum westerly drift velocities of the neutral gas near 95 km (Lauter and Entzian, 1966; Lauter and Sprenger, 1967). The total amount of ozone (Dobson, 1963), also plotted in this diagram, reveals no semiannual peaks. One would not expect completely parallel behavior between the D-region and total ozone since the latter is most sensitive to transport processes near the 20-km level whereas the former reacts to motions in the upper mesosphere. There are, however, certain events that indicate a coupling between stratospheric and mesospheric circulation patterns (Lauter and Sprenger, 1968).

Abnormal ionization changes in the D-region, resulting in a lowering of the ionospheric reflection layer at low frequencies, were observed during periods of abrupt stratospheric warming in late winter (Dieminger, 1952; Lauter, 1953; Bossolasco and Elena, 1960, 1963; Thomas, 1961; Gregory, 1965; Belrose, 1967; Shapley, 1967; Lauter and Sprenger, 1968; Sprenger and Schminder, 1968). Sprenger and Schminder (1966) point out the anomalous drift directions that exist in the D-region during such warming events and their correlation with the stratospheric vortex behavior at 10 mb (about 30 km) obtained from the Berlin weather charts (Scherhag et al., 1958). An example is shown in Fig. 6.33. According to this diagram, the anomalous behavior of the ionospheric drifts shows effects of transient eddies similar to the 30-km winds. The eddy effect reveals itself mainly in a change of the diurnal tide (Fig. 6.34), which is

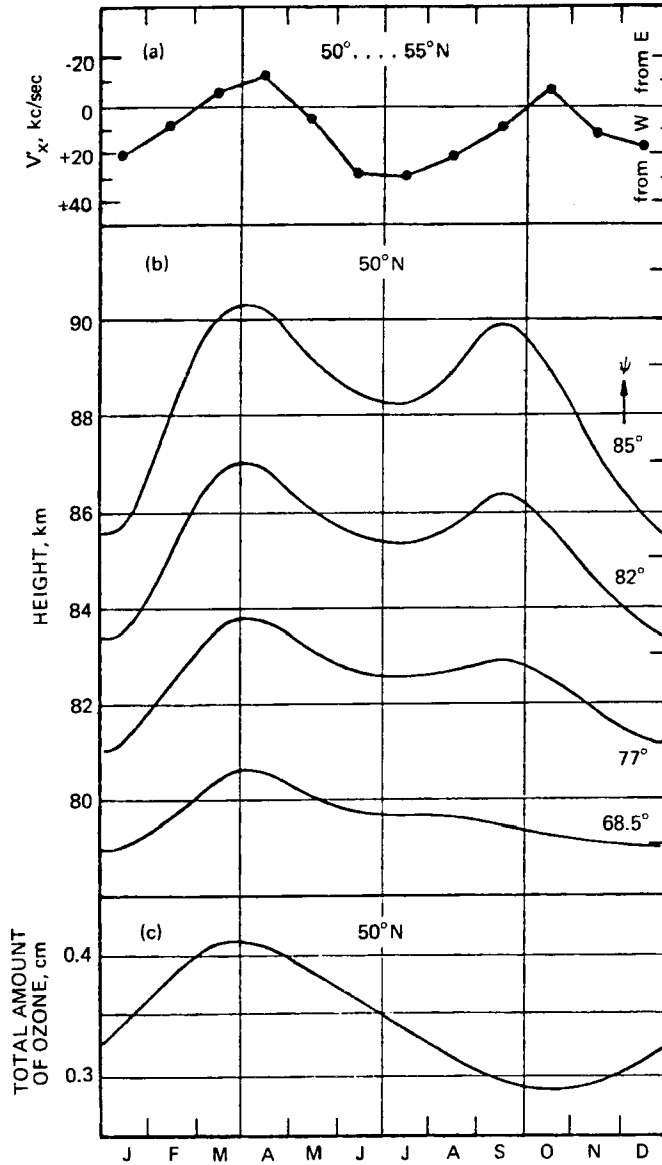


Fig. 6.32 Seasonal variations (a) of the zonal component V'_x of prevailing drift at the 95-km level (Lauter and Sprenger, 1967), (b) of the 155 kc/sec phase heights h' at different constant solar zenith angles ψ (Lauter and Entzian, 1966), and (c) of the total amount of atmospheric ozone (Dobson, 1963). [From E. A. Lauter and K. Sprenger, *Meteorological Monographs*, 9(31): 131 (1968).]

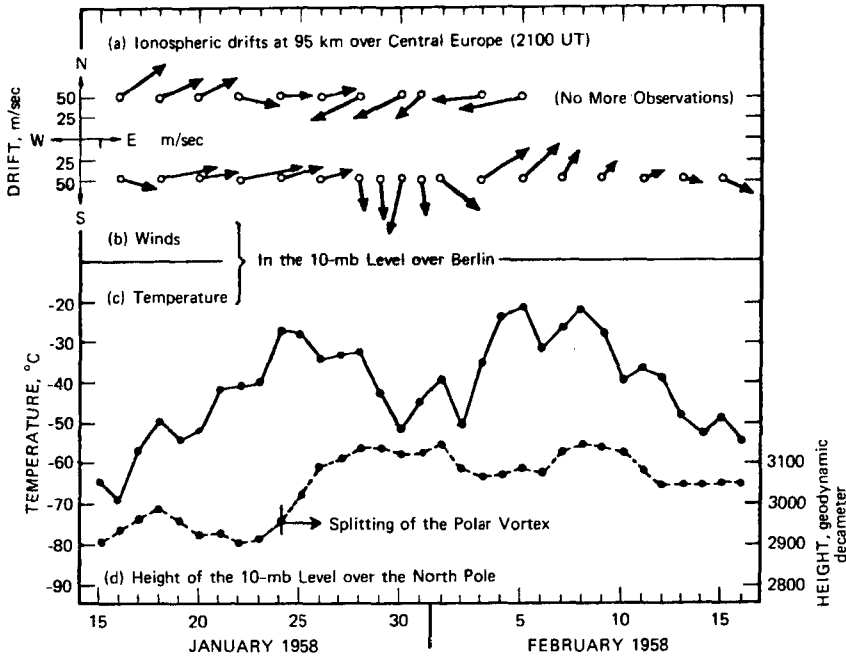


Fig. 6.33 Stratospheric warming event, January–February 1958, which has been connected for the first time with an observed anomaly of drift direction in the lower ionosphere (10-mb data from Scherhag et al., 1958). [From E. A. Lauter and K. Sprenger, *Meteorological Monographs*, 9(31): 136 (1968).]

expected to respond to the change in the thermal structure of the atmosphere beneath the level of observation. In corroboration of this Fraser (1968) reported a close correlation between midwinter stratospheric warming over Antarctica (at 36 km over McMurdo Sound) and height variations of the zonal zero velocity contour near 80 km (see Fig. 6.58), measured over Birdling's Flat at 44°S, 173°E (New Zealand). Stratospheric warming is paralleled by a decrease in the height of this contour.

Sprenger and Schminder (1967) reported on the presence of a 26-month cycle in drift velocities measured in the D-region. The maximum amplitude of the westerly wind maximum was found in midlatitudes (northern hemisphere) during January 1958, September 1960, November 1962, and January 1965 (see Lauter and Sprenger, 1968). The mean amplitude of this 26-month oscillation is about 3.5 m/sec, which is in good agreement with estimates from the stratosphere by Angell and Korshover (1965). According to Fig. 6.35, the phase of the oscillation seems to be progressing downward from the ionosphere to the lower stratosphere in midlatitudes. It was mentioned in Part 1, Chap. 3, that the biennial oscillation is reflected in the variation of eddy-transport processes. The winter anomaly of the D-region thus appears to respond to such changes in eddy processes even over long periods of time. From these

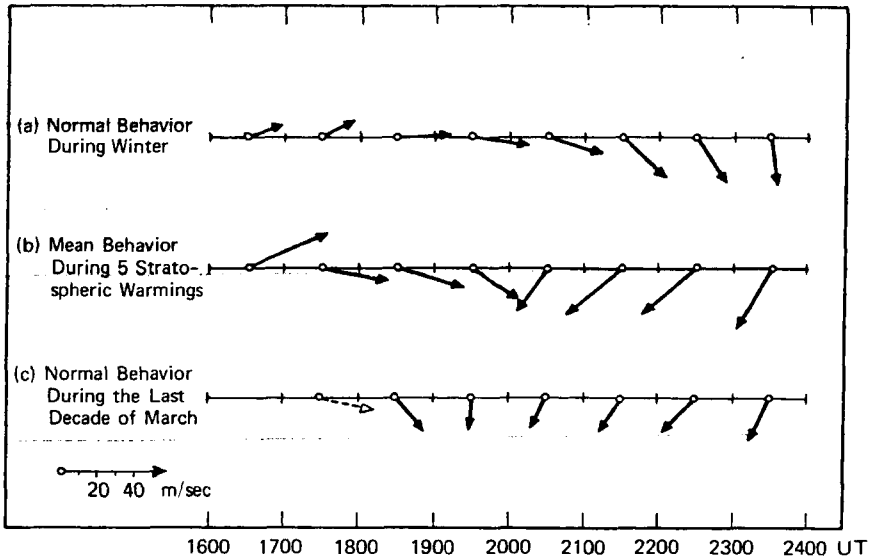


Fig. 6.34 Mean diurnal variation of the drift vector in the lower ionosphere during five stratospheric warming events (b) compared with the normal variation (a) during winter and (c) during late March. [From E. A. Lauter and K. Sprenger, *Meteorological Monographs*, 9(31): 137 (1968).]

data it would appear that the stratopause (near 50 km) is not the ultimate source region of the 26-month wind oscillation as, for instance, suggested by Belmont et al. (1969). But then, however, the single data point shown in Fig. 6.35 for 1962 is not very conclusive. One might arrive at the same quasi-periodicity in the D-region drift patterns if there were an upward phase propagation from the stratopause with the same rate as the downward propagation in the stratosphere. If, however, the downward phase propagation indeed held throughout the mesosphere, as implied by Fig. 6.35, the trapping of wave energy as a cause of the quasi-biennial wind oscillation (J. M. Wallace and Kousky, 1968b) would have to be validated for mesospheric layers. According to Dickinson (1969), planetary Rossby waves are only moderately attenuated in their upward propagation to the mesopause during midwinter (damping by a factor of 2), whereas at the equinoxes the damping factor has the order of magnitude of 10. Whether or not such upward propagation may trap enough energy to account for a downward progression of a westerly wind maximum through the mesosphere, as implied by Fig. 6.35, is still open to investigation.

In Table 6.1 the mean residence time of N_2O in the atmosphere has been given as 4 years, similar to that of CO_2 . Bates and Hayes (1967) deduced a mean residence time of 70 years from concentration measurements of N_2O in the troposphere and from estimates of vertical exchange coefficients K_{zz} derived from the distribution of other trace substances. They assumed, furthermore, that photodissociation above 20 km is the main sink of nitrous oxide. Summarizing, one may state that the

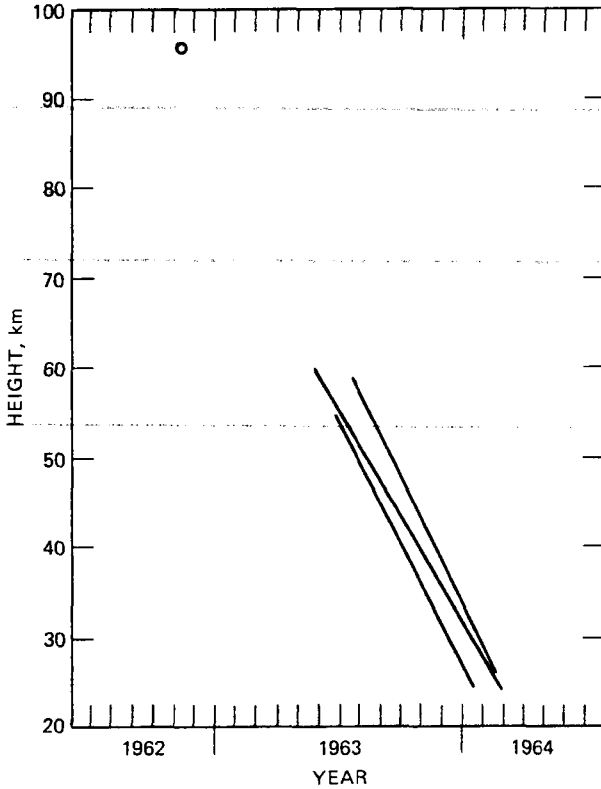


Fig. 6.35 Variation with height of the phase of the 26-month zonal wind oscillation in temperate latitudes with phase being defined by the time of wind maximum from the west. Solid lines: Regression lines derived from rocketsonde results of three stations of the North American Meteorological Rocket Network (Angell and Korshover, 1965). Circle: Mean phase in the lower ionosphere derived from the results of Sprenger and Schminder (1967b) in central Europe. [From E. A. Lauter and K. Sprenger, *Meteorological Monographs*, 9(31): 134 (1968).]

application of nitrogen compounds as tracers of atmospheric motions is still limited. More measurements on a global basis will be needed before these compounds can be used effectively for transport studies.

THE HALOGENS

Chlorine (Cl_2) and chloride (Cl^-) have been identified in air samples. Chlorine occurs as a gaseous constituent; Cl^- occurs in aerosols and precipitation (see Junge, 1963a). Most of the Cl^- is clearly of maritime origin, stemming largely from sea-salt particles. This is evident from the almost logarithmic decrease of $[\text{Cl}^-]$ in precipitation within the first few hundred kilometers from the coast, found by DeBary and Junge

(1963) over Europe. Coastal values of [Cl] in precipitation are higher in winter by a factor of 2 to 3 than in summer because of the higher frequency of storms. There usually is also a marked decrease with height of [Cl] in aerosol over the ocean, which points toward the ocean surface as a source of these particles (Durbin, 1959; Durbin and White, 1961; Singleton and Durbin, 1962). Over land the vertical distribution of these particles appears to be more irregular; maximum values are usually several hundred meters above the ground (see also Podzimek, 1959).

Chlorine may be taken as a characteristic constituent of sea-salt particles advected inland (see, for example, Zerche and Hänsch, 1967). From sea-salt deposits observed far inland in central Europe (Schubert and Hänsch, 1963a, 1963b), Ertel (1965) derived conditions for the advective transport of such salt particles: The minimum depth of inland penetration, L_{\min} , of the sea salt is given as

$$L_{\min} = \frac{uH}{s} \quad (6.8)$$

where u is the mean wind speed of the mixing layer near the ground, s is the sinking velocity of the salt particles, and $H = K_m/s$ is the height of the "homogeneous salt-particle atmosphere" at the coast, K_m being the mean diffusion coefficient of the atmosphere under the given storm conditions.

From studies of the chlorine budget of small watersheds in New Hampshire, Juang and Johnson (1967) concluded that about two-thirds of the chloride input into the area under study stemmed from precipitation removal of atmospheric chloride; the rest most likely stemmed from a dry removal process whereby aerosol containing chloride impacts upon vegetation (see also Hanya, 1951; Eriksson, 1955; Zersche and Hänsch, 1967). The bulk of chloride in river water appears to be of atmospheric origin with only a small amount from direct rock weathering (Eriksson, 1959, 1960).

Gaseous chlorine had earlier been thought to be released from sea-salt particles in a reaction with O_3 (Cauer, 1951) or with H_2SO_4 (Eriksson, 1959, 1960). Junge's (1956, 1957) measurements over Florida cast some doubt on this hypothesis, pointing toward a widespread gaseous chlorine distribution in the atmosphere. Further evidence is presented by DeBary and Junge (1963), who show that the ratio ([Cl] in air):([Cl] in precipitation) increases significantly inland from the coast, the opposite of the distribution found for [Cl] in precipitation alone. Bossolasco and Cicconi (1961) noted from measurements in Europe that in the lower atmosphere the chlorine/sodium ratio increased with distance from the sea in dry air as well as in precipitation. Also, there do not seem to be any significant seasonal variations in this ratio. Georgii (1960a) found some anthropogenic sources of this chlorine.

More recently, Valach (1967) claimed volcanic action to be the dominant source of gaseous chlorine in the atmosphere. The average yearly volcanic production of chlorine was estimated to be 9×10^6 tons/year (Eriksson, 1959, 1960). Already 1.2×10^6 tons/year are released from the Valley of Ten Thousand Smokes in Alaska in the form of HCl. It would seem that gaseous chlorine should lend itself as a tracer constituent at least near such regions of concentrated release.

Iodine (I) is difficult to detect as gas (I_2) in the atmosphere. It is readily absorbed by aerosol, especially if the concentration of the latter approaches a value 1000 times larger than that of I_2 (see Junge, 1963a). This is probably why radioactive ^{131}I is washed out by precipitation processes. Such a washout seems to occur even when cumulonimbus clouds penetrate to atmospheric layers contaminated with ^{131}I well above the tropopause (List et al., 1964; Reiter and Mahlman, 1965b). The entrainment of stratospheric air into such high-reaching clouds would cause conditions that Junge considers favorable for almost complete absorption of iodine. More about ^{131}I will be said in Part 4.

The burning of seaweed and the West European iodine industry have been identified as sources of iodine (see Junge, 1963a, for references). According to Bolin (1959), considerable amounts of iodine may come from the ocean. Miyake and Tsunogai (1963) found experimentally that free iodine is released from seawater by photochemical oxidation of iodide under the influence of solar violet radiation (wavelength less than $560 m\mu$). The rate of release for the whole ocean surface has been estimated to be 0.4×10^6 tons/year. This value is in fair agreement with the global rate of iodine deposition by rain. Release may be enhanced by an iodine-rich organic film on the ocean surface (Duce et al., 1965). Such a photochemical release mechanism could also account for the enrichment of iodine (expressed, for instance, by the iodine/chlorine or iodine/bromine ratios) in air, rain, and river water as compared with ocean water. Duce et al. (1963), for instance, found ratios of iodine/chlorine and iodine/bromine in rain over Hawaii (average values of these ratios, 1.1×10^3 and 0.20, respectively) and in aerosol to be about two orders of magnitude larger than corresponding values for seawater. The bromine/chlorine ratio, on the other hand, is approximately equal for rain, aerosol, and seawater (about 5.4×10^3), which suggests that no fractionation occurs in the release of the latter two constituents.

Duce et al. (1965) also found that the aerosol iodine/chlorine ratio increases with altitude and with distance from the sea; at least this was true in their measurements over Hawaii. This may be due to continuing absorption of I_2 on aerosol particles along their path or to loss of chlorine from these particles. A more likely explanation of this iodine and bromine enrichment may be found in the fact that aerosol particles in the atmosphere containing these two elements are on the average smaller in size than chloride-rich particles (Duce et al., 1965, 1966; Winchester and Duce, 1966). Chloride seems to be the principal anion in the "giant" sea-spray particles ($1 \mu < r < 20 \mu$) whose residence time in the atmosphere is only a few days. These particles are effectively released into the atmosphere by the bursting of bubbles at the ocean surface (Jacobs, 1937; Paterson and Spillane, 1969). The hydrophilic characteristics of these giant nuclei may be affected to a certain extent by organic molecules, either present in a surface film on the ocean or introduced by anthropogenic water or air pollution or both (Pueschel et al., 1969). Large particles ($0.1 \mu < r < 1 \mu$) containing mostly $(NH_4)_2SO_4$ remain in the atmosphere approximately 20 to 40 days. Substantial bromine has been measured in particles with a radius even smaller than 0.1μ . If chloride falls out rapidly with giant aerosol particles, the

bromine and iodine content of the atmosphere will show a shift toward larger iodine/chlorine and bromine/chlorine values with increasing age of the air mass.

Silver iodide (AgI) is widely used in cloud seeding and weather modification. Certain types of ice-nuclei generators also develop NaI together with AgI (Mossop and Tuck-Lee, 1968). Numerous investigations of the diffusion processes by which these artificial nuclei are spreading in the atmosphere, especially in and near convective or orographic cloud systems or both, are being conducted. It would exceed the scope of this review to explore the potential use of AgI as a tracer of small and mesoscale motions (see Langèr et al., 1967; American Meteorological Society, 1968).

Schaefer (1966, 1968, 1969) speculated that lead from auto exhaust and traces of iodine in the atmosphere may react readily to form lead iodide, which produces very effective ice nuclei. The generation of such nuclei in regions of heavy automotive traffic may produce inadvertent weather modification effects.

Chlorine and iodine are the halogens that have received the most attention as atmospheric tracer constituents. Fluorine (F) and fluoride (F⁻) are also present, although in much smaller quantities. Hydrogen fluoride, for instance, is released at a rate of 0.2×10^6 tons/year in the Valley of Ten Thousand Smokes, Alaska; thus it is also of volcanic origin. The chlorine/fluorine ratio there is 6, whereas in seawater it is 10^4 (Rankama and Sahama, 1952). Fluorine has also been identified in precipitation (Valach, 1967). The chlorine/fluorine ratio there (≈ 11) was probably not influenced by artificial sources. This also would support the hypothesis stated earlier that gaseous chlorine in the atmosphere may be of volcanic origin. The compounds SF₆, C₄F₈, and CBrF₃ have been used as artificial gaseous tracers for air-pollution and -diffusion studies (Niemeyer and McCormick, 1968).

Bromine has received attention by Duce et al. (1963, 1965) mainly in rainwater analyses. The bromine/chlorine ratio, according to their investigation, seems to show a slight increase with increasing altitude similar to the iodine/chlorine ratio. A possible source of Br₂ may be photooxidation. Such oxidation, however, would be conceivable only under acid pH values (as may be the case in droplets containing a variety of aerosols) and not directly from the sea surface with a basic pH of 8.3 (for references, see Duce et al., 1965).

Duce et al. (1965) considered automotive air pollution (see also Seto et al., 1969) as an additional source of bromine, which may explain the much larger bromine/chlorine ratios in aerosol over land than over the ocean. Ethylene bromide (CH₂Br-CH₂Br), added to gasoline to remove PbO from engine cylinder walls, yields about 1.2 g of bromine per gallon of gasoline. Such Br₂ injection into the atmosphere may provide a considerable increase of bromine/chlorine ratios, especially in regions with large traffic concentrations. Lininger et al. (1966) found a correlation between lead and bromine in polluted air in Cambridge, Mass. This also points toward fuel combustion as a source for Br₂. Bromine concentrations there were about one order of magnitude higher than over Hawaii, and they agreed with values found in the Washington, D. C., area (Gordon and Larson, 1964).

Boron/chlorine ratios have been studied by Gast and Thompson (1959). These ratios are higher in rainwater than in seawater. Most atmospheric boron appears to

come from the sea surface by evaporation. There are, however, terrestrial sources to be considered as well.

From the foregoing discussion, it appears that the halogens are quite suitable as tracers of maritime and continental air masses and for transport processes in specific regions. Considerably more detailed measurements will be needed, however, before their full potential as tracers for atmospheric motions may be realized.

Besides the ones already discussed, many other chemical elements and compounds have been identified as trace substances in the atmosphere. Junge (1963a) has given an exhaustive review of such substances. The discussion in the next section will be restricted to nonradioactive chemical tracers that have been used or may be used in the study of atmospheric motion patterns at different scales.

SODIUM (Na) AND OTHER ALKALI METALS

The Sodium Airglow Layer

One definite source of sodium in the atmosphere is the ocean surface. Sodium ions are carried aloft in sea spray, along with anions, mainly Cl^- , following similar transport characteristics (for details, see Eriksson, 1960). Of more importance in terms of tracer studies than its tropospheric occurrence, however, is the presence of sodium at mesospheric and thermospheric levels, where it gives rise to day glow, night glow, and twilight phenomena. Detailed accounts of these were given by Chamberlain (1961). (For a short summary, see Newell, Wallace, and Mahoney, 1966.)

Earlier estimates with the van Rhijn method of height measurement (for details, see Chamberlain, 1961) indicated heights of the sodium emission region in excess of 200 km. Among other factors the patchiness of airglow regions may cause errors in the van Rhijn estimates of height. Triangulation of such patches usually yields considerably lower altitudes of sodium airglow, as do rocket measurements (70 to 110 km, according to several sources listed by Chamberlain, 1961; see also early estimates by Penndorf, 1947; Vegard and Tönsberg, 1940). From measurements with a rocket-borne day-airglow photometer on Sept. 26, 1964, over Wallops Island, Donahue and Meier (1967) found most of the sodium to be concentrated in a 5-km-thick layer centered at 92.4 km. In this layer 16×10^9 atoms of sodium per square centimeter were sampled. This compares with 6.2×10^9 atoms per square centimeter at 89 km found in preceding twilight measurements and characterizing a layer 8.8 km thick.

Junge et al. (1962) rejected earlier hypotheses on the possible terrestrial (see Chamberlain, 1961, p. 469) or solar origin of the high atmospheric sodium. According to their argument, diffusion coefficients known to exist in the stratosphere (see Table 1.1) would not be large enough to carry particulate matter of $0.1\text{-}\mu$ radius from the troposphere into the mesosphere in sufficient quantity to account for the observed airglow phenomena. Figure 6.36 shows the mixing ratio χ of such particles at height z in relation to the mixing ratio χ_0 at tropopause height (12 km) for various diffusion coefficients. Values of 10^3 and 10^4 cm^2/sec for diffusion coefficients are in agreement

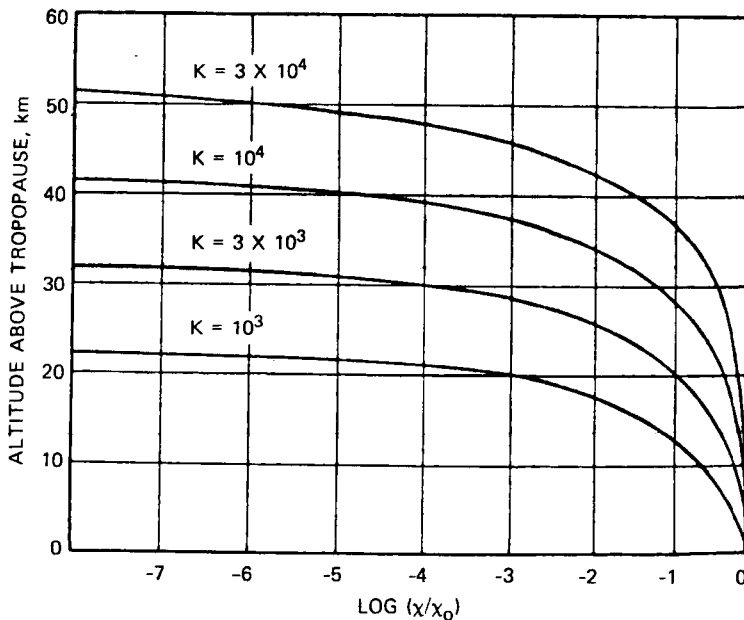


Fig. 6.36 A series of curves showing the decrease in the amount of particulate matter above the tropopause for a particle radius of 0.1μ and various assumed values of the diffusion coefficient K . The abscissa shows the logarithm of χ/χ_0 , where χ is the mixing ratio of particulate matter above the tropopause and χ_0 is the mixing ratio of particulate matter at the tropopause (taken as 12 km). [From C. E. Junge, O. Oldenberg, and J. T. Wasson, *Journal of Geophysical Research*, 67(3): 1030 (1962).]

with those derived by Spar (H.A.S.P., 1960) from the spread of a tungsten, ^{185}W , cloud and correspond to coefficients in the tropical stratosphere at 20 km and in the midlatitude stratosphere, respectively.

Junge et al. concluded that high atmospheric sodium is supplied by meteors and also by micrometeorites (cosmic dust). Meteors are known to evaporate mainly in the altitude range between 70 and 120 km, where most of the sodium airglow emission seems to occur. Speculation about the origin of ionospheric sodium, however, still continues (Vallance Jones, 1966). Hunten (1964) claims that meteoric sodium would contribute only slightly to the total sodium abundance in the upper atmosphere. Furthermore, the sodium/potassium ratio is about the same in the sodium layer as in seawater (Fig. 6.37), whereas other likely sources, such as meteorites, show a potassium abundance that is about five times greater than the sodium abundance. Thus a large part of sodium in the sodium layer appears to be of marine origin.

Similar to the oxygen emission discussed in Chap. 5, the sodium emission shows marked seasonal and latitudinal variations that allow certain inferences on upper atmospheric circulation patterns and transport processes (Newell, Wallace, and Mahoney, 1966). T. N. Davis and Smith (1965) reported on night-glow measurements

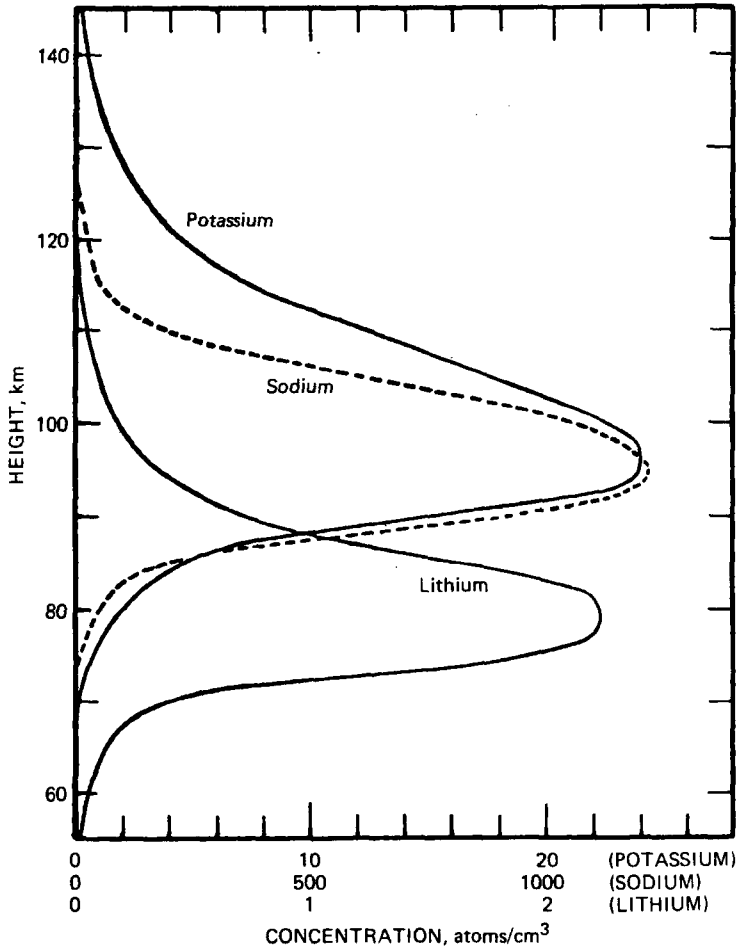


Fig. 6.37 Vertical distributions of the three alkali metals measured at Saskatoon, Saskatchewan, Canada. Note the three different concentration scales. [From D. M. Hunten, *Science*, 145: 29 (1964). Copyright 1964 by the American Association for the Advancement of Science.]

of sodium emission at $\lambda = 5893 \text{ \AA}$ taken mainly in the southern hemisphere. Hardly any diurnal variation was found in this emission. Hunten and Wallace (1967) suggested a factor of 1.43 for daytime enhancement of sodium during April as compared with twilight estimates. During June no enhancement was detected. Donahue and Meier (1967), on the other hand, found a daytime enhancement in excess of a factor of 2 from their Wallops Island measurements in September 1964, quoted earlier.

Seasonal variation shows a minimum in summer and a maximum in winter (see also Vallance Jones, 1963; Barbier, 1965b), in agreement with data from the northern

hemisphere reported by Newell et al. and shown in Fig. 6.38 (see also L. L. Smith and Steiger, 1968). This annual change is consistent with the variations in electron densities of the F₂-layer shown in Fig. 5.11, which suggested upwelling motions in the summer hemisphere and subsidence in the winter hemisphere, even though the F-layer is found at still higher levels (about 250 km) than the sodium emission layer. There does not seem to be any effect of solar activity on yearly averages of sodium night-glow intensity. Barbier (1965a), however, reported on a decreasing trend of these intensities between 1954 and 1964. Such a trend, to my knowledge, has not been reported elsewhere.

Figure 6.39 gives the average 5893-Å emission measurements made on board the *Eltanin* (T. N. Davis and Smith, 1965) at night, mainly during the period May 24 and Sept. 1, 1962. The higher values that occur in the southern hemisphere correspond to the seasonal change of this phenomenon mentioned previously. A comparison of this diagram with Fig. 5.9 shows that the individual peaks of the 5893-Å emission are out of phase with those of the 6300-Å red line. The cause for this may lie in the photochemistry of the phenomenon.

Chapman (1939) postulated the reaction



(with the rate coefficient of 4×10^{-11} cm³/sec assumed by Donahue and Meier, 1967). The term ²P refers to the state of electronic excitation. The following additional reactions may also be of importance (Hunten, 1964; for references see Chamberlain, 1961; Vallance Jones, 1963):



(with the rate coefficient of 6.5×10^{-12} cm³/sec, assumed by Donahue and Meier, 1967)



Reactions might also involve hydrogen, for example,



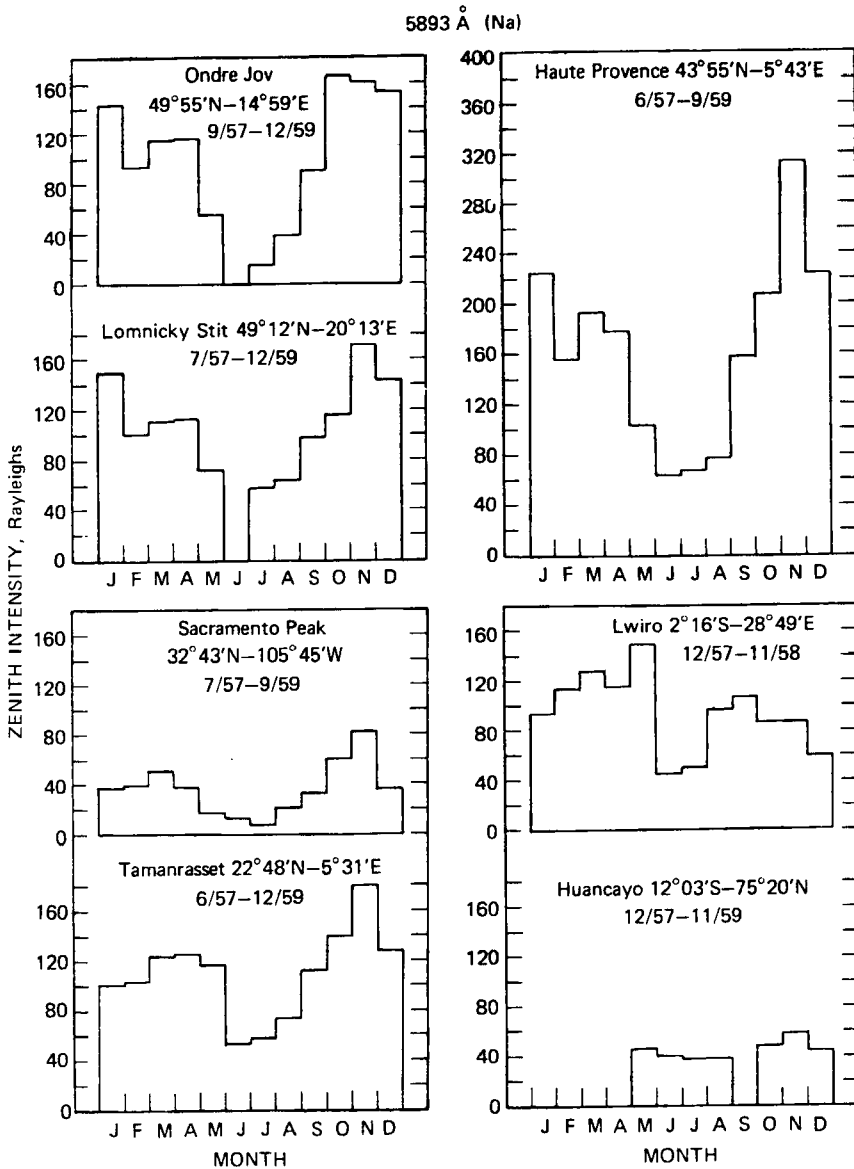


Fig. 6.38 Monthly values of the zenith intensity of the sodium component of night glow. Blank months indicate insufficient data. [From R. E. Newell, J. M. Wallace, and J. R. Mahoney, *Tellus*, 18(2-3): 374 (1966).]

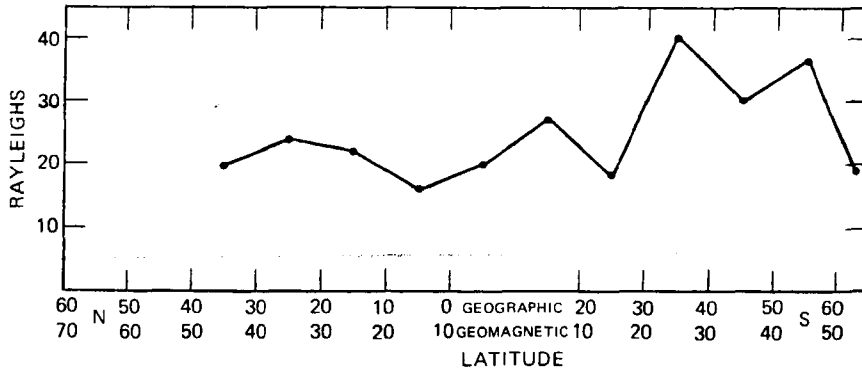


Fig. 6.39 Nightly average of hourly averages of the sodium group (sodium D 5893 Å and OH): 10° latitude averages vs. latitude, measured on board the *Eltanin*. [From T. N. Davis and L. L. Smith, *Journal of Geophysical Research*, 70(5): 1136 (1965).]

(For additional information, especially on ionization and recombination, see Blamont and Donahue, 1964.) The hydrogen emission occurs in several spectral bands of night glow. Its seasonal trend appears to be similar to that of the sodium airglow.

The “forbidden” oxygen red line is generated by a $^3P_2 - ^1D_2$ transition of atomic oxygen (see Chamberlain, 1961, Appendix VI). This transition thus depends on the concentration of [O], which is competitively influenced by reactions 6.9, 6.11, and 6.13. These reactions also depend on the concentrations of [Na], [NaO], and [NaO₂]. The ratio [NaO]/[NaO₂] varies only with temperature, whereas [Na]/[NaO] also depends on density (Chamberlain, 1961, p. 468). Changes in the photochemical equilibrium near the mesopause may be expected if the temperature minimum shifts by a few kilometers; large seasonal changes in the sodium emission may result. The latitudinal variations in the sodium emission, shown in Fig. 6.39, therefore, may not simply be interpreted as the effect of vertical “circulation wheels” with upwelling and sinking motions. The complex temperature (and density) structure near the mesopause may have a decisive influence on the airglow patterns. The horizontal details of this structure are not yet known, however, to a degree of resolution that would allow further interpretation of the data.

This is brought to light in a study by Blamont and Donahue (1964): They found a pronounced seasonal variation of the height of the layer of sodium twilight glow (Fig. 6.40). Measurements by Bullock and Hunten (1961) have been entered into this diagram for comparison. There also is an inverse correlation between the altitude of the twilight layer and the intensity of the sodium day glow (Fig. 6.41). The latter shows a marked seasonal variation in middle latitudes with a maximum of intensity during summer when the sodium twilight layer is found at low elevations (see also Vallance Jones, 1966) (Fig. 6.42). At high latitudes (Tromsø, Norway), sodium day glow reveals hardly any seasonal variation. Twilight glow has a much smaller seasonal

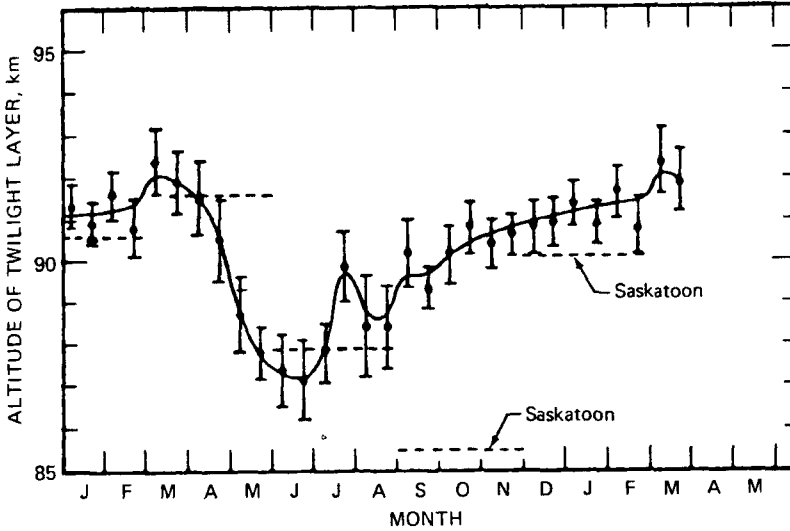


Fig. 6.40 Average altitude of twilight layer at Haute Provence 1954–1963; morning and evening data have been lumped. Results of Bullock and Hunten at Saskatoon are shown for comparison. [From J. E. Blamont and T. M. Donahue, *Journal of Geophysical Research*, 69(19): 4110 (1964).]

trend with an intensity minimum indicated in summer, also substantiated for the southern hemisphere (Gadsden, 1964a; Hunten, 1964).

From the seasonal variations in both sodium day and night glow, it would appear that variations of the atmospheric structure and transport processes near the mesopause have an important effect on these two airglow phenomena (Gadsden, 1964b). That these seasonal trends are out of phase for day and night glow confirms the opinion expressed before that these effects are overshadowed by the complex photochemistry of this region.

According to Donahue and Meier (1967), photochemistry alone cannot account for the thinly layered structure of the sodium region detected from rocket measurements. In a model computation these two investigators assume a source of sodium and NaO to be present in an even thinner aerosol layer. From this “dust horizon” sodium and other volatile constituents (such as calcium, potassium, and magnesium) would evaporate at an enhanced rate during daylight hours and would be carried away by eddy diffusion. The sodium distribution then would be controlled by the source strength, by diffusion, and by photochemistry (mainly Eqs. 6.9 and 6.12). (For details of the computation, see the original paper by Donahue and Meier.)

The thin dust layer that serves as a source of sodium may be generated by processes similar to the ones causing the noctilucent-cloud layer (see Fig. 2.19), whereby the turbopause (or at least a sharp gradient in the vertical eddy diffusion coefficient) helps to form a dust ledge. Note that the sodium layer observed by Donahue and Meier occurs in the general vicinity of the mesopause. (Vertical

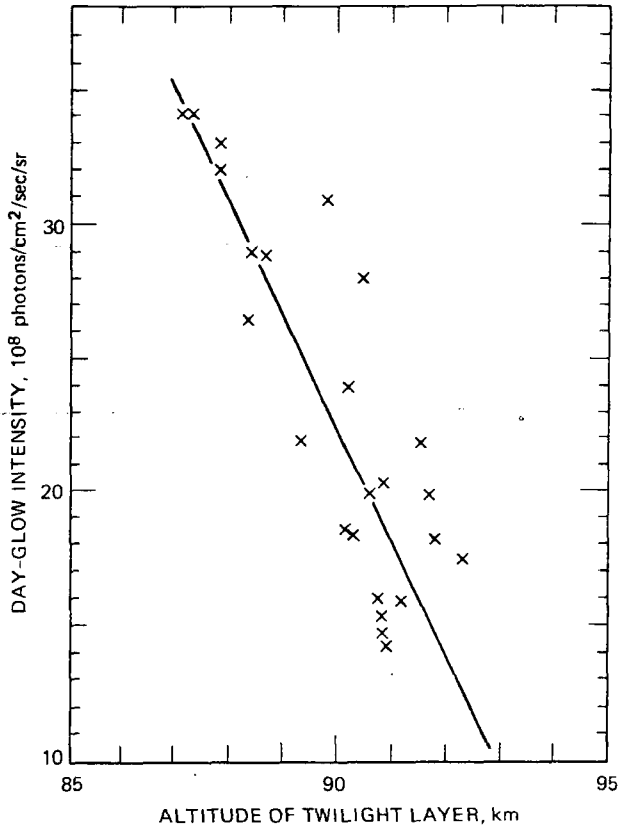


Fig. 6.41 Correlation of day-glow intensity with altitude of twilight layer. Points are taken from semimonthly averages. [From J. E. Blamont and T. M. Donahue, *Journal of Geophysical Research*, 69(19): 4110 (1964).]

temperature profiles were not given by the two investigators but may be inferred from the standard atmosphere as given by Environmental Science Services Administration et al., 1966.) Donahue (1966) suggested that at least part of the dust particles are electrically charged and are moved by wind-shear-generated electric fields similar to those causing the sporadic E-layer (Whitehead, 1961). Hanson and Donaldson (1967) speculated that Na^+ ions would be moved downward by easterlies (upward by westerlies until a wind reversal occurs) until they recombine, thus constituting a source of atomic sodium. This source region could be quite narrow if in reaction 6.12 O_3 is assumed to increase rapidly with decreasing altitude. Which of the aforementioned effects, a vertical gradient in the eddy diffusion coefficient or an ion transport in the presence of magnetic and electric fields, is the dominant one in generating a sharply defined sodium layer will still have to be determined. The presence of aerosol particles

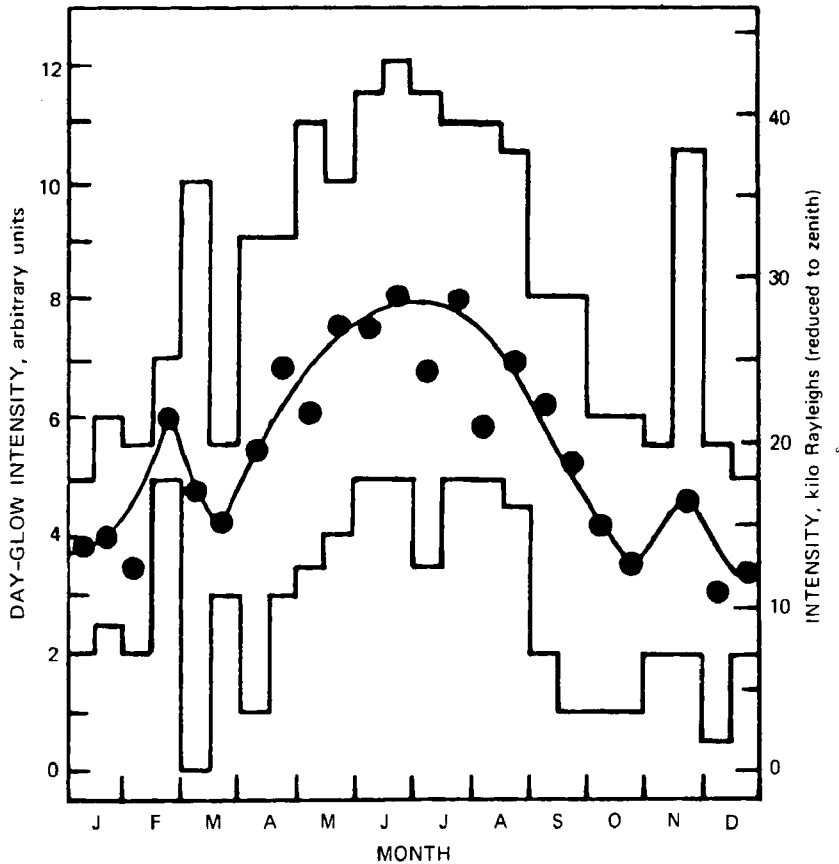


Fig. 6.42 Sodium day-glow intensity at Haute Provence for a solar elevation angle of 30° (20° November–February). Extreme readings are indicated as well as averages from August 1961 to January 1964. [From J. E. Blamont and T. M. Donahue, *Journal of Geophysical Research*, 69(19): 4107 (1964).]

with $\tau > 0.1 \mu$ enhances the recombination of ions and electrons in the D-region (Parthasarathy and Rai, 1966). Thus it is to be expected that the sodium layers affect the detailed structuring of the ionospheric D-region.

Transport effects also become apparent from a correlation between stratospheric warming episodes and sodium abundance estimated from twilight measurements over Canada (Hunten and Godson, 1967). Figure 6.43 may serve as an example. The sodium abundance has been estimated with the assumption that the ratio between day glow (not measured) and twilight abundance was 1.75. (For details the reader is referred to the original paper by Hunten and Godson.) From Fig. 6.43 and from other examples given by the two investigators, it appears that sodium abundance increases with the stratospheric warming events and remains high as long as the temperature

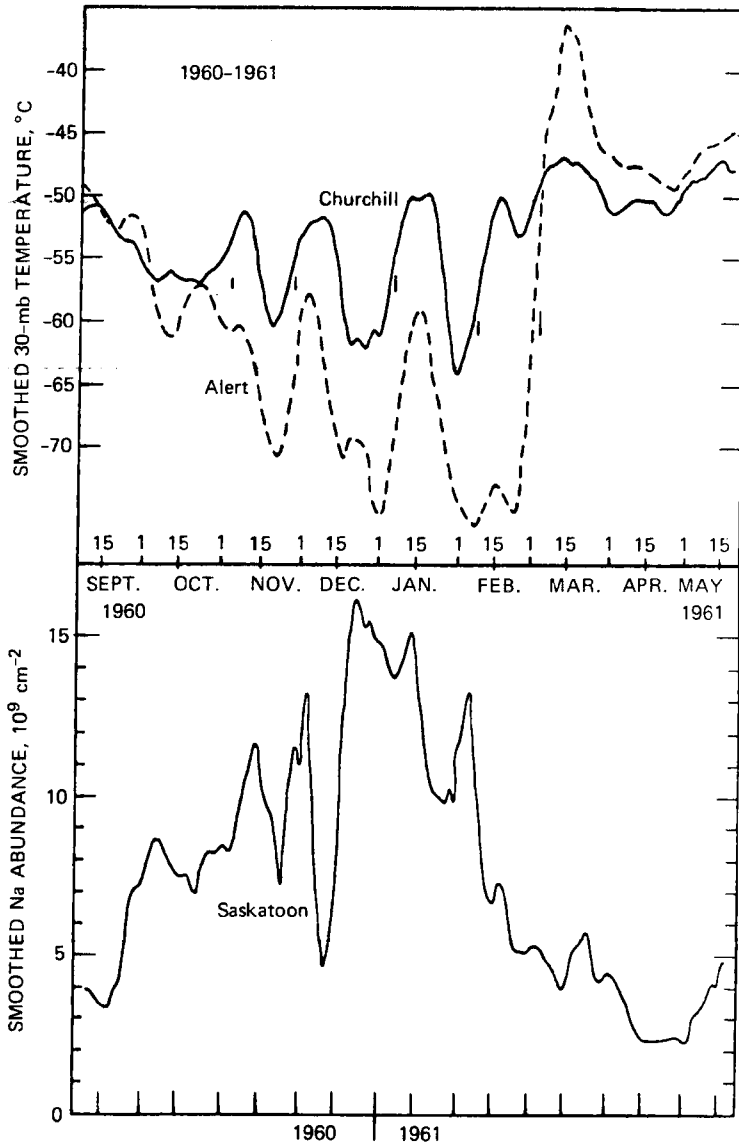


Fig. 6.43 Upper curves: 10-day running means of 30-mb temperatures for the 1960–1961 winter. Lower curve: smoothed sodium abundance. [From D. M. Hunten and W. L. Godson, *Journal of the Atmospheric Sciences*, 24(1): 81 (1967).]

continues to fluctuate. Afterward the sodium values begin to approach the considerably lower summer values. This would imply that large-scale eddy processes which are active near the polar-night jet stream and which are especially large during the breakdown period of the polar-night vortex (Mahlman, 1966, 1967) extend also far into the mesosphere. This conclusion is corroborated in a study by Shapley and Beynon (1965) of D-region absorption of radio waves during winter. This study also reveals a correlation with 10-mb temperature rises. (The peak height of the D-region is near 90 km.) These findings are of special interest because it is commonly believed that above 70 to 75 km tidal effects dominate atmospheric motion patterns (Newell, Wallace, and Mahoney, 1966). Even though the latter conclusion still has to be accepted, it would now appear that eddy transport processes that are dominant at stratopause level still exercise a certain amount of forcing upon the motions near the mesopause (G. E. Chapman, 1969).

Hunten and Godson (1967) speculated that the late-winter maximum in the twilight abundance of sodium may be produced by upwelling of aerosol-rich air from lower levels in large-scale eddy processes. This would imply that the sea surface may not be rejected as a possible source of some of the meso- and thermospheric sodium (Hunten, 1964; Vallance Jones, 1966). We have seen earlier that in the stratosphere the eddy transports are directed downward in middle latitudes (see, for example, Part 1, Fig. 3.11). It would be reasonable to assume that the vertical transports reverse their sign near the maximum wind layer near the stratopause. As Geisler and Dickinson (1967) have pointed out, an enhancement of the twilight intensity could also be achieved by a downward transport of atomic oxygen in eddy motions of 1 to 10 cm/sec since [O] influences reaction 6.9. Thus there is still some ambiguity in estimating the effects of large-scale eddy motions on the sodium airglow at twilight.

From rocket measurements it appears that the twilight and day-glow layers are located at the same height (Meier, 1966; Hunten and Wallace, 1967) or at least are not greatly separated (Vallance Jones, 1966). If evaporation of sodium from an "aerosol reservoir" during the daytime hours is held responsible for the day-glow phenomenon (see Hunten and Godson, 1967; Donahue and Meier, 1967), the summer maximums of day-glow intensity described earlier, opposed to the winter maximums of the twilight, may find a natural explanation.

Artificial-Tracer Experiments

Sodium has also been used as an artificial tracer of motions in the upper atmosphere (Coté, 1963; Jarrett et al., 1963a, 1963b; F. J. Smith, 1963; Rosenberg, 1964, 1966). Sodium or lithium vapors released from rockets cause intensive airglow trails. An example is given in Fig. 6.44 (Manning, 1961). Photogrammetry of these trails yields information on winds and turbulence at altitudes between 90 and 170 km (Albritton et al., 1962). Sodium and potassium vapor trails have also been used to measure upper atmosphere temperatures from Doppler-line broadening (Lory-Chanin, 1965; Shepherd, 1969).

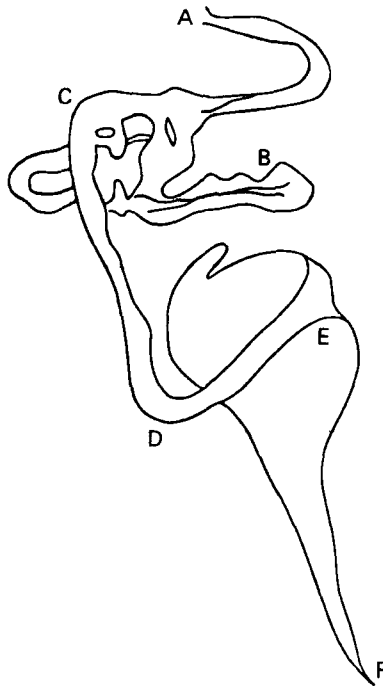


Fig. 6.44 Contours of a sodium vapor trail released on Apr. 19, 1961, over the eastern United States between 70- and 140-km altitude. Letters signify points of interest. [From E. J. Manring, 1961, reproduced in E. R. Reiter, *Beitraege zur Physik der Atmosphaere (West Germany)*, 36: 169 (1963).]

Authier (1964, 1965) reported about aluminum oxide (AlO) tracer experiments from rockets to study the temperature structure of the thermosphere (see also Rosenberg, 1964; Rosenberg, Golomb, and Allen, 1964; Rosenberg and Edwards, 1964; Golomb and MacLeod, 1966; Harang, 1964, 1969). Such compounds are not restricted in use during the twilight hours. Wind profiles can be measured throughout the night and also during daytime by observing the drift of smoke trails and puffs. The release of liquid trimethyl aluminum or triethyl aluminum generates AlO, Al₂O, and Al₂O₃; the Al₂O₃ is visible as smoke of submicron-size particles (Beaudoin et al., 1967; Marshall, 1969). The AlO radiance produced by grenade experiments yields larger cloud radii than expected from diffusion processes. Lloyd and Sheppard (1966) suggested a correction in the measured radii for the blast-wave effect of the grenade explosion (see also Rosenberg, 1962; Groves, 1962).

The radical CN, also tested in similar experiments, failed to show an emission. The release of nitric oxide, NO, produced measurable luminous trails (Pressman et al., 1957; Golomb, 1962a; Golomb et al., 1968). Föppl et al. (1965, 1967) reported on the use of barium, strontium, magnesium, and aluminum in rocket-borne tracer

experiments probing the lower thermosphere. They also suggested an interplanetary tracer experiment using calcium, barium, strontium, or europium. Experiments with one or the other of these metallic tracers have been described by Armstrong (1963a, 1963b, 1963c), Sheppard and Lloyd (1964), and Haerendel et al. (1967). Explosions of TNT in the 200- to 220-km altitude range also have been reported to produce traceable luminous clouds (Harang, 1964). Other chemical compounds have been used successfully (see Rosenberg, 1964, for details). Interesting experiments have been conducted by releasing barium during twilight at altitudes from 120 to 400 km. Barium produces a neutral cloud and an ionized cloud, the latter diffusing along the earth's magnetic field lines (Lloyd and Golomb, 1967; Lüst, 1968). Estimates on atmospheric density, scale height, temperature, and electric fields could be made from these observations.

Chemical releases have been used successfully to generate free electrons or to deplete electrons in certain regions of the ionosphere. Generation of free electrons, for instance, was accomplished by releases of cesium nitrate and aluminum powder (J. W. Wright, 1962; Golomb, 1962b; Rosenberg and Golomb, 1964; C. H. Murphy et al., 1967). Depletion of electrons occurred with rocket releases of sulfur hexafluoride, SF₆ (Rosenberg, 1962; Golomb et al., 1964). The ionospheric anomalies thus generated may be tracked by radio waves and thus yield wind information.

Artificially generated ion clouds appear to have a longer lifetime (sometimes more than 2 hr) under sunlit conditions but are shorter in the absence of ionizing radiation. The electron clouds produced during Project Firefly behaved similarly to sporadic E-layers, showing some evidence of a vertical gradient of drift velocities in the 95- to 115-km region.

Nonchemical tracers, such as radar-reflective fine chaff (Morris, 1967; Morris and Kays, 1969), and parachutes (Kays and Olsen, 1967) ejected from rockets have been used successfully to determine the fine-scale vertical structure of the mesospheric wind field and its changes with time. The latter measurements need considerable correction. Falling spheres (Robin balloons) have been used to measure detailed wind profiles in the upper stratosphere (Engler, 1968).

From the rate of growth of a vapor trail laid by a rocket, small-scale diffusion coefficients can be computed. Results are shown in Fig. 6.45 (Manning et al., 1961; see also Fooks, 1964; Golomb and MacLeod, 1966). From this diagram it is evident that diffusion coefficients increase rapidly with height in the thermosphere. The scatter of the data points in the lower part of the diagram and their departure from the computed values are attributed to the presence of turbulent motions, which may enhance the diffusion by orders of magnitude (Rosenberg, 1963). Blamont and Barat (1967), for instance, estimated from sodium-trail experiments a coefficient of turbulent diffusion of the order of 10^8 cm²/sec at 105 km, whereas the coefficient of molecular diffusion is only 2×10^6 cm²/sec at the same altitude. Diffusive separation, especially of argon and nitrogen, seems to occur above the turbopause, i.e., the height at which the turbulent and molecular diffusion coefficients become equal in magnitude (about 110 km) (Meadows-Reed and Smith, 1964; Nier et al., 1964; Rosenberg, 1968).

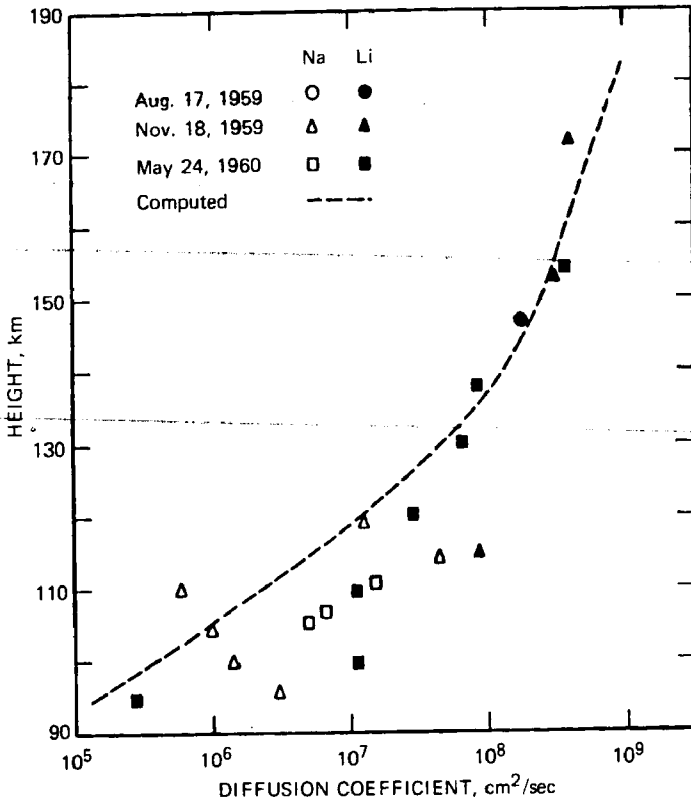


Fig. 6.45 Diffusion coefficients in the upper atmosphere determined by measuring the rate of growth of a vapor trail laid by a rocket (from Manring et al., 1961). These diffusion coefficients are compared with a theoretical curve calculated assuming that the trail grows entirely by molecular diffusion. There is a large scatter in the points for heights below 110 km, and the values are greater than the theory indicates. This would be expected if the rate of growth were increased by irregular air movements, perhaps of a turbulent type. [From G. F. Fooks, *Annales de Géophysique (France)*, 20(4): 417 (1964).]

From alkali-vapor-trail experiments, the initially smooth trails have been found to develop a globular structure a minute or so after release up to heights of 95 to 100 km (see also Blamont and Jager, 1961). These globules grow to diameters of 0.5 to 1 km within approximately 2 min. Afterward they grow more slowly. It is assumed, therefore, that 0.5 to 1 km constitutes the characteristic macroscale of turbulence, i.e., the characteristic eddy sizes. The microscale of turbulence has been estimated by Blamont et al. (1968) (see also Zimmerman et al., 1962):

$$\ell = \frac{2\pi}{k_M} \quad (6.17)$$

where $k_M = 0.5 \ell / \eta$

$$\eta = (\nu^3 / \epsilon)^{1/4}$$

= the microscale according to Kolmogorov (1958)

k_M = wave number of the microscale

ϵ = rate of dissipation of turbulent kinetic energy

ν = coefficient of viscosity

Structure function estimates of sodium vapor trails and trimethylaluminum trails yielded values of ℓ ranging from 16 m at 80 km (Fort Churchill) to 470 ± 70 m at 100 km (Hammaguir, Algeria). These estimates may still be questioned because Blamont et al. found macroscales of turbulence in this height range to be of similar magnitudes. Horizontal scales of ionospheric irregularities in the E- and F-regions found by Essex and Hibberd (1968) are of the same general magnitude, with a tendency to increase in size with height.

Above this turbulent layer the vapor trails remain smooth. The transition between the turbulent and the nonturbulent layers, occurring at the turbopause, is quite abrupt, within 1 km (see Fig. 6.45). It may shift its altitude, but it seems to be normally located between 100 and 120 km (Champion and Zimmerman, 1962; Champion, 1963; Golomb and MacLeod, 1966; McGrattan, 1967). The Reynolds number in this transition region is ≈ 2000 (for references see Fooks, 1964). Barat and Blamont (1969) noted weak anisotropy of turbulence below 100 km. Above this level isotropic conditions seem to prevail in which viscous effects and molecular diffusion dominate.

Large-scale winds deduced from alkali-trail experiments appear to be quite irregular. Large shifts in wind speed and wind direction occur in relatively shallow layers (Edwards et al., 1962; Manring et al., 1962; Ragsdale and Wasko, 1962; Manring and Bedinger, 1968). This is indicated in the hodographs shown in Fig. 6.46, which were obtained from two rocket firings only 3 days apart (crosses indicate the centers of the hodographs). Yet the wind patterns on these 2 days are quite different. Even during periods as short as 2 hr, winds in thin layers (about 5 km thick) may vary considerably, the deviations from the mean being of the same order as the mean values themselves. Such irregularities seem to occur mainly between heights of about 70 and 130 km (Kochanski, 1964). Vertical scales of these wind fluctuations are of the order of 6 km, and horizontal scales are of the order of 250 km (for references see Fooks, 1964). Hines (1960, 1963) considered these irregularities to be the effect of internal atmospheric gravity waves. Figure 6.47 contains estimates of the vertical wavelengths of these irregularities (Zimmerman, 1964). Although, especially during summer, Hines' theory seems to establish valid minimum conditions for the vertical structure of these wind fluctuations up to 130 km (data points are mainly scattered to the right of this limiting line), beyond this level the wind structure follows rather closely the scale height of the 1959 Air Research and Development Command (ARDC) model atmosphere (Minzner et al., 1959) that has been entered for reference. Zimmerman (1964) does not attempt to explain this observation, but it may have to do with the large values of molecular diffusion observed above this level (see Fig. 6.45) leading to

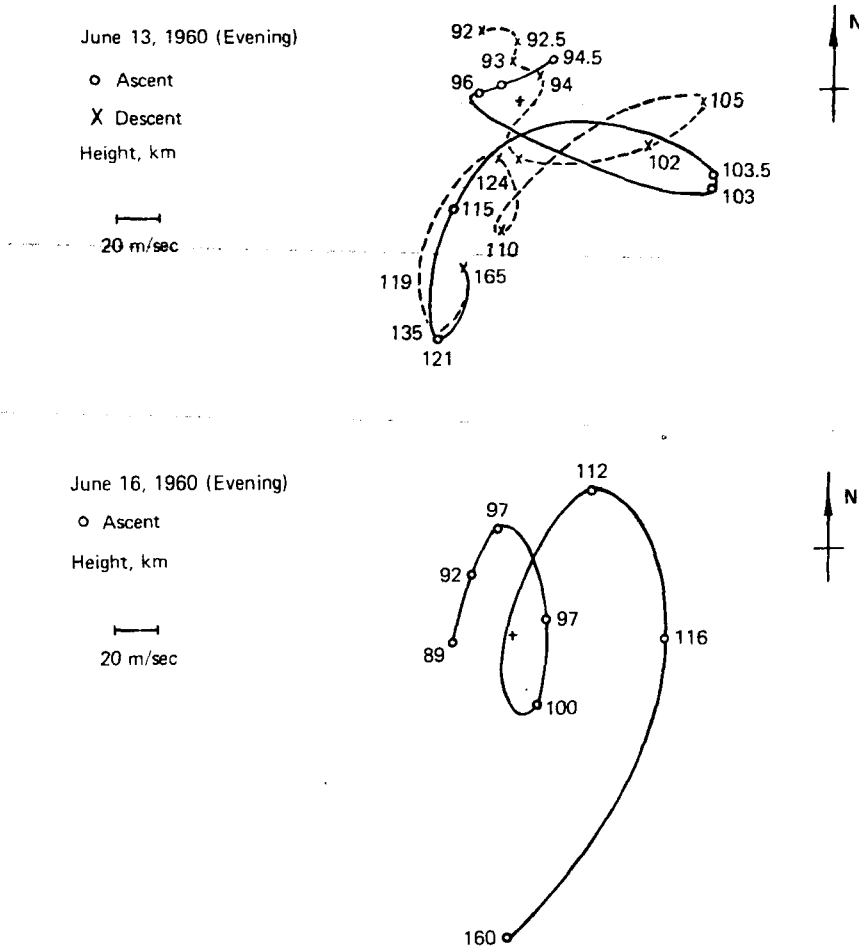


Fig. 6.46 Typical hodographs obtained from alkali-trail experiments. Heights, in kilometers, are marked next to observation points. Wind directions are given by vectors from centers of plots (marked by +) to data points. [From G. F. Fooks, *Annales de Géophysique (France)*, **20**(4): 419 (1964).]

an absence of organized small-scale turbulence. For winter the agreement is less convincing. It should be mentioned, however, that this model atmosphere conforms essentially to summer conditions.

Kochanski (1964) summarized the results of 25 sodium cloud experiments over Wallops Island (Fig. 6.48). Figure 6.49 shows wind vectors of the principal velocity maximums near 100 to 111 km and of the upper maximums near 140 km (not always observed) of these soundings. In agreement with Fig. 6.46, winds in the region of the principal maximum appear to be predominantly northwesterly during summer (see

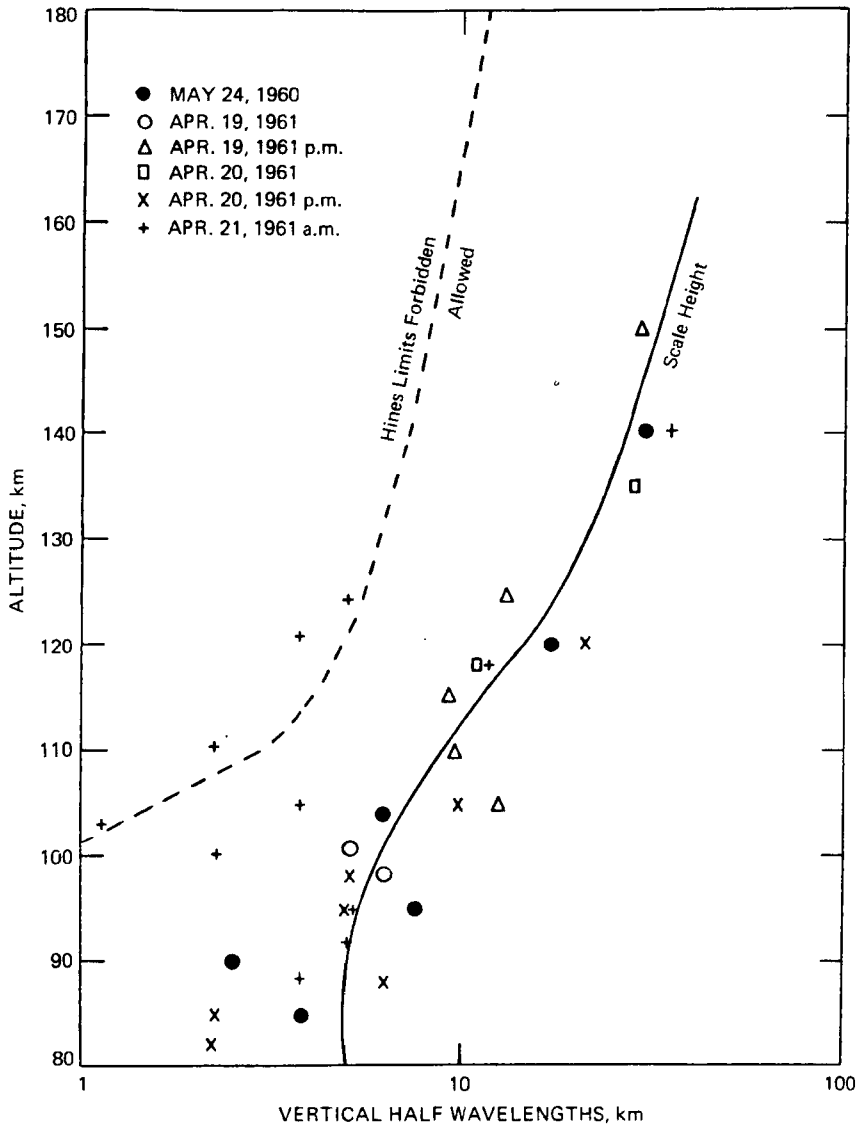


Fig. 6.47a Summer measurements of vertical half wavelengths, defined as the distance from one inflection point in the vertical wind profile to the next inflection point. The data are from the NASA Report NASS-215. (From S. P. Zimmerman, Report AFCRL-64-364, p. 376, Air Force Cambridge Research Laboratory, 1964.)

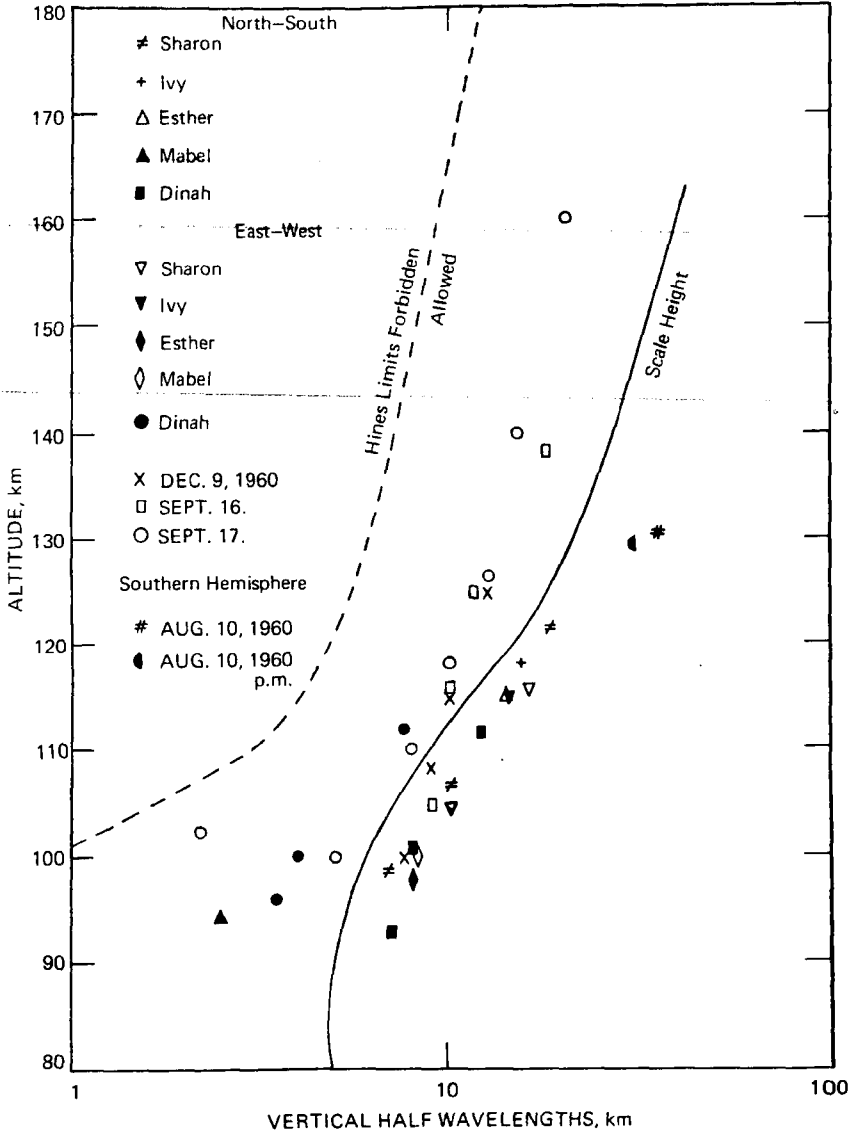


Fig. 6.47b Winter measurements of vertical half wavelengths. The data labeled with names are from Rosenberg, Edwards, and Wright (1964a), measured during December 1962; the data dated December and September are from the NASA Report NAS5-215; and the August 1960 data points are from Groves at Woomera, Australia. The superposed curves are the same as in Fig. 6.47a. (From S. P. Zimmerman, Report AFCRL-64-364, p. 377, Air Force Cambridge Research Laboratory, 1964.)

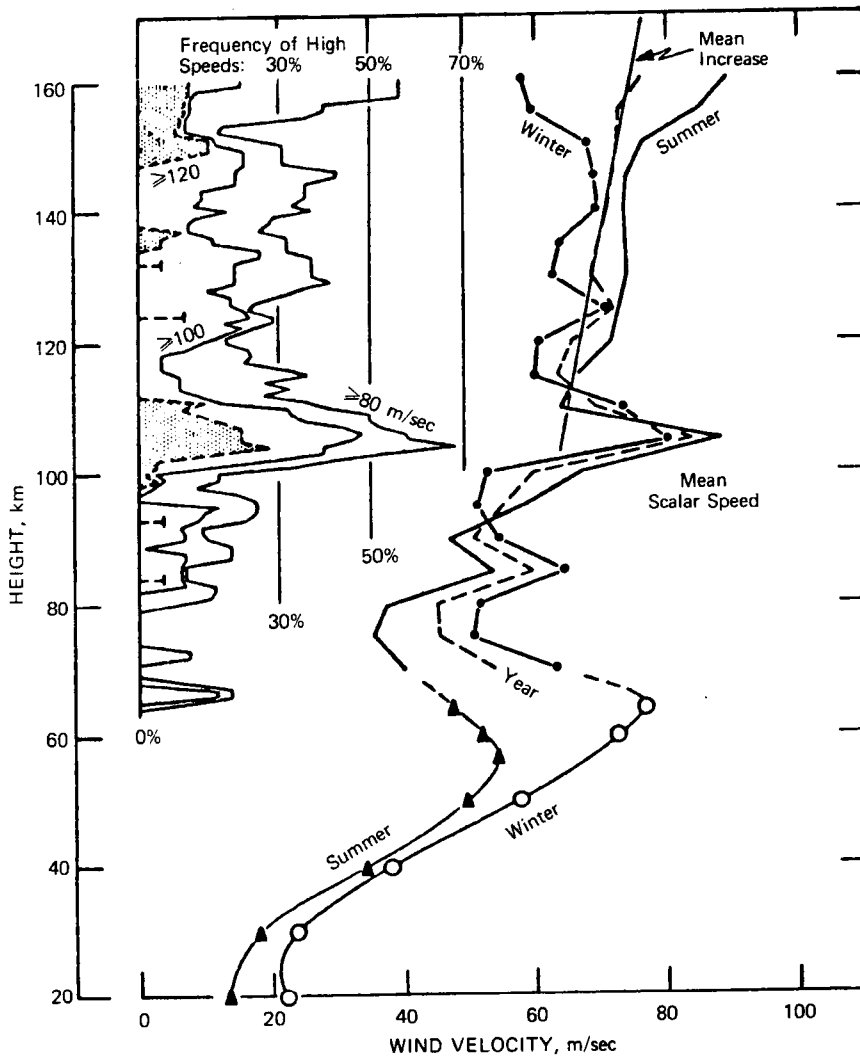


Fig. 6.48 Averages of the absolute value of wind velocity regardless of direction (i.e., the mean scalar speed), the upper part is based on 25 sodium cloud experiments over Wallops Island. Inset shows the frequency of occurrence of speeds over 80, 100, and 120 m/sec. [From A. Kochanski, *Journal of Geophysical Research*, 69(17): 3656 (1964).]

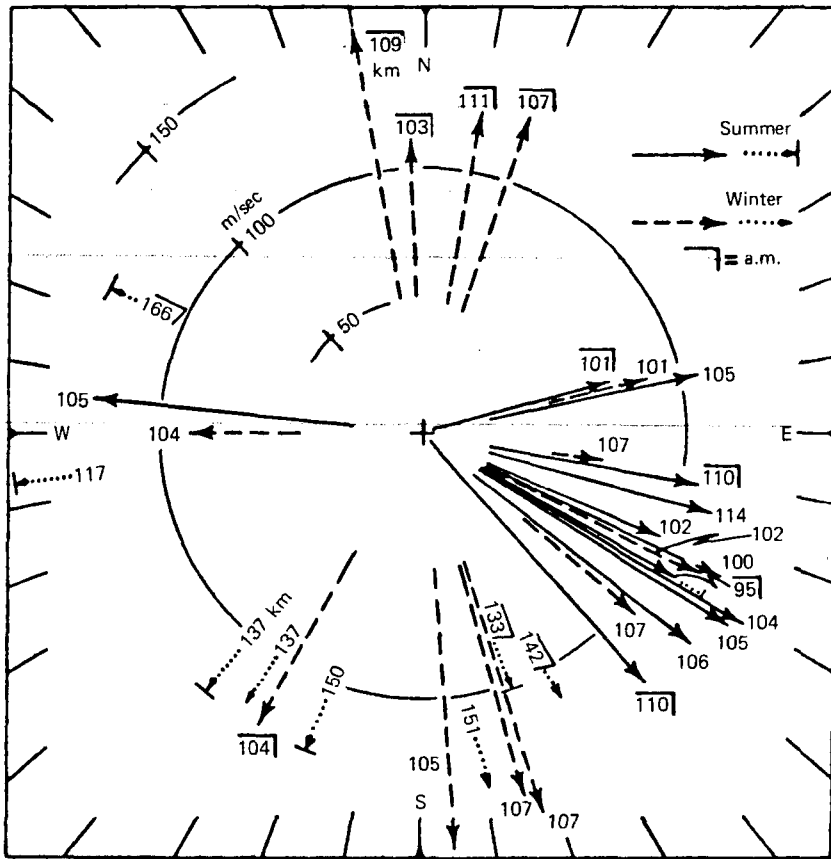


Fig. 6.49 Hodograph of winds of the principal maximum of velocity near 100 km (solid arrows for summer and dashed arrows for winter) and of the upper maximum near 140 km (short dotted arrows). Velocities (in m/sec) are given by radial distance from the center of the diagram. Numbers near tips of arrows are heights of wind maximums in kilometers. [From A. Kochanski, *Journal of Geophysical Research*, 69(17): 3653 (1964).]

also Spizzichino, 1964; Murphy, 1969; Montgomery et al., 1968). Strong north and south winds and also northwesterly winds seem to occur in this region during winter. These winds fit the general-circulation model at 100 km developed earlier by Kochanski (1963) and shown in Fig. 6.50.

The significance of the maximum wind level near 100 km is seen in Fig. 6.48. Speeds equal to or greater than 80 m/sec were observed near this level in nearly 70% of all cases, and in 88% of the measured soundings this feature attains some prominence. This principal maximum is located at, or slightly below, the level of diffusive separation (see earlier remarks). On either side of this wind maximum is a pronounced wind-speed minimum. Kochanski (1964) attributed the principal wind maximum

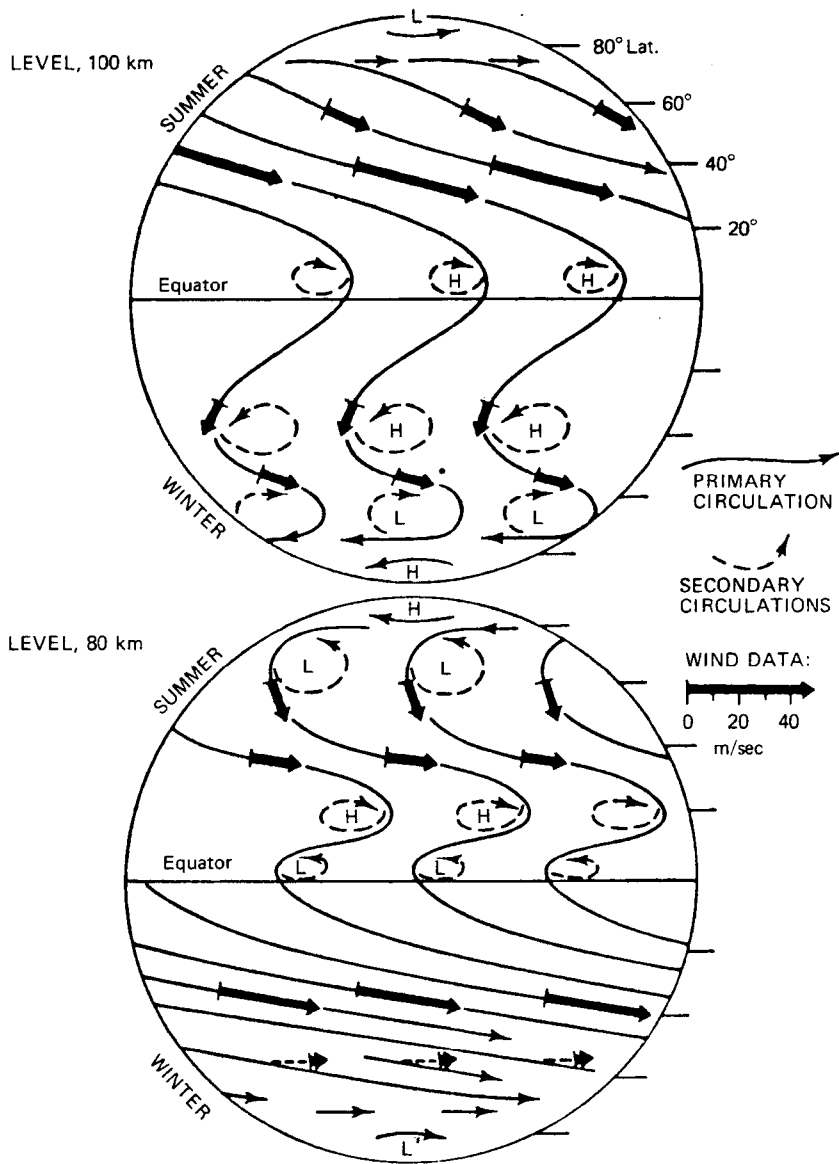


Fig. 6.50 Tentative model of planetary circulation at 100 and 80 km. Heavy arrows represent winds from Jodrell Bank and Adelaide placed as if these two stations were in the same hemisphere. Solid lines are streamlines of the primary circulation; dashed lines are hypothetical closed circulations of the second order. [From A. Kochanski, *Journal of Geophysical Research*, 68(1): 219 (1963).]

observed over Wallops Island during summer and winter to a standing wave phenomenon. These waves would be of planetary dimensions, meaning that the eddies shown in Fig. 6.50 for the winter circulation would be mainly standing eddies, at least in this altitude range. Such reasoning would corroborate the conclusions reported earlier about a correlation between late winter stratospheric warmings and sodium abundance which may be thought of as an effect of transport processes in planetary scale eddies. We shall see later that tidal effects also have considerable influence on this region.

A wind maximum near 100 km has been found in widely separated regions. It appears in the data from Ft. Churchill (Canada); Sardinia; Eglin, Fla. (30°N , 86.5°W); Barbados (13.1°N , 57.3°W); and Yuma, Ariz. (32.9°N , 114.3°W). Rosenberg, et al. (1964a, 1964b) report that shears on either side of this wind maximum show a good correlation with sporadic E-layer formation. From successive vapor-trail releases during the night of Dec. 3, 1963, over Eglin Air Force Base, Fla., variations in this maximum wind layer as well as in the vertical wind shears were studied (Figs. 6.51 and 6.52). The sporadic E-layer during that night shifted with the shearing layers (Fig. 6.53) (see also J. W. Wright et al., 1967). This is in accordance with Whitehead's (1962) theory on sporadic E formation: Strong vertical wind shears in the horizontal east-west component (as indicated in the time section of Fig. 6.52, right side) and the natural magnetic field will stratify ionized species into relatively high vertical-gradient values (see also MacLeod, 1964, 1966; Matsushita and Reddy, 1967; Rishbeth and Garriott, 1969; Reddy and Matsushita, 1968b). Other ionospheric wind measurements confirmed these findings (e.g., C. H. Murphy et al., 1966; C. H. Murphy and Bull, 1968b).

There appears to be a general downward propagation of the wind maximums during the night, both in the N-S and E-W wind components (C. H. Murphy et al., 1966; C. H. Murphy and Bull, 1967, 1968a, 1968c; C. H. Murphy, 1969; Maeda and Maeda, 1969; Chimonas and Axford, 1968; Justus and Montgomery, 1969; J. W. Wright, 1968). A clockwise rotation of wind direction with height appears to prevail near the 100-km level in middle latitudes of the northern hemisphere, with a vertical wavelength of 12 to 15 km (Rosenberg and Edwards, 1964; Justus and Edwards, 1965; Bedinger, 1966; C. H. Murphy and Bull, 1968a). Such rotation seems to be absent, or at least much less pronounced, in tropical regions (C. H. Murphy et al., 1966) and reversed in the southern hemisphere to a counterclockwise rotation (Jarrett et al., 1963b, Bedinger, 1966; Groves, 1966). This strongly suggests the dominant presence of tidal effects in this region (see Chap. 1; Lindzen, 1967; Zimmerman and Marcos, 1967). The possible effect of upward-propagating gravity waves should not be discounted, however, in explaining these shearing layers (Kato and Matsushita, 1968). Woodrum and Justus (1968) were able to extract from chemical-release trail data obtained over Eglin, Fla., between October 1962 and November 1965, the diurnal and semidiurnal tides (see also, Hines, 1966). An example is shown in Fig. 6.54. The clockwise rotation of the wind vector with height observed over this station and mentioned earlier appears to be due mainly to the diurnal tide (see Fig. 6.55). Tidal theory seems to fit the data adequately. From Figs. 6.54 and 6.55, the prevailing wind

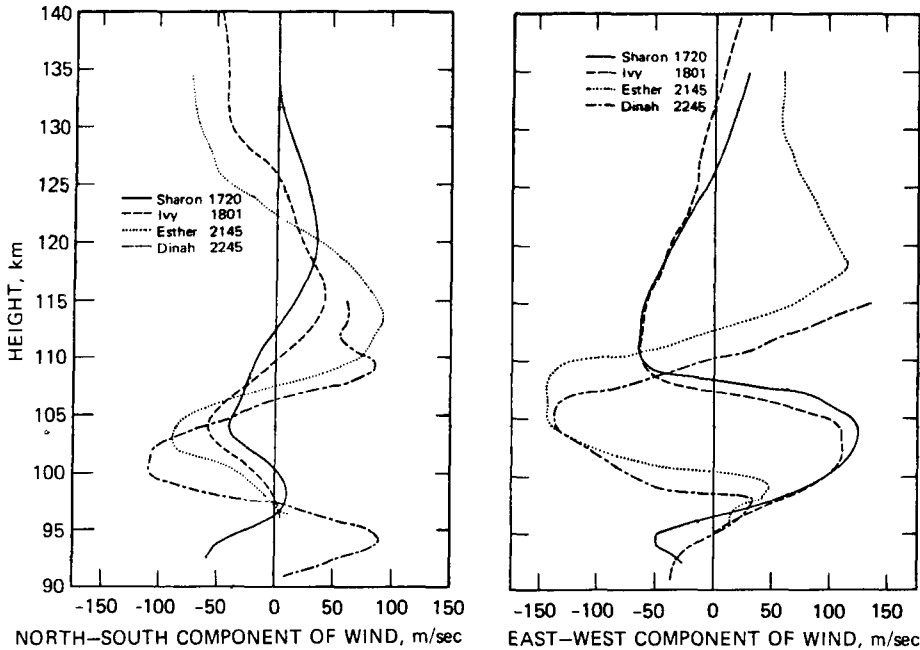


Fig. 6.51 Wind velocity profile, Eglin, Fla., Dec. 3 1963. Times of soundings are given in central standard time. (a) North-south components of the wind velocity as a function of altitude for the four releases (indicated by code names). (b) East-west components of the wind velocity as a function of altitude for the four releases. (From N. W. Rosenberg, H. D. Edwards, and J. W. Wright, Report AFCRL-64-881, p. 176, Air Force Cambridge Research Laboratory, 1964.)

also appears to change with altitude in wavelike fashion with a vertical wavelength of 27 ± 5 km.

This tidal effect upon winds in the ionosphere and the resulting variability of winds along vertical profiles make it exceedingly difficult to deduce the neutral wind field from observations of geomagnetically quiet daily observations. Such observations would yield an effective wind that, by virtue of its ion drifts, would cause an electric current and the observed magnetic-field variations. This effective wind would represent a weighted mean over the "dynamo region" of the ionosphere, the weighting factors depending on the distribution of conductivity in this region. It would be difficult to extract the detailed layering of the neutral wind field in the same region from this effective wind (Sugiura, 1968).

Chapter 1 mentions that metallic ions of meteoritic origin (Champion, 1968) (and in the case of Na^+ possibly of terrestrial origin) are present in the E-region. This is corroborated by the correlation that exists between lidar backscatter from aerosol particles between 110 and 140 km and the presence of sporadic E (Fiocco, 1965). Skylight polarization during the twilight hours, which depends to a certain degree on the presence of dust in the upper atmosphere, does not reveal a significant correlation

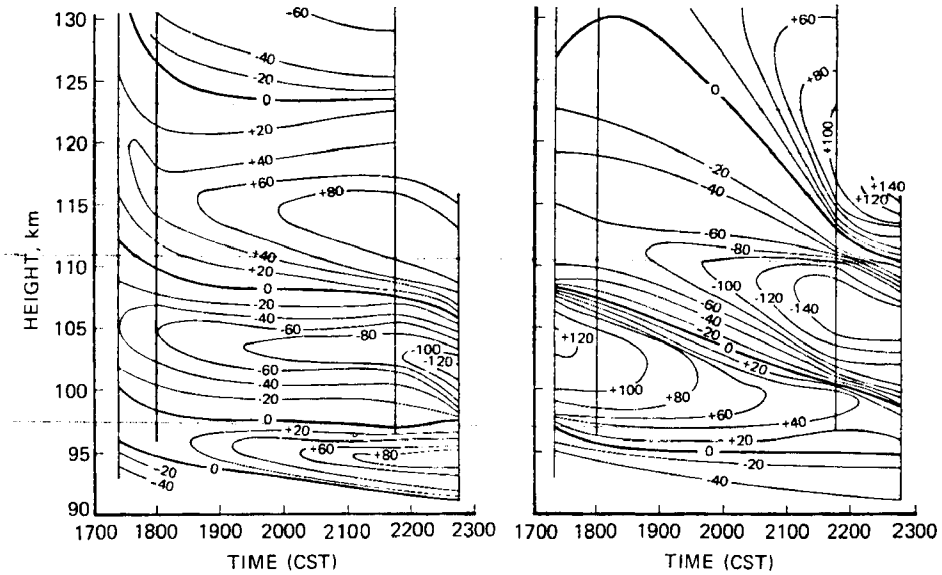


Fig. 6.52 (a) North-south wind contours (m/sec) from 1720 to 2245 CST on Dec. 3, 1962, over Eglin Air Force Base, Fla., as a function of altitude. (b) East-west wind contours from 1720 to 2245 CST on Dec. 3, 1962, over Eglin Air Force Base, Fla., as a function of altitude. (From N. W. Rosenberg, H. D. Edwards, and J. W. Wright, Report AFCRL-64-881, p. 177, Air Force Cambridge Research Laboratory, 1964.)

with sporadic E (Dietze and Kohl, 1966). J. W. Wright (1967) indicated a possible connection between large meteor showers and the high frequency of occurrence of blanketing sporadic E. The metallic ions play an important role in the formation of sporadic E-layers, whereby long-lived ions [lifetime of Na^+ at 100 km is of the order of several weeks or more (Lehmann and Wagner, 1966)] are subject to a vertical convergence mechanism inherent in the neutral wind field (MacLeod, 1966; Chirmonas and Axford, 1968). Such ion convergence is most frequently produced by vertical shears in the horizontal wind but may also be brought about by a vertical gradient in the vertical neutral wind component (for details, see MacLeod, 1968). The recombination rates of ions normally present in the E-region (NO^+ , O_2^+) are too fast to permit the high electron number densities observed in nighttime sporadic E (Wright et al., 1967).

Ionosonde measurements also indicate a considerable microstructure in sporadic E-layers (Reddy and M. M. Rao, 1968; Reddy, 1968). "Blobs" of higher ionization are embedded in the Es-layer and have much smaller vertical dimensions yet than the thin sporadic E-layer. (The small thickness of the latter is confirmed by rocket measurements. See, for example, Sagalyn and Smiddy, 1964.) Horizontal dimensions of these blobs may be on the order of several hundred meters.

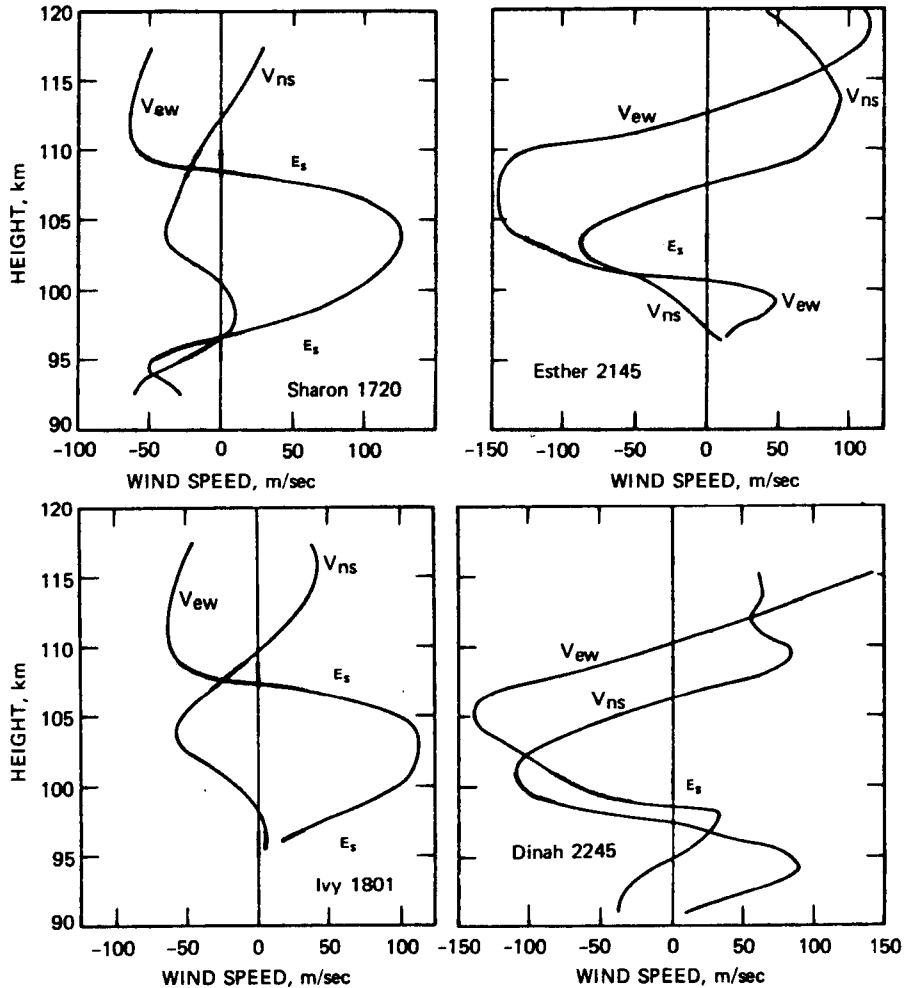


Fig. 6.53 North-south and east-west plots of wind speed as a function of altitude showing correlation with observed altitudes of sporadic E. (From N. W. Rosenberg, H. D. Edwards, and J. W. Wright, Report AFCRL-64-881, p. 178, Air Force Cambridge Research Laboratory, 1964.)

In Fig. 6.56 the seasonal variation of sporadic E appears to be similar to that of sodium day glow (see Fig. 6.42). Fort Belvoir, Va., even shows secondary maximums of sporadic E in autumn and winter (E. K. Smith, 1968), slightly earlier than the maximums of sodium day glow observed over Haute Provence. The southern hemisphere observations from Christchurch (New Zealand) also reveal a secondary winter maximum. According to E. K. Smith (1967, 1968), the coupling of conjugate regions of sporadic E may explain, at least in part, this odd seasonal behavior. There also appears to be a correlation between sporadic E and heavy thunderstorm activity

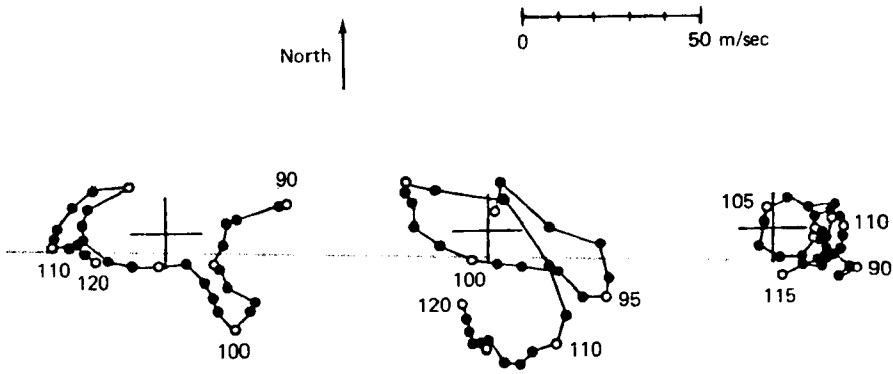


Fig. 6.54 The computed prevailing wind (a), diurnal tide at dawn or dusk (b), and semidiurnal tide at dawn or dusk (c). Solid dots represent winds at 1-km altitude intervals. Open circles indicate 5-km height intervals. Numbers give heights in kilometers. The magnitude and direction of the wind vectors are represented by lines drawn from the crosses in each figure to the individual dots. A speed scale is shown at the top of the figure. [From A. Woodrum and C. G. Justus, *Journal of Geophysical Research*, 73(2): 474 (1968).]

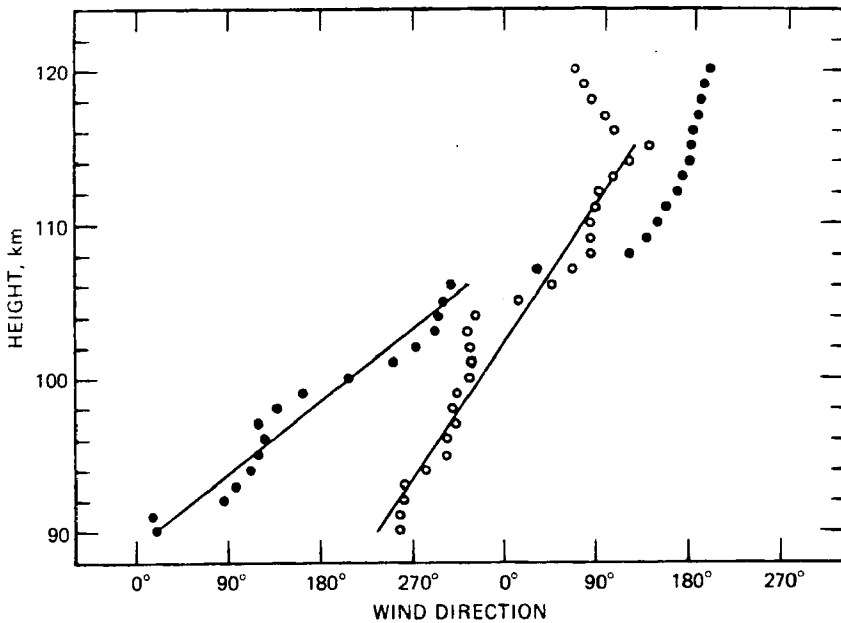


Fig. 6.55 Direction vs. altitude for the computed prevailing (○) and diurnal tide (●) winds. The straight lines through the prevailing and diurnal data were fitted by least squares to the altitude intervals indicated. [From A. Woodrum and C. G. Justus, *Journal of Geophysical Research*, 73(2): 475 (1968).]

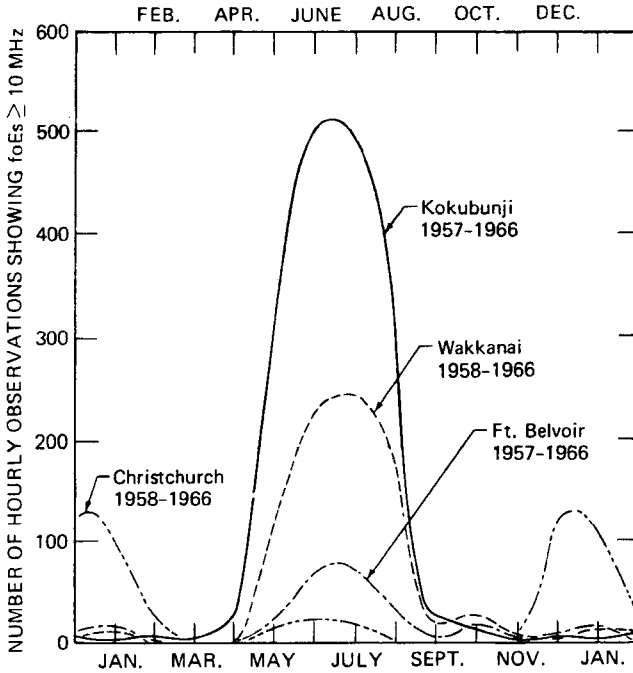


Fig. 6.56 Seasonal variation of intense sporadic E (critical frequencies, $f_oE_s > 10$ MHz) as observed at four ionosonde stations. (From E. K. Smith, paper presented at Second Seminar on the Cause and Structure of Temperate Latitude Sporadic E, Vail, Colo., June 19–22, 1968.)

(Rastogi, 1957, 1962; Sartor, 1967). The dominant factor in intense sporadic E generation, however, remains the wind field and, in particular, the vertical wind shear. The similarity with the seasonal trend of sodium day glow suggests that the downward transport of ions [such as postulated by MacLeod (1966) and Donahue and Meier (1967)] is responsible for both phenomena.

As mentioned in Part I (see Fig. 3.64), there is a quasi-biennial cycle in the occurrence of intense sporadic E. When that diagram is compared with Fig. 6.35, it appears that years with maximum westerlies near mesopause level during autumn are characterized by minimum sporadic E activity during the preceding summer.

Reddy and Matsushita (1968a, 1968b) pointed out a variation of strong (blanketing) sporadic E (frequencies at $f_bE_s \geq 4.0$ Mc/sec) parallel to the sunspot cycle, whereas weak sporadic E-layers ($f_bE_s \leq 4.0$ Mc/sec) tend to increase in frequency of occurrence with decreasing sunspot activity. Both correlations agree with the wind-shear theory of sporadic E formation: Strong E-layers are formed by strong wind shears. Wind shears appear to increase by about 40 to 60% from solar minimum to solar maximum, with the exception of the Grand Bahama station, where this increase is only 20 to 25% (Fig. 6.57). This same increase of the diurnal and semidiurnal wind components in the E-region has been postulated by Matsushita

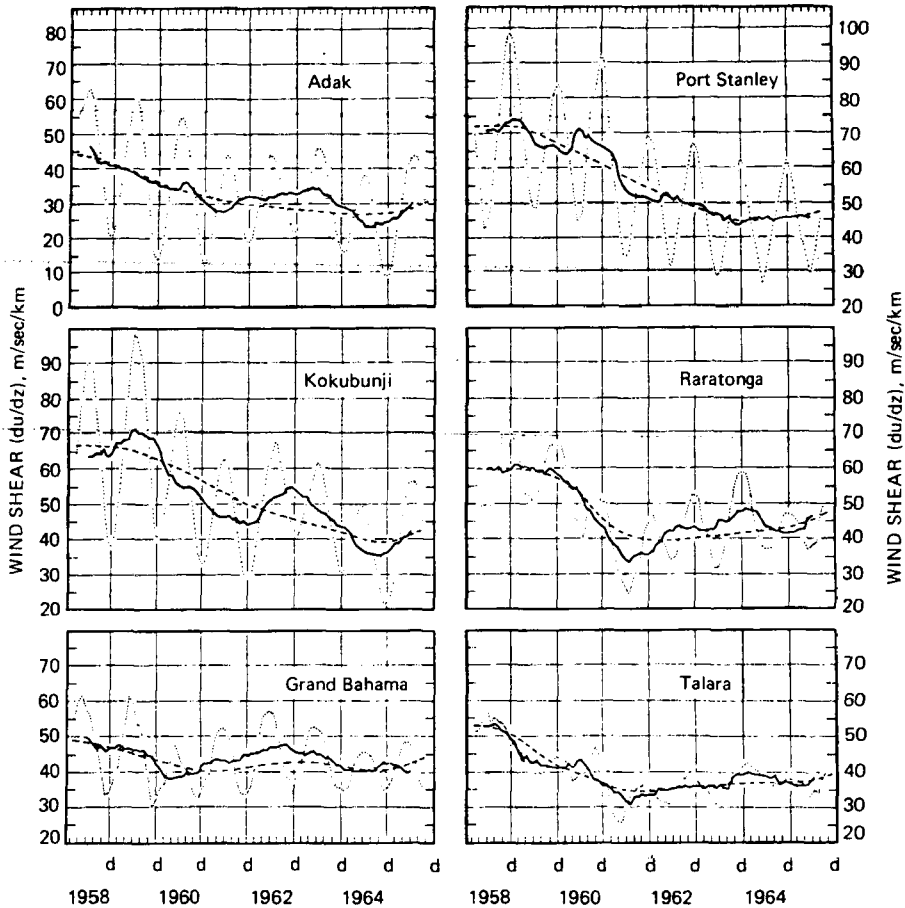


Fig. 6.57 Solar-cycle variation of neutral wind shears in the E-region near 110 km at noon. Dotted curves give 6-month running averages; solid curves give 12-month running averages of the noontime wind shears. The broken lines are manually drawn mean curves to show the long-term variation at each station. [From C. A. Reddy and S. Matsushita, *Journal of Geophysical Research*, 73(5): 1656 (1968).]

(1966) from a study of the variation of ionospheric current systems with the solar cycle. The negative correlation between weak Es and solar activity may be explained by the fact that such Es-layers are detectable only if the background electron density of the E-layer is relatively small, as is the case near the sunspot minimums. What causes the change in wind shears with the solar cycle is still subject to speculation. Possibly the tidal winds and gravity waves are stronger near maximums of solar activity.

Above 140 km wind shears are rather weak. Wind profiles generally lack short-wavelength oscillations in this region, in agreement with Hines' (1960) theory,

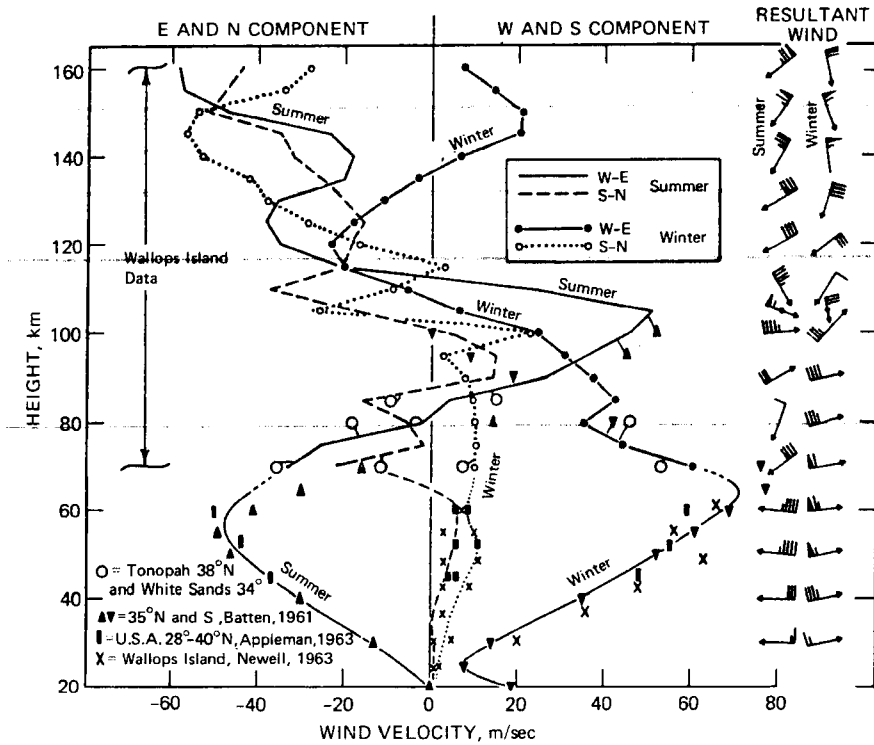


Fig. 6.58 Resultant components of the wind near 38°N latitude. The upper part is based on 2.5 sodium-cloud experiments, mainly from Wallops Island. Arrows indicate the resultant winds. [From A. Kochanski, *Journal of Geophysical Research*, 69(17): 3655 (1964).]

according to which internal gravity waves should subside at these altitudes, permitting only long modes. [A maximum gravity wave effect on electron densities at 230 km has, however, been found following nuclear explosions (Kotadia, 1967; Kotadia et al., 1968). (For traveling disturbances in the F_2 -region, see Breitling and Kupferman, 1967; Kanellakos, 1967; Albee and Kanellakos, 1968.) Magnetohydrodynamic waves in conjunction with nuclear explosions may propagate at even greater heights (B. L. Murphy and Kahalas, 1968).] Winds measured at these altitudes, therefore, should represent mainly general drifts. This holds for the upper wind maximum found near 140 km in several soundings (Figs. 6.48 and 6.49). These drifts are also evident from the resultant winds and mean components shown for summer and winter in Fig. 6.58. This diagram also contains data compiled by Batten (1961), Appleman (1963), and Newell (1963b).

The monsoonal character of the stratospheric circulation with its maximum effect near the stratopause (50 to 60 km) is clearly evident from this diagram. From chaff experiments at high latitudes (Morris, 1967; Morris and Kays, 1969), the

mesospheric easterly wind maximum of summer appears to be located at higher levels there (in the 75- to 80-km region) than in midlatitudes as shown in Fig. 6.58. Maximum easterly components of 92 m/sec were observed at 80 km over Fort Greely, Alaska, in July 1967. Zonal components of motion predominate to levels up to 100 km. At higher altitudes meridional components may even exceed the zonal ones. In the region 90 to 110 km, westerlies prevail during summer and winter over middle latitudes (Wallops Island). Data from Barbados (C. H. Murphy and Bull, 1968b; Murphy, 1969) shown in Fig. 6.59 indicate a prevalence of easterlies below 105 km during summer. (Easterly winds in this diagram are indicated as positive.) During winter meridional components gain some influence. These wind speeds and directions near the 100-km wind maximum, and slightly above, are in good agreement with drift-velocity measurements in the E-region using the fading method (Harnischmacher, 1964). Drift velocities in the D- and E-regions, using the close-spaced antenna method, were reported by Kent and Wright (1968) and fit well into the pattern shown in Fig. 6.58 (see also J. W. Wright, 1968; Goodwin, 1968), as do southern hemisphere data obtained by Fraser (1968), allowing for symmetry about the equator. From these ionospheric data, it may be seen that a 12-hr tidal wave has some importance in shaping the wind field (see Fig. 6.54). Comparisons of the E-region drifts with meteor-trail observations in the range of the semidiurnal tide show good agreement (Müller, 1968). Between 115 and 190 km, seasonal changes appear again. In summer, winds are mainly from the northeast. In winter, they are from the northeast between 115 and 135 km from the northwest above this layer (Kochanski, 1966).

In Fig. 6.48 a mean increase of wind speeds (regardless of directions and discounting the individual wind maximums described previously) has been found for the yearly average above 100 km. If this mean increase is extrapolated to 300 km we arrive at speeds of 100 m/sec. These agree well with observed regular movements in the F-region of the ionosphere. Over England drifts of 80 m/sec have been observed (predominantly from the west by day and from the east by night); over Australia 120 m/sec have been measured (Ratcliffe, 1960). Over India westerlies of 132 m/sec on the average have been observed in the E-region and of 161 m/sec in the F-region. These values are higher than those reported from other stations (Deshpande and Rastogi, 1966). Ionospheric east winds during day and west winds during night have been observed over Ghana, again showing an increase from the E-region (about 100 km) to the F-region (about 300 km) (Koster and Katsriku, 1966). (For a theoretical explanation of westerlies in the F-region, see Matuura, 1968.)

Atmospheric motions observed during the sodium-vapor experiments may be decomposed into general (large-scale) drifts, tidal components, and gravity waves. According to Kochanski (1964), the following estimates on the relative contributions hold:

	90 to 125 km	>130 km	160 km
General drifts	34%	Dominating	85%
Tidal components	26%		
Gravity waves	40%		

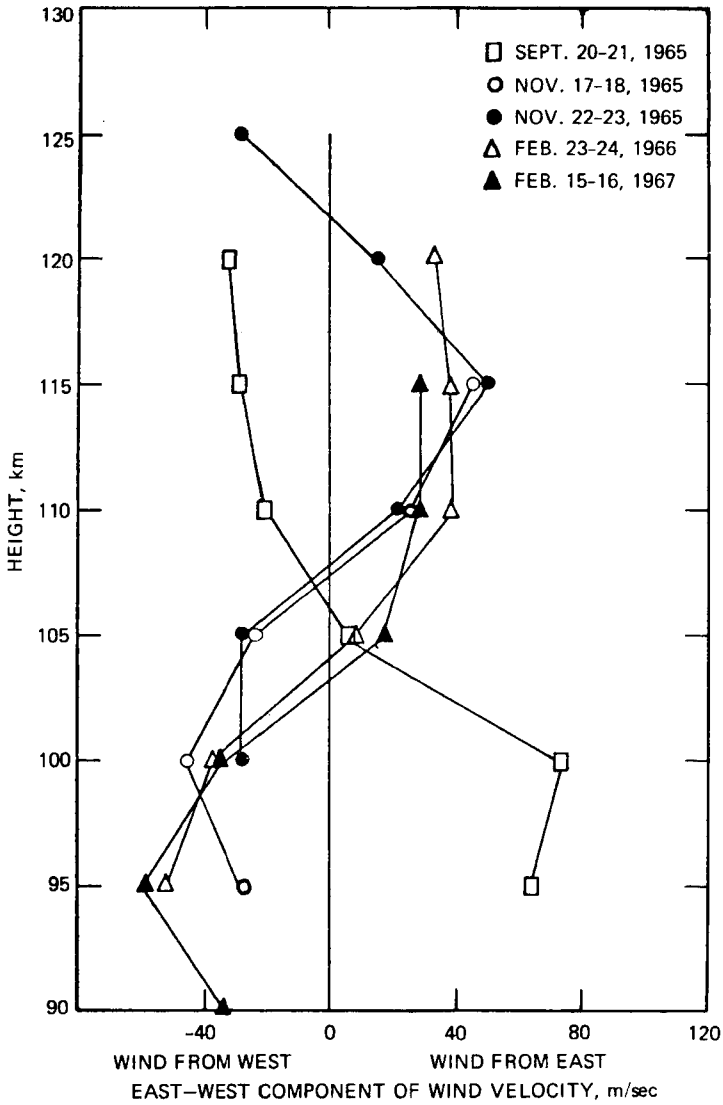


Fig. 6.59 Mean zonal wind profiles for five nights over Barbados (easterlies greater than 0). (From C. H. Murphy and G. V. Bull, in Proceedings of the 3rd National Conference on Aerospace Meteorology, New Orleans, La., May 6-9, 1968, p. 494.)

These findings are confirmed in a later study by Kochanski (1966) containing results from additional sodium-vapor experiments. The observed irregularities of motions near the "predominant wind maximum" (about 100 km) thus are due mainly to the dominant effects of gravity waves and tidal motions.

Other Alkali Metals and Metals in the Upper Atmosphere

Lithium, potassium, and calcium are other metals that have been identified in airglow measurements (for references, see Vallance Jones, 1963, 1966; Kvitte, 1969). The height distributions of sodium, potassium, and lithium, estimated by Sullivan and Hunten (1964), are shown in Fig. 6.60 (see also Fig. 6.37) together with the

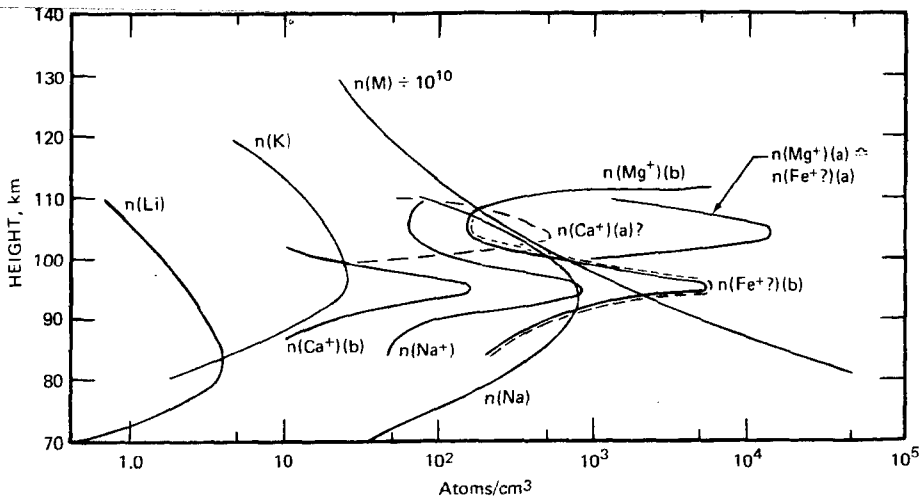


Fig. 6.60 Summary of reported height distributions of metallic atoms and ions in the upper atmosphere. Curves for $n(\text{Na})$, $n(\text{Li})$, and $n(\text{K})$ are from Sullivan and Hunten (1964); $n(\text{Mg}^+)(a)$ and $n(\text{Ca}^+)(a)$ are from Istomin (1963); and $n(\text{Mg}^+)(b)$, $n(\text{Ca}^+)(b)$, $n(\text{Na}^+)$, and $n(\text{Fe}^+)(b)$ are from Narcisi and Bailey (1965a). [From A. Vallance Jones, *Annales de Géophysique (France)*, 22(2): 194 (1966).]

distributions of other metallic elements. Rocket measurements have confirmed the presence of such ions (Narcisi and Bailey, 1965c, and Fig. 1.38). Potassium has a large natural abundance. Its peak almost coincides with the sodium layer. Lithium, on the other hand, is less abundant than sodium, and its peak occurs at a lower level. A significant amount of lithium seems to have been introduced into the atmosphere by the 1958 Johnston Island tests and by the Russian tests of 1961 (see also Ghosh and Mitra, 1966). This is shown in Fig. 6.61. Apparently the lithium cloud introduced into the atmosphere in 1958, which contained ^6Li and ^7Li (see Gadsden, 1962, 1964b;

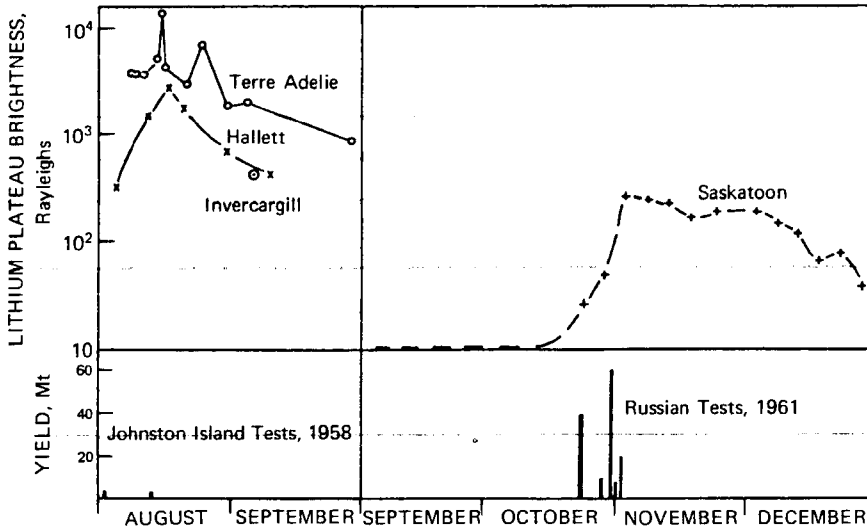


Fig. 6.61 Summary of lithium twilight observations as reported after the Johnston Island high-altitude tests of 1958 and the U.S.S.R. test series of 1961. [From A. Vallance Jones, *Planetary and Space Science (England)*, 10: 124 (1963).]

Nguyen-Huu-Doan, 1964), was transported southward toward Antarctica by winds of about 10 m/sec in the 60- to 120-km region (see Gadsden, 1964a). Only 3 to 4 days elapsed between the explosion and the initial rise in lithium brightness. Such winds are in agreement with those derived from the sodium experiments (Fig. 6.58), from meteor-trail observations (see Gadsden, 1964b), and also with Kochanski's (1963) circulation model (Fig. 6.50) (see also Gadsden, 1964a).

Gault and Rundle (see Vallance Jones, 1966) reported on large increases in lithium brightness observed at Saskatoon during March 1 to 6 following a rocket seeding experiment over Fort Churchill on Feb. 28 (Fig. 6.62). Rather weak general drifts must have prevailed in the lithium region over this area during the time in question to permit continued enhancement for several days. The tidal or wave components, on the other hand, may have been quite large, as suggested by the differences in the morning and afternoon values near the peak of the observed twilight phenomenon.

Seasonal variations of lithium brightness show maximums during autumn and winter over Saskatoon, Canada, and minimums during summer. Thus they appear to run parallel with the weak seasonal variations of sodium twilight emission and inverse to the variations of sodium day glow. According to Hunten (1964), a lithium maximum appears to recur in November, and a secondary maximum has been observed in 2 years out of 3 during early February. There may be a correlation between these two maximums and micrometeoritic dust showers (Dole, 1962). The observed lithium

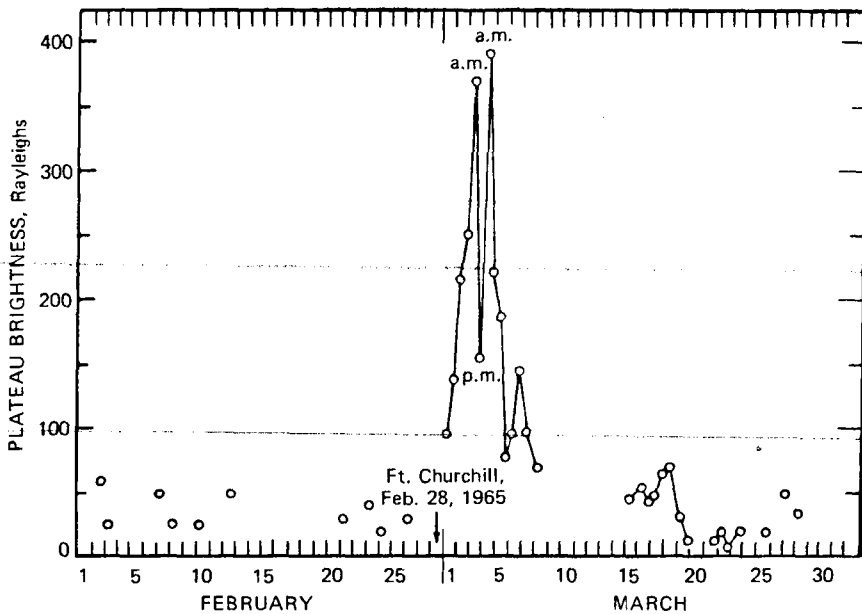


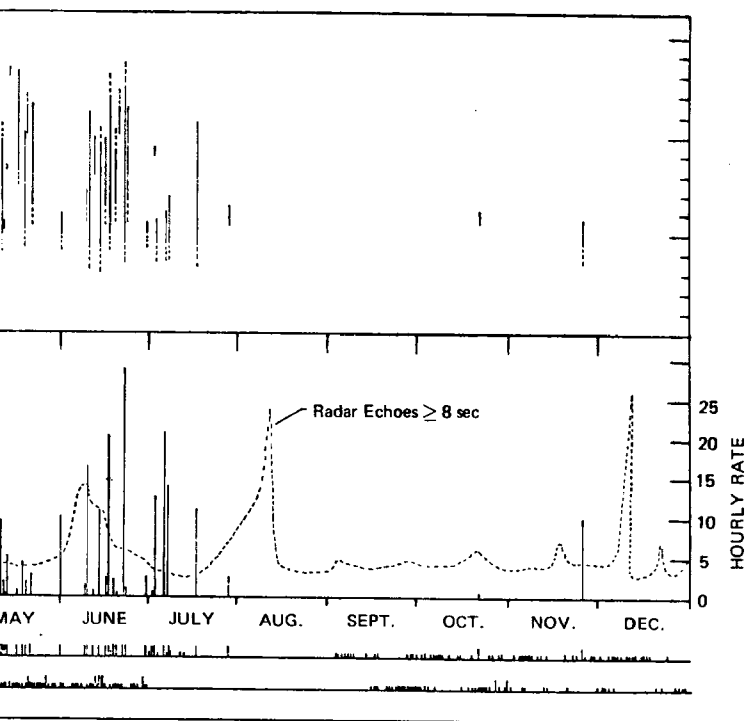
Fig. 6.62 Variation in lithium brightness at Saskatoon February–March 1965 following lithium injection February 28 at Fort Churchill. [From A. Vallance Jones, *Annales de Géophysique (France)*, 22(2): 193 (1966).]

abundance is too large to be of marine origin, whereas it would agree with abundance in micrometeorites. The latter, however, would contribute only a small percentage to the total abundance of sodium in the upper atmosphere (Sullivan and Hunten, 1964).

Junge et al. (1962) estimated that it would take 5 to 20 years for material to be transported from the 60- to 80-km region to 20 km. This estimate was derived from rhodium ^{102}Rh measurements (see Part 4). Gadsden (1964b) found the residence time of sodium in the meso- and stratosphere to be near 100 years and that of lithium of thermonuclear origin to be at least 1 or 2 years.

Calcium spectral lines have been observed sporadically in twilight spectra (Vallance Jones, 1958; Weill, 1966; Markham and Anctil, 1967; see also Vallance Jones, 1963, 1966 for references), but no use of them has been made as yet in studies of atmospheric motions (see Fig. 6.60). There are discrepancies in altitudes and abundances of the Ca^+ layers estimated by Istomin (1963) and by Narcisi and Bailey (1965a). Weill (1966) reported on a seasonal variation in the Ca II twilight emission found in Antarctica with a maximum in early June. Broadfoot (1967) attributed the spring and summer maximum of calcium emission observed in the northern hemisphere in the altitude range of 100 to 280 km to the increase in meteoric activity during this time of the year (Fig. 6.63). Such a correlation between calcium twilight emission and radar meteor echoes confirms the extraterrestrial origin of calcium in the upper atmosphere.

SODIUM (Na) AND OTHER ALKALI METALS



1964-1966 (three bottom lines). Each vertical line indicates a twilight record, and in the lower graph the vertical lines represent the maximum intensity observed during a daily meteor rate from radar echoes with a duration greater than 8 sec (from Millman). The dashed line indicates the range of altitude in the line of sight through which the earth's shadow of 29 km was assumed. [From A. L. Broadfoot, *Planetary and Space Science*

Markham and Ancia (1967) concluded from aircraft observations of the Ca II lines that the emitting source may be rather limited in its horizontal extent. This would explain the sporadic nature of optical observations of calcium emission in the upper atmosphere and would also support the postulated meteoritic source of calcium.

Aluminum has about the same abundance in meteorites as calcium. The Al I lines at 3944 to 3962 Å, however, have not yet been observed in airglow phenomena.

According to Istomin (1963), the ratio $[Mg^+]/[Ca^+]$ is 25 ± 8 as measured by rocket-borne mass spectrometers. This is close to the $[Mg]/[Ca] = 15$ of meteorites. Peaks of the magnesium layer were found at 105 km by Istomin and at 95 km by Narcisi and Bailey (1965a) with a second layer near 110 km (Figs. 6.60 and 1.38). The Mg^+ lines at 2796 to 2803 Å, however, cannot be observed from the ground.

The origin of these trace substances in the upper atmosphere is still much debated (Junge et al., 1962; Vallance Jones, 1966). For sodium, opinions are torn between an oceanic and a meteoritic source. If $[Na]/[K]$ abundance ratios in the ionosphere and in the oceans may be taken as indicators, Sullivan and Hunten (1964) have argued that at least 90% of the sodium must be of terrestrial origin.

It seems reasonable to assume that calcium, magnesium, and iron identified in the upper atmosphere (Fig. 6.60) are injected into these layers in the form of meteors or cosmic dust. More observations will be needed, however, especially on seasonal and local variations of these elements, to improve upon this hypothesis of their origin. If meteoric sources are involved, we should also be able to identify a number of additional elements in the upper atmosphere (Vallance Jones, 1966).

DUST

In the preceding chapters various aerosol layers such as the Junge layer near 20 km and the sodium layer near 90 km, have been described in detail. It has been pointed out that terrestrial as well as extraterrestrial sources may be held responsible for the formation of the various dust layers in the atmosphere. In this section a summary is given of dust particles, other than the ones described before, as tracers of atmospheric motions.

General Comments

The size distributions of aerosols have been studied by numerous authors. A detailed account has been given by Junge (1963a). Particles with radii greater than 0.1μ seem to follow a general distribution law.

$$\frac{dN}{d(\log r)} = cr^{-\beta} \quad (6.18)$$

where N is the total concentration of aerosol particles with radii smaller than r , c is a

constant, and β is approximately 3. A value of $\beta = 3.5$ was quoted earlier in this chapter for stratospheric aerosols in the size range $0.3 \mu < r < 3.0 \mu$.

From dimensional analysis, Friedlander (1960, 1961, 1965) (see also Welander, 1959) derived theoretical particle spectra that are in fair agreement with observations. The equilibrium range (equilibrium between coagulation and sedimentation effects) may actually contain two subranges in which distributions are proportional to r^{-2} and r^{-4} , characterizing the particle spectrum. These considerations apply to the upper end of the spectrum, with $r > 0.1 \mu$, where the particle distributions remain fairly constant with time. An upper limit of aerosol size of 20 to 30 μ should be expected from an equilibrium between diffusion and sedimentation. Much larger aerosols (up to 150 μ), however, are found regularly in the lower troposphere, indicating that this postulated equilibrium is not generally satisfied (Jaenicke and Junge, 1967; Blifford and Ringer, 1969; Junge et al., 1969). Rapid time variations of particle concentrations have been detected at the lower end of the spectrum ($r \ll 0.1 \mu$) which calls for sophisticated sampling techniques (Friedlander and Pasceri, 1965; Pasceri and Friedlander, 1965). The proportionality with r^{-4} seems to hold for particle sizes down to $r \approx 0.05 \mu$ (Clark and Whitby, 1967; Junge, 1969; Yamamoto and Tanaka, 1969). Near this radius value a maximum of $dN/d(\log r)$ seems to exist (Twomey and Severynse, 1964).

Pueschel and Noll (1967) showed that the large number of particles less than 0.1 μ (about 90% of the total number of aerosols present in a sample) contribute only approximately 5% to light extinction. The effect of aerosols on visibility thus comes mainly from the upper end of the spectrum (see also McCaldin et al., 1969; Horvath and Noll, 1969). For these particles both size and refractive index, influencing the extinction, depend on the relative humidity (Hänel, 1968). The particle-size distribution also affects the Mie scattering (Bary and Bullrich, 1961), which, in turn, can be probed by lidar (Barrett and Ben-Dov, 1967; Viezee and Oblanas, 1969). The development of such instrumentation will greatly aid in diffusion studies using aerosols as tracers.

Extraterrestrial Dust Sources

From the previous discussions it is evident that the nuclei detected in the noctilucent-cloud layer may be of meteoric origin. The same holds for the metallic ions identified in the E-region of the ionosphere (Figs. 1.38 and 1.39), even though the origin of the sodium in the sodium layer is still under dispute. It is feasible, as we have stated before, that a large part of this sodium comes from terrestrial sources.

Meteor trails appear between 70 or 80 to 120 km and contain ionized material that may be detected by radar. Fiocco (1967) contended that meteoric influx thus may contribute significantly to the background ionization of the E-layer. These trails give an indication of wind velocities and their variability in this altitude range when the Doppler shift of the return signal is measured (Barnes, 1968a, 1968b; Barnes and Pazniokas, 1968).

Rosinski and Pierrard (1964) believe vaporized material from meteors may form secondary particles that may serve as precipitation nuclei (for meteoric-particle ablation computations, see Kornblum, 1969a). Thus they are supporting Bowen's (1953, 1956) hypothesis, according to which there is a certain lag correlation between worldwide precipitation anomalies and the occurrence of meteor showers. An evaluation of this hypothesis will have to take a critical look at transport processes by Lorentz forces acting on charged particles in the D-region and by eddy processes in the meso- and stratosphere. If the Bowen hypothesis can be made responsible for an extraterrestrial cloud-seeding effect, exchange processes should be able to move nucleating material from the mesopause region into the vicinity of the tropopause within 30 (Bowen) to 65 days (Rosinski and Pierrard) (see also H. Maruyama and Kitagawa, 1967). This would require average downward transport velocities of the meteoric debris of 1 to 2 cm/sec. Furthermore, diffusion of the debris should not yet have caused uniform mixing throughout the stratosphere and mesosphere; so significant increases in precipitation nuclei at tropopause level could be expected with the appropriate time lag. All these requirements may be difficult to prove. Above all, J. E. Erickson (1969) has estimated that visible meteor streams (showers) contribute only on the order of 1% of the total meteor mass influx into the earth's atmosphere; therefore a significant source variability is questionable. There may, however, be a strong variability in the downward eddy-transport processes, which leads to variations in local dust-particle concentrations. The enhanced meteor shower activity during May and June of 1963 produced no increase in precipitation over the United States. Quite the contrary: between June and September 1963 below-normal precipitation was recorded (Dycus and Martin, 1969). Volz and Goody (1962) also found no correlation between stratospheric dust causing atmospheric turbidity and the occurrence of meteor showers. Rau and Schmidt (1961) pointed out a correlation between ice-nuclei concentrations and air masses whereby concentration increases were recorded in polar air after cold-front passages. Descending air in anticyclones also brought about concentration increases. Such variable vertical transport processes obliterate any significant correlations with meteor showers (Rau, 1960).

Gokhale and Goold (1969) investigated the nucleating properties of dust particles collected above 80 km. They found that these particles are substantially inferior as ice nuclei when compared with AgI or clay particles of terrestrial origin, even at temperatures of -20°C . Considerable supersaturation would be required to activate the extraterrestrial particles collected at high altitudes. Aircraft measurements of ice nuclei by Cadle et al. (1969) revealed a marked decrease of nuclei concentrations above the tropopause and a more uniform distribution in the stratosphere. This evidence further discredits the precipitation hypotheses by Bowen and Rosinski and Pierrard.

The evaporating meteors and meteorites themselves serve as sources of trace substances detected by rocket measurements or from airglow observations, as discussed before. Terminal fall velocities of small particles are shown in Fig. 6.16. Shafir and Humi (1967) and Shafir et al. (1967) also demonstrated that particles in the size range 0.1 to 100 μ will reach terminal velocities around 80 to 100 km (see also

Kornblum, 1969a, 1969b). Large particles may be subject to fragmentation during this braking process from their original (near-orbital) velocity, thus further enhancing the small-particle population in this region. Such fragmentation should be highly effective with most meteoroids, which turn out to be rather weak in structure ("dust balls" according to Fiocco and Colombo, 1964). Fragmentation also would explain the presence of the dust layer between 110 and 140 km detected by Fiocco and Colombo (1964) by the use of a ruby laser (see also Deirmendjian, 1965).

A number of estimates have been made on the rate of meteoric influx into the earth's atmosphere and on the density of hard interplanetary matter. It turns out that particles below a certain size (depending on their dielectric constant) should escape from the planetary space since the radiation pressure effect would exceed the sun's gravitational pull (Biermann, 1967; Schmidt and Elsässer, 1967; Newkirk, 1967). This limit is indicated by an arrow in Fig. 6.64. The upper size limit given in this diagram indicates micrometeorites that will barely survive passage through the atmosphere. Particles larger than this upper limit will be subject to fragmentation and ablation as they enter the earth's atmosphere (Whipple, 1950, 1951; Kornblum, 1969b). In Fig. 6.64 estimates by Allen (1946), Hulst (1947), Elsässer (1954), Beard (1959), Blackwell and Ingham (1961), Giese (1962), and Giese and Siedentopf (1962) are compared with those by Newkirk (1967) (marked HAO). Observations of the zodiacal light, which extends as a diffuse luminous cone along the ecliptic plane and may be seen after twilight and before dawn, also yield estimates on interplanetary dust. The fact that the zodiacal light is partly polarized would suggest that, in addition to dust particles, interplanetary electrons contribute to its existence (Elsässer, 1963). For various contributions to the problem of zodiacal light and interplanetary matter, see Weinberg, 1967. The solar "F-corona" also allows estimates on interplanetary dust as it is produced by light-scattering dust particles present along the line of sight. Polarization of the F-corona is small (Ney, 1967).

From Fig. 6.64 we may also estimate the particle-size distribution $n \propto r^{-p}$. A value of $p \approx 2$ (Soberman and Hemenway, 1965) to 3 seems to fit most of the observations. In the noctilucent-cloud layer, $3 < p < 4$ seems to hold (Witt et al., 1963; Hemenway et al., 1964; see also Kornblum, 1969b). Particle-size distributions in the Junge layer are given earlier in this chapter.

Biermann (1967) estimated the lifetime of particles with radii $0.01 \mu \leq r \leq$ several μ to be of the order of 10^7 sec. Smaller particles have shorter lifetimes, signifying an escape from our planetary system under the force of radiation pressure. Figure 6.64 indicates a slightly larger limiting size; so does an estimate by Schmidt and Elsässer (1967). Ney (1967) quoted the limiting size to be 0.5μ . Particles larger than this limiting escape size will orbit around the sun and slowly spiral into the sun. (This is known as the Poynting–Robertson effect. See, for example, Schmidt and Elsässer, 1967.)

The earth's gravitational and magnetic fields may trap solar-orbiting particles contained in the zodiacal cloud, thus leading to an enhancement of particle densities within the earth's magnetosphere (Schmidt and Elsässer, 1967). This is also suggested in Fig. 6.64 by the fact that several meteor and satellite observations yield larger

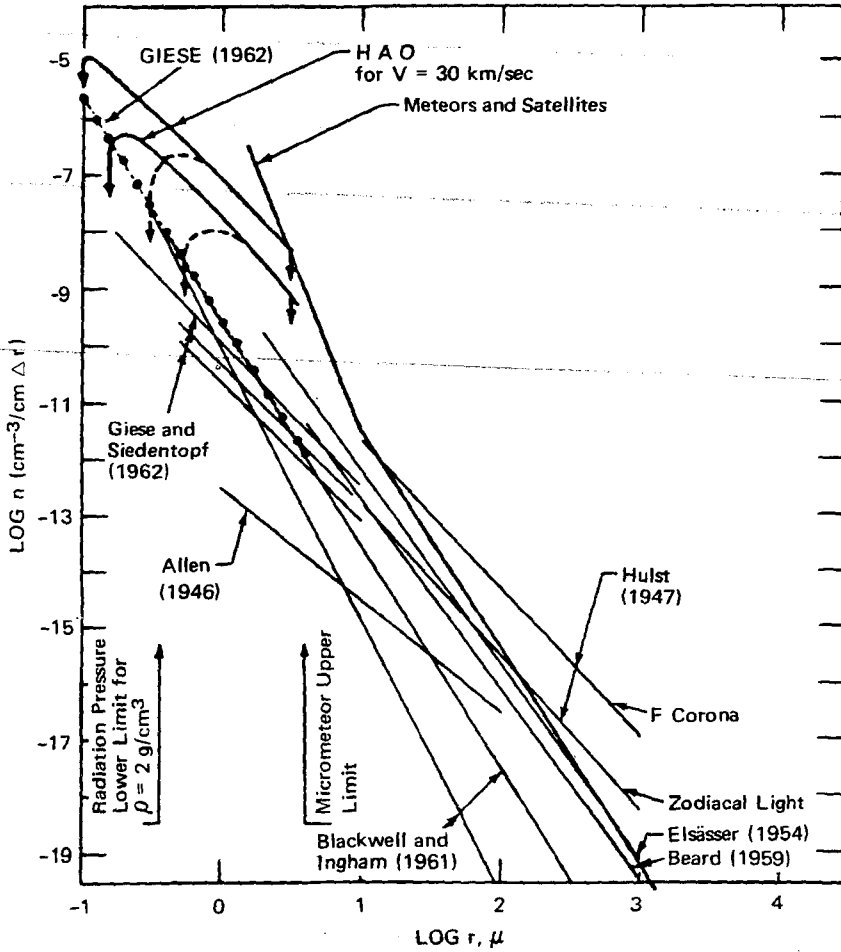


Fig. 6.64 Comparison of the concentration of interplanetary dust particles as inferred by Newkirk (1967) (labeled HAO) with the concentrations determined from satellites (Alexander et al., 1963) and visual and radar meteors (Whipple, 1961a) as well as with the various determinations from the photometry of the zodiacal light. The fact that the zodiacal light concentrations are approximately a factor of 1000 lower than those determined by Newkirk's analysis is taken as evidence for a local gravitational condensation of the interplanetary dust in the neighborhood of the earth. Note that the model inferred by Allen (1946) refers only to the concentration required if all the particles are of a given radius between 1 and 100 μ rather than a true size distribution. [From G. Newkirk Jr., Meteor Orbits and Dust, Report NASA-SP-135, p. 356, National Aeronautics and Space Administration, 1967.]

particle concentrations than measurements of the zodiacal light. A geocentric condensation of interplanetary dust was also suggested by Jager (1955), Beard (1959), Hibbs (1961), Singer (1961), and Whipple (1961a, 1961b, 1963). The magnitude of this condensation, according to Fig. 6.64, is larger for small particles (a factor of 10^3 over zodiacal densities) than for large particles. For particles with r greater than 10μ , the Poynting–Robertson effect apparently has not reduced the eccentricities and changed the axes of the orbits sufficiently for them to be captured by the earth. Small particles will take circular orbits more rapidly and therefore will be captured more effectively by the earth (see Newkirk and Eddy, 1964; Newkirk, 1967). Singer (1964) suggested that beyond 2 earth radii it may actually be the dust particles that determine the ambient density (their concentration depending on the geocentric velocities with which they travel in their orbits) and not so much the gaseous atmosphere.

Recent rocket and satellite observations did not confirm the existence of a geocentric “dust-belt,” thus indicating dust concentrations that are several orders of magnitude smaller than those obtained from earlier experiments (Fechtig et al., 1968; see also D’Aiutolo, 1964; Clifton and Naumann, 1966; Naumann, 1966; McDonnell, 1967). It may well be that the dust concentration around the earth and also the meteoric influx are variable between wide limits. Crozier’s (1966) data, for instance, suggest that the influx of magnetic spherules into the atmosphere was substantially higher in 1963 (especially in June of that year) than should be expected from a 9-year average. In a recent paper Bandermann and Singer (1969) suggested that the “dust-belt” found in earlier but not in recent observations might have been a consequence of the measurement techniques.

Estimates of the deposition rate of meteoric material on the earth vary (Table 6.2). Figure 6.65 shows influx estimates ($-\gamma$ is the flux of particles in the dimensions stated along the ordinate) as a function of particle size obtained from the “Venus Flytrap” sounding rocket (Hemenway and Soberman, 1962), from satellites (Alexander et al., 1963), from visual and radar meteors (Whipple, 1961a), from zodiacal light (Hulst, 1947), and from visual meteors (Watson, 1941, 1956). The integral from 0.1 to $10^4 \mu$ of this influx has been estimated by Newkirk (1967). Results are shown in Table 6.2. Newkirk explains his relatively low influx estimates with the argument that above 100 km a significant fraction of particles in the size range $0.3 \mu < r < 3 \mu$, identified there by various authors, is in geocentric quasi-closed orbits and does not contribute to meteoric influx toward the earth. These smaller values of flux arrived at by Newkirk also agree with some of the deposition-rate estimates of meteoric dust settling through the air or deposited at the ground. An alternate explanation for relatively low deposition rates, according to Newkirk (1967), would be that the majority of meteoric particles are too fragile to survive passage through the atmosphere.

Newkirk (1967) and Matsushima (1968) attributed the excessively high deposition rates estimated by Rosen (1964) and by Fiocco and Colombo (1964) to the misapplied assumption that all aerosol $0.5 \mu \leq r \leq 2 \mu$ at 20 km is of meteoric origin. They contend that only 1 to 10% of the stratospheric aerosol is meteoric. The relatively large aerosol concentrations detected by optical radar near 120 km could be

Table 6.2
RATE OF INFALL OF EXTRATERRESTRIAL MATERIAL ON THE EARTH

Reference	Rate	Remarks
Ney (1967)	1/30 particles/cm ² /sec or 10 ⁷ tons/year on whole earth.	Particles greater than 0.5 μ with particle density ρ = 1.
Newkirk (1967)	2 × 10 ⁻¹⁵ g/cm ² /sec or 10 ³ tons/day or 3 × 10 ⁵ tons per year on whole earth.	0.1 to 10 ⁴ μ from light scattering, satellite, and visual and radar meteor observations.
Dubin and McCracken (1962) Dubin (1960) LaGow and Alexander (1960)	About 10 ⁴ tons/day (summarized by Newkirk, 1967) or about 3.6 × 10 ⁶ tons/year.	Satellite measurements extrapolated to the radiation pressure limit of particle size.
Whipple (1961a) Crozier (1960) Laevatsu and Mellis (1961) Pettersson (1960) Crozier (1961) Thiel and Schmidt (1961) Crozier (1962) F. W. Wright and Hodge (1962) Rosen (1964)	About 10 ⁵ tons/year (summarized by Newkirk, 1967).	Settling through atmosphere or deposited on the ground or both.
Fiocco and Colombo (1964)	4 × 10 ⁶ tons/year.	Estimates from aerosol distributions 0.5 μ < r < 2 μ near 20 km.
Pettersson and Fredriksson (1958)	2 × 10 ⁷ tons/year. 2.4 to 5 × 10 ³ tons/year.	Estimates from aerosol above 100 km. Deep-sea meteoric spherules, mostly iron-nickel. Other meteoric spherules probably do not survive in ocean water; therefore the excessively low deposition estimates.
Carleton (1962)	5 × 10 ⁻¹⁶ g/cm ² /sec or 0.8 × 10 ⁵ tons/year.	From twilight estimates of dust by Volz and Goody (1962) assuming constant dust-mixing ratios above 30 km.
Bhandari et al. (1968)	Less than 550 tons/day or 2 × 10 ⁵ tons/year; probably less than 50 tons/day or 1.8 × 10 ⁴ tons/year.	Balloon-borne mesh impactor flown at 23.8 km, sampling particles 1 to 100 μ in diameter that have not burned up during entry.

Table 6.2 (Continued)

Reference	Rate	Remarks
Shedlovsky and Paisley (1966). Fiocco (1967)	Less than 9×10^4 tons/year. 4.4×10^3 tons/day or 1.6×10^6 tons/year.	Airplane samples, 19 to 21 km. If all incoming micro-meteorites had a velocity of 40 km/sec at 200-km height, this flux could account for background ionization of the E-layer. According to Erickson (1968), this velocity assumption is too large by a factor of 2, at least for photographic meteors.
Hodge et al. (1964) Brocas and Picciotto (1967)	About 2×10^5 tons/year. 3 to 10×10^6 tons/year.	Spherules on Greenland ice cap. From nickel deposits in Antarctic ice.

particles with r about 0.1μ produced by fragmentation (see earlier statements in this chapter) and escaping detection by direct sampling devices.

Hodge and F. W. Wright (1968) suggested that spherules found in the stratosphere and in the polar ice caps are too abundant to be micrometeorites. They may, to a large percentage, be ablation products of larger meteoroids, possibly comet fragments, which would not be in circular orbits around the earth as most of the small particles seem to be. Hamilton and Bull (1966) arrived at particle-size distributions for the Greenland ice cap and for the South Pole deposits of $3.5 < p < 6$ for $n \propto r^{-p}$.

Terrestrial Sources

Natural as well as anthropogenic sources of aerosols will have to be considered in estimating aspects of atmospheric motions.

Among naturally generated aerosols we already have identified volcanic activity as contributing at times significantly to particle concentrations found in the Junge layer. Deposition rates of volcanic dust (spherules) have been estimated by Hodge et al. (1964) from deposits on the Greenland ice cap. Their analysis yields approximately 5×10^4 tons/year on a worldwide basis. Stratospheric transport processes probably contribute most effectively to the global deposition of volcanic debris. It is of interest to note that a large fraction of volcanic fumes (95%, Anonymous, 1969; Cadle et al., 1969) consists of sulfuric acid droplets. Violent eruptions, such as the one of Mount Agung, thus could greatly enhance the sulfur concentrations found in the Junge layer. Ammonia (NH_3) was also found to be abundant in volcanic fumes.

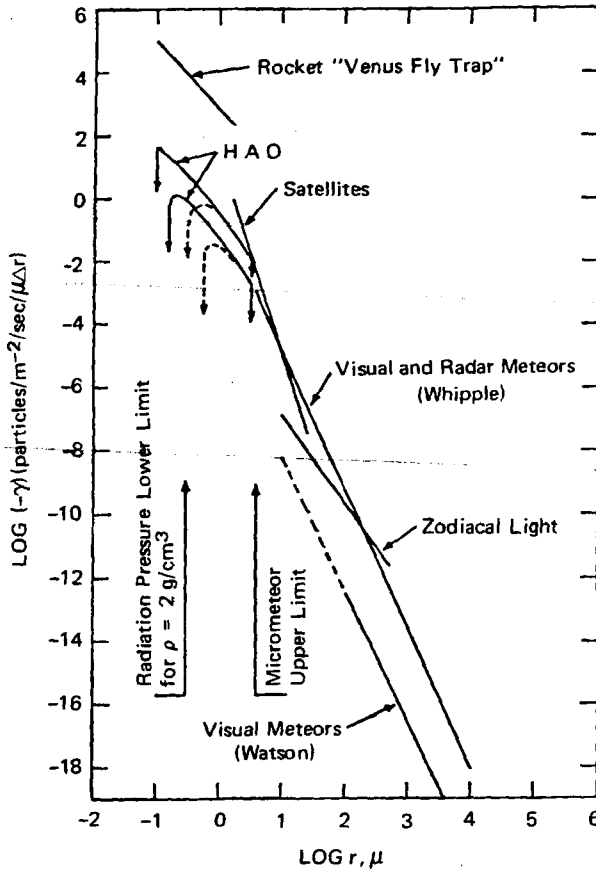


Fig. 6.65 Comparison of the meteoric influx rates inferred by Newkirk and Eddy (1964) (labeled HAO) with the fluxes determined from the rocket "Venus Flytrap" (Hemenway and Soberman, 1962), from satellites (Alexander, et al. 1963), from visual and radar meteors (Whipple, 1961a), from zodiacal light (Hulst, 1947), and from visual meteors (Watson, 1941). The higher HAO curves refer to the results of Sept. 10, 1960, and the lower curves to Oct. 3, 1960. For $k_{zz} = 2000 \text{ cm}^2/\text{sec}$, the solid HAO curves apply; for $k_{zz} = 10,000 \text{ cm}^2/\text{sec}$, the dashed curves apply. (k_{zz} is the vertical eddy diffusion coefficient.) The lower size limit of particles to remain in the solar system against radiation pressure and the upper size limit of particles to survive passage through the atmosphere (Whipple, 1950; 1951) are indicated. [From G. Newkirk and J. A. Eddy, *Journal of the Atmospheric Sciences*, 21(1): 55 (1964).]

Volcanic dust has a noticeable effect on atmospheric transmissivity; it may cause a decrease of surface temperatures. Volcanic activity has been held responsible for the temperature declines in 1787, 1816 (the "year without a summer"), 1837, 1884, 1893, and 1912 (Anonymous, 1969). Stratospheric dust also causes abnormal polarization of sky light (Volz, 1969b; Unz, 1969).

Large forest fires constitute a natural source of aerosols that will be confined mainly to the troposphere (Hobbs and Radke, 1969; Hobbs and Locatelli, 1969). The Canadian forest fires of the latter part of September 1950, for instance, carried smoke over the North Atlantic into Europe, where the turbidity gave rise to abnormal optical phenomena (blue sun) (C. D. Smith, 1950; Wexler, 1950; Bull, 1951; Elsley, 1951; Runge, 1951; Rodewald, 1952; Haarländer, 1959). Dust storms, especially over North Africa, transport considerable amounts of aerosol. Under conditions of the so-called "Dimmerfoehn," a southerly to southwesterly chinook wind observed in the Alps with midtropospheric air trajectories leading out of the Sahara desert, African dust is carried far into Europe (Streiff-Becker, 1942; Berenger, 1963; R. Reiter, 1964, p. 226).

From a study by Prospero (1968), it appears that African dust can also be identified over Barbados in the Antilles after having crossed the Atlantic in the trade-wind regime. Figure 6.66 indicates a distinct summer maximum for this trace substance. A sharp onset of the transport season during the later part of May is evident

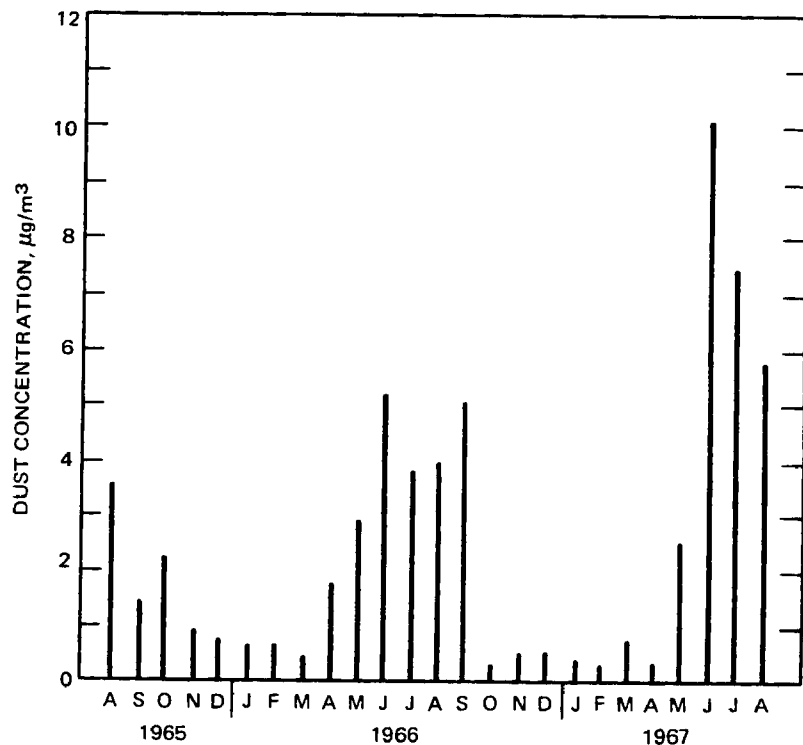


Fig. 6.66 Monthly average atmospheric dust concentration, Barbados, August 1965–August 1967. The dust concentrations indicated are corrected for rain losses; a 50% mass collection efficiency is assumed for the dust suspended in the air passing through the mesh area. [From J. M. Prospero, *Bulletin of the American Meteorological Society*, 49(6): 647 (1968).]

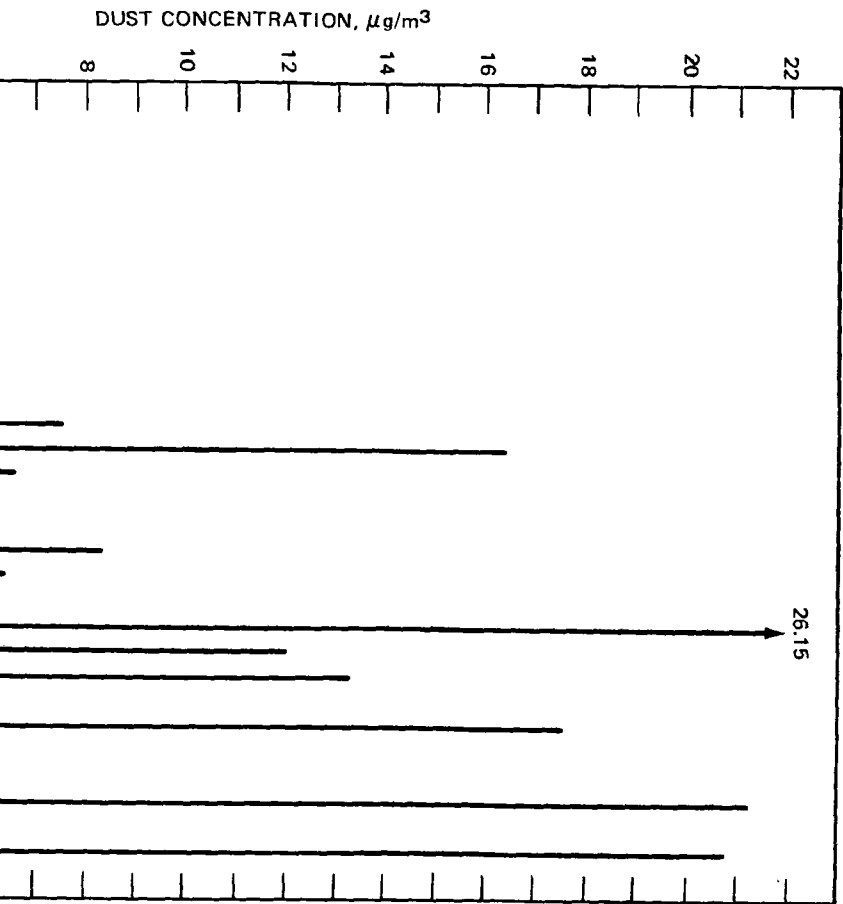
from Fig. 6.67. A contamination of these observations by local dust sources has to be discounted because of the difference in chemical composition between local soils and collected dust (Delany et al., 1967). Land masses surrounding the Caribbean and the Gulf of Mexico also seem unlikely sources of this seasonal dust-fall phenomenon (Hastenrath, 1966). Prospero and Bonatti (1969) reported on shipboard measurements and analyses of dust in the eastern equatorial Pacific. Marked differences were encountered in the chemical composition of the dust collected north and south of the intertropical convergence (ITC) zone, which suggested dust sources in Mexico on the one side and sources in Peru, Chile, and Ecuador on the other side of the ITC zone. In view of these studies, it appears desirable to explore the usefulness of dust as a tracer for large-scale atmospheric motions.

Dust devils (Sinclair, 1969; Logan, 1969) contribute toward the aerosol content of the lower troposphere under thermally unstable conditions, although their effectiveness will be orders of magnitude smaller than that of dust storms. The latter may spread debris over considerable depths in the troposphere. Danielsen (1968), for instance, reported on flight observations of dust that was mixed throughout the layer between the ground and ≤ 500 mb. Scorer (1968) also provided illustrations of natural air pollution by dust and by blizzards. One should surmise that geographic regions in which sand-dune formation is observed (Lettau, 1967; Hanna, 1969) are effective sources of terrestrial dust: Heavy particulate matter is deposited in the form of dunes, whereas small particles become airborne and are transported over great distances. The presence of dunes would indicate that winds of sufficient strength are frequently present from a prevailing direction to warrant such transport processes and dispersal of aerosols in the planetary boundary layer.

Organic aerosol in the form of pollen may serve as a tracer, especially when isolated sources are involved. From a biometeorological point of view, this tracer is of importance because it may cause allergic reactions in a wide segment of the population. Ragweed pollen especially appears to have allergenic properties. Gatz and Dingle (1963) (see also Dingle and Gatz, 1966) studied the behavior of this species of pollen in rain-out situations. The pollen grains of ragweed are of uniform size (20μ) and are easily determined in rainwater samples. They may, therefore, be regarded as a tracer of low-tropospheric air that has been transported upward in convective motions and entrained into convective systems. The observed fluctuation of pollen concentrations during certain rainfall episodes does not fit established washout models (Greenfield, 1957). Gatz and Dingle suggest that these fluctuations may be indicative of surges of entrainment of polluted air occurring during the precipitation event. Such surges would make the application of a simple washout model to the interpretation of aerosol concentrations in rainwater a highly questionable procedure.

Certain spores, such as the ones of white pine blister rust, are released mainly at night when the atmosphere is stably stratified and diffusion is suppressed. Arsdel (1967) showed that smoke tracer experiments portray very well the spreading of these spores and the ensuing blister-rust infections on trees. The lake-breeze effects of Lake Michigan and Lake Superior carry the spores out over the water; thus pines nearest the shore rarely reveal infections. The return flow aloft, however, carries the spores 10 to

DUST



17 miles inland, where they are deposited by downdrafts and cause numerous infections high up in the trees.

The spread of certain virus diseases, such as the foot-and-mouth disease, appears to depend significantly on wind and precipitation conditions. P. B. Wright (1969) suggested that the virus when released into the air attaches itself to particles. It becomes subject to dry deposition as well as to wet removal by washout.

Pollen grains have been used successfully as artificial tracers in small- and mesoscale dispersion experiments. Raynor et al. (1966) described dyeing techniques that suggest the use of pollen in multiple-tracer studies. Fluorescent particles in different colors (Morton, 1967) lend themselves to similar experiments.

Smaller aerosol particles, such as Aitken nuclei ($<0.2 \mu$), may become useful as tracers of atmospheric motions once their sources are better understood and a number of problems are resolved. Ice-nuclei counts taken at intervals of only a few minutes on July 10-11, 1963, at Hilo, Hawaii, indicate a very strong variability in the concentrations, sometimes as much as an order of magnitude within minutes (Price and Pales, 1964). Local circulations, such as mountain-slope winds, seem to play an important role in these variations (Nagamoto et al., 1967); so does the turbulent exchange coefficient (R. Reiter et al., 1968). Onshore winds usually carried low ice-nuclei counts, which suggests the presence of local sources on the island. However, measurements by Droessler and Heffernan (1965) in the same region could not verify such local terrestrial sources. No volcanic origin of these ice nuclei is suggested (Price and Pales, 1963). Kline (1963) and Kapoor et al. (1969) found that land surfaces serve as important ice-nuclei sources, whereas oceanic regimes reveal low count rates. Airborne measurements made by Twomey and Wojciechowski (1969) confirm these conclusions and, furthermore, establish a lifetime of cloud nuclei of about 3 days as they drift out over the ocean. Hogan et al. (1967) arrived at similar results, showing that off-shore winds over the U. S. east coast carry approximately 10 times more ice nuclei than midoceanic air masses over the Atlantic. Other authors, however, contend that moist oceanic air contains more ice nuclei than dry continental air. Battan and Riley (1960) arrived at this conclusion from measurements on top of Mount Bigelow, Ariz. It could very well be, however, that moist oceanic air picked up nuclei on its overland trajectory, whereas dry air came from the upper troposphere by subsidence and therefore was relatively clean. Bird et al. (1961) concluded that ice nuclei in the southern hemisphere stem mainly from the ocean. Brier and Kline (1959) and Kline (1960) also made note of maritime sources. Ryan and Scott (1969) found that ice nuclei might be released by evaporation of small precipitation particles. Georgii (1960b) speculated that air pollution over continents may inactivate part of the ice nuclei, thus leading to higher counts in pollution-free maritime air.

From airborne ice-nuclei measurements over Australia, Bigg (1967) found streaks of high concentrations in the upper and lower troposphere (Fig. 6.68) (see also Droessler, 1964; Droessler et al., 1967). He rules out aircraft exhaust or dust storms in the Australian interior (Bigg and Miles, 1964; Soulage, 1957). This leaves him with an extraterrestrial source of nuclei (see also Bigg and Giutronich, 1967) that might be responsible for a certain stratospheric burden of small particles. The transport and

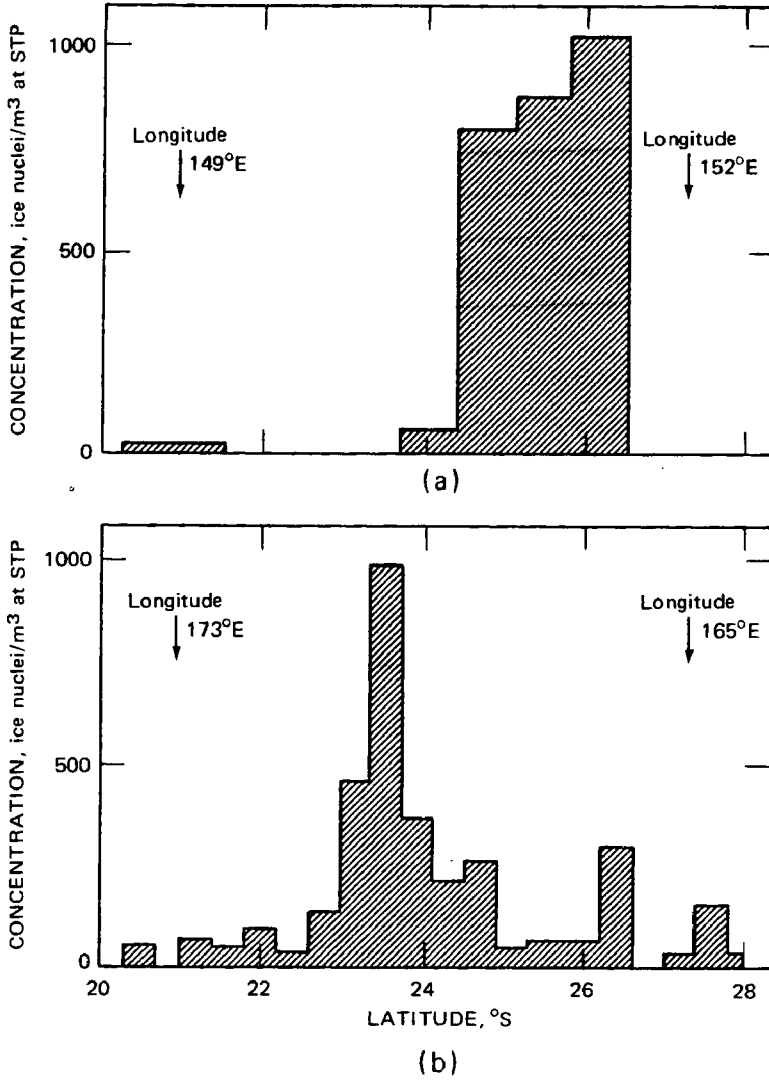


Fig. 6.68 Groups of high ice-nucleus concentrations (concentrations measured when sample was cooled to -15°C): (a) June 8, 1963, altitude 3650 m; (b) Sept. 6, 1963, altitude 10,700 m. [From E. K. Bigg, *Journal of the Atmospheric Sciences*, 24(2): 227 (1967).]

chemical processes leading to the formation of the Junge layer might conceivably influence a stratospheric ice-nuclei source. Coating of an ice nucleus by sulfate would inactivate it. Extraterrestrial nuclei, therefore, would have to traverse the sulfate layer quickly in order to retain their nucleating properties (Bigg and Miles, 1964). Bigg (1967) (see also Bigg and Miles, 1964) did not find an effect of Mount Agung debris

on his ice nuclei counts; thus he discounts volcanic sources for these nuclei. Transport processes in the jet-stream region, such as indicated by Fig. 4.9, may account for streaks of ice nuclei of stratospheric origin within the troposphere. Unfortunately, no details of analysis are available in Bigg's (1967) data. [For summaries on ice nuclei, see Mason (1957) and Fletcher (1962).]

Mészáros (1968) found that over a continental location (Hungary) about half of the sulfate and ammonium particles collected by impactors belonged to the Aitken size range ($r < 0.3 \mu$), whereas the majority of chloride particles fell into larger size ranges. Experiments by Bricard et al. (1968) suggest that Aitken nuclei may form from gaseous pollutants, such as SO_2 (see also discussion of the Junge layer). According to Junge and Scheich (1969), most of the water-soluble compounds of aerosols are associated with particles smaller than 0.1μ , whereas the total mass of the aerosol is primarily made up of larger particles. Nuclei formation in originally aerosol-free air appears to be enhanced by the presence of radioactive substances.

Among the large aerosol particles, the giant salt nuclei of marine origin, probably produced by bursting bubbles (Jacobs, 1937; Day, 1964; Paterson and Spillane, 1969), deserve mentioning since their distribution in the lower atmosphere and their ratio against other aerosols may be indicative of the air-mass history (for observed and theoretical distributions, see Toba, 1965a, 1965b, 1966; Junge et al., 1969). This is, for instance, shown by the large increase in the number of large hygroscopic particles during the Indian monsoon season (Fig. 6.69) (Sekhon and Ramana Murty, 1966; Ramana Murty et al., 1967). Sea-salt deposits have been observed far inland in Northern Germany following the passage of cyclonic disturbances with strong on-shore

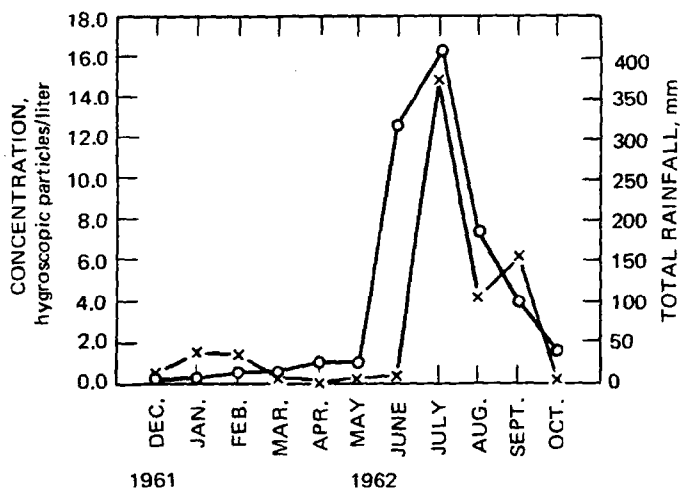


Fig. 6.69 Monthly mean concentration of giant hygroscopic aerosols (○) and total monthly rainfall (x). Measurements made December 1961 to October 1962. [From Bh. V. Ramana Murty, A. K. Roy, and R. K. Kapoor, *Tellus*, 19(1): 138 (1967).]

winds (Schubert and Hänsch, 1963b). From field and laboratory experiments investigating the growth of seawater aerosols as a function of humidity. Pueschel et al. (1969) concluded that organic molecules attached to sea-spray droplets may significantly alter the hydrophilic nature of these droplets as compared to those containing pure NaCl. Anthropogenic water or air pollution may have similar effects on the giant sea-salt nuclei, thus possibly contributing toward inadvertent weather modification.

Giant nuclei of continental origin may serve as tracers of local circulations, such as of mountain waves and chinook winds. Hoidale and S. M. Smith (1968) (see also Hoidale and Blanco, 1970) presented analyses over South Central New Mexico in which soil particles were identified with relatively large mineral concentrations (3 to 10% for various mineral compounds). Knowledge of soil conditions along surface-air trajectories permits the use of these particles as tracers of air motions. Rosinski and Kerrigan (1969) found that giant aerosol particles (presumably picked up by winds from the earth's surface) are present in significant numbers in convective clouds of severe continental thunderstorms. These particles begin to collect cloud droplets as soon as they enter the cloud base. Some of the giant aerosol particles appear to act as ice-forming nuclei at temperatures as warm as -6°C and may thus play a role in hail formation.

Anthropogenic sources of dust and of aerosols in general may be of an inadvertent nature, such as air pollution from industrial sources, or may have been caused deliberately for small-scale diffusion studies and other tracer experiments. It would go beyond the scope of this review to include all implications of impurities caused by air pollution. For more details the reader is referred to standard literature available in this field (e.g., Junge, 1963a; H. L. Green and Lane, 1964; Scorer, 1968; Air Conservation Commission, 1965; Moses, 1969; and others).

Wait (1946) inferred from measurements of electric conductivity made on board the *Carnegie* between 1915 and 1928 that the global burden of fine particles produced by industrial pollution is increasing rapidly. (Electric conductivity is expected to decrease with increasing small-particle concentrations since the latter will capture ions present in the atmosphere.) Gunn (1964), in careful measurements over the North Atlantic, pointed out that by 1962 only a 5% decrease in conductivity (increase in particle pollution) could be observed; thus Wait's pessimistic estimates have to be rejected. Schilling (1964) commented that during the years of atmospheric nuclear testing prior to 1962 relatively high conductivity values could be expected because of the ionizing effect of radioactive debris. Conductivity measurements during this period may be used more effectively as an indicator of radioactive debris than of small-particle pollution.

The seasonal distribution of anthropogenic dust deposition varies widely, depending on location, precipitation, wind regime, and proximity of industrial sources. Forests and parks tend to decrease aerosol concentrations (Zenker, 1954). Summer maximums can be expected away from big cities with industrial pollution and home incineration (Mrose and Zier, 1967). Metropolitan areas usually show larger dust concentrations (Löbner, 1965). Dust deposits may go as high as several kilograms per

100 m² per month (Teichert, 1956). Concentrations in urban areas with industrial and home pollution usually reveal winter maximums (Steinhauser, 1959b, 1960b; Dietze, 1965; Steinhauser and Chalupa, 1966; Ball and Panofsky, 1967), but even here exceptions may exist (Steinhauser, 1966). Precipitation analyses reveal similar seasonal variations (Podzimek et al., 1963). The variations of the vertical exchange coefficients through the course of the year, showing a summer maximum and a winter minimum, exercise a dominant influence on the aerosol distribution (McCormick and Kurfis, 1966). Owing to the sensitive dependence of particle concentrations on meteorological parameters, such as precipitation, wind direction, and speed, large variations in monthly mean values of aerosol deposition may exist from year to year (Carnuth, 1967).

The diurnal variation of aerosol deposition in a metropolitan region (Vienna, Austria) has been studied by Steinhauser (1962). During spring and summer the air appears to be cleanest in the afternoon (between 1400 and 1700 local time) and dirtiest in the morning (between 0500 and 0800 local time). This situation is obviously due to convective motions and atmospheric stability (see also Fiedler, 1966). During fall and winter relatively clean conditions prevail during night and in the afternoon and dirty conditions during the morning and evening hours. This rather complex diurnal variation is caused by a combination of atmospheric parameters and source-strength variations (coal burning in households and automotive traffic generating pollutants and whirling up dust).

The "sunrise effect" on condensation nuclei (showing an increase of concentrations at, or shortly after, sunrise) may at least in part be overshadowed by anthropogenic nuclei sources. Convective motions and photochemical processes may be of importance, too, in producing this effect (Müller and Thams, 1962). Specifically, exposure of SO₂ to ultraviolet light produces a nucleating effect more so than the exposure of H₂S or ammonia (Verzár and Evans, 1959; Hoppe, 1961).

As would be expected, ionizing radiation in the presence of radioactive particles in the atmosphere may cause large increases in the concentration of condensation nuclei. Strongest ionization in the atmospheric layers close to the ground should be expected in the early morning hours under stable stratification when natural radioactive decay products exercise their ionizing influence (Sekikawa and Kojima, 1969). Again, SO₂ appears to be affected by radiation in producing condensation nuclei (Megaw and Wiffen, 1961).

It was mentioned earlier that man-made air pollution may produce an inadvertent weather modification effect. Large-scale burning of organic material, such as sugar cane, may be considered an effective source of anthropogenic cloud nuclei, even more so than urban pollution and combustion products (Twomey, 1960; Squires, 1966; Twomey and Warner, 1967; Warner and Twomey, 1967; S. A. Changnon, 1968, 1969; Ogden, 1969; Schaefer, 1966, 1968, 1969). A tendency of cane fires to reduce rainfall has been commented on by Warner (1968). The adverse effect could be brought about by an increase in cloud-droplet concentrations per cubic centimeter (hence a decrease in droplet size) with an increase in condensation nucleus population (Twomey and Warner, 1967). Abel et al. (1969) reported that the exposure of aerosol

particles to organic vapors changes their subsequent growth behavior in water vapor. This effect may also have a bearing on inadvertent weather modification by man-made pollution. Nuclei are also produced by aircraft flying in the upper troposphere and lower stratosphere, as is evident from the formation of cloud fields from contrails that have been observed on occasion (Georgi, 1960). Additional effects of man-made aerosols may be found in a reduction of direct solar radiation and in an ensuing decrease of potential evaporation (Monteith, 1967; McCormick and Ludwig, 1967; Bryson, 1968; Charlson and Pilat, 1969).

Any of the aforementioned anthropogenic aerosols may serve as tracers for small- and large-scale atmospheric motions provided they can be identified with a specific source region (see, for example, analyses of aerosols in the vicinity of various industries reported by Pötzl, 1967).

Various types of aerosols have been introduced deliberately into the atmosphere to serve as tracers for local flow conditions and for diffusion experiments. The use of dyed pollen for such purposes was mentioned earlier. Fluorescent particles, which are produced in different colors (Morton, 1967), lend themselves to a wide range of applications. The most widely applied fluorescent pigment is zinc sulfide. (For a description of the characteristics of various fluorescent pigments, see Robinson et al., 1959; Gussman and Sacco, 1964; Leighton et al., 1965; Ludwick, 1966; Niemeyer and McCormick, 1968.) Concentrations of zinc sulfide can be recorded on a real-time basis, and therefore they can give a reliable indication of diffusion from a given source in field experiments (Fuquay et al., 1963; Nickola et al., 1967; Goldberg, 1968). Since the phosphorescence of some such pigments may decay with exposure to sunlight, care may have to be exercised in their use for large-scale flow experiments. Even though quantitative diffusion estimates may be impossible on such scales, qualitative information can still be obtained. Droessler et al. (1967), for instance, reported on the release of zinc sulfide in the jet stream over Australia. Some of the material was detected in air samples taken at the ground as far downstream as New Zealand. Airborne samplers also picked up fluorescent particles over a wide region during this experiment. Part of the downward transport may have occurred by precipitation processes. A certain correlation between fluorescent-particle observations at the ground and increases in ice-nuclei counts suggests that a stratospheric source of the latter may have been important (see earlier discussion of ice nuclei in this chapter). Since fluorescent particles can also be detected in precipitation, they lend themselves to tracer experiments in moist convective processes and in the control of cloud-seeding experiments (Morgan, 1967).

Large dust particles in the form of glass microspheres (100 to 200 μ in diameter) have been used to determine fallout patterns as a function of size distribution (Hage, 1961, 1964; Csanady, 1964).

Constant-density balloons can be regarded as the largest man-made tracers of atmospheric motions. They have been used successfully to portray mesoscale local circulation systems, such as the seabreeze (Hass et al., 1967), mountain waves (Wooldridge and Lester, 1969), or motions in the planetary boundary layer (Dickson and Angell, 1968; Angell, Pack, and Dickson, 1968; Angell et al., 1968; Druyan,

1968). In estimating vertical velocity components and their fluctuations from such balloon observations, we must be careful, however, since, because of the buoyant restoring forces active in proportion to the distance from the equilibrium level, the balloon trajectory will not correspond to actual air motions.

On a global scale constant-density balloons, such as the ones used in the GHOST project over the southern hemisphere, provide valuable information on Lagrangian spectra of large-scale atmospheric motions (Reiter, 1969a; Wooldridge and Reiter, 1970; Lalley and Lichfield, 1969; Solot, 1968; Lalley and Reed, 1969; Lalley, 1968). It is not clear at this time whether the seasonal shift of GHOST balloons toward the equator during autumn (of the southern hemisphere) and toward the pole in spring reflects the action of a mean meridional motion or the tendency of these balloons to congregate in the jet stream and follow its seasonal migration (Solot and Angell, 1969).

Removal of Aerosols by Precipitation

Aerosols are efficiently removed from the atmosphere by precipitation. A summary of such processes has been given by the U. S. Weather Bureau (1955), Facy (1962), Junge (1963a), the U. S. Atomic Energy Commission (1968), and others. It would exceed the scope of this report to list extensively the pertinent literature in this field.

We have already commented on the removal of pollen by rain. In more general terms, Rosinski (1967) contends that particles 1.5 to 5μ in diameter are very effectively scavenged by ice crystals in the presence of liquid water: Aerosol particles are transported in the direction of the growing ice phase (by the so-called Stefan flow) as demonstrated by Vittori and Prodi (1967) (see also Goldsmith et al., 1961; Podzimek, 1961; Vittori et al., 1969). This flow of particles toward lower water-vapor pressure, produced by bombardment of the aerosol particles by vapor molecules, is effective also in the presence of growing cloud droplets (Severynse, 1963). Aerosol particles larger than 5μ , according to Rosinski, are scavenged mainly by impact (for impact scavenging of pollen, see J. R. Starr, 1967; for mobility of particles, see Gussman, 1969). Coefficients for washout (below the cloud) and rain out (in the cloud) have been determined by Makhon'ko (1967) from the decrease of contaminant concentration in precipitation and air as a function of duration of precipitation. From his investigations it turns out that rain out of gaseous contaminants is by one order of magnitude less effective than that of aerosols. A similar conclusion might be drawn from analyses made by Khemani and Ramana Murty (1968) over Delhi, showing that Cl^-/Na^+ ratios usually are less than 1.8 in rains from convective clouds and larger than this value in precipitation from stratiform clouds. Droplets in the latter might have more time to absorb gaseous constituents. If precipitation evaporates before reaching the ground, an enrichment in aerosol concentrations may be expected. Such an effect has been observed downwind from evaporating cumulus clouds (Radke and Hobbs, 1969). The effectiveness of precipitation in removing aerosol may be seen from the

inverse seasonal variation of precipitation and of the turbidity coefficient, β , the latter being a function of the Mie scatter efficiency of aerosols (Yamamoto et al., 1968). Figure 6.70 shows the relation between these two parameters very clearly. Flowers et al. (1969), on the other hand, found no significant reduction of turbidity following precipitation over the United States. (Geographic distributions of turbidity presented by these authors point toward the influence of anthropogenic sources.) The washout effect is also evident from the changes in aerosol particle-size spectra observed by Carnuth and R. Reiter (1966) in precipitation but not in fog.

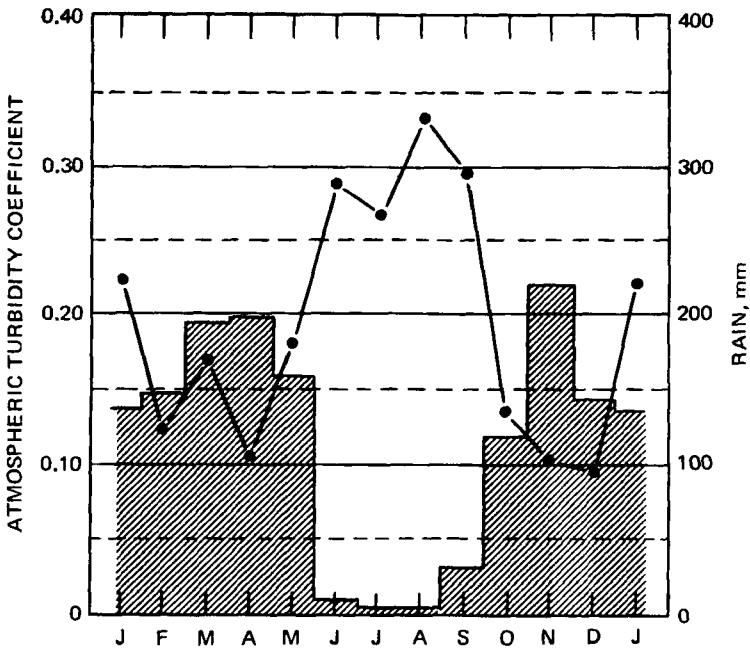


Fig. 6.70 The relation between the monthly average value of the atmospheric turbidity coefficient (●) and monthly amounts of precipitation (histogram) for Leopoldville-Binza. [From G. Yamamoto, M. Tanaka, and K. Arai, *Journal of the Meteorological Society of Japan*, 46(4): 297 (1968).]

Chemical analysis of the soluble material washed out in rain indicates that continental aerosols contribute the majority of this material in precipitation over land. [This may be inferred from an analysis of $\text{Ca}^{2+}/\text{Cl}^-$ ratios, which attain average values in excess of 20 over the desert regions of the southwestern United States and fall generally below 1 in oceanic and coastal regions (Junge and Werby, 1958; Gambell, 1962).] The industrial origin of some of the washed-out material has been ascertained by Mrose (1961) from data collected in central Europe. (For Indian data, see Handa, 1969a, 1969b.) A moderate washout effect on Aitken nuclei has been observed by Müller (1963). Local sources of such nuclei may, however, easily compensate for this

wash-out loss. Gatz et al. (1969) and Dingle et al. (1969) reported on an interesting experiment during which indium, ^{115}In , was used as a tracer for wash-out processes. The rare-earth element was released from an aircraft into a convective precipitation system with a pyrotechnical flare. Neutron activation allows a convenient identification of the tracer in precipitation samples. Further development of this or similar methods will enhance weather-modification research and the understanding of convective storm systems.

7 CONCLUSIONS AND OUTLOOK

The preceding chapters, especially those which deal with phenomena in the atmospheric layers above the stratopause, reveal one basic fact: chemists, ionospheric physicists, rocket engineers, and meteorologists have amassed a wealth of information. It is exceedingly difficult to piece these tidbits of sometimes controversial evidence together into a consistent pattern of the general circulation of the atmosphere at high altitudes, mainly because there still exists a communications gap between the aforementioned groups of scientists and investigators. The chemist is mainly concerned with reaction rates and relative concentrations of constituents; he relies heavily on laboratory simulation of the atmosphere. The ionospheric physicist deals with "plasma" problems, whereas the meteorologist concentrates on the neutral atmosphere as measured by balloons and interprets its motions in the form of trajectories. He regards the aeronomist as one who frequently lacks sufficient data from the "ignorosphere" of atmospheric strata; hence he may be hard pressed at times to distinguish fact from fiction. The rocket specialist, not infrequently, collects data that are difficult to interpret in the light of existing atmospheric "models," and therefore he is often shrugged off as one who suffers from instrumental problems.

The difficulties arising from insufficient communication between these various fields of science will rapidly be alleviated by concerted efforts for a better understanding of our environment. A number of problems will have to be solved before such an understanding can be achieved. Many observations of aerosol particle concentrations, ion densities, etc., reveal a surprisingly "layered" meso-structure of the mesosphere that reminds us of similar conditions in the troposphere as investigated,

for instance, by Danielsen (1959) and others. It seems to me that synoptically coordinated global measurements of drift velocities obtained from ionospheric sounding techniques, luminous trail experiments, falling sphere or chaff measurements, and other sensor applications could provide enough detailed information to help to unravel some of the discrepancies between observed and measured tidal motions in the upper atmosphere. Some of the observed meso- and microscale layering of tracers in the upper atmosphere could conceivably be produced by the effects of turbulent mixing on a vertical gradient of the atmospheric constituent that is being mixed, concentrating the gradient at the upper and lower boundaries of the turbulent layer (Reiter, 1968).

There are open questions of a still more basic nature. The large-scale seasonal behavior of the mesosphere is slowly beginning to emerge from the data collected in the D-region and in the sodium layer. Some of the evidence is still controversial, however, and it is even more so for the thermosphere. Gravity waves and tidal motions are heavily masking the sparse information on drift velocities and directions in this region. Small-scale diffusion, waves, tides, and large-scale mean motion all appear to work together in dispersing atmospheric trace constituents as well as atomic debris introduced into the high atmosphere. Noctilucent-cloud formation, airglow phenomena, and the possible "cloud seeding" effect by extraterrestrial particles could be explored more rigorously if the eddy scales and mean magnitudes of these upper-atmospheric transport processes were better known. The intricate photochemistry of the natural constituents complicates our quest for small- and large-scale diffusion patterns as a function of ϕ , λ , z , and t . Artificial tracers injected into a well-defined coordinate point, which could be followed over considerable distance and time, exceeding the capabilities of present luminescent trail experiments, could shed some light on these bothersome problems.

The practical impact of more sophisticated answers than presently available to the preceding problems would come mainly in the field of telecommunication, which is intimately linked to the behavior of the ionosphere. There are, however, problem areas closer to earth that warrant attention and vigorous exploration.

It has been mentioned that the Junge layer near 18 to 20 km suggests a rather distinct behavior of atmospheric flow patterns. Air masses of tropical origin tend to spread out quasi-horizontally in this altitude region, covering a wide range of geographic latitudes. The dryness of the stratosphere in this altitude range, the spread of ozone, and the intrusion of clean air after the January 1968 Chinese atomic test may be mentioned together with the aerosol distribution in support of this statement. It comes to mind that this atmospheric layer is earmarked for heavy supersonic air-transport (SST) traffic in the 1970s (Finger and McInturff, 1970). What will happen if thousands of tons of water vapor are thrust into this region of the atmosphere along narrow and heavily traveled air-traffic lanes? Will this vapor eventually accumulate faster than it can be removed by small-scale diffusion and by large-scale eddy transport processes? Will it spread out horizontally, causing a blanket of relatively high moisture content? What will be the effects of such a blanket on the

atmospheric radiation balance? Clearly the assumptions by Manabe and Wetherald (1967) of a uniform water-vapor distribution in the stratosphere will have to be abandoned in such an estimate. Will the Junge aerosol, which in all likelihood is hygroscopic, absorb this excess moisture and thereby grow in size to form a haze layer that might have effects on atmospheric transmissivity similar to those of volcanic debris after heavy eruptions? Will the Junge aerosol, if increased in size by water absorption, settle at a faster rate than at present, and could the Junge layer, from such an effect, disappear entirely?

To answer these questions, we have to find out more about the behavior of the eddy diffusion coefficients K_{zz} , K_{yy} , and K_{yz} in this region as a function of height, season, and scale. Accurate wind measurements on a global basis will help in estimating the effects of large-scale eddy processes on the dispersion of atmospheric trace constituents. More reliable information, however, could be obtained from experiments using artificial tracers released into this region from well-known point sources or by the deployment of constant-density balloons. Numerical models of the general circulation should be checked against the results of such tracer experiments. Finally, the effects of water vapor introduced into the Junge layer along air-traffic corridors upon the radiation balance and upon atmospheric circulation patterns should be estimated from numerical-model experiments.

It is needless to say that such an investigation will have to be carried out on a global basis since the pollution to be expected from SST traffic will also have global dimensions. Research efforts along these lines may well be incorporated into a "Global Atmospheric Research Project." A "Global Atmospheric Tracer Experiment," if properly executed, not only appears feasible in exploring the puzzling details of the 20-km region but also may yield scientific data not otherwise attainable from routine observation networks.

Not only is our knowledge of transport processes vague in the 20-km region of the stratosphere but also it is lacking in detail even in the region near the tropopause. Many studies have followed the intrusions of radioactive debris, of ozone, and even of stratospheric sulfate into the troposphere via the "tropopause gap" near well-developed jet streams. The return-flow processes of tropospheric air, which, for reasons of continuity, replenish the stratospheric reservoir, are less well understood. At least part of the return flow, it seems, is accomplished by intrusions of (moist) tropospheric air into the stratosphere within the same jet-stream systems that cause the stratosphere-to-troposphere mass flow. This specific return-flow mechanism, however, does not tell the whole story. A considerable amount of tropospheric air may seep into the stratosphere through the rising branch of the Hadley cell in tropical latitudes. Again, the detailed behavior of the Junge layer, and especially mass-flow estimates in this layer, will have a significant bearing on the solution of the return-flow problem. Tracer experiments in the upper tropical troposphere as well as in jet streams of extratropical latitudes could conceivably yield information on the relative importance of these two return-flow processes. The water-vapor and ozone budgets of the stratosphere could be balanced more satisfactorily if the transport processes in the tropopause region were better known on a global basis.

Last, but not least, there are many important problem areas that have not even been touched upon in this review. Among them is the question of the chemical interaction of anthropogenic pollutants with themselves and with atmospheric constituents which allows for the full range of meteorological variables: radiation, temperature, pressure, concentrations, turbulence conditions, and precipitation in various forms. Application of atmospheric transport processes thus plays a fundamental role in air-pollution research, which has become a prime area of concern for our generation.

LIST OF SYMBOLS

NOTE: In order to keep with the standard notation used in meteorological literature, I have used one symbol to signify different variables. Confusion is avoided by proper explanation in the text.

$[B]_{(i)}$	Quantity "B" averaged over coordinate "i"
$[N]$	Concentration of chemical constituent "N"
A	Area
a	Constant
b	Exponent
$b(\mu)$	Amplitude factor
C	Speed of sound
c	Concentration of tracer; constant
c_p	Specific heat at constant pressure
c_v	Specific heat at constant volume
$D(\Delta h)$	Structure function
d_0	Exchange rate
$F_{(n)}$	Normalized spectrum function
F_y, F_z	Flux of tracer
f	Coriolis parameter
g	Acceleration of gravity
H	Scale height of atmosphere
Δh	Height increment
J_i	Dissociation rates
K	Exchange coefficient

K_E	Kinetic energy
$K_{yy}, K_{yz},$ K_{zy}, K_{zz}	Eddy diffusion coefficients
k	Wave number
k_i	Reaction rates
k_x, k_z	Horizontal and vertical wave numbers
L_{\min}	Minimum transport distance of aerosol
l	Scale of motion; observed solar radiation; microscale of turbulence
l'	Solar radiation in dust-free atmosphere
l_0	Solar constant
l_y, l_z	Horizontal and vertical mixing lengths
N	Refractivity of radio waves
n	Hemispheric wave number; frequency (cycles per hour); number of observations
P	Potential vorticity
p	Pressure; exponent
Q	Source release rate (e.g., g/sec); source function
Q_z	Vertical component of absolute vorticity
R	Gas constant
$R(\tau)$	Autocorrelation function with time lag τ
r	Particle radius
S	Source function
s	Arbitrary parameter; specific humidity; sinking velocity of particle
T	Linke turbidity factor; absolute temperature
t	Time coordinate
U	Wind component normal to mountain ridge
u	Cartesian wind-speed component, positive toward east
V	Total speed
V_ℓ	Wind-speed component along mixing path ℓ
v	Cartesian wind-speed component, positive toward north
w	Cartesian wind-speed component, positive upward
X_r	Distance along x of diffusing particles from center of gravity of cluster
x	Cartesian coordinate, positive eastward
Y_r	Distance along y of diffusing particles from center of gravity of cluster
y	Cartesian coordinate, positive northward
z	Cartesian coordinate, positive upward
α	Slope angle of mixing path; exponent
β	Exponent
Γ	$(1/\rho)/(\partial\rho/\partial z)$; gamma function
γ	$(c_p/c_v) = 1.4$ ratio of specific heats
γ_s	Dimensionless constant
ϵ	Rate of dissipation
η	Kolmogorov microscale of turbulence
θ	Potential temperature

κ	Poisson's constant
λ	Geographic longitude
λ_x, λ_z	Horizontal and vertical wavelengths
μ	$\sin \phi$
ν	Coefficient of viscosity
ρ	Density
Σ, Σ_M	Lidar backscatter
σ^2	Variance of particle dispersion
σ_H^2	Variance of height fluctuations
σ_u, σ_v	Standard deviations of velocity component fluctuations
σ_y, σ_z	Standard deviations of displacement of particles
τ	Time lag in correlation function; time of half restoration of chemical equilibrium; tropospheric residence time
$\phi_{cc}(k)$	Energy spectrum of wind as a function of wave number
$\phi_{HH}(k)$	Spectrum function of geopotential height
ϕ	Geographic latitude
χ	(c/ρ) = mixing ratio of tracer
χ_w	Water-vapor mixing ratio
ψ	Zenith angle

REFERENCES

- Abel, N., P. Winkler, and C. E. Junge, 1969, Studies of Size Distributions and Growth with Humidity of Natural Aerosol Particles, final scientific report, Max-Planck-Institut für Chemie, Mainz, Germany.
- Ahmed, S. J., and A. Halim, 1961, Total Atmospheric Ozone and Geomagnetic Activity, *J. Geophys. Res.*, **66**(10): 3213-3218.
- Air Conservation Commission, 1965, Air Conservation, American Association for the Advancement of Science, Publication No. 80.
- Akasofu, S.-I., and S. Chapman, 1963, The Enhancement of the Equatorial Electrojet During Polar Magnetic Substorms, *J. Geophys. Res.*, **68**(9): 2375-2382.
- Albee, P. R., and D. P. Kanellakos, 1968, A Spatial Model of the F-Region Ionospheric Traveling Disturbance Following a Low-Altitude Nuclear Explosion, *J. Geophys. Res.*, **73**(3): 1039-1053.
- Albritton, D. L., L. C. Young, H. D. Edwards, and J. L. Brown, 1962, Position Determination of Artificial Clouds in the Upper Atmosphere, Report AFCRL-62-826, pp. 81-86, Air Force Cambridge Research Laboratories.
- Aldaz, L., 1965, Atmospheric Ozone in Antarctica, *J. Geophys. Res.*, **70**(8): 1767-1773.
- , 1969, Flux Measurements of Atmospheric Ozone Over Land and Water, *J. Geophys. Res.*, **74**(28): 6943-6976.
- Alexander, W. M., C. W. McCracken, L. Secretan, and O. E. Berg, 1963, Review of Direct Measurements of Interplanetary Dust from Satellites and Probes, in *Space Research, III*, W. Priester (Ed.), pp. 891-917, North-Holland Publishing Co., Amsterdam.
- Allen, C. W., 1946, The Spectrum of the Corona at the Eclipse of 1940, October 1, *Mon. Notices, Roy. Astron. Soc.*, **106**: 137-150.
- Altshuller, A. P., 1958, Natural Sources of Gaseous Pollutants in the Atmosphere, *Tellus*, **10**(4): 479-492.
- American Meteorological Society, 1968, Proceedings of the First National Conference on Weather Modification, April 28–May 1, 1968, Albany, New York.

- Anderson, A. D., and W. Francis, 1966, The Variation of the Neutral Atmospheric Properties with Local Time and Solar Activity from 100 to 10,000 km, *J. Atmos. Sci.*, 23(1): 110-124.
- Angell, J. K., and J. Korshover, 1964, Quasi-Biennial Variations in Temperature, Total Ozone, and Tropopause Height, *J. Atmos. Sci.*, 21(5): 479-492.
- , and J. Korshover, 1965, A Note on the Variation with Height of the Quasi-Biennial Oscillation, *J. Geophys. Res.*, 70(16): 3851-3856.
- , and J. Korshover, 1967, Biennial Variation in Springtime Temperature and Total Ozone in Extratropical Latitudes, *Mon. Weather Rev.*, 95(11): 757-762.
- , and J. Korshover, 1968, Additional Evidence for Quasi-Biennial Variations in Tropospheric Parameters, *Mon. Weather Rev.*, 96(11): 778-784.
- , J. Korshover, and G. F. Cotten, 1969, Quasi-Biennial Variations in the "Centers of Action," *Mon. Weather Rev.*, 97(12): 867-872.
- , D. H. Pack, and C. R. Dickson, 1968, A Lagrangian Study of Helical Circulations in the Planetary Boundary Layer, *J. Atmos. Sci.*, 25(5): 707-717.
- , D. H. Pack, W. A. Hass, and W. H. Hoecker, 1968, Tetroon Flights Over New York City, *Weather*, 23(5): 184-191.
- Anonymous, 1958, Current Data on CO₂ in Scandinavia, *Tellus*, 10(1): 176; (2): 287-288; (3): 407-408; (4): 506-507.
- , 1959, CO₂ Values in Scandinavia, *Tellus*, 11(1): 145-146; (2): 265-266; (3): 373.
- , 1960, CO₂ Values in Scandinavia, May-July 1959, *Tellus*, 12(1): 119.
- , 1966, Atmospheric Emissions from Nitric Acid Manufacturing Processes, U. S. Department of Health, Education, and Welfare, Public Health Service, Division of Air Pollution, Cincinnati, Ohio.
- , 1969, Volcanic Aerosols, *NCAR (Nat. Cent. Atmos. Res.) Quart.*, No. 22.
- Appleman, H. S., 1963, The Climatological Wind and Wind Variability Between 45 and 60 Kilometers, *J. Geophys. Res.*, 68(12): 3611-3617.
- Armendariz, M., and L. J. Rider, 1966, Wind Shear for Small Thickness Layers, *J. Appl. Meteorol.*, 5(6): 810-815.
- Armstrong, E. B., 1963a, Observations of Luminous Clouds Produced in the Upper Atmosphere by Exploding Grenades. I. Atomic Emission, *Planet. Space Sci.*, 11: 733-742.
- , 1963b, Observations of Luminous Clouds Produced in the Upper Atmosphere by Exploding Grenades. II. Emission of A10 Bands from Sunlit Clouds, *Planet. Space Sci.*, 11: 743-750.
- , 1963c, Observations of Luminous Clouds Produced in the Upper Atmosphere by Exploding Grenades. III. Continuous Spectra from Night-Time Glows, *Planet. Space Sci.*, 11: 751-758.
- Arsdel, E. P. van, 1967, The Nocturnal Diffusion and Transport of Spores, *Phytopathology*, 57(11): 1221-1229.
- Astapenko, P. D., 1964, Atmospheric Processes in the High Latitudes of the Southern Hemisphere (translated from Russian: Izdatel'stvo Akademii Nauk SSSR Moskva, 1960), Israel Program for Scientific Translations, Jerusalem.
- Atlas, D., et al., 1966, Tropopause Detected by Radar, Instrumentation Paper No. 120, Report AF-CRL-66-714, Air Force Cambridge Research Laboratories.
- Attmannspacher, W., 1963, Project Cell Structure of the Atmosphere, Scientific Report No. 2, Deutscher Wetterdienst, Zentralamt, Offenbach a.M.
- Authier, B., 1964, Mesures de température de l'ionosphère a partir de la fluorescence de molécules produites artificiellement au moyen de fusées, *Ann. Geophys.*, 20(4): 353-382.
- , 1965, Fluorescence crépusculaire du monoxyde d'aluminium formé par émission ionosphérique de triméthyl aluminium, *Ann. Geophys.*, 21(2): 273-275.
- Azcarraga, A., and L. S. Muniosguren, 1969, Meteorological Rockets in Spain, in *Stratospheric Circulation*, W. L. Webb (Ed.), pp. 519-527, Academic Press, Inc., New York.
- Bainbridge, A. E., H. E. Suess, and I. Friedman, 1961, Isotropic Composition of Atmospheric Hydrogen and Methane, *Nature*, 192: 648.
- Baker, D. J., and R. O. Waddoups, 1967, Rocket Measurement of Midlatitude Night Airglow Emissions, *J. Geophys. Res.*, 72(19): 4881-4885.

- , and R. O. Waddoups, 1968, Correction to paper by D. Baker and R. Waddoups, Rocket Measurement of Midlatitude Night Airglow Emissions, *J. Geophys. Res.*, 73(7): 2546-2547.
- Ball, R. J., and H. A. Panofsky, 1967, Air Pollution at Johnstown, Pennsylvania, Final Report, College of Earth and Mineral Sciences Experiment Station, Public Health Service.
- Ballard, N., R. Valenzuela, M. Izquierdo, J. S. Randhawa, R. Morla, and J. F. Bettle, 1969, Solar Eclipse: Temperature, Wind and Ozone in the Stratosphere, *J. Geophys. Res.*, 74(2): 711-712.
- Ballif, J. R., and S. V. Venkateswaran, 1962, A Study of Hydroxyl (OH) and Sodium (Na) Emission from the Night Sky, Report, Institute of Geophysics and Planetary Physics, University of California, May.
- Bandermann, L. W., and S. F. Singer, 1969, Interplanetary Dust Measurements Near the Earth, *Rev. Geophys.*, 7(4): 759-797.
- Bangerl, A., and F. Steinhauser, 1959, Die Verteilung des SO₂-Gehaltes der Luft im Stadtgebiet von Wien, *Arch. Meteorol., Geophys. Bioklimatol.*, 10: 132-153.
- Bannon, J. K., R. Frith, and H. C. Shellard, 1952, Humidity of the Upper Troposphere and Lower Stratosphere over Southern England, *Geophys. Memoirs*, No. 88.
- , and L. P. Steele, 1960, Average Water-Vapour Content of the Air, *Geophys. Memoirs*, No. 102.
- Barat, J., and J. Blamont, 1969, Structure of the Turbulent Field From 90 to 120 Km, in *Atmospheric Emissions*, B. M. McCormac and A. Omholt (Eds.), pp. 507-514, Van Nostrand-Reinhold Co., New York.
- Barbier, D., 1965a, Variations de l'intensité des principales radiations de la luminescence atmosphérique nocturne avec le cycle solaire, *Ann. Geophys.*, 21(2): 265.
- , 1965b, La lumière du ciel nocturne aux îles kerguelen, *Ann. Geophys.*, 21(3): 299-302.
- , J. Volut, and J. Pelissier, 1963, Observations de la lumière du ciel nocturne aux îles kerguelen, *Ann. Geophys.*, 19(2): 184-187.
- Barclay, F. R., M. J. W. Elliott, P. Goldsmith, and J. V. Jelley, 1960, A Direct Measurement of the Humidity in the Stratosphere Using a Cooled Vapour Trap, *Quart. J. Roy. Meteorol. Soc.*, 86(368): 259-264.
- Barnes, A. A., Jr., 1961, The General Circulation of the Stratosphere, in *Radioactive Fallout from Nuclear Weapons*, p. 204, USAEC Report TID-7632.
- , 1968a, Winds and Densities from Radar Meteor Trail Returns, 80 to 120 km, *Meteorol. Monogr.*, 9(31): 190-195.
- , 1968b, The Application of Radar Meteor Trail Data to Aerospace Operational Problems, in *Proceedings of the Third National Conference on Aerospace Meteorology, New Orleans, La., May 6-9*, pp. 169-172, American Meteorological Society, Boston, Mass.
- , and J. J. Pazniokas, 1968, Proceedings of the Workshop on Methods of Obtaining Winds and Densities from Radar Meteor Trail Returns, Special Report No. 75, Report AFCRL-68-0228, Air Force Cambridge Research Laboratories.
- Barrett, E. W., and O. Ben-Dov, 1967, Application of Lidar to Air Pollution Measurements, *J. Appl. Meteorol.*, 6(3): 500-515.
- , L. R. Herndon, and H. J. Carter, 1950, Some Measurements of the Distribution of Water Vapour in the Stratosphere, *Tellus*, 2(4): 302-311.
- Bartel, A. W., and J. W. Temple, 1952, Ozone in Los Angeles and Surrounding Areas, *Ind. Eng. Chem.*, 44: 857-861.
- Barth, Ch. A., 1964, Three-Body Reactions, *Ann. Geophys.*, 20(2): 182-196.
- , 1966, Rocket Measurement of Nitric Oxide in the Upper Atmosphere, *Planet. Space Sci.*, 14: 623-630.
- Bary, E. de, and K. Bullrich, 1961, Einfluss der Aerosolgrößenverteilung auf die Intensität der gestreuten Strahlung eines Luftvolumens, *Z. Meteorol.*, 15: 55.
- , and F. Rössler, 1966, Size Distributions of Atmospheric Aerosols Derived from Scattered Radiation Measurements Aloft, *J. Geophys. Res.*, 71(4): 1011-1016.

- Batchelor, G. K., 1950, The Application of the Similarity Theory of Turbulence to Atmospheric Diffusion, *Quart. J. Roy. Meteorol. Soc.*, **76**(328): 133-146.
- Bates, D. R., and P. B. Hayes, 1967, Atmospheric Nitrous Oxide, *Planet. Space Sci.*, **15**: 189-197.
- , and M. Nicolet, 1950, The Photochemistry of Atmospheric Water Vapor, *J. Geophys. Res.*, **55**(3): 301-327.
- , and M. Nicolet, 1965, Atmospheric Hydrogen, *Planet. Space Sci.*, **13**: 905-909.
- Batey, P. H., G. R. Court, and J. Sayers, 1965, Afterglow Measurements of the Rate Coefficients for the Reactions $O^+ + O_2 \rightarrow O_2^+ + O$ and $O^+ + N_2 \rightarrow NO^+ + N$, *Planet. Space Sci.*, **13**: 911-917.
- Battan, L. J., and J. J. Riley, 1960, Ice-Crystal Nuclei and Maritime Air, *J. Meteorol.*, **17**(6): 675-676.
- Batten, E. S., 1961, Wind Systems in the Mesosphere and Lower Ionosphere, *J. Meteorol.*, **18**(3): 283-291.
- Bcan, B. R., 1966, Radio Studies of Atmospheric Water Vapor, dissertation, Colorado State University, May 1966.
- , B. A. Cahoon, C. A. Samson, and G. D. Thayer, 1966, *A World Atlas of Atmospheric Radio Refractivity*, ESSA Monograph 1, U. S. Government Printing Office, Washington.
- Beard, D. B., 1959, Interplanetary Dust Distribution, *Astrophys. J.*, **129**: 496-506.
- Beaudoin, P. E., D. Golomb, T. M. Noel, N. W. Rosenberg, and W. K. Vickery, 1967, Observation of Mesosphere Winds and Turbulence with Smoke Trails, *J. Geophys. Res.*, **72**(14): 3729-3733.
- Bedinger, J. F., 1966, Compendium of Wind Data from the Vapor Trail Technique, G.C.A. Report 66-7-N, NASA Contract NASW-1083, March.
- Begemann, F., 1963, The Tritium Content of Atmospheric Hydrogen and Atmospheric Methane, in *Earth Science and Meteoritics*, J. Geiss and E. D. Goldberg (Eds.), pp. 169-187, North-Holland Publishing Co., Amsterdam.
- , and I. Friedman, 1968a, Tritium and Deuterium in Atmospheric Methane, *J. Geophys. Res.*, **73**(4): 1149-1153.
- , and I. Friedman, 1968b, Isotopic Composition of Atmospheric Hydrogen, *J. Geophys. Res.*, **73**(4): 1139-1147.
- Beilke, S., and H.-W. Georgii, 1968, Investigation on the Incorporation of Sulfur Dioxide into Fog- and Rain-Droplets, *Tellus*, **20**(3): 435-442.
- Belmont, A. D., L. W. Engberg, D. G. Dartt, W. C. C. Shen, and D. N. Hovland, 1969, Mean Circulation Features of the Equatorial Stratosphere, Final Report, Control Data Corp., Minneapolis.
- , G. W. Nicholas, and W. C. Shen, 1968, Comparison of 15- μ TIROS VII Data with Radiosonde Temperatures, *J. Appl. Meteorol.*, **7**(2): 284-289.
- Belrose, J. S., 1967, The "Berlin" Warming, *Nature*, **214**: 660-664.
- Benson, S. W., and A. E. Axworthy, 1965, Reconsiderations of the Rate Constants from the Thermal Decomposition of Ozone, *J. Chem. Phys.*, **42**: 2614-2615.
- Berenger, M., 1963, Contribution à l'étude des lithométéores, *La Meteorol.*, **72**: 347-374.
- Berger, R., and W. F. Libby, 1969, Equilibration of Atmospheric Carbon Dioxide with Seawater: Possible Enzymatic Control of Rate, *Science*, **164**(3886): 1395-1397.
- Berggren, R., 1965, The Vertical Distribution of Ozone over Arosa on 16 April, 1962, and the Synoptic Situation, *Tellus*, **17**(2): 180-193.
- , and K. Labitzke, 1966, A Detailed Study of the Horizontal and Vertical Distribution of Ozone, *Tellus*, **18**(4): 761-772.
- , and K. Labitzke, 1968, The Distribution of Ozone on Pressure Surfaces, *Tellus*, **20**(1): 88-97.
- Berson, F. A., and R. N. Kulkarni, 1968, Sunspot Cycle and the Quasi-Biennial Oscillation, *Nature*, **217**: 1133-1134.
- Beyers, N. J., and B. T. Miers, 1965, Diurnal Temperature Change in the Atmosphere Between 30 and 60 Km over White Sands Missile Range, *J. Atmos. Sci.*, **22**(3): 262-266.

- , and B. T. Miers, 1968, A Tidal Experiment in the Equatorial Stratosphere over Ascension Island, *J. Atmos. Sci.*, **25**(1): 155-159.
- , B. T. Miers, and R. J. Reed, 1966, Diurnal Tide Motions near the Stratopause During 48 Hours at White Sands Missile Range, *J. Atmos. Sci.*, **23**(3): 325-333.
- Bhandari, N., R. Arnold, and D. W. Parkin, 1968, Cosmic Dust in the Stratosphere, *J. Geophys. Res.*, **73**(5): 1837-1845.
- Biermann, L., 1967, Theoretical Considerations of Small Particles in Interplanetary Space, Report NASA-SP-150, pp. 279-286, National Aeronautics and Space Administration.
- Bigg, E. K., 1964, Atmospheric Stratification Revealed by Twilight Scattering, *Tellus*, **16**(1): 76-83.
- , 1967, Cross-Sections of Ice Nucleus Concentrations at Altitude over Long Paths, *J. Atmos. Sci.*, **24**(2): 226-229.
- , and J. Giutronich, 1967, Ice Nucleating Properties of Meteoric Material, *J. Atmos. Sci.*, **24**(1): 46-49.
- , and G. T. Miles, 1963, Stratospheric Ice Nucleus Measurements from Balloons, *Tellus*, **15**(2): 162-166.
- , and G. T. Miles, 1964, The Results of Large-Scale Measurements of Natural Ice Nuclei, *J. Atmos. Sci.*, **21**(4): 396-403.
- Bird, I., G. Cresswell, J. Humble, D. Norris, and E. K. Bigg, 1961, Atmospheric Ice Nuclei in High Southern Latitudes, *J. Meteorol.*, **18**(4): 563-564.
- Bischof, W., 1960, Periodical Variations of the Atmospheric CO₂ Content in Scandinavia, *Tellus*, **12**(2): 216-226.
- , 1962, Variations in Concentrations of Carbon Dioxide in the Free Atmosphere, *Tellus*, **14**(1): 87-90.
- , 1965, Carbon Dioxide Concentrations in the Upper Troposphere and Lower Stratosphere. I, *Tellus*, **17**(3): 398-402.
- , and B. Bolin, 1966, Space and Time Variations of the CO₂ Content of the Troposphere and Lower Stratosphere, *Tellus*, **18**(2-3): 155-159.
- Bishop, K. F., H. J. Delafield, A. E. Eggleton, C. O. Peabody, and B. T. Taylor, 1962, The Tritium Content of Atmospheric Methane, in *Tritium in the Physical and Biological Sciences*, Symposium Proceedings, Vienna, 1961, pp. 1-55, International Atomic Energy Agency, Vienna, 1962 (STI/PUB/39).
- Blackwell, D. E., and M. F. Ingham, 1961, Observations of the Zodiacal Light from a Very High Altitude Station, Pts. I-III, *Mon. Notices, Roy. Astron. Soc.*, **122**: 113-165.
- Blamont, J. E., and J. Barat, 1967, Introduction d'un modèle pour la structure des mouvements de l'atmosphère entre 85 et 110 km d'altitude, *Ann. Geophys.*, **23**(2): 173-195.
- , and T. M. Donahue, 1964, Sodium Dayglow: Observation and Interpretation of a Large Diurnal Variation, *J. Geophys. Res.*, **69**(19): 4093-4127.
- , and C. de Jager, 1961, Upper Atmospheric Turbulence near the 100 Km Level, *Ann. Geophys.*, **17**: 134-144.
- , H. Teitelbaum, and J. Barat, 1968, L'échelle interne de la turbulence atmosphérique de 80 à 100 km déterminée à partir de la fonction de structure des inhomogénéités (1), *Ann. Geophys.*, **24**(1): 115-122.
- Blankenship, J. R., and P. J. Crutzen, 1966, A Photochemical Model for the Space-Time Variations of the Oxygen Allotropes in the 20 to 100 Km Layer, *Tellus*, **18**(2-3): 160-175.
- Blifford, I. H., Jr., and L. D. Ringer, 1969, The Size and Number Distribution of Aerosols in the Continental Troposphere, *J. Atmos. Sci.*, **26**(4): 716-726.
- Blumen, W., and R. G. Hendl, 1969, On the Role of Joule Heating as a Source of Gravity-Wave Energy Above 100 Km, *J. Atmos. Sci.*, **26**(2): 210-217.
- Boer, G. J., Jr., and J. R. Mahoney, 1968, Further Results on the Velocity Structure in the 30-60 Km Region Deduced from Paired Robin Soundings, Final Scientific Report to AFCRL, Massachusetts Institute of Technology.

- Bojkov, R. D., 1966, Differences in the Vertical Ozone Distribution Deduced from Umkehr and Ozonesonde Data at Goose Bay, *J. Appl. Meteorol.*, 5(6): 872-877.
- , 1967a, The Vertical Distribution of Atmospheric Ozone and Some Relationship Between Its Variations and the Total Ozone Amount, *Z. Meteorol.*, 19(11-12): 355-362.
- , 1967b, Vertical Ozone Distribution over South Africa, *J. Geophys. Res.*, 72(22): 5585-5593.
- , 1968a, The Ozone Variations During the Solar Eclipse of 20 May 1966, *Tellus*, 20(3): 417-421.
- , 1968b, Mean Pole-to-Pole Vertical Ozone Distribution, McGill University, *Meteorology*, 90: 221-240.
- , 1969a, Differences in Dobson Spectrophotometer and Filter Ozonometer Measurements of Total Ozone, *J. Appl. Meteorol.*, 8(3): 362-368.
- , 1969b, Computing the Vertical Ozone Distribution from Its Relationship with Total Ozone Amount, *J. Appl. Meteorol.*, 8(2): 284-292.
- , and A. D. Christie, 1966, Vertical Ozone Distribution over New Zealand, *J. Atmos. Sci.*, 23(6): 791-798.
- Bolin, B., 1959, Note on the Exchange of Iodine Between the Atmosphere, Land and Sea, *Int. J. Air Pollution*, 2: 127-131.
- , 1960, On the Exchange of Carbon Dioxide Between the Atmosphere and the Sea, *Tellus*, 12(3): 274-281.
- , 1964, Gross-Atmospheric Circulation as Deduced from Radioactive Tracers, *Research in Geophysics*, Vol. 2, pp. 479-508, M.I.T. Press, Cambridge, Mass.
- , 1966, Forändringar av Lufthavets Koldioxidhalt-ett Globalt Luftfororeningsproblem (Changes of the Carbon Dioxide Content of the Atmosphere—a Global Air Pollution Problem), Naturvetenskap, Stockholm, Sweden.
- , and E. Eriksson, 1959, Changes in the Carbon Dioxide Content of the Atmosphere and Sea Due to Fossil Fuel Combustion, *Rosby Memorial Volume*, B. Bolin (Ed.), pp. 130-142, Rockefeller Institute Press and Oxford University Press.
- , and C. D. Keeling, 1963, Large-Scale Atmospheric Mixing as Deduced from the Seasonal and Meridional Variations of Carbon Dioxide, *J. Geophys. Res.*, 68(13): 3899-3920.
- Bolle, H. J., 1965, Stratospheric Water Vapor Determination by Absorption in Single Lines, *Beitr. Phys. Atmos.*, 38: 41-50.
- Bossolasco, M., and G. Cicconi, 1961, Vergleichende Untersuchungen über die chemische Zusammensetzung des Luft und des Niederschlages, *Geofis. Pura Appl.*, 50: 81-93.
- , and A. Elena, 1960, The Anomalous Ionospheric Absorption on Winter Days, *Geofis. Pura Appl.*, 47(3): 89-100.
- , and A. Elena, 1963, Absorption de la couche D et temperature de la mesosphere, *Compt. Rend., Ser. B*, 256: 4491-4493.
- Bosua, T. A., 1963, Die Invloed van die stoflag van vulkamese corsprong op die Sonstraling ontvage te Pretonia, *Newsletter*, No. 172, pp. 113-116, Republic of South Africa Weather Bureau.
- Boville, B. W., 1966, Planetary Waves in the Stratosphere and Their Upward Propagation, *Space Research*, VII, pp. 20-29, North-Holland Publishing Co., Amsterdam.
- , and F. K. Hare, 1961, Total Ozone and Perturbations in the Middle Stratosphere, *Quart. J. Roy. Meteorol. Soc.*, 87(374): 490-501.
- , and F. K. Hare, 1963, Total Ozone and Perturbations in the Middle Stratosphere, *Quart. J. Roy. Meteorol. Soc.*, 89(379): 157-159.
- Bowen, E. G., 1953, The Influence of Meteoritic Dust on Rainfall, *Aust. J. Phys.*, 6: 490-497.
- , 1956, The Relation Between Rainfall and Meteor Showers, *J. Meteorol.*, 13(2): 142-151.
- Bowman, G. G., 1968, Movements of Ionospheric Irregularities and Gravity Waves, *J. Atmos. Terrest. Phys.*, 30(5): 721-734.
- Brabets, R. I., 1963, Ozone Measurement Survey in Commercial Jet Aircraft, Technical Report ADS-5, pp. 1-54, Illinois Institute of Technology Research Institute Technical Center, Chicago, Ill.

- Bray, J. R., 1959, An Analysis of the Possible Recent Change in Atmospheric Carbon Dioxide Concentration, *Tellus*, 11(2): 220-230.
- Breiland, J. G., 1964, Vertical Distribution of Atmospheric Ozone and Its Relation to Synoptic Meteorological Conditions, *J. Geophys. Res.*, 69(18): 3801-3808.
- , 1965, A Case Study of the Vertical Distribution of Atmospheric Ozone, *J. Appl. Meteorol.*, 4(3): 357-364.
- , 1967, Comparison of the Vertical Distribution of Thermal Stability in the Lower Stratosphere with the Vertical Distribution of Atmospheric Ozone, *J. Atmos. Sci.*, 24(5): 569-576.
- , 1968, Some Large-Scale Features of the Vertical Distribution of Atmospheric Ozone Associated with the Thermal Structure of the Atmosphere, *J. Geophys. Res.*, 73(16): 5021-5028.
- , 1969, Variations in the Vertical Distribution of Atmospheric Ozone During the Passage of a Short Wave in the Westerlies, *J. Geophys. Res.*, 74(18): 4501-4510.
- , and H. T. May, 1969, Vertical Distributions of Ozone over Albuquerque, New Mexico, Department of Physics and Astronomy, The University of New Mexico, Sept. 15, 1969.
- Breitling, W. L., and R. A. Kupferman, 1967, Traveling Ionospheric Disturbances Associated with Nuclear Detonations, *J. Geophys. Res.*, 72(1): 307-315.
- Brewer, A. W., 1949, Evidence for a World Circulation Provided by the Measurements of Helium and Water Vapour Distribution in the Stratosphere, *Quart. J. Roy. Meteorol. Soc.*, 75(326): 351-363.
- , 1960, The Transfer of Atmospheric Ozone into the Troposphere, Scientific Report, Planetary Circulations Project, Massachusetts Institute of Technology.
- , 1966, The Rate of Production of Ozone in the Lower Stratosphere, *Meteorol.*, 80: 195-198.
- , K. P. B. Thomson, and A. W. Wilson, 1966, Scattered Ultraviolet Light in the Stratosphere, *Quart. J. Roy. Meteorol. Soc.*, 92(393): 415.
- , and A. W. Wilson, 1965, Measurements of Solar Ultraviolet Radiation in the Stratosphere, *Quart. J. Roy. Meteorol. Soc.*, 91(390): 452-461; 93(396): 267.
- , and A. W. Wilson, 1968, The Regions of Formation of Atmospheric Ozone, *Quart. J. Roy. Meteorol. Soc.*, 94(401): 249-265.
- Bricard, J., F. Billard, and G. Madelaine, 1968, Formation and Evolution of Nuclei of Condensation that Appear in Air Initially Free of Aerosols, *J. Geophys. Res.*, 73(14): 4487-4496.
- Brier, G. W., and D. B. Kline, 1959, Ocean Water as a Source of Ice Nuclei, *Science*, 130(3377): 717-718.
- Briggs, J., and W. T. Roach, 1963, Aircraft Observations Near Jet Streams, *Quart. J. Roy. Meteorol. Soc.*, 89(380): 225-247.
- Broadfoot, A. L., 1967, Twilight Ca^+ Emission from Meteor Trails up to 280 Km, *Planet. Space Sci.*, 15: 503-514.
- , and K. R. Kendall, 1968, The Airglow Spectrum, 3,100–10,000 Å, *J. Geophys. Res.*, 73(1): 426-428.
- Brocas, J., and E. Picciotto, 1967, Nickel Content of Antarctic Snow: Implications of the Influx Rate of Extraterrestrial Dust, *J. Geophys. Res.*, 72(8): 2229-2236.
- Brousailles, F. J., and J. F. Morrissey, 1967, Stratospheric Humidity Sensing with the Alpha Radiation Hygrometer, Instrumentation Paper No. 133, Report AFCRL-67-0604, Air Force Cambridge Research Laboratories.
- Brown, C. W., and C. D. Keeling, 1965, The Concentration of Atmospheric Carbon Dioxide in Antarctica, *J. Geophys. Res.*, 70(24): 6077-6086.
- Brown, F., P. Goldsmith, H. F. Green, A. Holt, and A. G. Parham, 1961, Measurements of the Water Vapour, Tritium and Carbon-14 Content of the Middle Stratosphere over Southern England, *Tellus*, 13(3): 407-416.
- Bryson, R. A., 1968, All Other Factors Being Constant. . ., *Weatherwise*, 21: 56-61.

- Buch, H. S., 1954, Hemispheric Wind Conditions During the Year 1950, Final Report, Part 2, Massachusetts Institute of Technology.
- Buell, C. E., 1958, The Correlation Between Wind and Height on an Isobaric Surface, *J. Meteorol.*, 15(3): 309-316.
- , 1960, The Structure of Two-Point Wind Correlations in the Atmosphere, *J. Geophys. Res.*, 65(10): 3353-3366.
- Buettner, K. J. K., 1967, Valley Wind, Sea Breeze, and Mass Fire: Three Cases of Quasi-Stationary Airflow, *Proceedings of the Symposium on Mountain Meteorology, June 26, 1967, Fort Collins, Colorado*, Atmospheric Science Paper No. 122, pp. 103-129, Colorado State University.
- , J. Businger, and R. Charlson, 1962, Discussion of paper by J. Kroening and E. P. Ney, "Atmospheric Ozone," *J. Geophys. Res.*, 67(11): 4508-4509.
- Bull, G. A., 1951, Blue Sun and Blue Moon, *Meteorol. Mag.*, 80(943): 1-4.
- Bullock, W. R., and D. M. Hunten, 1961, Vertical Distribution of Sodium in the Upper Atmosphere, *Can. J. Phys.*, 39: 976.
- Bureau of Census, 1967, *Statistical Abstract of the United States*, 88th Annual Edition, U. S. Department of Commerce, Washington, D. C.
- Burkard, O., 1962, Recombination in the Upper Ionosphere, *J. Atmos. Terrest. Phys.*, 24: 145-153.
- Burov, M. I., 1959, Fotogrammetricheskii method opredeleniya serebristych oblakov, Trudi Soveshchaniya Po Serebristym Oblakam, Tartu.
- Byron-Scott, R., 1967, A Stratospheric General Circulation Experiment Incorporation Diabatic Heating and Ozone Photochemistry, *Meteorology*, 87: 201 pp. plus Appendixes.
- Cadle, R. D., 1963, Rates of Chemical Reactions in the Sub-Ionospheric Atmosphere, *J. Geophys. Res.*, 68(13): 3977-3986.
- , 1967, Role of Methylene in the Production of Atmospheric Tritiated Methane, *J. Geophys. Res.*, 72(8): 2251-2253.
- , R. Bleck, J. P. Shedlovsky, I. H. Blifford, J. Rosinski, and A. L. Lazrus, 1969, Trace Constituents in the Vicinity of Jet Streams, *J. Appl. Meteorol.*, 8(3): 348-356.
- , W. H. Fischer, E. R. Frank, and J. P. Lodge, Jr., 1968, Particles in the Antarctic Atmosphere, *J. Atmos. Sci.*, 25(1): 100-103.
- , A. L. Lazrus, and J. P. Shedlovsky, 1969, Comparison of Particles in the Fume from Eruptions of Kilauea, Mayon, and Arenal Volcanoes, *J. Geophys. Res.*, 74(13): 3372-3378.
- Calfee, R. F., and D. M. Gates, 1966, Calculated Slant-Path Absorption and Distribution of Atmospheric Water Vapor, *Appl. Opt.*, 5: 287-292.
- Callendar, G. S., 1940, Variations of the Amount of Carbon Dioxide in Different Air Currents, *Quart. J. Roy. Meteorol. Soc.*, 66(283): 395-400.
- , 1958, On the Amount of Carbon Dioxide in the Atmosphere, *Tellus*, 10(2): 243-248.
- Campbell, E. S., and C. Nudelman, 1960, Reaction Kinetics, Thermodynamics and Transport Processes in the Ozone Oxygen System, Report AFOSR-TN-60-502, New York University.
- Canales, F. C., 1965, Relations entre la répartition verticale de l'ozone atmosphérique et l'évolution de la situation météorologique en Europe occidentale, *Pure Appl. Geophys.*, 62: 215-223.
- Carleton, N. P., 1962, The Relation of the Recent Atmospheric Dust Measurements of Volz and Goody to the Problem of Meteoric Influx, *J. Atmos. Sci.*, 19(5): 424-426.
- Carnuth, W., 1967, Zur Abhängigkeit des Aerosolpartikelspektrums von meteorologischen Vorgängen und Zuständen, *Arch. Meteorol., Geophys. Bioklimatol., Ser. A*, 16(4): 321-343.
- , and R. Reiter, 1966, Simultaneous Measurements of the Aerosol Particle Size Spectra at 700, 1,800, and 3,000 M Above Sea-Level, *J. Rech. Atmos.*, 2: 261-268.
- Carver, J. H., B. H. Horton, and F. G. Burger, 1966, Nocturnal Ozone Distribution in the Upper Atmosphere, *J. Geophys. Res.*, 71(17): 4189-4192.

- Caton, W. M., W. J. Welch, and S. Silver, 1967, Absorption and Emission in the 8-Millimeter Region by Ozone in the Upper Atmosphere, *J. Geophys. Res.*, **72**(24): 6137-6148.
- Cauer, H., 1951, Some Problems of Atmospheric Chemistry, *Compendium of Meteorology*, pp. 1126-1138, American Meteorological Society.
- Chagnon, C. W., and C. E. Junge, 1961, The Vertical Distribution of Sub-Micron Particles in the Stratosphere, *J. Meteorol.*, **18**(6): 746-753.
- Chamberlain, J. W., 1961, *Physics of the Aurora and Airglow*, International Geophysics Series, Vol. 2, Academic Press, Inc., New York.
- Champion, K. S. W., 1963, Atmospheric Structure and Its Variation in the Lower Thermosphere, Report by COSPAR Working Group 4, 6th Planetary Meeting, Warsaw, June 1963.
- , 1967, Variations with Season and Latitude of Density, Temperature and Composition in the Lower Thermosphere, Air Force Surveys in Geophysics No. 192, Report AFCRL-67-0161, Air Force Cambridge Research Laboratories.
- , 1968, Composition of the Mesosphere and Lower Thermosphere, *Meteorol. Monogr.*, **9**(31): 47-56.
- , F. A. Marcos, and J. Slowey, 1967, New Model Atmospheres Giving Latitudinal and Seasonal Variations in the Thermosphere, Air Force Surveys in Geophysics No. 194, Report AFCRL-67-0330, Air Force Cambridge Research Laboratories.
- , and S. P. Zimmerman, 1962, Winds and Turbulence at 200,000 to 400,000 Feet from Chemical Releases, Report AFCRL-62-826, pp. 57-67, Air Force Cambridge Research Laboratories.
- Chandra, C., 1963, Electron Density Distribution in the Upper F-Region, *J. Geophys. Res.*, **68**(7): 1937-1942.
- Changnon, S. A., Jr., 1968, The La Porte Weather Anomaly—Fact or Fiction? *Bull. Amer. Meteorol. Soc.*, **49**(1): 4-11.
- , 1969, Recent Studies on the Urban Effects on Precipitation in the United States, *Bull. Amer. Meteorol. Soc.*, **50**(6): 411-421.
- Chapman, G. E., 1969, Stratospheric–Mesospheric Circulation Patterns and D-Region Absorption, USAEC Report MIT-2241-53, Massachusetts Institute of Technology.
- Chapman, S., 1939, Notes on Atmospheric Sodium, *Astrophys. J.*, **90**: 309-316.
- , 1956, The Electrical Conductivity of the Ionosphere, *Nuovo Cim., Suppl.*, **4**: 1385-1412.
- , and P. C. Kendall, 1965, Noctilucent Clouds and Thermospheric Dust: Their Diffusion and Height Distribution, *Quart. J. Roy. Meteorol. Soc.*, **91**(388): 115-131.
- Charlson, R. J., and M. J. Pilat, 1969, Climate: The Influence of Aerosols, *J. Appl. Meteorol.*, **8**(6): 1001-1002.
- Charney, J. G., and P. G. Drazin, 1961, Propagation of Planetary-Scale Disturbances from the Lower into the Upper Atmosphere, *J. Geophys. Res.*, **66**(1): 83-109.
- Chimonas, G., and W. I. Axford, 1968, Vertical Movement of Temperate-Zone Sporadic E-Layers, *J. Geophys. Res.*, **73**(1): 111-117.
- Christie, A. D., 1969a, The Genesis and Distribution of Noctilucent Cloud, *J. Atmos. Sci.*, **26**(1): 168-176.
- , 1969b, A Condensation Model of Noctilucent Cloud Formation, *Space Research*, **IX**, pp. 175-182, North-Holland Publishing Co., Amsterdam.
- , 1969c, Noctilucent Clouds in North America, in *Stratospheric Circulation*, W. L. Webb (Ed.), pp. 241-258, Academic Press Inc., New York.
- Christophe-Glaume, J., 1965, Étude de la raie 5577 Å de l'oxygène dans la luminescence atmosphérique nocturne, *Ann. Geophys.*, **21**(1): 1-57.
- Clark, J., and W. Hitschfeld, 1964, Heating Rates Due to Ozone Computed by the Curtis–Godson Approximation, *Quart. J. Roy. Meteorol. Soc.*, **90**(383): 96-100.
- Clark, W. E., and K. T. Whitby, 1967, Concentration and Size Distribution Measurements of Atmospheric Aerosols and a Test of the Theory of Self-Preserving Size Distributions, *J. Atmos. Sci.*, **24**(6): 677-687.

- Clarke, J. F., 1969, A Meteorological Analysis of Carbon Dioxide Concentrations Measured at a Rural Location, *Atmos. Environ.*, **3**(4): 375-383.
- Clifton, S., and R. J. Naumann, 1966, Pegasus Satellite Measurements of Meteoroid Penetration (Feb. 16–Dec. 31, 1965), NASA Technical Memorandum, Report NASA-TM X-1316, National Aeronautics and Space Administration.
- Clyne, M. A. A., and B. A. Thrush, 1963, Rates of Elementary Processes in the Chain Reaction Between Hydrogen and Oxygen, 2. Kinetics of the Reaction of Hydrogen Atoms with Molecular Oxygen, *Proc. Roy. Soc. (London), Ser. A*, **275**: 559-566.
- Cole, A. E., 1967, Mean Monthly Atmospheres for 15°N, Air Force Surveys in Geophysics No. 189, Report AFCRL-67-0120, Air Force Cambridge Research Laboratories.
- , 1969, Recent Meteorological Rocket Data and an International Standard Atmosphere to 50 Kilometers, Air Force Surveys in Geophysics No. 209, Report AFCRL-69-0001, Air Force Cambridge Research Laboratories.
- , and A. J. Kantor, 1964, Horizontal and Vertical Distributions of Atmospheric Density up to 90 Km, Air Force Surveys in Geophysics No. 157, Report AFCRL-64-483, Air Force Cambridge Research Laboratories.
- , and A. J. Kantor, 1968, Spatial Variations in Stratospheric and Mesospheric Wind Fields, in *Proceedings of the Third National Conference on Aerospace Meteorology, May 6–9, New Orleans, La.*, pp. 465-471, American Meteorological Society, Boston, Mass.
- , and A. J. Kantor, 1969, Small Scale Variations in Stratospheric and Mesospheric Winds, in *Stratospheric Circulation*, W. L. Webb (Ed.), pp. 453-468, Academic Press Inc., New York.
- Collis, R. T. H., and M. G. H. Ligda, 1966, Note on Lidar Observations of Particulate Matter in the Stratosphere, *J. Atmos. Sci.*, **23**(2): 255-257.
- Cook, G. E., and D. W. Scott, 1966, Exospheric Densities Near Solar Minimum Derived from the Orbit of Echo 2, *Planet. Space Sci.*, **14**: 1149-1165.
- COSPAR Working Group IV, 1965, *COSPAR International Reference Atmosphere (CIRA) 1965*, North-Holland Publishing Co., Amsterdam.
- Coté, O. R., 1963, Wind, Diffusion and Turbulence: Analysis of Sodium Vapor Trails in the 80 to 140 Km Region of the Atmosphere, pp. 1-4, paper presented at American Institute of Aeronautics and Astronautics and American Meteorological Society Meeting on Meteorological Support for Aerospace Testing and Operations, July 10–12, 1963, Fort Collins, Colorado.
- , 1968, Fluid Dynamics Analog Studies Related to the Dispersion of Particles in the Upper Atmosphere, USAEC Report SC-CR-67-2812, GCA Corporation.
- Craig, H., 1957, The Natural Distribution of Radiocarbon and the Exchange Time of Carbon Dioxide Between Atmosphere and Sea, *Tellus*, **19**(1): 1-17.
- Craig, R. A., 1965, *The Upper Atmosphere. Meteorology and Physics*, International Geophysics Series, Vol. 8, Academic Press Inc., New York.
- , and J. H. Clark, 1969, Stratospheric Ozone and Circulation, Department of Meteorology, Final Report, Report AFCRL-69-0217, Florida State University.
- , J. J. DeLuisi, and P. R. Sticksel, 1967, Ozone Distribution over Tallahassee, Florida, *J. Geophys. Res.*, **72**(6): 1661-1667.
- , J. J. DeLuisi, and I. Stuetzer, 1967, Comparison of Chemiluminescent and Umkehr Observations, *J. Geophys. Res.*, **72**(6): 1667-1671.
- Crozier, W. D., 1960, Black, Magnetic Spherules in Sediments, *J. Geophys. Res.*, **65**(9): 2971-2977.
- , 1961, Micrometeorite Measurements: Satellite and Ground Level Data Compared, *J. Geophys. Res.*, **66**(9): 2793-2795.
- , 1962, Five Years of Continuous Collection of Black, Magnetic Spherules from the Atmosphere, *J. Geophys. Res.*, **67**(6): 2543-2548.
- , 1966, Nine Years of Continuous Collection of Black, Magnetic Spherules from the Atmosphere, *J. Geophys. Res.*, **71**(2): 603-611.
- Crutzen, P. J., 1969, Determination of Parameters Appearing in the "Dry" and the "Wet" Photochemical Theories for Ozone in the Stratosphere, *Tellus*, **21**(3): 368-388.
- Csanady, G. T., 1964, An Atmospheric Dust Fall Experiment, *J. Atmos. Sci.*, **21**(2): 222-225.

- Cumme, G., R. Knuth, and Ch. U. Wagner, 1966, Zur Frage der aus Langwellenabsorptionsmessungen erschlossenen Elektronenkonzentrationsprofile in der unteren Ionosphäre während des Sonnenaufganges, *Schriftenr. Nat. Kom. Geod. Geophys. Deut. Dem. Rep., Reihe, II(1)*: 99-138.
- Curtis, A. R., 1952, Discussion of a Paper by Goody, *Quart. J. Roy. Meteorol. Soc.*, **78**(338): 638-640.
- Dachs, J., 1969, On Nightglow Intensity Variations Connected with Vertical Movements in the Upper Atmosphere, in *Atmospheric Emissions*, B. M. McCormac and A. Omholt (Eds.), pp. 515-517, Van Nostrand-Reinhold Co., New York.
- D'Aiutolo, C. T., 1964, Review of Meteoroid Environment Based on Results from Explorer XIII and Explorer XVII Satellites, *Space Research*, IV, p. 858, John Wiley & Sons, Inc., New York.
- Danielsen, F. F., 1959, The Laminar Structure of the Atmosphere and Its Relation to the Concept of a Tropopause, *Arch. Meteorol., Geophys. Bioklimatol., Ser. A*, **11**(3): 293-332.
- , 1961, Trajectories: Isobaric, Isentropic and Actual, *J. Meteorol.*, **18**(4): 479-486.
- , 1964, Radioactivity Transport from Stratosphere to Troposphere, *Mineral Ind.*, **33**: 1-7.
- , 1967, Transport and Diffusion of Stratospheric Radioactivity Based on Synoptic Hemispheric Analyses of Potential Vorticity, Final Report, USAEC Report NYO-3317-3, Pennsylvania State University.
- , 1968, Stratospheric-Tropospheric Exchange Based on Radioactivity, Ozone and Potential Vorticity, *J. Atmos. Sci.*, **25**(3): 502-518.
- , and R. T. Duquet, 1967, A Comparison of FPS-16 and GMD-1 Measurements and Methods of Processing Wind Data, *J. Appl. Meteorol.*, **6**(5): 824-836.
- , and E. R. Reiter, 1960, Bemerkungen en E. Kleinschmidt: Nicht-adiabatische Abkühlung im Bereich "des jet stream," *Beitr. Phys. Atmos.*, **32**(3 and 4): 265-273.
- Dave, J. V., and C. L. Mateer, 1967, A Preliminary Study on the Possibility of Estimating Total Atmospheric Ozone from Satellite Measurements, *J. Atmos. Sci.*, **24**(4): 414-427.
- , and C. L. Mateer, 1968, The Effect of Stratospheric Dust on the Color of the Twilight Sky, *J. Geophys. Res.*, **73**(22): 6897-6914.
- Davis, D. R., and C. E. Dean, 1966, Low-Level Tropospheric Ozone, *Mon. Weather Rev.*, **94**(3): 179-182.
- Davis, T. N., and L. L. Smith, 1965, Latitudinal and Seasonal Variations in the Night Airglow, *J. Geophys. Res.*, **70**(5): 1127-1138.
- Day, J. A., 1964, Production of Droplets and Salt Nuclei by the Bursting of Air-Bubble Films, *Quart. J. Roy. Meteorol. Soc.*, **90**(383): 72-78; (386): 498.
- DeBary, E., and C. Junge, 1963, Distribution of Sulfur and Chlorine over Europe, *Tellus*, **15**(4): 370-381.
- Defant, A., 1921a, Die Zirkulation der Atmosphaere in den gemässigten Breiten der Erde, *Geograf. Ann.*, **3**: 209-266.
- , 1921b, Die Bestimmung der Turbulenzgrössen der atmosphaerischen Zirkulation ausser-tropischer Breiten, *Sitzungsber. Akad. Wiss., Vienna*, **130**: 383-403.
- , and F. Defant, 1958, *Physikalische Dynamik der Atmosphaere*, Akademische Verlagsgesellschaft m.b.H., Frankfurt a.M.
- Deirmendjian, D., 1965, Note on Laser Detection of Atmospheric Dust Layers, *J. Geophys. Res.*, **70**(3): 743-745.
- Deland, R. J., 1965, Some Observations of the Behavior of Spherical Harmonics, *Mon. Weather Rev.*, **93**(5): 307-312.
- Delany, A. C., D. W. Parkin, J. J. Griffin, F. D. Goldberg, and B. E. F. Reimann, 1967, Airborne Dust Collected at Barbados, *Geochim. Cosmochim. Acta*, **31**: 885-909.
- DeLuisi, J. J., 1967, The Effect of Haze upon Umkehr Measurements, Report No. 67-3, Report AFCRL-67-0367, Department of Meteorology, Florida State University.
- , 1969, A Study of the Effect of Haze upon Umkehr Measurements, *Quart. J. Roy. Meteorol. Soc.*, **95**(403): 181-187.

- DeMandel, R. E., 1968, An Investigation of the Mesoscale Structure of Upper-Air Winds Measured with the FPS-16/Jimsphere System, in *Proceedings of the Third National Conference on Aerospace Meteorology, New Orleans, La., May 6-9*, pp. 154-159, American Meteorological Society, Boston, Mass.
- Deshpande, M. R., and R. G. Rastogi, 1966, Ionospheric Horizontal Drifts Within the Equatorial Electrojet Region in India, *Ann. Geophys.*, **22**(3): 418-421.
- Dickinson, R. E., 1969, Vertical Propagation of Planetary Rossby Waves Through an Atmosphere with Newtonian Cooling, *J. Geophys. Res.*, **74**(4): 929-938.
- , and J. F. Geisler, 1968, Vertical Motion Field in the Middle Thermosphere from Satellite Drag Densities, *Mon. Weather Rev.*, **96**(9): 606-616.
- , C. P. Lagos, and R. E. Newell, 1968, Dynamics of the Neutral Gas in the Thermosphere for Small Rossby Number Motions, *J. Geophys. Res.*, **73**(13): 4299-4313.
- Dickson, C. R., and J. K. Angell, 1968, Eddy Velocities in the Planetary Boundary Layer as Obtained from Tetroon Flights at Idaho Falls, *J. Appl. Meteorol.*, **7**(6): 986-993.
- Dieminger, W., 1952, Über die Ursache der exzessiven Ionisation in der Ionosphäre an Wintertagen, *J. Atmos. Terrest. Phys.*, **2**: 340-349.
- , G. Rose, H. Schwentek, and H. U. Widdel, 1967, The Morphology of Winter Anomaly of Absorption, *Space Research*, **VII**, pp. 228-239, North-Holland Publishing Co., Amsterdam.
- Dietze, G., 1956, Gössenverteilung des atmosphärischen Aerosols und Himmelslicht-Polarisation, *Z. Meteorol.*, **10**: 354-363.
- , 1965, Der Staubgehalt der Luft bei verschiedenen meteorologischen Bedingungen, *Z. Meteorol.*, **18**(1-2): 39-42.
- , 1969, Zones of the Visibility of a Noctilucent Cloud, *Tellus*, **21**(3): 436-442.
- , and G. Kohl, 1966, Zu den Beziehungen zwischen optischen und elektrischen Eigenschaften ionosphärischer Schichten, *Z. Meteorol.*, **18**(5-7): 212-218.
- , and H. Seidel, 1967, Über die Sondierung stratosphärischer und mesosphärischer Staubschichten mit Laserimpulsen, *Z. Meteorol.*, **19**(7-8): 202-211.
- Dillemath, F. J., D. R. Skidmore, and C. C. Schubert, 1960, The Reaction of Ozone with Methane, *J. Phys. Chem.*, **64**: 1496-1499.
- Dingle, A. N., and D. Gatz, 1966, Air Cleansing by Convective Rains, *J. Appl. Meteorol.*, **5**(2): 160-168.
- , D. F. Gatz, and J. W. Winchester, 1969, A Pilot Experiment Using Indium as Tracer in a Convective Storm, *J. Appl. Meteorol.*, **8**(2): 236-240.
- Dittmann, E., 1966, Modellrechnung zur Wasserdampfausbreitung von einer verdunstenden Seeoberfläche, Thesis, Meteorological Institut, University of Bonn, Germany.
- Dobson, G. M. B., 1956, Origin and Distribution of the Poly-Atomic Molecules in the Atmosphere, *Proc. Roy. Soc. (London), Ser. A*, **236**: 187-192.
- , 1963, *Exploring the Atmosphere*, Clarendon Press, Oxford.
- , 1966, Annual Variation of Ozone in Antarctica, *Quart. J. Roy. Meteorol. Soc.*, **92**(394): 549-553.
- , A. W. Brewer, and B. M. Cwilong, 1946, Meteorology of the Lower Atmosphere, *Proc. Roy. Soc. (London), Ser. A*, **185**: 144-175.
- , D. N. Harrison, and J. Lawrence, 1929, *Proc. Roy. Soc. (London), Ser. A*, **190**: 137.
- , and C. W. B. Normand, 1962, Comments on Paper by H. C. Willett, "The Relationship of Total Atmospheric Ozone to the Sunspot Cycle," *J. Geophys. Res.*, **67**(10): 4095.
- Doherty, R. H., 1968, Importance of Associative Detachment and Dissociative Attachment in the Lower Ionosphere as Shown by LF Radio Measurements, *J. Geophys. Res.*, **73**(7): 2429-2440.
- Dole, S. H., 1962, The Gravitational Concentration of Particles in Space Near the Earth, *Planet. Space Sci.*, **9**: 541-553.
- Donahue, T. M., 1966, On the Ionospheric Conditions in the D Region and Lower E Region, *J. Geophys. Res.*, **71**(9): 2237-2242.

- , and R. R. Meier, 1967, Distribution of Sodium in the Daytime Upper Atmosphere as Measured by a Rocket Experiment, *J. Geophys. Res.*, **72**(11): 2803-2829.
- Douppnik, J. R., and J. S. Nisbet, 1968, Fluctuations of Electron Density in the Daytime F-Region, *J. Atmos. Terrest. Phys.*, **30**(5): 931-961.
- Droessler, E. G., 1964, A Note on Ice Nuclei Storms, *J. Atmos. Sci.*, **21**(6): 701-702.
- , and K. J. Heffernan, 1965, Ice Nucleus Measurements in Hawaii, *J. Appl. Meteorol.*, **4**(4): 442-445.
- , K. J. Heffernan, and E. K. Bigg, 1967, A Stratospheric Air Tracer Experiment Using Zinc Sulfide, *J. Appl. Meteorol.*, **6**(2): 373-379.
- Drozdov, O. A., and A. S. Grigor'eva, 1965, The Hydrologic Cycle in the Atmosphere (translated from Russian), Israel Program for Scientific Translations, Jerusalem.
- Druyan, L. M., 1968, A Comparison of Low-Level Trajectories in an Urban Atmosphere, *J. Appl. Meteorol.*, **7**(4): 583-590.
- Dubin, M., 1960, IGY Micrometeorite Measurements, in *Space Research*, H. Kallmann-Bijl (Ed.), pp. 1042-1058, North-Holland Publishing Co., Amsterdam.
- , and C. W. McCracken, 1962, Measurements of Distributions of Interplanetary Dust, *Astron. J.*, **67**: 248-256.
- Duce, R. A., J. T. Wasson, J. W. Winchester, and F. Burns, 1963, Atmospheric Iodine, Bromine and Chlorine, *J. Geophys. Res.*, **68**(13): 3943-3948.
- , J. W. Winchester, and T. W. Van Nahl, 1965, Iodine, Bromine and Chlorine in the Hawaiian Marine Atmosphere, *J. Geophys. Res.*, **70**(8): 1775-1799.
- , J. W. Winchester, and T. W. Van Nahl, 1966, Iodine, Bromine and Chlorine in Winter Aerosols and Snow from Barrow, Alaska, *Tellus*, **18**(2-3): 238-248.
- Dufay, M., 1949, Recherches sur les spectres des éclairs. 2. Étude du spectra dans les regions violette et ultraviolette, *Ann. Geophys.*, **5**: 255-263.
- Durbin, W. G., 1959, Some Observations of the Vertical and Horizontal Distribution of Chloride Particles, *Geofis. Pura Appl.*, **42**: 11-20.
- , and G. D. White, 1961, Measurements of the Vertical Distribution of Atmospheric Chloride Particles, *Tellus*, **13**(2): 260-275.
- Dutsch, H. U., Das atmosphärische Ozon als Indikator für Strömungen in der Stratosphäre, *Arch. Meteorol., Geophys. Bioklimatol., Ser. A*, **9**: 87-119.
- , 1960, Vertical Ozone Distribution from Umkehr Observations, *Arch. Meteorol., Geophys. Bioklimatol., Ser. A*, **11**: 240-251.
- , 1962a, Ozone Distribution and Stratospheric Temperature Field over Europe During the Sudden Warming in January/February 1958, *Beitr. Phys. Atmos.*, **35**: 87-107.
- , 1962b, Mittelwerte und wetterhafte Schwankungen des atmosphärischen Ozongehaltes in verschie denen Höhen über Arosa, *Arch. Meteorol., Geophys. Bioklimatol., Ser. A*, **13**(2): 167-185.
- , 1963, Ozone and Temperature in the Stratosphere, *Meteorol. Abh. Inst. Meteorol. Geophys., Freie Univ., Berlin*, **36**: 271-290.
- , 1964, Uniform Evaluation of Umkehr Observations from the World Ozone Network. Part III. Worldwide Ozone Distribution at Different Levels and Its Variation with Season from "Umkehr" Observations, National Center for Atmospheric Research.
- , 1965, Vertical Ozone Distribution over Arosa, Report AFCRL-65-419, Lichtklimatisches Observatorium, Arosa, Switzerland, and National Center for Atmospheric Research.
- , 1966, Two Years of Regular Ozone Soundings over Boulder, Colorado, NCAR Technical Notes, Report NCAR-TN-10, National Center for Atmospheric Research.
- , 1968, The Photochemistry of Stratospheric Ozone, *Quart. J. Roy. Meteorol. Soc.*, **94**(402): 483-497.
- , 1969, Atmospheric Ozone and Ultraviolet Radiation, in *World Survey of Climatology*, Vol. IV, H. Landsberg (Ed.), Elsevier, Amsterdam.

- Dycus, R. D., and C. D. Martin, 1969, Rainfall and the Meteoroid Influx to Earth, *J. Atmos. Sci.*, **26**(4): 782-783.
- Dyer, A. J., and B. Hicks, 1965, Stratospheric Transport of Volcanic Dust Inferred from Solar Radiation Measurements, *Nature*, **208**: 131-133.
- , and B. Hicks, 1968, Global Spread of Volcanic Dust from the Bali Eruption of 1963, *Quart. J. Meteorol. Soc.*, **94**(402): 545-554.
- Eady, E. T., 1949, Long Waves and Cyclone Waves, *Tellus*, **1**(3): 33-52.
- Eddy, J. A., P. J. Lena, and R. M. MacQueen, 1969, The Far Infrared Transmission of the Upper Atmosphere, *J. Atmos. Sci.*, **26**(6): 1318-1328.
- Edwards, H. D., M. M. Cooksey, R. N. Fuller, D. L. Albritton, and N. W. Rosenberg, 1962, Upper Atmosphere Wind Measurements Determined from Twelve Rocket Experiments, AFCRL-62-826, pp. 69-79, Air Force Cambridge Research Laboratories.
- Effenberger, E., 1951, Messmethoden zur Bestimmung des CO₂-Gehaltes der Atmosphäre und die Bedeutung derartiger Messungen für die Biometeorologie und Meteorologie, *Ann. Meteorol.*, **4**(10-11): 417-427.
- Eliassen, E., and B. Machenhaur, 1965, A Study of Fluctuations of the Atmospheric Planetary Flow Patterns Represented by Spherical Harmonics, *Tellus*, **17**(2): 220-238.
- Elsässer, H., 1954, Die räumliche Verteilung der Zodiakallichtmaterie, *Z. Astrophys.*, **33**: 274-285.
- , 1963, The Zodiacal Light, *Planet. Space Sci.*, **11**: 1015-1033.
- Elsley, E. M., 1951, Alberta Forest Fire Smoke—24 September, 1950, *Weather*, **6**(1): 22-24.
- Elterman, L., 1966, An Atlas of Aerosol Attenuation and Extinction Profiles for the Troposphere and Stratosphere, Environmental Research Paper No. 241, Report AFCRL-66-828, Air Force Cambridge Research Laboratories.
- , 1967, Aerosol Measurements in the Troposphere and Stratosphere, Environmental Research Paper No. 253, Report AFCRL-67-0003, Air Force Cambridge Research Laboratories.
- , 1968, UV, Visible, and IR Attenuation for Altitudes to 50 km, 1968, Environmental Research Paper No. 285, Report AFCRL-68-0153, Air Force Cambridge Research Laboratories.
- , and A. B. Campbell, 1964, Atmospheric Aerosol Observations with Searchlight Probing, *J. Atmos. Sci.*, **21**(4): 457-458.
- Endlich, R. M., R. C. Singleton, K. A. Drexhage, and R. L. Mancuso, 1969, Studies of Vertical Wind Profiles at Cape Kennedy, Florida, NASA Contractor Report, Report NASA-CR-61263, National Aeronautics and Space Administration.
- Engler, N., 1968, Wind Detail from Falling Spheres, *J. Geophys. Res.*, **73**(10): 3323.
- Environmental Science Services Administration, National Aeronautics and Space Administration, and U. S. Air Force, 1966, *U. S. Standard Atmosphere Supplements*, U. S. Government Printing Office, Washington.
- Erickson, J. E., 1968, Velocity Distribution of Sporadic Photographic Meteors, *J. Geophys. Res.*, **73**(12): 3721-3726.
- , 1969, Mass Influx and Penetration Rate of Meteor Streams, *J. Geophys. Res.*, **74**(2): 576-585.
- Eriksson, E., 1954, Report on an Informal Conference in Chemistry held at the Meteorological Institute, University of Stockholm, May 24-26, 1954, *Tellus*, **6**(3): 302-307.
- , 1955, Airborne Salts and the Chemical Composition of River Waters, *Tellus*, **7**(2): 243-250.
- , 1959, The Yearly Circulation of Chloride and Sulfur in Nature; Meteorological, Geochemical and Pedological Implications, Part I, *Tellus*, **11**(4): 376-403.
- , 1960, The Yearly Circulation of Chloride and Sulfur in Nature; Meteorological, Geochemical and Pedological Implications, Part II, *Tellus*, **12**(1): 63-109.
- , 1963a, Possible Fluctuations in Atmospheric Carbon Dioxide Due to Changes in the Properties of the Sea, *J. Geophys. Res.*, **68**(13): 3871-3876.
- , 1963b, The Yearly Circulation of Sulfur in Nature, *J. Geophys. Res.*, **68**(13): 4001-4008.
- Ertel, H., 1965, Advektive Reichweite von Meersalzablagerungen im küstennahen Binnenland, *Z. Meteorol.*, **18**(1-2): 43-45.

- Essenwanger, O., 1963, On the Derivation of Frequency Distributions of Vector Wind Shear Values for Small Shear Intervals, *Geofis. Pura Appl.*, **56**: 216-224.
- , 1965, Statistical Parameters and Percentile Values for Vector Wind Shear Distributions of Small Increments, *Arch. Meteorol., Geophys. Bioklimatol., Ser. A*, **15**(1): 50-61.
- , 1967a, Comments on "Mesoscale Structure of 11-20 Km Winds," *J. Appl. Meteorol.*, **6**(3): 591-593.
- , 1967b, The Negative Binomial Distribution Applied to Atmospheric Parameters, in Proceedings of the Twelfth Conference on the Design and Experiments in Army Research Development and Testing, Report ARO-D-67-2, pp. 221-242.
- , and N. Billions, 1965, On Wind Distributions for Smaller Shear Intervals, Report RR-TR-65-4, U. S. Army Missile Command.
- Essex, E. A., and F. H. Hibberd, 1968, Frequency and Spatial Correlations of Fading Radio Echoes from the Ionosphere, *J. Atmos. Terrest. Phys.*, **30**(5): 1019-1031.
- Evans, W. F. J., D. M. Hunten, E. J. Llewellyn, and A. Vallance Jones, 1968, Altitude Profile of the Infrared Atmospheric System of Oxygen in Dayglow, *J. Geophys. Res.*, **73**(9): 2885-2896.
- Fabian, P., and C. E. Junge, 1970, Global Rate of Ozone Destruction at the Earth's Surface, *Arch. Meteorol., Geophys. Bioklimatol., Ser. A*, **19**(2): 161-172.
- Facy, L., 1962, Radioactive Precipitations and Fallout, in *Nuclear Radiation in Geophysics*, H. Israel and A. Krebs (Eds.), pp. 202-240, Springer-Verlag, Berlin.
- Farkas, E., 1969, Comments on "Biennial Variation in Springtime Temperature and Total Ozone in Extratropical Latitudes," *Mon. Weather Rev.*, **97**(8): 613-615.
- Farley, D. T., J. P. McClure, D. L. Sterling, and J. L. Green, 1967, Temperature and Composition of the Equatorial Ionosphere, *J. Geophys. Res.*, **72**(23): 5837-5851.
- Faust, H., 1960, Die Schwachwindsschicht in der unteren Stratosphäre als Nullschicht, *Meteorol. Rundsch.*, **13**: 77.
- , 1963, The Null-Layer Conception in Stratosphere and Mesosphere, Especially in Spring and Fall, U. S. Department of the Army, European Research Office, Project Cell Structure of the Atmosphere, Scientific Report No. 1, 4th year.
- , 1966, In der Vertikalen abwechselnd auftretende Tendenz zu West- und Ostwind, *Meteorol. Rundsch.*, **19**(5): 147-151.
- , 1967a, Interaction Between the Different Layers of the Homosphere, *Arch. Meteorol., Geophys. Bioklimatol., Ser. A*, **16**: 12.
- , 1967b, Zur Frühjahrs-Windumstellung in Stratosphäre und Mesosphäre, *Pure Appl. Geophys.*, **66**: 156-158.
- , 1967c, Stratosphärische Temperaturen im Nord- und Südpolargebiet, *Meteorol. Rundsch.*, **20**(3): 89-91.
- , 1967d, Meridionalschnitte des Zonalwindes bis 60 km Höhe von 60°N bis 10°S, *Meteorol. Rundsch.*, **20**(4): 104-108.
- , 1968, *Der Aufbau der Erdatmosphäre*, Friedrich Vieweg & Sohn, Braunschweig, Germany.
- , and W. Attmannspacher, 1961, Die allgemeine Zirkulation der außertropischen Breiten bis 60 km Höhe auf der Basis der Nullschichtkonzeption, *Meteorol. Rundsch.*, **14**: 6.
- , and W. Attmannspacher, 1962a, Project Cell Structure of the Atmosphere, *Ber. Deut. Wetterdienst, Offenbach*.
- , and W. Attmannspacher, 1962b, Forschungsprojekt Zellstruktur der Atmosphäre, *Ber. Deut. Wetterdienst, Offenbach*.
- Fechtig, H., U. Gerloff, and J. H. Weihrauch, 1968, Results of Cosmic-Dust Collection of Luster, 1965, *J. Geophys. Res.*, **73**(16): 5029-5037.
- Fehsenfeld, F. C., P. D. Goldan, A. L. Schmeltekopf, and E. E. Ferguson, 1965a, Laboratory Measurement of the Rate of the Reaction $O^+ + O_2 \rightarrow O_2^+ + O$ at Thermal Energy, *Planet. Space Sci.*, **13**: 579-582.
- , A. L. Schmeltekopf, and E. E. Ferguson, 1965b, Some Measured Rates for Oxygen and Nitrogen Ion-Molecule Reactions of Atmospheric Importance, Including $O^+ + N_2 \rightarrow NO^+ + N$, *Planet. Space Sci.*, **13**: 219-223.

- , A. L. Schmeltekopf, and E. E. Ferguson, 1965c, Correction in the Laboratory Measurement of the Rate Constant for $N_2^+ + O_2 \rightarrow N_2 + O_2^+$ at 300°K, *Planet. Space Sci.*, **13**: 919-920.
- Fenimore, C. P., and C. W. Jones, 1958, Determination of Hydrogen Atoms in Rich, Flat, Premixed Flames by Reaction with Heavy Water, *J. Phys. Chem.*, **62**: 693-697.
- Fenn, R. W., 1960, Measurements of the Concentration and Size Distribution of Particles in the Arctic Air of Greenland, *J. Geophys. Res.*, **65**(10): 3371-3376.
- , H. E. Gerber, and W. Dieter, 1963, Measurements of the Sulphur and Ammonium Component of the Arctic Aerosol of the Greenland Icecap, *J. Atmos. Sci.*, **20**(5): 466-468.
- Ferguson, A. F., and D. Parkinson, 1963, The Hydroxyl Bands in the Nightglow, *Planet. Space Sci.*, **11**: 149-159.
- Ferguson, E., 1967, Ionospheric Ion-Molecule Reaction Rates, *Rev. Geophys.*, **5**(3): 305-327.
- Fichtl, G. H., D. W. Camp, and W. W. Vaughan, 1969, Detailed Wind and Temperature Profiles, in *Clear Air Turbulence and Its Detection*, Y.-H. Pao and A. Goldburg (Eds.), pp. 308-333, Plenum Press, Inc., New York.
- Fiedler, R., 1966, Die Aerosolkonzentration in mittleren Saaletal bei Strahlungswetter in Abhängigkeit von Tageszeit und Jahreszeit, *Z. Meteorol.*, **18**(8-10): 302-319.
- Finger, F. G., M. F. Harris, and S. Teweles, 1965, Diurnal Variation of Wind, Pressure and Temperature in the Stratosphere, *J. Appl. Meteorol.*, **4**: 632-635.
- , R. B. Mason, and S. Teweles, 1964, Diurnal Variation in Stratospheric Temperatures and Heights Reported by the United States Weather Bureau Outrigger Radiosonde, *Mon. Weather Rev.*, **92**: 243-250.
- , and R. M. McInturff, 1968, The Diurnal Temperature Range of the Middle Stratosphere, *J. Atmos. Sci.*, **25**(6): 1116-1128.
- , and R. M. McInturff, 1970, Meteorology and the Supersonic Transport, *Science*, **167**(3914): 16-25.
- , and H. M. Woolf, 1966, An Experiment Designed to Determine the Diurnal Temperature and Wind Variation and to Detect Possible Errors in Rocketsonde Temperature Measurements in the Upper Stratosphere, NASA Technical Memorandum Report NASA-TM-X-1298, National Aeronautics and Space Administration.
- , and H. M. Woolf, 1967, Diurnal Variation of Temperature in the Upper Stratosphere as Indicated by a Meteorological Rocket Experiment, *J. Atmos. Sci.*, **24**(2): 230-239.
- Fiocco, G., 1965, Optical Radar Results and Ionospheric Sporadic E, *J. Geophys. Res.*, **70**(9): 2213-2215.
- , 1967, On the Production of Ionization by Micrometeorites, *J. Geophys. Res.*, **72**(13): 3497-3501.
- , and G. Colombo, 1964, Optical Radar Results and Meteoric Fragmentation, *J. Geophys. Res.*, **69**(9): 1795-1803.
- , and G. Grams, 1964, Observations of the Aerosol Layer at 20 Km by Optical Radar, *J. Atmos. Sci.*, **21**(3): 323-324.
- , and G. Grams, 1969, Optical Radar Observations of Mesospheric Aerosols in Norway During Summer 1966, *J. Geophys. Res.*, **74**(10): 2453-2458.
- , and L. D. Smullins, 1963, Detection of Scattering Layers in the Upper Atmosphere by Optical Radar, *Nature*, **199**: 1275-1276.
- Fischer, W. H., J. P. Lodge, Jr., J. B. Pate, and R. D. Cadle, 1969, Antarctic Atmospheric Chemistry, *Science*, **164**: 66-67.
- Fitzsimmons, R. V., and E. J. Bair, 1964, Distribution and Relaxation of Vibrationally Excited Oxygen in Flash Photolysis of Ozone, *J. Chem. Phys.*, **40**: 451-458.
- Fletcher, N. H., 1962, *The Physics of Rainclouds*, Cambridge University Press.
- Flohn, H., and D. Henning, 1964, Stratosphärische Staubwolken vulkanischer Herkunft, *Meteorol. Rundsch.*, **17**: 89.
- Flowers, E., and H. Viebrock, 1965, Solar Radiation: An Anomalous Decrease of Direct Solar Radiation, *Science*, **148**: 493-494.

- Flowers, E. C., R. A. McCormick, and K. R. Kurfis, 1969, Atmospheric Turbidity over the United States, 1961–1966, *J. Appl. Meteorol.*, **8**(6): 955-962.
- Fogle, B., 1966, Recent Advances in Research on Noctilucent Clouds, *Bull. Amer. Meteorol. Soc.*, **47**(10): 781-787.
- , 1968, The Climatology of Noctilucent Clouds According to Observations Made from North America During 1964–1966, *Meteorol. Mag.*, **97**: 193-204.
- Foner, S. N., and R. L. Hudson, 1962, Mass Spectrometry of the H₂O Free Radical, *J. Chem. Phys.*, **36**: 2681-2692.
- Fonselius, S., 1954, Amino Acids in Rainwater, *Tellus*, **6**(1): 90.
- , 1958, Coordinates and Map of CO₂ and Chemical Stations, *Tellus*, **10**(1): 170-171.
- , F. Koroleff, and K. Buch, 1955, Microdetermination of CO₂ in the Air with Current Data for Scandinavia, *Tellus*, **7**(2): 258-265.
- , and K. E. Wärme, 1960, A Method to Make Standard CO₂ Samples for Infrared Gas Analysis and the Operation of an IRGA Analyser for Air Samples from the Scandinavian Network, *Tellus*, **12**(2): 227-230.
- Fooks, G. F., 1964, Dynamic Processes in the Lower Ionosphere and Their Variation with Height, *Ann. Geophys.*, **20**(4): 417-424.
- Föppl, H., G. Haerndel, L. Haser, J. Loidl, P. Lütjens, R. Lust, F. Melzner, B. Meyer, H. Neuss, and E. Rieger, 1967, Artificial Strontium and Barium Clouds in the Upper Atmosphere, *Planet. Space Sci.*, **15**: 357-372.
- , G. Haerndel, J. Loidl, R. Lust, F. Melzner, B. Meyer, H. Neuss, and E. Rieger, 1965, Preliminary Experiments for the Study of the Interplanetary Medium by the Release of Metal Vapour in the Upper Atmosphere, *Planet. Space Sci.*, **13**: 95-114.
- Fraser, G. J., 1968, Seasonal Variation of Southern Hemisphere Mid-Latitude Winds at Altitudes of 70–100 Km, *J. Atmos. Terrest. Phys.*, **30**(5): 707-719.
- Friedlander, S. K., 1960, Similarity Considerations for the Particle-Size Spectrum of a Coagulating, Sedimenting Aerosol, *J. Meteorol.*, **17**(5): 479-483.
- , 1961, Theoretical Considerations for the Particle-Size Spectrum of the Stratospheric Aerosol, *J. Meteorol.*, **18**(6): 753-759.
- , 1965, Theory of Self-Preserving Size Distributions in a Coagulating Dispersion, in *Radioactive Fallout from Nuclear Weapons Tests*, Alfred W. Klement (Ed.), AEC Symposium Series, No. 5 (CONF-765), Germantown, Md., pp. 253-259.
- , and R. E. Pasceri, 1965, Measurements of the Particle Size Distribution of the Atmospheric Aerosol: I. Introduction and Experimental Methods, *J. Atmos. Sci.*, **22**(5): 571-576.
- Friend, J. P., 1966, Properties of the Stratospheric Aerosol, *Tellus*, **18**(2-3): 465-473.
- , H. W. Feely, P. W. Krey, J. Spar, and A. Walton, 1961, The High Altitude Sampling Program. Discussion of HASP Results, Report DASA-1300, Vol. 3, August, Defense Atomic Support Agency.
- Fritz, S., 1951, Ozone Measurements During Sudden Ionospheric Disturbances, *Arch. Meteorol., Geophys. Bioklimatol., Ser. A*, **4**: 343-350.
- Fukushima, M., 1967, Some Investigations of the Effect of Mountain Wave on the Distribution of the Atmospheric Refractive Index, *J. Meteorol. Soc. Jap.*, **45**(4): 332-341.
- Funk, J. P., and G. L. Garnham, 1962, Australian Ozone Observations and a Suggested 24-Month Cycle, *Tellus*, **14**(4): 378-382.
- Fuquay, J. J., Ch. L. Simpson, M. L. Barad, and J. H. Taylor, 1963, Results of Recent Field Programs in Atmospheric Diffusion, *J. Appl. Meteorol.*, **2**(1): 122-128.
- Gadsden, M., 1962, Observations of Lithium in Twilight After a High Altitude Thermonuclear Explosion, *Ann. Geophys.*, **18**(4): 392-393.
- , 1964a, On the Twilight Sodium Emission. I. Observations from a Southern Hemisphere Station, *Ann. Geophys.*, **20**: 261-271.
- , 1964b, On the Twilight Sodium Emission. II. A Theoretical Model of Sodium Abundance, *Ann. Geophys.*, **20**: 383-396.

- Gaigerov, S. S., Yu. P. Kosheikov, D. A. Tarasenko, and E. G. Shvidkovsky, 1969, Properties of the Atmosphere up to 80 Km, in *Stratospheric Circulation*, W. L. Webb (Ed.), pp. 323-338, Academic Press Inc., New York.
- Galbally, I., 1969, An Evaluation of the Ehmert Technique for Measuring Ozone Profiles in the Atmospheric Surface Layer, *J. Geophys. Res.*, **74**(28): 6869-6872.
- Gambell, A. W., Jr., 1962, Indirect Evidence of the Importance of Water-Soluble Continentally Derived Aerosols, *Tellus*, **14**(1): 91-95.
- Gast, J. A., and Th. G. Thompson, 1959, Evaporation of Boric Acid from Sea Water, *Tellus*, **11**(3): 344-347.
- Gattinger, R. L., and A. Vallance Jones, 1966, The $^1\Delta_g-^3\Sigma_g-O_2$ Bands in the Twilight and Day Airglow, *Planet. Space Sci.*, **14**: 1-14.
- Gatz, D. F., and A. N. Dingle, 1963, Washout of Ragweed Pollen by Rainfall, *J. Geophys. Res.*, **68**(12): 3641-3648.
- , A. N. Dingle, and J. W. Winchester, 1969, Detection of Indium as an Atmospheric Tracer by Neutron Activation, *J. Appl. Meteorol.*, **8**(2): 229-235.
- Gebhart, R., 1967, Über das Strahlungsgleichgewicht der Mesosphäre, *Beitr. Phys. Atmos.*, **40**: 204-215.
- , 1968, Photochemical, Advective and Turbulent Effects on the Meridional Distribution of Ozone. A Study of the Time-Dependent Problem, *Arch. Meteorol., Geophys. Bioklimatol., Ser. A*, **17**: 301-335.
- Gee, J. H., 1967, A Note on the Effect of Directional Wind Shear on Medium-Scale Atmospheric Diffusion, *Quart. J. Roy. Meteorol. Soc.*, **93**(396): 237-242.
- Geisler, J. E., and R. E. Dickinson, 1967, Comment on "Upper-Atmosphere Sodium and Stratospheric Warming at High Latitudes," *J. Atmos. Sci.*, **24**(6): 720-721.
- , and R. E. Dickinson, 1968, Vertical Motions and Nitric Oxide in the Upper Mesosphere, *J. Atmos. Terrest. Phys.*, **30**: 1505-1521.
- General Electric Company, 1963, Ozone, Nitric Oxide and Radiation Effects on a Supersonic Transport, Final Report, Contract No. FA-WA-4181, Space Science Laboratory.
- Georges, T. M., 1968, HF Doppler Studies of Traveling Ionospheric Disturbances, *J. Atmos. Terrest. Phys.*, **30**(5): 735-746.
- Georgi, J., 1960, Flugzeug-Kondensfahne erzeugt ausgedehntes Wolkenfeld, *Z. Meteorol.*, **14**(4): 102.
- Georgii, H.-W., 1960a, Untersuchungen über atmosphärische Spurenstoffe und ihre Bedeutung für die Chemie der Niederschläge, *Geofis. Pura Appl.*, **47**: 155-171.
- , 1960b, The Influence of Climate and Weather Elements on the Activity of Natural Freezing Nuclei, Geophysics Monograph No. 5, pp. 233-239, American Geophysics Union.
- , 1963, Oxides of Nitrogen and Ammonia in the Atmosphere, *J. Geophys. Res.*, **68**(13): 3963-3970.
- , and D. Jost, 1964, Untersuchung über die Verteilung von Spurengasen in der freien Atmosphäre, *Pure Appl. Geophys.*, **59**: 217-224.
- Ghosh, S. N., 1968, Distributions and Lifetimes of N and NO Between 100 and 280 Kilometers, *J. Geophys. Res.*, **73**(1): 309-318.
- , and V. Mitra, 1966, Enhancement of Li I Line (6708Å) in the Twilight Airglow Due to Thermonuclear Explosions, *Ann. Geophys.*, **22**(4): 609-613.
- Giese, R. H., 1962, Light Scattering by Small Particles and Models of Interplanetary Matter Derived from the Zodiacal Light, *Space Sci. Rev.*, **1**: 589-611.
- , and H. Siedentopf, 1962, Optische Eigenschaften von Modellen der interplanetaren Materie, *Z. Astrophys.*, **54**: 200-216.
- Gille, J. C., 1968, On the Possibility of Estimating Diurnal Temperature Variation at the Stratopause from Horizon Radiance Measurements, *J. Geophys. Res.*, **73**(6): 1863-1868.
- Godshall, F. A., L. J. Allison, J. Hansen, and G. Warnecke, 1969, The Association of Monthly Average Cloud Cover, Derived from Meteorological Satellite Data and Sea Surface

- Temperature with the Large Scale Circulation over the Tropical Pacific Ocean, paper presented at the AMS-RMS Conference on the Global Circulation of the Atmosphere, London, England, Aug. 25 to 29, 1969.
- Godson, W. L., 1955, The Computation of Infra-Red Transmission by Atmospheric Water Vapour, *J. Meteorol.*, 12(3): 272-284.
- , 1960, Total Ozone and the Middle Stratosphere over Arctic and Subarctic Areas in Winter and Spring, *Quart. J. Roy. Meteorol. Soc.*, 86(369): 301-317.
- , 1962, The Representation and Analysis of Vertical Distributions of Ozone, *Quart. J. Roy. Meteorol. Soc.*, 88(377): 220-232.
- , 1963, A Comparison of Middle-Stratosphere Behaviour in the Arctic and Antarctic, with Special Reference to Final Warmings, *Meteorol. Abh., Inst. Meteorol. Geophys., Freie Univ. Berlin*, 36: 161-206.
- Goetz, A., 1966, Microphysical and Chemical Aspects of Sea Fog and Oceanic Haze, Report ARG67-FR-456, Atmospheric Research Group, Altadena, Calif.
- Gokhale, N. R., and J. Goold, Jr., 1969, Ice-Nucleating Properties of Dust Collected Above 80 Kilometers, *J. Geophys. Res.*, 74(23): 5374-5378.
- Goldberg, L. J., 1968, Application of the Microaerofluorometer to the Study of Dispersion of a Fluorescent Aerosol into a Selected Atmosphere, *J. Appl. Meteorol.*, 7(1): 68-72.
- Goldsmith, P., 1964, Measurements of Humidity up to 30 Km Using a New Hygrometer, paper presented at the International Atmospheric Ozone Symposium, Albuquerque, New Mexico, September.
- , H. J. Delafield, and L. C. Cox, 1961, Measurement of the Deposition of Submicron Particles in Gradients of Vapour Pressure and of the Efficiency of this Mechanism in the Capture of Particulate Matter by Cloud Droplets in Nature, *Geofis. Pura Appl.* 50: 278-280.
- Golomb, D., 1962a, Generation of a Luminous Trail in the Night Sky, Research Report, Report AFCRL-62-826, pp. 103-111, Space Physics Laboratory.
- , 1962b, Artificial Electron Removal from the F-Layer, Report AFCRL-62-862, pp. 113-121, Air Force Cambridge Research Laboratories.
- , and R. E. Good, 1967, Upper Atmosphere O-Atom Densities by Wind Tunnel Simulation of Nitric Oxide Releases, *J. Geophys. Res.*, 71(23): 5753-5756.
- , R. E. Good, and R. S. Mabee, 1968, Air Densities in the Lower Thermosphere from Jet Radii, *J. Geophys. Res.*, 73(9): 3017-3023.
- , and M. MacLeod, 1966, Diffusion Coefficients in the Upper Atmosphere from Chemiluminous Trails, *J. Geophys. Res.*, 71(9): 2299-2307.
- , N. W. Rosenberg, C. Aharonian, J. A. F. Hill, and H. L. Alden, 1965, Oxygen Atom Determination in the Upper Atmosphere by Chemiluminescence of Nitric Oxide, *J. Geophys. Res.*, 70(5): 1155-1173.
- , N. W. Rosenberg, J. W. Wright, and R. A. Barnes, 1964, Formation of an Electron Depleted Region in the Ionosphere by Chemical Releases, in Proceedings of the Fourth International Space Science Symposium, Warsaw, June 4-10, 1963, *Space Research*, IV, pp. 389-398, John Wiley & Sons, Inc., New York.
- Goodwin, G. L., 1968, Fourier Analyses and Interpretation of D- and E-Region Winds, *J. Atmos. Terrest. Phys.*, 30(5): 995-1017.
- Gordon, C. M., and R. E. Larson, 1964, Activation Analysis of Aerosols, *J. Geophys. Res.*, 69(14): 2881-2885.
- Gordon, W. E., 1967, F-Region and Magnetosphere, Backscatter Results, *Rev. Geophys.*, 5(2): 191-205.
- Gossard, E. E., and M. R. Paulson, 1968, A Case Study of a Periodic Structure in the Atmosphere Near the 90 Km Level, *J. Atmos. Terrest. Phys.*, 30(5): 885-896.
- Götz, F. W. P., 1951, Ozone in the Atmosphere, *Compendium of Meteorology*, pp. 275-291, American Meteorological Society, Boston, Mass.
- Goyer, G. G., and R. D. Watson, 1968, Laser Techniques for Observing the Upper Atmosphere, *Bull. Amer. Meteorol. Soc.*, 49(9): 890-895.

- Grams, G., and G. Fiocco, 1967, Stratospheric Aerosol Layer During 1964 and 1965, *J. Geophys. Res.*, 72(14): 3523-3542.
- Grantham, D. D., and A. J. Kantor, 1967, Distribution of Radar Echoes over the United States, Report AFCRL-67-0232, Air Force Cambridge Research Laboratories.
- Grasnick, K.-H., and W. Hoebbel, 1967, Final Warmings and Ozone Variations, paper presented at 14th General Assembly of the International Union of Geodesy and Geophysics, Lucerne, Switzerland, Sept. 25–Oct. 7, 1967.
- Green, A. E. S., L. R. Peterson, and S. S. Prasad, 1969, Semi-Empirical Cross Sections and the Airglow and Aurora, in *Atmospheric Emissions*, B. M. McCormac and A. Omholt (Eds.), pp. 523-532, Van Nostrand-Reinhold Co., New York.
- Green, H. L., and W. R. Lane, 1964, *Particulate Clouds: Dusts, Smokes and Mists*, Van Nostrand Co., Inc., New York.
- Green, J. S. A., 1965, Atmospheric Tidal Oscillation: An Analysis of the Mechanics, *Proc. Roy. Soc. (London)*, Ser. A, 288: 564-574.
- Greenfield, S. M., 1957, Rain Scavenging of Particulate Matter from the Atmosphere, *J. Meteorol.*, 14(2): 115-125.
- Greenhow, J. S., and J. E. Hall, 1960, Diurnal Variation of Density and Scale Height in the Upper Atmosphere, *J. Atmos. Terrest. Phys.*, 18: 203-214.
- , and A. C. B. Lovell, 1960, The Upper Atmosphere and Meteors, in *Physics of the Upper Atmosphere*, J. A. Ratcliffe (Ed.), pp. 513-549, Academic Press Inc., New York and London.
- , and E. L. Neufeld, 1956, The Height Variation of the Upper Atmosphere Winds, *Phil. Mag.*, 1: 1157-1171.
- , and E. L. Neufeld, 1961, Winds in the Upper Atmosphere, *Quart. J. Roy. Meteorol. Soc.*, 87(374): 472-489.
- Greer, R. G. H., and G. T. Best, 1967, A Rocket-Borne Photometric Investigation of the Oxygen Lines at 5577 Å and 6300 Å, the Sodium D-Lines and the Continuum at 5300 Å in the Night Airglow, *Planet. Space Sci.*, 15: 1857-1881.
- Gregory, J. B., 1965, The Influence of Atmospheric Circulation on Mesospheric Electron Densities in Winter, *J. Atmos. Sci.*, 22(1): 18-23.
- , 1968, Solar Influences and Their Variations, *Meteorol. Monogr.*, 9(31): 19-31.
- Griggs, M., 1963, Measurements of the Vertical Distribution of Atmospheric Ozone at Nairobi, *Quart. J. Roy. Meteorol. Soc.*, 89(380): 284-286.
- Grigorevskii, V. M., 1964, Correlation Between the Period of Rotation of Satellite 1958 61 and Solar Activity, *Planet. Space Sci.*, 12: 1121-1128.
- Gringorten, I. I., H. A. Salmela, I. Solomon, and J. Sharp, 1966, Atmospheric Humidity Atlas—Northern Hemisphere, Air Force Surveys in Geophysics, No. 186, Report AF-CRL-66-621, Air Force Cambridge Research Laboratories.
- Groves, G. V., 1962, Initial Expansion to Ambient Pressure of Chemical Explosive Releases in the Upper Atmosphere, Report AFCRL-62-826, pp. 15-43, Air Force Cambridge Research Laboratories.
- , 1966, Variations in Upper Atmosphere Wind, Temperature, and Pressure at Woomera During the Night of 29/30 April 1965, *Space Research*, VII, p. 977, Humanities Press, New York.
- Gruner, P., 1958, Dämmerungserscheinungen, *Handb. Geophys.*, 8: 432-526.
- Gunn, R., 1964, The Secular Increase of the Worldwide Fine Particle Pollution, *J. Atmos. Sci.*, 21(2): 168-181.
- Gupta, P. K. S., 1964, Characteristic Pattern of Total Ozone During Recent Winters at New Delhi, *Beitr. Phys. Atmos.*, 37: 161-173.
- Gussman, R. A., 1969, On the Aerosol Particle Slip Correction Factor, *J. Appl. Meteorol.*, 8(6): 999-1001.
- , and A. M. Sacco, 1964, Notes on a Method of Establishing the Size Distribution of Meteorological Tracer Aerosols, *J. Appl. Meteorol.*, 3(5): 638-640.
- Gutnick, M., 1961, How Dry is the Sky? *J. Geophys. Res.*, 66(9): 2867-2871.

- , 1962, Mean Annual Mid-Latitude Moisture Profiles to 31 Km, Air Force Surveys in Geophysics, No. 147, July.
- Haagen-Smit, A. J., 1958, Air Conservation, *Science*, 128(3329): 869-878.
- Haarländer, H., 1959, Zum Problem der Verfrachtung radioaktiver Spurenstoffe in der Atmosphäre, *Ber. Deut. Wetterdienstes, Offenbach*, No. 55.
- Haerendel, G., R. Lüst, and E. Rieger, 1967, Motion of Artificial Ion Clouds in the Upper Atmosphere, *Planet. Space Sci.*, 15: 1-18.
- Hage, K. D., 1961, The Influence of Size Distribution on the Ground Deposit of Large Particles Emitted from an Elevated Source, *Int. J. Air Water Pollut.*, 4: 24-32.
- , 1964, Comments on "An Atmospheric Dust Fall Experiment," *J. Atmos. Sci.*, 21(6): 704-705.
- Haines, A., and B. Musgrave, 1964, Chemical State of Tritium in the Atmosphere and Sources of Tritiated Methane, in *Radioactive Fallout from Nuclear Weapons Tests*, Alfred W. Klement (Ed.), AEC Symposium Series, No. 5 (CONF-765), pp. 144-149.
- , and B. Musgrave, 1968, Tritium Content of Atmospheric Methane and Ethane, *J. Geophys. Res.*, 73(4): 1167-1173.
- Hall, L. A., C. W. Chagnon, and H. E. Hinteregger, 1967, Daytime Variations in the Composition of the Upper Atmosphere, *J. Geophys. Res.*, 72(13): 3425-3427.
- Hamilton, W. L., and C. Bull, 1966, A Comparison of the Dust Flux in the Upper Atmosphere and on the Polar Ice Sheets, *J. Geophys. Res.*, 71(10): 2679-2683.
- Hampson, J., 1964, Photochemical Behavior of the Ozone Layer, Canadian Armament Research and Development Establishment, TN, 1627/64.
- Handa, B. K., 1969a, Chemical Composition of Monsoon Rains over Calcutta, Part I, *Tellus*, 21(1): 95-100.
- , 1969b, Chemical Composition of Monsoon Rains over Calcutta, Part II, *Tellus*, 21(1): 101-106.
- Hänel, G., 1968, The Real Part of the Mean Complex Refractive Index and the Mean Density of Samples of Atmospheric Aerosol Particles, *Tellus*, 20(3): 371-379.
- Hann, J., and R. Süring, 1939, *Lehrbuch der Meteorologie*, Vol. I, Verlag Withbald Keller, Leipzig.
- Hanna, S. R., 1969, The Formation of Longitudinal Sand Dunes by Large Helical Eddies in the Atmosphere, *J. Appl. Meteorol.*, 8(6): 874-883.
- Hanson, W. B., and J. S. Donaldson, 1967, Sodium Distribution in the Upper Atmosphere, *J. Geophys. Res.*, 72(21): 5513-5514.
- Hanya, T., 1951, Average Composition of Japanese Fresh Waters and Some Consideration on It, in *Scientific Hydrology*, pp. 516-518, International Union of Geodesy and Geophysics.
- Harang, O., 1964, Excitation of A10 Bands in the Sunlit Atmosphere and the Determination of the Temperature from the Distribution Among the Vibrational Levels, *Planet. Space Sci.*, 12: 567-571.
- , 1969, Summary on Spectroscopy of Rocket Releases, in *Atmospheric Emissions*, B. M. McCormac and A. Omholt (Eds.), pp. 489-499, Van Nostrand-Reinhold Co., New York.
- Harnischmacher, E., 1964, Évolution dans le temps des vents dans la région E, *Ann. Geophys.*, 20(4): 425-446.
- Harris, B., 1964, Volcanic Particles in the Stratosphere, *Aust. J. Phys.*, 17: 472-479.
- Harris, I., 1966, Horizontal Energy Transport in the Thermosphere, *Trans. Amer. Geophys. Union*, 47: 459.
- , and W. Priester, 1962, Time-Dependent Structure of the Upper Atmosphere, *J. Atmos. Sci.*, 19(4): 286-301.
- , and W. Priester, 1965, On the Diurnal Variation of the Upper Atmosphere, *J. Atmos. Sci.*, 22(1): 3-10.
- , and W. Priester, 1968, The Structure of the Thermosphere and Its Variations, *Meteorol. Monogr.*, 9(31): 72-81.
- , and W. Priester, 1969, On the Semiannual Variation of the Upper Atmosphere, *J. Atmos. Sci.*, 26(2): 233-240.

- Harris, M. F., F. G. Finger, and S. Teweles, 1965, Frictional and Thermal Influences in the Solar Semidiurnal Tide, *Mon. Weather Rev.*, **94**: 427-447.
- H.A.S.P., 1960, High Altitude Sampling Program, Report DASA-532, pp. 1-252, Defense Atomic Support Agency, Washington, D.C.
- Hass, W. A., W. H. Hoecker, D. H. Pack, and J. K. Angell, 1967, Analysis of Low-Level Constant Volume Balloon (Tetron) Flights over New York City, *Quart. J. Roy. Meteorol. Soc.*, **93**(398): 483-493.
- Hastenrath, S. L., 1966, On General Circulation and Energy Budget in the Area of the Central American Seas, *J. Atmos. Sci.*, **23**(6): 694-711.
- Hatrúwitz, B., 1961, Frictional Effects and the Meridional Circulation in the Mesosphere, *J. Geophys. Res.*, **66**(8): 2381-2391.
- , 1964, Tidal Phenomena in the Upper Atmosphere, Technical Note No. 58, Report WMO 146.TP.69, World Meteorological Organization.
- Hedin, A. E., C. P. Avery, and C. D. Tschetter, 1964, An Analysis of Spin Modulation Effects on Data Obtained with a Rocket-Borne Mass Spectrometer, *J. Geophys. Res.*, **69**(21): 4637-4648.
- , and A. O. Nier, 1965, Diffusive Separation in the Upper Atmosphere, *J. Geophys. Res.*, **70**(5): 1273-1274.
- Helliwell, N. C., J. K. Mackenzie, and M. J. Kerley, 1957, Some Further Observations from Aircraft of Frost Point and Temperature up to 50,000 Feet, *Quart. J. Roy. Meteorol. Soc.*, **83**(356): 257-262.
- Hemenway, C. L., E. F. Fullam, R. A. Skrivanek, R. K. Soberman, and G. Witt, 1964, Electron Microscope Studies of Noctilucent Cloud Particles, *Tellus*, **16**(1): 96-102.
- , and R. K. Soberman, 1962, Studies of Micrometeorites Obtained from a Recoverable Sounding Rocket, *Astron. J.*, **67**: 256-266.
- , R. K. Soberman, and G. Witt, 1964, Sampling of Noctilucent Cloud Particles, *Tellus*, **16**(1): 84-88.
- Hering, W. S., 1964, Ozonesonde Observations over North America, Vol. I, Research Report, Report AF-CRL-64-30(I), pp. 1-512, Air Force Cambridge Research Laboratories.
- , and T. R. Borden, Jr., 1964, Ozonesonde Observations over North America, Vol. 2, Environmental Research Paper No. 38, Report AFCRL-64-30(II), Air Force Cambridge Research Laboratories.
- , and T. R. Borden, Jr., 1965a, Ozonesonde Observations over North America, Vol. 3, Environmental Research Paper No. 133, Report AFCRL-64-30(III), Air Force Cambridge Research Laboratories.
- , and T. R. Borden, Jr., 1965b, Mean Distributions of Ozone Density over North America, 1963-1964, Environmental Research Paper No. 162, Report AFCRL-65-913, Air Force Cambridge Research Laboratories.
- , and T. R. Borden, Jr., 1967, Ozonesonde Observations over North America, Vol. 4, Environmental Research Paper No. 279, Report AFCRL-64-30(IV), Air Force Cambridge Research Laboratories.
- , C. N. Touart, and T. R. Borden, Jr., 1967, Ozone Heating and Radiative Equilibrium in the Lower Stratosphere, *J. Atmos. Sci.*, **24**(4): 402-413.
- Herman, B. M., and D. N. Yarger, 1969, Estimating the Vertical Atmospheric Ozone Distribution by Inverting the Radiative Transfer Equation for Pure Molecular Scattering, *J. Atmos. Sci.*, **26**(1): 153-162.
- Hernandez, G. J., 1965, Data Previous to the International Geophysical Year I: 5577 [OI] Line at Sacramento Peak, New Mexico, Research Report, Report AFCRL-65-319, Air Force Cambridge Research Laboratories.
- , and S. M. Silverman, 1964, A Re-examination of Lord Rayleigh's Data on the Airglow 5577 Å [OI] Emission, *Planet. Space Sci.*, **12**: 97-112.
- , and J. P. Turtle, 1965, Nightglow 5577 Å [OI] Line Kinetic Temperatures, *Planet. Space Sci.*, **13**: 901-904.

- Hesstvedt, E., 1959, Mother of Pearl Clouds in Norway, *Geofis. Publ.*, 20(10): 29.
- , 1961, Note on the Nature of Noctilucent Clouds, *J. Geophys. Res.*, 66(6): 1985-1987.
- , 1963, On the Determination of Characteristic Times in a Pure Oxygen Atmosphere, *Tellus*, 15(1): 82-88.
- , 1964, On the Water Vapor Content in the High Atmosphere, *Geofis. Publ.*, 25(3): 18.
- , 1965a, On the Spatial Distribution of Some Hydrogen Components in the Mesosphere and Lower Thermosphere, *Tellus*, 17(3): 341-349.
- , 1965b, The Ozone Distribution over the Equator and Its Dependence on Vertical Motions, *Tellus*, 17(2): 177-179.
- , 1965c, Some Characteristics of the Oxygen-Hydrogen Atmosphere, *Geofis. Publ.*, 26(1): 30 pp.
- , 1967a, On the Moisture Content Near the Mesopause and Its Relation to the Formation of Noctilucent Clouds, paper presented at 14th General Assembly of the International Union of Geodesy and Geophysics, Lucerne, Switzerland, Sept. 25–Oct. 7, 1967.
- , 1967b, On the Effect of Vertical Eddy Diffusion on Atmospheric Composition in the Mesosphere and Lower Thermosphere, report under Contract No. DAJA37-67-C-0848, European Research Office, U. S. Army.
- , 1967c, On the Dissociation of Water Vapor in the Mesosphere and Lower Thermosphere—a Theoretical Study, preliminary report under Contract No. DAJA37-67-C-0848, European Research Office, U. S. Army.
- , 1968a, On the Photochemistry of Ozone in the Ozone Layer, report under Contract No. DAJA37-67-C-0848, European Research Office, U. S. Army.
- , 1968b, On the Effect of Vertical Eddy Transport on Atmospheric Composition in the Mesosphere and Lower Thermosphere, *Geofis. Publ.*, 27(4): 35 pp.
- , 1969a, Air Glow and Vertical Eddy Transport, in *Atmospheric Emissions*, B. M. McCormac and A. Omholt (Eds.), pp. 501-505, Van Nostrand-Reinhold Co., New York.
- , 1969b, The Physics of Nacreus and Noctilucent Clouds, in *Stratospheric Circulation*, W. L. Webb (Ed.), pp. 209-217, Academic Press Inc., New York.
- , 1969c, The Effect of Vertical Eddy Transport on the Composition of the Mesosphere and Lower Thermosphere, in *Stratospheric Circulation*, W. L. Webb (Ed.), pp. 307-316, Academic Press Inc., New York.
- , and U. B. Jansson, 1968, On the Effect of Vertical Eddy Transport on the Distribution of Neutral Nitrogen Components in the D-Region, report under Contract No. DAJA37-67-C-0848 with European Research Office, U. S. Army, University of Oslo.
- Heuvel, A. P. van den, and B. J. Mason, 1963, The Formation of Ammonium Sulphate in Water Droplets Exposed to Gaseous Sulphur Dioxide and Ammonia, *Quart. J. Roy. Meteorol. Soc.*, 89(380): 271-275.
- Hibbs, A. R., 1961, The Distribution of Micrometeorites Near the Earth, *J. Geophys. Res.*, 66(2): 371-377.
- Hidy, G. M., and J. R. Brock, 1967, Photophoresis and the Descent of Particles Into the Lower Stratosphere, *J. Geophys. Res.*, 72(2): 455-460.
- Hilsenrath, E., L. Seiden, and P. Goodman, 1969, An Ozone Measurement in the Mesosphere and Stratosphere by Means of a Rocket Sonde, *J. Geophys. Res.*, 74(28): 6873-6880.
- Hines, C. O., 1959, An Interpretation of Certain Ionospheric Motions in Terms of Atmospheric Waves, *J. Geophys. Res.*, 64(12): 2210-2211.
- , 1960, Internal Atmospheric Gravity Waves at Ionospheric Heights, *Can. J. Phys.*, 38: 1441-1481.
- , 1963, The Upper Atmosphere in Motion, *Quart. J. Roy. Meteorol. Soc.*, 89(379): 1-42.
- , 1965, Comments on "The Rotational Speed of the Upper Atmosphere Determined from Changes in Satellite Orbits," by D. G. King-Hele, *Planet. Space Sci.*, 13: 169-172.
- , 1966, Diurnal Tide in the Upper Atmosphere, *J. Geophys. Res.*, 71(5): 1453-1475.
- , 1968a, Tidal Oscillations, Shorter Period Gravity Waves and Shear Waves, *Meteorol. Monogr.*, 9(31): 114-121.

- , 1968b, A Possible Source of Waves in Noctilucent Clouds, *J. Atmos. Sci.*, 25(5): 937-942.
- , 1968c, Some Consequences of Gravity-Wave Critical Layers in the Upper Atmosphere, *J. Atmos. Terrest. Phys.*, 30(5): 837-843.
- , 1968d, An Effect of Molecular Dissipation in Upper Atmospheric Gravity Waves, *J. Atmos. Terrest. Phys.*, 30(5): 845-849.
- , 1968e, An Effect of Ohmic Losses in Upper Atmospheric Gravity Waves, *J. Atmos. Terrest. Phys.*, 30(5): 851-856.
- , and R. Raghava Rao, 1968, Validity of Three-Station Methods of Determining Ionospheric Motions, *J. Atmos. Terrest. Phys.*, 30(5): 979-993.
- Hinteregger, H. E., 1964, Notes on Wright's Interpretation of Temporal Variation on O/N₂ Ratio in the Thermosphere, *J. Geophys. Res.*, 69(13): 2854-2856.
- Hitschfeld, W., and J. T. Houghton, 1961, Radiative Transfer in the Lower Stratosphere Due to the 9.6 Micron Band of Ozone, *Quart. J. Roy. Meteorol. Soc.*, 87(374): 562-577.
- , and J. T. Houghton, 1962, Radiative Transfer in the Lower Stratosphere Due to the 9.6 Micron Band of Ozone, *Quart. J. Roy. Meteorol. Soc.*, 88(376): 193-195.
- , and J. T. Houghton, 1963, Radiative Transfer in the Lower Stratosphere Due to the 9.6 Micron Band of Ozone (Discussions), *Quart. J. Roy. Meteorol. Soc.*, 89(379): 159-160.
- Hobbs, P. V., and J. D. Locatelli, 1969, Ice Nuclei from a Natural Forest Fire, *J. Appl. Meteorol.*, 8(5): 833-834.
- , and L. F. Radke, 1969, Cloud Condensation Nuclei from a Simulated Forest Fire, *Science*, 163: 279-280.
- Hodge, P. W., and F. W. Wright, 1968, Studies of Particles of Extraterrestrial Origin. 6. Comparison of Previous Influx Estimates and Present Satellite Flux Data, *J. Geophys. Res.*, 73(24): 7589-7592.
- , F. W. Wright, and C. C. Langway, Jr., 1964, Studies of Particles of Extraterrestrial Origin. 3. Analysis of Dust Particles from Polar Ice Deposits, *J. Geophys. Res.*, 69(14): 2919-2931.
- Hoffmann, W. F., 1967, Infrared Astronomy, in *The Encyclopedic of Atmospheric Sciences and Astrogeology*, R. W. Fairbridge (Ed.), pp. 478-480, Reinhold Publishing Co., New York.
- Hogan, A. W., J. M. Bishop, A. L. Aymer, B. W. Harlow, J. C. Klepper, and G. Lupo, 1967, Aitken Nuclei Observations over the North Atlantic Ocean, *J. Appl. Meteorol.*, 6(4): 726-727.
- Hoidale, G., and S. M. Smith, 1968, Analysis of the Giant Particle Component of the Atmosphere over an Interior Desert Basin, *Tellus*, 20(2): 251-268.
- Hoidale, G. B., and A. J. Blanco, 1970, Temporal Variations in the Nature of Atmospheric Dust Above an Interior Desert Basin, *Arch. Meteorol., Geophys. Bioklimatol., Ser. A.*, 19(1): 71-88.
- Holton, J. R., and R. S. Lindzen, 1968, A Note on "Kelvin" Waves in the Atmosphere, *Mon. Weather Rev.*, 96(6): 385-386.
- Hooke, W. H., 1968, Ionospheric Irregularities Produced by Internal Atmospheric Gravity Waves, *J. Atmos. Terrest. Phys.*, 30(5): 795-823.
- Hoover, T. E., and D. C. Berkshire, 1969, Effects of Hydration on Carbon Dioxide Exchange Across an Air-Water Interface, *J. Geophys. Res.*, 74(2): 456-464.
- Hoppe, W., 1961, Bildung von Kondensationskernen durch UV-Strahlung in verschiedenen Gasen, *Geofis. Pura Appl.*, 50: 129-139.
- Hopwood, J. M., 1969, A Note on the Quasi-Biennial Oscillation at Darwin, *Aust. Meteorol. Mag.*, 16(3): 114-117.
- Horiuchi, G., 1962, On the Negative Ion in Mesosphere, *J. Meteorol. Soc. Jap.*, 40(5): 300-302.
- Horvath, H., and K. E. Noll, 1969, The Relationship Between Atmospheric Light Scattering Coefficient and Visibility, *Atmos. Environ.*, 3(5): 543-550.
- Höschele, K., 1966, Der zeitliche Verlauf und die örtliche Verteilung der SO₂-Konzentrationen in einem Stadtgebiet mit einer Analyse der Einflussgrößen, *Meteorol. Rundsch.*, 19(1): 14-22.
- Houghton, D. D., and W. L. Jones, 1968, A Numerical Model for Linearized Gravity and Acoustic Waves, *Bull. Amer. Meteorol. Soc.*, 49(8): 845.

- Houghton, J. T., 1963, Absorption in the Stratosphere by Some Water Vapor Lines in the ν_2 Band, *Quart. J. Roy. Meteorol. Soc.*, **89**(381): 332-338.
- , 1969, Absorption and Emission by Carbon-Dioxide in the Mesosphere, *Quart. J. Roy. Meteorol. Soc.*, **95**(403): 1-20.
- Hulst, H. C. van de, 1947, Zodiacal Light in the Solar Corona, *Astrophys. J.*, **105**: 471-488.
- Hunt, B. G., 1964, A Non-Equilibrium Investigation into the Diurnal Photochemical Atomic Oxygen and Ozone Variations in the Mesosphere, Technical Note PAD 82, Australian Weapons Research Establishment.
- , 1965, Influence of Metastable Oxygen Molecules on Atmospheric Ozone, *J. Geophys. Res.*, **70**(19): 4990-4991.
- , 1966a, Photochemistry of Ozone in a Moist Atmosphere, *J. Geophys. Res.*, **71**(5): 1385-1399.
- , 1966b, The Need for a Modified Photochemical Theory of the Ozonosphere, *J. Atmos. Sci.*, **23**(1): 88-95.
- , 1969, Experiments with a Stratospheric General Circulation Model. III. Large-Scale Diffusion of Ozone Including Photochemistry, *Mon. Weather Rev.*, **97**(4): 287-306.
- , and S. Manabe, 1968, Experiments with a Stratospheric General Circulation Model. II. Large-Scale Diffusion of Tracers in the Stratosphere, *Mon. Weather Rev.*, **96**(8): 503-539.
- Hunten, D. M., 1964, Metallic Emissions from the Upper Atmosphere, *Science*, **145**: 26-31.
- , and W. L. Godson, 1967, Upper-Atmospheric Sodium and Stratospheric Warmings at High Latitudes, *J. Atmos. Sci.*, **24**(1): 80-87.
- , and M. B. McElroy, 1966, Quenching of Metastable States of Atomic and Molecular Oxygen and Nitrogen, *Rev. Geophys.*, **4**(3): 303-328.
- , and M. B. McElroy, 1968, Metastable $O_2(^1\Delta)$ as a Major Source of Ions in the D Region, *J. Geophys. Res.*, **73**(7): 2421-2428.
- , and L. Wallace, 1967, Rocket Measurements of the Sodium Dayglow, *J. Geophys. Res.*, **72**(1): 69-79.
- Huppi, E. R., and A. T. Stair, Jr., 1969, Sunset to Sunrise Variations of the OH Emission of the Night Sky, in *Atmospheric Emissions*, B. M. McCormac and A. Omholt (Eds.), pp. 471-475, Van Nostrand-Reinhold Co., New York.
- Iozenas, V. A., V. A. Krasnopol'skiy, A. P. Kuznetsov, and A. I. Lebedinskiy, 1969a, Study of the Planetary Distribution of Ozone from Ultraviolet Spectra Measured on Satellites, *Izv. Akad. Nauk SSSR Fiz. Atmos. Okeana*, **5**(4): 395-403.
- , V. A. Krasnopol'skiy, A. P. Kuznetsov, and A. I. Lebedinskiy, 1969b, Studies of the Earth's Ozonosphere from Satellites, *Izv. Atmos. Oceanic Phys.*, **5**(2): 149-159 (English translation).
- Istomin, V. G., 1963, Ions of Extraterrestrial Origin in the Earth's Ionosphere, *Planet. Space Sci.*, **11**: 173-181.
- , M. Ya. Marov, and V. V. Mikhnevich, 1969, Scientific and Practical Aspects of the Earth's Upper Atmosphere Structure and Parameter Variations, *Meteorol. Gid.*, **6**: 3-9 (English translation), Report JPRS-48560, Joint Publications Research Service.
- Jacchia, L. G., 1964, Influence of Solar Activity on the Earth's Upper Atmosphere, *Planet. Space Sci.*, **12**: 355-378.
- , 1966, Density Variations in the Heterosphere, *Ann. Geophys.*, **22**(1): 75-85.
- , J. Slowey, and F. Verniani, 1967, Geomagnetic Perturbations and Upper-Atmosphere Heating, *J. Geophys. Res.*, **72**(5): 1423-1434.
- Jacobs, M. B., 1959, Concentration of Sulfur-Containing Pollutants in a Major Urban Area, Atmospheric Chemistry of Chlorine and Sulfur Compounds, *Geophysics Monograph No. 3*, pp. 81-87, American Geophysics Union.
- Jacobs, W. C., 1937, Preliminary Report on the Study of Atmospheric Chlorides, *Mon. Weather Rev.*, **65**: 147-151.
- Jaenicke, R., and C. Junge, 1967, Studien zur oberen Grenzgröße des natürlichen Aerosoles, *Beitr. Phys. Atmos.*, **40**: 129-143.

- Jaffe, L. S., and H. D. Estes, 1963, Ozone Toxicity Hazard in Cabins of High Altitude Aircraft—A Review and Current Program, *Aerospace Med.*, 633-642.
- Jager, C. de, 1955, The Capture of Zodiacal Dust by the Earth, *Mem. Soc. Roy. Sci. Liège*, 15: 174-182.
- Jarrett, A. H., G. J. McGrattan, and J. A. Rees, 1963a, The Measurement of High Altitude Wind Velocities from Vapour Releases. I. Projector Method, *Planet. Space Sci.*, 11: 1309-1310.
- , G. J. McGrattan, and F. J. Smith, 1963b, The Measurement of High Altitude Wind Velocities from Vapour Releases. III. Trails Released from Flights SL16 and SL63 at Woomera, *Planet. Space Sci.*, 11: 1319-1324.
- Jesse, O., 1896, Die Höhe der leuchtenden Nachtwolken, *Astron. Nachr.*, 140: 161-168.
- Johnson, F. S., 1968, System for Collecting Worldwide Lower Thermosphere Data, *Meteorol. Monogr.*, 9(31): 208-212.
- Jones, L. M., and J. W. Peterson, 1968, Falling Sphere Measurements, 30 to 120 km, *Meteorol. Monogr.*, 9(31): 176-189.
- Jones, W. L., 1969, Atmospheric Internal Gravity Waves and Tides, in *Stratospheric Circulation*, W. L. Webb (Ed.), pp. 469-482, Academic Press Inc., New York.
- Joseph, J., 1967, Detection of Noctilucent Clouds in the Twilight Layer from Satellites, *J. Geophys. Res.*, 72(15): 4020-4026.
- Juang, F. H. T., and N. M. Johnson, 1967, Cycling of Chlorine Through a Forested Watershed in New England, *J. Geophys. Res.*, 72(22): 5641-5647.
- Junge, C. E., 1956, Recent Investigations in Air Chemistry, *Tellus*, 8(1): 127-139.
- , 1957, Chemical Analysis of Aerosol Particles and of Gas Traces on the Island of Hawaii, *Tellus*, 9(4): 528-537.
- , 1960, Sulfur in the Atmosphere, *J. Geophys. Res.*, 65(1): 227-237.
- , 1962a, Global Ozone Budget and Exchange Between Stratosphere and Troposphere, *Tellus*, 14(4): 363-377.
- , 1962b, Note on the Exchange Rate Between the Northern and Southern Atmosphere, *Tellus*, 14(2): 242-246.
- , 1962c, 3.1 Neuere Ergebnisse der Luftchemie und ihre Bedeutung für die Meteorologie. Meteorologische Tagung in Hamburg, 1962, *Ber. Deut. Wetterdienstes*, 91: 80-88.
- , 1963a, *Air Chemistry and Radioactivity*, International Geophysics Series, Vol. 4, Academic Press Inc., New York and London.
- , 1963b, Sulfur in the Atmosphere, *J. Geophys. Res.*, 68(13): 3975-3976.
- , 1963c, Studies of Global Exchange Processes in the Atmosphere by Natural and Artificial Tracers, *J. Geophys. Res.*, 68(13): 3849-3856.
- , 1969, Comments on "Concentration and Size Distribution Measurements of Atmospheric Aerosols and a Test of the Theory of Self-Preserving Size Distributions," *J. Atmos. Sci.*, 26(3): 603-608.
- , C. W. Chagnon, and J. E. Manson, 1961, Stratospheric Aerosols, *J. Meteorol.*, 18(1): 81-108.
- , and G. Czeplak, 1968, Some Aspects of the Seasonal Variation of Carbon Dioxide and Ozone, *Tellus*, 20(3): 422-434.
- , and J. E. Manson, 1961, Stratospheric Aerosol Studies, *J. Geophys. Res.*, 66(7): 2163-2182.
- , O. Oldenberg, and J. T. Wasson, 1962, On the Origin of the Sodium Present in the Upper Atmosphere, *J. Geophys. Res.*, 67(3): 1027-1040.
- , E. Robinson, and F. L. Ludwig, 1969, A Study of Aerosols in Pacific Air Masses, *J. Appl. Meteorol.*, 8(3): 340-347.
- , and T. G. Ryan, 1958, Study of the SO₂ Oxidation in Solution and Its Role in Atmospheric Chemistry, *Quart. J. Roy. Meteorol. Soc.*, 84(359): 46-55.
- , and G. Scheich, 1969, Studien zur Bestimmung des Säuregehaltes von Aerosolteilchen, *Atmos. Environ.*, 3(4): 423-441.
- , and R. T. Werby, 1958, The Concentration of Chloride, Sodium, Potassium, Calcium and Sulphate in Rainwater over the United States, *J. Meteorol.*, 15(5): 417-425.

- Jurica, G. M., 1966, Radiative Heating in the Troposphere and Lower Stratosphere, *Mon. Weather Rev.*, **94**(9): 573-579.
- Jurkevich, I., 1964, Effects of Ozone, Nitrogen Oxides, and Solar Ultraviolet Radiation on the Supersonic Transport, Technical Information Series, Report R64SD2, pp. 1-70.
- Jursa, A. S., M. Nakamura, and Y. Tanaka, 1965, Molecular Oxygen Distribution in the Upper Atmosphere, *J. Geophys. Res.*, **70**(11): 2699-2702.
- Justus, C. G., and H. E. Edwards, 1965, Tables of Observed Winds in the 70-170 Km Region of the Upper Atmosphere, Georgia Institute of Technology, Engineering Experiment Station Report, July.
- , and J. B. Montgomery III, 1969, A Pilot Study of the Irregular Winds at Chemical Release Altitudes, Technical Report No. AFWL-TR-68-132, Air Force Weapons Laboratory.
- , and R. G. Roper, 1968, Some Observations of Turbulence in the 80 to 110 Km Region of the Upper Atmosphere, *Meteorol. Monogr.*, **9**(31): 122-128.
- Kanellakos, D. P., 1967, Discussion of paper by W. J. Breiting, R. A. Kupferman, and G. J. Gassman, "Travelling Ionospheric Disturbances Associated with Nuclear Detonations," *J. Geophys. Res.*, **72**(21): 5579-5582.
- Kantor, A. J., 1969a, Winds, Temperatures and Densities over Thule, Greenland, at 25 to 65 Kilometers, Environmental Research Paper No. 297, Report AFCRL-69-0025, Air Force Cambridge Research Laboratories.
- , 1969b, Strong Wind and Vertical Wind Shear Above 30 Km, Environmental Research Paper No. 303, Report AFCRL-69-0346, Air Force Cambridge Research Laboratories.
- Kanwisher, J., 1960, pCO₂ in Sea Water and Its Effect on the Movement of CO₂ in Nature, *Tellus*, **12**(2): 209-215.
- , 1963, Effect of Wind on CO₂ Exchange Across the Sea Surface, *J. Geophys. Res.*, **68**(13): 3921-3928.
- Kao, S.-K., 1965, Some Aspects of the Large-Scale Turbulence and Diffusion in the Atmosphere, *Quart. J. Roy. Meteorol. Soc.*, **91**(387): 10-17.
- , 1967, Some Aspects of the Large-Scale Turbulence and Diffusion in the Atmosphere, *Quart. J. Roy. Meteorol. Soc.*, **93**(397): 387-390.
- , 1968, Relative Dispersion of Particles in a Stratified Rotating Atmosphere, *J. Atmos. Sci.*, **25**(3): 481-487.
- , and A. A. Al-Gain, 1968, Large-Scale Dispersion of Clusters of Particles in the Atmosphere, *J. Atmos. Sci.*, **25**(2): 214-221.
- , and W. S. Bullock, 1964, Lagrangian and Eulerian Correlations and Energy Spectra of Geostrophic Velocities, *Quart. J. Roy. Meteorol. Soc.*, **90**(384): 166-174.
- , and W. S. Bullock, 1967, Lagrangian and Eulerian Correlations and Energy Spectra of Geostrophic Velocities, *Quart. J. Roy. Meteorol. Soc.*, **93**(397): 387-390.
- , and W. R. Hill, 1970, Characteristics of the Large-Scale Dispersion of Particles in the Southern Hemisphere, *J. Atmos. Sci.*, **27**(1): 126-132.
- , and D. C. Powell, 1969, Large-Scale Dispersion of Clusters of Particles in the Atmosphere. II. Stratosphere, *J. Atmos. Sci.*, **26**(4): 734-740.
- , and E. E. Sands, 1966, Energy Spectrums, Mean and Eddy Kinetic Energies of the Atmosphere Between Surface and 50 Kilometers, *J. Geophys. Res.*, **71**(22): 5213-5219.
- , and H. D. Woods, 1964, Energy Spectra of Meso-Scale Turbulence Along and Across the Jet Stream, *J. Atmos. Sci.*, **21**(5): 513-519.
- Kaplan, L. D., 1960, The Influence of Carbon Dioxide Variations on the Atmospheric Heat Balance, *Tellus*, **12**(2): 204-208.
- Kapoor, R. K., R. S. Sekhon, A. S. Ramachandra Murty, and Bh. V. Ramana Murty, 1969, Ice-Forming Nuclei and Their Dominant Source Region, *J. Meteorol. Soc. Jap.*, **47**(3): 219-226.
- Kasten, F., 1968, Falling Speed of Aerosol Particles, *J. Appl. Meteorol.*, **7**(5): 944-947.
- Kato, S., and S. Matsushita, 1968, Space Charge Waves and Ionospheric Irregularities, *J. Atmos. and Terrest. Phys.*, **30**: 857-869.

- Kaufman, F., 1964, Aeronomic Reactions Involving Hydrogen, a Review of Recent Laboratory Studies, *Ann. Geophys.*, **20**: 106-114.
- Kays, M., and R. O. Olsen, 1967, Improved Technique for Deriving Wind Profiles from Rocketsonde Parachutes, *J. Geophys. Res.*, **72**(16): 4035-4040.
- Keeling, C. D., 1958, The Concentration and Isotopic Abundances of Atmospheric Carbon Dioxide in Rural Areas, *Geochim. Cosmochim. Acta.*, **13**: 322-334.
- , 1960, The Concentration and Isotopic Abundances of Carbon Dioxide in the Atmosphere, *Tellus*, **12**(2): 200-203.
- , 1965, Carbon Dioxide in Surface Waters of the Pacific Ocean. 2. Calculation of the Exchange with the Atmosphere, *J. Geophys. Res.*, **70**(24): 6099-6102.
- , 1968, Carbon Dioxide in Surface Ocean Waters. 4. Global Distribution, *J. Geophys. Res.*, **73**(14): 4543-4553.
- , T. B. Harris, and E. M. Wilkins, 1968, Concentration of Atmospheric Carbon Dioxide at 500 and 700 Millibars, *J. Geophys. Res.*, **73**(14): 4511-4528.
- , and L. S. Waterman, 1968, Carbon Dioxide in Surface Ocean Waters. 3. Measurements on Lusiad Expedition 1962-1963, *J. Geophys. Res.*, **73**(14): 4529-4541.
- Kelley, J. J., Jr., 1964, An Analysis of Carbon Dioxide in the Arctic Atmosphere at Point Barrow, Alaska, Technical Report ONR Contract 477(24)NR307-252, Department of Atmospheric Science, University of Washington, Seattle.
- , 1969a, Investigations of Atmospheric Trace Gases and Suspended Particulate Matter on Mount Olympus, Washington, *J. Geophys. Res.*, **74**(2): 435-443.
- , 1969b, Observations of Carbon Dioxide in the Atmosphere over the Western United States, *J. Geophys. Res.*, **74**(6): 1688-1693.
- , and E. LaChapelle, 1966, Atmospheric Carbon Dioxide Variations on Mount Olympus, Washington, *J. Geophys. Res.*, **71**(8): 2173-2175.
- , and J. D. McTaggart-Cowan, 1968, Vertical Gradient of Net Oxidant Near the Ground Surface at Barrow, Alaska, *J. Geophys. Res.*, **73**(10): 3328-3330.
- Kellogg, W. W., 1961, Warming of the Polar Mesosphere and Lower Ionosphere in the Winter, *J. Meteorol.*, **18**(3): 373-381.
- , 1964, Meteorological Soundings in the Upper Atmosphere, Technical Note No. 60, WMO-No. 153.TP.73, World Meteorological Organization.
- , 1968, Research on the Lower Fringe of Space, *Meteorol. Monogr.*, **9**(31): 2-6.
- Keneshea, T. J., 1962, A Computer Program for Solving the Reaction Rate Equation in the E Ionospheric Region, Research Report, Report AFCRL-62-828, Air Force Cambridge Research Laboratories.
- , 1963, A Solution to the Reaction Rate Equations in the Atmosphere Below 150 Kilometers, Research Report, Report AFCRL-63-711, pp. 1-127, Air Force Cambridge Research Laboratories.
- , 1967, A Technique for Solving the General Reaction-Rate Equations in the Atmosphere, Environmental Research Paper No. 263, Report AFCRL-67-0221, Air Force Cambridge Research Laboratories.
- , and R. J. Fowler, 1966, Computed Electron, Ion and Neutral Density Profiles for the Solar Eclipse of 12 November, 1966, Environmental Research Paper No. 233, Report AFCRL-66-741, Air Force Cambridge Research Laboratories.
- Kennedy, J. S., and W. Nordberg, 1967, Circulation Features of the Stratosphere Derived from Radiometric Temperature Measurements with the TIROS VII Satellite, *J. Atmos. Sci.*, **24**(6): 711-719.
- Kent, G. S., and R. W. H. Wright, 1968, Movements of Ionospheric Irregularities and Atmospheric Winds, *J. Atmos. Terrest. Phys.*, **30**(5): 657-691.
- Khemani, L. T., and Bh. V. Ramana Murty, 1968, Chemical Composition of Rain Water and Rain Characteristics at Delhi, *Tellus*, **20**(2): 284-292.

REFERENCES

- King, G. A. M., 1964, The Dissociation of Oxygen and High Level Circulation in the Atmosphere, *J. Atmos. Sci.*, 21(3): 231-237.
- , 1967, Discussion of paper by B. Machlum, "On the 'Winter Anomaly' in the Midlatitude D Region," *J. Geophys. Res.*, 72(23): 6118-6119.
- King-Hele, D. G., 1964, The Rotational Speed of the Upper Atmosphere Determined from Changes in Satellite Orbits, *Planet. Space Sci.*, 12: 835-853.
- Kinisky, J. J., W. D. Komhyr, and C. L. Mateer, 1961, Measurements of Atmospheric Ozone at Edmonton, Canada, 53°34'N:113°31'W—July 1, 1957 to June 30, 1960, Canadian Meteorological Memoirs, No. 8.
- Kitaoka, T., 1963, Some Considerations on the Stratospheric Circulation Related to the Cause of the Aleutian High, *Meteorol. Abh., Inst. Meteorol. Geophys., Freie Univ. Berlin*, 36: 121-152.
- Kleinschmidt, E., Jr., 1959, Nicht-adiabatische Abkühlung im Bereich der Jetstream, *Beitr. Phys. Atmos.*, 32(1-2): 94-108.
- Kline, D. B., 1960, Recent Observations of Freezing Nuclei Variations at Ground Level, *Geophysics Monograph No. 5*, pp. 240-246, American Geophysical Union.
- , 1963, Evidence of Geographical Differences in Ice Nuclei Concentrations, *Mon. Weather Rev.*, 91(10-12): 681-686.
- Knudsen, W. C., 1968, Geographic Distribution of F-Region Electrons with About 10-EV Energy, *J. Geophys. Res.*, 73(3): 841-856.
- Koch, W. L., 1961, Meteorological Requirements for Supersonic Transport Aircraft, a working paper, Contract No. FAA/BRD-139, pp. 1-14, FAA, Bureau of Research and Development.
- Kochanski, A., 1963, Circulation and Temperatures at 70 to 100 Kilometers Height, *J. Geophys. Res.*, 68(1): 213-226.
- , 1964, Atmospheric Motions from Sodium Cloud Drifts, *J. Geophys. Res.*, 69(17): 3651-3662.
- , 1966, Atmospheric Motions from Sodium Cloud Drifts at Four Locations, *Mon. Weather Rev.*, 94(4): 199-212.
- Kolmogorov, A. N., 1958, Die lokale Struktur der Turbulenz in einer inkompressiblen zähen Flüssigkeit bei sehr grossen REYNOLDSschen Zahlen, in *Sammelband zur Statistischen Theorie der Turbulenz*, H. Goering (Ed.), pp. 71-76, Akademie-Verlag, Berlin.
- Komhyr, W. D., 1961, Measurements of Atmospheric Ozone at Moosonee, Canada—July 1, 1957, to July 31, 1960, Canadian Meteorological Memoirs, No. 6.
- Koprova, L. I., 1968, The Statistical Characteristics of the Vertical Structure of the Aerosol Attenuation Coefficient, *Izv., Atmos. Oceanic Phys.*, 4(8): 895-901.
- Kornblum, J. J., 1969a, Micrometeoroid Interaction with the Atmosphere, *J. Geophys. Res.*, 74(8): 1893-1907.
- , 1969b, Concentration and Collection of Meteoric Dust in the Atmosphere, *J. Geophys. Res.*, 74(8): 1908-1919.
- Koster, J. R., and I. K. Katsriku, 1966, Some Equatorial Ionospheric E- and F-Region Drift Measurements at Tamale, *Ann. Geophys.*, 22(3): 440-447.
- Kosters, J. J., T. G. Kyle, and D. G. Murcray, 1969, Attenuation of the Direct Solar Beam by Aerosols, *J. Geophys. Res.*, 74(13): 3379-3383.
- Kotadia, K. M., 1967, Ionospheric Effects of Nuclear Explosions—I, *Ann. Geophys.*, 23(1): 1-11.
- , K. G. Jani, and U. Rawer, 1968, Ionospheric Effects of Nuclear Explosions—II, *Ann. Geophys.*, 24(1): 91-100.
- Koyama, T., 1963, Gaseous Metabolism in Lake Sediments and Paddy Soils and the Production of Atmospheric Methane and Hydrogen, *J. Geophys. Res.*, 68(13): 3971-3974.
- , 1964, Biogeochemical Studies on Lake Sediments and Paddy Soils and the Production of Atmospheric Methane and Hydrogen, in *Recent Researches in the Fields of Hydrosphere, Atmosphere and Nuclear Geochemistry*, p. 143, Water Research Laboratory, Nagoya University, Japan.
- Krassovsky, V. I., 1963, Hydroxyl Emission in the Upper Atmosphere, *Planet. Space Sci.*, 10: 7-17.

- , 1965, Ionospheric Winds and the Distribution of Charged Particles in the Geomagnetic Field, *Planet. Space Sci.*, **13**: 469-470.
- Kreutz, W., 1941, Kohlensäuregehalt der unteren Luftschichten in Abhängigkeit von Witterungsfaktoren, *Angew. Botanik*, **23**: 89-117.
- Kroening, J. L., 1965, Stratosphere and Troposphere: Transport of Material Between Them, *Science*, **147**: 862-864.
- , and E. P. Ney, 1962, Atmospheric Ozone, *J. Geophys. Res.*, **67**(5): 1867-1875.
- Krueger, A. J., 1969, Atmospheric Absorption Anomalies in the Ultraviolet Near an Altitude of 50 Kilometers, *Science*, **166**(3908): 998-1000.
- Kuhn, W. R., and J. London, 1969, Infrared Radiative Cooling in the Middle Atmosphere (30-110 Km), *J. Atmos. Sci.*, **26**(2): 189-204.
- Kulkarni, P. V., 1965, On the Height of the 5577 Å [OI] Airglow Layer in Hawaii, *Ann. Geophys.*, **21**(1): 58-67.
- , and W. R. Steiger, 1967, Correlations Among Night Airglow Radiations, *Ann. Geophys.*, **23**(1): 125-131.
- Kulkarni, R. N., 1962, Comparison of Ozone Variations and of Its Distribution with Height over Middle Latitudes of the Two Hemispheres, *Quart. J. Roy. Meteorol. Soc.*, **88**(378): 522-534; **90**(385): 348-350.
- , 1963, Some Ozone-Weather Relationships in the Middle Latitude of the Southern Hemisphere, *Quart. J. Roy. Meteorol. Soc.*, **89**(382): 478-489; **90**(385): 348-350.
- , 1966a, The Vertical Distribution of Atmospheric Ozone and Possible Transport Mechanisms in the Stratosphere of the Southern Hemisphere, *Quart. J. Roy. Meteorol. Soc.*, **92**(393): 363-374.
- , 1966b, Breakdown of the Biennial Variation of Ozone and of Lower Stratospheric Temperature in the Middle Latitudes of the Southern Hemisphere, *Nature*, **210**: 286-287.
- , 1968a, Ozone Fluctuations in Relation to Upper Air Perturbations in the Middle Latitudes of the Southern Hemisphere, *Tellus*, **20**(2): 305-313.
- , 1968b, Day and Night Measurements of Ozone in the Southern Hemisphere, *Quart. J. Roy. Meteorol. Soc.*, **94**(401): 266-278.
- Kvifte, G. J., 1967, Hydroxyl Rotational Temperatures and Intensities in the Nightglow, *Planet. Space Sci.*, **15**: 1515-1523.
- , 1969, Twilight Observations, in *Atmospheric Emissions*, B. M. McCormac and A. Omholt (Eds.), pp. 399-410, Van Nostrand-Reinhold Co., New York.
- Kyle, T. G., D. G. Murcray, F. H. Murcray, and W. J. Williams, 1969, Abundance of Methane in the Atmosphere Above 20 Kilometers, *J. Geophys. Res.*, **74**(13): 3421-3425.
- Labitzke, K., 1968, Midwinter Warmings in the Upper Stratosphere in 1966, *Quart. J. Roy. Meteorol. Soc.*, **94**(401): 279-291.
- Laboratory of Astrophysics and Physical Meteorology, 1960, Preliminary Report on Solar Observations from a U-2 Observatory, Johns Hopkins University.
- Laevatsu, T., and O. Mellis, 1961, Size and Mass Distribution of Cosmic Dust, *J. Geophys. Res.*, **66**(8): 2507-2508.
- Lagos, C. P., 1967, On the Dynamics of the Thermosphere, Planetary Circulations Project, Report No. 20, Massachusetts Institute of Technology.
- , 1969, Note on the Mechanism of the 5577 Å [OI] Emission at 100 Km, in *Atmospheric Emissions*, B. M. McCormac and A. Omholt (Eds.), pp. 519-521, Van Nostrand-Reinhold Co., New York.
- LaGow, H. E., and W. M. Alexander, 1960, Recent Direct Measurements of Cosmic Dust in the Vicinity of the Earth Using Satellites, in *Space Research*, H. Kallman-Bijl (Ed.), pp. 1033-1041, North-Holland Publishing Co., Amsterdam.
- Lalley, V. E., 1968, The Southern Hemisphere GHOST Flight Program, The First Year, *Space Research*, VIII, pp. 1002-1004, North-Holland Publishing Co., Amsterdam.

- , and E. W. Lichfield, 1969, Summary of Status and Plans for the GHOST Balloon Project, *Bull. Amer. Meteorol. Soc.*, 50(11): 867-874.
- , and R. J. Reed, 1969, Superpressure Balloon Flights in the Tropical Stratosphere, *Science*, 166(3906): 738-739.
- Langer, G., J. Rosinski, and C. P. Edwards, 1967, A Continuous Ice Nuclei Counter and Its Application to Tracking in the Troposphere, *J. Appl. Meteorol.*, 6(1): 114-125.
- Larkin, F. S., and B. A. Thrush, 1964, Recombination of Hydrogen Atoms in the Presence of Atmospheric Gases, *Discuss. Faraday Soc.*, 37: 113.
- Lauter, E. A., 1953, Variationen der D-Schichtdämpfung auf 245 kHz, *Z. Meteorol.*, 7: 321-330.
- , and G. Entzian, 1966, Überwachung der tiefen Ionosphäre mit Hilfe der Quasi-Phasenmessung im Langwellenbereich (100...200 kHz), *Schriftenr. Nat. Kom. Geod. Geophys. Deut. Dem. Rep., Reihe II*, 1: 67-97.
- , and P. Nitzsche, 1967, Seasonal Variations of Ionospheric Absorption Deduced from A3-Measurements in the Frequency Range 100...2000 Kc/s, *J. Atmos. Terrest. Phys.*, 29: 533-544.
- , and K. Sprenger, 1967, Erscheinungen in der D-Region in Zusammenhang mit Strukturänderungen des Neutralgases der Strato- und Mesosphäre, *Kleinheubacher Ber.*, 12: 297-307.
- , and K. Sprenger, 1968, D-Region Phenomena and Stratospheric-Mesospheric Coupling, *Meteorol. Monogr.*, 9(31): 129-139.
- , K. Sprenger, and G. Entzian, 1969, The Lower Ionosphere in Winter, in *Stratospheric Circulation*, W. L. Webb (Ed.), pp. 401-438, Academic Press Inc., New York.
- Lea, D. A., 1968, Vertical Ozone Distribution in the Lower Troposphere Near an Urban Pollution Complex, *J. Appl. Meteorol.*, 7(2): 252-267.
- Lehmann, H. R., and C. U. Wagner, 1966, Meteoritic Ions in the Lower Ionosphere, *J. Atmos. Terrest. Phys.*, 28: 617-625.
- Leighton, P. A., 1961, *Photochemistry of Air Pollution*, Academic Press Inc., New York.
- , W. A. Perkins, S. W. Grinnell, and F. X. Webster, 1965, The Fluorescent Particle Atmospheric Tracer, *J. Appl. Meteorol.*, 4(3): 334-348.
- Leistner, W., 1967, Über Ergebnisse von Messungen der mittelwelligen Ultraviolettstrahlung von Hamburg und vom Mt. Wilson (1740m) und die Beziehung zur Ozonosphäre und den Sonnenfleckenrelativzahlen, *Meteorol. Rundsch.*, 20(5): 135-141.
- LeVier, R. E., and L. M. Branscomb, 1968, Ion Chemistry Governing Mesospheric Electron Concentrations, *J. Geophys. Res.*, 73(1): 27-41.
- Lenhard, R. W., Jr., 1963, Variation of Hourly Winds at 35 to 65 Kilometers During One Day at Eglin Air Force Base, Florida, *J. Geophys. Res.*, 68(1): 227-234.
- Leone, I. A., and E. Brennan, 1969, The Importance of Moisture in Ozone Phytotoxicity, *Atmos. Environ.*, 3(4): 399-406.
- Leovy, C., 1964, Simple Models of Thermally Driven Mesospheric Circulation, *J. Atmos. Sci.*, 21(4): 327-341.
- , 1967, Energetics of the Middle Atmosphere, Paper given at Survey Symposium on Measurements in the Upper Atmosphere (ICMUA, IAMAP), paper presented at 14th General Assembly of the International Union of Geodesy and Geophysics, Lucerne, Switzerland, Sept. 25-Oct. 7, 1967.
- , 1969, Atmospheric Ozone: An Analytic Model for Photochemistry in the Presence of Water Vapor, *J. Geophys. Res.*, 74(2): 417-426.
- Lettau, H. H., 1967, Small to Large-Scale Features of Boundary Layer Structure over Mountain Slopes, in *Proceedings of the Symposium on Mountain Meteorology, June 26, 1967, Fort Collins, Colorado*, Atmospheric Science Paper No. 122, pp. 1-74, Colorado State University.
- Lieth, H., 1963, The Role of Vegetation in the Carbon Dioxide Content of the Atmosphere, *J. Geophys. Res.*, 68(13): 3887-3898.
- , 1965, Versuch einer kartographischen Darstellung der Produktivität der Pflanzendecke auf der Erde, pp. 72-79, Geographisches Taschenbuch. Franz Steiner Verlag GmbH, Wiesbaden.

- Lindzen, R. S., 1965, The Radiative-Photochemical Response of the Mesosphere to Fluctuations in Radiation, *J. Atmos. Sci.*, **22**(5): 469-478.
- , 1967, Thermally Driven Diurnal Tide in the Atmosphere, *Quart. J. Roy. Meteorol. Soc.*, **93**(395): 18-42.
- , 1968, Lower Atmospheric Energy Sources for the Upper Atmosphere, *Meteorol. Monogr.*, **9**(31): 37-46.
- , and R. Goody, 1965, Radiative and Photochemical Processes in Mesospheric Dynamics: Part I. Models for Radiative and Photochemical Processes, *J. Atmos. Sci.*, **22**(4): 341-348.
- , and T. Matsuno, 1968, On the Nature of the Large Scale Wave Disturbances in the Equatorial Lower Stratosphere, *J. Meteorol. Soc. Jap.*, **46**(3): 215-221.
- Lininger, R. L., R. A. Duce, J. W. Winchester, and W. R. Matson, 1966, Chlorine, Bromine, Iodine and Lead in Aerosols from Cambridge, Massachusetts, *J. Geophys. Res.*, **71**(10): 2457-2464.
- Linscott, I., C. L. Hemenway, and G. Witt, 1964, Calcium Film Indicator of Moisture Associated with Noctilucent Cloud Particles, *Tellus*, **16**(1): 110-113.
- List, R. J., K. Telegadas, and G. J. Ferber, 1964, Meteorological Evaluation of the Sources of Iodine-131 in Pasteurized Milk, *Science*, **146**: 59-64.
- Lloyd, K. H., and D. Golomb, 1967, Observations on the Release of a Cloud of Barium Atoms and Ions in the Upper Atmosphere, Environmental Research Paper No. 268, Report AFCRL-67-0144, Air Force Cambridge Research Laboratories.
- , and L. M. Sheppard, 1966, Atmospheric Structure at 130-200 Km Altitude from Observations on Grenade Glow Clouds During 1962-1963, *Aust. J. Phys.*, **19**: 323-342.
- Löbner, A., 1965, Schwebstoffkonzentrationen in der atmosphärischen Luft verschiedener Länder, *Staub*, **25**(6): 221-224.
- Lockhart, L. B., R. A. Baus, P. King, and I. H. Blifford, 1959, *Atmospheric Radioactivity Studies at the U. S. Naval Research Laboratories*, Hearings Before the Joint Committee on Atomic Energy, 86th Congress, Vol. 1, pp. 561-574, U. S. Government Printing Office, Washington.
- , R. L. Patterson, Jr., A. W. Saunders, Jr., and R. W. Black, 1960, Fission Product Radioactivity in the Air Along the 80th Meridian (West) During 1959, *J. Geophys. Res.*, **65**(12): 3987-3997.
- Lodge, J. P., Jr., A. J. MacDonald, Jr., and E. Vihman, 1960, A Study of the Composition of Marine Atmospheres, *Tellus*, **12**(2): 184-187.
- Logan, S. E., 1969, A Simple Analytical Model for the Dust Devil, USAEC Report UCRL-50667, University of California, Lawrence Radiation Laboratory.
- Lomax, J. B., and D. L. Nielson, 1968, Observation of Acoustic-Gravity Wave Effects Showing Geomagnetic Field Dependence, *J. Atmos. Terrest. Phys.*, **30**(5): 1033-1050.
- London, J., 1962, The Distribution of Total Ozone over the Northern Hemisphere, *Sun at Work*, Vol. 7, 2nd Quarter, Arizona State University.
- , 1963a, The Distribution of Total Ozone in the Northern Hemisphere, *Beitr. Phys. Atmos.*, **36**: 254-263.
- , 1963b, Ozone Variations and Their Relation to Stratospheric Warming, *Meteorol. Abh., Inst. Meteorol. Geophys., Freie Univ. Berlin*, **36**: 299-310.
- , 1967a, The Worldwide Distribution of Atmospheric Ozone, paper presented at the 14th General Assembly of the International Union of Geodesy and Geophysics, Lucerne, Switzerland, Sept. 25-Oct. 7, 1967 (IAMAP-C1-2).
- , 1967b, The Average Distribution and Time Variation of Ozone in the Stratosphere and Mesosphere, *Space Research*, VII, pp. 173-185.
- , 1969, A Discussion of the Structure of the Energy Budget of the Upper Atmosphere, *Annals of the IGSY*, Vol. 5, Solar-Terrestrial Physics: Terrestrial Aspects, pp. 3-22, M.I.T. Press.
- , and M. W. Haurwitz, 1963, Ozone and Sunspots, *J. Geophys. Res.*, **68**(3): 795-801.
- , and C. Prabhakara, 1963, The Effect of Stratospheric Transport Processes on the Ozone Distribution, *Meteorol. Abh., Inst. Meteorol. Geophys., Freie Univ. Berlin*, **36**: 291-297.

- Long, M. J., 1966, A Preliminary Climatology of Thunderstorm Penetrations of the Tropopause in the United States, *J. Appl. Meteorol.*, **5**(4): 467-473.
- Loon, H. van, and R. L. Jenne, 1969, The Half-Yearly Oscillations in the Tropics of the Southern Hemisphere, *J. Atmos. Sci.*, **26**(2): 218-232.
- Lorius, C., G. Baudin, J. Cittanova, and R. Platzler, 1969, Impuretés solubles contenues dans la glace de l'Antarctique, *Tellus*, **21**(1): 136-148.
- Lory-Chanin, M.-L., 1965, Structure physique des raies de résonance émises par un nuage artificiel d'alcalins et mesure de la température de l'ionosphère, *Ann. Geophys.*, **21**(3): 303-346.
- Lovill, J. E., 1968, The Vertical Distribution of Ozone and Atmospheric Transport Processes over the San Francisco Bay Area, Report under NSF Grant GP-4248 and Department of the Navy, Order No. IPR 10-64-8050-WEPS, San Jose State College.
- , and A. Miller, 1968, The Vertical Distribution of Ozone over the San Francisco Bay Area, *J. Geophys. Res.*, **73**(16): 5073-5079.
- Ludwick, J. D., 1966, Atmospheric Diffusion Studies with Fluorescein and Zinc Sulfide Particles as Dual Tracers, *J. Geophys. Res.*, **71**(6): 1553-1559.
- Lüst, R., 1968, Relative Motion of Ion and Neutral Clouds, *Meteorol. Monogr.*, **9**(31): 148-151.
- MacLeod, M. A., 1964, Wind Shear Theory of Sporadic E, Environmental Research Paper No. 15, Report AFCRL-64-364, pp. 309-321, Air Force Cambridge Research Laboratories.
- , 1966, Sporadic E Theory. I. Collision-Geomagnetic Equilibrium, *J. Atmos. Sci.*, **23**(1): 96-109.
- , 1968, The Influence of the Neutral Wind Field on the Distribution of Ionization in the E-Region, *Meteorol. Monogr.*, **9**(31): 139-147.
- MacQueen, R. M., 1968, A Note on the Stratospheric Infrared Sky Radiance, *J. Atmos. Sci.*, **25**(2): 335-337.
- Maeda, H., and H. Murata, 1968, Electric Currents Induced by Nonperiodic Winds in the Ionosphere, *J. Geophys. Res.*, **73**(3): 1077-1092.
- Maeda, K., 1963, On the Heating of Polar Night Mesosphere, *Meteorol. Abh., Inst. Meteorol. Geophys., Freie Univ. Berlin*, **36**: 451-506.
- , and H. Maeda, 1969, Stratosphere-Ionosphere Coupling, in *Stratospheric Circulation*, W. L. Webb (Ed.), pp. 339-389, Academic Press Inc., New York.
- Maehlum, B., 1967, On the "Winter Anomaly" in the Mid-Latitude D Region, *J. Geophys. Res.*, **72**(9): 2287-2299.
- Mahlman, J. D., 1965a, Relation of Stratospheric-Tropospheric Mass Exchange Mechanisms to Surface Radioactivity Peaks, *Arch. Meteorol., Geophys. Bioklimatol., Ser. A*, **15**: 1-25.
- , 1965b, Relation of Tropopause-Level Index Changes to Radioactive Fallout Fluctuations, Department of Atmospheric Science, Technical Paper No. 70, pp. 84-109, Colorado State University.
- , 1966, Atmospheric General Circulation and Transport of Radioactive Debris, Atmospheric Science Paper No. 103, Colorado State University.
- , 1967, Further Studies on Atmospheric General Circulation and Transport of Radioactive Debris, Atmospheric Science Paper No. 110, Colorado State University.
- Mahoney, J. R., 1966, A Study of Energy Sources for the Thermosphere, Planetary Circulations Project, Report No. 17, Massachusetts Institute of Technology.
- , 1968, A Numerical Study of the Variable Structure of the Lower Thermosphere, *Meteorol. Monogr.*, **9**(31): 90-97.
- , and G. J. Boer, Jr., 1968, Horizontal and Vertical Scales of Winds in the 30- to 60-Km Region, in *Proceedings of the Third National Conference on Aerospace Meteorology, New Orleans, La., May 6-9*, pp. 457-464, American Meteorological Society, Boston, Mass.
- Makhon'ko, K. P., 1967, Simplified Theoretical Notion of Contaminant Removal by Precipitation from the Atmosphere, *Tellus*, **19**(3): 467-476.

- Manabe, S., 1967, On the Response of Numerical Models of the Atmosphere upon the Variation of Stratospheric Water Vapor, paper presented at the 14th General Assembly of the International Union of Geodesy and Geophysics, Lucerne, Switzerland, Sept. 25–Oct. 7, 1967.
- , and R. T. Wetherald, 1967, Thermal Equilibrium of the Atmosphere with a Given Distribution of Relative Humidity, *J. Atmos. Sci.*, **24**(3): 241-259.
- Manring, F. J., 1961, Optical Tracers for Atmosphere Soundings, *Aerosp. Eng.*, **20**(9): 8-9, 34-36.
- , and J. F. Bedinger, 1968, Techniques and Precisions Associated with Chemical Trail Requirements, *Meteorol. Monogr.*, **9**(31): 196-200.
- , J. F. Bedinger, and H. Knaflich, 1961, Some Measurements of Winds and of the Coefficient of Diffusion in the Upper Atmosphere, *Space Research*, II, pp. 1107-1124, North-Holland Publishing Co., Amsterdam.
- , J. F. Bedinger, and H. Knaflich, 1962, Measurement of Winds in the Upper Atmosphere During April 1961, *J. Geophys. Res.*, **67**(10): 3923-3925.
- Mariani, F., 1963, Evidence for the Effect of Corpuscular Radiation on the Ionosphere, *J. Atmos. Sci.*, **20**(6): 479-491.
- Markham, T. P., and R. E. Anctil, 1967, An Airborne Measurement of the Spatial Extent of Ca II in Twilight, *Planet. Space Sci.*, **15**: 589-590.
- Marov, M. Ya., 1966, The Density of the Upper Atmosphere, *Ann. Géophys.*, **22**(1): 65-74.
- Marshall, J. C., 1969, Behavior of Smoke Trails, 30 to 70 km, *J. Appl. Meteorol.*, **8**(4): 641-648.
- Martell, E. A., 1963, On the Inventory of Artificial Tritium and Its Occurrence in Atmospheric Methane, *J. Geophys. Res.*, **68**(13): 3759-3770.
- , and P. T. Drevinsky, 1960, Atmospheric Transport of Artificial Radioactivity, *Science*, **132**: 1523-1531.
- Martin, D. W., 1956, Contribution to the Study of Atmospheric Ozone, General Circulation Project, Science Report No. 6, Massachusetts Institute of Technology.
- , and A. W. Brewer, 1959, A Synoptic Study of Day-To-Day Changes of Ozone Over the British Isles, *Quart. J. Roy. Meteorol. Soc.*, **85**(366): 393-403.
- Maryama, H., and T. Kitagawa, 1967, Relation of Meteor Stream to Natural Ice Nuclei and Precipitation, *J. Meteorol. Soc. Jap.*, **45**(1): 126-136.
- Maryama, T., 1967, Large Scale Disturbances in the Equatorial Lower Stratosphere, *J. Meteorol. Soc. Jap.*, **45**(5): 391-408.
- , 1968a, Upward Transport of Westerly Momentum Due to Large-Scale Disturbances in the Equatorial Lower Stratosphere, *J. Meteorol. Soc. Jap.*, **46**(5): 404-417.
- , 1968b, Time Sequence of Power Spectra of Disturbances in the Equatorial Lower Stratosphere in Relation to the Quasi-Biennial Oscillation, *J. Meteorol. Soc. Jap.*, **46**(5): 327-342.
- , 1969, Long-Term Behaviour of Kelvin Waves and Mixed Rossby-Gravity Waves, *J. Meteorol. Soc. Jap.*, **47**(4): 245-254.
- , and M. Yanai, 1967, Evidence of the Large-Scale Wave Disturbances in the Equatorial Lower Stratosphere, *J. Meteorol. Soc. Jap.*, **45**(2): 196-199.
- Mason, B. J., 1957, *The Physics of Clouds*, Clarendon Press, Oxford.
- Masterbrook, H. J., 1963a, The Status of Water Vapor Observations Above 20 Km and Implications As to the General Circulation, paper presented at the Upper Atmosphere Meteorology Symposium, International Union of Geodesy and Geophysics, Berkeley, Calif., August.
- , 1963b, Frost Point Hygrometer Measurement in the Stratosphere and the Problem of Moisture Contamination, in *Humidity and Moisture*, Vol. 2, pp. 480-485, Reinhold Publishing Co., New York.
- , 1966, Water Vapor Observations at Low, Middle, and High Latitudes During 1964 and 1965, Report NRL-6447, Naval Research Laboratory.
- , 1968, Water Vapor Distribution in the Stratosphere and High Troposphere, *J. Atmos. Sci.*, **25**(2): 299-311.

- , and J. E. Dinger, 1960, The Measurement of Water-Vapour Distribution in the Stratosphere, Report NRL-5551, Naval Research Laboratory.
- , and J. E. Dinger, 1961, Distribution of Water Vapor in the Stratosphere, *J. Geophys. Res.*, **66**(5): 1437-1444.
- Mateer, C. L., and H. U. Dütsch, 1964, Uniform Evaluation of Umkehr Observations from the World Ozone Network. I. Proposed Standard Umkehr Evaluation Technique, National Center for Atmospheric Research, Boulder, Colo.
- , and W. L. Godson, 1960, The Vertical Distribution of Atmospheric Ozone over Canadian Stations from Umkehr Observations, *Quart. J. Roy. Meteorol. Soc.*, **86**(370): 512-518.
- Matsushita, S., 1968, Discussion of paper by J. M. Rosen, "The Vertical Distribution of Dust to 30 Kilometers," *J. Geophys. Res.*, **73**(9): 3085-3088.
- Matsushita, S., 1966, Sporadic E and Ionospheric Currents, *Radio Sci.*, **1**: 204-212.
- , and C. A. Reddy, 1967, A Study of Blanketing Sporadic E at Middle Latitudes, *J. Geophys. Res.*, **72**(11): 2903-2916.
- Matuura, N., 1968, Effect of the Ionosphere on the Upper Atmospheric Rotation, *J. Atmos. Terrest. Phys.*, **30**(5): 763-778.
- McCaldin, R. O., L. W. Johnson, and N. T. Stephens, 1969, Atmospheric Aerosols, *Science*, **166**(3903): 381-382.
- McCormac, B. M., and A. Omholt (Eds.), 1969, *Atmospheric Emissions*, Van Nostrand-Reinhold Co., New York.
- McCormick, R. A., and K. R. Kurfis, 1966, Vertical Diffusion of Aerosols over a City, *Quart. J. Roy. Meteorol. Soc.*, **92**(393): 392-397.
- , and J. H. Ludwig, 1967, Climate Modification by Atmospheric Aerosols, *Science*, **156**: 1358-1359.
- , and C. Xintaras, 1962, Variation of Carbon Monoxide Concentrations as Related to Sampling Interval, Traffic and Meteorological Factors, *J. Appl. Meteorol.*, **1**(2): 237-243.
- McDonnell, J. A. M., 1967, Detection of Meteoritic Dust from a Sounding Rocket, *J. Geophys. Res.*, **72**(23): 6110-6112.
- McGrath, W. D., and J. J. McGarvey, 1967, The Production, Deactivation and Chemical Reactions of O(¹D) Atoms, *Planet. Space Sci.*, **15**: 427-455.
- McGrattan, G. J., 1967, A Suggested Test of a Theory of Atmospheric Turbulence, *Planet. Space Sci.*, **15**: 811-812.
- McLone, R. R., 1967, On the Form of Noctilucent Clouds, *Pure Appl. Geophys.*, **67**: 233-238.
- Meadows-Reed, E., and C. R. Smith, 1964, Mass Spectrometric Investigations of the Atmosphere Between 100 and 227 Kilometers Above Wallops Island, Virginia, *J. Geophys. Res.*, **69**(15): 3199-3207.
- Meetham, A. R., 1937, The Correlation of the Amount of Ozone with Other Characteristics of the Atmosphere, *Quart. J. Roy. Meteorol. Soc.*, **63**(268): 289.
- Megaw, W. J., and R. D. Wiffen, 1961, The Generation of Condensation Nuclei by Ionizing Radiation, *Geofis. Pura Appl.*, **50**: 118-128.
- Meier, R. R., 1966, Rocket Determination of the Daytime Sodium Distribution in the Upper Atmosphere, Ph. D. Thesis, University of Pittsburgh.
- Meinel, M. P., and A. B. Meinel, 1963, Late Twilight Glow of the Ash Stratum from the Eruption of Agung Volcano, *Science*, **142**: 582-583.
- , and A. B. Meinel, 1964, Height of the Glow Stratum from the Eruption of Agung on Bali, *Nature*, **201**: 657-658.
- Merilees, P., 1966, Harmonic Representation Applied to Large Scale Atmospheric Waves, Scientific Report No. 3, McGill University.
- Mesinger, F., and O. Milovanović, 1963, The Expansion of Clusters of Particles Under the Action of Atmospheric Macro-turbulence, *Geofis. Pura Appl.*, **55**: 164-174.
- Mészáros, E., 1968, On the Size Distribution of Water Soluble Particles in the Atmosphere, *Tellus*, **20**(3): 443-448.

- Midorikawa, B., 1957, The Distribution of CO₂ Concentration of the Air in Some Plant Communities, *Jap. J. Ecol.*, **7**: 72-76.
- Miers, B. T., 1965, Wind Oscillations Between 30 and 60 Km over White Sands Missile Range, New Mexico, *J. Atmos. Sci.*, **22**(4): 382-387.
- , 1967, Stratospheric Winds over Panama, *J. Geophys. Res.*, **72**(20): 5149-5152.
- Mikhnevich, V. V., 1964, Atmospheric Density Variations at Altitudes over 200 Km, *Planet. Space Sci.*, **12**: 1111-1120.
- Miller, A., and C. D. Ahrens, 1969, Ozone Within and Below the West Coast Temperature Inversion, Report No. 6, NSF Grant GA-1090, San Jose State College.
- Miller, A. J., 1967, Note on the Vertical Motion in the Lower Stratosphere, *Beitr. Phys. Atmos.*, **40**(1-2): 29-48.
- , H. M. Woolf, and F. G. Finger, 1968, Small-Scale Wind and Temperature as Evidenced by Meteorological Rocket Systems, in *Proceedings of the Third National Conference on Aerospace Meteorology, New Orleans, La., May 6-9*, pp. 478-487, American Meteorological Society, Boston, Mass.
- Mills, A., and H. C. Urey, 1940, The Kinetics of Isotopic Exchange Between Carbon Dioxide, Bicarbonate Ions, Carbonate Ions and Water, *J. Amer. Chem. Soc.*, **62**: 1019-1026.
- Minzner, R. A., K. S. W. Champion, and H. L. Pond, 1959, The ARDC Model Atmosphere, 1959, Air Force Surveys in Geophysics, No. 115, Air Force Cambridge Research Laboratories.
- Mirtov, B. A., 1964, Gaseous Composition of the Atmosphere (Izdatel'stvo Akademii Nauk SSSR, Moskva, 1961), Israel Program for Scientific Translations, Jerusalem, 1964.
- Mitchell, J. M., Jr., 1962, Comments on paper by H. C. Willet, "The Relationship of Total Atmospheric Ozone to the Sunspot Cycle," *J. Geophys. Res.*, **67**(10): 4093-4094.
- Mitra, A. P., 1969, Photochemistry of Ozone, in *Stratospheric Circulation*, W. L. Webb (Ed.), pp. 263-306, Academic Press Inc., New York.
- Miyake, Y., and S. Tsunogai, 1963, Evaporation of Iodine from the Ocean, *J. Geophys. Res.*, **68**(13): 3989-3994.
- Molla, A. C., Jr., and C. J. Loisel, 1962, On the Hemispheric Correlations of Vertical and Meridional Wind Components, *Geofis. Pura Appl.*, **51**: 166-170.
- Möller, F., 1963, On the Influence of Changes in the CO₂ Concentration in Air on the Radiation Balance of the Earth's Surface and on the Climate, *J. Geophys. Res.*, **68**(13): 3877-3886.
- , 1964, "Reply"—Comments on paper by F. Möller, *J. Geophys. Res.*, **69**(8): 1663-1664.
- Monteith, J. L., 1967, Local Differences in the Attenuation of Solar Radiation over Britain, *Quart. J. Roy. Meteorol. Soc.*, **92**(392): 254-262; **93**(397): 382.
- Montgomery, J. B., III, C. G. Justus, and H. D. Edwards, 1968, Winds Observed from November 1965 Through December 1967 in the 70 to 230 Km Region of the Upper Atmosphere, Final Report, Report AFCRL-68-0503, Georgia Institute of Technology.
- Montgomery, R. B., 1959, Salinity and the Residence Time of Subtropical Oceanic Surface Water, *Rosby Memorial Volume*, pp. 143-146, Rockefeller Institute Press and Oxford University Press.
- Moore, C. B., J. R. Smith, and A. Gaalswyk, 1954, On the Use of Constant-Level Balloons to Measure Horizontal Motions in the Atmosphere, *J. Meteorol.*, **11**(3): 167-172.
- Moore, J. G., and C. R. Nagaraja Rao, 1965, Observations of the Day Airglow During the Total Solar Eclipse of 30 May, 1965, *Ann. Geophys.*, **23**(2): 197-206.
- Moos, H. W., and W. G. Fastie, 1967, Rocket Photometry of the Far UV Twilight Airglow, *J. Geophys. Res.*, **72**(21): 5165-5171.
- More, W. B. de and O. F. Raper, 1964, Deactivation of O(¹D) in the Atmosphere, *Astrophys. J.*, **139**: 1381-1383.
- Moreno, H., and I. Stack, 1964, The Atmospheric Extinction on Cerro Toledo During 1963, *Publ. Astron. Soc. Pac.*, **76**: 55-56.
- Morgan, G., Jr., 1967, The Detection of Zinc Sulfide in Melted Snow Samples, *J. Appl. Meteorol.*, **6**(5): 924-928.

- Morris, J. E., 1967, Wind Measurements in the Subpolar Mesosphere Region, *J. Geophys. Res.*, **72**(24): 6123-6129.
- , and M. D. Kays, 1968, Circulation in the Arctic Mesosphere in Summer, Report ECOM-5181, U. S. Army Electronics Command, Atmospheric Sciences Laboratory, White Sands Missile Command.
- , and M. D. Kays, 1969, Circulation in the Arctic Mesosphere in Summer, *J. Geophys. Res.*, **74**(2): 427-434.
- , and B. T. Miers, 1969, A Climatology of the Upper Atmosphere, in *Stratospheric Circulation*, W. L. Webb (Ed.), pp. 533-553, Academic Press Inc., New York.
- Morton, J. D., 1967, Comments on "Dyed Pollen Grains and Spores as Tracers in Dispersion and Deposition Studies," *J. Appl. Meteorol.*, **6**(4): 725.
- Moses, H., 1969, Mathematical Urban Air Pollution Models, USAEC Report ANL/ES-RPY-1, Argonne National Laboratory.
- Mossop, S. C., 1963, Stratospheric Particles at 20 Km, *Nature*, **199**: 325.
- , 1964, Volcanic Dust Collected at an Altitude of 20 Km, *Nature*, **203**: 824-827.
- , and C. Tuck-Lee, 1968, The Composition and Size Distribution of Aerosols Produced by Burning Solutions of AgI and NaI in Acetone, *J. Appl. Meteorol.*, **7**(2): 234-240.
- Mrose, H., 1961, Ergebnisse von Spurenstoffbestimmungen im Niederschlag, *Z. Meteorol.*, **15**(1): 46-54.
- , and M. Zier, 1967, Staubausfall und Luftverunreinigung, *Z. Meteorol.*, **19**(7-8): 252-254.
- Muench, H. S., 1968, Large-Scale Disturbances in the Summertime Stratosphere, *J. Atmos. Sci.*, **25**(6): 1108-1115.
- Mukammal, E. I., 1963, Ozone as a Cause of Tobacco Injury, manuscript of the Canada Department of Transport, Toronto, Ontario.
- Müller, H. G., 1968, Simultaneous Observations of Meteor Winds and Ionospheric Drifts, *J. Atmos. Terrest. Phys.*, **30**(5): 701-706.
- Müller, W., 1963, Die Änderung Kondensationskernkonzentration bei Niederschlägen, Nebel und Gewittern, *Geofis. Pura Appl.*, **55**: 200-208.
- , and J. C. Thams, 1962, Zum Problem des Sonnenaufgangseffektes der Kondensationskerne, *Geofis. Pura Appl.*, **52**: 214-226.
- Munczak, F., 1960, On the Appearance of Ninhydrinpositive Substances in the Atmosphere, *Tellus*, **12**: 282-292.
- Münnich, K. O., and T. C. Vogel, 1963, Investigation of Meridional Transport in the Troposphere by Means of Carbon-14 Measurements, in *Radioactive Dating*, Symposium Proceedings, Athens, 1962, pp. 189-197, International Atomic Energy Agency, Vienna (STI/PUB/68).
- Murakami, T., 1962, Stratospheric Wind, Temperature, and Isobaric Height Conditions During the IGY Period—Part I, Report No. 5, Massachusetts Institute of Technology.
- Murcray, D. G., T. G. Kyle, and W. J. Williams, 1969, Distribution of Water Vapor in the Stratosphere as Derived from Setting Sun Absorption Data, *J. Geophys. Res.*, **74**(23): 5369-5373.
- , F. H. Murcray, and W. J. Williams, 1966, Further Data Concerning the Distribution of Water Vapour in the Stratosphere, *Quart. J. Roy. Meteorol. Soc.*, **92**(391): 159-161.
- , F. H. Murcray, W. J. Williams, and F. E. Leslie, 1960, Water Distribution Above 90,000 Feet, *J. Geophys. Res.*, **65**(11): 3641-3649.
- Murgatroyd, R. J., 1957, Winds and Temperatures Between 20 Km and 100 Km—A Review, *Quart. J. Roy. Meteorol. Soc.*, **83**(358): 417-458.
- , 1965a, Tracers and Transfer Problems in the Lower Stratosphere, *Quart. J. Roy. Meteorol. Soc.*, **91**(390): 421-424.
- , 1965b, General Climatology and Standard Atmospheres, Technical Note No. 70, pp. 170-199, World Meteorological Organization.
- , 1968, Temperature, Density and Pressure Variations in the Stratosphere and Mesosphere, *Meteorol. Monogr.*, **9**(31): 37-71.

- , 1969, Estimations from Geostrophic Trajectories of Horizontal Diffusivity in the Mid-Latitude Troposphere and Lower Stratosphere, *Quart. J. Roy. Meteorol. Soc.*, **95**(403): 40-62.
- , P. Goldsmith, and W. B. H. Hollings, 1955, Some Measurements of Humidity from Aircraft Up to Heights of About 50,000 Feet over Southern England, *Quart. J. Roy. Meteorol. Soc.*, **81**(350): 533-537.
- , and R. M. Goody, 1958, Sources and Sinks of Radiative Energy from 30 to 90 Km, *Quart. J. Roy. Meteorol. Soc.*, **84**(361): 225-234.
- , and F. Singleton, 1961, Possible Meridional Circulation in the Stratosphere and Mesosphere, *Quart. J. Roy. Meteorol. Soc.*, **87**(372): 125-135; **88**(375): 105-107.
- Murphy, B. L., and S. L. Kahalas, 1968, Antipodal Effect due to Magnetohydrodynamic Wave Propagation After the Starfish Detonation of July 9, 1962, *J. Geophys. Res.*, **73**(5): 1858-1860.
- Murphy, C. H., 1969, Seasonal Variation of Winds over Barbados, West Indies, *J. Geophys. Res.*, **74**(1): 339-347.
- , and G. V. Bull, 1967, Nighttime Variation of Ionospheric Winds over Barbados, West Indies, *J. Geophys. Res.*, **72**(19): 4831-4837.
- , and G. V. Bull, 1968a, Ionospheric Winds over Yuma, Arizona, Measured by Gun-Launched Projectiles, *J. Geophys. Res.*, **73**(9): 3005-3015.
- , and G. V. Bull, 1968b, General Properties of Ionospheric Winds, in *Proceedings of the Third National Conference on Aerospace Meteorology, New Orleans, La., May 6-9*, pp. 488-494, American Meteorological Society.
- , and G. V. Bull, 1968c, Gun-Launched Probes over Barbados, *Bull. Amer. Meteorol. Soc.*, **49**(6): 640-644.
- , G. V. Bull, and H. D. Edwards, 1966, Ionospheric Winds Measured by Gun-Launched Projectiles, *J. Geophys. Res.*, **71**(19): 4535-4544.
- , G. V. Bull, and J. W. Wright, 1967, Motions of an Electron-Ion Cloud Released at 100 Km from a Gun-Launched Projectile, *J. Geophys. Res.*, **72**(13): 3511-3514.
- Murray, R., and B. J. Moffitt, 1969, Monthly Patterns of the Quasi-Biennial Pressure Oscillation, *Weather*, **24**(10): 382-389.
- Nagamoto, C. T., J. Rosinski, and G. Langer, 1967, Ice Nuclei Concentration in Hawaii During the Period 7 January to 10 March, 1967, *J. Appl. Meteorol.*, **6**(6): 1123-1125.
- Narcisi, R. S., 1966, Ion Composition Measurements and Related Ionospheric Processes in the D and Lower E Regions, Environmental Research Paper, No. 230, Report AFCRL-66-715, and *Ann. Geophys.*, **22**(2): 224-234.
- , and A. D. Bailey, 1965a, Mass Spectrometry in the D-Region Ionosphere—Apparatus, Techniques and First Measurements, Report AFCRL-65-81, Air Force Cambridge Research Laboratories.
- , and A. D. Bailey, 1965b, Mass Spectrometry in the D-Region Ionosphere—Apparatus, Techniques and First Measurements, Environmental Research Paper, No. 82, Report AFCRL-65-81, Air Force Cambridge Research Laboratories.
- , and A. D. Bailey, 1965c, Mass Spectrometric Measurements of Positive Ions at Altitudes from 64 to 112 Kilometers, Environmental Research Paper, No. 140, Report AFCRL-65-682, and *J. Geophys. Res.*, **70**(15): 3687-3700.
- , A. D. Bailey, and L. D. Lucca, 1966, Composition Measurements of Sporadic E in the Nighttime Lower Ionosphere, paper presented at the *Seventh International Space Science Symposium*, Vienna, May 10-19, North-Holland Publishing Co., Amsterdam.
- National Aeronautics and Space Administration, United States Air Force, and United States Weather Bureau, 1962, *U. S. Standard Atmosphere, 1962*, U. S. Government Printing Office, Washington, D. C.
- Naumann, R. J., 1966, The Near Earth Meteoroid Environment, NASA Technical Note, Report NASA-TND-3717, National Aeronautics and Space Administration.

- Nelson, R. A., 1968, Response of the Ionosphere to the Passage of Neutral Atmospheric Waves, *J. Atmos. Terrest. Phys.*, **30**(5): 825-835.
- Neporent, B. S., M. S. Kiseleva, A. G. Makogonenko, and V. I. Shlyakhov, 1968, Stratospheric Humidity as Determined from the Absorption of Solar Radiation by a Resolved Spectral Structure of Water Vapor, *Izv. Atmos. Oceanic Phys.*, **4**(8): 826-834.
- Newell, R. E., 1961, The Transport of Trace Substances in the Atmosphere and Their Implications for the General Circulation of the Stratosphere, *Geofis. Pura Appl.*, **49**: 137-158.
- , 1963a, Transfer Through the Tropopause and Within the Stratosphere, *Quart. J. Roy. Meteorol. Soc.*, **89**(380): 167-204.
- , 1963b, Preliminary Study of Quasi-Horizontal Eddy Fluxes from Meteorological Rocket Network Data, *J. Atmos. Sci.*, **20**(3): 213-225.
- , 1964a, The Circulation of the Upper Atmosphere, *Sci. Amer.*, **210**(3): 62-74.
- , 1964b, Further Ozone Transport Calculations and the Spring Maximum in Ozone Amount, *Pure Appl. Geophys.*, **59**: 191-206.
- , 1964c, Stratospheric Energetics and Mass Transport, *Pure Appl. Geophys.*, **58**: 145-156.
- , 1964d, A Note on the 26-Month Oscillation, *J. Atmos. Sci.*, **21**(3): 320-321.
- , 1967, Stratosphere and Mesosphere, *Trans. Amer. Geophys. Union*, **48**(2): 436-449.
- , 1968a, The General Circulation of the Atmosphere Above 60 Km, *Meteorol. Monogr.*, **9**(31): 98-113.
- , 1968b, Semi-Annual Variation in Thermospheric Density, *Nature*, **217**: 150-151.
- , H. W. Brandli, and D. A. Widen, 1966, Concentration of Ozone in Surface Air over Greater Boston in 1965, *J. Appl. Meteorol.*, **5**(5): 740-741.
- , and R. E. Dickinson, 1967, On the Application of a Proposed Global System for Measuring Meteor Winds, *Pure Appl. Geophys.*, **68**: 162-172.
- , J. W. Kidson, and D. G. Vincent, 1969, Annual and Biennial Modulations in the Tropical Hadley Cell Circulation, *Nature*, **222**(5188): 76-78.
- , J. R. Mahoney, and R. W. Lenhard, Jr., 1966, A Pilot Study of Small-Scale Wind Variations in the Stratosphere and Mesosphere, *Quart. J. Roy. Meteorol. Soc.*, **92**(391): 41-54; **94**(402): 602-603 (1968).
- , and A. J. Miller, 1968, Vertical Velocity Variability in the Lower Stratosphere, *J. Appl. Meteorol.*, **7**(3): 516-518.
- , J. M. Wallace, and J. R. Mahoney, 1966, The General Circulation of the Atmosphere and Its Effects on the Movement of Trace Substances, Part 2, *Tellus*, **18**(2-3): 363-380.
- Newkirk, G., Jr., 1956, Photometry of the Solar Aureole, *J. Opt. Soc. Amer.*, **46**: 1028-1037.
- , 1967, Meteoric Dust in the Stratosphere Determined by Optical Scattering Techniques, in *Meteor. Orbits and Dust*, G. S. Hawkins (Ed.), Smithsonian Contributions to Astrophysics, Vol. II, Report NASA-SP-135, pp. 349-358, National Aeronautics and Space Administration.
- , and J. A. Eddy, 1963, Influx of Meteor Particles in the Upper Atmosphere of the Earth as Determined from Stratospheric Coronagraph Observations, in *Space Research*, III, W. Priester, (Ed.), pp. 143-154, North-Holland Publishing Co., Amsterdam.
- , and J. A. Eddy, 1964, Light Scattering by Particles in the Upper Atmosphere, *J. Atmos. Sci.*, **21**(1): 35-60.
- , and J. L. Kroening, 1965, Aerosols in the Stratosphere: A Comparison of Techniques of Estimating Their Concentration, *J. Atmos. Sci.*, **22**(5): 567-570.
- Ney, F. P., 1967, Zodiacal Cloud, in *The Encyclopedia of Atmospheric Sciences and Astrogeology*, R. W. Fairbridge (Ed.), pp. 1161-1162, Reinhold Publishing Corporation, New York.
- , and J. Kroening, 1962, Author's Reply to the Preceding Discussion, *J. Geophys. Res.*, **67**(11): 4510-4511.
- Nguyen-Huu-Doan, 1964, Étude spectrophotométrique de la lumière du ciel nocturne et crépusculaire dans le visible. II, *Ann. Géophys.*, **20**(1): 1-21.
- Nickola, P. W., M. O. Rankin, M. F. Scoggins, and E. M. Shenn, 1967, A System for Recording Air Concentrations of Zinc Sulfide Fluorescent Pigment on a Real-Time Scale, *J. Appl. Meteorol.*, **6**(2): 430-433.

- Nicolet, M., 1958, La dissociation de l'oxygène dans la haute atmosphère, *Arch. Meteorol., Geophys. Bioklimatol., Ser. A*, **10**: 301-304.
- , 1960, The Properties and Constitution of the Upper Atmosphere, in *Physics of the Upper Atmosphere*, J. A. Ratcliffe (Ed.), pp. 17-71, Academic Press, Inc., New York and London.
- , 1965a, Nitrogen Oxides in the Chemosphere, *J. Geophys. Res.*, **70**(3): 679-690.
- , 1965b, Ionospheric Processes and Nitric Oxide, *J. Geophys. Res.*, **70**(3): 691-702.
- Niemeyer, L. E., and R. A. McCormick, 1968, Some Results of Multiple-Tracer Diffusion Experiments at Cincinnati, *J. Air Pollut. Contr. Ass.*, **18**(6): 403-405.
- Nier, A. O., J. H. Hoffman, C. Y. Johnson, and J. C. Holmes, 1964, Neutral Constituents of the Upper Atmosphere: The Minor Peaks Observed in a Mass Spectrometer, *J. Geophys. Res.*, **69**(21): 4629-4636.
- Nolan, G. F., 1967, A Study of Mesoscale Features of Summertime Minimum Wind Fields in the Lower Stratosphere, Environmental Research Paper, No. 275, Report AFCRL-67-0601, Air Force Cambridge Research Laboratories.
- Nordberg, W., 1964, Rocket Soundings in the Mesosphere, *Astronaut. Aeronaut.*, **2**(5): 48-58.
- , 1966, Recent Observations of the Structure of the Upper Stratosphere and Mesosphere, Publication in Meteorology No. 80, pp. 293-323, McGill University.
- , L. Katchen, J. Theon, and W. S. Smith, 1965, Rocket Observations of the Structure of the Mesosphere, *J. Atmos. Sci.*, **22**(6): 611-622.
- Nucciotti, F., G. Simonini, and O. Vittori, 1968, Inquinanti chimici nelle precipitazioni di alcuni aeroporti e stazioni del Servizio Meteorologico A. M., Part I: SO₃, NO₂ + NO₃, NH₄, *Riv. Meteorol. Aeronaut.*, **28**(3): 50-62.
- Ogden, T. L., 1969, The Effect on Rainfall of a Large Steelworks, *J. Appl. Meteorol.*, **8**(4): 585-591.
- Okita, T., 1968, Concentration of Sulfate and Other Inorganic Materials in Fog and Cloud Water and in Aerosol, *J. Meteorol. Soc. Jap.*, **46**(2): 120-127.
- Oort, A. H., 1963, On the Energy Cycle in the Lower Stratosphere, Report No. 9, Massachusetts Institute of Technology.
- Orville, R. E., 1967, Ozone Production During Thunderstorms, Measured by the Absorption of Ultraviolet Radiation from Lightning, *J. Geophys. Res.*, **72**(14): 3557-3561.
- Östlund, H. G., 1959, Isotopic Composition of Sulfur in Precipitation and Sea-Water, *Tellus*, **11**(4): 478-480.
- , and J. Alexander, 1963, Oxidation Rate of Sulfide in Sea Water, a Preliminary Study, *J. Geophys. Res.*, **68**(13): 3995-3997.
- Paetzold, H. K., 1955, New Experimental and Theoretical Investigations on the Atmospheric Ozone Layer, *J. Atmos. Terrest. Phys.*, **7**: 128-140; Selected Meteorological Paper No. 9, Radiation, Part 2, Meteorological Society of Japan.
- , 1963, On the Problem of Solar Activity Effects on the Lower Terrestrial Atmosphere, *Meteorol. Abh., Inst. Meteorol. Geophys., Freie Univ. Berlin*, **36**: 353-363.
- , and F. Piscalar, 1961, Meridionale Ozonverteilung und stratosphärische Zirkulation, *Naturwissenschaften*, **48**: 474.
- Pales, J. C., and C. D. Keeling, 1965, The Concentration of Atmospheric Carbon Dioxide in Hawaii, *J. Geophys. Res.*, **70**(24): 6053-6076.
- Palmén, E., and D. Söderman, 1966, Computation of the Evaporation from the Baltic Sea from the Flux of Water Vapor in the Atmosphere, *Geophysica*, **8**(4): 261-279.
- Panchev, S., 1967, *Random Functions and Turbulence* (in Russian), pp. 385-388, Hydrometeorological Press, Leningrad.
- , 1968, Coefficient of Horizontal Macroturbulent Exchange in the Atmosphere, *J. Atmos. Sci.*, **25**(5): 933-935.
- Parthasarathy, R., and D. B. Rai, 1966, Effect of Meteoric Dust on the Effective Recombination Coefficient in the Lower Ionosphere, *Radio Sci.*, **1**(12): 1401-1408.
- Pasceri, R. E., and S. K. Friedlander, 1965, Measurements of the Particle Size Distribution of the

- Atmospheric Aerosol: II. Experimental Results and Discussion, *J. Atmos. Sci.*, **22**(5): 577-584.
- Pasquill, F., 1962, *Atmospheric Diffusion*, D. Van Nostrand Company, Ltd., London.
- Paterson, M. P., and K. T. Spillane, 1969, Surface Films and the Production of Sea-Salt Aerosols, *Quart. J. Roy. Meteorol. Soc.*, **95**(405): 526-534.
- Paton, J., 1949, Luminous Night Clouds, *Meteorol. Mag.*, **78**(930): 354-357.
- , 1969, Noctilucent Clouds over Western Europe During 1968, *Meteorol. Mag.*, **98**: 219-222.
- Peixoto, J. P., 1960, Hemispheric Temperature Conditions During the Year 1950, Scientific Report No. 4, Massachusetts Institute of Technology.
- Peng, L., 1963, Stratospheric Wind, Temperature and Isobaric Height Conditions During the IGY Period— Part II, Report No. 10, Massachusetts Institute of Technology.
- Penn, S., 1964, A Case Study Using Ozone to Determine Structure and Air Motions at the Tropopause, *J. Appl. Meteorol.*, **3**(5): 581-586.
- , 1965, Ozone and Temperature Structure in a Hurricane, *J. Appl. Meteorol.*, **4**(2): 212-216.
- , 1966, Temperature and Ozone Variations near Tropopause Level over Hurricane Isbell, October 1964, *J. Appl. Meteorol.*, **5**(4): 407-410.
- Penndorf, R., 1947, Der Ozongehalt der mittleren Stratosphäre, *Z. Meteorol.*, **1**: 345-357.
- , 1954, The Vertical Distribution of Mie Particles in the Troposphere, Geophysical Research Paper No. 25, pp. 1-12, Air Force Cambridge Research Laboratories.
- Perl, G., 1965, Das bodennahe Ozon in Arosa, seine regelmässigen und unregelmässigen Schwankungen, *Arch. Meteorol., Geophys. Bioklimatol., Ser. A*, **14**: 449-458.
- Petersen, H. L., and C. B. Kretschmer, 1960, Kinetics of Recombination of Atomic Oxygen at Room Temperature, Report AD-283044.
- Peterson, J. T., and R. A. Bryson, 1968, Atmospheric Aerosols: Increased Concentrations During the Last Decade, *Science*, **162**: 120-121.
- Petterson, H., 1960, Cosmic Spherules and Meteoritic Dust, *Sci. Amer.*, **202**: 123-132.
- , and K. Fredriksson, 1958, Magnetic Spherules in Deep-Sea Deposits, *Pacific Sci.*, **12**: 71-81.
- Pilipowskyj, S., J. A. Weinman, B. R. Clemesha, G. S. Kent, and R. W. Wright, 1968, Investigation of the Stratospheric Aerosol by Infrared and Lidar Techniques, *J. Geophys. Res.*, **73**(24): 7553-7560.
- Pinus, N. Z., 1963, Statistical Characteristics of the Horizontal Component of the Wind Velocity at Heights of 6-12 Km, *Bull. Acad. Sci., USSR, Geophys. Ser.*, 105-107.
- , E. R. Reiter, G. N. Shur, and N. K. Vinnichenko, 1967, Power Spectra of Turbulence in the Free Atmosphere, *Tellus*, **19**(2): 206-213.
- Pittock, A. B., 1965, Possible Destruction of Ozone by Volcanic Material at 50 Mb, *Nature*, **207**: 182.
- , 1966, A Thin Stable Layer of Anomalous Ozone and Dust Content, *J. Atmos. Sci.*, **23**(5): 538-542.
- , 1968, Seasonal and Year-To-Year Ozone Variations from Soundings over Southeastern Australia, *Quart. J. Roy. Meteorol. Soc.*, **94**(402): 563-575.
- , 1969, A Statistical Approach to the Synoptic Climatology of Vertical Ozone Distributions, *J. Appl. Meteorol.*, **8**(2): 308-311.
- Plass, G. N., 1956, The Carbon Dioxide Theory of Climatic Change, *Tellus*, **8**(2): 140-154.
- , 1964, Comments on paper by F. Möller, "On the Influence of Changes in the CO₂ Concentrations in Air on the Radiation Balance of the Earth's Surface and on the Climate," *J. Geophys. Res.*, **69**(8): 1663-1664.
- Podzimek, J., 1959, Relation Between Concentration of Giant Chloride Nuclei and Exchange in the Atmosphere, *Geofis. Pura Appl.*, **42**: 133-139.
- , 1961, Über die Bindung der Aerosolteilchen auf der Oberfläche der Wolkenelemente, *Geofis. Pura Appl.*, **50**: 161-168.
- , L. Šrámek, and E. Volfová, 1963, Chemical Analyses of Precipitation Collected Around Hradec Kralove, *Trav. Inst. Geophys. Acad. Tchécoslovaque Sci., Geofys. Sb.*, No. 195, pp. 493-520.

- Pötzl, K., 1967, Methoden zur Analyse anorganischer Schwebstoffe und ihre Anwendung zur Untersuchung von Industriestäuben, *Zentralbl. Biol. Aerosol. Forsch.*, **13**(5/6): 1-16.
- Prabhakara, C., 1962, Effects of Non-Photochemical Processes on the Meridional Distribution and Total Amount of Ozone in the Atmosphere, Ph. D. Thesis, New York University.
- , 1963, Effects of Non-Photochemical Processes on the Meridional Distribution and Total Amount of Ozone in the Atmosphere, *Mon. Weather Rev.*, **91**(9): 411-432.
- , 1969a, Feasibility of Determining Atmospheric Ozone from Outgoing Infrared Energy, *Mon. Weather Rev.*, **97**(4): 307-314.
- , 1969b, Remote Sensing of Atmospheric Ozone Using the 9.6 Region, National Aeronautics and Space Administration, Goddard Space Flight Center, Preprint X-622-69-467, 30 pp.
- Pressman, J., L. M. Aschenbrand, F. F. Marmo, A. Jursa, and M. Zelikoff, 1957, A Synthetic Atmospheric Chemiluminescence Caused by the Release of NO at 106 Km, in *The Threshold of Space*, p. 235, Pergamon Press, Inc., New York.
- Price, S., and J. C. Pales, 1963, Local Volcanic Activity and Ice Nuclei Concentrations on Hawaii, *Arch. Meteorol., Geophys. Bioklimatol., Ser. A*, **13**(3-4): 398-407.
- , and J. C. Pales, 1964, Ice Nucleus Counts and Variations at 3.4 Km and Near Sea Level in Hawaii, *Mon. Weather Rev.*, **92**(5): 207-221.
- Priester, W., and D. Cattani, 1962, On the Semi-Annual Variation in Geomagnetic Activity and Its Relation to Solar Corpuseular Radiation, *J. Atmos. Sci.*, **19**(2): 121-126.
- Prospero, J. M., 1968, Atmospheric Dust Studies on Barbados, *Bull. Amer. Meteorol. Soc.*, **49**(6): 645-653.
- , and E. Bonatti, 1969, Continental Dust in the Atmosphere of the Eastern Equatorial Pacific, *J. Geophys. Res.*, **74**(13): 3362-3371.
- Pueschel, R. F., R. J. Charlson, and N. C. Ahlquist, 1969, On the Anomalous Deliquescence of Sea-Spray Aerosol, *J. Appl. Meteorol.*, **8**(6): 995-998.
- , and K. E. Noll, 1967, Visibility and Aerosol Size Frequency Distribution, *J. Appl. Meteorol.*, **6**(6): 1045-1052.
- Quiroz, R. S., and A. J. Miller, 1967, Note on the Semi-Annual Wind Variation in the Equatorial Stratosphere, *Mon. Weather Rev.*, **95**(9): 635-641.
- Radke, L. F., and P. V. Hobbs, 1969, Measurement of Cloud Condensation Nuclei, Light Scattering Coefficient, Sodium-Containing Particles, and Aitkin Nuclei in the Olympic Mountains of Washington, *J. Atmos. Sci.*, **26**(2): 281-288.
- Ragsdale, G. C., and P. E. Wasko, 1962, Wind Flow in the 80-400 Km Altitude Region of the Atmosphere, Report MTP-AERO-62-49, National Aeronautics and Space Administration, George C. Marshall Space Flight Center.
- Ramana Murty, Bh. V., A. K. Roy, and R. K. Kapoor, 1967, Sources of Origin and Meteorological Importance of Hygroscopic and Ice-Forming Nuclei, *Tellus*, **19**(1): 136-142.
- Ramanadham, K. R., 1963a, Atmospheric Ozone and Some Problems of the Stratosphere, Symposium on Atmospheric Ozone II, International Union of Geodesy and Geophysics Monograph No. 19, p. 1.
- , 1963b, Bi-Annual Variation of Atmospheric Ozone over the Tropics, *Quart. J. Roy. Meteorol. Soc.*, **89**(382): 540-542; **91**(389): 381.
- , 1965, The 26-Month Cycle and Atmospheric Ozone, in *International Atmospheric Ozone Symposium*, Albuquerque, Aug. 31, 1964, pp. 1-6, World Meteorological Organization, Geneva.
- Randhawa, J. S., 1967, Mesospheric Ozone Measurements During Solar Eclipse, Report ECOM-5131, Atmospheric Sciences Laboratory, White Sands Missile Range.
- , 1968, Mesospheric Ozone Measurements During a Solar Eclipse, *J. Geophys. Res.*, **73**(2): 493-495.
- , 1969a, Ozone Measurements from a Stable Platform near the Stratopause Level, *J. Geophys. Res.*, **74**(18): 4588-4590.
- , 1969b, Ozone Measurements from a Stable Platform near the Stratopause Level, Report ECOM-5242, Atmospheric Sciences Laboratory, White Sands Missile Range, March 1969.

- Rangarajan, S., 1964, Ozone Variations Associated with the Equatorial Stratospheric Wind Oscillations, *Indian J. Meteorol. Geophys.*, **15**: 565-578.
- , 1969, A Worldwide Anomaly in the Concentration of Ozone Above 40 Km, *J. Atmos. Sci.*, **26**(3): 613-616.
- Rankama, K., and Th. G. Sahama, 1952, *Geochemistry*, The University of Chicago Press, Chicago.
- Rao, G. L., and B. R. Rao, 1969, A Statistical Study of Horizontal Drifts and Anisotropy of Irregularities in the F₂ Region, *J. Atmos. Sci.*, **26**(3): 580-586.
- Rao, N. N., 1967, Ionospheric Electron Content and Irregularities Deduced from BI-C Satellite Transmissions, *J. Geophys. Res.*, **72**(11): 2929-2942.
- Rao, P. B., 1968, Electron Concentrations and Electron and Ion Temperatures in the F Region for Magnetically Quiet and Disturbed Conditions, *J. Geophys. Res.*, **73**(5): 1661-1678.
- Raschke, E., 1967, A Quasi-Global Analysis of the Mean Relative Humidity of the Upper Troposphere, *Tellus*, **19**(2): 214-218.
- , and W. R. Bandeen, 1967, A Quasi-Global Analysis of Tropospheric Water Vapor Content from TIROS IV Radiation Data, *J. Appl. Meteorol.*, **6**(3): 468-481.
- Rasmussen, R. A., 1965, Terpenes: Their Analysis and Fate in the Atmosphere, Ph. D. Thesis, Washington University.
- Rasool, S. I., 1961, Effects de l'activité solaire sur l'ozone atmosphérique et la hauteur de la tropopause, *Geofis. Pura Appl.*, **48**: 93-101.
- , 1963, Effects of Assumed Changes in the Near Ultraviolet Radiation on the Photochemical Distribution of Atmospheric Ozone and on the Heating Rates in the Stratosphere, National Aeronautics and Space Administration Institute for Space Studies Report.
- Rastogi, R. G., 1957, Thunderstorms and Sporadic E Layer Ionization, *Indian J. Meteorol. Geophys.*, **8**(1): 43-54.
- , 1962, Thunderstorms and Sporadic E Layer Ionization over Ottawa, Canada, *J. Atmos. Terrest. Phys.*, **24**: 533-540.
- Ratcliffe, J. A., 1960, *Physics of the Upper Atmosphere*, Academic Press Inc., New York and London.
- , and K. Weeks, 1960, The Ionosphere, in *Physics of the Upper Atmosphere*, J. A. Ratcliffe (Ed.), pp. 377-470, Academic Press Inc., New York and London.
- Rau, W., 1960, Die zeitlichen Änderungen des atmosphärischen Gefrierkerngehaltes und ihre Beziehungen zu den Meteorströmen und zur atmosphärischen Zirkulation, *Geofis. Pura Appl.*, **46**: 110-124.
- , and M. Schmidt, 1961, Registrierung des atmosphärischen Gefrierkerngehalts in Weissenau von Juli 1957 bis August 1959, *Beitr. Phys. Atmos.*, **34**: 274-320.
- Rawcliffe, R. D., and D. D. Elliott, 1966, Latitude Distribution of Ozone at High Altitudes, Deduced from a Satellite Measurement of the Earth's Radiance at 2840 Å, *J. Geophys. Res.*, **71**(21): 5077-5091.
- , G. E. Meloy, R. M. Friedman, and E. H. Rogers, 1963, Measurement of Vertical Distribution of Ozone from a Polar Orbiting Satellite, *J. Geophys. Res.*, **68**(24): 6425-6429.
- Raynor, G., L. A. Cohen, J. V. Hayes, and E. C. Ogen, 1966, Dyed Pollen Grains and Spores as Tracers in Dispersion and Deposition Studies, *J. Appl. Meteorol.*, **5**(5): 728-729.
- Reddy, C. A., 1968, Physical Significance of the E_s Parameters f_hE_s, fl_{E_s}, and f₀E_s. 2. Causes of Partial Reflection from E_s, *J. Geophys. Res.*, **73**(17): 5627-5647.
- , and S. Matsushita, 1968a, Solar Cycle Variation of Blanketing Sporadic E, *J. Geophys. Res.*, **73**(5): 1641-1660.
- , and S. Matsushita, 1968b, The Variations of Neutral Wind Shears in the F-Region as Deduced from Blanketing E_s, *J. Atmos. and Terrest. Phys.*, **30**: 747-762.
- , and M. M. Rao, 1968, On the Physical Significance of the F_s Parameters f_hF_s, fl_{F_s}, and f₀F_s, *J. Geophys. Res.*, **73**(1): 215-224.
- Reed, E. I., 1968, A Night Measurement of Mesospheric Ozone by Observations of Ultraviolet Airglow, *J. Geophys. Res.*, **73**(9): 2951-2957.

- , and R. Scolnik, 1965, A Nighttime Measurement of Atmospheric Ozone Above 40 Km, in *International Atmospheric Ozone Symposium*, Albuquerque, Aug. 31, p. 27, World Meteorological Organization, Geneva.
- Reed, R. J., 1950, The Role of Vertical Motions in Ozone-Weather Relationships, *J. Meteorol.*, 7(4): 263-267.
- , 1962, Some Features of the Annual Temperature Regime in the Tropical Stratosphere, *Mon. Weather Rev.*, 90(6): 211-215.
- , 1964, A Tentative Model of the 26-Month Oscillation in Tropical Latitudes, *Quart. J. Roy. Meteorol. Soc.*, 90(386): 441-466.
- , 1966, Zonal Wind Behavior in the Equatorial Stratosphere and Lower Mesosphere, *J. Geophys. Res.*, 71(18): 4223-4233.
- , 1968a, Tidal Motions 30-60 Km, Publication in Meteorology No. 90, pp. 147-152, McGill University.
- , 1968b, Quasi-Regular Stratospheric Motions, Publication in Meteorology No. 90, pp. 153-159, McGill University.
- , and K. E. German, 1965, A Contribution to the Problem of Stratospheric Diffusion by Large-Scale Mixing, *Mon. Weather Rev.*, 93(5): 313-321.
- , D. J. McKencie, and J. C. Vyverberg, 1966, Further Evidence of Enhanced Diurnal Tidal Motions Near the Stratopause, *J. Atmos. Sci.*, 23(2): 247-251.
- , and M. J. Oard, 1969, A Comparison of Observed and Theoretical Diurnal Tidal Motions Between 30 and 60 Kilometers, *Mon. Weather Rev.*, 97(6): 456-459.
- Reeves, R. R., G. Manella, and P. Harteck, 1960, Rate of Recombination of Oxygen Atoms, *J. Chem. Phys.*, 32: 632-633.
- Regener, V. H., 1957, The Vertical Flux of Atmospheric Ozone, *J. Geophys. Res.*, 62(2): 221-228.
- , and L. Aldaz, 1969, Turbulent Transport Near the Ground as Determined from Measurements of the Ozone Flux and the Ozone Gradient, *J. Geophys. Res.*, 74(28): 6935-6942.
- Reger, E., and H. Siedentopf, 1950, Staubmessungen in der freien Atmosphäre, *Z. Meteorol.*, 4: 136-142.
- Reid, G. C., 1964, Physical Processes in the D Region of the Ionosphere, *Rev. Geophys.*, 2(2): 311-334.
- , 1968, The Formation of Small-Scale Irregularities in the Ionosphere, *J. Geophys. Res.*, 73(5): 1627-1640.
- Reiter, E. R., 1958, The Layer of Maximum Wind, *J. Meteorol.*, 15(1): 27-43.
- , 1963a, A Case Study of Radioactive Fallout, Atmospheric Science Technical Paper No. 42, Colorado State University.
- , 1963b, A Case Study of Radioactive Fallout, *J. Appl. Meteorol.*, 2(6): 691-705.
- , 1963c, Exploratory Study of the Physical Nature of Certain Mesosstructural Details in Vertical Wind Profiles, Atmospheric Science Technical Paper No. 47, Colorado State University.
- , 1963d, Die Feinstruktur der Atmosphäre und ihre Messung, *Beitr. Phys. Atmos.*, 36(1/2): 157-172.
- , 1966, Large Scale Atmospheric Transport Processes of Radioactive Debris, Report COO-1340-8, Colorado State University.
- , 1967, Meteorological Conditions at the Fort St. Vrain Nuclear Generating Station, Report to the Public Service Company of Colorado.
- , 1968, The Nature of Clear-Air Turbulence: A Review, in *Clear Air Turbulence and Its Detection*, Y.-H. Pao and A. Goldberg (Eds.), pp. 7-33, Plenum Press, New York.
- , 1969a, Atmospheric Transport Processes, Part I: Energy Transfers and Transformations, USAEC Report TID-24868.
- , 1969b, Mean and Eddy Motions in the Atmosphere, *Mon. Weather Rev.*, 97(3): 200-204.
- , and A. Burns, 1965, Atmospheric Structure and Clear-Air Turbulence, Atmospheric Science Technical Paper No. 65, Colorado State University.
- , M. E. Glasser, and J. D. Mahlman, 1967, The Role of the Tropopause in Stratospheric—

- Tropospheric Exchange Processes, Atmospheric Science Paper No. 107, Colorado State University.
- , and P. F. Lester, 1967, The Dependence of the Richardson Number on Scale Length, Atmospheric Science Paper No. 111, Colorado State University.
- , and J. D. Mahlman, 1964a, Atmospheric Transport Processes Leading to Radioactive Fallout over the United States, November 1962, in *Radioactive Fallout from Nuclear Weapons Tests*, Alfred W. Klement (Ed.), AEC Symposium Series, No. 5 (CONF-765), Germantown, Md., pp. 450-463.
- , and J. D. Mahlman, 1964b, Heavy Radioactive Fallout over the Southern United States, November 1962, Atmospheric Science Technical Paper No. 58, pp. 21-49, Colorado State University.
- , and J. D. Mahlman, 1965a, Heavy Radioactive Fallout over the Southern United States, November 1962, *J. Geophys. Res.*, 70(18): 4501-4520.
- , and J. D. Mahlman, 1965b, Heavy Iodine-131 Fallout over the Midwestern United States, May 1962, Atmospheric Science Technical Paper No. 70, pp. 1-53, Colorado State University.
- , and A. Nania, 1964, Jet-Stream Structure and Clear-Air Turbulence (CAT), *J. Appl. Meteorol.*, 3(3): 247-260.
- Reiter, R., 1964, *Felder, Ströme und Aerosole in der unteren Troposphäre nach Untersuchungen im Hochgebirge bis 3000 m NN*, Dietrich Steinkopff Verlag, Darmstadt.
- , 1966, Further Experimental Evidence for the Importance, with Respect to Thunderstorm Electrification, of NO_3^- Ions Contained in Precipitation, *J. Atmos. Terrest. Phys.*, 28: 1065-1080.
- , W. Carnuth, and R. Sládovič, 1968, Effects of Atmospheric Fine Structure Characteristics on the Vertical Distribution of Aerosols, *Arch. Meteorol., Geophys. Bioklimatol., Ser. A*, 17: 336-365.
- Remsberg, E. E., and J. A. Weinman, 1969, Analysis of a Stratospheric Haze Phenomenon Photographed on the Gemini V Spaceflight, unpublished.
- Renzetti, N. A., 1959, Ozone in Los Angeles Atmosphere, in *Ozone Chemistry and Technology*, pp. 230-262, American Chemical Society, Washington, D. C.
- Revelle, R., and H. E. Suess, 1957, Carbon Dioxide Exchange Between Atmosphere and Ocean, and the Question of an Increase of Atmospheric CO_2 During the Past Decades, *Tellus*, 9(1): 18-27.
- Ripperton, L. A., 1965, Ozone and Ozone Precursors in the Atmosphere of Chapel Hill, North Carolina, *J. Geophys. Res.*, 70(20): 5009-5016.
- Rishbeth, H., 1968, On Explaining the Behavior of the Ionospheric F Region, *Rev. Geophys.*, 6(1): 33-71.
- , and O. K. Garriott, 1969, *Introduction to Ionospheric Physics*, International Geophysics Series, Vol. 14, Academic Press Inc., New York.
- Roach, F. E., 1969, The Night Glow and the F Region Ionosphere, in *Atmospheric Emissions*, B. M. McCormac and A. Omholt (Eds.), pp. 439-447, Van Nostrand-Reinhold Co., N. Y.
- Robinson, E., J. A. MacLeod, and C. E. Lapple, 1959, A Meteorological Tracer Technique Using Uranine Dye, *J. Meteorol.*, 16(1): 63-67.
- , and R. C. Robbins, 1968a, Evaluation of CO Data Obtained on *Eltanin* Cruise 27, 29 and 31, *Antarctic J. U. S.*, 3(5): 194-197.
- , and R. C. Robbins, 1968b, Source, Abundance, and Fate of Gaseous Atmospheric Pollutants, Final Report, SRI Project PR-6755, American Petroleum Institute.
- Rodewald, M., 1952, Die blaue Sonne vom 27. September 1950, *Naturwiss. Rundsch.*, 5(1): 8-15.
- Rodgers, C. D., 1967, The Radiative Heat Budget of the Troposphere and Lower Stratosphere, Planetary Circulations Project, Report No. A2, Massachusetts Institute of Technology.
- Rodionov, S. F., B. N. Movchan, A. L. Osherovich, V. A. Gulyŭ, Kh. K. Kumykov, A. K. Suslov, A. Kh. Shukurov, and L. N. Yurganov, 1967, The Shadowing Effect in the Ozone Region of the Solar Spectrum in May 1966, *Izv. Atmos. and Oceanic Phys.*, 3(12): 1280-1291.

- Rosen, J. M., 1964, The Vertical Distribution of Dust to 30 Kilometers, *J. Geophys. Res.*, **69**(21): 4673-4676.
- , 1967, Stratospheric Dust, Atmospheric Physics Annual Progress Report, University of Minnesota.
- , 1968, Simultaneous Dust and Ozone Soundings over North and Central America, *J. Geophys. Res.*, **73**(2): 479-486.
- Rosenberg, N. W., 1962, Chemical Releases in the Upper Atmosphere (Project Firefly), A Summary Report, Report AFCRL-62-826, pp. 1-14, Air Force Cambridge Research Laboratories.
- , 1963, Chemical Releases in the Upper Atmosphere (Project Firefly), A Summary Report, *J. Geophys. Res.*, **68**(10): 3057-3063.
- , 1964, Project Firefly 1962-1963, Environmental Research Paper No. 15, Report AFCRL-64-364, Air Force Cambridge Research Laboratories.
- , 1966, Chemical Releases at High Altitudes, Environmental Research Paper No. 209, Report AFCRL-66-490, Air Force Cambridge Research Laboratories.
- , 1968, Statistical Analysis of Ionospheric Winds—II, *J. Atmos. Terrest. Phys.*, **30**(5): 907-917.
- , and H. D. Edwards, 1964, Observations of Ionospheric Wind Patterns Through the Night, *J. Geophys. Res.*, **69**(13): 2819-2826.
- , H. D. Edwards, and J. W. Wright, 1964a, Ionospheric Winds: Motions into Night and Sporadic E Correlations, Environmental Research Paper No. 67, Report AFCRL-64-881, Air Force Cambridge Research Laboratories.
- , H. D. Edwards, and J. W. Wright, 1964b, Ionospheric Winds and Sporadic E Correlations, Environmental Research Paper No. 15, Report AFCRL-64-364, pp. 291-307, Air Force Cambridge Research Laboratories.
- , and D. Golomb, 1964, Generation and Properties of High Altitude Chemical Plasma Clouds, Environmental Research Paper No. 26, Report AFCRL-64-522, Air Force Cambridge Research Laboratories, and *Progr. Astronaut. Aeronaut.*, **12**: 395-408.
- , D. Golomb, and E. F. Allen, Jr., 1964, Resonance Radiation of A10 from Trimethyl Aluminum Released into the Upper Atmosphere, *J. Geophys. Res.*, **69**(7): 1451-1454.
- , and S. P. Zimmerman, 1967, Correlation Between the 5577 Å [OI] Night Airglow Intensity and Solar Activity, *Planet. Space Sci.*, **15**: 863-872.
- Rosinski, J., 1967, Insoluble Particles in Hail and Rain, *J. Appl. Meteorol.*, **6**(6): 1066-1074.
- , and T. C. Kerrigan, 1969, The Role of Aerosol Particles in the Formation of Raindrops and Hailstones in Severe Thunderstorms, *J. Atmos. Sci.*, **26**(4): 695-715.
- , and J. M. Pierrard, 1964, Condensation Products of Meteor Vapors and Their Connection with Noctilucent Clouds and Rainfall Anomalies, *J. Atmos. Terrest. Phys.*, **26**: 51-66.
- Rossmann, F., 1950, Luftelektrische Messungen mittels Segelflugzeugen, *Ber. Deut. Wetterd.*, **15**: 1-54.
- Rubin, M. J., and W. Weyant, 1963, The Mass and Heat Budget of the Antarctic Atmosphere, *Mon. Weather Rev.*, **91**(10-12): 487-493.
- Runge, H., 1951, Blaue Sonne, blauer Mond, *Z. Meteorol.*, **5**(2): 60-62.
- Ryan, B. F., and W. D. Scott, 1969, Ice Nuclei and the Onset of Rainfall, *J. Atmos. Sci.*, **26**(3): 611-612.
- Sagalyn, R. C., and M. Smiddy, 1964, Rocket Investigation of the Electrical Structure of the Lower Ionosphere, Environmental Research Paper No. 61, Report AFCRL-64-841, Air Force Cambridge Research Laboratories, and *Space Research*, IV, pp. 371-387, North-Holland Publishing Co., Amsterdam.
- Sartor, J. D., 1967, Remote Sensing of Radio Emission from Convective Clouds Including Transmission via Sporadic E, *Mon. Weather Rev.*, **95**(12): 871-877.
- Schaefer, V. J., 1966, Ice Nuclei from Automobile Exhaust and Iodine Vapor, *Science*, **154**: 1555.
- , 1968, Ice Nuclei from Auto Exhaust and Organic Vapors, *J. Appl. Meteorol.*, **7**(1): 148-149.

- , 1969, The Inadvertent Modification of the Atmosphere by Air Pollution, *Bull. Amer. Meteorol. Soc.*, **50**(4): 199-206.
- Scherhag, R., 1960, Stratospheric Temperature Changes and the Associated Changes in Pressure Distribution, *J. Meteorol.*, **17**(6): 575-582.
- , et al., 1958, Daily and Monthly Northern Hemisphere 10 Mb Synoptic Weather Maps, *Meteorol. Abh., Inst. Meteorol. Geophys., Freie Univ., Berlin* (continuing series).
- Schiff, H. I., 1964, Reactions Involving Nitrogen and Oxygen, *Ann. Géophys.*, **20**(1): 115-127.
- , 1968, Reactions Related to Atmospheric Ozone Chemistry, *Meteorol. Monogr.*, **9**(31): 32-36.
- , and L. R. Megill, 1964, The Influence of Metastable Oxygen Molecules on Ozone and Airglow, *J. Geophys. Res.*, **69**(23): 5120-5121.
- Schilling, G. F., 1964, Comments on "The Secular Increase of the World-Wide Fine Particle Pollution," *J. Atmos. Sci.*, **21**(6): 703-704.
- , 1968, Density and Temperature Variations in the Intervening Layer (90–150 Km), *Meteorol. Monogr.*, **9**(31): 82-89.
- Schmidlin, F. J., 1969, A Statistical Comparison of Winter–Summer Rocketsonde–Radiosonde Temperatures in the 20- to 34-Kilometer Region of the Stratosphere, *Mon. Weather Rev.*, **97**(8): 607-612.
- Schmidt, Th., and H. Elsässer, 1967, Dynamics of Submicron Particles ($a < 10^{-5}$ Cm) in Interplanetary Space, Report NASA-SP-150, pp. 287-289, National Aeronautics and Space Administration.
- Schofield, K., 1967, An Evaluation of Kinetic Rate Data for Reactions of Neutrals of Atmospheric Interest, *Planet. Space Sci.*, **15**: 643-670.
- Schove, D. J., 1969, The Biennial Oscillation, Tree Rings and Sunspots, *Weather*, **24**(1): 390-397.
- Schröder, W., 1966a, Zur geographischen Verteilung der leuchtenden Nachtwolken, *Meteorol. Rundsch.*, **19**(5): 151-153.
- , 1966b, Zur täglichen Häufigkeit der leuchtenden Nachtwolken, *Meteorol. Rundsch.*, **19**(1): 26-27.
- , 1966c, Bibliographical Notes on Noctilucent Clouds, I and II, *Meteorol. Rundsch.*, **19**(6): 174-175.
- , 1966d, Untersuchungen über die leuchtenden Nachtwolken, *Beitr. Phys. Atmos.*, **39**: 50-54.
- , 1967a, Zur Breitenwanderung der leuchtenden Nachtwolken, *Meteorol. Rundsch.*, **20**(2): 54-55.
- , 1967b, Untersuchungen über die leuchtenden Nachtwolken in Deutschland, *Meteorol. Rundsch.*, **20**(1): 29-30.
- , 1967c, Studien der leuchtenden Nachtwolken (NLC) im Jahre 1966, *Meteorol. Rundsch.*, **20**(3): 92-93.
- , 1967d, Zur weiträumigen Häufigkeit der leuchtenden Nachtwolken, *Z. Meteorol.*, **19**(3-4): 109-111.
- , 1967e, Katalog deutscher Beobachtungen von leuchtenden Nachtwolken für die Jahre 1885-1956, *Z. Meteorol.*, **19**(9-10): 301-303.
- , 1968a, Analyse der täglichen Häufigkeit der leuchtenden Nachtwolken, *Meteorol. Rundsch.*, **21**(1): 28-30.
- , 1968b, Mesosphärische Zirkulation und leuchtende Nachtwolken, *Meteorol. Rundsch.*, **21**(2): 54-56.
- , 1968c, Katalog deutscher Beobachtungen von leuchtenden Nachtwolken für die Jahre 1885-1956, *Z. Meteorol.*, **20**(11/12): 372-379.
- Schröer, E., 1947, Über Zusammenhänge zwischen Sauerstoffatmosphäre und ionisierten Schichten und eine den Mögel-Dellinger Effekt verursachende Wellenstrahlung, *Z. Meteorol.*, **1**: 110-113.
- Schubert, G., and W. Hänsch, 1963a, Gegenüberstellung einiger meteorologischer Elements von Schwerin/Mecklenburg während der beiden Sturmperioden in der 2. Februar Dekade 1962.

- , and W. Hänsch, 1963b, Beobachtung von Meersalzablagerung tief im Landesinnern von Mecklenburg nach dem zweiten Sturmtief am 16.17. Februar 1962, *Z. Meteorol.*, **16**: 276-277.
- Scoggins, J. R., 1963, An Evaluation of Detailed Wind Data that is Measured by the FPS-16 Radar/Spherical Balloon Technique, NASA Technical Note TN-D-1572, National Aeronautics and Space Administration.
- , 1965, Spherical Balloon Wind Sensor Behavior, *J. Appl. Meteorol.*, **4**(1): 139-145.
- Scorer, R. S., 1968, *Air Pollution*, Pergamon Press, London.
- Scott, W. D., D. Lamb, and D. Duffy, 1969, The Stratospheric Aerosol Layer and Anhydrous Reactions Between Ammonia and Sulfur Dioxide, *J. Atmos. Sci.*, **26**(4): 727-733.
- Seiler, W., and C. Junge, 1967, Entwicklung eines Messverfahrens zur Bestimmung kleiner Mengen von Kohlenoxyd (CO), *Meteorol. Rundsch.*, **20**(6): 175-176.
- , and C. Junge, 1969, Decrease of Carbon Monoxide Mixing Ratio Above the Polar Tropopause, *Tellus*, **21**(3): 447-449.
- Seitz, H., B. Davidson, J. P. Friend, and H. W. Feely, 1968, Numerical Models of Transport, Diffusion and Fallout of Stratospheric Radioactive Material, Final Report on Project Streak, USAEC Report NYO-3654-4, Isotopes Inc.
- Sekhon, R. S., and Bh. V. Ramana Murty, 1966, Some Characteristic Features of Hygroscopic and Non-Hygroscopic Aerosols at Delhi, *J. Atmos. Sci.*, **23**(6): 771-777.
- Sekihara, K., 1961, Solar Activity and Atmospheric Ozone, *J. Meteorol. Soc. Jap.*, **39**(6): 315-323.
- Sekikawa, T., and H. Kojima, 1969, Charged Fraction and Charged Equilibrium on the Submicron Aerosol Particles in the Atmosphere, *J. Meteorol. Soc. Jap.*, **47**(5): 329-334.
- Sellers, W. D., and D. N. Yarger, 1969, The Statistical Prediction of the Vertical Ozone Distribution, *J. Appl. Meteorol.*, **8**(3): 357-361.
- Seto, Y.-B., R. A. Duce, and A. H. Woodcock, 1969, Sodium-To-Chlorine Ratio in Hawaiian Rains as a Function of Distance Inland and of Elevation, *J. Geophys. Res.*, **74**(4): 1101-1103.
- Severynse, G. T., 1963, Removal of Aerosol Particles from the Atmosphere by Growing Cloud Droplets, *Geofis. Pura Appl.*, **55**: 151-163.
- Shafirir, U., S. Abarbanel, and M. Humi, 1967, A Note on the Dynamical Interaction of Small Interplanetary Particles with the Earth's Upper Atmosphere, *J. Atmos. Sci.*, **24**(5): 582-585.
- , and M. Humi, 1967, Interplanetary Particles and Noctilucent Clouds, *J. Atmos. Sci.*, **24**(5): 577-581.
- Shah, G. M., 1966, Apparent Variation of Ozone During Nighttime, *J. Atmos. Sci.*, **23**(5): 535-537; **25**(6): 1174.
- , 1967, Quasi-Biennial Oscillation in Ozone, *J. Atmos. Sci.*, **24**(4): 396-401.
- Shapiro, R., and F. Ward, 1962, A Neglected Cycle in Sunspot Numbers? *J. Atmos. Sci.*, **19**(6): 506-508.
- Shapley, A. H., 1967, Ionization Changes Coupled to Stratospheric Effects, in *Space Research*, VII, p. 245, North-Holland Publishing Co., Amsterdam.
- , and W. J. G. Bynon, 1965, "Winter Anomaly" in Ionospheric Absorption and Stratospheric Warmings, *Nature*, **206**: 1242-1243.
- Shaw, J. H., 1959, A Determination of the Abundance of Nitrous Oxide, Carbon Monoxide, and Methane in Ground Level Air at Several Locations near Columbus, Ohio, Scientific Report No. 1, pp. 1-38, Air Force Cambridge Research Center.
- Shedlovsky, J. P., and S. Paisley, 1966, On the Meteoritic Component of Stratospheric Aerosol, *Tellus*, **18**(2): 499-503.
- Shen, W. C., G. W. Nicholas, and A. D. Belmont, 1968, Antarctic Stratospheric Warmings During 1963 Revealed by 15- μ TIROS VII Data, *J. Appl. Meteorol.*, **7**(2): 268-283.
- Shepherd, G. G., 1969, Airglow Spectroscopic Temperatures, in *Atmospheric Emissions*, B. M. McCormac and A. Omholt (Eds.), pp. 411-422, Van Nostrand-Reinhold Co., New York.
- Sheppard, L. M., and K. H. Lloyd, 1964, Atmospheric Density and the Diffusion of Grenade Glow Clouds, *Planet. Space Sci.*, **12**: 317-318.

- Shimizu, M., 1962, Vertical Distribution of Atmospheric Ozone at Tateno and Other Four Stations in and near Japan, *J. Meteorol. Soc. Jap.*, **40**(3): 136-147.
- , 1964, Ozone Changes Related to Tropospheric and Stratospheric Disturbances, *J. Meteorol. Soc. Jap.*, **42**(1): 26-42.
- Shur, G. N., 1962, Experimental Investigations of the Energy Spectrum of Atmospheric Turbulence, *Tr. Tsent. Aerolog. Observ.*, No. 43.
- Sidle, A. B., 1967, Amino Acid Content of Atmospheric Precipitation, *Tellus*, **19**(1): 128-135.
- Silverman, S. M., 1969, Night Airglow Phenomenology, in *Atmospheric Emissions*, B. M. McCormac and A. Omholt (Eds.), pp. 383-397, Van Nostrand-Reinhold Co., New York.
- Sinclair, P. C., 1969, General Characteristics of Dust Devils, *J. Appl. Meteorol.*, **8**(1): 32-45.
- Singer, S. F., 1961, Dust Shell Around the Earth (Abstract), *J. Geophys. Res.*, **66**(8): 2560-2561.
- , 1964, What Determines the Lifetime of Trapped Protons? in *Space Science*, IV, P. Muller (Ed.), pp. 681-689, North-Holland Publishing Co., Amsterdam.
- Singleton, F., and W. G. Durbin, 1962, Aircraft Observations of the Horizontal Distribution of Chloride Particles and Their Relation to Drop-Growth Processes in Clouds, *Quart. J. Roy. Meteorol. Soc.*, **88**(377): 315-323; **89**(381): 430-431.
- Sissenwine, N., M. Dubin, and H. Wexler, 1962, The U. S. Standard Atmosphere, 1962, *J. Geophys. Res.*, **67**(9): 3627-3630.
- , D. D. Grantham, and H. A. Salmela, 1968a, Mid-Latitude Humidity to 32 Km, *J. Atmos. Sci.*, **25**(6): 1129-1140.
- , D. D. Grantham, and H. A. Salmela, 1968b, Humidity up to the Mesopause, Air Force Surveys in Geophysics No. 206, Report AFCRL-68-0550, Air Force Cambridge Research Laboratories.
- Skeib, G., and Ch. Popp, 1961, Messungen des Gesamtzongehaltes der Atmosphäre in Mirny, Antarktika, *Z. Meteorol.*, **15**: 287-291.
- Skrivaneck, R. A., 1969, Rocket Sampling of Noctilucent Clouds, in *Stratospheric Circulation*, W. L. Webb (Ed.), pp. 219-239, Academic Press Inc., New York.
- , and R. K. Soberman, 1964, Simulation of Ring Patterns Observed with Noctilucent Cloud Particles, *Tellus*, **16**(1): 114-117.
- Slack, F. F., 1967, Scintillation Studies Using the Early Bird Synchronous Satellite 136-MHz Signal, Environmental Research Paper No. 278, Report AFCRL-67-0655, Air Force Cambridge Research Laboratories.
- Slocum, G., 1955, Has the Amount of Carbon Dioxide in the Atmosphere Changed Significantly Since the Beginning of the Twentieth Century? *Mon. Weather Rev.*, **83**(10): 225-231.
- Smith, C. D., 1950, The Widespread Smoke Layer from Canadian Forest Fires During Late September 1950, *Mon. Weather Rev.*, **78**(9): 180-184.
- Smith, E. K., 1967, A Suggested Conjugate Point Dependence for Intense Temperate Latitude Sporadic E, in Conjugate Point Symposium, June 13-18, 1967, Boulder, Colo., Institute for Telecommunication Sciences and Aeronomy.
- , 1968, Some Unexplained Features in the Statistics for Intense Sporadic E, paper presented at Second Seminar on the Cause and Structure of Temperate Latitude Sporadic E, Vail, Colorado, June 19-22, 12 pp.
- , and S. Matsushita, 1962, *Ionospheric Sporadic E*, The MacMillan Company, New York.
- , and S. Weintraub, 1953, The Constants in the Equations for Atmospheric Refractive Index at Radio Frequencies, *Proc. Inst. Radio. Eng.*, **41**: 1035-1037.
- Smith, F. J., 1963, The Measurement of High Altitude Wind Velocities from Vapour Releases, II. Computer Method, *Planet. Space Sci.*, **11**: 1311-1317.
- Smith, L. B., 1969, Observations of Atmospheric Density, Temperature, and Winds over Kauai, Report SC-RR-68-523, Sandia Laboratories.
- Smith, L. L., and W. R. Steiger, 1968, Night Airglow Intensity Variations in the [OI] 5577 Å, [OI] 6300 Å, and NaI 5890-96 Å Emission, *J. Geophys. Res.*, **73**(7): 2531-2538.
- Smith, R. M., 1968, A Preview on the Determination of Mass Return Flow of Air and Water Vapour into the Stratosphere Using Tritium as a Tracer, *Tellus*, **20**(1): 76-81.

- Smith, R. W., 1969, Predawn Enhancement over Britain, in *Atmospheric Emissions*, B. M. McCormac and A. Omholt (Eds.), pp. 485-488, Van Nostrand-Reinhold Co., New York.
- Smith, W. L., 1967, An Iterative Method for Reducing Tropospheric Temperature and Moisture Profiles from Satellite Radiation Measurements, *Mon. Weather Rev.*, **95**(6): 363-369.
- Smith, W. S., L. Katchen, P. Sacher, P. Swartz, and J. Theon, 1964, Temperature, Pressure, Density and Wind Measurements with the Rocket Grenade Experiment, 1960-1963, NASA Technical Report NASA-TR-R-211, National Aeronautics and Space Administration, October.
- , L. Katchen, and J. S. Theon, 1968, Grenade Experiments in a Program of Synoptic Meteorological Measurements, *Meteorol. Monogr.*, **9**(31): 170-175.
- Soberman, R. K., S. A. Chrest, J. J. Manning, L. Rey, T. G. Ryan, R. A. Skrivanek, and N. Wilhelm, 1964, Techniques of Rocket Sampling of Noctilucent Cloud Particles, *Tellus*, **16**(1): 89-95.
- , and C. L. Hemenway, 1965, Meteoric Dust in the Upper Atmosphere, *J. Geophys. Res.*, **70**(19): 4943-4949.
- Solot, S. B., 1968, GHOST Balloon Data, Report NCAR-TN-34 (several volumes), National Center for Atmospheric Research.
- , and J. K. Angell, 1969, Mean Meridional Air Flow Implied by 200-Mb GHOST Balloon Flights in Temperate Latitudes of the Southern Hemisphere, *J. Atmos. Sci.*, **26**(6): 1299-1305.
- Soulage, G., 1957, Sur l'activité glaucogène des fumées d'échappement d'avions, *Bull. Obs. Puy de Dôme*, **4**: 113-114.
- Sparrow, J. G., 1967, Note on the Diurnal Cycle in the Equatorial Stratosphere, *J. Appl. Meteorol.*, **6**(2): 441-444.
- , E. P. Ney, G. B. Burnett, and J. W. Stoddart, 1968, Airglow Observations from OSO-B2 Satellite, *J. Geophys. Res.*, **73**(3): 857-866.
- , and E. L. Unthank, 1964, Biennial Stratospheric Oscillations in the Southern Hemisphere, *J. Atmos. Sci.*, **21**(6): 592-596.
- Spencer, N. W., G. R. Carignan, and D. R. Tausch, 1968, Recent Measurements of the Lower Thermosphere Structure, *Meteorol. Monogr.*, **9**(31): 201-207.
- Spindler, G. B., 1966, Observations on the Release of Nitric Oxide in the E-Region, *Planet. Space Sci.*, **14**: 53-64.
- Spizzichino, A., 1964, Méthodes de mesure des vents dans la basse ionosphère, *Ann. Géophys.*, **20**(4): 397-416.
- , and C. Taieb, 1964, Contribution à l'étude des mouvements des couches E sporadiques, *Ann. Géophys.*, **20**(2): 197-200.
- Sprenger, K., and R. Schminder, 1966, Vergleich von Ionosphären-driftmessungen im Langwellenbereich an zwei 300 km voneinander entfernten Stationen, *Kleinheubacher Ber.*, **11**: 79-87.
- , and R. Schminder, 1967, Evidence of a 26-Month Wind Oscillation in the Lower Ionosphere over Central Europe, *Z. Meteorol.*, **19**: 168-170.
- , and R. Schminder, 1968, On the Significance of Ionospheric Drift Measurements in the LF Range, *J. Atmos. Terrest. Phys.*, **30**(5): 693-700.
- Squires, P., 1966, An Estimate of the Anthropogenic Production of Cloud Nuclei, *J. Rech. Atmos.*, Nos. 2-3: 297-308.
- Staley, D. O., 1962, On the Mechanism of Mass and Radioactivity Transport from Stratosphere to Troposphere, *J. Atmos. Sci.*, **19**(6): 450-467.
- Starr, J. R., 1967, Deposition of Particulate Matter by Hydrometeors, *Quart. J. Roy. Meteorol. Soc.*, **93**(398): 516-521.
- Starr, V. P., 1968, *Physics of Negative Viscosity Phenomena*, McGraw-Hill Book Company, Inc., New York.
- , and J. P. Peixoto, 1958, On the Global Balance of Water Vapor and the Hydrology of Deserts, *Tellus*, **10**(2): 188-194.

- , J. P. Peixoto, and A. R. Crisi, 1965, Hemispheric Water Balance for the IGY, *Tellus*, 17(4): 463-472.
- Steinhauser, F., 1958, Der Kohlendioxyd-Gehalt der Luft in Wien und seine Abhängigkeit von verschiedenen Faktoren, *Ber. Deut. Wetterd.*, 51: 17-19.
- , 1959a, Ergebnisse von Registrierungen des Ozongehaltes der Luft in Wien, *Arch. Meteorol., Geophys. Bioklimatol.*, 11(3): 368-382.
- , 1959b, Messungen der Staubablagerung in Wien, *Idöjárás*, 63(2): 94-99.
- , 1960a, Ergebnisse von Messungen des CO₂-Gehaltes der Luft in Österreich, *Wetter Leben*, 12(9-10): 263-269.
- , 1960b, Messungen der Luftverschmutzung in Wien, *Arch. Meteorol., Geophys. Bioklimatol., Ser. B*, 10(2): 200-209.
- , 1962, Der Tagesgang der Luftverschmutzung in Wien, *Arch. Meteorol. Geophys. Bioklimatol., Ser. B*, 12(1): 109-122.
- , 1964, Über den Gehalt an chemischen Beimengungen von Luft und Niederschlägen, *Idöjárás*, 68(6): 348-363.
- , 1966, Die Staubablagerungen im Stadtgebiet von Graz, *Wetter Leben*, 18: 99-104.
- , 1967, Über die Änderungen der SO₂-Ablagerungen aus der Luft in Wien von 1958-1966, *Wetter Leben*, 19: 47-56.
- , and K. Chalupa, 1965, Die SO₂-Ablagerung aus der Luft im Stadtgebiet von Graz, *Wetter Leben*, 17: 45-66.
- , and K. Chalupa, 1966, Ergebnisse von Messungen der Staubablagerungen in Österreich, *Wetter Leben*, 18: 177-185.
- Stephens, J. J., and E. R. Reiter, 1966, Estimating Refractive Index Spectra in Regions of Clear Air Turbulence, Electrical Engineering Research Laboratory, Report No. P-12, The University of Texas.
- Stewart, D. A., 1968, Eddy Flux of Sensible Heat at Different Levels in the Stratosphere, *Arch. Meteorol., Geophys. Bioklimatol.*, 17: 101-113.
- , and O. M. Essenwanger, 1968, Zur interpretation aerologischer Korrelationen und deren Zusammenhang mit speziellen Schichten, *Meteorol. Rundsch.*, 21(5): 134-138.
- Stewart, K. H., 1967, Satellite Techniques for Observing Height Profiles of Ozone, Manuscript G.16209/AVM/9/67/250, Meteorology Office, Great Britain.
- Sticksel, P. R., 1966, The Vertical Distribution of Ozone over Tallahassee, Florida, Report 66-3, Florida State University.
- Stinson, R., A. I. Weinstein, and E. R. Reiter, 1964, Details of Wind Structure from High Resolution Balloon Soundings, NASA Technical Memorandum, Report NASA TM-x-53115, National Aeronautics and Space Administration.
- Størmer, C., 1935, Measurements of Luminous Night Clouds in Norway, 1933 and 1934, *Astrophys. Norv.*, 1(3): 87-114.
- , 1940, Height of Mother-Of-Pearl Clouds Observed in Southern Norway During 1926-1934, *Nature*, 145: 221-222.
- Stranz, D., 1961, Ozone Measurements During Solar Eclipse, *Tellus*, 13(2): 276-279.
- Streff-Becker, R., 1942, Neue Untersuchungen über Föhn in den Schweizer Alpen, *Schweiz. Naturforsch. Gesellsch., Denkschriften*, 74(4): 244-278.
- Stroud, W. G., W. Nordberg, W. R. Bandeen, F. L. Bartman, and P. Titus, 1960, Rocket Grenade Measurements of Temperature and Winds in the Mesosphere over Churchill, Canada, *J. Geophys. Res.*, 65(8): 2307-2323.
- Sturrock, R. F., 1960, Measurements of Atmospheric Ozone During the International Geophysical Year at Alert, N.W.T. (82°30'N; 62°20'W), *Can. Meteorol. Memoirs*, No. 4.
- Sugiura, M., 1968, Ionospheric Winds and Associated Geomagnetic Variations, *Meteorol. Monogr.*, 9(31): 152-157.
- Sullivan, H. M., and D. M. Hunten, 1964, Lithium, Sodium, Potassium in the Twilight Airglow, *Can. J. Phys.*, 42: 1325-1335.

- , W. D. Komhyr, and C. L. Mateer, 1961, Measurements of Atmospheric Ozone at Resolute, Canada (74°43'N; 94°59'W): July 7, 1957 to December 31, 1959, *Can. Meteorol. Memoirs*, No. 7.
- Suomi, V. E., and P. M. Kuhn, 1958, An Economical Net Radiometersonde, *Tellus*, 10(1): 160-163.
- Swider, W., Jr., 1969a, Upper Atmospheric Emission Processes, in *Atmospheric Emissions*, B. M. McCormac and A. Omholt (Eds.), pp. 367-382, Van Nostrand-Reinhold Co., New York.
- , 1969b, Ionization Rates Due to the Attenuation of 1-100 Å Nonflare Solar X Rays in the Terrestrial Atmosphere, *Rev. Geophys.*, 7(3): 573-594.
- Taffe, W. J., 1969, The Variation of the Upper Atmospheric Scale Height and Its Effect on Atmospheric Tidal Wavelengths, Environmental Research Paper No. 304, Report AFCRL-69-0350, Air Force Cambridge Research Laboratories.
- Takahashi, T., 1961, Carbon Dioxide in the Atmosphere and in Atlantic Ocean Water, *J. Geophys. Res.*, 66(2): 477-494.
- , 1967, Carbon Dioxide Cycle in the Sea and Atmosphere, in *The Encyclopedia of Atmospheric Sciences and Astrogeology*, R. W. Fairbridge (Ed.), pp. 131-136, Reinhold Publishing Corporation, New York.
- Takeuchi, D. M., 1966, Size Distribution of Marine Aerosols at Mau (Hawaii), Report ARG67-FR-456, pp. A-1 to A-22, Atmospheric Research Group, Altadena, Calif.
- Tarrant, R. F., K. C. Lu, C. S. Chên, and W. B. Bollen, 1968, Nitrogen Content of Precipitation in a Coastal Oregon Forest Opening, *Tellus*, 20(3): 554-556.
- Tatarski, V. I., 1961, *Wave Propagation in a Turbulent Medium*, McGraw-Hill Book Company, Inc., New York.
- Teichert, F., 1955, Vergleichende Messung des Ozongehaltes der Luft am Erboden und in 80 m Höhe, *Z. Meteorol.*, 9: 21-27.
- , 1956, Ergebnisse einer regionalen Staubuntersuchung mit Hilfe von Staubbechern, *Z. Meteorol.*, 10: 369-373.
- Telford, J. W., 1960, Freezing Nuclei Above the Tropopause, *J. Meteorol.*, 17(1): 86-88.
- Teweles, S., 1964, Stratospheric-Mesospheric Circulation, in *Research in Geophysics*, Vol. 2, H. Odishaw (Ed.), pp. 509-528, M.I.T. Press, Cambridge, Mass.
- , 1967, Upper Atmosphere Investigations Require Coordinated Approach, *Bull. Amer. Meteorol. Soc.*, 48(4): 262-264.
- Theon, J. S., 1968, Short Term Temperature Variation in the Atmosphere Below 120 Km, in *Proceedings of the Third National Conference on Aerospace Meteorology*, New Orleans, La., May 6-9, pp. 449-456, American Meteorological Society, Boston, Mass.
- , and J. J. Horvath, 1968, Observations of the Southern Hemisphere Stratosphere and Mesosphere, *J. Geophys. Res.*, 73(14): 4475-4480.
- , W. Nordberg, L. B. Katchen, and J. J. Horvath, 1967, Some Observations on the Thermal Behavior of the Mesosphere, *J. Atmos. Sci.*, 24(4): 428-438.
- Thiel, E., and R. A. Schmidt, 1961, Spherules from the Antarctic Ice Cap, *J. Geophys. Res.*, 66(1): 307-310.
- Thomas, L., 1961, Year to Year Changes in the Winter-Anomaly of Ionospheric Absorption, *J. Atmos. Terrest. Phys.*, 21: 215-217.
- , 1969, Ionospheric Phenomena Related to Airglow, in *Atmospheric Emissions*, B. M. McCormac and A. Omholt (Eds.), pp. 423-435, Van Nostrand-Reinhold Co., New York.
- Thompson, M. C., Jr., A. W. Kirkpatrick, and W. B. Grant, 1968, Measurements of Radio Refractive Index Microstructure of the Near-Ground Atmosphere, *J. Geophys. Res.*, 73(20): 6425-6435.
- Thyer, N., and K. J. K. Buettner, 1962, On Valley and Mountain Winds, 3, Technical Report, University of Washington.
- Tinsley, B. A., 1969, Hydrogen and Helium in the Upper Atmosphere, in *Atmospheric Emissions*, B. M. McCormac and A. Omholt (Eds.), pp. 539-544, Van Nostrand-Reinhold Co., New York.

- Titheridge, J. E., 1963, Large-scale Irregularities in the Ionosphere, *J. Geophys. Res.*, **68**(11): 3399-3417.
- , 1968a, Periodic Disturbances in the Ionosphere, *J. Geophys. Res.*, **73**(1): 243-252.
- , 1968b, Nighttime Changes in the Electron Content of the Ionosphere, *J. Geophys. Res.*, **73**(9): 2985-2993.
- Toba, Y., 1965a, On the Giant Sea-Salt Particles in the Atmosphere. I. General Features of the Distribution, *Tellus*, **17**(1): 131-145.
- , 1965b, On the Giant Sea-Salt Particles in the Atmosphere. II. Theory of the Vertical Distribution in the 10-M Layer over the Ocean, *Tellus*, **17**(3): 365-381.
- , 1966, On the Giant Sea-Salt Particles in the Atmosphere. III. An Estimate of the Production and Distribution over the World Ocean, *Tellus*, **18**(1): 132-145.
- Tohmatsu, T., and T. Nagata, 1963, Dynamical Studies of the Oxygen Green Line in Airglow, *Planet. Space Sci.*, **10**: 103-116.
- Tromp, S. W., 1963, *Medical Biometeorology*, Elsevier Publishing Company, Netherlands.
- Tucker, G. B., 1964, Zonal Winds over the Equator, *Quart. J. Roy. Meteorol. Soc.*, **90**(386): 405-423.
- Tuller, S. E., 1968, World Distribution of Mean Monthly and Annual Precipitable Water, *Mon. Weather Rev.*, **96**(11): 785-797.
- Twomey, S., 1960, On the Nature and Origin of Natural Cloud Nuclei, *Bull. Obs. Puy de Dôme*, 1-19.
- , 1969, Comments on "Estimating the Vertical Ozone Distribution," *J. Atmos. Sci.*, **26**(5): 1154.
- , and G. T. Severynse, 1964, Size Distributions of Natural Aerosols Below 0.1 Micron, *J. Atmos. Sci.*, **21**(5): 558-564.
- , and J. Warner, 1967, Comparison of Measurements of Cloud Droplets and Cloud Nuclei, *J. Atmos. Sci.*, **24**(6): 702-703.
- , and T. A. Wojciechowski, 1969, Observations of the Geographical Variation of Cloud Nuclei, *J. Atmos. Sci.*, **26**(4): 684-688.
- United States Atomic Energy Commission, 1968, *Meteorology and Atomic Energy, 1968*, D. H. Slade (Ed.), USAEC Report TID-24190.
- United States Weather Bureau, 1955, *Meteorology and Atomic Energy*, U. S. Government Printing Office, Washington.
- Unz, F., 1969, Die Konzentration des Aerosols in Troposphäre und Stratosphäre aus Messungen der Himmelsstrahlung im Zenit, *Beitr. Phys. Atmos.*, **42**(1): 1-35.
- Valach, R., 1967, The Origin of the Gaseous Form of Natural Atmospheric Chlorine, *Tellus*, **19**(3): 509-516.
- Vallance Jones, A., 1958, Calcium and Oxygen in the Twilight Airglow, *Ann. Geophys.*, **14**: 179.
- , 1963, Metallic Emissions in the Twilight and Their Bearing on Atmospheric Dynamics, *Planet. Space Sci.*, **10**: 117-127.
- , 1966, Abundance of Metallic Atoms in the Atmosphere, *Ann. Geophys.*, **22**(2): 189-197.
- , and R. L. Gattinger, 1963, The Seasonal Variation and Excitation Mechanism of the 1.58μ $^1\Delta_g$ - $^3\Sigma_g^-$ Twilight Airglow Band, *Planet. Space Sci.*, **11**: 961-974.
- Vassy, A., 1962, L'ozone et la mésosphère—quelques problèmes actuels, *Beitr. Phys. Atmos.*, **35**: 160-164.
- , and O. Tanaevsky, 1964, Radioactivité artificielle et ozone, traceurs en météorologie dynamique, *Pure Appl. Geophys.*, **59**: 239-242.
- Vassy, E., 1963, Comparison of Ozone Variations of the Two Hemispheres, *Quart. J. Roy. Meteorol. Soc.*, **89**(379): 154-155.
- Vegard, L., and E. Tönsberg, 1940, Investigations on the Auroral Twilight Luminescence Including Temperature Measurements in the Ionosphere, *Geophys. Publ.*, **13**(1).
- Venkateswaran, S. V., J. G. Moore, and A. J. Krueger, 1961, Determination of the Vertical Distribution of Ozone by Satellite Photometry, *J. Geophys. Res.*, **66**(6): 1751-1772.

- Verzár, F., and H. D. Evans, 1959, Production of Atmospheric Condensation Nuclei by Sunrays, *Geofis. Pura Appl.*, **43**: 259-268.
- Viebrock, H. J., and E. C. Flowers, 1968, Comments on the Recent Decrease in Solar Radiation at the South Pole, *Tellus*, **20**(3): 400-411.
- Viezee, W., and J. Oblanas, 1969, Lidar-Observed Haze Layers Associated with Thermal Structure in the Lower Atmosphere, *J. Appl. Meteorol.*, **8**(3): 369-375.
- Vigroux, E., M. Migeotte, and P. Vermande, 1965, Variations saisonnières de l'ozone atmosphérique, *Ann. Géophys.*, **21**(4): 500-504.
- , M. Migeotte, and P. Vermande, 1966, Variations de l'ozone atmosphérique, *Ann. Géophys.*, **22**(1): 15-22.
- Vincent, D. G., 1968, Mean Meridional Circulations in the Northern Hemisphere Lower Stratosphere During 1964 and 1965, *Quart. J. Roy. Meteorol. Soc.*, **94**(401): 333-349.
- Vincent, R. A., 1969, Short Period Phase Height Oscillations in the E-Region, *J. Atmos. Terrest. Phys.*, **31**: 607-609.
- Vinnichenko, N. K., N. Z. Pinus, and G. N. Shur, 1965, Some Results of the Experimental Turbulence Investigations in the Troposphere, in *Proceedings of the International Colloquium on Atmospheric Turbulence and Radio Wave Propagation*, A. M. Yaglom and V. I. Tatarski (Eds.), pp. 65-75, Publishing House Nauka, Moscow, 1967.
- Vittori, O., and F. Nucciotti, 1967, Concentrazioni di SO₂ ed S totale nei bassi strati ed inversioni termiche, *Riv. Meteorol. Aeronaut.*, **27**(3): 54-61.
- , and V. Prodi, 1967, Scavenging of Atmospheric Particles by Ice Crystals, *J. Atmos. Sci.*, **24**(5): 533-538.
- , V. Prodi, G. Morgan, and G. Cesari, 1969, Natural Tracer Distribution in Hailstones, *J. Atmos. Sci.*, **26**(1): 148-152.
- Volz, F. E., 1964, Twilight Phenomena Caused by the Eruption of Agung Volcano, *Science*, **144**: 1121-1122.
- , 1965a, Note on the Global Variation of Stratospheric Turbidity Since the Eruption of Agung Volcano, *Tellus*, **17**(4): 513-515.
- , 1965b, Atmospheric Haze Layers and Brightness of the Horizon, *Tellus*, **17**(2): 166-176.
- , 1969a, Stratospheric Dust Striations, *Bull. Amer. Meteorol. Soc.*, **50**(1): 16.
- , 1969b, Neutral Points of Sky Polarization in Spring and Summer 1968, *J. Geophys. Res.*, **74**(8): 1920-1921.
- , and R. M. Goody, 1962, The Intensity of the Twilight and Upper Atmospheric Dust, *J. Atmos. Sci.*, **19**(5): 385-406.
- Wagner, C.-U., 1963, The Concentration of Negative Ions of Oxygen and Its Combinations in the Ionosphere, *Geofis. Pura Appl.*, **54**: 105-118.
- Wait, G. R., 1946, Some Experiments Relating to the Electrical Conductivity of the Lower Atmosphere, *J. Wash. Acad.*, **36**: 321-343.
- Walker, J. C. G., and N. W. Spencer, 1968, Temperatures of the Earth's Upper Atmosphere, *Science*, **162**(3861): 1437-1442.
- Wallace, J. M., and V. E. Kousky, 1968a, Long Term Variation in Wave Activity in the Tropical Stratosphere and Its Relation to Mean Zonal Wind Patterns, *Bull. Amer. Meteorol. Soc.*, **49**(8): 845.
- , and V. E. Kousky, 1968b, On the Relation Between Kelvin Waves and the Quasi-Biennial Oscillation, *J. Meteorol. Soc. Jap.*, **46**(6): 496-502.
- , and R. E. Newell, 1966, Eddy Fluxes and the Biennial Stratospheric Oscillation, *Quart. J. Roy. Meteorol. Soc.*, **92**(394): 481-489.
- Wallace, L., 1962, The OH Nightglow Emission, *J. Atmos. Sci.*, **19**(1): 1-16.
- Walshaw, C. D., 1955, Line Width in the 9.6 μ Band of Ozone, *Proc. Phys. Soc. (London), Ser. A*, **68**: 530-534.
- , 1957, Integrated Absorption by the 9.6 Band of Ozone, *Quart. J. Roy. Meteorol. Soc.*, **83**: 315-321; Selected Meteorology Paper No. 9, *Radiation*, Part 2, Meteorological Society of Japan.

- Wanta, R. C., W. B. Moreland, and H. E. Heggstad, 1961, Tropospheric Ozone: An Air Pollution Problem Arising in the Washington, D. C. Metropolitan Area, *Mon. Weather Rev.*, 89(8): 289-296.
- Warmbt, W., 1965, Ozonmessungen über der Meeresoberfläche im Nordatlantik und im Seegebiet von Westgrönland, *Z. Meteorol.*, 18(3-4): 151-156.
- , and F. Teichert, 1956, Ozonmessungen Dresden-Wahnsdorf und Fichtelberg 1954/55, *Z. Meteorol.*, 10: 264-277.
- Warner, J., 1968, A Reduction in Rainfall Associated with Smoke from Sugar-Cane Fires—An Inadvertent Weather Modification? *J. Appl. Meteorol.*, 7(2): 247-251.
- , and S. Twomey, 1967, The Production of Cloud Nuclei by Cane Fires and the Effect on Cloud Droplet Concentration, *J. Atmos. Sci.*, 24(6): 704-706.
- Wasko, P. E., and T. A. King, 1963, Earth's Aerospace Properties from 100 to 100,000 Km Altitude (Preliminary), Report MTP-AERO-63-2, National Aeronautics and Space Administration, George C. Marshall Space Flight Center.
- Watson, F. G., 1941, *Between the Planets*, The Blakiston Company.
- , 1956, *Between the Planets* (revised edition), Harvard University Press, Cambridge, Mass.
- Wayne, R. P., 1967, The Photochemical Formation of Electronically Excited Oxygen Molecules in the Atmosphere, *Quart. J. Roy. Meteorol. Soc.*, 93(395): 69-79.
- Webb, W. L., 1965, Scale of Stratospheric Detail Structure, *Space Research*, V, pp. 997-1007, North-Holland Publishing Co., Amsterdam.
- , 1966a, *Structure of the Stratosphere and Mesosphere*, International Geophysics Series, Vol. 9, Academic Press Inc., New York.
- , 1966b, Stratospheric Tidal Circulations, *Rev. Geophys.*, 4(3): 363-375.
- , 1966c, Circulation of the Middle and Upper Atmosphere, paper presented at the *Seventh International Space Science Symposium*, May 10-19, Vienna, North-Holland Publishing Co., Amsterdam.
- , 1968, Meteorological Rocket Measurements in the Mesosphere, *Meteorol. Monogr.*, 9(31): 158-169.
- , 1969, Exploration of the Stratospheric Circulation, in *Stratospheric Circulation*, W. L. Webb (Ed.), pp. 5-25, Academic Press Inc., New York.
- , J. Giraytys, H. B. Tolefson, R. C. Forsberg, R. I. Vick, O. H. Daniel, and R. L. Tucker, 1966, Meteorological Rocket Network Probing of the Stratosphere and Lower Mesosphere, *Bull. Amer. Meteorol. Soc.*, 47(10): 788-799.
- Weill, G., 1966, Quelques observations de l'émission crépusculaire des raies H et K du calcium ionisé, *Ann. Géophys.*, 22(2): 266-271.
- Weill, G. M., 1969, $\text{NI}(\text{S} - \text{D})$ Radiation in the Night Airglow and Low Latitude Aurora, in *Atmospheric Emissions*, B. M. McCormac and A. Omholt (Eds.), pp. 449-470, Van Nostrand-Reinhold Co., New York.
- Weinberg, J. L., 1967, The Zodiacal Light and the Interplanetary Medium, Report NASA-SP-150, National Aeronautics and Space Administration.
- Weinert, R. A., 1967, The Movement and Dispersion of Volcanic Dust from the Eruption of Mount Agung, Bali, 17th March 1963, *Aust. Meteorol. Mag.*, 15(4): 225-229.
- Weinstein, A. I., and E. R. Reiter, 1965, Mesoscale Structure of 11-20 Km Winds, Report CR-61080, National Aeronautics and Space Administration.
- , E. R. Reiter, and J. R. Scoggins, 1966, Mesoscale Structure of 11-20 Km Winds, *J. Appl. Meteorol.*, 5(1): 49-57.
- Weinstock, B., 1969, Carbon Monoxide: Residence Time in the Atmosphere, *Science*, 166(3902): 224-225.
- Welander, P., 1959, A Theoretical Power-Law for the Size Distribution of Small Particles or Drops Falling Through the Atmosphere, *Tellus*, 11(2): 197-201.
- Wexler, H., 1950, The Great Smoke Pall—September 24-30, 1950, *Weatherwise*, 3(6): 129-134.
- , W. B. Moreland, and W. S. Weyant, 1960, A Preliminary Report on Ozone Observations at Little America, Antarctica, *Mon. Weather Rev.*, 88(2): 43-54.

- Whipple, F. L., 1950, The Theory of Micrometeorites, I: In An Isothermal Atmosphere, *Proc. Nat. Acad. Sci.*, **36**: 687-695.
- , 1951, The Theory of Micro-Meteorites, II: In Heterothermal Atmospheres, *Proc. Nat. Acad. Sci.*, **37**: 19-30.
- , 1961a, The Particulate Contents of Space, in *Medical and Biological Aspects of the Energies of Space*, P. Campbell (Ed.), pp. 49-70, Columbia University Press, New York.
- , 1961b, The Dust Cloud About the Earth, *Nature*, **189**: 127-128.
- , 1963, On Meteoroids and Penetration, *J. Geophys. Res.*, **68**(17): 4929-4939.
- Whitehead, J. D., 1961, The Formation of Sporadic E Layer in the Temperate Zones, *J. Atmos. Terrest. Phys.*, **20**: 49-61.
- , 1962, The Formation of a Sporadic E Layer from a Vertical Gradient in Horizontal Wind, in *Ionospheric Sporadic E*, E. K. Smith and S. Matsushita (Eds.), The Macmillan Company, New York.
- Whitten, R. C., and I. G. Poppoff, 1964, Ion Kinetics in the Lower Ionosphere, *J. Atmos. Sci.*, **21**(2): 117-133.
- Wiin-Nielsen, A., 1967, On the Annual Variation and Spectral Distribution of Atmospheric Energy, *Tellus*, **19**(4): 540-559.
- Wilkins, E. M., 1961, Seasonal Variations in Atmospheric Carbon Dioxide Concentration, *J. Geophys. Res.*, **66**(4): 1314-1315.
- Willett, H. C., 1962, The Relationship of Total Atmospheric Ozone to the Sunspot Cycle, *J. Geophys. Res.*, **67**(2): 661-670.
- , 1968, Remarks on the Seasonal Changes of Temperature and of Ozone in the Arctic and the Antarctic Stratospheres, *J. Atmos. Sci.*, **25**(3): 341-360.
- , and J. Prohaska, 1965, Further Evidence of Sunspot—Ozone Relationships, *J. Atmos. Sci.*, **22**(5): 493-497.
- Williamson, E. J., and J. T. Houghton, 1965, Radiometric Measurements of Emission from Stratospheric Water Vapor, *Quart. J. Roy. Meteorol. Soc.*, **91**(389): 330-338.
- Wilson, A. T., 1959a, Organic Nitrogen in New Zealand Snows, *Nature*, **183**: 318-319.
- , 1959b, Surface of the Ocean as a Source of Airborne Nitrogenous Material and Other Plant Nutrients, *Nature*, **184**: 99-101.
- Winchester, J. W., and R. A. Duce, 1966, Coherence of Iodine and Bromine in the Atmosphere of Hawaii, Northern Alaska, and Massachusetts, *Tellus*, **18**(2-3): 287-291.
- Wisse, J. A., and A. J. Meerburg, 1969, Ozone Observations at Base King Baudouin in 1965 and 1966, *Arch. Meteorol., Geophys. Bioklimatol., Ser. A*, **18**(1-2): 41-54.
- Witt, G., 1962, Height, Structure, and Displacement of Noctilucent Clouds, *Tellus*, **14**(1): 1-18.
- , 1968, Optical Characteristics of Mesospheric Aerosol Distributions in Relation to Noctilucent Clouds, *Tellus*, **20**(1): 98-114.
- , C. L. Hemenway, N. Lange, S. Modin, and R. K. Soberman, 1964, Composition Analysis of Particles from Noctilucent Clouds, *Tellus*, **16**(1): 103-109.
- , C. L. Hemenway, and R. K. Soberman, 1963, Collection and Analysis of Particles from the Mesopause, in *Space Research*, IV, P. Muller (Ed.), pp. 197-204, North-Holland Publishing Co., Amsterdam.
- Woodrum, A., and C. G. Justus, 1968, Atmospheric Tides in the Height Region 70 to 120 Kilometers, *J. Geophys. Res.*, **73**(2): 467-478.
- Woodriddle, G., and P. F. Lester, 1969, Detailed Observations of Lee Waves and a Comparison with Theory, Atmospheric Science Paper No. 138, Colorado State University.
- , and E. R. Reiter, 1970, Large Scale Atmospheric Circulation Characteristics as Evident from GHOST Balloon Data, *J. Atmos. Sci.*, **27**(2): 183-194.
- Worth, J. J. B., L. A. Ripperton, and C. R. Berry, 1967, Ozone Variability in Mountainous Terrain, *J. Geophys. Res.*, **72**(8): 2063-2068.
- Wright, F. W., and P. W. Hodge, 1962, Space Density of Dust in the Atmosphere, *Nature*, **195**: 269.

- Wright, J. W., 1962, The Lifetime and Movement of Artificially-Produced Electron Clouds Observed with Spaced Ionosondes, Report AFCRL-62-826, pp. 87-101, Air Force Cambridge Research Laboratories.
- , 1964, Diurnal and Seasonal Variations of the Atmosphere near the 100 Kilometer Level, *J. Geophys. Res.*, **69**(13): 2851-2853.
- , 1967, Sporadic E as an Indicator of Wind Structure in the Lower Ionosphere and the Influx of Meteors, *J. Geophys. Res.*, **72**(19): 4821-4829.
- , 1968, The Interpretation of Ionospheric Radio Drift Measurements—I. Some Results of Experimental Comparisons with Neutral Wind Profiles, *J. Atmos. Terrest. Phys.*, **30**(5): 919-930.
- , C. H. Murphy, and G. V. Bull, 1967, Sporadic E and the Wind Structure of the E-Region, *J. Geophys. Res.*, **72**(5): 1443-1460.
- Wright, P. B., 1969, Effects of Wind and Precipitation on the Spread of Foot-and-Mouth Disease, *Weather*, **24**(6): 204-213.
- Yaalon, D. H., 1964, The Concentration of Ammonia and Nitrate in Rain Water over Israel in Relation to Environmental Factors, *Tellus*, **16**(2): 200-204.
- Yaglom, A. M., and V. I. Tatarski, 1967, Atmospheric Turbulence and Radio Wave Propagation, in *Proceedings of the International Colloquium, Moscow, June 15-22*, Publishing House Nauka, Moscow.
- Yamamoto, G., and M. Tanaka, 1969, Determination of Aerosol Size Distribution from Spectral Attenuation Measurements, *Appl. Opt.*, **8**(2): 447-453.
- , M. Tanaka, and K. Arao, 1968, Hemispherical Distribution of Turbidity Coefficients as Estimated from Direct Solar Radiation Measurement, *J. Meteorol. Soc. Jap.*, Ser. II, **46**(4): 287-300.
- Yanai, M., and Y. Hayashi, 1969, Large-Scale Equatorial Waves Penetrating from the Upper Troposphere into the Lower Stratosphere, *J. Meteorol. Soc. Jap.*, **47**(3): 167-182.
- , and T. Maruyama, 1966, Stratospheric Wave Disturbances Propagating over the Equatorial Pacific, *J. Meteorol. Soc. Jap.*, **44**(5): 291-294.
- , T. Maruyama, T. Nitta, and Y. Hayashi, 1968, Power Spectra of Large-Scale Disturbances over the Tropical Pacific, *J. Meteorol. Soc. Jap.*, **46**(4): 308-323.
- Yano, K., 1967, A Long-Term Aspect of the Seasonal Variation in the Nightglow 5577 Intensity at Middle Latitudes, *Planet. Space Sci.*, **15**: 1091-1093.
- Yerg, D. G., 1951, Ionospheric Wind Systems and Electron Concentrations of the F Layer, *J. Meteorol.*, **8**(4): 244-250.
- Young, Ch., and E. S. Epstein, 1962, Atomic Oxygen in the Polar Winter Mesosphere, *J. Atmos. Sci.*, **19**(6): 435-443.
- Zahn, U. von, 1967, Mass Spectrometric Measurements of Atomic Oxygen in the Upper Atmosphere: A Critical Review, *J. Geophys. Res.*, **72**(23): 5933-5937.
- Zak, J. A., and H. A. Panofsky, 1968, Estimation of Stratospheric Flow from Satellite 15-Micron Radiation, *J. Appl. Meteorol.*, **7**(1): 136-140.
- Zander, R., and M. Bottema, 1967, Water Vapor in the Stratosphere, *J. Geophys. Res.*, **72**(22): 5749-5751.
- Zenker, H., 1954, Waldeinfluss auf Kondensationskerne und Lufthygiene, *Z. Meteorol.*, **8**: 150-159.
- Zerche, M., and W. Hänsch, 1967, Ergebnisse über die Bestimmung des Chloridgehaltes im Niederschlagswasser in Schwerin/Meckl. *Z. Meteorol.*, **19**: 97-101.
- Zimmerman, S. P., 1964, Small-Scale Wind Structure Above 100 Km, Environmental Research Paper No. 15, Report AFCRL-64-364, pp. 375-378, Air Force Cambridge Research Laboratories.
- , K. S. W. Champion, and N. W. Rosenberg, 1962, Molecular and Turbulent Diffusion in the Upper Atmosphere, Report AFCRL-62-826, pp. 45-55, Air Force Cambridge Research Laboratories.

- , and F. A. Marcos, 1967, Measurements of Tidal Oscillations Above 120 Kilometers, Environmental Research Paper No. 266, Report AFCRL-67-0131, Air Force Cambridge Research Laboratories.
- Zipf, E. C., and W. G. Fastie, 1963, Symposium on Airborne Eclipse Observations, Douglas Aircraft Company, Santa Monica, Calif.

AUTHOR INDEX

- Abarbanel, S., 344
Abel, N., 284, 297
Aharonian, C., 315
Ahlquist, N. C., 338
Ahmed, S. J., 156, 157, 297
Ahrens, C. D., 116, 132, 332
Air Conservation Commission, 283, 297
Akasofu, S.-I., 156, 297
Albee, P. R., 261, 297
Albritton, D. L., 243, 297, 310
Aldaz, L., 113, 147, 148, 151, 297, 340
Alden, H. L., 315
Alexander, J., 191, 336
Alexander, W. M., 272, 273, 274, 276, 297, 326
Al-Gain, A. A., 14, 17, 18, 19, 20, 23, 323
Allen, C. W., 271, 272, 297
Allen, E. F., Jr., 244, 342
Allison, L. J., 314
Altshuller, A. P., 218, 297
American Meteorological Society, 232, 297
Anctil, R. E., 266, 268, 330
Anderson, A. D., 31, 298
Angell, J. K., 159, 162, 227, 229, 285, 286, 298, 308, 318, 346
Anonymous 1958, 96, 298
Anonymous 1959, 96, 298
Anonymous 1960, 96, 298
Anonymous 1966, 218, 298
Anonymous 1969, 204, 275, 276, 298
Appleman, H. S., 261, 298
Arao, K., 287, 353
Armendariz, M., 47, 298
Armstrong, E. B., 245, 298
Arnold, R., 301
Arsdel, E. P. van, 278, 298
Aschenbrand, L. M., 338
Astapenko, P. D., 210, 298
Atlas, D., 69, 298
Attmannspacher, W., 214, 215, 298, 311
Authier, B., 244, 298
Avery, C. P., 318
Axford, W. I., 254, 256
Axworthy, A. E., 59, 300
Aymer, A. L., 320
Azcarraga, A., 25, 298
Bailey, A. D., 61, 264, 266, 268, 334
Bainbridge, A. E., 189, 298
Bair, E. J., 59, 312
Baker, D. J., 170, 172, 182, 298, 299
Ball, R. J., 284, 299
Ballard, N., 144, 299
Ballif, J. R., 58, 299
Bandeem, W. R., 65, 67, 73, 339, 347
Bandermann, L. W., 273, 299
Bangerl, A., 193, 194, 299
Bannon, J. K., 65, 75, 299
Barad, M. L., 313
Barat, J., 245, 247, 299, 301
Barbier, D., 173, 175, 179, 235, 236, 299

- Barclay, F. R., 75, 299
 Barnes, A. A., Jr., 140, 269, 299
 Barnes, R. A., 315
 Barrett, E. W., 77, 78, 269, 299
 Bartel, A. W., 115, 299
 Barth, Ch. A., 114, 222, 299
 Bartman, F. L., 347
 Bary, E. de, 205, 269, 299
 Batchelor, G. K., 19, 300
 Bates, D. R., 58, 59, 182, 228, 300
 Batey, P. H., 114, 300
 Battan, L. J., 280, 300
 Batten, E. S., 261, 300
 Baudin, G., 329
 Baus, R. A., 328
 Bean, B. R., 69, 300
 Beard, D. B., 271, 272, 273, 300
 Beaudoine, P. E., 244, 300
 Bedinger, J. F., 247, 254, 300, 330
 Begemann, F., 189, 190, 191, 300
 Beilke, S., 192, 300
 Belmont, A. D., 95, 228, 300, 344
 Belrose, J. S., 225, 300
 Ben-Dov, O., 269, 299
 Benson, S. W., 59, 300
 Berenger, M., 277, 300
 Berg, O. E., 297
 Berger, R., 96, 300
 Berggren, R., 113, 129, 130, 135, 136, 137, 300
 Berkshire, D. C., 96, 320
 Berry, C. R., 352
 Berson, F. A., 162, 300
 Best, G. T., 170, 316
 Bettie, J. F., 299
 Beyers, N. J., 35, 39, 40, 41, 300, 301
 Beynon, W. J. G., 243, 344
 Bhandari, N., 274, 301
 Biermann, L., 271, 301
 Bigg, E. K., 196, 199, 200, 280, 281, 282, 301, 309
 Billard, F., 303
 Billions, N., 47, 311
 Bird, I., 280, 301
 Bischof, W., 96, 97, 98, 99, 102, 301
 Bishop, J. M., 320
 Bishop, K. F., 189, 190, 191, 301
 Black, R. W., 328
 Blackwell, D. E., 271, 272, 301
 Blamont, J. E., 238, 239, 240, 241, 245, 246, 247, 299, 301
 Blanco, A. J., 283, 320
 Blankenship, J. R., 114, 118, 301
 Bleck, R., 304
 Blifford, I. H., Jr., 269, 301, 304, 328
 Blumen, W., 32, 301
 Boer, G. J., Jr., 44, 48, 301, 329
 Bojkov, R. D., 114, 121, 122, 139, 140, 144, 148, 149, 151, 302
 Bolin, B., 95, 97, 102, 104, 105, 106, 107, 109, 110, 111, 112, 120, 231, 301, 302
 Bolle, H. J., 84, 302
 Bollen, W. B., 348
 Bonatti, E., 278, 338
 Borden, T. R., Jr., 120, 121, 125, 130, 318
 Bossolasco, M., 225, 230, 302
 Bosua, T. A., 209, 302
 Bottema, M., 78, 353
 Boville, B. W., 34, 142, 143, 302
 Bowen, E. G., 270, 302
 Bowman, G. G., 49, 302
 Brabets, R. I., 113, 302
 Brandli, H. W., 146, 335
 Branscomb, L. M., 114, 327
 Bray, J. R., 96, 97, 102, 303
 Breiland, J. G., 130, 132, 133, 136, 303
 Breitling, W. L., 261, 303
 Brennan, E., 115, 327
 Brewer, A. W., 74, 75, 114, 118, 120, 141, 143, 303, 308, 330
 Bricard, J., 282, 303
 Brier, G. W., 280, 303
 Briggs, J., 129, 303
 Broadfoot, A. L., 168, 266, 267, 303
 Brocas, J., 275, 303
 Brock, J. R., 205, 319
 Brousaides, F. J., 78, 303
 Brown, C. W., 97, 102, 104, 303
 Brown, F., 76, 303
 Brown, J. L., 297
 Bryson, R. A., 207, 209, 285, 303, 337
 Buch, H. S., 7, 304
 Buch, K., 313
 Buell, C. E., 11, 304
 Buettner, K. J. K., 100, 117, 304, 348
 Bull, C., 275, 317
 Bull, G. A., 277, 304
 Bull, G. V., 254, 262, 263, 334, 353
 Bullock, W. R., 238, 239, 304
 Bullock, W. S., 18, 20, 323
 Bullrich, K., 269, 299
 Bureau of Census, 116, 304
 Burger, F. G., 304
 Burkard, O., 224, 304

- Burnett, G. B., 346
 Burns, A., 15, 340
 Burns, F., 309
 Burov, M. I., 89, 304
 Businger, J., 304
 Byron-Scott, R., 120, 304
 Cadle, R. D., 114, 189, 199, 211, 212,
 214, 270, 275, 304, 312
 Cahoon, B. A., 300
 Calfee, R. F., 82, 304
 Callendar, G. S., 96, 304
 Camp, D. W., 312
 Campbell, A. B., 195, 310
 Campbell, E. S., 59, 304
 Canales, F. C., 138, 304
 Carignan, G. R., 346
 Carleton, N. P., 274, 304
 Carnuth, W., 284, 287, 304, 341
 Carter, H. J., 299
 Carver, J. H., 144, 304
 Caton, W. M., 113, 143, 305
 Cattani, D., 156, 338
 Cauer, H., 230, 305
 Cesari, G., 350
 Chagnon, C. W., 195, 196, 197, 203, 305,
 317, 322
 Chalupa, K., 193, 284, 347
 Chamberlain, J. W., 114, 170, 233, 236,
 238, 305
 Champion, K. S. W., 31, 61, 62, 247, 255,
 305, 332, 353
 Chandra, C., 42, 305
 Changnon, S. A., Jr., 284, 305
 Chapman, G. E., 176, 224, 243, 305
 Chapman, S., 42, 91, 92, 93, 156, 214,
 236, 297, 305
 Charlson, R. J., 285, 304, 305, 338
 Charney, J. G., 49, 305
 Chen, C. S., 348
 Chimonas, G., 254, 256, 305
 Chrest, S. A., 346
 Christie, A. D., 89, 92, 122, 302, 305
 Christophe-Glaume, J., 173, 174, 175,
 305
 Cicconi, G., 230, 302
 Cittanova, J., 329
 Clark, J., 144, 305
 Clark, J. H., 120, 306
 Clark, W. E., 205, 269, 305
 Clarke, J. F., 99, 306
 Clemesha, B. R., 337
 Clifton, S., 273, 306
 Clyne, M. A. A., 59, 306
 Cohen, L. A., 339
 Cole, A. E., 25, 26, 27, 31, 32, 33, 44, 52,
 306
 Collis, R. T. H., 195, 306
 Colombo, G., 271, 273, 274, 312
 Cook, G. E., 32, 34, 306
 Cooksey, M. M., 310
 COSPAR Working Group IV, 61, 306
 Cote, O. R., 24, 243, 306
 Cotten, G. F., 162, 298
 Court, G. R., 300
 Cox, L. C., 315
 Craig, H., 106, 306
 Craig, R. A., 114, 120, 139, 223, 306
 Cresswell, G., 301
 Crisi, A. R., 347
 Crozier, W. D., 273, 274, 306
 Crutzen, P. J., 58, 114, 118, 301, 306
 Csanady, G. T., 285, 306
 Cumme, G., 224, 307
 Curtis, A. R., 144, 307
 Cwilong, B. M., 308
 Czeplak, G., 109, 111, 112, 163, 164,
 165, 322
 Dachs, J., 175, 307
 D'Aiutolo, C. T., 273, 307
 Daniel, O. H., 49, 351
 Danielsen, E. F., 20, 23, 44, 55, 65, 129,
 130, 135, 201, 278, 290, 307
 Dartt, D. G., 300
 Dave, J. V., 114, 197, 307
 Davidson, B., 217, 344
 Davis, D. R., 115, 148, 307
 Davis, T. N., 173, 178, 234, 236, 238, 307
 Day, J. A., 282, 307
 Dean, C. E., 115, 148, 307
 DeBary, E., 229, 230, 307
 Defant, A., 9, 11, 307
 Defant, F., 9, 307
 Deirmendjian, D., 271, 307
 Delafield, H. J., 301, 315
 Deland, R. J., 34, 307
 Delany, A. C., 278, 307
 DeLuisi, J. J., 114, 306, 307
 DeMandel, R. E., 47, 308
 Deshpande, M. R., 262, 308
 Dickinson, R. E., 39, 43, 222, 223, 224,
 225, 228, 243, 308, 314, 335
 Dickson, C. R., 285, 298, 308
 Dieminger, W., 224, 225, 308
 Dieter, W., 312
 Dietze, G., 90, 195, 205, 256, 284, 308
 Dilleuth, F. J., 85, 189, 308

- Dinger, J. E., 76, 78, 331
 Dingle, A. N., 278, 288, 308, 314
 Dittmann, E., 72, 308
 Dobson, G. M. B., 75, 117, 136, 150, 154,
 156, 157, 225, 226, 308
 Doherty, R. H., 144, 224, 308
 Dole, S. H., 265, 308
 Donahue, T. M., 233, 235, 236, 238, 239,
 240, 241, 243, 259, 301, 308, 309
 Donaldson, J. S., 240, 317
 Douppnik, J. R., 180, 309
 Drazin, P. G., 49, 305
 Drevinsky, P. T., 163, 330
 Drexhage, K. A., 310
 Droessler, E. G., 280, 285, 309
 Drozdov, O. A., 11, 13, 72, 309
 Druyan, L. M., 285, 309
 Dubin, M., 274, 309, 345
 Duce, R. A., 231, 232, 309, 328, 344, 352
 Dufay, M., 117, 309
 Duffy, D., 344
 Duquet, R. T., 44, 55, 307
 Durbin, W. G., 230, 309, 345
 Dütsch, H. U., 58, 113, 114, 115, 118, 119,
 120, 123, 130, 136, 138, 139, 143, 144,
 145, 146, 156, 309, 331
 Dycus, R. D., 270, 310
 Dyer, A. J., 196, 197, 199, 209, 310
 Eady, E. T., 5, 7, 310
 Eddy, J. A., 78, 199, 201, 202, 205, 273,
 276, 310, 335
 Edwards, C. P., 327
 Edwards, H. D., 39, 244, 247, 250, 254,
 255, 256, 257, 297, 310, 332, 334, 342
 Edwards, H. E., 254, 323
 Effenberger, E., 96, 102, 310
 Eggleton, A. E., 301
 Elena, A., 225, 302
 Eliassen, E., 34, 310
 Elliott, D. D., 122, 145, 339
 Elliott, M. J. W., 299
 Elsässer, H., 271, 272, 310, 343
 Elsley, E. M., 277, 310
 Elterman, L., 195, 310
 Endlich, R. M., 48, 310
 Engberg, L. W., 300
 Engler, N., 245, 310
 Entzian, G., 224, 225, 226, 327
 Environmental Science Services
 Administration, 25, 31, 44, 45, 61, 90,
 214, 240, 310
 Epstein, E. S., 168, 169, 353
 Erickson, J. E., 270, 275, 310
 Eriksson, E., 96, 97, 106, 192, 195, 230,
 233, 302, 310
 Ertel, H., 230, 310
 Essenwanger, O., 47, 215, 216, 311, 347
 Essex, E. A., 172, 247, 311
 Estes, H. D., 113, 322
 Evans, H. D., 284, 350
 Evans, W. F. J., 168, 311
 Fabian, P., 147, 311
 Facy, L., 286, 311
 Farkas, E., 157, 311
 Farley, D. T., 39, 311
 Fastie, W. G., 168, 176, 332, 354
 Faust, H., 25, 173, 214, 215, 218, 311
 Fechtig, H., 273, 311
 Feely, H. W., 217, 313, 344
 Fehsenfeld, F. C., 114, 311, 312
 Fenimore, C. P., 59, 312
 Fenn, R. W., 192, 312
 Ferber, G. J., 328
 Ferguson, A. F., 182, 312
 Ferguson, E. E., 224, 311, 312
 Fichtl, G. H., 48, 312
 Fielder, R., 284, 312
 Finger, F. G., 31, 34, 35, 290, 312, 318, 332
 Fiocco, G., 91, 195, 196, 198, 200, 201,
 207, 208, 212, 255, 269, 271, 273, 275,
 312, 316
 Fischer, W. H., 210, 304, 312
 Fitzsimmons, R. V., 59, 312
 Fletcher, N. H., 282, 312
 Flohn, H., 200, 312
 Flowers, E. C., 209, 210, 211, 212, 287,
 312, 313, 350
 Fogle, B., 89, 90, 313
 Foner, S. N., 59, 313
 Fonselius, S., 96, 190, 313
 Fooks, G. F., 245, 246, 247, 248, 313
 Föppl, H., 244, 313
 Forsberg, R. C., 49, 351
 Fowler, R. J., 224, 324
 Francis, W., 31, 298
 Frank, E. R., 304
 Fraser, G. J., 227, 262, 313
 Fredriksson, K., 274, 337
 Friedlander, S. K., 205, 269, 313, 336
 Friedman, I., 189, 190, 298, 300
 Friedman, R. M., 339
 Friend, J. P., 7, 211, 217, 313, 344
 Frith, R., 299
 Fritz, S., 157, 313
 Fukushima, M., 69, 70, 313
 Fullam, E. F., 91, 318

- Fuller, R. N., 310
Funk, J. P., 159, 313
Fuquay, J. J., 285, 313
Gaalswyk, A., 332
Gadsden, M., 239, 264, 265, 266, 313
Gaigerov, S. S., 25, 314
Galbally, I., 147, 314
Gambell, A. W., Jr., 287, 314
Garnham, G. L., 159, 313
Garriott, O. K., 58, 179, 180, 223, 254, 341
Gast, J. A., 232, 314
Gates, D. M., 82, 304
Gattinger, R. L., 168, 314, 349
Gatz, D. F., 278, 288, 308, 314
Gault, W. A., 265
Gebhart, R., 29, 120, 145, 314
Gee, J. H., 22, 314
Geisler, J. E., 43, 222, 223, 224, 225, 243, 308, 314
General Electric Company, 113, 314
Georges, T. M., 52, 314
Georgi, J., 285, 314
Georgii, H.-W., 191, 192, 218, 220, 222, 230, 280, 300, 314
Gerber, H. E., 312
Gerloff, U., 311
German, K. E., 3, 4, 5, 6, 7, 9, 11, 12, 17, 74, 87, 162, 340
Ghosh, S. N., 223, 264, 314
Giese, R. H., 271, 272, 314
Gille, J. C., 95, 314
Giraytys, J., 49, 351
Giutronich, J., 280, 301
Glasser, M. E., 205, 340
Godshall, F. A., 162, 314
Godson, W. L., 115, 138, 140, 141, 144, 214, 241, 242, 243, 315, 321, 331
Goetz, A., 218, 315
Gokhale, N. R., 270, 315
Goldan, P. D., 311
Goldberg, E. D., 307
Goldberg, L. J., 285, 315
Goldsmith, P., 78, 86, 286, 299, 303, 315, 334
Golomb, D., 169, 170, 244, 245, 247, 300, 315, 328, 342
Good, R. E., 170, 315
Goodman, P., 319
Goodwin, G. L., 49, 53, 262, 315
Goody, R. M., 157, 168, 197, 200, 207, 270, 274, 328, 334, 350
Goold, J., Jr., 270, 315
Gordon, C. M., 232, 315
Gordon, W. E., 39, 315
Gossard, E. E., 49, 315
Götz, F. W. P., 157, 315
Goyer, G. G., 195, 315
Grams, G., 91, 195, 196, 198, 200, 201, 207, 208, 212, 312, 316
Grant, W. B., 348
Grantham, D. D., 82, 83, 84, 86, 316, 345
Grasnick, K.-H., 161, 316
Green, A. E. S., 61, 316
Green, H. F., 303
Green, H. L., 190, 283, 316
Green, J. L., 311
Green, J. S. A., 35, 316
Greenfield, S. M., 278, 316
Greenhow, J. S., 39, 48, 171, 173, 179, 316
Greer, R. G. H., 170, 316
Gregory, J. B., 44, 225, 316
Griffin, J. J., 307
Griggs, M., 136, 316
Grigor'eva, A. S., 11, 13, 72, 309
Grigorevskii, V. M., 156, 316
Gringorten, I. I., 86, 316
Grinnell, S. W., 327
Groves, G. V., 244, 250, 254, 316
Gruner, P., 197, 316
Gulyi, V. A., 341
Gunn, R., 283, 316
Gupta, P. K. S., 136, 316
Gussman, R. A., 285, 286, 316
Gutnick, M., 76, 77, 81, 83, 86, 91, 316, 317
Haagen-Smit, A. J., 115, 317
Haarländer, H., 277, 317
Hacrendel, G., 245, 313, 317
Hage, K. D., 285, 317
Haines, A., 189, 190, 191, 317
Halim, A., 156, 157, 297
Hall, J. E., 39, 316
Hall, L. A., 61, 317
Hamilton, W. L., 275, 317
Hampson, J., 58, 317
Handa, B. K., 287, 317
Hänel, G., 269, 317
Hann, J., 95, 96, 317
Hanna, S. R., 278, 317
Hänsch, W., 230, 283, 343, 344, 353
Hansen, J., 314
Hanson, W. B., 240, 317
Hanya, T., 230, 317
Harang, O., 244, 245, 317

- Hare, F. K., 142, 143, 302
 Harlow, B. W., 320
 Harnischmacher, E., 262, 317
 Harris, B., 209, 317
 Harris, I., 32, 34, 39, 42, 43, 44, 317
 Harris, M. F., 34, 312, 318
 Harris, T. B., 103, 324
 Harrison, D. N., 75, 308
 Harteck, P., 59, 340
 Haser, L., 313
 H.A.S.P., 234, 318
 Hass, W. A., 285, 298, 318
 Hastenrath, S. L., 278, 318
 Haurwitz, B., 27, 35, 89, 179, 318
 Haurwitz, M. W., 156, 157, 328
 Hayashi, Y., 157, 353
 Hayes, J. V., 339
 Hayes, P. B., 228, 300
 Hedin, A. E., 61, 62, 318
 Heffernan, K. J., 280, 309
 Heggstad, H. E., 351
 Helliwell, N. C., 75, 318
 Hemenway, C. L., 91, 92, 271, 273, 276,
 318, 328, 346, 352
 Hendl, R. G., 32, 301
 Henning, D., 200, 312
 Hering, W. S., 120, 121, 125, 130, 143, 318
 Herman, B. M., 114, 318
 Hernandez, G. J., 171, 173, 175, 318
 Herndon, L. R., 299
 Hesstvedt, E., 58, 59, 60, 61, 77, 86, 87,
 88, 89, 91, 114, 162, 182, 224, 319
 Heuvel, A. P van den, 193, 319
 Hibberd, F. H., 172, 247, 311
 Hibbs, A. R., 273, 319
 Hicks, B., 196, 197, 199, 209, 310
 Hidy, G. M., 205, 319
 Hill, J. A. F., 315
 Hill, W. R., 23
 Hilsenrath, E., 144, 319
 Hines, C. O., 48, 49, 52, 53, 54, 92, 173,
 247, 249, 250, 254, 261, 319, 320
 Hinteregger, H. E., 61, 317, 320
 Hitschfeld, W., 143, 144, 305, 320
 Hobbs, P. V., 277, 286, 320, 338
 Hodge, P. W., 274, 275, 320, 352
 Hoebbel, W., 161, 316
 Hoecker, W. H., 298, 318
 Hoffman, J. H., 336
 Hoffmann, W. F., 95, 113, 143, 320
 Hogan, A. W., 280, 320
 Hoidale, G. B., 283, 320
 Hollings, W. B. H., 334
 Holmes, J. C., 336
 Holt, A., 303
 Holton, J. R., 157, 320
 Hooke, W. H., 49, 320
 Hoover, T. E., 96, 320
 Hoppe, W., 284, 320
 Hopwood, J. M., 158, 320
 Horiuchi, G., 224, 320
 Horton, B. H., 304
 Horvath, H., 269, 320
 Horvath, J. J., 25, 348
 Höschele, K., 193, 320
 Houghton, D. D., 52, 320
 Houghton, J. T., 27, 73, 74, 78, 97, 143,
 320, 321, 352
 Hovland, D. N., 300
 Hudson, R. L., 59, 313
 Hulst, H. C. van de, 271, 272, 273, 276,
 321
 Humble, J., 301
 Humi, M., 92, 270, 344
 Hunt, B. G., 58, 59, 114, 120, 122, 144,
 321
 Hunten, D. M., 114, 168, 223, 234, 235,
 236, 238, 239, 241, 242, 243, 264,
 265, 266, 268, 304, 311, 321, 347
 Huppi, E. R., 183, 321
 Ingham, M. F., 271, 272, 301
 Iozenas, V. A., 114, 123, 321
 Istomin, V. G., 39, 264, 266, 268, 321
 Izquierdo, M., 299
 Jacchia, L. G., 32, 156, 173, 321
 Jacobs, M. B., 193, 321
 Jacobs, W. C., 231, 282, 321
 Jaenicke, R., 269, 321
 Jaffe, L. S., 113, 322
 Jager, C. de, 246, 273, 301, 322
 Jami, K. G., 325
 Jansson, U. B., 224, 319
 Jarrett, A. H., 243, 254, 322
 Jelley, J. V., 299
 Jenne, R. L., 31, 32, 329
 Jesse, O., 89, 322
 Johnson, C. Y., 336
 Johnson, F. S., 61, 322
 Johnson, L. W., 331
 Johnson, N. M., 230, 322
 Jones, C. W., 59, 312
 Jones, L. M., 44, 322
 Jones, W. L., 52, 320, 322
 Joseph, J., 90, 322
 Jost, D., 191, 192, 220, 222, 314

- Juang, F. H. T., 230, 322
 Junge, C. E., 76, 96, 104, 109, 111, 112, 113, 145, 147, 148, 163, 164, 165, 185, 188, 189, 190, 191, 192, 195, 196, 197, 201, 203, 205, 218, 229, 230, 231, 233, 234, 266, 268, 269, 282, 283, 286, 287, 297, 305, 307, 311, 321, 322, 344
 Jurica, G. M., 73, 323
 Jurkevich, I., 113, 323
 Jursa, A. S., 61, 323, 338
 Justus, C. G., 39, 55, 254, 258, 323, 332, 352
 Kahalas, S. L., 261, 334
 Kanellakos, D. P., 261, 297, 323
 Kantor, A. J., 25, 31, 44, 52, 84, 306, 316, 323
 Kanwisher, J., 95, 97, 106, 109, 323
 Kao, S.-K., 14, 15, 17, 18, 19, 20, 23, 48, 323
 Kaplan, L. D., 97, 323
 Kapoor, R. K., 280, 282, 323, 338
 Kasten, F., 199, 202, 323
 Katchen, L. B., 336, 346, 348
 Kato, S., 254, 323
 Katsriku, I. K., 262, 325
 Kaufman, F., 59, 324
 Kays, M. D., 39, 245, 261, 324, 333
 Keeling, C. D., 96, 97, 99, 100, 102, 103, 104, 105, 106, 107, 108, 109, 110, 111, 112, 302, 303, 324, 336
 Kelley, J. J., Jr., 96, 99, 100, 113, 116, 324
 Kellogg, W. W., 27, 31, 168, 169, 324
 Kendall, K. R., 168, 303
 Kendall, P. C., 91, 92, 93, 214, 305
 Keneshea, T. J., 58, 114, 180, 223, 224, 324
 Kennedy, J. S., 95, 324
 Kent, G. S., 262, 324, 337
 Kerley, M. J., 318
 Kerrigan, T. C., 283, 342
 Khemani, L. T., 286, 324
 Kidson, J. W., 162, 335
 King, G. A. M., 179, 180, 181, 224, 325
 King, P., 328
 King, T. A., 44, 351
 King-Hele, D. G., 173, 325
 Kinisky, J. J., 138, 325
 Kirkpatrick, A. W., 348
 Kiseleva, M. S., 335
 Kitagawa, T., 270, 330
 Kitaoka, T., 75, 76, 77, 78, 81, 84, 325
 Kleinschmidt, E., Jr., 65, 325
 Klepper, J. C., 320
 Kline, D. B., 280, 303, 325
 Knaflich, H., 330
 Knudsen, W. C., 180, 325
 Knuth, R., 307
 Koch, W. L., 113, 325
 Kochanski, A., 247, 248, 251, 252, 253, 261, 262, 264, 265, 325
 Kohl, G., 256, 308
 Kojima, H., 284, 344
 Kolmogorov, A. N., 247, 325
 Komhyr, W. D., 138, 325, 348
 Koprova, L. I., 195, 325
 Kornblum, J. J., 199, 270, 271, 325
 Koroleff, F., 313
 Korshover, J., 159, 162, 227, 229, 298
 Koshelkov, Yu. P., 314
 Koster, J. R., 262, 325
 Kusters, J. J., 201, 325
 Kotadia, K. M., 261, 325
 Kousky, V. E., 52, 157, 161, 228, 350
 Koyama, T., 188, 189, 325
 Krasnopol'skiy, V. A., 321
 Krassovsky, V. I., 173, 182, 325, 326
 Kretschmer, C. B., 59, 337
 Kreutz, W., 96, 326
 Krey, P. W., 313
 Kroening, J. L., 117, 201, 204, 212, 326, 335
 Krueger, A. J., 182, 326, 349
 Kuhn, P. M., 205, 348
 Kuhn, W. R., 97, 326
 Kulkarni, P. V., 170, 179, 326
 Kulkarni, R. N., 114, 138, 142, 148, 150, 154, 158, 162, 300, 326
 Kumykov, Kh. K., 341
 Kupferman, R. A., 261, 303
 Kurfis, K. R., 284, 313, 331
 Kuznetsov, A. P., 321
 Kvifte, G. J., 183, 264, 326
 Kyle, T. G., 85, 189, 201, 325, 326, 333
 Labitzke, K., 27, 113, 129, 135, 136, 137, 300, 326
 Laboratory of Astrophysics and Physical Meteorology, 75, 326
 LaChapelle, E., 99, 100, 324
 Laevatsu, T., 274, 326
 Lagos, C. P., 43, 171, 308, 326
 LaGow, H. E., 274, 326
 Lalley, V. E., 286, 326, 327
 Lamb, D., 344
 Lane, W. R., 190, 283, 316

- Lange, N., 352
 Langer, G., 232, 327, 334
 Langway, C. C., Jr., 320
 Lapple, C. E., 341
 Larkin, F. S., 59, 327
 Larson, R. E., 232, 315
 Lauter, E. A., 224, 225, 226, 227, 228,
 229, 327
 Lawrence, J., 75, 308
 Lazrus, A. L., 304
 Lea, D. A., 116, 117, 327
 Lebedinskiy, A. I., 321
 Lehmann, H. R., 256, 327
 Leighton, P. A., 115, 285, 327
 Leistner, W., 155, 327
 LeLevier, R. E., 114, 327
 Lena, P. J., 310
 Lenhard, R. W., Jr., 39, 327, 335
 Leone, I. A., 115, 327
 Leovy, C., 89, 92, 114, 120, 121, 122,
 144, 327
 Leslie, F. E., 333
 Lester, P. F., 47, 285, 341, 352
 Lettau, H. H., 278, 327
 Libby, W. F., 96, 300
 Lichfield, E. W., 286, 327
 Lieth, H., 97, 327
 Ligda, M. G. H., 195, 306
 Lindzen, R. S., 35, 36, 37, 38, 39, 40,
 41, 49, 55, 56, 157, 161, 254, 320, 328
 Lininger, R. L., 232, 328
 Linscott, I., 91, 328
 List, R. J., 231, 328
 Llewellyn, E. J., 311
 Lloyd, K. H., 244, 245, 328, 344
 Löbner, A., 283, 328
 Locatelli, J. D., 277, 320
 Lockhart, L. B., 163, 328
 Lodge, J. P., Jr., 191, 304, 312, 328
 Logan, S. E., 278, 328
 Loidl, J., 313
 Loisel, C. J., 3, 128, 138, 332
 Lomax, J. B., 52, 328
 London, J., 97, 123, 127, 138, 144,
 156, 157, 158, 162, 163, 326, 328
 Long, M. J., 84, 329
 Loon, H. van, 31, 32, 329
 Lorius, C., 211, 329
 Lory-Chanin, M.-L., 243, 329
 Lovell, A. C. B., 171, 173, 179, 316
 Lovill, J. E., 132, 134, 329
 Lu, K. C., 348
 Lucca, L. D., 334
 Ludwick, J. D., 285, 329
 Ludwig, F. L., 322
 Ludwig, J. H., 285, 331
 Lupo, G., 320
 Lüst, R., 313, 317, 329
 Lütjens, P., 313
 Mabee, R. S., 315
 MacDonald, A. J., Jr., 328
 Machenhaur, B., 34, 310
 Mackenzie, J. K., 318
 MacLeod, J. A., 341
 MacLeod, M. A., 244, 245, 247, 254,
 256, 259, 315, 329
 MacQueen, R. M., 200, 310, 329
 Madelaine, G., 303
 Maeda, H., 180, 254, 329
 Maeda, K., 27, 254, 329
 Machlum, B., 224, 329
 Mahlman, J. D., 3, 66, 67, 68, 70, 71,
 130, 138, 147, 205, 231, 243, 329,
 340, 341
 Mahoney, J. R., 39, 44, 48, 52, 233, 234,
 237, 243, 301, 329, 335
 Makhon'ko, K. P., 286, 329
 Makogonenko, A. G., 335
 Manabe, S., 73, 74, 97, 98, 120, 143, 291,
 321, 330
 Mancuso, R. L., 310
 Manella, G., 59, 340
 Manning, J. J., 346
 Manring, E. J., 243, 244, 245, 246,
 247, 330
 Manson, J. E., 197, 322
 Marcos, F. A., 254, 305, 354
 Mariani, F., 180, 330
 Markham, T. P., 266, 268, 330
 Marmo, F. F., 338
 Marov, M. Ya., 173, 321, 330
 Marshall, J. C., 244, 330
 Martell, E. A., 85, 86, 163, 189, 330
 Martin, C. D., 270, 310
 Martin, D. W., 118, 141, 330
 Maruyama, H., 270, 330
 Maruyama, T., 157, 330, 353
 Mason, B. J., 193, 282, 319, 330
 Mason, R. B., 312
 Mastenbrook, H. J., 73, 76, 78, 79, 80, 81,
 82, 84, 85, 86, 87, 91, 330, 331
 Mateer, C. L., 114, 140, 145, 197, 214,
 307, 325, 331, 348
 Matson, W. R., 328

AUTHOR INDEX

- Matsuno, T., 157, 328
Matsushima, S., 273, 331
Matsushita, S., 182, 254, 259, 261,
323, 331, 339, 345
Matuura, N., 262, 331
May, H. T., 130, 303
McCaldin, R. O., 269, 331
McClure, J. P., 311
McCormac, B. M., 167, 331
McCormick, R. A., 185, 186, 187, 232,
284, 285, 313, 331, 336
McCracken, C. W., 274, 297, 309
McDonnell, J. A. M., 273, 331
McElroy, M. B., 114, 168, 223, 321
McGarvey, J. J., 114, 331
McGrath, W. D., 114, 331
McGrattan, G. J., 247, 322, 331
McIntosh, B. A., 267
McInturff, R. M., 34, 35, 290, 312
McKencie, D. J., 340
McLone, R. R., 91, 331
McTaggart-Cowan, J. D., 113, 116, 324
Meadows-Reed, E., 245, 331
Meerburg, A. J., 149, 151, 152, 153,
155, 352
Meetham, A. R., 141, 331
Megaw, W. J., 284, 331
Megill, L. R., 114, 343
Meier, R. R., 233, 235, 236, 239, 243,
259, 309, 331
Meinel, A. B., 200, 331
Meinel, M. P., 200, 331
Mellis, O., 274, 326
Meloy, G. E., 339
Melzner, F., 313
Merilees, P., 34, 331
Mesinger, F., 18, 19, 21, 22, 331
Mészáros, E., 282, 331
Meyer, B., 313
Midorikawa, B., 96, 332
Miers, B. T., 25, 35, 39, 40, 41, 300, 301,
332, 333
Migeotte, M., 350
Mikhnevich, V. V., 156, 321, 332
Miles, G. T., 199, 280, 281, 301
Miller, A., 116, 132, 329, 332
Miller, A. J., 3, 31, 44, 128, 138, 139,
332, 335, 338
Millman, P. M., 267
Mills, A., 96, 332
Milovanović, O., 18, 19, 21, 22, 331
Minzner, R. A., 247, 332
Mirtov, B. A., 113, 332
Mitchell, J. M., Jr., 156, 332
Mitra, A. P., 58, 120, 332
Mitra, V., 264, 314
Miyake, Y., 231, 332
Modin, S., 352
Moffitt, B. J., 162, 334
Molla, A. C., Jr., 3, 128, 138, 332
Möller, F., 98, 332
Monteith, J. L., 285, 332
Montgomery, J. B., III, 39, 252, 254,
323, 332
Montgomery, R. B., 97, 332
Moore, C. B., 23, 332
Moore, J. G., 176, 332, 349
Moos, H. W., 168, 332
More, W. B. de, 59, 332
Moreland, W. B., 351
Moreno, H., 209, 332
Morgan, G., Jr., 285, 332, 350
Morla, R., 299
Morris, J. E., 25, 39, 245, 261, 333
Morrisey, J. F., 78, 303
Morton, J. D., 280, 285, 333
Moses, H., 283, 333
Mossop, S. C., 202, 205, 212, 232, 333
Movchan, B. N., 341
Mrose, H., 283, 287, 333
Muench, H. S., 34, 333
Mukammal, E. I., 115, 333
Müller, H. G., 262, 333
Müller, W., 284, 287, 333
Munczak, F., 190, 218, 333
Muniosguren, L. S., 25, 298
Münnich, K. O., 163, 333
Murakami, T., 7, 333
Murata, H., 180, 329
Murcay, D. G., 76, 78, 201, 325, 326,
333
Murcay, F. H., 326, 333
Murgatroyd, R. J., 2, 18, 24, 27, 28, 30,
31, 32, 75, 89, 92, 162, 167, 168, 171,
173, 215, 218, 333, 334
Murphy, B. L., 261, 334
Murphy, C. H., 39, 245, 252, 254, 262,
263, 334, 353
Murray, R., 162, 334
Musgrave, B., 189, 190, 191, 317
Nagamoto, C. T., 280, 334
Nagaraja Rao, C. R., 176, 332
Nagata, T., 169, 170, 171, 173, 177, 349
Nakamura, M., 323

- Nania, A., 22, 341
 Narcisi, R. S., 61, 63, 91, 264, 266, 268, 334
 National Aeronautics and Space Administration, 31, 45, 61, 310, 334
 Naumann, R. J., 273, 306, 334
 Nelson, R. A., 49, 335
 Neporent, B. S., 78, 335
 Neufeld, E. L., 39, 48, 316
 Neuss, H., 313
 Newell, R. E., 5, 12, 25, 26, 27, 28, 29, 32, 39, 48, 49, 51, 61, 114, 138, 139, 140, 141, 142, 145, 146, 157, 159, 161, 162, 215, 224, 233, 234, 236, 237, 243, 261, 308, 335, 350
 Newkirk, G., Jr., 199, 201, 202, 204, 205, 271, 272, 273, 274, 276, 335
 Ney, E. P., 117, 271, 274, 326, 335, 346
 Nguyen-Huu-Doan, 265, 335
 Nicholas, G. W., 300, 344
 Nickola, P. W., 285, 335
 Nicolet, M., 58, 59, 90, 169, 176, 182, 223, 300, 336
 Nielson, D. L., 52, 328
 Niemeyer, L. E., 232, 285, 336
 Nier, A. O., 61, 245, 318, 336
 Nisbet, J. S., 180, 309
 Nitta, T., 353
 Nietzsche, P., 224, 327
 Noel, T. M., 300
 Nolan, G. F., 215, 336
 Noll, K. E., 269, 320, 338
 Nordberg, W., 25, 31, 324, 336, 347, 348
 Normand, C. W. B., 156, 157, 308
 Norris, D., 301
 Nucciotti, F., 192, 336, 350
 Nudelman, C., 59, 304
 Oard, M. J., 39, 340
 Oblanas, J., 269, 350
 Ogden, E. C., 339
 Ogden, T. L., 284, 336
 Okita, T., 192, 193, 336
 Oldenberg, O., 234, 322
 Olsen, R. O., 245, 324
 Omholt, A., 167, 331
 Oort, A. H., 7, 336
 Orville, R. E., 117, 336
 Osheroovich, A. L., 341
 Östlund, H. G., 191, 336
 Pack, D. H., 285, 298, 318
 Paetzold, H. K., 120, 123, 156, 336
 Paisley, S., 197, 275, 344
 Pales, J. C., 97, 99, 100, 102, 280, 336, 338
 Palmén, E., 71, 336
 Panchev, S., 11, 13, 14, 17, 336
 Panofsky, H. A., 95, 284, 299, 353
 Parham, A. G., 303
 Parkin, D. W., 301, 307
 Parkinson, D., 182, 312
 Parthasarathy, R., 224, 241, 336
 Pasceri, R. E., 205, 269, 313, 336
 Pasquill, F., 17, 18, 337
 Pate, J. B., 312
 Paterson, M. P., 231, 282, 337
 Paton, J., 89, 90, 337
 Patterson, R. L., Jr., 328
 Paulson, M. R., 49, 315
 Paznoikas, J. J., 269, 299
 Peabody, C. O., 301
 Peixoto, J. P., 7, 72, 337, 346, 347
 Pelissier, J., 299
 Peng, L., 7, 337
 Penn, S., 128, 129, 337
 Penndorf, R., 195, 196, 233, 337
 Perkins, W. A., 327
 Perl, G., 147, 148, 149, 337
 Petersen, H. L., 59, 337
 Peterson, J. T., 207, 209, 337
 Peterson, J. W., 44, 322
 Peterson, L. R., 316
 Petterson, H., 274, 337
 Picciotto, E., 275, 303
 Pierrard, J. M., 270, 342
 Pilat, M. J., 285, 305
 Pilipowskyj, S., 204, 337
 Pinus, N. Z., 14, 15, 16, 337, 350
 Piscalar, F., 120, 336
 Pittock, A. B., 129, 135, 148, 151, 212, 337
 Plass, G. N., 97, 98, 337
 Platzter, R., 329
 Podzimek, J., 230, 284, 286, 337
 Pond, H. L., 332
 Popp, Ch., 123, 345
 Poppoff, I. G., 224, 352
 Pötzl, K., 285, 338
 Powell, D. C., 18, 323
 Prabhakara, C., 28, 114, 162, 163, 328, 338
 Prasad, S. S., 316
 Pressman, J., 244, 338
 Price, S., 280, 338
 Priestler, W., 32, 34, 39, 42, 43, 44, 156, 317, 338

- Prodi, V., 286, 350
 Prohaska, J., 156, 352
 Prospero, J. M., 277, 278, 279, 338
 Pueschel, R. F., 231, 269, 283, 338
 Quiroz, R. S., 31, 338
 Radke, L. F., 277, 286, 320, 338
 Raghava Rao, R., 49, 320
 Ragsdale, G. C., 247, 338
 Rai, D. B., 224, 241, 336
 Ramachandra Murty, A. S., 323
 Ramana Murty, Bh. V., 282, 286, 323, 324, 338, 344
 Ramanathan, K. R., 150, 157, 158, 338
 Randhawa, J. S., 39, 144, 299, 338
 Rangarajan, S., 145, 160, 339
 Rankama, K., 232, 339
 Rankin, M. O., 335
 Rao, B. R., 39, 179, 339
 Rao, G. L., 39, 179, 339
 Rao, M. M., 256, 339
 Rao, N. N., 173, 339
 Rao, P. B., 44, 339
 Rao, R. R. (see Raghava Rao, R.)
 Raper, O. F., 59, 332
 Raschke, E., 65, 72, 73, 339
 Rasmussen, R. A., 116, 190, 339
 Rasool, S. I., 156, 157, 339
 Rastogi, R. G., 259, 262, 308, 339
 Ratcliffe, J. A., 61, 95, 170, 171, 179, 182, 223, 224, 262, 339
 Rau, W., 270, 339
 Rawcliffe, R. D., 122, 144, 145, 339
 Rawer, U., 325
 Raynor, G., 280, 339
 Reddy, C. A., 254, 256, 259, 261, 331, 339
 Reed, E. I., 144, 339, 340
 Reed, R. J., 3, 4, 5, 6, 7, 9, 11, 12, 17, 25, 31, 39, 40, 41, 44, 74, 87, 128, 160, 161, 162, 286, 301, 327, 340
 Rees, J. A., 322
 Reeves, R. R., 59, 340
 Regner, V. H., 140, 147, 163, 164, 340
 Reger, E., 195, 196, 340
 Reid, G. C., 145, 173, 340
 Reimann, B. E. F., 307
 Reiter, E. R., 2, 14, 15, 16, 18, 22, 23, 44, 46, 47, 55, 57, 65, 66, 67, 68, 69, 70, 71, 75, 130, 138, 147, 205, 231, 244, 286, 290, 307, 337, 340, 341, 347, 351, 352
 Reiter, R., 220, 221, 277, 280, 287, 304, 341
 Remsberg, E. E., 85, 341
 Renzetti, N. A., 115, 341
 Revelle, R., 106, 341
 Rey, L., 346
 Rider, L. J., 47, 298
 Rieger, E., 313, 317
 Riley, J. J., 280, 300
 Ringer, L. D., 269, 301
 Ripperton, L. A., 115, 341, 352
 Rishbeth, H., 43, 58, 179, 180, 223, 254, 341
 Roach, F. E., 180, 341
 Roach, W. T., 129, 303
 Robbins, R. C., 187, 188, 341
 Robinson, E., 187, 188, 285, 322, 341
 Rodewald, M., 277, 341
 Rodgers, C. D., 144, 341
 Rodionov, S. F., 144, 341
 Rogers, E. H., 339
 Roper, R. G., 39, 55, 323
 Rose, G., 308
 Rosen, J. M., 199, 206, 207, 212, 214, 273, 274, 342
 Rosenberg, N. W., 39, 175, 243, 244, 245, 250, 254, 255, 256, 257, 300, 310, 315, 342, 353
 Rosinski, J., 270, 283, 286, 304, 327, 334, 342
 Rössler, F., 205, 299
 Rossmann, F., 195, 196, 342
 Roy, A. K., 282, 338
 Rubin, M. J., 150, 342
 Rundle, H. N., 265
 Rungc, H., 277, 342
 Ryan, B. F., 280, 342
 Ryan, T. G., 195, 322, 346
 Sacco, A. M., 285, 316
 Sacher, P., 346
 Sagalyn, R. C., 256, 342
 Sahama, Th. G., 232, 339
 Salmela, H. A., 82, 83, 86, 316, 345
 Samson, C. A., 300
 Sands, E. E., 48, 323
 Sartor, J. D., 259, 342
 Saunders, A. W., Jr., 328
 Sayers, J., 300
 Schaefer, V. J., 232, 284, 342, 343
 Scheich, G., 282, 322
 Scherhag, R., 34, 225, 227, 343
 Schiff, H. I., 58, 59, 114, 343

- Schilling, G. F., 54, 55, 283, 343
 Schmeltekopf, A. L., 311, 312
 Schmidlin, F. J., 31, 343
 Schmidt, M., 270, 339
 Schmidt, R. A., 274, 348
 Schmidt, Th., 271, 343
 Schminder, R., 225, 227, 229, 346
 Schofield, K., 58, 343
 Schove, D. J., 162, 343
 Schröder, W., 89, 90, 92, 343
 Schröer, E., 168, 343
 Schubert, C. C., 85, 189, 308
 Schubert, G., 230, 283, 343, 344
 Schwentek, H., 308
 Scoggins, J. R., 44, 344, 351
 Scoggins, M. F., 335
 Scolnik, R., 144, 340
 Scorer, R. S., 278, 283, 344
 Scott, D. W., 32, 34, 204, 205, 306
 Scott, W. D., 280, 342, 344
 Secretan, L., 297
 Seidel, H., 195, 308
 Seiden, L., 319
 Seiler, W., 188, 344
 Seitz, H., 215, 217, 344
 Sekhon, R. S., 282, 323, 344
 Sekihara, K., 157, 344
 Sekikawa, T., 284, 344
 Sellers, W. D., 114, 344
 Seto, Y.-B., 232, 344
 Severynse, G. T., 269, 286, 344, 349
 Shafrir, U., 92, 270, 344
 Shah, G. M., 144, 158, 160, 344
 Shapiro, R., 157, 344
 Shapley, A. H., 225, 243, 344
 Sharp, J., 316
 Shaw, J. H., 188, 344
 Shedlovsky, J. P., 197, 275, 304, 344
 Shellard, H. C., 299
 Shen, W. C., 95, 300, 344
 Shenn, E. M., 335
 Shepherd, G. G., 183, 243, 344
 Sheppard, L. M., 244, 245, 328, 344
 Shimizu, M., 123, 138, 345
 Shlyakhov, V. I., 335
 Shukurov, A. Kh., 341
 Shur, G. N., 15, 16, 337, 345, 350
 Shvidkovsky, E. G., 314
 Sidle, A. B., 190, 345
 Sidentopf, H., 195, 196, 271, 272, 314, 340
 Silver, S., 305
 Silverman, S. M., 173, 175, 318, 345
 Simonini, G., 336
 Simpson, Ch. L., 313
 Sinclair, P. C., 278, 345
 Singer, S. F., 273, 299, 345
 Singleton, F., 28, 30, 89, 92, 162, 167, 168, 171, 215, 218, 230, 334, 345
 Singleton, R. C., 310
 Sissenwine, N., 78, 81, 82, 83, 84, 85, 86, 87, 91, 142, 345
 Skeib, G., 123, 345
 Skidmore, D. R., 85, 189, 308
 Skrivanek, R. A., 91, 318, 345, 346
 Slack, F. F., 170, 345
 Sládovič, R., 341
 Slocum, G., 96, 345
 Slowey, J., 305, 321
 Smiddy, M., 256, 342
 Smith, C. D., 277, 345
 Smith, C. R., 245, 331
 Smith, E. K., 69, 182, 257, 259, 345
 Smith, F. J., 243, 322, 345
 Smith, J. R., 332
 Smith, L. B., 345
 Smith, L. L., 173, 176, 178, 179, 234, 236, 238, 307, 345
 Smith, R. M., 75, 76, 345
 Smith, R. W., 180, 346
 Smith, S. M., 283, 320
 Smith, W. L., 69, 346
 Smith, W. S., 44, 171, 336, 346
 Smullins, L. D., 195, 312
 Soberman, R. K., 91, 271, 273, 276, 318, 346, 352
 Söderman, D., 71, 336
 Solomon, I., 316
 Solot, S. B., 23, 286, 346
 Soulage, G., 280, 346
 Spar, J., 234, 313
 Sparrow, J. G., 34, 160, 170, 173, 346
 Spencer, N. W., 39, 61, 346, 350
 Spillane, K. T., 231, 282, 337
 Spindler, G. B., 170, 173, 346
 Spizzichino, A., 182, 252, 346
 Sprenger, K., 224, 225, 226, 227, 228, 229, 327, 346
 Squires, P., 284, 346
 Šrámek, L., 337
 Stack, I., 209, 332
 Stair, A. T., Jr., 183, 321
 Staley, D. O., 163, 346
 Starr, J. R., 286, 346

- Starr, V. P., 2, 72, 346, 347
Steele, L. P., 65, 299
Steiger, W. R., 173, 176, 179, 236, 326
Steinhauser, F., 96, 100, 101, 102, 147, 148, 149, 193, 194, 284, 299, 347
Stephens, J. J., 69, 347
Stephens, N. T., 331
Sterling, D. L., 311
Stewart, D. A., 215, 216, 347
Stewart, K. H., 144, 347
Sticksel, P. R., 130, 306, 347
Stinson, R., 44, 347
Stoddart, J. W., 346
Stormer, C., 77, 89, 347
Stranz, D., 144, 156, 347
Streiff-Becker, R., 277, 347
Stroud, W. G., 91, 168, 347
Stuetzer, I., 114, 306
Sturrock, R. F., 138, 347
Suess, H. E., 106, 298, 341
Sugiura, M., 180, 255, 347
Sullivan, H. M., 138, 264, 266, 268, 347, 348
Suomi, V. E., 205, 348
Süring, R., 95, 96, 317
Suslov, A. K., 341
Swartz, P., 346
Swider, W., Jr., 61, 223, 348
Taeusch, D. R., 346
Taffe, W. J., 39, 348
Taieb, C., 182, 346
Takahashi, T., 95, 105, 348
Takeuchi, D. M., 205, 348
Tanaevsky, O., 148, 349
Tanaka, M., 269, 287, 353
Tanaka, Y., 323
Tarasenko, D. A., 314
Tarrant, R. F., 218, 348
Tatarski, V. I., 47, 48, 69, 348, 353
Taylor, B. T., 301
Taylor, J. H., 313
Teichert, F., 113, 147, 284, 348, 351
Teitelbaum, H., 301
Telegadas, K., 328
Telford, J. W., 348
Temple, J. W., 115, 299
Teweles, S., 31, 173, 215, 312, 318, 348
Thams, J. C., 284, 333
Thayer, G. D., 300
Theon, J. S., 25, 44, 91, 224, 320, 336, 346, 348
Thiel, E., 274, 348
Thomas, L., 180, 223, 225, 348
Thompson, M. C., Jr., 69, 348
Thompson, Th. G., 232, 314
Thomson, K. P. B., 303
Thrush, B. A., 59, 306, 327
Thyer, N., 100, 348
Tinsley, B. A., 94, 348
Titheridge, J. E., 172, 180, 349
Titus, P., 347
Toba, Y., 282, 349
Tohmatsu, T., 169, 170, 171, 173, 177, 349
Tofelson, H. B., 49, 351
Tonsberg, E., 233, 349
Touart, C. N., 318
Tromp, S. W., 190, 349
Tschetter, C. D., 318
Tsunogai, S., 231, 332
Tucker, G. B., 161, 349
Tucker, R. L., 49, 351
Tuck-Lee, C., 232, 333
Tuller, S. E., 72, 349
Turtle, J. P., 171, 318
Twomey, S., 114, 269, 280, 284, 349, 351
United States Air Force, 45, 310, 334
United States Atomic Energy Commission, 18, 286, 349
United States Weather Bureau, 18, 286, 334, 349
Unthank, E. L., 160, 346
Unz, F., 200, 276, 349
Urey, H. C., 96, 332
Valach, R., 230, 232, 349
Valenzuela, R., 299
Vallance Jones, A., 168, 234, 235, 236, 238, 243, 264, 265, 266, 268, 311, 314, 349
Van Nahl, T. W., 309
Vassy, A., 123, 148, 349
Vassy, E., 150, 349
Vaughan, W. W., 312
Vegard, L., 233, 349
Venkateswaran, S. V., 58, 144, 299, 349
Vermande, P., 350
Verniani, F., 321
Verzár, F., 284, 350
Vick, R. I., 49, 351
Vickery, W. K., 300
Viebrock, H. J., 209, 210, 211, 212, 312, 350
Viezee, W., 269, 350
Vigroux, E., 139, 145, 350

- Vihman, E., 328
 Vincent, D. G., 28, 75, 123, 335, 350
 Vincent, R. A., 53, 162, 350
 Vinnichenko, N. K., 15, 16, 337, 350
 Vittori, O., 192, 286, 336, 350
 Vogel, T. C., 163, 333
 Volfová, E., 337
 Volut, J., 299
 Volz, F. E., 197, 200, 201, 207, 208, 270,
 274, 276, 350
 Vyverberg, J. C., 340
 Waddoups, R. O., 170, 172, 182, 298, 299
 Wagner, C.-U., 145, 256, 307, 327, 350
 Wait, G. R., 283, 350
 Walker, J. C. G., 39, 350
 Wallace, J. M., 52, 157, 159, 161, 228,
 233, 234, 237, 243, 335, 350
 Wallace, L., 58, 182, 235, 243, 321, 350
 Walshaw, C. D., 113, 143, 350
 Walton, A., 313
 Wanta, R. C., 115, 351
 Ward, F., 157, 344
 Warmbt, W., 113, 147, 351
 Wärme, K. E., 96, 313
 Warnecke, G., 314
 Warner, J., 284, 349, 351
 Wasko, P. E., 44, 247, 338, 351
 Wasson, J. T., 234, 309, 322
 Waterman, L. S., 105, 107, 324
 Watson, F. G., 273, 276, 351
 Watson, R. D., 195, 315
 Wayne, R. P., 58, 114, 351
 Webb, W. L., 25, 35, 39, 43, 44, 48,
 49, 76, 144, 173, 214, 351
 Webster, F. X., 327
 Weeks, K., 171, 179, 182, 224, 339
 Weihrauch, J. H., 311
 Weill, G. M., 179, 266, 351
 Weinberg, J. L., 271, 351
 Weinert, R. A., 209, 351
 Weinman, J. A., 85, 337, 341
 Weinstein, A. I., 44, 55, 347, 351
 Weinstock, B., 188, 351
 Weintraub, S., 69, 345
 Welander, P., 269, 351
 Welch, W. J., 305
 Werby, R. T., 287, 322
 Wetherald, R. T., 73, 74, 97, 98, 143,
 291, 330
 Wexler, H., 123, 150, 151, 277, 345, 351
 Weyant, W. S., 150, 342, 351
 Whipple, F. L., 271, 272, 273, 274, 276,
 352
 Whitby, K. T., 205, 269, 305
 White, G. D., 230, 309
 Whitehead, J. D., 240, 254, 352
 Whitten, R. C., 224, 352
 Widdel, H. U., 308
 Widen, D. A., 146, 335
 Wiffen, R. D., 284, 331
 Wiin-Nielsen, A., 14, 352
 Wilhelm, N., 346
 Wilkins, E. M., 103, 104, 324, 352
 Willett, H. C., 150, 154, 156, 352
 Williams, W. J., 326, 333
 Williamson, E. J., 78, 352
 Wilson, A. T., 218, 352
 Wilson, A. W., 118, 120, 143, 303
 Winchester, J. W., 231, 308, 309, 314,
 328, 352
 Winkler, P., 297
 Wisse, J. A., 149, 151, 152, 153, 155, 352
 Witt, G., 89, 90, 91, 92, 271, 318, 328, 352
 Wojciechowski, T. A., 280, 349
 Woodcock, A. H., 344
 Woodrum, A., 254, 258, 352
 Woods, H. D., 15, 323
 Wooldridge, G., 14, 23, 285, 286, 352
 Woolf, H. M., 31, 35, 312, 332
 Worth, J. J. B., 148, 352
 Wright, F. W., 274, 275, 320, 352
 Wright, J. W., 180, 245, 250, 254, 255,
 256, 257, 262, 315, 334, 342, 353
 Wright, P. B., 280, 353
 Wright, R. W., 262, 324, 337
 Xintaras, C., 185, 186, 187, 331
 Yaalon, D. H., 218, 353
 Yaglom, A. M., 69, 353
 Yamamoto, G., 269, 287, 353
 Yanai, M., 157, 330, 353
 Yano, K., 175, 176, 353
 Yarger, D. N., 114, 318, 344
 Yerg, D. G., 179, 353
 Young, Ch., 168, 169, 353
 Young, L. C., 297
 Yurganov, L. N., 341
 Zahn, U. von, 61, 353
 Zak, J. A., 95, 353
 Zander, R., 78, 353
 Zelikoff, M., 338
 Zenker, H., 283, 353
 Zerche, M., 230, 353
 Zier, M., 283, 333
 Zimmerman, S. P., 175, 246, 247, 249,
 250, 254, 305, 342, 353, 354
 Zipf, E. C., 176, 354

SUBJECT INDEX

- Abu-Ahmedabad, India, 158, 165
Acoustic waves, 49
Adelaide, Australia, 253
Aeroplancton, 190
Aerosol, 191, 193, 195, 197, 199, 204 f.,
210 ff., 214 f., 224, 229, 231, 240, 255,
269, 286
anthropogenic sources of, 283
as a catalytic sink for ozone, 212
concentrations, 205, 214
deposition, diurnal variation of, 284
extraterrestrial origin of, 185
laminae of, 201
layer (see Junge layer)
ledge, 218
mixing ratios of, 200
organic, 278
refractive index, 269
size distributions of, 91, 268 f.
stratospheric origin, 195
tropospheric origin, 195
Agl (see Silver iodide)
Agung Volcano, Bali, (see Mount Agung,
Bali)
Ahmadābād, India (see Abu-Ahmedabad)
Ahmedabad, India (see Abu-Ahmedabad)
Air pollution, 73, 116, 132, 185, 192, 205,
231 f., 278, 280, 283 f., 292
Airglow, 94, 114, 168 ff., 175 ff., 233 f.,
238 ff., 243, 264 ff., 270 f., 290
drift of patterns, 179
emission (5577Å), altitude distribution
of, 169
diurnal variation of, 171
effect of high atmospheric circulation
patterns on, 176
seasonal variations of, 173, 176
variation with latitude and season, 173
patches, 170, 172
patterns, 238
predawn enhancement of the oxygen red
line, 180
trails, 243
ultraviolet, 168
Aitken nuclei, 193, 280, 282, 287
Alaska, 99 f., 195, 198, 208, 230, 232, 262
Albedo, 157, 161
Alberta, 154
Albrook Field, Canal Zone, 121 f., 125
Albuquerque, New Mexico, 121, 125, 130,
132 f.
Aldehydes, 115
Alert, Canada, 142
Algeria, 174, 247
Alkali metals, 233, 235, 264
Alkaline tracer experiments, 182
Alkali-trail experiments, 246 ff.
AlO (see Aluminum oxide)
Al₂O, 244
Al₂O₃, 244

- Alps, 277
 Aluminum, 244, 268
 Aluminum oxide, 244
 Aluminum powder, 245
 Amarillo, Texas, 132
 Amino acids, 190
 Ammonia, 193, 195, 204, 218 ff., 275, 284
 Amundsen-Scott Base, Antarctica, 151, 154 f., 209 f.
 Angular momentum transport, 179
 rotation, 24
 Antarctic stratospheric vortex (see Polar night vortex)
 Antarctica, 97, 123, 150 ff., 163, 209 ff., 227, 265 f., 275
 CO₂ over, 102
 subsidence motions over, 29, 151, 154
 Antilles, West Indies, 277
 ARCAS Robin measurements, 52
 Arctic, 75, 99, 102, 104
 Argentine Island, Antarctica, 150
 Argon, 245
 Arizona, 132, 173, 176, 178, 254, 280
 Aromatic compounds, 190
 Arosa, Switzerland, 147 ff., 156 f., 159, 165
 Ascending motions, 92, 122, 142, 167
 Ascension Island, 158
 Ascension rate of balloon, 134
 Asia, 72
 Aspendale, Australia, 150, 154, 158 ff.
 Atlantic, 277, 280
 Atmospheric composition, interdiurnal variability of, 61
 nuclear testing, 283
 Auroral displays, 154
 Australia, 25, 150, 154, 158 ff., 174, 208 f., 250, 253, 262, 280, 285
 Austria, 100 f., 147 ff., 193 f., 284
 Autocorrelation coefficients, 14
 Automotive traffic, 185
 Averages, zonal, time, 3
 Avogadro's number, 163
 Bacteria, 190
 Bahamas, West Indies, 259
 Bali, 143, 196 f., 199, 207 ff., 275, 281
 Balloon, constant-density, 23, 285, 291
 constant-level, 23
 contamination of the atmosphere by the ascending, 77 f.
 degassing of the ascending, 81
 Baltic Sea, 98 f.
 Barbados, West Indies, 254, 262 f., 277, 279
 Barium, 244 f.
 Baroclinic regions, 20, 130
 Base King Baudouin, Antarctica, 149, 152 f., 155
 Bedford, Massachusetts, 135
 Berlin, Germany, 227
 Bicarbonate ions, 95
 Biennial oscillation, 52, 157 f., 160, 162, 214, 227 ff.
 temperature maximums, 160
 variation of cloud cover in the tropics, 162
 variation of ozone, 157, 159
 breakdown of, 158
 "Biennial wave," poleward progression of, 159
 Billows, 91
 Binza, Democratic Republic of the Congo, 287
 Biosphere, 97
 Birdling's Flat, New Zealand, 227
 Blue Hill Observatory, Milton, Massachusetts, 207
 Blue sun, 277
 Boise, Idaho, 132 f.
 Boron, 232
 Boron/chlorine ratio, 232
 Boston, Massachusetts, 146
 Boulder, Colorado, 135, 139, 145 f.
 Boundary layer (see Mixing layer, adiabatic)
 Br₂, 232
 Braking of satellites, 156
 Brewer-Dobson circulation model, 75
 Brisbane, Australia, 150, 154, 158 ff.
 Bromine, 231 f.
 Bromine/chlorine ratio, 231 f.
 Brownsville, Texas, 130, 133
 Bubbler ozonesonde measurements, 136
 Burrwood, Louisiana, 68
 C (see Carbon, isotopes of)
 Ca (see Calcium)
 Calcium, 61, 239, 245, 264, 266, 268
 emission, 266 ff.
 in the upper atmosphere, extraterrestrial origin of, 266
 Calcium/chloride ratio, 287
 California, 78, 81 ff., 85 f., 91, 102, 116, 134, 188
 Camden, Australia, 174
 Canada, 140, 142, 154, 168, 207, 214, 235, 241, 247, 254, 265 f., 277

- Canal Zone, 121 f., 125
 Canton Island, 158
 Carbon, isotopes of (^{12}C , ^{13}C , ^{14}C), 96, 111
 Carbon dioxide, 27, 75, 95 f., 105, 112, 143 ff., 148, 185, 189, 228
 "air pollution" by, 98
 in the atmosphere, residence time, 106
 "buffering" effect of the oceans, 97
 consumption of, by land vegetation, 110
 diurnal variation of, 96 ff.
 equilibrium temperature reached under various concentrations, 97
 exchange between atmosphere and sea, 95 f.
 heating rate, 74
 industrial sources, 109
 infrared bands, 27, 95, 97, 168
 interdiurnal variation of, 96
 interhemispheric exchange of, 100
 latitudinal fluctuations of, 97, 105
 longitudinal variations in partial pressure, 106
 monthly average concentration of atmospheric, 102, 104
 near the ocean surface, concentration of, 107
 partial pressure of, 96, 105 f., 108
 seasonal trend in concentrations, 102
 107
 partial pressure, 106
 secular trend of, 96 ff., 109
 sinks of, 107, 109 ff.
 as a function of latitude, 110
 sources of, 105, 107, 109 ff.
 as a function of latitude, 110
 transfer into the ocean, 109
 turnover time of the total, 97
 variation near the ground, 96
 Carbon monoxide, 95, 185 ff.
 diurnal variation of, 185
 industrial sources of, 187
 ocean sources, 187
 residence times of, 188
 traffic sources of, 187
 tropospheric burden of, 188
 Carbonate ions, 95
 Carbonic acid, 95
 Carbonic anhydrase, 96
 Caribbean, 278
 Carnegie, 283
 CAT (see Clear air turbulence)
 CBrF_3 , 232
 Cesium nitrate, 245
 C_4F_8 , 232
 CH_2 (see Methylene)
 CH_4 (see Methane)
 Chaff, radar reflective, 245, 261, 290 f.
 Chappius bands, 143
 $\text{CH}_2\text{Br}-\text{CH}_2\text{Br}$ (see Ethylene bromide)
 Chemical reactions in the high atmosphere, 58 f.
 tracers, 185
 Chemiluminescent releases, 173
 Chico, California, 81 ff., 86, 91
 Chile, 208 f., 278
 Chinese nuclear test, 215, 290
 Chinook winds, 283
 Chloride, 229 ff., 233
 precipitation removal of atmospheric, 230
 Chlorine, 229 f., 232
 volcanic source of, 230, 232
 Chlorine/fluorine ratio, 232
 Chlorine/sodium ratio, 230, 286
 Christchurch, New Zealand, 122, 257, 259
 Christmas Island, 162
 CH_3T (see Methane, tritiated)
 Churchill, Canada (see Fort Churchill, Canada)
 Cl^- (see Chloride)
 Cl_2 (see Chlorine)
 Clay particles, 270
 Clear air turbulence, 15, 129
 Close-spaced antenna method, 262
 Cloud cover, large-scale variations in, 98, 157, 162
 nuclei, anthropogenic, 284
 lifetime of, 280
 seeding, 270, 285, 290
 CN, 244
 CO (see Carbon monoxide)
 CO_2 (see Carbon dioxide)
 Cold fronts, 136
 outbreaks, 123
 "Cold trap" of the equatorial tropopause, 75
 College, Alaska, 195
 Collision frequencies between neutrals and ions, 42
 Colorado, 78, 121 ff., 125, 130, 132 f., 135, 139, 145 f., 150, 174
 Combustion, fossil-fuel, 97, 107
 processes, home, industrial, 96, 185

- Comet fragments, 275
- Computer modeling of chemical reactions, 58
- Concentrations of chemical compound, 3, 17 f., 118
- Condensation nuclei, 205
- Conductivity measurements, 283
- Congo, Democratic Republic of, 150, 287
- Constant specific humidity surfaces, 66
- Continuity equation, 2
- Contrails, 285
- Convective motions, 148, 284
precipitation processes, 70
- Convergence of meridians, 6
- Coordinate system, Eulerian, Lagrangian, 14, 18, 20
geographic, curvilinear, 2
- Copenhagen, Denmark, 102
- Coriolis parameter, 12
- Coronagraph, 199, 201
- Corpuscular radiation, 156 f.
- Correlation, between ozone and stratospheric circulation characteristics, 161
between ozone and temperature, 138, 141
between temperature and the meridional wind component, 216
between thermal stability and ozone concentrations, 130
between total amount of ozone and ozone in a layer, 140
between tropical wind systems, ozone, the time of breakdown of the northern hemisphere polar vortex, and the direction of motion of the stratospheric warming centers, 161
between tropopause height and amounts of total ozone, 138
functions, 11
- Cosmic dust, 234, 268
- Cosmic radiation, 224
- Countergradient flux, 165
- Cumulonimbus clouds, 231
- Cyclogenetic processes, 147
- Czechoslovakia, 174
- Dalarö, Sweden, 98 f.
- Danube River, 194
- Davos, Switzerland, 208
- Day glow, 58, 233, 240, 243
spectrum, 222
- Del Rio, Texas, 132
- Denmark, 102
- Density distribution, 31
diurnal wave, 39
exospheric, 44
seasonal variation of, 31
semiannual variation in, 32
semidiurnal wave, 39
upper atmospheric, 44
- Denver, Colorado, 78, 132
- Descending motions in the stratosphere, 92, 122, 128, 150
- Diffusion, 2, 3, 12, 17 f., 20, 22, 24, 28, 61, 74, 96, 100, 102, 162, 165, 201, 239, 245, 247, 269, 290
coefficients, 3, 86 f., 92 f., 135 f., 165, 230, 234, 239, 245 f., 291
model, 215
- Dilution, short-term, of contaminants, 18
- Dimmerfoehn, 277
- Dinitrogen hexoxide, 218
- Dinitrogen pentoxide, 218
- Dinitrogen tetraoxide, 218
- Dinitrogen trioxide, 218
- Dishpan experiments, 24
- Dispersion, 14, 18 f., 24, 39, 43, 55
- Dissipation of turbulent kinetic energy, 16, 247
- Dissociation of atmospheric constituents, 57
rate, 58, 60 f., 118
- Diurnal temperature wave, 43
- D-layer (see D-region)
- Dobson spectrophotometer, 114
units, 123, 127
- Dodge City, Kansas, 68
- Doppler shift, 269
- Doppler-line broadening, 243
- Downslope currents, 148
- Drag measurements, 31
- D-region, 91, 144, 222 ff., 241, 243, 262, 270, 290
anomalies in the, 224
ionization, 224
26-month cycle of drift velocities in the, 227
winter anomaly of the, 223 ff., 227
- "Dry sky" conditions, 91
- Dry stratosphere, 74
- Dumont d'Urville, Antarctica, 155
- Dust, 93, 197, 202, 206 f., 212, 214, 218, 240, 255
anthropogenic sources of, 283
belt, geocentric, 273
devils, 278
extraterrestrial source for stratospheric,

- 199 f., 269
 interplanetary, 271
 layer between 110 and 140 km, 271
 ledge, 92, 214, 239
 mixing ratio of, 200
 particles of volcanic origin, 207
 sedimentation of, 269
 storms, 278, 280
 Earth's radiance, 145
 Earth's radius, 6
 East Germany, 147
 Easterly stratospheric wind, 34, 160
 Echo satellite (1960 Iota 1), 144
 Echo II satellite, 32, 34
 Eclipse, 144, 156, 177
 Ecuador, 278
 Eddy exchange coefficient, 8f., 11 ff., 20,
 23 f., 107, 162, 164, 214, 218, 228
transport, 2, 4 ff., 9, 11, 18, 24, 28 f., 34,
 71 f., 75, 82 ff., 92, 99, 109, 118, 123,
 133, 139 ff., 151, 162, 165, 167, 179 f.,
 196, 205, 212, 214 f., 218, 224 f., 227,
 243, 254, 270
 Edmonton, Alberta, Canada, 154
 Eglin Air Force Base, Florida, 25, 44, 63,
 254 ff.
 El Paso, Texas, 132
 E-layer (see E-region)
 Electric conductivity, 283
 Electromagnetic wave absorption, 223
 Electron clouds, 245
 concentration, 42, 144, 223
 temperatures, thermospheric diurnal varia-
 tion of, 39
 Electronic excitation, 58, 168, 171, 177,
 223, 236
 Electrons, depletion of, 245
Eltanin, 188, 236, 238
 England, 75, 78, 83, 191, 253, 262
 Enzymes, 96
 Eppley normal-incidence pyrhelimeter,
 201
 Equator, 7, 75, 105, 111, 167, 262, 286
 Equivalent potential temperature, 20
 E-region, 52, 54, 172, 223, 247, 255 f.,
 262, 269, 275
 drifts, 262
 microstructure in sporadic, 256
 seasonal dependence, 182
 solar-cycle variation of neutral wind
 shears in, 260
 sporadic (see Sporadic E)
- Escape rates, 94
 Eskdalemuir, Scotland, 154
 Ethylene bromide, 232
 Europe, 97, 224, 227, 230, 277, 287
 Europium, 245
 Evaporation, 65, 71 f.
 Exchange, between northern and southern
 hemispheres, 104, 189
 between stratosphere and troposphere,
 164
 Exosphere, 31 f.
 Explorer IX satellite, drag of, 44 f.
 "Explosive" warming (see Stratospheric
 circulation model, warming)
 F (see Fluorine)
 F⁻ (see Fluoride)
 Fading method, 262
 Fall velocities of small particles, terminal,
 270
 Falling spheres, 25, 31, 48, 290
 "Fast Fourier transform," 48
 F-corona, 271
 Fe (see Iron)
 Feedback mechanism within the earth-
 atmosphere system, 162
 Fickian diffusion (see Diffusion)
 F-layer (see F-region)
 Florida, 25, 44, 63, 82, 121, 125, 135, 230,
 254 ff.
 Fluorescent particles, 280, 285
 Fluoride, 232
 Fluorine, 232
 Flux, countergradient, 3, 5, 7
 of energy from troposphere to strato-
 sphere, 139
 Foot-and-mouth disease, 280
 "Forbidden" oxygen red line (see Airglow)
 Forest fires, 190, 277
 Fort Belvoir, Virginia, 257, 259
 Fort Churchill, Canada, 207, 214, 247, 254,
 265 f.
 Fort Collins, Colorado, 121 ff., 125, 130,
 132, 150
 Fort Greely, Alaska, 262
 Fort Worth, Texas, 68
 FPS-16 radar wind soundings, 44, 48, 57
 France, 173 ff., 239, 241, 257
 Free electrons, generation of, 245
 F-region, 42, 44, 52 ff., 172 f., 179 f., 236,
 247, 262
 anomalously strong, 173
 diurnal variation of vertical velocities in,

- 180
 winter anomaly in, 223
 F₁-region, 176 f.
 F₂-region, 180, 224, 236
 anomalous seasonal and latitudinal variation, 180
 winter anomaly of, 224
 French Southern and Antarctic territories, 174
 Fritz Peak, Colorado, 174
 Frost-point hygrometer, 78
 Gamma function, 48
 Garmisch, Germany, 200 f.
 Gary, Indiana, 191
 Gas constant, 136
 exchange between ocean and atmosphere, 109
 Gemini V, 84
 General circulation, 1, 9, 24, 31, 75, 185, 252 f.
 Geomagnetic activity, 157
 Geomagnetic field, 53, 180
 Geomagnetic index, 44 f.
 Geomagnetic variations, semiannual, 156
 Geopotential decameters, 13
 Geopotential height, 11, 13
 Germany, 191, 196, 220 ff., 227, 282
 Ghana, 262
 GHOST balloon, 14, 23, 286
 Giant nuclei, 193, 283
 Giant salt nuclei, 282
 Glass microspheres, 285
 GMD soundings, 44
 Grand Bahama, Bahamas, West Indies, 259
 Grand Junction, Colorado, 132 f.
 Gravity, inertia waves, 44, 47, 53 f., 92, 132, 261
 waves, 49, 52 f., 55, 91, 173, 247, 254, 260, 262, 264, 290
 Green airglow (see Airglow)
 Greenland, 83 ff., 192, 275
 Grenade experiments, 25, 173, 244
 Growth rings in trees as climatological indicators, 162
 Gulf of Mexico, 70, 278
 H (see Hydrogen)
 Hadley circulation, 205, 291
 Haleakala, Hawaii, 173, 176, 178
 Hallet Station, Antarctica, 151, 153, 155
 Halley Bay, Antarctica, 150 f., 153 ff.
 Halogens, 229, 232 f.
 Hammaguir, Algeria, 247
 Hartley bands, 143
 Haute Provence, France, 173 ff., 239, 241, 257
 Hawaii, 31, 97, 99 f., 102, 165, 173, 176, 178, 207, 209, 231, 280
 Haze layer, 57, 84
 HCl, 230
 Heat budget, 97 f., 113
 Heat flux, 3, 5, 7 f., 12, 28, 43, 161, 167, 215
 Heating rates, 120, 144, 169
 Helium, 61, 75
 Heterosphere, 61
 Hilo, Hawaii, 280
 H₂O, 59
 H₂O₂, 59
 H₃O⁺, 61, 91
 H₅O₂⁺, 61, 91
 Hodograph, 47
 Home incineration, 100
 Homogeneous atmosphere, 96
 Homogeneous salt-particle atmosphere, 230
 Homosphere, 61
 H₂S, 191, 195, 202, 205 f., 284
 half-life of, 195
 oxidation of, 207
 HT, 189
 Huancayo, Peru, 174
 Huggins bands, 143
 Humidity, "motorboating," 66 ff., 70 f.
 seasonal variations of, 75
 transport of specific, 72
 Hungary, 282
 Hurricanes, 129
 Hyderabad, India, 195, 197
 Hydrocarbons, 115
 Hydrodynamic tracers, 115
 Hydrogen, 58 f., 61, 87 f., 94, 236
 atomic, 182
 compounds, 118, 120
 fluoride, 232
 half-life times, 87
 variations of, with season, 94
 with solar cycle, 94
 Hydromagnetic effects, 173
 Hydroxyl radical, 58 f., 114, 182, 236, 238
 emission in the infrared, 183
 seasonal trend in the intensities of, 183
 I (see Iodine)
 Ice crystals, 286
 Ice nuclei, 199, 232, 270, 280, 283
 Iceland, 142

- Idaho, 132 f.
 Impactor collectors, 205
 In (see Indium)
 India, 158, 165, 195, 197
 Indian monsoon, 282
 Indiana, 191
 Indium, 288
 Industrial pollution (see Air pollution)
 Industrialization, 96
 Inertial gravity waves (see Gravity, inertia waves)
 Intertropical convergence (ITC) zone, 212, 278
 Iodide, photochemical oxidation of, 231
 Iodine, 231 f.
 Iodine/bromine ratio, 231
 Iodine/chlorine ratio, 231 f.
 Ion drag, 42 f.
 Ion temperatures, thermospheric diurnal variation of, 39
 Ionosonde measurements, 256
 Ionosphere, 44, 53, 58, 176, 179, 222, 227, 247, 255, 262, 268 f.
 "dynamic region" of, 255
 inversion in, 55
 Ionospheric absorption, current systems, 32, 156
 disturbance, 52
 drifts, anomalous behavior of the, 225
 east winds, 262
 seasonal variations of, 225
 west winds, 262
 IRIS (Infrared Interferometer Spectrometer), 114
 Iron, 61, 268, 274
 Isentropic charts, 137
 surface, 5, 7, 20, 22, 44, 66 f., 129, 135 f., 215
 trajectory (see Trajectory, isentropic)
 Isobaric surface (see Surface, isobaric)
 Isobaric trajectory (see Trajectory, isobaric)
 Isopycnic layer, 31, 215, 218
 Isotropy, 11, 13
 Italy, 154, 157 f., 254
 ITC (see Intertropical convergence zone)
 Jackson, Mississippi, 71
 Japan, 69, 75, 77, 84, 142, 154, 157 f., 174, 259
 Jet axis, 76, 129
 core, 66, 75, 128
 maximum, 154, 205
 stream, 15, 22 f., 66, 75, 84, 92, 123, 128, 130, 136, 141, 147 f., 153, 205, 214, 282, 285 f., 291
 stream front, 66, 128 ff.
 Jimsphere, 48
 Jodrell Bank, England, 253
 Johnston Island, 264 f.
 Joule heating, 32
 Junge layer, 195 f., 200 f., 204, 207, 210 f., 214, 218, 268, 271, 275, 281, 290 f.
 temporal variation of the stratospheric, 201
 Kampala, Uganda, 218
 Kansas, 68
 Katmai, Alaska, 208
 Keflavík, Iceland, 142
 Kelvin waves, 157, 159
 Kenya, 136
 Kerguelén, Îles des, French Southern and Antarctic territories, 174
 Kinetic energy spectra, 11, 14, 16
 Kinshasa (See Léopoldville)
 Kisaraza, Japan, 69
 Kitt Peak, Arizona, 173, 176, 178
 Klagenfurt, Austria, 100 f.
 Kodaikānal, India, 158
 Kokubunji, Japan, 259
 Kronogård, Sweden, 90
 Lagrangian spectrum, 14
 Lake Charles, Louisiana, 68
 Lake Michigan, 278
 Lake Superior, 278
 Land-sea distribution, 65
 Lander, Wyoming, 132
 Laser, 205, 271
 Lausanne, Switzerland, 208
 Lead, 232
 iodide, 232
 Lee waves, orographic, 70, 77, 92, 283, 285
 Léopoldville, Democratic Republic of the Congo, 150, 287
 Lexington, Massachusetts, 195 f., 198, 201, 208
 Li (see Lithium)
 Lidar, 91, 195, 197, 204, 207, 255, 269
 Light extinction, 269
 Linke turbidity factor, 207, 209
 Lithium, 264
 brightness, seasonal variations of, 265
 of thermonuclear origin, 266
 twilight observations, 265
 vapor, 243

- Little America, Antarctica, 151, 155
 Long waves (see Planetary waves)
 Lorentz forces, 270
 Los Angeles, California, 102, 116
 Louisiana, 68, 70
 Luminous clouds, 245
 trails, 244, 290
 Macquarie Island, Australia, 150, 154
 Magnesium, 239, 244, 268
 Magnetic field, 53, 254
 Magnetic lines, 42, 245
 Magnetic variations, 255
 Magneto-hydrodynamic waves, 261
 Magnetosphere, 271
 Malaya, 97
 Marcus Island, 142
 Martinique, West Indies, 208
 Mass spectrometer, 61
 Massachusetts, 135, 146, 174, 195 f., 198,
 201, 207 f., 212
 Matsushima, Japan, 69
 Mauna Loa, Hawaii, 97, 99 f., 102, 165,
 207, 209
 McMurdo Sound, Antarctica, 227
 Mean circulation model above 100 km, 175
 Mean meridional circulations, 1 f., 29, 31,
 75, 92, 139 f., 168, 179, 210, 212, 214 f.,
 224 f.
 Mesopause, 25, 27, 31, 39, 49, 52 f., 55, 74,
 87, 89, 92 f., 167, 175 f., 179, 228,
 238 f., 243, 270
 rising motions near, 92
 temperatures, 27, 91
 water-vapor mixing ratio at, 91
 Mesoscale motions, 70, 117
 Mesosphere, 27 f., 31, 35, 39, 44, 49, 86 f.,
 94, 113, 144, 155, 167 f., 171, 173, 176,
 223 ff., 228, 233, 243, 266, 270
 Mesospheric circulation, 89, 170, 245
 easterly wind maximum of summer, 262
 equilibrium temperature, 145
 temperature, 57, 145, 161, 168
 water vapor, 86
 Messina, Italy, 154
 Metals, 61, 195, 245, 255 f., 264, 269
 Meteor observations, 271
 radar echoes, 267, 273
 showers, 256, 270
 trails, 171, 173, 262, 265, 269
 Meteoric activity, 266
 debris, downward transport velocities of,
 270
 influx rates, 270 f., 273, 276
 spherules, 274
 Meteorites, 268
 Meteorological Rocketsonde Network, 44,
 173, 229
 Meteors, 91, 224, 234, 268, 270
 visual, 273, 276
 Methane, 58, 85 f., 188, 191
 oxidation of, 85 f., 185
 residence times, 189
 sinks of, 188
 source of, 188
 tritiated, 189 f.
 Methylene, 189 f.
 Mexico, 278
 Mg^+ , 61
 $[Mg^+]/[Ca^+]$ ratio, 268
 Micrometeorites, 91, 93, 234, 266, 275
 Middlesex, England, 191
 Midland, Texas, 132 f.
 Mic scatter, 269, 287
 Milton, Massachusetts, 207
 Minneapolis, Minnesota, 207
 Minnesota, 207
 Mirny, Antarctica, 123
 Mississippi, 71
 Missouri, 191
 Mixing layer, adiabatic, 71, 133, 148, 278,
 285
 depth of, 133
 marine, 97
 Mixing length, 3 f.
 Mixing path, 5
 Mixing ratio, 2 f., 5, 71, 76, 78, 82, 85 f.
 Mixing surface, 4
 slope of, 4 f., 7, 12
 Model of the upper atmospheric circulation,
 177
 Moist adiabatic processes, 20, 23
 Moisture (see Water vapor)
 Molecular diffusion, 246 f.
 Monsoon, summer, 72
 Monsoonal wind regime in stratosphere and
 mesosphere, 25, 261
 Montgomery stream function, 136 f.
 Moosonee, Ontario, 143
 Mother-of-pearl clouds, 73, 76, 81
 "Motorboating" humidity (see Humidity,
 "motorboating")
 Mount Abu, India, (see Abu-Ahmedabad,
 India)
 Mount Agung, Bali, 135, 196 f., 199, 207 ff.,
 275, 281

- Mount Bigelow, Arizona, 280
 Mount Olympus, Washington, 99 f.
 Mount Pelée, Martinique, West Indies, 208
 Mount Stromlo, Australia, 208
 Mountain breeze, 148, 280
 waves (see Lee waves, orographic)
 N (see Nitrogen)
 Na (see Sodium)
 [Na]/[NaO] ratio, 238
 NaCl, 283
 Nacreous clouds, 76, 81
 NaI, 232
 Nairobi, Kenya, 136
 Nandi Island, Fiji, 158
 Nantucket Island, Massachusetts, 196
 NaO, 236, 238 f.
 [NaO]/[NaO₂] ratio, 238
 NaO₂, 238
 Natural gas, 188
 Neosho, Missouri, 191
 New Mexico, 25, 48, 62, 78, 121, 125, 130,
 132 f., 170, 172, 283
 New York, 193
 New York City, New York, 193
 New Zealand, 122, 188, 227, 257, 259, 285
 NH₃ (see Ammonia)
 NH₄⁺, 218
 (NH₄)₂SO₄, 231
 Nickel, 274
 Night glow, 58, 168, 170, 182, 233 f., 237
 NIMBUS III IRIS (Infrared Interferometer
 Spectrometer), 114
 Nitrates, 218
 Nitric oxide, 218 f., 222 ff., 244
 Nitrogen, 58, 61, 180, 218, 220, 223, 245
 oxides of, 115
 Nitrogen dioxide, 218 f., 223
 ground-level source of, 220
 mixing ratios, 222
 Nitrogen trioxide, 218
 Nitrous oxide, 218 f., 228
 photodissociation, 228
 residence time of, 228
 NLC (see Noctilucent clouds)
 NO (see Nitric oxide)
 NO⁺, 61, 256
 NO₂ (see Nitrogen dioxide)
 NO₃ (see Nitrogen trioxide)
 NO₃⁻ ions, 218, 220 f.
 washout removal of, 220
 N₂O (see Nitrous oxide)
 N₂O₃ (see Dinitrogen trioxide)
 N₂O₄ (see Dinitrogen tetraoxide)
 N₂O₅ (see Dinitrogen pentoxide)
 N₂O₆ (see Dinitrogen hexoxide)
 Noctilucent clouds, 25, 73, 86 f., 89 ff.,
 145, 162, 179, 200, 214, 239, 269, 271,
 290
 diurnal variations, 90
 rocket samples of, 91
 North Africa, 277
 North America, 49, 120, 224, 229
 North Atlantic, 277, 283
 Northern hemisphere, 185, 188 ff., 199, 235
 Norway, 150, 154, 183, 238
 Nuclear explosions, 261
 Nuclear tests, high-altitude, 52
 Number density, 42, 60 f., 93
 O (see Oxygen)
 O₃ (see Ozone)
 Oakland, California, 134
 Oberhausen, Germany, 191
 Ocean surface temperatures, 162
 Oceanic thermocline, 97
 OH (see Hydroxyl radical)
 Oklahoma, 68
 Oklahoma City, Oklahoma, 68
 Olefins emitted by plants, 116
 photochemical oxidation of, 116
 Olympia, Washington, 132 f.
 Ondrejov, Czechoslovakia, 174
 Ontario, 143
 Optical radar (see Lidar)
 Oregon, 132
 Organic material, decay of, 195
 Orographic cloud systems, 232
 Oxidant concentrations, 115, 132 f.
 Oxygen, 58 f., 61, 143, 157, 167, 180, 182,
 189, 223 f., 236, 238
 atomic, 27, 58, 61, 85, 95, 144, 167 ff.,
 175, 179
 electronic excitation state of, 59, 114, 167
 emission (5577 Å, 6300 Å) (see Airglow)
 green line, 5577 Å (see Airglow)
 infrared emission of, 168
 ions, 61, 145, 224, 256
 photochemical reactions with hydrogen, 182
 photodissociation of, 114
 recombination process of atomic, 168, 176
 red line, "forbidden" (see Airglow)
 6300 Å (see Airglow)
 seasonal variations in the 1.58-μ emission,
 168
 Ozonagram, 115 f.

- Ozone, 7, 12, 28 f., 32, 34, 39, 56, 58 f., 75,
113, 116 f., 121, 127 ff., 132, 134 ff.,
143, 145, 157, 164, 167, 182, 185, 189,
195 f., 207, 212, 214, 224 f., 230, 240,
291
in air pollution, 115
balloon measurements of, 39
budget, 141
catalytic destruction effect on, 135
destruction at the ground, 147, 153, 163
dissociation of, 114, 141, 144, 156, 168
diurnal variation of, 144, 148
effects on temperature, 142
half-life of, 113
heating, 39
hemispheric differences, 148
infrared bands of, 113, 143
interdiurnal variation of, 139, 150
ions, 225
latitudinal gradients in total, 150
maximum, latitude dependence of the,
118
in the mesosphere, 144
"moist" reactions, 120
nonequilibrium concentration of, 115,
119, 122
number densities, 120 ff.
peak, 114, 122 f., 139, 141, 143, 153
photochemical equilibrium of, 118, 145,
162
theory of, 114, 117 ff., 122 f., 142, 145
time constants for, 120
production by thunderstorms, 117
profiles, satellite-observed, 58
reactions with nitrogen, 114
relaxation time of, 115, 118
residence time of, 147 f., 163
satellite measurements of, 114
seasonal variation of, 145
soundings, 114, 130
spring maximum of, 122 f., 145, 147,
149 f., 158
surface concentrations, 145, 153, 155,
163
time of half-restoration of, 115, 118
transport, 138, 141, 148, 211
from the stratosphere to the troposphere,
163
theoretical models of, 162
variations, solar relations of, 155 f.
winter maximum of surface, 211
Ozonesonde Network, 120, 136
Ozonometer M-83, 114
Ozonosphere, 128, 155 f.
Pacific, 106, 188, 278
Panama, 206 f., 212
Particle dispersion, 17 ff.
Particles, falling speed of spherical, 202
PbO, 232
Peru, 174, 278
pH value, 96, 195, 232
Photochemistry, 56, 58, 136, 182, 239
Photoelectrons, 180
Photophoretic forces, 205
Planetary boundary layer (see Mixing
layer, adiabatic)
Planetary waves, 14, 18, 23 f., 34, 49, 128,
139, 210, 218, 224
Plume, 17 f.
Point Barrow, Alaska, 99 f.
Point Mugu, California, 116
Poisson's constant, 136
Poland, 208
Polar front jet stream, 75, 163
Polar night jet stream, 243
Polar night vortex, breakdown of the strato-
spheric, 25, 138, 147 ff., 196, 243
excentricity of, 210
Pole, 27, 75, 92, 111, 167 f.
Pollen, 190, 218, 278, 280, 286
dyed, 285
ragweed, 278
Potassium, 239, 264
Potential gradient, 220
Potential temperature, 66, 115, 133
Potential vorticity, 115, 129 f., 133, 135
Power spectra of velocity, 17
Poynting-Robertson effect, 271, 273
Precipitable water, 207
Precipitation, 71 f.
nuclei, 270
Pretoria, South Africa, 149, 151
Project Firefly, 245
Project Streak, 215
Puget Sound, 100
Purple twilight, 197
Quasi-biennial wind oscillation (see Biennial
oscillation)
Radar meteors, 266, 276
signals, backscatter of, 69
Radiation budget, 97 f., 113
diffuse, 212
direct solar, 207, 210 ff.
flux, 57, 143, 145, 185
pressure effect, 271

- Radiative equilibrium temperatures, 143
 Radiative heating, 27, 29, 75
 Radio refractive index, 69
 Radio refractivity, 57, 69
 Radioactive debris, 56, 66, 70, 139, 147 f.,
 163, 205, 214, 218, 282 ff., 291
 Radioactive fallout, spring maximum of,
 123
 Radiocarbon data, 106
 Radiometer, 69, 73, 144, 205
 Rainout, pollen in, 278
 Rare-earth element, 288
 Rate of dissipation of kinetic energy, 20
 Reaction rate, 59, 118
 Recombination rate, 58
 Refractometer, 69
 Relaxation times, 136, 144 f., 155
 Resolute, Canada, 142
 Retz, Austria, 100 f.
 Reynolds number, 247
 Rh (see Rhodium)
 Rhodium, 266
 Richardson numbers, 55 f.
 Robin falling sphere, 44
 Rocket measurements, 61, 144, 182, 222,
 229, 233, 239, 243 ff., 247, 264, 270,
 273
 seeding experiment, 265
 Rocky Mountains, 123
 Rome, Italy, 157 f.
 Rossby waves, planetary, 228
 Ruby laser (see Laser), 271
 Russia (see Soviet Union)
 S (see Sulfur)
 $^{32}\text{S}/^{34}\text{S}$ isotope ratio, 191
 Sahara, 277
 Salem, Oregon, 132
 Salt Lake City, Utah, 132 f.
 San Francisco, California, 188
 Sardinia, Italy, 254
 Saskatchewan, Canada, 235, 265 f.
 Saskatoon, Saskatchewan, Canada, 235,
 265 f.
 Satellite drag observations, 32, 54, 173
 Satellite observations, 271, 273
 Satellites, 31 f., 54, 65, 69, 72, 84, 145,
 162, 173, 271, 273
 "Scale height" of the atmosphere, 54
 Scandinavia, 96, 102
 Scattering ratio, 208
 Scotland, 154
 Sea fog, 218
 Sea salt, 191, 229 f.
 Sea spray, 218, 231, 283
 Seabreeze, 285
 Searchlight techniques, 195
 Seattle, Washington, 132
 Sendai, Japan, 69
 SF_6 (see Sulfur hexafluoride)
 Shreveport, Louisiana, 68, 70
 Silver iodide, 232, 270
 Sky radiance, 204
 Skylight polarization, 255, 276
 Small-ion concentration, 204
 Smoke tracer experiments, 278
 trails, 244
 SO_2 (see Sulfur dioxide)
 SO_4^{2-} (see Sulfate)
 $\text{S}_2\text{O}_8^{2-}$ anions, 211
 Sodium, 224, 233 f., 237 ff., 254 f., 264,
 266, 268 f., 290
 airglow emission, 233 f., 236, 238 f., 241,
 243, 257, 259
 as an artificial tracer, 243
 cloud experiments, 92, 244 f., 247, 261 f.,
 264 f.
 emission, seasonal variations, 234
 meteoric, 234
 thermospheric, 243
 Sodium/potassium ratio, 234, 268
 Solar activity, 236, 260
 constant, 207
 cycle (see Sunspot cycle), 179, 260
 flux in the 10.7-cm wave band, 44 f.
 UV emission, 157
 violet radiation, 231
 X rays, 223
 Source release rate, 17
 South Africa, 149, 151, 209
 South American Andes, 208
 South Pole, 29, 105, 110, 123, 151, 153,
 209 ff., 275
 South Pole station, Antarctica, 151
 Southern hemisphere, 188 ff., 199, 209,
 235, 262, 280
 Soviet Union, 13, 78, 114, 144, 195, 208,
 264
 Space vehicles, 73
 Specific heat, 48, 52, 136
 Specific humidity, 70 f.
 conservation of, 65
 Spectral densities, 48
 Spectrographic absorption measurements,
 82
 Spectrum function, 12 ff., 47 f.
 Speed of sound, 48, 52

- Sporadic E, 44, 61, 175 f., 182, 240, 245, 254 ff., 259
 blanketing, 256
 formation, theory on, 254
 occurrence with wind shears, 182
 quasi-biennial cycle in the occurrence of intense, 259
 seasonal variation of, 257
 intense, 259
- Spores, 278
- Sr (see Strontium)
- Srinagar, India, 165
- Standard Atmosphere, U. S., 61
- Standard deviation, 13, 17 f., 22, 139
- Stefan flow, 286
- Stockholm, Sweden, 98
- Straits of Juan de Fuca, 100
- Stratonull layer, 214 f.
- Stratopause, 27, 31 f., 39, 44, 49, 95, 113, 144 f., 228, 243, 261
 maximum wind layer near, 243
- Stratosphere, 1, 3, 7, 18, 22, 24, 27 ff., 31, 39, 44, 48 f., 58, 66, 70, 72, 74 f., 77 f., 81 ff., 86 f., 91, 102, 113, 115, 117, 122 f., 128, 136, 139, 141 f., 145, 147, 150 f., 153, 155, 157, 162, 167, 173, 189, 196, 199 ff., 205, 207, 211 f., 214 f., 225, 227 f., 231, 233 f., 243, 245, 266, 270, 282
 diurnal temperature in, 34
 "dry," 73, 78, 214
 "wet," 78
- Stratospheric circulation, monsoonal character of the, 261
- Stratospheric circulation model, one-cell, 163
 two-cell, 28, 163, 167
- Stratospheric ice-nuclei source, 281
- Stratospheric moisture, latitudinal variations of, 84
 seasonal trend of, 82
- Stratospheric temperature, density, semi-annual cycle in, 31
 distribution, 27, 34, 95
- Stratospheric vortex (see Polar night vortex)
- Stratospheric warming, 34, 138, 147, 149 f., 215, 225, 227 f., 241, 254
- Stratospheric-tropospheric exchange processes, 66, 129, 135, 147, 153, 164 f., 291
- Streamlines, 70
- Strontium, 215, 217, 244 f.
- Structure function, 47 f., 247
- Subtropical jet stream, 75, 163
- Sudden warming (see Stratospheric warming)
- Sugar cane, burning of, 284
- Sulfate, 191 ff., 195, 197, 199, 201, 211 f., 214, 281, 291
 layer, 136, 195, 202, 205, 207, 212, 214, 218, 281
- Sulfur, 191, 197, 199, 205, 207, 212, 275
- Sulfur dioxide, 191, 193, 195, 202, 205 ff., 212, 282, 284
 annual variation, 193
 diurnal cycle of, 193
 half-life, 195
 mixing ratios, 192
 oxidation of, 207
 photochemical oxidation of, 195, 218
 rainout of gaseous, 192
 washout of gaseous, 192
- Sulfur hexafluoride, 232, 245
 mixing ratios, 197
 oceanic, 191
 volcanic, 191, 204
- Sulfuric acid droplets, 202, 275
- "Sunrise effect" on condensation nuclei, 284
- Sunspot activity, 157, 259
 cycle, 44, 94, 155, 157, 179, 260
 latitude, 156
 number, 156 f., 168, 175
- Supersonic transport flights, 73, 98, 290 f.
- Surface, isobaric, 20, 22
- Sweden, 90, 98 f.
- Switzerland, 147 ff., 156 f., 159, 165, 208
- Tallahassee, Florida, 121, 125, 135
- Tamanrasset, Algeria, 174
- Tateno, Japan, 77, 154, 157 f.
- Tatoosh Island, Washington, 130, 132 f.
- Temperature distribution, exospheric, 44
 mesopause, 31, 89, 92
 peak near 50 km, 142
 semiannual variation in, 32, 44
 stratospheric, 161
 at the thermopause, diurnal variation of, 42
 tidal effects on, 35
 tropopause, 75
 variations, diurnal, 44
- Terminal velocities, small extraterrestrial particles, 92
- Terpenes, 190
- Terre Adelie, Antarctica, 212
- Texas, 68, 130, 132 f.

- Thermal electrons**, 177
Thermal wind equation, 31
Thermopause, 32
 diurnal temperature variations near, 39
Thermosphere, 25, 27, 29, 31 f., 39, 43 f.,
 93 f., 171 f., 233, 244 f.
 bulges in, 61
 solar response of, 44
Thermospheric circulation, 175
Three-atom gases, 185
Three-body collisions, 58, 61
Thule, Greenland, 83 ff.
Thunderstorms, 84, 218, 283
 "Tidal jet," 39
Tidal wind, 39, 260
Tide, diurnal, 225, 258
 diurnal thermal, 56
 semidiurnal, 258, 262
Tides, 35, 39, 43, 55 f., 171, 173, 225,
 254 f., 258, 262, 264 f., 290
TIROS IV, 73
TNT, 245
Tokyo, Japan, 69
Torishima, Japan, 154
Tracers, artificial, 243, 291
Trajectory, 20, 22, 55, 66, 70, 117, 210 f.
 isentropic, 20, 23, 65, 130
 isobaric, 14, 18, 23
Triethyl aluminum, 244
Trimethyl aluminum, 244
 trails, 247
Trinidad, West Indies, 78, 80 ff.
Tritium, 75 f., 189 f.
 half-life of, 189
 units, 189
Tromsø, Norway, 150, 154, 238
Tropopause, 78, 82, 123, 129 f., 132, 136,
 147, 163, 165, 167, 188 f., 196 f., 201,
 205 f., 212, 214, 231, 234, 270, 291
 gap, 141, 153, 205, 291
Troposphere, 1, 7, 9, 18, 23 f., 44, 49, 52,
 65, 69 f., 75, 86, 102, 109, 115, 123, 128,
 139, 145, 151, 165, 199, 201, 205, 211,
 233, 269, 277, 282
Tucson, Arizona, 132
Tungsten, 7, 28, 234
Turbidity, 207, 210, 270, 277
 coefficient, 287
 seasonal variations in, 207
Turbopause, 61, 92 f., 239, 245, 247
Turbosphere, 61
Turbulence, 3, 13, 15, 39, 56 f., 69, 165,
 245 ff.
Turbulent mixing, 55, 70 f., 75, 86, 130, 136
Twilight (see Airglow)
U-2 aircraft, 129, 197
Uganda, 218
Ultraviolet radiation, 32, 39, 42, 95, 113,
 118, 143, 155, 180, 182, 284
Umkehr measurements, 114, 149
 method, 141, 145
United States, 188, 244, 270, 280, 287
University of New Mexico, 130, 132
Upslope breeze, diurnal, 99
USSR, European (see Soviet Union)
Utah, 132 f.
Valley breezes, 99
Valley of Ten Thousand Smokes, Alaska,
 230, 232
Van Allen radiation belts, 180
van Rhijn method of height measurement,
 233
Vapor trail, 243, 245 f.
Vaporization of meteors, 73
 "Venus Flytrap" sounding rocket, 273, 276
Vienna, Austria, 100 f., 147 ff., 193 f., 284
Virginia, 25, 233, 235, 248, 251, 254, 257,
 259, 261 f.
Virus diseases, 280
Viscosity, coefficient of, 247
 hydromagnetic, 54
 molecular, 54
Volcanic activity, 275
Volcanic debris, 135
Volcanic dust, 275 f.
Volcanic fumes, 202, 232, 275
Vorticity component, vertical, 133
W (see Tungsten)
Wakkanai, Japan, 259
Wallops Island, Virginia, 25, 233, 235, 248,
 251, 254, 261 f.
Wank Peak, Germany, 220 f.
Warsaw, Poland, 208
Washington, 99 f., 130, 132 f.
Washington, D. C., 78, 80 ff., 85, 208
Washout, 205, 286, 288
Water, 62, 72
Water vapor, 3, 27, 56 f., 59, 65, 69 f.,
 72 ff., 78, 83 ff., 98, 143, 145, 162,
 185, 189, 212, 290
 budget of the upper stratosphere, 58
 dissociation of, 87
 distribution from photochemical equi-
 librium, 92
 half-life times, 87, 92
 ions, 61

- Waters, upwelling coastal, 106
"Weather flecking" of tobacco leaves, 148
Wembley, Middlesex, England, 191
West Indies, 78, 80 ff., 208, 254, 259,
262 f., 277, 279
White pine blister rust, 278
White Sands, New Mexico, 25, 48, 62, 170,
172
Wind distribution, diurnal and tidal effects
on, 35
fluctuations, average vertical wavelength
of, 48
mesoscale, 48
maximum near 100 km, 252, 254, 264
minimum in mean zonal, 214 f.
Window, 118, 143
Woomera, Australia, 25, 250
Wyoming, 132
"Year without a summer," 276
Yuma, Arizona, 254
Zinc sulfide, 285
Zodiacal cloud, 271
Zodiacal light, 271 ff.
Zugspitze Peak, Germany, 220 f.

NOTICE

This book was prepared under the sponsorship of the United States Government. Neither the United States nor the United States Atomic Energy Commission, nor any of their employees, nor any of their contractors, subcontractors, or their employees, makes any warranty, express or implied, or assumes any legal liability or responsibility for the accuracy, completeness or usefulness of any information, apparatus, product or process disclosed, or represents that its use would not infringe privately owned rights.